VOL. 554 NOS. 1 + 2 AUGUST 2
7th Int. Symp. on LC–MS,
SFC–MS, CE–MS and MS–MS
Montreux, Oct. 31–Nov. 2, 1990

RNAL OF HROMATOGRAPHY

DING ELECTROPHORESIS AND OTHER SEPARATION METHODS

SYMPOSIUM VOLUMES

ELSEVIER

Scope. The *Journal of Chromatography* publishes papers on all aspects of chromatography, electrophoresis and related methods. Contributions consist mainly of research papers dealing with chromatographic theory, instrumental development and their applications. The section *Biomedical Applications*, which is under separate editorship, deals with the following aspects: developments in and applications of chromatographic and electrophoretic techniques related to clinical diagnosis or alterations during medical treatment; screening and profiling of body fluids or tissues with special reference to metabolic disorders; results from basic medical research with direct consequences in clinical practice; drug level monitoring and pharmacokinetic studies; clinical toxicology; analytical studies in occupational medicine.

Submission of Papers. Manuscripts (in English; *four* copies are required) should be submitted to: Editorial Office of *Journal of Chromatography*, P.O. Box 681, 1000 AR Amsterdam, The Netherlands, Telefax (+31-20) 5862 304, or to: The Editor of *Journal of Chromatography, Biomedical Applications*, P.O. Box 681, 1000 AR Amsterdam, The Netherlands. Review articles are invited or proposed by letter to the Editors. An outline of the proposed review should first be forwarded to the Editors for preliminary discussion prior to preparation. Submission of an article is understood to imply that the article is original and unpublished and is not being considered for publication elsewhere. For copyright regulations, see below.

Publication. The *Journal of Chromatography* (incl. *Biomedical Applications*) has 38 volumes in 1991. The subscription prices for 1991 are:

J. Chromatogr. (incl. *Cum. Indexes, Vols. 501–550*) + *Biomed. Appl.* (Vols. 535–572):
Dfl. 7220.00 plus Dfl. 1140.00 (p.p.h.) (total *ca.* US$ 4519.00)

J. Chromatogr. (incl. *Cum. Indexes, Vols. 501–550*) only (Vols. 535–561):
Dfl. 5859.00 plus Dfl. 810.00 (p.p.h.) (total *ca.* US$ 3604.75)

Biomed. Appl. only (Vols. 562–572):
Dfl. 2387.00 plus Dfl. 330.00 (p.p.h.) (total *ca.* US$ 1468.75).

Subscription Orders. The Dutch guilder price is definitive. The US$ price is subject to exchange-rate fluctuations and is given as a guide. Subscriptions are accepted on a prepaid basis only, unless different terms have been previously agreed upon. Subscriptions orders can be entered only by calender year (Jan.–Dec.) and should be sent to Elsevier Science Publishers, Journal Department, P.O. Box 211, 1000 AE Amsterdam, The Netherlands, Tel. (+31-20) 5803 642, Telefax (+31-20) 5803 598, or to your usual subscription agent. Postage and handling charges include surface delivery except to the following countries where air delivery via SAL (Surface Air Lift) mail is ensured: Argentina, Australia, Brazil, Canada, Hong Kong, India, Israel, Japan*, Malaysia, Mexico, New Zealand, Pakistan, PR China, Singapore, South Africa, South Korea, Taiwan, Thailand, USA. * For Japan air delivery (SAL) requires 50% additional charge of the normal postage and handling charge. For all other countries airmail rates are available upon request. Claims for missing issues must be made within three months of our publication (mailing) date, otherwise such claims cannot be honoured free of charge. Back volumes of the *Journal of Chromatography* (Vols. 1–534) are available at Dfl. 208.00 (plus postage). Customers in the USA and Canada wishing information on this and other Elsevier journals, please contact Journal Information Center, Elsevier Science Publishing Co. Inc., 655 Avenue of the Americas, New York, NY 10010, USA, Tel. (+1-212) 633 3750, Telefax (+1-212) 633 3990.

Abstracts/Contents Lists published in Analytical Abstracts, Biochemical Abstracts, Biological Abstracts, Chemical Abstracts, Chemical Titles, Chromatography Abstracts, Clinical Chemistry Lookout, Current Contents/Life Sciences, Current Contents/Physical, Chemical & Earth Sciences, Deep-Sea Research/Part B: Oceanographic Literature Review, Excerpta Medica, Index Medicus, Mass Spectrometry Bulletin, PASCAL-CNRS, Pharmaceutical Abstracts, Referativnyi Zhurnal, Research Alert, Science Citation Index and Trends in Biotechnology.

See inside back cover for Publication Schedule, Information for Authors and information on Advertisements.

0021-9673/91/$03.50

This issue is printed on acid-free paper.

Printed in The Netherlands

For Contents, see p. VII

JOURNAL OF CHROMATOGRAPHY

VOL. 554 (1991)

JOURNAL of CHROMATOGRAPHY

INCLUDING ELECTROPHORESIS AND OTHER SEPARATION METHODS

SYMPOSIUM VOLUMES

ELSEVIER
AMSTERDAM — OXFORD — NEW YORK — TOKYO

J. Chromatogr., Vol. 554 (1991)

Castle of Chillon, beginning of 19th century

0021-9673/91/$03.50

Printed in The Netherlands

SYMPOSIUM VOLUME

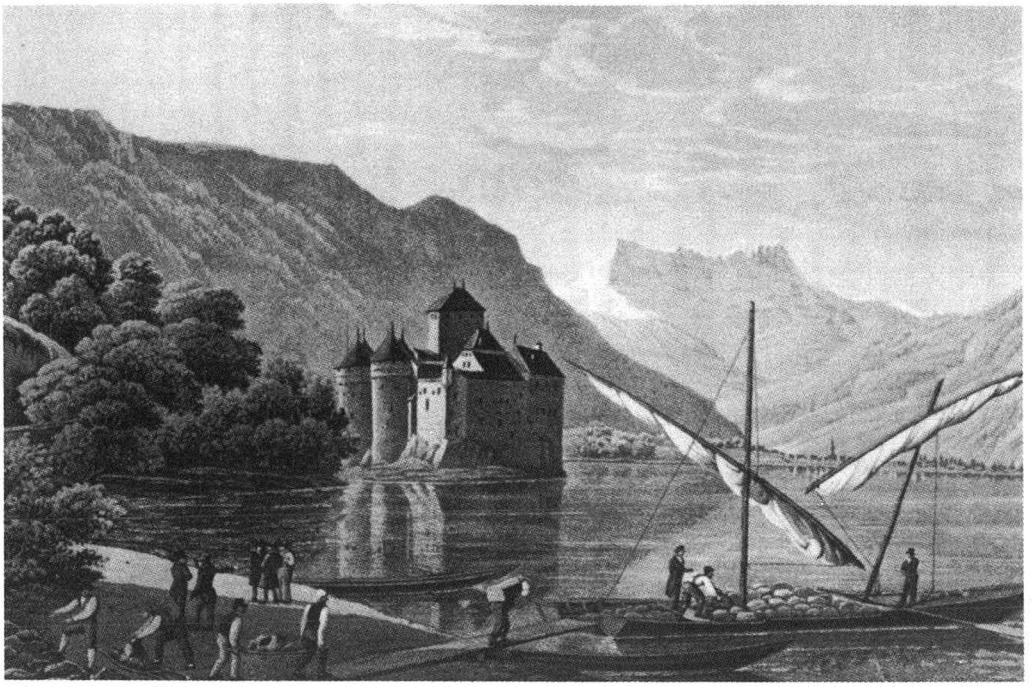

7TH INTERNATIONAL SYMPOSIUM ON LIQUID CHROMATOGRAPHY–MASS SPECTROMETRY,

SUPERCRITICAL FLUID CHROMATOGRAPHY–MASS SPECTROMETRY, CAPILLARY ELECTROPHORESIS–MASS SPECTROMETRY AND TANDEM MASS SPECTROMETRY

Montreux (Switzerland), October 31–November 2, 1990

Guest Editor

J. VAN DER GREEF

(Leiden and Zeist)

VOL. 554, NOS 1+2 JOURNAL OF CHROMATOGRAPHY AUGUST 21, 1991

CONTENTS

7TH INTERNATIONAL SYMPOSIUM ON LIQUID CHROMATOGRAPHY–MASS SPECTROMETRY, SUPERCRITICAL FLUID CHROMATOGRAPHY–MASS SPECTROMETRY, CAPILLARY ELECTROPHORESIS–MASS SPECTROMETRY AND TANDEM MASS SPECTROMETRY, MONTREUX, OCTOBER 31–NOVEMBER 2, 1990

In articles with more than one author, the name of the author to whom correspondence should be addressed is indicated in the article heading by a 6-pointed asterisk (*).

Journal of Chromatography, 554 (1991) 1–2
Elsevier Science Publishers B.V., Amsterdam

FOREWORD

The *7th International Symposium on Liquid Chromatography–Mass Spectrometry, Supercritical Fluid Chromatography–Mass Spectrometry, Capillary Electrophoresis–Mass Spectrometry and Tandem Mass Spectrometry*, held in Montreux from October 31 to November 2, 1990, again showed the rapidly growing interest in this field of research. This was clearly reflected by the attendance of about 240 persons, the largest number so far in this series.

The scientific level of the symposium was very high, and good discussions were held, demonstrating, among other things, that the number of liquid chromatography–mass spectrometry (LC–MS) users is growing enormously, outnumbering the people in LC–MS development.

Basically, the combination of methods consists of the separation unit, the interface and the mass spectrometer. Although the emphasis was more on the last two aspects in the past, in this symposium developments were reported in all three areas, and this also reflects the fact that strong emphasis is placed on developing practical applications.

Separation techniques receiving greatest attention at present are based on LC, supercritical fluid chromatography and capillary electrophoresis. Several "incompatible" LC systems have been investigated. In particular, ion-pair and ion-exchange chromatography, coupled with electrospray interfacing, is apparently becoming a practical reality. The problem of non-volatile buffers in the mobile phase was addressed by several research groups. The replacement by volatile buffer systems was demonstrated, as was on-line mobile phase switching, miniaturization for low-flow-rate interfaces and the use of hybrid separation methods, such as pseudo-electrochromatography, which allows voltage programming across a packed fused-silica column.

A similar hybrid approach is also being adopted in interface development. At present, the four most widely used interfaces are particle beam, thermospray, continuous-flow fast atom bombardment (FAB) and electrospray. The recently introduced interfaces are often combinations of the various underlying basic principles.

Thermospray is still the most popular interface for routine use, because it operates at conventional flow-rates and can handle compounds with a wide polarity range. The particle-beam method is advancing strongly, because it is robust and very straightforward to use. While the instrumental aspects of continuous-flow FAB are hardly developing, it appears to provide a useful analytical tool for polar compounds in the m/z range <2500. The heated nebulizer interface is clearly performing very well, being robust and, as a consequence, an attractive approach in high-throughput applications. The major interest with respect to new instrumental design centred on electrospray and ion spray techniques. In particular, they open up avenues to the detection of high-molecular-weight proteins and glycoproteins. Two manufacturers presented data on an antibody of 148 000 dalton, yielding molecular weight information with a triple quadrupole instrument.

Developments in mass analysers are also a strong influence in the field of combination methods. Recent work on ion traps demonstrates the high mass capability at 45 000 dalton, high sensitivity and extremely good MS–MS performance of these

devices. Further, high resolution and array detection was shown by a magnetic sector instrument with both thermospray and electrospray.

Analyte characteristics are very important for the overall success of any LC–MS approach. Derivatization was shown to improve detection performance substantially in both the particle-beam and thermospray techniques. The latter was demonstrated in even a fully automated system, exhibiting satisfactory quantification performance. A remarkable observation was that different folding of macromolecules probably results in differences in charge distribution in the electrospray technique. An interesting discussion was held on the basic mechanism of ionization in electrospray and on the nomenclature to be used in LC–MS.

The conclusion to be drawn from this symposium is that LC–MS and related combination methods have a great future, because all building blocks —separation, interfacing, ionization and mass analysis— are undergoing vigorous development, while the basic instrumentation is already a very useful analytical tool in many laboratories.

The next meeting will be held in Ithaca, NY, July 17–19, 1991, and the next European LC–MS meeting will be held on November 4–6, 1992, in Montreux.

Leiden (Netherlands) JAN VAN DER GREEF

Journal of Chromatography, 554 (1991) 3–26
Elsevier Science Publishers B.V., Amsterdam

CHROMSYMP. 2220

Strategies in developing interfaces for coupling liquid chromatography and mass spectrometry

W. M. A. NIESSEN* and U. R. TJADEN
Division of Analytical Chemistry, Center for Bio-Pharmaceutical Sciences, P.O. Box 9502, 2300 RA Leiden (Netherlands)
and
J. VAN DER GREEF
Division of Analytical Chemistry, Center for Bio-Pharmaceutical Sciences, P.O. Box 9502, 2300 RA Leiden and TNO–CIVO Institutes, P.O. Box 360, 3700 AJ Zeist (Netherlands)

ABSTRACT

Considerable progress has been made over the last 20 years in coupling liquid chromatography and mass spectrometry. A large number of interfaces have been developed and, although only a few have found widespread application, the developments in interfacing are worth reviewing. The developments in interfacing are categorized along three lines: efforts to introduce 1 ml/min of an aqueous mobile phase into the mass spectrometer vacuum system, efforts to achieve analyte enrichment in the interface and efforts to combine interfacing and liquid-based soft ionization techniques. These lines are explored, with special attention being given to the most successful interfaces. Some similarities between the various interfaces are revealed.

INTRODUCTION

The on-line combination of liquid chromatography and mass spectrometry (LC–MS) has been under investigation for about 20 years. The first paper on LC–MS came from the Russian group of Tal'roze *et al.* [1] in 1972. The development of LC–MS has continued via various landmarks and led to a vast number of papers on successful applications that have appeared during the last few years and to several successful and commercially available LC–MS interfaces. The subject has been extensively reviewed [2–6]. This paper can also be considered as a review on LC–MS, but attention is especially focused on the developments in interface technology. In that respect, it is more or less a free interpretation of the history of LC–MS.

In developing on-line LC–MS three fundamental compatibility problems had to be solved, *viz.*, the amount of solvent eluting from the LC column, the composition of the LC mobile phase and the nature of the analytes. Interfaces have been developed to be placed between the LC column outlet and the mass analyser to solve the incompatibility between the LC solvent and the MS high vacuum. Over 25 different interface approaches have been described (see Table I). In the development of these

0021-9673/91/$03.50

TABLE I

HISTORICAL OVERVIEW OF LC–MS INTERFACES

Important features of the various interfaces, *i.e.*, nebulization, analyte enrichment and liquid-based ionization, are indicated.

Year	Type	Nebulization	Enrichment	Liquid-based ionization
1972	Stopped flow		+	
1972	Capillary inlet			
1974	Moving belt	±	+	
1974	Pneumatic nebulizer in atmospheric-pressure source	+		
1975	Solvent vapour separator membrane		+	
1976	Liquid ion evaporation	+		+
1978	Crossed beam	+		
1978	Jet separator		+	
1979	Vacuum nebulizer	+	+	
1980	Direct liquid introduction	+		±
1981	Conical tip	+		
1981	Continuous sample preconcentrator	+	+	
1982	Rotating disk		+	
1983	Helium	+		
1983	Thermospray	+		+
1984	Monodisperse aerosol generator	+	+	
1985	Electrospray	+		+
1985	Frit FAB			+
1986	Continuous-flow FAB			+
1986	Particle beam	+	+	
1986	Heated nebulizer	+		±
1987	Thermabeam	+	+	
1987	Gas nebulized	+		
1987	Ionspray	+		+
1988	Atmospheric-pressure spray	+		+
1989	Frit-EI/CI			

LC–MS interfaces over the past 20 years three development lines can be distinguished, which are concerned with efforts (i) to introduce 1 ml/min of an aqueous mobile phase into the MS vacuum system, (ii) to achieve analyte enrichment in the interface and (iii) to develop liquid-based ionization techniques. These lines are explored and discussed below. As a result, similarities in different LC–MS interfaces are recognized and the possibilities and limitations of the various LC–MS interfaces become clearer and can more readily be explained.

AN INTERFACE FOR LC–MS

The most important feature of an LC–MS interface is to provide a means for the transition of analyte molecules from the liquid state to the high vacuum of the mass spectrometer. During this transition as much analyte as possible must be transferred, while the mobile phase constituents can be partially or completely removed. In

this respect, the LC–MS interface can be characterized by the transfer efficiency and the enrichment factor. The transfer efficiency Y is defined as

$$Y = (Q_{MS}/Q_{LC}) \cdot 100\% \quad (1)$$

where Q_{LC} and Q_{MS} are the amount of analyte eluting from LC column and the amount introduced into the mass spectrometer, respectively. Note that the amount of analyte introduced into the MS system is difficult to define unambigiously, because with some interfaces the analyte is transferred as neutral molecules that are subsequently ionized, whereas with other interfaces ionization is an integral part of the transfer step and the ions are preferentially extracted from the interface.

The enrichment factor E is the ratio of the analyte concentration in the MS flow and that in the LC flow, defined as

$$E = (Q_{MS}/F_{MS})/(Q_{LC}/F_{LC}) \quad (2)$$

where F_{LC} and F_{MS} are the flow-rate from the LC column and the flow-rate introduced into the mass spectrometer, respectively. Again, F_{MS} is sometimes difficult to define, because of the features of the interface. For some interfaces these aspects are discussed in more detail below.

The mass spectrometer is a mass-flow-sensitive detector, which means that the response R is directly proportional to the mass flow, dm/dt:

$$R = \tau(dm/dt) \quad (3)$$

where τ is the response factor. As the mass flow is the change of mass per unit time, eqn. 3 can be written as

$$R = \tau\, C(t)\, F_{MS} \quad (4)$$

where $C(t)$ is the analyte concentration profile *e.g.*, a nearly Gaussian peak from the LC column, and

$$F_{MS} = F_{LC}\, S \quad (5)$$

where S is the splitting ratio. It is important to appreciate some of the features of this equation. As under normal LC–MS conditions F_{MS} is constant, the response is directly proportional to the analyte concentration:

$$R = \tau'\, C(t) \quad (6)$$

where τ' is the response factor multiplied by the constant factor $F_{LC}S$. This conclusion seems obvious, but the linearity in eqn. 6 can be wrongly interpreted in the sense that the mass spectrometer under certain conditions act as a concentration-sensitive device. LC–MS experiments in which the flow-rate F_{MS} is varied cannot readily be

performed. With most interfaces the range of possible flow-rate variation is narrow and, more important, a change in F_{MS} results in a change in the pressure conditions in the source, which in turn influences the ionization efficiency, the ion extraction efficiency and via the pressure in the analyser the ion transmission, *i.e.*, not only the flow-rate varies but also the response factor changes.

The extraction of ions from the source may complicate the evaluation of the influence of the flow-rate and the amount injected on the response. With various ionization techniques operative in atmospheric-pressure ion sources, for instance, the ions produced are preferentially sampled into the mass analyser. However, the ion extraction efficiency is not directly proportional to the concentration of ions in the source over a wide range, which may be due to space charging and possibly some other effects. As is discussed in more detail below, the ion sampling system of atmospheric-pressure ion sources act as an analyte-enrichment interface.

In real-life analytical applications it is generally the analyte concentration in the sample that is the key factor. In selecting the separation conditions for a particular problem to be solved with a particular LC–MS interface, optimum tuning of flow-rate, column diameter and separation efficiency is needed in order to achieve the highest mass flow to the mass spectrometer.

INTRODUCTION OF 1 ml/min OF LIQUID INTO A VACUUM

In this section the various attempts to develop an LC–MS interface that allows the direct introduction of 1 ml/min of an aqueous mobile phase into the MS vacuum system are reviewed.

Obviously, the most straightforward way of coupling LC and MS is by inserting the column outlet capillary directly into the MS vacuum system. This approach has been theoretically and experimentally explored by Tal'roze and co-workers [1,7,8]. In order to cope with the limited pumping capacity of a conventional MS vacuum system, only part of the column effluent could be introduced (typically 1%, *i.e.*, the maximum solvent load to the mass spectrometer is 10 μl/min). As a consequence, for this interface no analyte enrichment takes place ($E = 1$) and the maximum transfer efficiency is 1%, as Q_{MS} can be written as

$$Q_{MS} = S\,Q_{LC} \tag{7}$$

($S = 0.01$ for the capillary inlet). The effective transfer efficiency is analyte dependent (see below).

The outlet of the capillary is heated in order to provide heat for the evaporation of the solvent. This interface is called a capillary inlet interface (see Fig. 1), although the confusing term "direct liquid introduction" is also often used. There is no LC–MS interface that is theoretically so well understood as the capillary inlet. This is a result of the work of Tal'roze and co-workers [1,7,8], Arpino and co-workers [9,10] and Bruins and Drenth [11]. Prototypes of the capillary inlet interface have been described by at least fourteen different groups, but no commercial capillary inlet interface is available. The capillary inlet interfaces have been used in combination with various LC column types, *i.e.*, open bed, conventional packed, microbore, packed microcapillary and open-tubular columns.

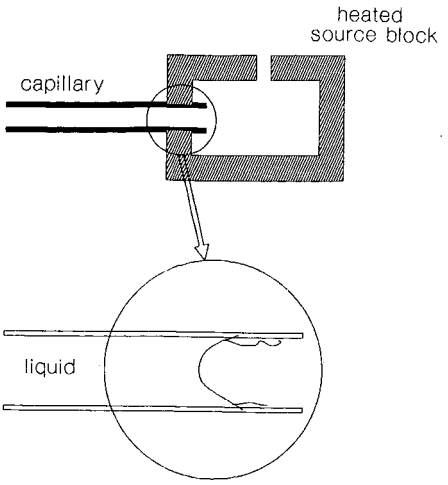

Fig. 1. Schematic diagram of the capillary inlet interface. The enlargement shows the general problem of the capillary inlet interface in the analysis of less volatile analytes.

From the theoretical understanding of the interface, the limitations of the capillary inlet are readily indicated. The position of the liquid–vapour transition depends on the solvent properties, the temperature and the tube inside diameter. For a homogeneously heated capillary, Arpino *et al.* [9] derived an equation to calculate this position in terms of the ratio of the length l of the capillary possessed by the vapour and the length $(L-l)$ of the capillary occupied by the liquid:

$$\frac{l}{L-l} = \frac{M\,\eta_1(P_v^2 - P_s^2)}{2\,\rho\,R\,T\,\eta_g[(P_i - P_v) + 4\,\gamma/d_c]} \tag{8}$$

where L is the length of the capillary, M is the molecular weight of the liquid (in kg/mol), η_1 the viscosity of the liquid, P_v the saturated vapour pressure of the liquid, P_s is the ion source pressure, η_g the viscosity of the vapour, P_i the inlet pressure, γ the surface tension of the liquid and d_c is the inside diameter of the capillary. As the vapour pressure of common LC solvents is considerably higher than common ion source pressures, the length l will always be larger than zero, which means that in practical situations the evaporation of the eluent will always take place inside the capillary. The volatile solvent evaporates whereas non-volatile impurities in the liquid stream precipitate at the inner wall of the capillary (see Fig. 1). The most important group of non-volatile "impurities" in the effluent stream is the analytes of interest. As a result, the application of the capillary inlet interface is restricted to fairly volatile analytes that are generally amenable to gas chromatographic (GC)–MS analysis.

The problem with the analyte evaporation can be avoided by the use of nebulization methods: the eluent is dispersed as an aerosol in either an atmospheric- or a reduced-pressure chamber, and the droplets are desolvated as a result of the more efficient evaporation of the solvent from the greatly enlarged surface area of the liquid created by the aerosol. The analyte molecules are transferred essentially unheated to

the gas phase, where they can be subjected to a gas-phase ionization method, *e.g.*, chemical ionization (CI), or where ions are produced by ion evaporation (IEV, see below).

Various nebulization methods have been explored for their potential in LC–MS coupling (see Table II). Ultrasonic nebulizers, where a piezoelectric crystal has been used to impose artificial instabilities on the liquid jet produced at a diaphragm, have been explored by Christensen *et al.* [12] and by Willoughby [13]. No significant improvement relative to conventional DLI (see below) was observed. Electrospray, where a solvent is nebulized as a result of charging the liquid by means of applying a potential difference, typically 3 kV, between the capillary and a counter electrode, appears to be limited to low flow-rates, *i.e.*, below 10 μl/min.

Pneumatic nebulization (PN) is the best-know nebulization technique; it is also used in other analytical techniques, such as atomic absorption and emission spectrometry. For LC–MS, PN has first been used in atmospheric-pressure (AP) ion sources to study AP-CI [14] and AP-IEV [15]. Later, various PN systems in reduced-pressure regions were described, where the nebulization is performed either directly into the ion source [16–18] or an additional pumping stage is applied between the nebulizer and the ion source [19,20]. The latter interface is also called a vacuum nebulizer (see Fig. 2b).

The disintegration of a liquid jet has only been explored in reduced-pressure regions. The use of a disintegrating liquid jet to transfer non-volatile analytes from the liquid to the gas phase was first described by Melera [21] and subsequently further developed by Arpino and co-workers [9,10]. The liquid jet is formed at a diaphragm with a 2–5-μm pinhole. The minimum flow-rate $F_{\text{jet,min}}$ at which a stable liquid jet is formed at a diaphragm is given by

$$F_{\text{jet,min}} = \frac{\pi d_{\text{jet}}^2}{4}\left(\frac{8\gamma}{\rho d_{\text{jet}}}\right)^{1/2} = 0.015\, d_{\text{jet}}^{3/2} \tag{9}$$

TABLE II

NEBULIZATION TECHNIQUES APPLIED IN LC–MS

Technique	Abbreviation
Disintegration of a liquid jet	DLI
Ultrasonic nebulization	
Pneumatic nebulization	PN
Applied in: medium-pressure ion sources	
atmospheric-pressure ion sources	
vacuum nebulizers	
effluent deposition in moving-belt interfacing	
particle-beam interface	
ion-evaporation system	
ionspray interface	
Electrical atomization	ES
Thermal nebulization	TS
Combinations of these techniques	

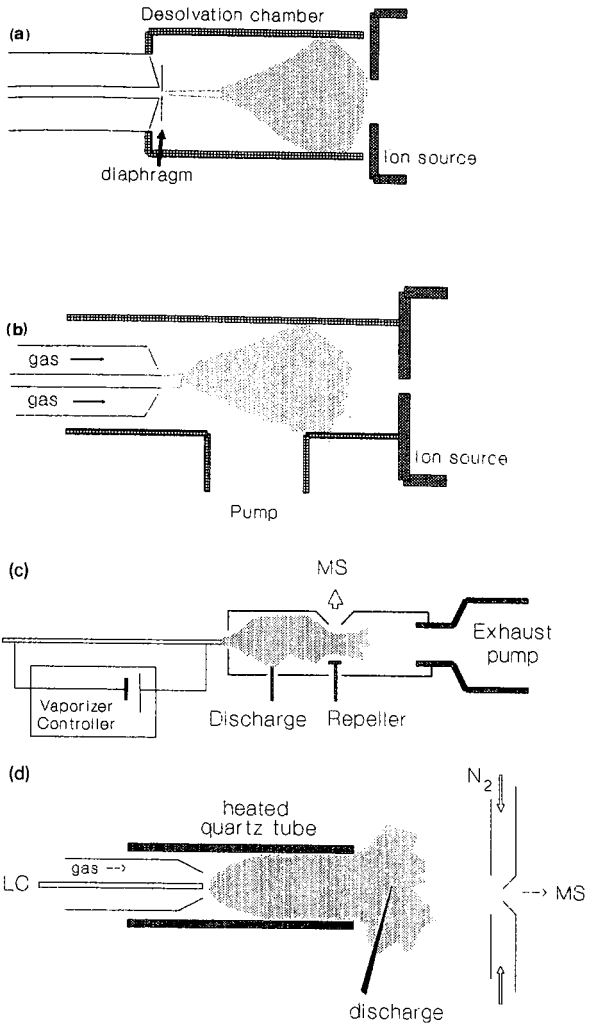

Fig. 2. Various nebulizer interfaces for LC–MS. (b) Vacuum nebulizer: a pneumatic nebulizer with an additional heated pumping stage between the nebulizer and the ion source. (a) Direct liquid introduction: a liquid jet nebulizer with a heated desolvation chamber between the nebulizer and the ion source. (c) Thermospray: a thermal nebulizer with an exhaust pump line containing a liquid nitrogen trap at the ion source opposite to the nebulizer. (d) Heated nebulizer: pneumatic nebulizer with a heated quartz desolvation chamber in an atmospheric pressure ion source, also showing the special ion sampling system with the nitrogen curtain gas.

The right-hand side of eqn. 9 is valid for solvents commonly used in reversed-phase LC. The droplets are typically twice the diaphragm diameter in size [22]. They are subsequently desolvated in a heated desolvation chamber and the gas mixture is mass analyzed using CI with the solvent as the reagent gas. This LC–MS interface is known as the direct liquid introduction (DLI) system (see Fig. 2a); it is commercially available from various manufacturers. Usually, 10–50 μl/min of liquid are introduced,

necessitating the use of a split in combination with conventional LC columns (splitting ratio 0.01–0.05). The most important drawback of the DLI system is frequent clogging of the pinhole [23,24].

It is interesting to note the similarities between the DLI [9,10,23,24] and the PN interface [16–20]. With both systems the nebulization is performed in a reduced-pressure region. In most instances, a heated desolvation chamber is used to achieve heat transfer to the droplets in the low-pressure vapour phase. Analyte ionization is achieved by solvent-mediated CI. It has been demonstrated by Arpino and Beaugrand [10] for DLI, but it also holds for the PN, that the maximum amount of liquid that can be introduced is limited to *ca.* 100 μl/min. This upper limit is not limited by the pumping capacity of the MS vacuum system, as a vacuum system suitable for high liquid flow-rates was used for these experiments [10], but is actually the result of the inefficient heat transfer from the desolvation chamber wall to the droplets, *i.e.*, the limited heat conductance of the low-pressure vapour.

There are two ways to solve the problems with the heat transfer to the droplets, *i.e.*, nebulization in a heated atmospheric pressure region or preheating the liquid prior to the nebulization. Both approaches lead to additional problems. With the former approach the analytes have to be efficiently transferred from an atmospheric pressure region into the high vacuum region (see the next section). With the latter approach both efficient pumping and sufficient heating power must be provided. The high pumping efficiency needed with the latter approach is achieved by directly pumping the ion source by means of a mechanical pump equipped with a liquid nitrogen trap in the exhaust pump line.

Sufficient heat must be transferred to the liquid to achieve almost complete evaporation after the nebulization; evaporation inside the capillary should be avoided because of the risk of precipitation of non-volatiles (*cf.*, Fig. 1). Experiments performed by Arpino and Beaugrand [10] with preheating the liquid prior to liquid jet formation by means of a heated liquid recirculating through the DLI probe were not successful; insufficient heat was transferred in this way. A more successful approach resulted from experiments with the rapid evaporation of the column effluents as is achieved in thermospray [25]. To provide sufficient heating power the use of lasers and hydrogen flames was explored, but it later appeared that indirect or direct electrical heating of a narrow-bore (typically 0.15 mm I.D.) column outlet capillary also resulted in sufficiently rapid vaporization of the column effluent [25,26]. With the thermospray (TS) interface over 1 ml/min of an aqueous mobile phase can directly be introduced into the MS vacuum system without solvent evaporation problems due to heat-transfer limitations.

In the TS interface (see Fig. 2c) heat is transferred directly from the vaporizer capillary to the liquid. As a result, the liquid starts to evaporate inside the vaporizer, resulting in disruption of the liquid phase by the formation of vapour bubbles that rapidly expand owing to the high temperature. In this way the risk of analyte precipitation is greatly reduced because the liquid is efficiently kept away from the heated surface after the onset of the evaporation. A stream of vapour and superheated liquid droplets is produced, which traverses the ion source to the exhaust pump. Ions that are produced in the source may be sampled by a sampling cone and mass analysed. In practice, the amount of heat transferred to the liquid is sufficient for complete evaporation, but the kinetics of the vaporization are sufficiently slow that part of the liquid

emerges from the vaporizer as small droplets, which may act as carriers for the non-volatile analytes (see below). However, as these droplets consist of superheated liquid, problems may arise with the decomposition of thermolabile compounds, especially with those which readily undergo thermal solvolysis, *e.g.*, with compounds that contain a glycoside binding. As an example, the TS mass spectrum of a 5-methoxypodophyllotoxin-4-β-D-glycoside (mol.wt. 606) in Fig. 3b shows no protonated molecule, but an intense fragment ion resulting from the loss of the sugar group. Many other examples of thermal degradation effects can be found in literature.

Nevertheless, the TS interface has become the most widely used LC–MS interface [27,28]. Over 300 papers have appeared and the number of papers on TS actually exceeds the number of papers devoted to all other LC–MS interfaces.

Two interfaces used in an atmospheric-pressure ion source are closely related to TS, *viz.*, the heated nebulizer [29,30] and the atmospheric-pressure spray (APS) interface [31,32]. The heated nebulizer is a pneumatic nebulizer equipped with a heated quartz desolvation chamber; it is used in combination with a discharge electrode for AP-CI (see Fig. 2d). The APS interface consists of an indirectly electrically heated vaporizer; it is used with a discharge electrode for AP-CI and also in the buffer

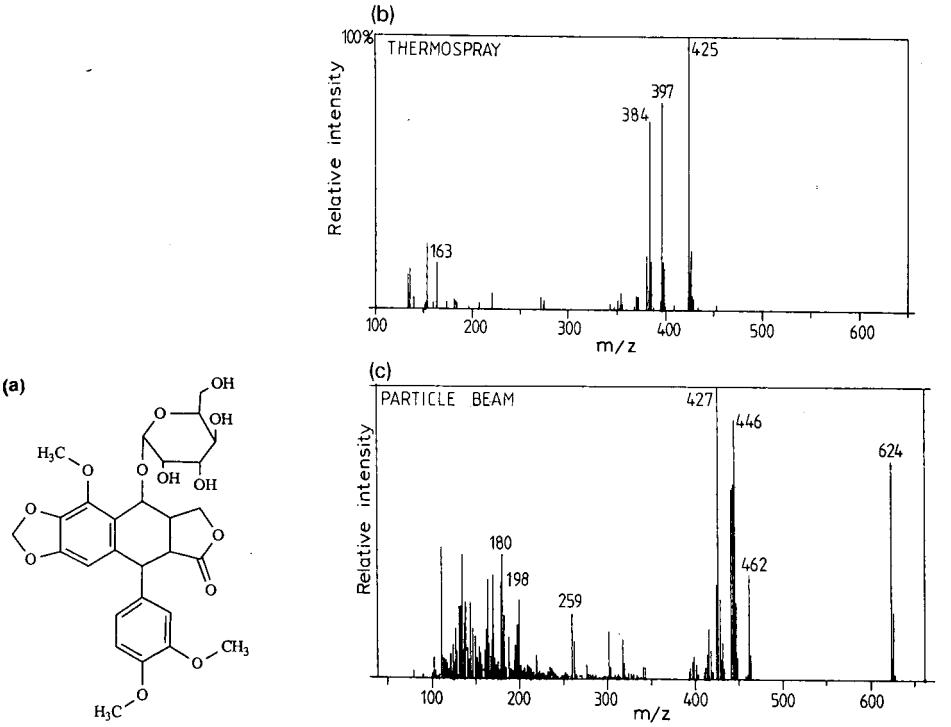

Fig. 3. (a) Structure of a 5-methoxypodophyllotoxin-4-β-D-glycoside (mol.wt. 606) and mass spectra obtained with (b) a thermospray and (c) a particle beam interface. Conditions: Finnigan MAT (San José, CA, USA) TSQ-70 instrument, equipped with either a Finnigan MAT thermospray interface or a Hewlett-Packard Model 59980A particle-beam interface (column bypass mode). Solvent, methanol–water (40:60) at 1.2 ml/min (thermospray) or 0.5 ml/min (particle beam). Thermospray in discharge-on mode (1 kV), vaporizer temperature 90°C, block temperature 230°C. Particle beam in ammonia CI mode, desolvation chamber 50°C, source temperature 250°C.

TABLE III

MAXIMUM ALLOWABLE FLOW-RATES OF SOME LC–MS INTERFACES

Interface	Flow-rate (μl/min)	Interface	Flow-rate (μl/min)
Capillary inlet	10	Ionspray	200
Direct liquid introduction	50	Particle beam	500
Pneumatic nebulizers in medium-pressure ion sources	50	Thermospray	2000
		Heated nebulizer (APCI)	2000
Electrospray	10	Atmospheric-pressure spray	2000

ionization mode (see below). Obviously, the TS interface itself can also be used in combination with a discharge electrode for AP-CI.

The TS interface, and the related heated nebulizer and the APS interfaces, are the end of the first line of development: how to introduce 1 ml/min of aqueous solvents into the MS vacuum system (see Table III).

ANALYTE ENRICHMENT: REMOVAL OF SOLVENT PRIOR TO THE MS VACUUM

The incompatibility problem with respect to the flow-rate, as discussed in the previous section, was also met in coupling packed GC columns with a mass spectrometer [33,34]. The interfaces developed for GC–MS, such as the Watson–Biemann fritted glass or effusion interface, the membrane interface and the jet separator, are based on gas-phase analyte enrichment. In the interface the ratio of the amounts of analyte and carrier gas are improved by selective removal of the carrier gas (*cf.*, eqn. 2). Typically 30–70% of the amount of analyte can be transferred from the GC column to the mass spectrometer with an enrichment factor of 10–20 [33,34].

Various analyte enrichment interfaces have also been developed for LC–MS, *e.g.*, the moving belt interface (MBI), the particle beam interface (PBI) and vacuum nebulizers (see Fig. 2b). The PBI resembles a jet separator for GC–MS. Very high enrichment factors have been achieved with the MBI and PBI, as essentially all the solvent is removed prior to introduction of the analytes into the mass spectrometer; the vacuum nebulizers are less efficient. However, the transfer efficiency of these interfaces is limited. The analyte-enrichment approach seems to be the most versatile means of LC–MS coupling, especially from the MS point of view. It makes LC and MS virtually independent and opens up the possibility of obtaining both CI and EI spectra of the analytes.

The approaches to analyte enrichment in MBI and PBI are widely different, although similar problems are met. With the MBI (see Fig. 4a) the column effluent is deposited on a continuously moving endless belt, from which the solvent is evaporated prior to the flash desorption of the analytes into the ion source [35,36]. The deposition of the eluent is most efficiently performed by means of either pneumatic or thermospray nebulization. The desorption of the analytes from the belt is mostly done by flash evaporation, although desorption by fast atom bombardment (FAB) directly from the belt has also been described [37,38]. After the flash evaporation, analyte ionization is performed by either EI or CI. The transfer efficiency in the flash

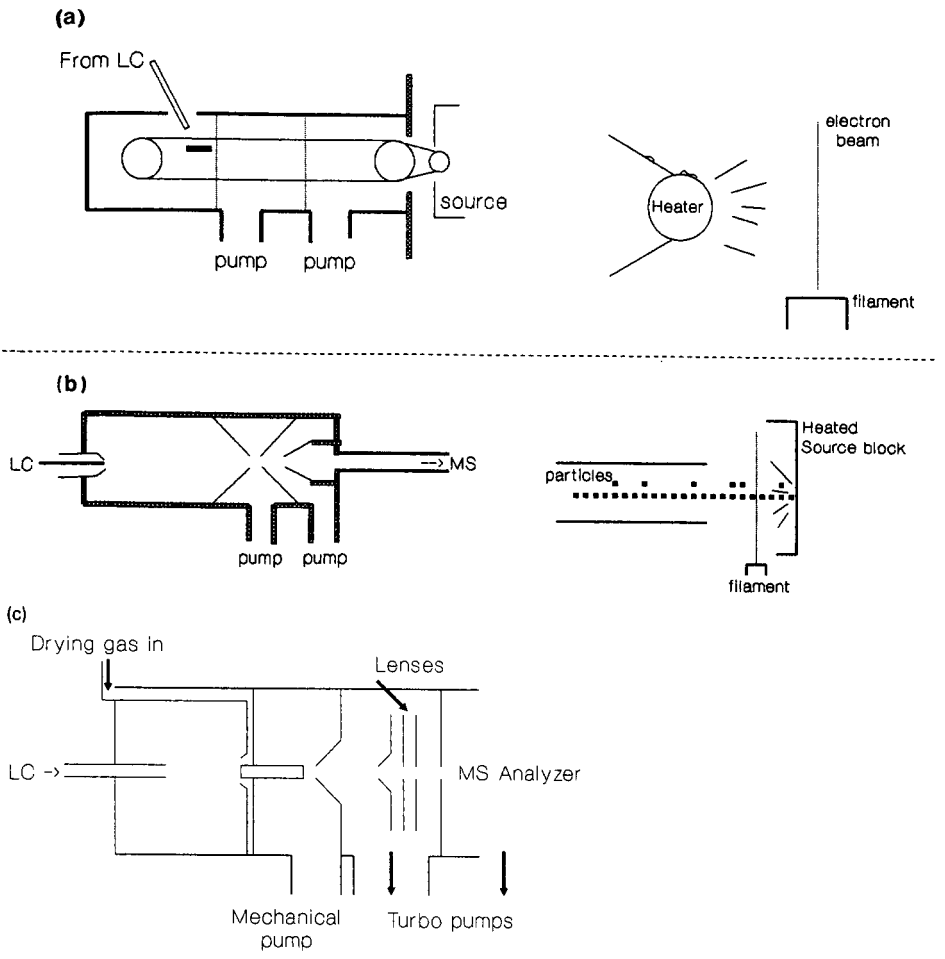

Fig. 4. Schematic diagram of some analyte-enrichment interfaces for LC–MS: (a) moving belt interface; (b) particle beam interface; (c) one-stage differentially pumped system for electrospray.

evaporation step in the ion source is determined by the analyte volatility and by interaction between the analyte and the belt surface [35,36,39]. Volatility-enhancing derivatization procedures, such as ion-pair formation or methylation [40], have successfully been applied to improve the detectability of less volatile analytes.

In the PBI (see Fig. 4b) the LC column effluent is nebulized by means of pneumatic or thermospray nebulization [41,42]. Droplet desolvation takes place in a slightly heated desolvation chamber which essentially is at atmospheric pressure. Helium is used for the nebulization, as it provides a high thermal conductivity. The non-volatile molecules nucleate to form sub-micrometer particles, which are subsequently separated from the solvent molecules in a two-stage momentum separator. The particles are transferred to the ion source, where they collide with the heated surface of the source and are volatilized. Subsequently, the analyte molecules are

ionized by EI or CI. Similarly to the situation in the MBI, the transition of the analyte from the liquid or solid state to the gas phase is thermally induced in the PBI. The potential of volatility-enhancing derivatization procedures to improve analyte detectability in PBI LC–MS has recently been explored [43].

From the description above, some corresponding features of the MBI and the PBI can be deduced. With both interfaces the nebulization takes place at atmospheric pressure. The solvent is subsequently removed completely prior to the introduction of the analyte molecules into the MS ion source. Although the heat transfer in the atmospheric-pressure desolvation chamber is improved relative to the medium-pressure chambers as used in vacuum nebulizers and DLI, the maximum flow-rate of aqueous solvents is still limited to *ca.* 0.5 ml/min, unless preheating of the solvent is applied, *i.e.*, unless thermospray nebulization is performed. The transition of the analyte molecules to the gas phase is thermally induced. As a consequence, the applicability range is limited to fairly volatile thermally stable compounds, although the short duration of the heating in the flash evaporation from the belt surface or at the ion source surface allows the analysis of compounds that are not amenable to GC analysis. As an example, the ammonia CI mass spectrum of a 5-methoxypodophyllotoxin-4-β-D-glycoside (mol.wt. 606) is given in Fig. 3c. With the PBI no thermal hydrolysis takes place; an intact ammoniated molecule is observed for this compound in addition to structure-informative fragment peaks. However, some of the fragments might be due to thermally induced reactions.

The universal or thermospray EI interface, recently developed by Vestec [44], is closely related to the PBI. It consists of a thermospray nebulizer, a spray chamber to remove the large droplets from the aerosol, a countercurrent gas diffusion membrane separator to remove most of the solvent molecules and a two-stage momentum separator (see Fig. 5). It thus combines various analyte enrichment approaches employed in GC–MS coupling.

An important aspect that should be addressed in relation to the MBI and PBI, but also to some other interfaces, *e.g.*, interfaces used in atmospheric-pressure sources, is the transition from an atmospheric-pressure chamber to the high-vacuum region. Three different approaches have been used. In the PBI and the MBI a two-stage differentially pumped system equipped with mechanical pumps is used. With the MBI the belt traverses a series of two narrow slits in the baffles between these pumping stages (Fig. 4a), whereas with the PBI molecular beam technology is applied in an arrangement with a nozzle and two skimmers (Fig. 4b). Several one-stage differentially pumped systems with a nozzle-skimmer system (see Fig. 4c) have also been described, *e.g.*, for electrospray interfaces [45,46]. Such a system can also be considered as a gas-phase analyte-enrichment system. In the third approach the ionization of the analytes also takes place in the atmospheric-pressure source. The ions are extracted from the source into the high-vacuum mass analyzer through a small sampling aperture (typically 25 μm I.D.) (see Fig. 2d) [15,29,47]. The analyzer region is efficiently pumped by means of a cryogenic pump [29]. In order to prevent clogging or contamination of the ion sampling aperture, and to provide additional droplet desolvation, a countercurrent flowing nitrogen curtain gas is applied around the sampling aperture (see Fig. 2d) [47]. The latter is also applied in the electrospray-type systems (*cf.* Fig. 4c).

In conclusion, conventional analyte-enrichment interfaces, *i.e.*, MBI and PBI,

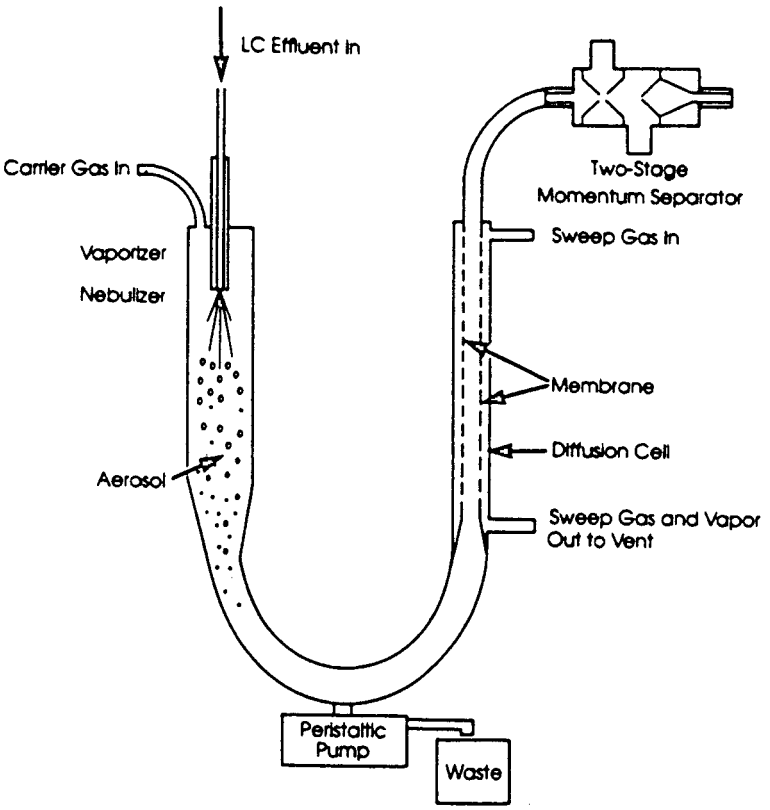

Fig. 5. Schematic diagram of the Vestec thermospray EI interface (reprinted with permission from Vestec, Houston, TX [44]).

are useful in providing EI and solvent-independent CI spectra for a limited range of compounds; the limitations are due to the necessity for volatilization of the analyte. The application range of MBI and PBI can be increased by applying other desorption techniques, as demonstrated by the experiments with FAB desorption in combination with MBI [37,38] and with PBI [48,49]. However, PBI and MBI with FAB ionization have not yet found widespread application.

WHY THE SOLVENT SHOULD NOT BE REMOVED IN LC–MS

In previous sections it was concluded that nebulization is an important step in the transfer of analytes and in the transition from the liquid phase to the gas phase. The early research on LC–MS was based on the assumption that ionization must follow the vaporization of the intact neutral molecules. By studying various liquid-phase ionization techniques, which at that time (1982) were mostly still in an early stage of development, Arpino and Guiochon [50] recognized the importance of the liquid in transferring the analytes and even assisting in the ionization. The ability of the DLI interface to transfer labile compounds to the gas phase, where they can be

ionized in ion–molecule reactions with the solvent as reagent gas (solvent-mediated CI), is believed to be strongly supported by the presence of the mobile phase [51]. The analyte molecules, preferentially present in the droplets, are softly desolvated and subjected to a desorption CI type of process [52]. In their review, entitled "Why the solvent should not be removed in LC–MS interfacing methods?" [50], Arpino and Guiochon concluded that preformed ions in solution can be transferred to the gas phase directly and mass analysed when sufficient energy is supplied to the liquid, *e.g.*, by means of particle bombardment (FAB, plasma desorption), laser radiation or electric fields. Vestal [53] later came to similar conclusions.

From this it may be concluded that solvent removal prior to ionization in the MS should not be complete, otherwise the liquid–gas transition must be thermally induced, limiting the applicability range as discussed for the PBI and the MBI in the previous section. For preformed ions in solution, *i.e.*, ionic compounds such as quaternary ammonium salts and compounds that readily undergo protolysis at acidic or basic functional groups, the nebulization may even result in additional liquid-based ionization techniques, such as FAB or IEV. The investigation and implementation of liquid-based ionization techniques in LC–MS is the third line of development; it is explored in more detail below.

LIQUID-BASED IONIZATION TECHNIQUES

Continuous-flow fast atom bombardment (CF-FAB) [54–56] is an implementation of FAB in LC–MS. The FAB matrix liquid, *e.g.*, glycerol, is added pre- or post-column to the LC mobile phase. Part of the eluent (5–15 μl/min) flows to the FAB target which is either a frit [54] or a modified FAB target [55]. As the liquid is bombarded at the target close to the outlet capillary, the actual mobile phase mixture acts as the FAB matrix solution. Subsequently, the evaporation of the volatile mobile phase constituents is achieved and the excess of glycerol is collected on a wick of compressed paper [57]. As a result of the dynamic nature and the composition of the FAB matrix at the CF-FAB target, various advantages over conventional FAB are observed, *e.g.*, improved detection limits, partly attributed to the reduction of matrix cluster ion intensities, and reduced ion suppression effects for mixtures of hydrophilic and hydrophobic peptides [56,58]. The CF-FAB technique appears to be limited with respect to the mass range of compounds that can be analysed. Whereas with conventional FAB mass spectra for peptides up to a molecular weight of 24 000 have been reported, the highest mass reported in CF-FAB is 5730 for bovine insulin with a low signal-to-noise ratio; in most reports compounds up to a molecular weight of *ca.* 2000 are analysed [56]. A clear explanation for this is lacking, but it most likely is a matrix related effect.

Other liquid-based ionization techniques are based on nebulization techniques, especially thermospray and electrospray. There is considerable debate on the mechanism of these techniques. The discussion here is mainly focused on TS.

The thermospray technique is not only a liquid introduction and nebulization technique, but also as a soft ionization technique [25,29]. This soft ionization method, called thermospray buffer ionization, is operative without a primary source of electrons when a volatile buffer, *e.g.*, ammonium acetate, is present in solution. The ionization mechanism is primarily explained by Vestal and co-workers [25,27,53] in

terms of ion evaporation (IEV) [15,60], while they suggest that some gas-phase ion–molecule reactions (CI) might also be involved [27]. Besides TS buffer ionization two other ionization modes can be applied in TS, *i.e.*, filament-on and discharge-on. Both modes resemble solvent-mediated CI. The ionization in APS buffer ionization appears to be similar to that in TS buffer ionization [32]. With the heated nebulizer [29,30] only discharge-on experiments have been reported, although buffer ionization is probably also possible. The possibility of buffer ionization in combination with a heated nebulizer interface was actually demonstrated at this symposium [61].

Various results in the literature shed more light on the TS ionization mechanism. First, it has been shown by various workers [62–65] that gas-phase ion–molecule reactions, *i.e.*, solvent-mediated CI, play an important role in the TS buffer ionization mechanism. For instance, the reagent gas composition in TS buffer ionization can be explained from equilibrium constants for gas-phase reactions [62]. A simple experiment to distinguish between ion evaporation of preformed ions and gas-phase ion–molecule reactions was described by Bursey *et al.* [64]: the relative acid–base order of aniline and ammonia reverses on going from the liquid to the gas phase. Aniline is not protonated by ammonia in the liquid phase, but it is in the gas phase, demonstrating the importance of gas-phase ion–molecule reactions in TS. The influence of the repeller potential on solvent and analyte mass spectra in TS buffer ionization is also most readily explained by ion–molecule reactions [65]. In conclusion, solvent-mediated CI is an important mechanism of analyte ionization in TS, not only in filament-on and discharge-on modes, but also in the TS buffer ionization mode. Ammonium ions and especially ammonium solvent cluster ions, produced as a result of the TS nebulization, form the CI reagent gas in the solvent-mediated CI mode operative in positive-ion TS buffer ionization [65], whereas in the negative ion mode the acetate-related ions play a major role [63].

The IEV mechanism was proposed by Iribarne and Thomson [15,60]. During the nebulization process charged droplets are produced owing to statistical fluctuations in the distribution of the positive and negative ions over the droplets on disruption of the liquid. Subsequent solvent evaporation results in an increasing electrical field at the droplet surface, finally permitting the emission of ions from the droplets, *i.e.*, field-induced ion evaporation [15,60]. This process is assumed to be similar to the field-induced desolvation mechanisms known from field desorption (FD) [66]. The IEV mechanism, and especially whether it is active in TS, has been questioned by Röllgen and co-workers [67,68]. Considering the ammonium acetate concentration commonly used in TS buffer ionization (0.1 mol/l), desolvation of the droplets will result in solid ammonium acetate particles with possibly included analyte molecules, instead of highly charged liquid droplets. The particles rapidly decompose owing to the low decomposition and volatilization temperature of ammonium acetate. Moreover, the actual electric fields at which ion evaporation can take place can be calculated to be much higher [68]. The removal of a solvated ion from the droplet surface under field stress would most likely generate a sequence of events in which a number of charges are removed from the droplet. Such a sequence is a typical electrohydrodynamic instability event, which takes place at the Rayleigh instability limit. The alternative mechanism suggested by Röllgen and co-workers [67,68] is based on soft desolvation of the ions by solvent evaporation from small charged droplets produced by either electrohydrodynamic or mechanical instabilities, or both.

Despite the questions with regard to the actual ionization mechanism, the abbreviation IEV is used here to describe the observation of ions from nebulized solutions containing preformed ions, *i.e.*, irrespective of whether these ions are produced by ion evaporation as described by Iribarne and Thomson [15,60], by soft desolvation as described by Röllgen and co-workers [67,68] or by any other yet unknown mechanism.

Reviewing the literature on TS, it appears that in the majority of applications under commonly used solvent conditions, *i.e.*, solvents containing 0.1 mol/l ammonium acetate, the ionization can be readily explained from gas-phase ion–molecule reactions, *i.e.*, CI. The IEV mechanism appears to have only a minor contribution to the TS ion production under these conditions. However, when the ammonium acetate concentration in the mobile phase is greatly reduced, IEV may become important. This view is supported by the comparative study of Voyksner [69] on nucleotides analysed with and without ammonium acetate. Compounds that are ionic in solution, such as sulphate conjugates [70] and sulphonated azo dyes [71,72], are preferentially analysed with a low concentration or even without ammonium acetate present in solution. For instance, the total ion current observed for the disulphonated azo dye Direct Red 81 (mol.wt. 675, disodium salt) first increases with increasing ammonium acetate concentration to a maximum at *ca.* 10^{-3} mol/l, but on further increase in the ammonium acetate concentration it decreases dramatically (see Fig. 6). With increasing ammonium acetate concentration, exceeding 10^{-3} mol/l, the intensity of the ion at *m/z* 630, $[M - 2Na + H]^+$, which is assumed to be produced by a gas-phase reneutralization reaction, also increases [71]. This means that the ammonium acetate concentration for IEV must be lower than that commonly applied in TS, *i.e.*, 10^{-3} instead of 0.1 mol/l. However, unlike other methods discussed below, some electrolyte in the solution appears to be necessary. An extensive set of experiments can be formulated based on these observations, *e.g.*, related to the influence of ionic strength, nature and charge of the ionic additive. It also appears to be important for IEV to tune the nebulization in such a way that smaller droplets are produced [72]; this aspect is addressed in more detail below.

The IEV ionization mechanism is also assumed to play a major role in two other liquid-based ionization techniques, *viz.*, electrospray and ionspray. The devel-

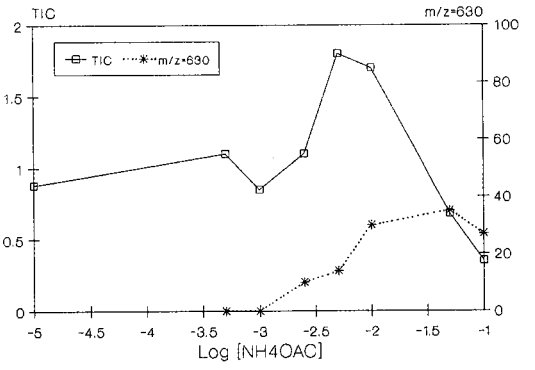

Fig. 6. Influence of the ammonium acetate concentration on the total ion current (TIC) and the ion intensity at *m/z* 630, $[M - 2Na + H]^+$, of the disulphonated azo dye Direct Red 81. Data for the plot obtained from ref. 71. TIC-axis: counts; *m/z* = 630 axis: relative abundance.

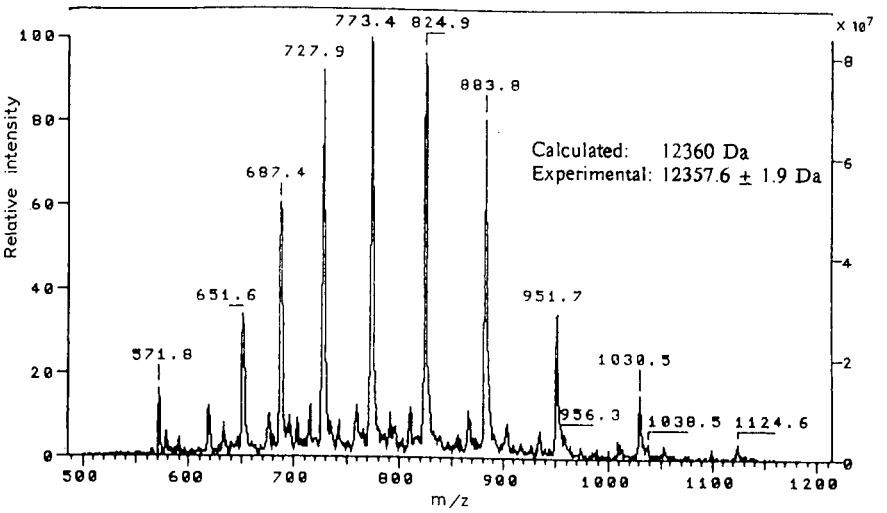

Fig. 7. Typical electrospray spectrum of cytochrome *c*. Conditions: Finnigan MAT TSQ-70 instrument equipped with a Finnigan MAT ESI system. Cytochrome *c* (10 pmol/μl, purchased from Fluka, Buchs, Switzerland) in methanol–water (50:50) at a constant infusion flow-rate of 1 μl/min. The spectrum is the average of 30 scans accumulated in 1 min.

opment of these techniques is based on initial experiments by Dole *et al.* [73] to produce macro-ions by desolvation of the charged droplets obtained in electrospraying dilute solutions of macromolecules, *i.e.*, the same mechanism later proposed by Röllgen and co-workers [67,68] from their experimental evidence and physical understanding of the process. Fenn and co-workers [74–77] continued this electrospray (ES) research, first using small molecules, but subsequently also larger molecules, such as polyethylene glycols and proteins. The results with the proteins, for which envelopes of multiply charged ions in the mass range between *m/z* 500 and 1500 were obtained, introduced a new era in the application of MS in the biological sciences. A typical ES mass spectrum for cytochrome *c* (mol.wt. 12 360), as obtained in the authors' laboratory, is given in Fig. 7. The ES interface operates at 1–5 μl/min. Although an LC–MS interface based on ES has been described [45], the research in ES now appears to be completely focused on the analysis of proteins and other biomacromolecules, which is partly due to the apparent incompatibility of ES with conventional LC in terms of flow-rate.

The ionspray (IS) interface is a modification of the ES concept; pneumatic nebulization is used to assist the electrospray [47]. As a result, the IS interface can accommodate larger solvent loads, *i.e.*, up to 200 μl/min, which more readily allows the coupling with LC, although improved performance is achieved at lower flow-rates. The IS interface can also be used for the analysis of proteins [78]; in these studies generally lower flow-rates, *e.g.*, 10 μl/min, are applied.

The solvent typically used in the analysis of proteins by ES and IS is methanol–water (50:50), often containing some acetic acid. It has recently been demonstrated that with such a solvent it is also possible to obtain multiply charged ions from large proteins in TS [79]. TS apparently is considerably less sensitive than ES and IS;

100–4000 pmol of protein are needed in TS, whereas 1–100 pmol are generally sufficient in ES and IS. However, as 100-μl injections at 1.3 ml/min are performed in TS and 1 μl/min infusion in ES, the sample concentration needed for the spectrum is similar with both techniques. It can be concluded that the overall ionization efficiency in TS is less than that in ES and IS: more analyte molecules are needed in TS than in ES to achieve a comparable signal-to-noise ratio in the spectrum. Unfortunately, the analysis of peptides is frequently limited by the available amount of sample.

From the results briefly indicated above, it can be concluded that the IEV ionization can be operative, irrespective of the nebulization technique. Multiply charged ions from proteins can be produced via electrospray, electrospray-assisted pneumatic nebulization (ionspray) and thermospray. However, it appears that the maximum of the ion envelope shifts to higher m/z values with an increasing solvent load to the source, presumably indicating the growing importance of gas-phase ion–molecule reneutralization reactions. Gas-phase ion–molecule reactions in an ES source have recently been investigated by Ikonomou *et al.* [80]. The data presented at this symposium by Voyksner [81] strongly emphasize the importance of gas-phase ion–molecule processes in ES also.

A similarity between most liquid-based ionization techniques discussed here, *viz.*, ES, IS and CF-FAB, is that they are low-flow-rate techniques. Low-flow-rate interfaces necessitate splitting, either post-column after a conventional LC column or pre-column in terms of a reduced injection volume for a microbore column. Splitting is a serious drawback, as it restricts the achievable detection limits (*cf.* eqn. 4). The larger sample loadability of a microcapillary packed column operated in the gradient elution mode by the application of on-column peak-focusing techniques may obviate these disadvantages. The low-flow-rate techniques can also benefit from high-efficiency separation techniques, such as capillary electrophoresis (CE); the narrow peaks result in improved $C(t)$ values (*cf.*, eqn. 4). On the other hand, the narrow peaks require rapid scanning of the mass spectrometer, *e.g.*, in order to acquire a sufficient number of peaks from the ion envelope of multiply charged protein ions to perform accurate molecular weight determinations in the analysis of unknowns. At present, most of these spectra are acquired, depending on the amount, in times from several seconds to even minutes, which is necessary from ion-statistical arguments to average the statistical distribution of charges over the molecule, and to average the statistical fluctuations in the peak heights which appear to be unavoidable when nebulization techniques are applied for analyte introduction. The application of array detectors, such as the PATRIC array detector [82], shows great promise in this respect, in terms of both sensitivity and acquisition speed, as recently demonstrated by Reinhoud *et al.* [83]. Considerable progress is to be expected in this area in the near future.

NEBULIZATION IN LC–MS

From the previous discussion it appears that two aspects of LC–MS interfacing are especially important: the nebulization and the liquid-based soft ionization methods.

Pneumatic nebulization is most widely used in LC–MS (see Table II); it is also the technique of choice in many other analytical techniques where nebulization is important.

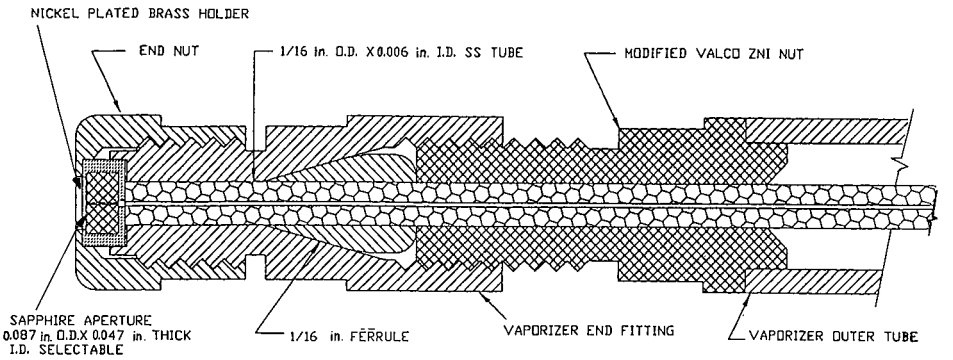

Fig. 8. Schematic diagram of the diaphragm-equipped thermospray interface (reprinted with permission from Vestec, Houston, TX, USA [85]).

In LC–MS the actual nebulization technique applied to produce the droplets is apparently less important. The maximum allowable flow-rate is found to be limited by the transfer of heat needed for the evaporation of the solvent, although with ES the flow-rate appears to be primarily limited by the nebulization process itself. The liquid-based soft ionization methods are operative irrespective of the way in which the droplets are produced, although the droplet size appears to be important, especially in IEV techniques. Droplet size decreases in the order liquid jet, pneumatic, thermospray, electrospray, although with both the liquid jet and the pneumatic nebulization, in principle, smaller droplets are achievable. For liquid jet nebulization the droplet size depends on the diaphragm diameter, but in practice also on the heat transferred to the liquid prior to the nebulization: the evaporation of solvent from heated droplets more readily produces sufficiently small droplets within the time frame available for the ionization. For pneumatic nebulization the droplet size depends on the gas speed relative to the liquid linear velocity, according to the equation given by Nukiyama and Tanasawa [84]. However, decreasing the droplet size with the liquid jet or the pneumatic nebulizers would lead to systems that are more prone to clogging.

An interesting development in the application of nebulization techniques in LC–MS is the exploration of combination techniques, although most possible combinations have not yet been investigated. For instance, the IS interface [47] is a combination of electrospray and pneumatic nebulization; it is a highly successful approach to LC–MS interfacing.

In an attempt to produce smaller droplets by TS, McLean and Freas [72] experimented with short, narrow-bore, fused-silica capillary restrictors at the outlet of the TS vaporizers (*cf.*, Arpino and Beaugrand [10]). The use of laser-drilled sapphire diaphragms at the outlet of the TS vaporizer has recently been introduced by Vestec [85] (see Fig. 8). Various aperture diameters can be selected, depending on the flow-rate to be introduced. The flow-rate that must be introduced in a conventional TS vaporizer capillary to achieve stable TS nebulization conditions depends on solvent properties, such as vapour pressure, viscosity and molecular weight, on the capillary diameter and on the temperature. In principle, stable liquid jets can be produced by means of vaporizers with smaller inside diameters, but the risk of clogging the vapor-

TABLE IV

OBJECTIVES IN DEVELOPING ON-LINE LC–MS

A universal detector LC
A free choice of LC solvent composition and flow-rate
Analysis of thermolabile and non-volatile analytes
Avoid analyte derivatization
Low detection limits
Identification of analytes

izer increases. With a vaporizer, with a sapphire diaphragm fitted at the outlet, the clogging is actually more likely to occur at the diaphragm, which can be replaced more readily than the complete vaporizer capillary. Using eqn. 9, it can be shown that for the common diaphragm diameters (25–75 μm I.D.) and flow-rates (1–1.5 ml/min), a stable liquid jet can be produced. The heat transferred in the vaporizer capillary to the liquid, prior to the formation of the liquid jet, ensures rapid solvent evaporation from the droplets produced upon jet disintegration. With the use of smaller diaphragms smaller droplets are produced: the common effect of decreasing droplet size with smaller diaphragms [22] is further enhanced by the more effective evaporation of the solvent from the smaller superheated droplets. As such, the TS vaporizers with a diaphragm can be considered as a combination technique: thermospray and liquid jet formation.

The reduction in the flow-rate in TS is expected to be beneficial for the sensitivity of the TS system. From a comparison of the detection limits for organophosphorus pesticides in DLI [86] and TS [87], this statement can be sustained. Parker *et al.* [86] reported for the DLI that 100 ng injected on-column was needed to detect the major peaks in the spectrum. Barcelo [87] reported an on-column detection limit of 20–50 ng for the TS. In judging these figures it must be emphasized that in DLI a splitting ratio of 0.01 was used, *i.e.*, 1 ng is introduced into the source, whereas in TS 20–50 ng are introduced into the source. It can be concluded that the ionization efficiency and/or the ion extraction efficiency in TS are considerably worse than in DLI. This may be due to the high pressures in the TS source, typically 2000 Pa, relative to the DLI (10 Pa). The transition region from the TS source at 2000 Pa to the analyser region at 10^{-3} Pa seems hardly optimized in this respect. Reduction of the flow-rate from the TS vaporizer would decrease the pressure in the source and could enhance the ion extraction efficiency, although it is unclear whether similar ionization efficiencies can indeed be achieved at the lower flow-rates and source pressures. Experiments performed in this area by Osterman *et al.* [88] are not well documented.

CONCLUSIONS

Some conclusions from the present discussion can be drawn by comparing the research objectives in developing on-line LC–MS, as summarized in Table IV, and the present state-of-the-art in LC–MS.

The coupling of LC and MS has become a successful analytical tool, but has not resulted in a universal detector for LC. Various steps in the LC–MS interfacing

show selectivity or discrimination towards certain analytes, especially the inherent properties of the ionization techniques used.

No free choice of LC solvent composition is possible. Most favourable solvents in LC–MS are reversed-phase LC solvents containing volatile buffer constituents. This limits the LC–MS application of several powerful LC techniques, such as ion-exchange and ion-pair LC, although some impressive results in this area have recently been described [89–92]; these techniques are especially useful for separating the type of analytes for which LC–MS would be most attractive. Pseudo-electro-microchromatography, as demonstrated by Verheij *et al.* [93], appears to be a powerful alternative for the analysis of ionic compounds; the technique is readily compatible with common low-flow-rate LC–MS interfaces. In target-compound analysis, valve-switching techniques, *e.g.*, phase-system switching, can be applied. Solving incompatibilities in this respect has been discussed in a previous paper [94]. In general, the use of non-volatile mobile phase constituents, *e.g.*, phosphate buffers, in routine LC–MS application is prohibited, which is a disadvantage limiting the practical use of LC–MS. This problem is not expected to be solved in a general way in the near future.

Thermolabile and non-volatile analytes can be handled in LC–MS. However, because mostly soft ionization techniques, *i.e.*, (solvent-mediated) CI, FAB and IEV, are applied in LC–MS, the information that can be achieved is limited. For many compounds no EI spectra can be produced. Tandem MS (MS–MS) and some other fragmentation-inducing techniques can be applied, but the spectra obtained are not as readily interpretable as EI spectra. As a result, identification of unknowns is not straightforward.

The desire to avoid analyte derivatization results from GC and GC–MS. However, in LC–MS analyte derivatization can be very useful, especially considering the fact that most ionization techniques used in LC–MS rely strongly on chemistry [94]. More attention should be paid to this aspect.

The detection limits achievable in LC–MS are generally insufficient, especially in the field of bioanalysis and environmental analysis, were the complexity of the sample matrix prevents the effective use of sample preconcentration techniques. Lower, preferably much lower, detection limits are needed in various application areas. This statement is nearly always true for a variety of analytical techniques, but certainly in LC–MS. A more profound study on the causes of the disappointing detection limits would be appropriate, but is beyond the scope of this paper.

The importance of miniaturization in LC has varied with time. Originally, the coupling of conventional LC columns to MS systems was pursued. The necessity for splitting in DLI stimulated the application of microcolumns. The interest decreased again with the introduction of the TS interface, capable of introducing the total effluent from a conventional LC column. However, a revival of the interest in microcolumns resulted from the introduction of low-flow-rate liquid-based soft ionization techniques, such as CF-FAB and ES. Considerable progress in this field can be expected in the near future. The various aspects of interfacing microcolumn separation techniques to mass spectrometry are discussed in more detail elsewhere [95].

LC–MS has acquired a place amongst the various applicable analytical techniques. Real problems are solved with LC–MS, sometimes with great elegance, but still many questions remain unanswered and many goals remain to be achieved. This paper has clarified some important technological aspects in LC–MS interface devel-

opments. It is hoped that it will give a better understanding of LC–MS, and will open up new research directions to improve the performance of LC–MS.

ACKNOWLEDGEMENT

5-Methoxypodophyllotoxin-4-β-D-glycoside was kindly provided by Dr. Harkes, MT–TNO, Zeist, Netherlands.

REFERENCES

1 V. L. Tal'roze, V. E. Skurat, I. G. Gorodetskii and N. B. Zolotai, *Russ. J. Phys. Chem.*, 46 (1972) 456.
2 P. J. Arpino and G. Guiochon, *Anal. Chem.*, 51 (1979) 682A.
3 D. E. Games, *Biomed. Mass Spectrom.*, 8 (1981) 454.
4 T. R. Covey, E. D. Lee, A. P. Bruins and J. D. Henion, *Anal. Chem.*, 58 (1986) 1451A.
5 K. Vekey, D. Edwards and L. F. Zerilli, *J. Chromatogr.*, 488 (1989) 73.
6 K. B. Tomer and C. E. Parker, *J. Chromatogr.*, 492 (1989) 189.
7 V. L. Tal'roze, V. E. Skurat and G. V. Karpov, *Russ. J. Phys. Chem.*, 43 (1969) 241.
8 V. L. Tal'roze, I. G. Gorodetskii, N. B. Zolotai, G. V. Karpov, V. E. Skurat and V. Ya. Maslennikova, *Adv. Mass Spectrom.*, 7 (1978) 858.
9 P. J. Arpino, P. Krien, S. Vajta and G. Devant, *J. Chromatogr.*, 203 (1981) 117.
10 P. J. Arpino and C. Beaugrand, *Int. J. Mass Spectrom. Ion Processes*, 64 (1985) 275.
11 A. P. Bruins and B. F. H. Drenth, *J. Chromatogr.*, 271 (1983) 71.
12 R. G. Christensen, E. White, V. S. Meiselman and H. S. Hertz, *J. Chromatogr.*, 271 (1983) 61.
13 R. C. Willoughby, *Ph.D. Thesis*, Georgia Institute of Technology, 1983.
14 E. C. Horning, D. I. Carroll, I. Dzidic, K. D. Haegele, M. G. Horning and R. N. Stillwell, *J. Chromatogr.*, 99 (1974) 13.
15 J. V. Iribarne and B. A. Thomson, *J. Chem. Phys.*, 64 (1976) 2287.
16 J. A. Apffel, U. A. Th. Brinkman, R. W. Frei and E. I. A. M. Evers, *Anal. Chem.*, 55 (1983) 2280.
17 K. Matsumoto, H. Kojima, K. Yasuda and S. Tsuge, *Org. Mass Spectrom.*, 20 (1985) 243.
18 F. S. Pullen, D. S. Ashton and M. A. Baldwin, *J. Chromatogr.*, 474 (1989) 335.
19 Y. Hirata, T. Takeuchi, S. Tsuge and Y. Yoshida, *Org. Mass Spectrom.*, 14 (1979) 126.
20 S. Tsuge, in M. V. Novotny and D. Ishii (Editors), *Microcolumn Separations*, Elsevier, Amsterdam, 1985, p. 217.
21 A. Melera, *Adv. Mass Spectrom.*, 8 (1980) 1597.
22 R. N. Berglund and B. Y. H. Liu, *Environ. Sci. Technol.*, 7 (1973) 147.
23 W. M. A. Niessen, *Chromatographia*, 21 (1986) 277.
24 W. M. A. Niessen, *Chromatographia*, 21 (1986) 342.
25 C. R. Blakley and M. L. Vestal, *Anal. Chem.*, 55 (1983) 750.
26 M. L. Vestal and G. J. Fergusson, *Anal. Chem.*, 57 (1985) 2373.
27 D. A. Garteiz and M. L. Vestal, *LC Mag.*, 3 (1985) 334.
28 P. J. Arpino, *Mass Spectrom. Rev.*, 9 (1990) 631.
29 *The API Book*, Sciex, Thornhill, Canada, 1989.
30 T. R. Covey, E. D. Lee and J. D. Henion, *Anal. Chem.*, 58 (1986) 2453.
31 M. Sakairi and H. Kambara, *Anal. Chem.*, 60 (1988) 774.
32 M. Sakairi and H. Kambara, *Anal. Chem.*, 61 (1989) 1159.
33 C. F. Simpson, *CRC Crit. Rev. Anal. Chem.*, 3 (1972) 1.
34 G. A. Junk, *Int. J. Mass Spectrom. Ion Phys.*, 8 (1972) 1.
35 J. van der Greef, W. M. A. Niessen and U. R. Tjaden, *Spectra*, 12, No. 1 (1989) 26.
36 P. J. Arpino, *Mass Spectrom. Rev.*, 8 (1989) 35.
37 P. Dobberstein, E. Korte, G. Meyerhoff and R. Pesch, *Int. J. Mass Spectrom. Ion Phys.*, 46 (1983) 185.
38 J. G. Stroh, J. Carter Cook, R. M. Milberg, L. Brayton, T. Kihara, Z. Huang, K. L. Rinehard, Jr., and I. A. S. Lewis, *Anal. Chem.*, 57 (1985) 985.
39 J. van der Greef, A. C. Tas, M. C. ten Noever de Brauw, M. Höhn, G. Meyerhoff and U. Rapp., *J. Chromatogr.*, 323 (1985) 81.
40 P. Vouros, E. P. Lankmayr, M. J. Hayes, B. L. Karger and J. M. McGuire, *J. Chromatogr.*, 251 (1982) 175.

41 R. C. Willoughby and R. F. Browner, *Anal. Chem.*, 56 (1984) 2626.
42 R. D. Voyksner, C. S. Smith and P. C. Knox, *Biomed. Environ. Mass Spectrom.*, 19 (1990) 523.
43 A. P. Tinke, R. A. M. van der Hoeven, W. M. A. Niessen, U. R. Tjaden and J. van der Greef, *J. Chromatogr.*, 554 (1991) 119.
44 M. L. Vestal, D. Winn, C. H. Vestal and J. G. Wilkes, in M. A. Brown (Editor), *Liquid Chromatography/Mass Spectrometry. Applications in Agricultural, Pharmaceutical and Environmental Chemistry (ACS Symposium Series*, Vol. 420), American Chemical Society, Washington, DC, 1990, p. 215.
45 C. M. Whitehouse, R. N. Dreyer, M. Yamashita and J. B. Fenn, *Anal. Chem.*, 57 (1985) 675.
46 R. D. Smith, J. A. Olivares, N. T. Nguyen and H. R. Udseth, *Anal. Chem.*, 60 (1988) 1948.
47 A. P. Bruins, T. R. Covey and J. D. Henion, *Anal. Chem.*, 59 (1987) 2642.
48 J. D. Kirk and R. F. Browner, *Biomed. Environ. Mass Spectrom.*, 18 (1989) 355.
49 P. E. Sanders, *Rapid Commun. Mass Spectrom.*, 4 (1990) 123.
50 P. J. Arpino and G. Guiochon, *J. Chromatogr.*, 251 (1982) 153.
51 M. Dedieu, C. Juin, P. J. Arpino and G. Guiochon, *Anal. Chem.*, 54 (1982) 2372.
52 M. A. Baldwin and F. W. McLafferty, *Org. Mass Spectrom.*, 7 (1973) 1353.
53 M. L. Vestal, *Mass Spectrom. Rev.*, 2 (1983) 447.
54 Y. Ito, T. Takeuchi, D. Ishii and M. Goto, *J. Chromatogr.*, 346 (1985) 161.
55 R. M. Caprioli, T. Fan and J. S. Cottrell, *Anal. Chem.*, 58 (1986) 2949.
56 R. M. Caprioli, *Anal. Chem.*, 62 (1990) 477A.
57 R. M. Caprioli, paper presented at the *36th ASMS Conference on Mass Spectrometry and Allied Topics, San Francisco, CA, 1988, p. 729.*
58 R. M. Caprioli, W. T. Moore and T. Fan, *Rapid Commun. Mass Spectrom.*, 1 (1987) 15.
59 C. R. Blakley, J. J. Carmody and M. L. Vestal, *J. Am. Chem. Soc.*, 102 (1980) 5931.
60 B. A. Thomson and J. V. Iribarne, *J. Chem. Phys.*, 71 (1979) 4451.
61 M. S. Bolgar, B. M. Warrack and G. C. DiDonato, presented at the *7th Montreux Symposium on LC–MS, Montreux, October 31–November 2, 1990.*
62 A. J. Alexander and P. Kebarle, *Anal. Chem.*, 58 (1986) 471.
63 C. E. Parker, R. W. Smith, S. J. Gaskell and M. M. Bursey, *Anal. Chem.*, 58 (1986) 1661.
64 M. M. Bursey, C. E. Parker, R. W. Smith and S. J. Gaskell, *Anal. Chem.*, 57 (1985) 2597.
65 C. E. M. Heeremans, R. A. M. van der Hoeven, W. M. A. Niessen, J. van der Greef and N. M. M. Nibbering, *Org. Mass Spectrom.*, 26 (1991) 519.
66 U. Giessmann and F. W. Röllgen, *Int. J. Mass Spectrom. Ion Phys.*, 38 (1981) 267.
67 G. Schmelzeisen-Redeker, L. Bütfering and F. W. Röllgen, *Int. J. Mass Spectrom. Ion Processes*, 90 (1989) 139.
68 F. W. Röllgen, H. Nehring and U. Giessmann, in A. Hedin, B. U. R. Sundqvist and A. Benninghoven (Editors), *Ion Formation from Organic Solids (IFOS V)*, Wiley, New York, 1989, p. 155.
69 R. D. Voyksner, *Org. Mass Spectrom.*, 22 (1987) 513.
70 D. Watson, G. W. Taylor and S. Murray, *Biomed. Mass Spectrom.*, 12 (1985) 610.
71 D. A. Flory, M. A. McLean, M. L. Vestal and L. D. Betowski, *Rapid Commun. Mass Spectrom.*, 1 (1987) 48.
72 M. A. McLean and R. B. Freas, *Anal. Chem.*, 61 (1989) 2054.
73 M. Dole, R. L. Hines, L. L. Mack, R. C. Mobley, L. D. Ferguson and M. B. Alice, *J. Chem. Phys.*, 49 (1968) 2240.
74 M. Yamashita and J. B. Fenn, *J. Phys. Chem.*, 88 (1984) 4451.
75 S. F. Wong, C. K. Meng and J. B. Fenn, *J. Phys. Chem.*, 92 (1988) 546.
76 C. K. Meng, M. Mann and J. B. Fenn, *Anal. Chem.*, 61 (1989) 1702.
77 J. B. Fenn, M. Mann, C. K. Meng, S. F. Wong and C. M. Whitehouse, *Mass Spectrom. Rev.*, 9 (1990) 37.
78 T. R. Covey, R. F. Bonner, B. I. Shushan and J. D. Henion, *Rapid Commun. Mass Spectrom.*, 2 (1988) 249.
79 K. Straub and K. Chan, *Rapid Commun. Mass Spectrom.*, 4 (1990) 267.
80 M. G. Ikonomou, A. T. Blades and P. Kebarle, *Anal. Chem.*, 62 (1990) 957.
81 R. D. Voyksner, presented at the *7th Montreux Symposium on LC–MS, Montreux, October 31–November 2, 1990.*
82 C. Brunnee, R. Pesch and E. Schröder, *Rapid Commun. Mass Spectrom.*, 4 (1990) 173.
83 N. J. Reinhoud, E. Schröder, U. R. Tjaden, W. M. A. Niessen, M. C. ten Noever de Brauw and J. van der Greef, *J. Chromatogr.*, 516 (1990) 147.

84 S. Nukiyama and Y. Tanasawa, *Trans. Soc. Mech. Eng. Jpn.*, 5 (1939) 68.
85 *Vestec Diaphragm Interface*, Vestec, Houston, TX, 1990.
86 C. E. Parker, C. A. Haney and J. R. Hass, *J. Chromatogr.*, 237 (1982) 233.
87 D. Barcelo, *Biomed. Environ. Mass Spectrom.*, 17 (1988) 363.
88 R. M. Osterman, C. R. Blakley, G. J. Fergusson and M. L. Vestal, in *Proceedings of the 35th ASMS Conference on Mass Spectrometry and Allied Topics, May 24–29, 1987, Denver, CO*, ASMS, East Lansing, MI, 1987, p. 364.
89 R. C. Simpson, C. C. Fenselau, M. R. Hardy, R. R. Townsend, Y. C. Lee and R. J. Cotter, *Anal. Chem.*, 62 (1990) 248.
90 J. J. Conboy, J. D. Henion, M. W. Martin and J. W. Zweigenbaum, *Anal. Chem.*, 62 (1990) 800.
91 K. W. M. Siu, R. Guevremont, J. C. Y. Le Blanc, G. J. Gardner and S. S. Berman, *J. Chromatogr.*, 554 (1991) 27.
92 R. E. A. Escott, P. G. McDowell and N. P. Porter, *J. Chromatogr.*, 554 (1991) 281.
93 E. R. Verheij, U. R. Tjaden, W. M. A. Niessen and J. van der Greef, *J. Chromatogr.*, 554 (1991) 339.
94 J. van der Greef, W. M. A. Niessen and U. R. Tjaden, *J. Chromatogr.*, 474 (1989) 5.
95 W. M. A. Niessen, U. R. Tjaden and J. van der Greef, in preparation.

Journal of Chromatography, 554 (1991) 27–38
Elsevier Science Publishers B.V., Amsterdam

CHROMSYMP. 2210

Electrospray interfacing for the coupling of ion-exchange and ion-pairing chromatography to mass spectrometry[a]

K. W. M. SIU*, R. GUEVREMONT, J. C. Y. LE BLANC[b], G. J. GARDNER and S. S. BERMAN
Institute for Environmental Chemistry, National Research Council of Canada, Montreal Road, Ottawa, Ontario K1A 0R9 (Canada)

ABSTRACT

Electrospray was evaluated as an interface for coupling ion-exchange and ion-pairing chromatography to mass spectrometry. Effective separation and good sensitivity were demonstrated for a liquid flow-rate as high as 50 μl/min and a matrix ion concentration as high as 10 m*M*. Minimum detectable amounts were estimated to be five to ten times poorer than those obtained in the absence of ion-exchange buffers or ion-pairing reagents. The minimum detectable amount for arsenobetaine after a dynamic ion-exchange separation was estimated to be about 20 pg.

INTRODUCTION

Almost all published work on liquid chromatography–mass spectrometry (LC–MS) using electrospray (ES) or ionspray (IS) interfacing has concentrated on reversed-phase separation [1] despite the fact that both ES and IS are only effective for ions that are pre-formed in solution. The popularity of reversed-phase separation stems partially from its effectiveness in separating relatively large analytes, such as some azodyes [2], peptides and proteins [1,3–5], and toxins [6], usually after the ionization of these species is suppressed in solution; another reason is the use of low-ionic-strength eluents, which are more compatible with ES and IS. The fact that ES and IS interfacing have rapidly become accepted techniques in LC–MS for biotechnology and environmental research demonstrates the effectiveness of this approach.

We have been interested in applying ES tandem MS to the determination of small, environmentally significant ions in complex matrices [7–9]. For these ions, reversed-phase chromatography is ineffective because they lack large hydrophobic side-chains, and ion exchange or ion pairing must be employed.

---

[a] NRCC 32 549. Portions of this study were reported in the *38th American Society for Mass Spectrometry Conference, Tucson, AZ, June 1990* and the *73rd Canadian Chemical Conference and Exhibition, Halifax, July 1990*.

[b] Present address: Department of Chemistry, Queen's University, Kingston, Ontario K7L 3N6, Canada.

In this paper, we report our experience in coupling ion-exchange and ion-pairing chromatography to tandem MS via an electrospray interface. The examples that we have chosen are a dynamic cation-exchange separation of several environmentally important organoarsenic ions in admixture and an ion-pairing separation of a mixture of six permissible food dyes.

EXPERIMENTAL

Instrumentation

Experiments were performed on a SCIEX TAGA, Model 6000E atmospheric pressure ionization, triple quadrupole mass spectrometer with an upper mass range of about m/z 1400. For ES interfacing, the corona discharge assembly was removed. The ES probe was mounted on a small movable platform to facilitate reproducible positioning. The optimum probe tip position was established from time to time but was generally found to be about 1–2 cm from the interface plate with the spray off-axis from the orifice. Ions desorbed from solution were heavily solvated. Under the high electric field established between the probe tip and the interface plate, they drifted towards the latter, and a small fraction was sampled via the orifice. Declustering of these sampled ions was accomplished by means of a mild collision-induced dissociation with nitrogen in the "lens" region. The declustered ions were then mass-analyzed by one or both quadrupoles.

Three types of probes were used over a span of several months during which this study was carried out: stainless steel (Hamilton, 33 gauge, *ca.* 100 μm I.D.), polyimide-clad fused silica (J & W, 50 μm I.D.), and aluminium-clad fused silica (SGE, 50 μm I.D.). Their performance was comparable. To facilitate coupling of the probe to standard LC coupling, it was mounted concentrically inside a 1/16 in. O.D. stainless-steel tube (used typically in gas chromatography) by means of epoxy glue. For IS experiments, the probe was fitted concentrically with a slightly wider stainless-steel tube (Hamilton, 22 gauge, *ca.* 400 μm I.D.) for the passage of the nitrogen nebulizer gas (20 p.s.i.) [10]. The stainless-steel tubes were electropolished before use. For the polarization of the spray probe, a Tennelec Model TC950 power supply (maximum voltage, 5 kV) was used in series with a 50-MΩ current-limiting resistor. The ES current was monitored by a laboratory-made digital microammeter that may be floated above ground. Electrical isolation of the probe was achieved by the use of fused silica or PEEK (polyether ether ketone, Upchurch) tubing for connection.

The lens and quadrupole voltages were optimized for ES. Full-scan mass spectra were usually acquired with a measurement time of 10 ms per step (typically one m/z unit) whereas selected ion or reaction monitoring was performed with a typical measurement time of 1 s per cycle. For MS–MS runs, argon was used as the target gas at a thickness of about $1.3 \cdot 10^{14}$ atoms per cm^2, which allowed on average fewer than one collision event per ion. The collision energy used was typically about 33 eV, laboratory frame.

Chromatographic separation was performed using two reciprocating piston pumps (Waters, Model 6000A) controlled via a gradient former (Waters, Model 680). Samples were introduced via a valve injector (Rheodyne, Model 7125) with a 20-μl sample loop. We prefer the use of regular-bore columns because of wider column selection. Two of these were used: a Hamilton PRP-1 column (5-μm packing, 15 cm

× 0.41 cm I.D.) for the separation of organoarsenic species and a Waters Novapak C_{18} column (4-μm packing, 15 cm × 0.39 cm I.D.) for the separation of food dyes. The typical flow-rate was 1 ml/min. To obtain the appropriate flow-rate for ES, the column effluent was split. About 5% (*ca.* 50 μl/min) was directed into the ES interface; the remaining 95% was routed to a UV–visible variable-wavelength detector (Waters, Model 450) or to waste. Effluent splitting was accomplished by means of a zero dead-volume tee union (SSI) and PEEK connection tubes of the appropriate length and internal diameter. Small changes in the split ratio were inconsequential as ES-MS is insensitive to small changes of flow-rate. When chromatographic separation was unnecessary, the samples were continuously infused by means of a syringe pump (Harvard Apparatus, Model 22) at typical flow-rates of 20–50 μl/min.

Reagents

Polypropylene glycol (PPG) 1000, sodium octanesulphonate and tetrabutylammonium phosphate (TBAP) were analytical grade (Aldrich). Myoglobin (horse heart) was available from Sigma. Arsenobetaine (AB), arsenocholine (AC) iodide, and te-

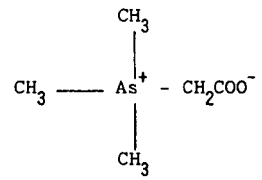

AB

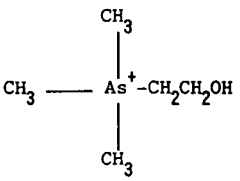

AC

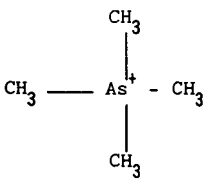

TMA

Fig. 1. Structure of organoarsenic species. AB = arsenobetaine; AC = arsenocholine; TMA = tetramethylarsonium.

tramethylarsonium (TMA) iodide (Fig. 1) were synthesized by W. R. Cullen (Department of Chemistry, University of British Columbia). The food dyes, Indigotine, Tartrazine, Sunset Yellow FCF, Amaranth, Fast Green FCF, and Brilliant Blue FCF (Fig. 2), were purified and donated by F. Lancaster (Health Protection Branch, Health and Welfare Canada). These are six out of ten synthetic food colours permitted in Canada. Organic solvents were LC grade. Water was distilled and deionized (DDW) by means of a commercial cartridge system (Cole-Palmer).

For the dynamic cation exchange of AB, AC and TMA, the PRP-1 column was pre-coated with octanesulphonate as described [11]. Optimum separation was obtained with an eluent of DDW–methanol (80:20) containing 1 m*M* sodium octanesulphonate and 10 m*M* ammonium citrate. For the determination of AB alone, an eluent of DDW–methanol (70:30) containing 10 m*M* sodium octanesulphonate and 0.5% acetic acid on the Novapak C_{18} column was found to work best. For the food dyes, an ion-pairing separation as recommended by Health and Welfare Canada [12] was used; the food dyes were separated in a linear gradient program from 50:50 to 40:60 DDW–methanol containing 5 m*M* TBAP in 12 min.

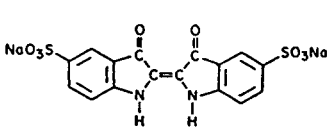

IND

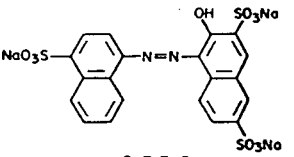

AMA

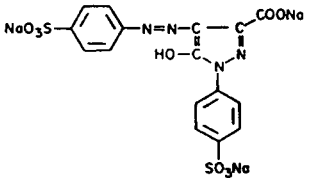

TAR

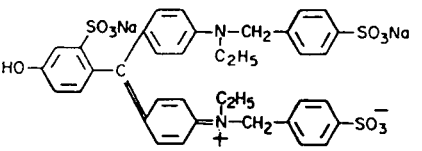

FAS

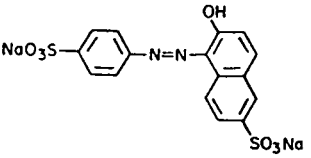

SUN

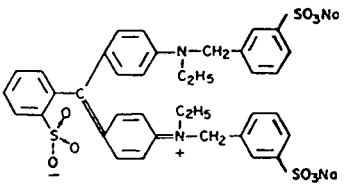

BRI

Fig. 2. Structure of permissible food dyes. IND = Indigotine; TAR = Tartrazine; SUN = Sunset Yellow FCF; AMA = Amaranth; FAS = Fast Green FCF; BRI = Brilliant Blue FCF.

RESULTS AND DISCUSSION

Before attempting to interface ion-exchange and ion-pairing separation to MS, preliminary investigations were performed to assess the compatibility of ES to the flow-rates and matrix ion concentrations that were necessary for these modes.

Fig. 3 shows the result of selected ion monitoring a 0.25 μM PPG 1000 solution in DDW–methanol (80:20) containing 1 mM ammonium acetate and adjusted to pH 10 with ammonia at a flow-rate of 50 μl/min. PPG 1000 is a mixture of polypropylene glycols containing different numbers of propylene units, with an average molecular weight in the vicinity of 1000 dalton. The ions monitored were two of the many singly charged ammonium adduct ions of PPG [13]. The experiment was conducted in part in IS, *i.e.*, a nitrogen nebulizer gas was added and its flow-rate was varied over a wide range (0 to 1000 and back to 0 ml/min) in a span of 10 min. The nitrogen flow-rate appeared to have little influence on response, which was relatively stable. Essentially identical results were obtained when the liquid flow-rate was lowered from 50 to 10 μl/min. Consequently, all further experiments were conducted with ES at a liquid flow-rate of 50 μl/min.

The presence of organic solvent appears to play a significant role in response stability. In our hands, it is possible to run samples of virtually 100% water as solvent at room temperature (Fig. 4) (and we do so when the presence of organic solvent is undesirable), but signal stability almost always improves when 10% or more methanol is introduced (Fig. 5). Others have reported that the electrospray of 100% aqueous solutions may be stabilized by operating at approximately 50°C [14].

Once the flow-rate compatibility question was answered, the next step was to determine the effect of the presence of significant concentrations of matrix ions as dictated by ion-exchange and ion-pairing chromatography. It was known that they would suppress analyte ion signal [15]; the question was how much. Fig. 6 shows the result of such an experiment on arsenobetaine. The variation of protonated AB response and ES current with the polarization voltage in the presence of varying

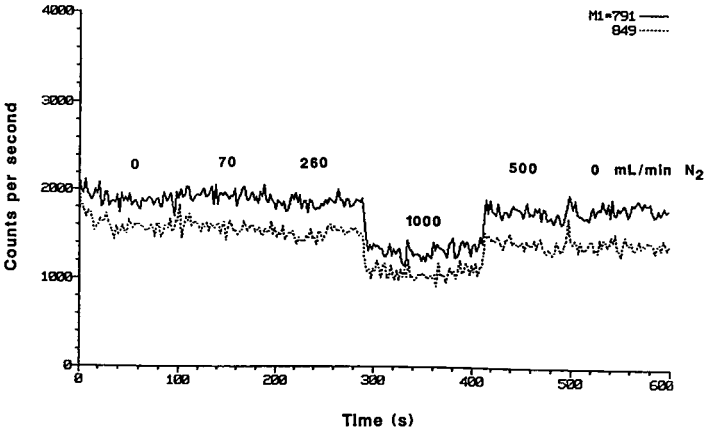

Fig. 3. PPG 1000 response *versus* time and nebulizer gas flow-rate. Conditions: 0.25 μM PPG 1000 solution in DDW–methanol (80:20) containing 1 mM ammonium acetate at pH 10 with ammonia; liquid flow-rate, 50 μl/min; nebulizer gas flow-rate as indicated.

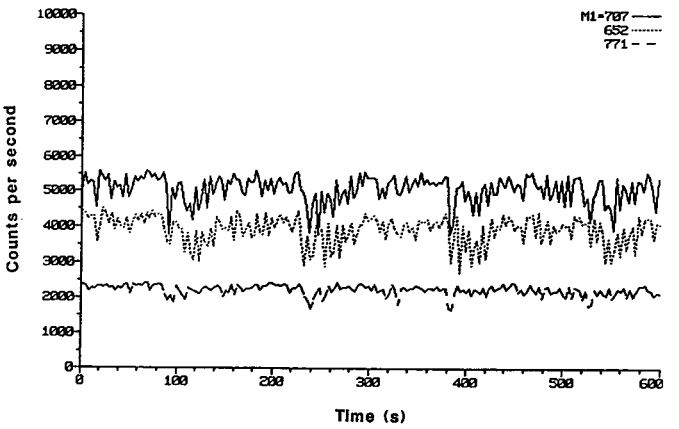

Fig. 4. ES response of myoglobin *versus* time. Conditions: 0.5 μM equine myoglobin in DDW containing 0.05% acetic acid; liquid flow-rate, 50 μl/min. The ions monitored are protonated myoglobin: m/z 652, 26 H^+; m/z 707, 24 H^+; m/z 771, 22 H^+.

amounts of matrix ions was monitored. As expected, the analyte response and ES current were functions of the applied voltage. The presence of matrix ions resulted in signal suppression, but the effect was relatively small even when a matrix ion concentration as high as 100 mM citrate was encountered. At the optimum voltage of about 3.5 kV, the AB response decreased by a factor of 8 when 100 mM ammonium citrate and 1 mM sodium octanesulphonate were added. Similar results were obtained for AC (Fig. 7); a suppression factor of about 5 at the optimum voltage was evident.

Thus it was apparent that ES is quite compatible with the flow-rates and matrices necessary for interfacing ion-exchange and ion-pairing chromatography to MS. The first real interfacing we attempted was the coupling of dynamic ion-exchange separation of AB, AC and TMA ion to tandem MS.

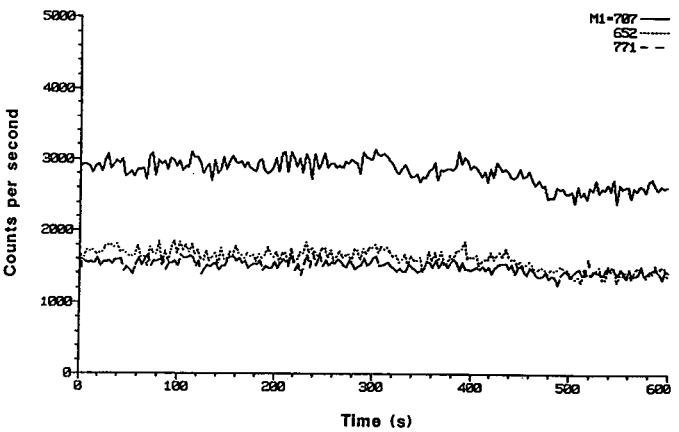

Fig. 5. ES response of myoglobin *versus* time. Conditions: 0.5 μM equine myoglobin in DDW–methanol (90:10) containing 0.05% acetic acid; liquid flow-rate, 50 μl/min. See Fig. 4 for ion assignment.

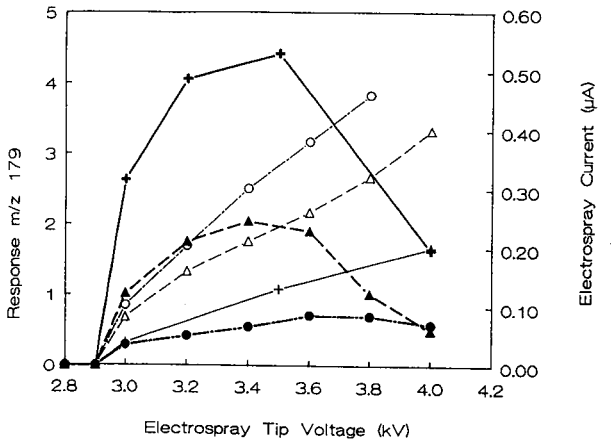

Fig. 6. ES results of AB solutions containing various concentrations of matrix ions. Open symbols, current; closed symbols, response; all solutions were 25 μM AB in DDW–methanol (80:20) plus the following: + and +, no ammonium citrate, no sodium octanesulphonate; ▲ and △ 10 mM ammonium citrate, 1 mM sodium octanesulphonate; ● and ○, 100 mM ammonium citrate, 1 mM sodium octanesulphonate.

AB, AC and TMA are organoarsenic species known to exist in marine fauna. The most powerful and often employed technique of these involatile species is LC–inductively coupled plasma (ICP) MS [16,17]. In solution, AC and TMA exist as simple cations. AB is a zwitterion in the crystallilne state, but is easily protonated in solution and exist as a cation. These ionic species are best separated by ion pairing or dynamic ion exchange. We preferred the use of poly(styrene–divinylbenzene)-type packing for AC and TMA to circumvent their strong interaction with surface silanol

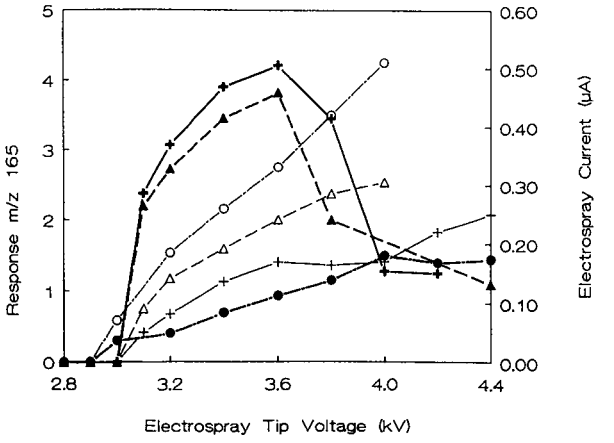

Fig. 7. ES results of AC solutions containing various concentrations of matrix ions. All solutions were 17 μM AC, all other conditions were identical to those in Fig. 6.

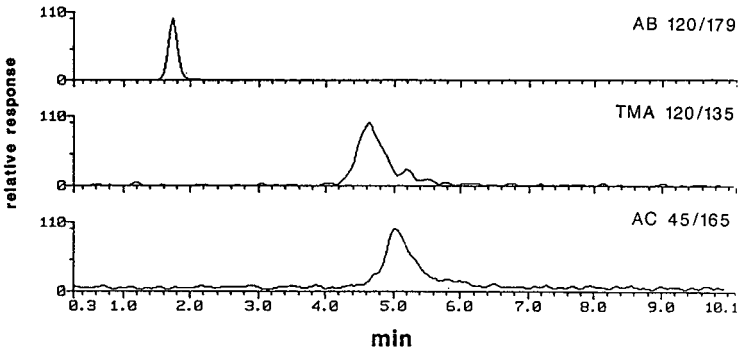

Fig. 8. Selected reaction monitoring of AB, AC and TMA. Analyte amounts, 1 ng each; column, PRP-1,5 μm; eluent, DDW–methanol (80:20) containing 1 m*M* sodium octanesulphonate and 10 m*M* ammonium citrate. The daughter/parent pair monitored are indicated in the figure.

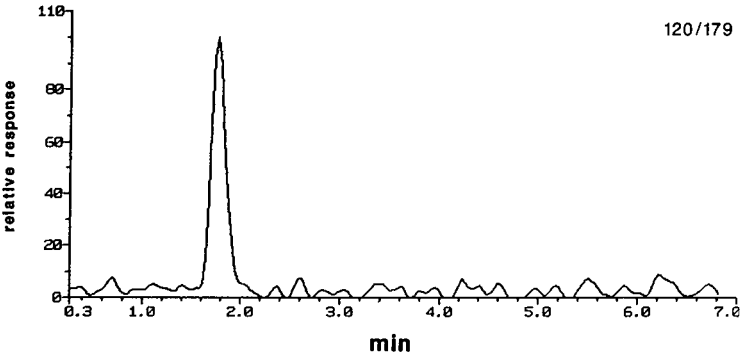

Fig. 9. Selected reaction monitoring of 100 pg AB. See Fig. 8 for conditions.

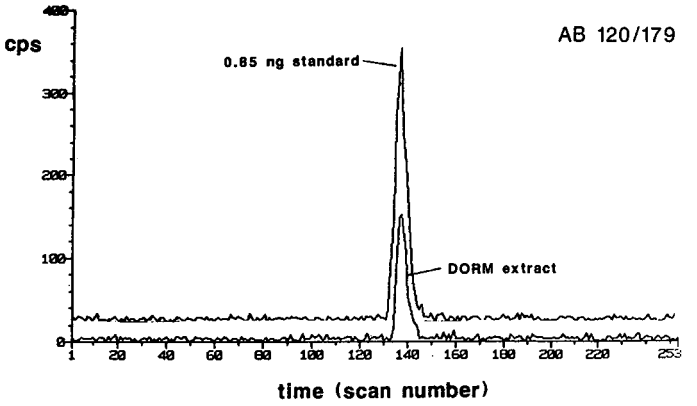

Fig. 10. Determination of AB in DORM. Column, Novapak C_{18}, 4 μm; eluent, DDW–methanol (70:30) containing 10 m*M* sodium octanesulphonate and 0.5% acetic acid.

groups on silica-based materials. The collision-induced dissociation pathways of the three organoarsenic species are well characterized [7,18]; the principal daughter ion for both protonated AB (*m/z* 179) and TMA (*m/z* 135) is the trimethylarsine ion (*m/z*

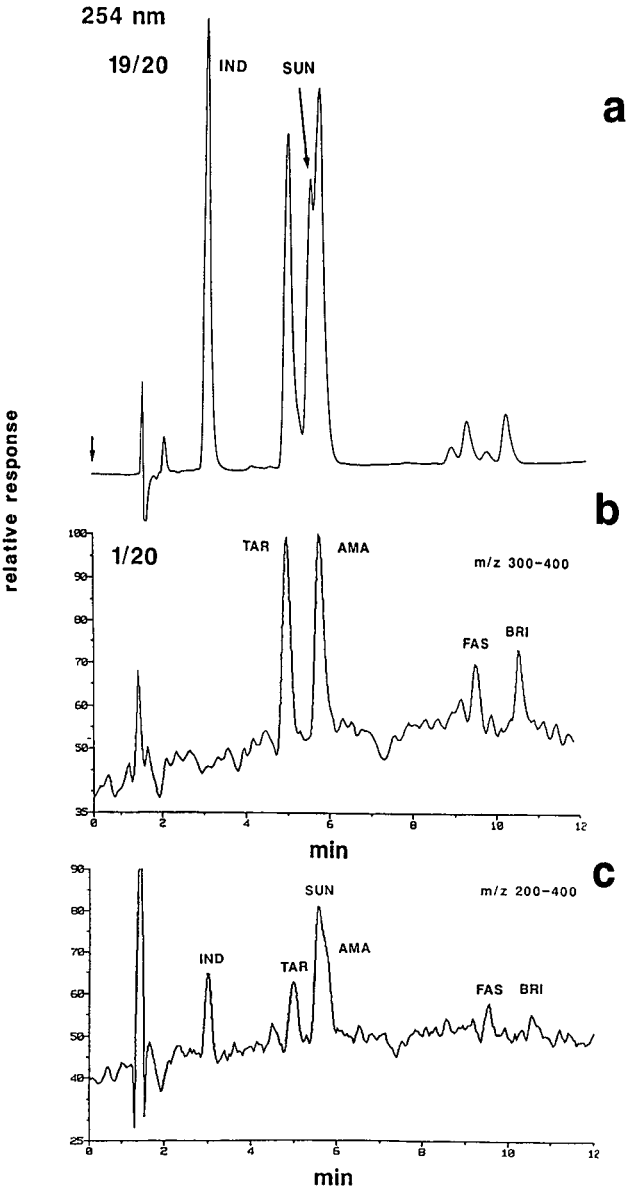

Fig. 11. Ion-pairing separation of food dyes. (a) UV–visible detection at 254 nm; (b) total ion chromatogram in the negative-ion detection mode from *m/z* 300 to 400; (c) total ion chromatogram from *m/z* 200 to 400. The split ratio between the UV–visible detector and the mass spectrometer was 19:1. Column, Novapak C_{18}, 4 μm; eluent, linear gradient from 50:50 to 40:60 DDW–methanol containing 5 m*M* TBAP in 12 min. See Fig. 2 for structures of the dyes.

120), and that for AC is at m/z 45, which is believed to be protonated ethylene oxide.

Fig. 8 shows selected reaction monitoring of 1 ng each of AB, AC and TMA via their parent/principal daughter pairs. Relatively strong interaction with the stationary phase was still apparent for TMA and AC, which were partially resolved. The best sensitivity was observed for AB whose minimum detectable amount (MDA) (defined as two times over noise) was estimated to be about 20 pg (Fig. 9).

This technique has been applied to the determination of AB in a dogfish muscle reference material (DORM-1, National Research Council of Canada) (Fig. 10). A weaker eluent was used to better retain AB. AB was extracted from the tissue by sonicating 0.3 g DORM-1 in 10 ml eluent for 30 min. The measured concentration of 15.7 ± 0.4 μg arsenic per g (four replicate analyses employing both standard calibration and additions) is practically identical to that obtained by LC–ICP-MS [16].

The next separation attempted was the ion-pairing separation of food dyes. The

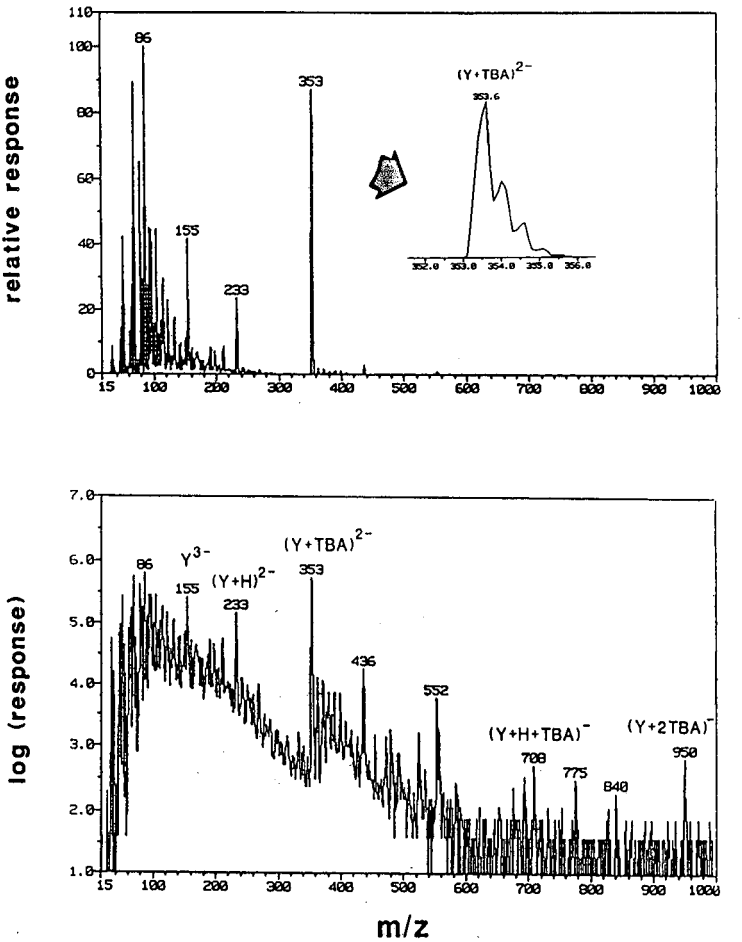

Fig. 12. Full-scan mass spectrum of a 935 μ*M* solution of Tartrazine in DDW–methanol (50:50) containing 5 m*M* TBAP. ES flow-rate, 50 μl/min; continuous infusion. Y stands for the fully ionized Tartrazine.

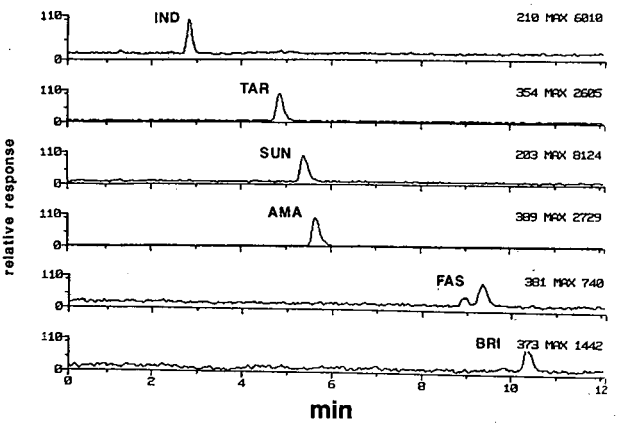

Fig. 13. Selected ion monitoring of the TBA adduct ion of food dyes. Chromatographic conditions are detailed in Fig. 11; analyte amounts, 5 ng each. The *m/z* monitored are shown in the figure.

food dyes contain good chromophores and are traditionally assayed by means of UV–visible detection after LC separation [12]. Fig. 11 shows the simultaneous output of the UV–visible detector and the mass spectrometer on injection of a mixture of the six dyes. The upper MS trace (Fig. 11b) is a total ion chromatogram in the negative-ion detection mode between *m/z* 300 and 400, which shows the presence of four of the six dyes. All six dyes were detected when the scan range was extended to measure from *m/z* 200 to 400 (Fig. 11c). The most prominent food dye ions under the given experimental conditions were the adduct ions of tetrabutylammonium (TBA) with the food dyes, which contain two to three sulphonate and/or carboxylate groups. For Tartrazine, which has three ionizable groups, the principal ion was at *m/z* 353 (Fig. 12) and identified as a doubly charged adduct ion between 1 unit of Tartrazine and 1 unit of TBA. Other Tartrazine-based ions were also present; the highest (triply) charged Tartrazine ion at *m/z* 155 is the principal ion when TBA or other ion-pair reagent is absent. The same trend was observed for the other food dyes. That the *m/z* ion of Tartrazine at *m/z* 353 is doubly charged is self-evident after the *m/z* scale is expanded to reveal resolution of the ^{13}C-containing ions by 0.5 *m/z* units. Fig. 13 shows selected ion monitoring of the TBA adduct ions of 5 ng each of the food dyes. MDAs of the food dyes were in the order of a few hundred of picograms. For Amaranth the MDA was estimated to be about 200 pg, *ca.* a factor of 10 better than that of UV–visible detection.

CONCLUSIONS

ES is a viable and valuable interface for coupling ion-exchange and ion-pairing chromatography to MS. The presence of ion-exchange buffers and ion-pairing reagents do raise the MDAs of analyte ions by suppressing analyte ion signals and/or raising background ion counts. This increase in MDAs is typically five to ten times above those obtained in the absence of matrix ions, which is the price one pays for employing ion-exchange and ion-pairing chromatography. Conboy *et al.* [19] have done impressive work in reducing the electrolyte concentration in their chromato-

graphic effluent by passing it through an ion-exchange fibre (much like Dionex ion chromatography) prior to ES. This may be the approach of choice when maximum sensitivity is desired.

REFERENCES

1 E. C. Huang, T. Wachs, J. J. Conboy and J. D. Henion, *Anal. Chem.*, 62 (1990) 713A.
2 P. O. Edlund, E. D. Lee, J. D. Henion and W. L. Budde, *Biomed. Environ. Mass Spectrom.*, 18 (1989) 233.
3 J. Henion, E. C. Huang and K. L. Duffin, *Proceedings of the 38th ASMS Conference on Mass Spectrometry and Applied Topics, Tucson, AZ, June 3–8, 1990*, ASMS, East Lansing, MI, p. 14.
4 J. J. Conboy, J. D. Henion, J. Crowther and J. Tolan, *Proceedings of the 38th ASMS Conference on Mass Spectrometry and Applied Topics, Tucson, AZ, June 3–8, 1990*, ASMS, East Lansing, MI, p. 146.
5 E. C. Huang and J. D. Henion, *Proceedings of the 38th ASMS Conference on Mass Spectrometry and Applied Topics, Tucson, AZ, June 3–8, 1990*, ASMS, East Lansing, MI, p. 148.
6 M. A. Quilliam, B. A. Thomson, G. J. Scott and K. W. M. Siu, *Rapid Commun. Mass Spectrom.*, 3 (1989) 145.
7 K. W. M. Siu, G. J. Gardner and S. S. Berman, *Rapid Commun. Mass Spectrom.*, 2 (1988) 69.
8 K. W. M. Siu, G. J. Gardner and S. S. Berman, *Rapid Commun. Mass Spectrom.*, 2 (1988) 201.
9 K. W. M. Siu, G. J. Gardner and S. S. Berman, *Anal. Chem.*, 61 (1989) 2320.
10 K. W. M. Siu, G. J. Gardner and S. S. Berman, *Org. Mass Spectrom.*, 24 (1989) 931.
11 R. M. Cassidy and S. Elchuk, *Anal. Chem.*, 54 (1982) 1558.
12 F. E. Lancaster, *Analytical Methods and Techniques for Colours in Foods*, Health and Welfare Canada, Ottawa, 1981, p. 11-1.
13 S. F. Wong, C. K. Meng and J. B. Fenn, *J. Phys. Chem.*, 92 (1988) 546.
14 M. H. Allen, F. H. Field and M. L. Vestal, *Proceedings of the 38th ASMS Conference on Mass Spectrometry and Applied Topics, Tucson, AZ, June 3–8, 1990*, ASMS, East Lansing, MI, p. 431.
15 T. R. Covey, A. P. Bruins and J. D. Henion, *Org. Mass Spectrom.*, 23 (1988) 178.
16 D. Beauchemin, M. E. Bednas, S. S. Berman, J. W. McLaren, K. W. M. Siu and R. E. Sturgeon, *Anal. Chem.*, 60 (1988) 2209.
17 Y. Shibata and M. Morita, *Anal. Sci.*, 5 (1989) 107.
18 B.P.-Y. Lau, P. Michalik, C. J. Porter and S. Krolik, *Biomed. Environ. Mass Spectrom.*, 14 (1987) 723.
19 J. J. Conboy, J. D. Henion, M. W. Martin and J. A. Zweigenbaum, *Anal. Chem.*, 62 (1990) 800.

Journal of Chromatography, 554 (1991) 39–46
Elsevier Science Publishers B.V., Amsterdam

CHROMSYMP. 2273

Liquid chromatography–mass spectrometry with ionspray and electrospray interfaces in pharmaceutical and biomedical research

A. P. BRUINS
University Centre for Pharmacy, A. Deusinglaan 2, 9713 AW Groningen (Netherlands)

ABSTRACT

Electrospray and ionspray techniques use samples that exist as ions or ion–molecule complexes in solution. After the dispersion of the solution into an electrically charged aerosol, the sample ions may escape from the solution into the gas phase in a region that is at atmospheric pressure. The sample ions are transported into the mass analyser which is operated under a high vacuum. Liquid chromatographs can be coupled to electrospray and ionspray interfaces. Flow injection or continuous infusion of a sample solution (both without the use of a separating column) may be preferred over on-line liquid chromatography–mass spectrometry in certain applications. Electrospray or ionspray is applicable to polar or ionic samples. Weakly polar and apolar samples are not ionized under electrospray or ionspray conditions. Applications of the techniques are in the fields of drug metabolism, natural product analysis and the determination of high molecular weights through the observation of multiply charged ions.

INTRODUCTION

The majority of samples in biomedical analyses are polar and thermally labile. Liquid chromatograpy (LC) can handle such samples. One-line LC–mass spectrometry (MS) is the logical choice if the advantages of LC are to be combined with the power of MS. The conventional gas phase ionization techniques that are routinely used in MS [electron impact (EI) and chemical ionization (CI)], require that the sample is present in the vapour phase, which can only be achieved through the input of a sufficient amount of heat. Although the time spent in the hot zones in moving-belt, particle-beam and thermospray LC–MS interfaces is short, limitations are imposed on the analysis of thermolabile samples.

Many samples of biological origin exist as ions in solution. Others can easily associate with ions in solution, such as H^+, Na^+, NH_4^+, acetate and Cl^-. Such samples are difficult to volatilize and ionize by EI or CI. The goal of newly developed ionization techniques for LC–MS is the transport of sample ions or ion–molecule complexes from the liquid phase (the effluent of the liquid chromatograph) into the mass analyser, without passage through the hot zones [1].

0021-9673/91/$03.50

Ions can be taken from the condensed phase into the gas phase or vacuum with the help of mechanical energy [fast atom bombardment (FAB), secondary ion mass spectrometry (SIMS)], electrical energy (field desorption [2], ion evaporation [3]) or photons.

On-line LC–MS with FAB or SIMS requires the continous transport of a sample solution to the liquid target surface as achieved in continuous-flow FAB, pioneered by Ito *et al.* [4].

The separation of ions from the condensed phase under the influence of electrical forces has been studied extensively in field desorption MS [2] and in electrohydrodynamic ionization from glycerol solution [5], but neither have been adapted for routine on-line LC–MS. The pioneering work by Iribarne *et al.* [3] on ion evaporation from small electrically charged water droplets had far-reaching consequences for on-line LC–MS. Present day LC–MS interfaces that use the ion evaporation principle are electrospray [6,7] and ionspray [8].

The operating principle of electrospray and ionspray is the dispersion of a sample solution into an electrically charged aerosol. In the case of electrospray, a phenomenon described by Zeleny in 1917 [9], nebulization takes place by the exposure of a liquid surface to a high electric field. In an electrospray LC–MS interface [10] a solution of the analyte is introduced into dry air or nitrogen at atmospheric pressure through a metal capillary tube that is held at a potential of several kilovolts relative to the walls of the ion source. The build-up of charge at the liquid surface creates such an instability in the liquid that coulomb repulsion forces are sufficient to overcome the surface tension: small (< 1 μm diameter) charged droplets separate from the liquid emerging from the capillary tube. The technique works best with flow-rates in the range below 5–10 μl/min and hence needs microbore columns or a split of the effluent from the liquid chromatograph. Dispersion of liquids by electrical forces alone, as is the case with electrospray, becomes more difficult if the percentage of water in the eluate is high. In the case of ionspray, the nebulizing action of the electric field is assisted by a high-velocity gas flow.

The ionspray LC–MS interface is essentially a concentric pneumatic nebulizer, exposed to an electric field. The nebulizing capillary is usually floated at 3 kV relative to the walls of the ion source. The input of mechanical energy in the nebulization step makes higher flow-rates (40 μl/min, compatible with 1 mm I.D. microbore columns) and higher percentages of water in the sample solution feasible. However, the best sensitivity is still obtained with flow-rates around 5 μl/min.

Once an electrically charged aerosol is formed, evaporation of solvents from the very small droplets takes place. The size of the droplets decreases, and the electric field at the liquid surface of the droplets increases. As a result, the liquid surface becomes so unstable that microdroplets containing a few ions, or ions with one or more shells of solvent, separate from the droplets [3,11]. A final desolvation of each microdroplet or solvated ion produces sample ions that are transported into the mass analyser.

Electrospray and ionspray ionization are carried out at atmospheric pressure for a number of reasons. First, the evaporation of solvents from droplets is more efficient at high pressure, due to the effective transfer of heat. Second, a reduced pressure combined with high electric fields gives rise to strong electrical discharges. In a discharge, both positive and negative-charge carriers are formed, that will recom-

bine with droplets having the opposite charge. As a result droplet charge is neutralized and the formation of sample ions from charged droplets can no longer take place. Third, the gas flow through a pneumatic nebulizer cannot be accommodated by the standard vacuum system of a mass spectrometer.

As often, new methods build upon experience gained a decade or more ago. In the case of LC–MS with atmospheric pressure ionization (API), analytical applications were published by Horning *et al.* in 1974 [12]. Their original API source was very sensitive, but in its original design it showed two drawbacks: ions were drawn into the mass analyser through a small 25 μm I.D. orifice, which was prone to plugging by dust particles or non-volatile materials; in addition, the expansion of ions and polar components of the LC eluent, such as water, tended to produce big cluster ions due to strong cooling in the free jet expansion stage.

Manufacturers of analytical mass spectrometers have not produced API sources as standard accessories for their instruments. Interest in LC–API-MS remained dormant for nearly 10 years until Henion *et al.* at Cornell University [13] revitalized the technique in co-operation with SCIEX, a manufacturer of API mass spectrometers designed for monitoring air quality. This instrument has a 100-μm orifice combined with fast cryogenic pumping. The penetration of dust and water vapour into the free jet expansion stage is prevented by a dry nitrogen gas curtain [14]. Fig. 1 shows the construction of an ionspray LC–MS interface with a SCIEX ion source. Basically ions are pushed to the right towards the small conical orifice by the voltages applied to various parts. At the same time dust and neutral molecules are pushed to the left by the flow of dry nitrogen gas. At the entrance of the conical orifice ions are drawn into the vacuum system of the mass spectrometer, together with a part of the dry nitrogen gas flow. In this simple and elegant construction, blockage of the orifice and the formation of clusters from ions and water molecules are prevented. The electrospray ion source constructed by Whitehouse *et al.* [10] makes use of a similar counter-current flow of dry nitrogen.

An API source with an electrospray or ionspray interface as described here can operate at room temperature, but an increased temperature (up to 80°C) may be advantageous for the handling of a high percentage of water in the eluent. In either case the temperature is probably low enough to prevent thermal degradation of the most difficult samples.

The early efforts on electrospray MS were directed at improvements of the hardware and the investigation of multiply charged ions of polyglycols [15]. The ionspray interface was used together with microbore LC for the support of environmental and biomedical studies. The determination of sulphonated azo dyes in waste water [16], the metabolism of steroids in race horses [17], contamination in pharmaceuticals [18] and the real-time monitoring of the products of an enzyme reaction [19] have demonstrated the versatility of the electrospray or ionspray ionization technique.

The emphasis by Wong *et al.* [15] on multiply charged ions was received with scepticism when the complicated spectra of polyethylene glycol oligomers were shown. A significant breakthrough was achieved with the presentation of series of multiply charged ions of pure samples, in particular proteins [20]. The ability to obtain a molecular weight in the range up to 100 000 and more with a simple quadrupole mass spectrometer has led to an overwhelming interest in electrospray and ion-

spray techniques. Manufacturers that were not convinced of the potential of API and electrospray/ionspray a few years ago have now modified their instruments.

Another new application of electrospray is the combination of capillary zone electrophoresis (CZE) with MS, developed by Smith *et al.* [21]. Electrophoretic separation techniques have been the theme of three *International symposia on High-Performance Capillary Electrophoresis* (Boston, MA, 1989; San Franciso, CA, 1990 and San Diego, CA, 1991) where attention was focused on the efficient separation of samples of biochemical, medial, pharmaceutical and biotechnological origins. CZE–MS of dynorphins may serve an a representative example from this new field [22].

Electrospray and ionspray are suited for polar and ionic compounds, but are not effective inonization techniques for weakly polar and apolar samples. Such weakly polar samples can still be ionized if the atmospheric pressure ion source can be adapted for use in the atmospheric pressure chemical ionization mode (APCI) instead of the electrospray mode [23].

EXPERIMENTAL

A NERMAG R3010 triple quadrupole mass spectrometer was modified for API [24]. The original transfer line for the gas chromatograph was removed. The API source is mounted on a 10 cm I.D. tube and flange which has replaced the gas chromatography inlet flange. Three vacuum stages are used [25]. The first stage is pumped by a 35 m^3/h rotary pump (Alcatel 2033). The second and third stages are the original ion source housing and analyser regions, each pumped by the original 700 l/s oil diffusion pumps. The pressures in the first, second and third stages are 1.7, $2 \cdot 10^{-3}$ and $1 \cdot 10^{-5}$ mbar, respectively.

Ions are drawn into the first stage through a 0.3 mm I.D. nozzle orifice in a 1 mm thick stainless-steel disk. The central portion of the beam of gas and ions is admitted into the second stage through a 1.4 mm I.D. skimmer orifice located 4 mm downstream from the nozzle. Ions are guided into the mass analyser by the use of a radio frequency only quadrupole mounted in the original source housing of the NERMAG R3010. The nozzle orifice is protected from particulate matter and solvent vapour by a dry nitrogen gas curtain [14] as shown in Fig. 1.

A Jasco FAMILIC 100N syringe pump and a Jasco injector with a 0.3-μl loop was used for the flow injection experiments. Methanol was used as the eluent at 5 μl/min. Samples were injected as solutions in methanol. A flow-rate of 5–10 μl/min of

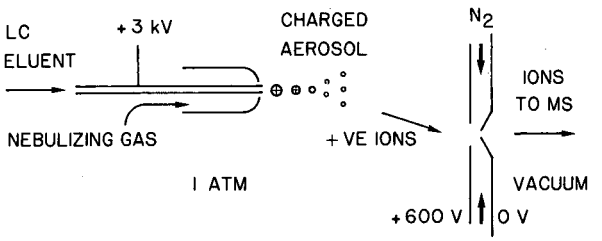

Fig. 1. Ionspray LC–MS interface in atmospheric pressure ion source with dry nitrogen gas curtain.

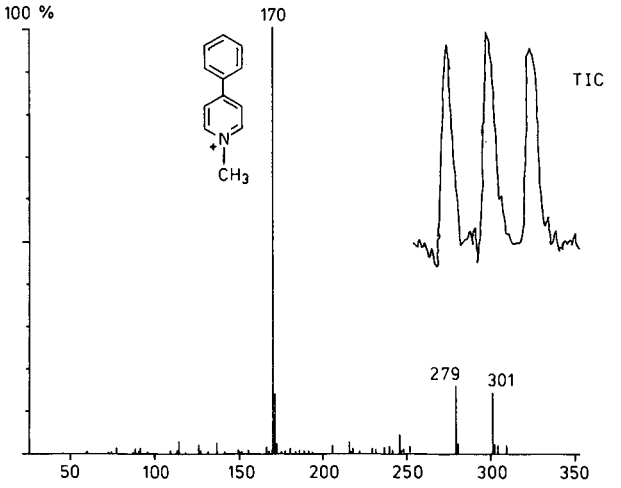

Fig. 2. Electrospray mass spectrum of MPP^+, with total ion current (TIC) trace (m/z 30–380) of three repeated 3-ng injections; m/z 279 and 301 are the MH^+ and $M \cdot Na^+$ ions of dibutyl phthalate. Sample courtesy of H. Rollema (University Centre for Pharmacy, Groningen, Netherlands).

the effluent from 2 and 4.6 mm I.D. columns was introduced into the ionspray interface via a splitter in on-line LC–MS experiments.

The instrument is entirely dedicated to LC–API-MS with ionspray for the support of research on drug metabolism, natural products and newly synthesized compounds.

RESULTS

Fig. 2 shows the electrospray sprectrum of MPP^+, a neurotoxin formed from 1-methyl-4-phenyl-1,2,3,6-tetrahydropyridine (MPTP), a byproduct of a designer

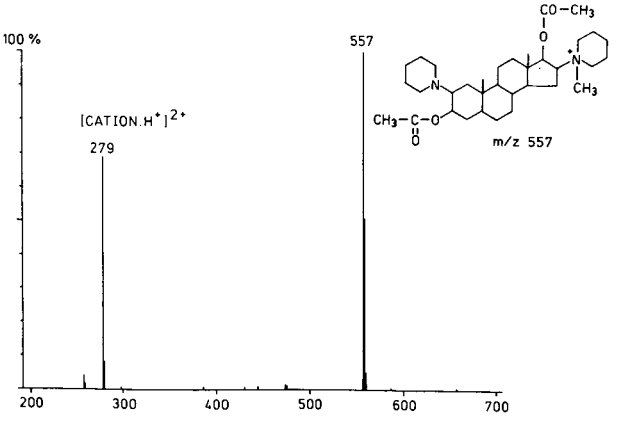

Fig. 3. Electrospray mass spectrum of 30 ng vecuronium bromide (ORG NC 45). Sample courtesy or Organon.

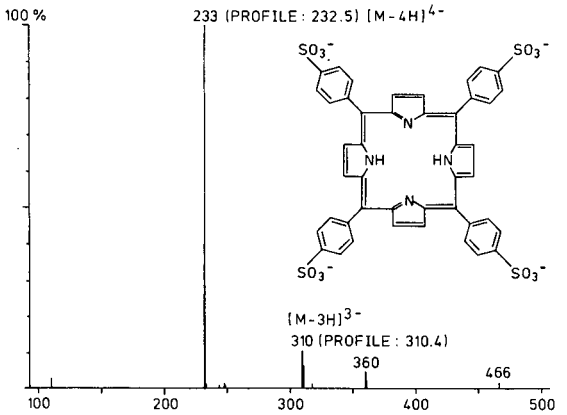

Fig. 4. Electrospray mass spectrum of 30 ng synthetic sulphonated *meso*-tetraphenylporphyrin (mol.wt. 934). Sample courtesy of J. Braams (University Centre for Pharmacy, Groningen, Netherlands) and R. J. B. J. Brouwers (Tjongerschans Hospital, Heerenveen, Netherlands).

drug synthesis. Continuous flow FAB of MPP^+ shows a SIMS sensitivity in the low nanogram range [26]. Electrospray gives low-nanogram full-spectrum sensitivity. Fig. 3 demonstrates the application of ionspray in the determination of multifunctional quaternary ammonium drugs. Vecuronium bromide undergoes extensive thermal demethylation during LC–MS with a moving belt [27]. Thermal dealkylation reactions are also a problem in thermospray [28]. The ion at *m/z* 279 is a doubly charged ion, corresponding to vecuronium protonated at the tertiary amino function. The mass spectrum in Fig. 3 shows the total absence of thermal degradation products. The ability of ionspray and electrospray to generate multiply charged ions from multifunctional molecules has already been mentioned in conjunction with the analysis of peptides [29]. On a more modest scale, the quadruply charged ion in the mass spec-

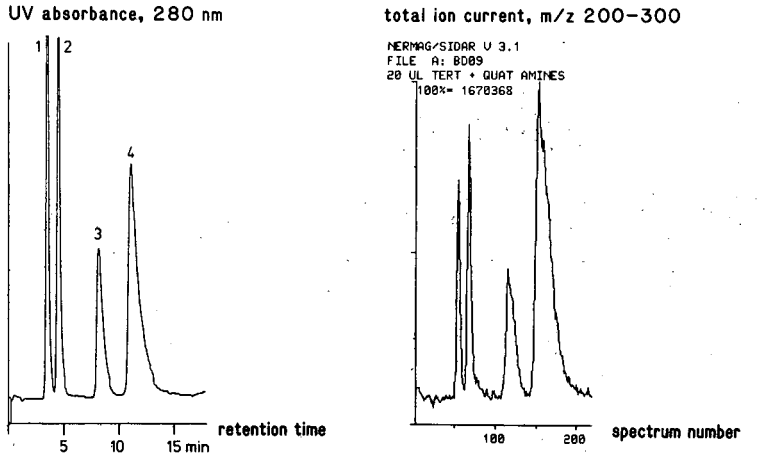

Fig. 5. HPLC separation with UV (left) and ionspray MS (right) detection of a mixture of dextrorphan (1), dextromethorphan (2), N-methyldextrorphan (3) and N-methyldextromethorphan (4). Injection: *ca.* 300 ng per component into HPLC system; *ca.* 3–30 ng into MS system. From ref. 30.

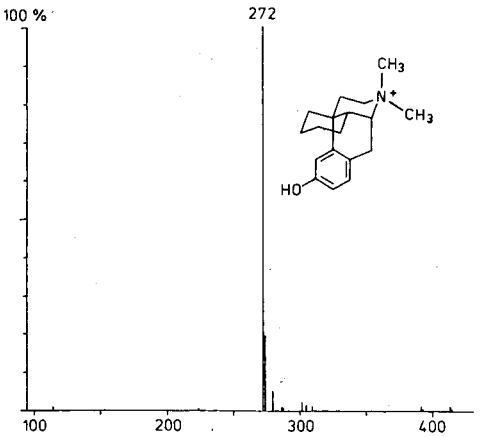

Fig. 6. Ionspray mass spectrum of N-methyldextrorphan. Sample courtesy of A. B. L. Lanting (University Centre for Pharmacy, Groningen, Netherlands).

trum of a synthetic tetrasulphonated porphyrin in Fig. 4 was one of the keys for the confirmation of the identity of this product.

Fig. 5 shows the on-line separation of a mixture of two morphinans (dextrorphan and dextromethorphan) and their *N*-methylated derivatives [30]. The mass spectrum of the third peak is presented in Fig. 6. A study of the metabolism of quaternary ammonium drugs in this department hinges on the ability of the ionspray LC–MS interface to produce clean spectra, without a trace of thermal dealkylation reactions. Details on metabolism, LC conditions and the LC–MS of samples obtained from biological materials will be published elsewhere.

CONCLUSIONS

Papers previously published and the examples shown here demonstrate that API with an electrospray or ionspray LC–MS interface is well suited for the support of biomedical research. The operation at room temperature (or up to 80°C at the most) is a significant advantage for thermolabile samples. The high mass capability and coupling with CZE make it a most promising new field.

REFERENCES

1 A. P. Bruins, *Adv. Mass Spectrom.*, 11 (1989) 23.
2 R. P. Lattimer and H.-R. Schulten, *Anal. Chem.*, 61 (1989) 1201A.
3 J. V. Iribarne, P. J. Dziedzic and B. A. Thomson, *Int. J. Mass Spectrom. Ion Phys.*, 50 (1983) 331.
4 Y. Ito, T. Takeuchi and D. Ishii, *J. Chromatogr.*, 346 (1985) 161.
5 K. D. Cook, *Mass Spectrom. Rev.*, 5 (1986) 467.
6 M. Yamashita and J. B. Fenn, J. Phys. Chem., 88 (1984) 4451.
7 M. L. Aleksandrov, L. N. Gall', N. V. Krasnov, V. I. Nikolaev, V. A. Pavlenko and V. A. Skurov, *Dokl. Akad. Nauk. S.S.S.R.*, 277 (1984) 379.
8 A. P. Bruins, T. R. Covey and J. D. Henion, *Anal. Chem.*, 59 (1987) 2642.
9 J. Zeleny, *Phys. Rev.*, 10 (1917) 1.
10 C. M. Whithouse, R. N. Dreyer, M. Yamashita and J. B. Fenn, *Anal. Chem.*, 57 (1985) 675.
11 F. W. Röllgen, E. Bramer-Weger and L. Bütfering, *J. Phys.*, 11 (1987) C6-253.

12 E. C. Horning, D. I. Carrol, I. Dzidic, K. D. Haegele, M. G. Horning and R. N. Stillwell, *J. Chromatogr.*, 99 (1974) 13.
13 J. D. Henion, B. A. Thomson and P. H. Dawson, *Anal. Chem.*, 54 (1982) 451.
14 D. A. Lane, B. A. Thomson, A. M. Lovett and N. M. Reid, *Adv. Mass Spectrom.*, 8 (1980) 1480.
15 S. F. Wong, C. K. Meng and J. B. Fenn, *J. Phys. Chem.*, 92 (1988) 546.
16 A. P. Bruins, L. O. G. Weidolf, J. D. Henion and W. L. Budde, *Anal. Chem.*, 59 (1987) 2647.
17 P. O. Edlund, L. Bowers and J. D. Henion, *J. Chromatogr.*, 487 (1989) 431.
18 R. D. Eckerlin, J. G. Ebel, J. D. Henion and T. R. Covey, *Anal. Chem.*, 61 (1989) 53A.
19 E. D. Lee, W. Mück, J. D. Henion and T. R. Covey, *J. Am. Chem. Soc.*, 111 (1989) 4600.
20 C. K. Meng, M. Mann and J. B. Fenn, *Z. Phys. D*, 10 (1988) 361.
21 R. D. Smith, C. J. Barinaga and H. R. Udseth, *Anal. Chem.*, 60 (1988) 1948.
22 E. D. Lee, W. Mück, J. D. Henion and T. R. Covey, *J. Chromatogr.*, 458 (1988) 313.
23 E. C. Huang, T. Wachs, J. J. Conboy and J. D. Henion, *Anal. Chem.*, 62 (1990) 713A.
24 A. P. Bruins and C. Beaugrand, *Proceedings of the 36th ASMS Conference on Mass Spectrometry and Allied Topics, June 5–10, 1988, San Francisco CA*, ASMS, East Lansing, MI, p. 1241.
25 A. P. Bruins, *Mass Spectrom. Rev.*, 10 (1991) 57.
26 T.-C. L. Wang, M.-C- Shih, S. P. Markey and M. W. Duncan, *Anal. Chem.*, 61 (1989) 1013.
27 T. R. Baker, P. Vouros and J. A. J. Martyn, *Org. Mass Spectrom.*, 24 (1989) 723.
28 D. Vicchio and A. L. Yergey, *Org. Mass Spectrom.*, 24 (1989) 1060.
29 T. R. Covey, R. F. Bonner, B. I. Shushan and J. D. Henion, *Rapid Commun. Mass Spectrom.*, 2 (1988) 249.
30 A. B. L. Lanting, B. F. H. Drenth, J. Bosman and A. P. Bruins, *Proceedings of the 37th ASMS Conference on Mass Spectrometry and Allied Topics, May 21–26, 1989, Miami Beach, FL*, ASMS, East Lansing, MI, p. 984.

Journal of Chromatography, 554 (1991) 47–59
Elsevier Science Publishers B.V., Amsterdam

CHROMSYMP. 2358

Source of band broadening in liquid chromatographic–fast atom bombardment mass spectrometric systems with precolumn addition of viscous matrix to the mobile phase

JEAN-PIERRE GAGNÉ, ALAIN CARRIER and MICHEL J. BERTRAND*
Regional Center for Mass Spectrometry, Department of Chemistry, University of Montreal, P.O. Box 6128, Stn A, Montreal H3C 3J7 (Canada)

ABSTRACT

The factors affecting band broadening in liquid chromatographic–fast atom bombardment mass spectrometric (LC–FAB-MS) systems using precolumn addition of glycerol to the mobile phase were investigated and their relative importance evaluated. The integrated LC–MS system is subject to three sources of band broadening, namely the chromatographic system, the interface and the mass spectrometer. The individual variances associated with these components can be used to estimate the total variance of the system. The factors affecting broadening in the chromatographic system were identified by examination of the Van Deemter plots obtained for several types of compounds at glycerol concentrations ranging from 0 to 20%. The plots reveal that the C term is significantly affected by an increase in glycerol concentration and that the main factor affecting broadening is a change in the diffusion coefficient, D_m. The increase in the variance associated with the dead volume of the chromatographic system, as measured with a non-retained species, indicates that the increase in the viscosity of the mobile phase on addition of glycerol also results, to a lesser extent, in band broadening as a consequence of the change in flow dynamics within the system. Investigation of the factors affecting band broadening in the interface show that the main source of broadening is the wetting of the probe tip, which is far more important than the dead volume introduced by the transfer capillary. The band broadening induced by the mass spectrometer in the LC–FAB-MS system is essentially related to the scanning speed used for the analysis.

INTRODUCTION

The technique of fast atom bombardment mass spectrometry (FAB-MS) has developed considerably since its introduction by Barber *et al.* [1] in 1981. From the initial applications in which an analyte was dissolved in a viscous matrix (glycerol, thioglycerol, diethanolamine, nitrobenzyl alcohol, etc.) and exposed to bombardment by a beam of fast-moving neutral particles, the technique was modified to allow the introduction of aqueous solutions in a continuous-flow mode (CF-FAB) [2] and then to interface liquid chromatography with mass spectrometry (LC–FAB-MS) [3]. Although aqueous solutions can be introduced in the continuous-flow or dynamic mode by passing the mobile phase through a fused-silica capillary that is located in the hollow shaft of the FAB probe [2,4,5], it is still necessary that a viscous matrix be present in the mobile phase for ionization to occur [2,4]. The addition of the viscous

0021-9673/91/$03.50

matrix can be made before (precolumn) the chromatographic separation [3,6–8] or after the separation by use of postcolumn devices [8–11]. Even if the postcolumn addition of the viscous matrix is favored by some groups, in most instances precolumn mixing with the mobile phase is still utilized and mostly involves the use of glycerol.

Some of the effects of precolumn addition have been mentioned occasionally in the literature [3,8,12,13] but only one study has focused on this subject [8]. The addition of a viscous matrix to the mobile phase can significantly alter the chromatographic separation. If the viscous matrix is introduced into the mobile phase before chromatography occurs, its presence can change the conditions within the column and affect the separation. If mixing of the viscous matrix occurs after the chromatography, dead-volume effects can be introduced into the system, leading to peak broadening, especially if capillary columns are used [8]. In order to identify and quantify the effects on the chromatographic performance of the precolumn addition of a viscous matrix, a systematic study was recently undertaken [14] in which the chromatographic behavior of six compounds in three chemical classes was examined as a function of increasing glycerol content (0–30%) in the mobile phase.

The results obtained [14] demonstrated that the retention times and capacity factors of the analytes decreased for all compounds as the glycerol content in the mobile phase increased. It was also observed that the number of theoretical plates decreased in the system and that the normalized peak widths increased for all compounds when the concentration of glycerol was increased from 5 to 30%. However, at lower glycerol contents in the mobile phase ($< 5\%$) the effects on compounds were different, depending on their k' values. Analytes with smaller capacity factors showed a net decrease in the number of theoretical plates and an increase in the normalized peak widths, whereas for compounds with higher capacity factors such as peptides these two chromatographic indicators were almost invariant. Further, the data obtained in that study showed that an increase in the glycerol content of the mobile phase caused a net decrease in resolution and an increase in the separation impedance of the system. Hence, it was concluded that the overall effect of the precolumn addition of a high concentration of viscous matrix to the mobile phase is detrimental to the performance of the chromatographic system. The factors most likely responsible for this are changes in the distribution of the analyte due to modifications in the chemical composition of the mobile phase and band broadening induced by the increase in the viscosity of the mobile phase.

The objective of this work was, first, to identify the factors responsible for the chromatographic band broadening observed on precolumn addition of a viscous matrix to the mobile phase and to quantify their relative contributions, and second, to evaluate the broadening caused by other components of the LC–FAB-MS system such as the interface. The identification and quantification of the relative importance of the chromatographic and mass spectrometric factors governing the overall separation performance of these systems should facilitate their optimization and design.

EXPERIMENTAL

Instrumentation

The liquid chromatographic system consisted of a Perkin-Elmer Model 410

pump connected to a Rheodyne Model 7125 injector with a 6-μl sample loop. Detection was achieved by a Perkin-Elmer LC-90 variable-wavelength (254 or 280 nm) detector. The chromatographic columns [Spherisorb ODS-2, d_p = 5 μm, 125 mm × 4.6 mm I.D. (CSC, Montreal); Perisorb RP-18, d_p = 40 μm, used as a precolumn] used were maintained at 25°C by a water-jacket regulated by a Haake (Berlin-Steglitz, Germany) circulator. Experiments involving continuous-flow FAB (CF-FAB) were performed on a Kratos MS-50TCTA mass spectrometer equipped with a standard Kratos FAB source and using a laboratory-built continuous-flow probe which has been described previously [4,5]. The scanning conditions of the instrument were dependent on the experiment being conducted. Viscosity measurements on all mobile phases used were performed using a capillary viscosimeter.

Chemicals

The peptides met-enkephalin and bradykinin were obtained from Sigma (St. Louis, MO, USA). Substituted phenolic compounds, such as phloroglucinol and *p*-hydroxybenzoic acid, and organic acids, such as 3,5-dihydroxybenzoic, vanillic and trifluoroacetic acid, were purchased from Aldrich (Milwaukee, WI, USA). Glass-distilled glycerol (>99.0%) was obtained from BDH (Toronto, Canada). All compounds were used without further purification and the mobile phases were prepared using high-performance liquid chromatographic-grade acetonitrile, acetic acid and distilled, deionized water obtained with a Milli-Q purification system (Millipore, Bedford, MA, USA).

Preparation of mobile phases

The eluents were carefully prepared by mixing volumes of distilled, deionized water and appropriate organic modifiers. The mobile phases used for peptide analysis contained fixed proportions of trifluoroacetic acid (TFA) (0.1) and acetonitrile (ACN) (30) and the proportion of water was adjusted to complement the volume of glycerol (GLY) in the solution (ACN–H_2O–GLY–TFA = 30:70 − x:x:0.1). A similar procedure was utilized for the mobile phases involved in the analysis of low-molecular-weight phenolic compounds and organic acids. The ratio of acetic acid (AcOH) to acetonitrile was fixed at 1:10 and water was used to complement the volume of glycerol in the solution (ACN–H_2O–GLY–AcOH = 10:90 − x:x:1). Sufficient amounts of each mixture were prepared to ensure that all experiments would be conducted with the same mobile phases. In all instances, the solvents were filtered (0.45-μm filter) and degassed prior to use.

Chromatographic measurements

All chromatographic experiments were carried out at 25°C after the chromatographic system had equilibrated for at least 90 min. Precise values for the volumetric flow-rate were measured for each experiment. The retention of sodium nitrate was taken as the dead volume and the average linear velocity was calculated using the length of the chromatographic column. The number of theoretical plates (N) was estimated from the widths at half-height of the peaks. The Van Deemter plots were generated by measuring the theoretical plate height (H) with linear velocities over the range 0.02–7 mm/s.

RESULTS AND DISCUSSION

In a multi-component system such as LC–FAB-MS, the introduction of an analyte corresponds to the introduction of a signal which is submitted to several operators as it travels through the system. If the operators in the system induce broadening of the signal and the output signal has a Gaussian distribution, it can be assumed that each component will independently contribute to broadening [15]. Therefore, the total broadening of the signal can be estimated by the total variance, σ_t^2, which is given by the sum of the individual variances, σ_i^2, [15–19] as shown in Fig. 1. Thus, the total variance (σ_t^2) of the LC–FAB-MS system is represented by the equation

$$\sigma_t^2 = \sigma_{chr}^2 + \sigma_{int}^2 + \sigma_{spec}^2 \quad (1)$$

where σ_{chr}^2, σ_{int}^2 and σ_{spec}^2 refer to the variances associated with the chromatographic system, the interface and the mass spectrometer, respectively. Each of the three components of the system can be considered as a dispersion–dilution operator that will contribute to the broadening of the chromatographic band. Based on this assumption, one can attempt to identify the factors in each of the sub-systems that contribute to band broadening and evaluate their relative importance.

The total variance in a chromatographic system, σ_{chr}^2, can be expressed as the sum of the variances σ_c^2 and σ_{ex}^2:

$$\sigma_{chr}^2 = \sigma_c^2 + \sigma_{ex}^2 \quad (2)$$

which represent the broadening occurring in the column and the broadening induced by components external to the column. The external contributions usually affect the broadening of the chromatographic band by the introduction of dead-volume effects. In systems utilizing conventional LC columns (150 mm × 4.6 mm I.D., d_p = 5 μm), the extra-column dispersion of the analyte due to dead volumes in connectors and detectors is usually of the order of 30–60 μl [17,20], which is small compared with the elution volume of the analyte.

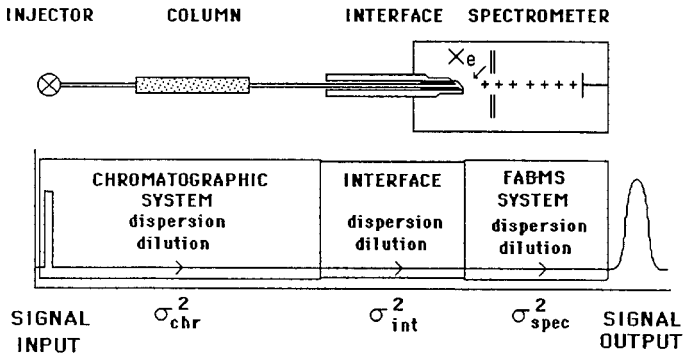

Fig. 1. Dispersion operators and associated variances, σ_{chr}^2, σ_{int}^2 and σ_{spec}^2, in an LC–FAB-MS system using precolumn addition of the viscous matrix.

The broadening that is induced within the chromatographic column is essentially due to the three kinetic effects, which are expressed as terms in the Van Deemter equation [21–24] that relates the height of a theoretical plate (H) to the average linear velocity of the mobile phase ($\bar{u}$). For the chromatographic system under analysis, the equation can be expressed [24] as

$$H = 2\lambda d_p + \frac{2\gamma D_m}{\bar{u}} + \frac{f_1(k')d_p^2\bar{u}}{D_m} + \frac{f_2(k')d_f^2\bar{u}}{D_s} \tag{3}$$

where λ and γ are constants, d_p and d_f represent the particle size and film thickness, D_m and D_s are the diffusion coefficients in the mobile and stationary phases and $f_1(k')$ and $f_2(k')$ are functions of the capacity factor k'. As the film thickness is usually considered to be small [23,25], the last term in eqn. 3 can be neglected, which leads to

$$H = 2\lambda d_p + \frac{2\gamma D_m}{\bar{u}} + \frac{(1 + 6\,k' + 11\,k'^2)d_p^2\bar{u}}{24(1 + k')^2 D_m} \tag{4}$$

where the last term on the right hand side of the equation is referred to as the C term. As the addition of a viscous matrix has been shown [14] to affect k' and D_m, it is interesting to determine the relative contributions of these two factors which appear in the C term of eqn. 4. Because the chromatographic variance σ^2_{chr} is related to H:

$$\sigma^2_{chr} = \frac{H\,t_r^2}{L} \tag{5}$$

where L is the length of the column, it is possible to identify the factors responsible for the decrease in efficiency that occurs in the chromatographic system when the concentration of a viscous matrix such as glycerol is increased.

A series of experiments were performed in order to evaluate the contribution of the kinetic factors to the band broadening which is observed when a viscous matrix is added to the mobile phase. In these experiments, Van Deemter plots were obtained for six compounds in three separate chemical classes as the concentration of glycerol in the mobile phase was increased from 0 to 30%. Fig. 2 shows typical plots obtained for the peptide met-enkephalin. The data in Fig. 2 indicate that as the concentration of glycerol is increased the C term in the Van Deemter equation steadily increases, as shown by the increase in the slopes with the glycerol content. A similar effect was observed for the peptide bradykinin. The same type of experiments were also conducted with several other analytes of lower molecular weight such as vanillic acid, 3,5-dihydroxybenzoic acid, p-hydroxybenzoic acid and phloroglucinol. Typical results obtained in those experiments are given in Fig. 3, where the Van Deemter plots at increasing glycerol concentration are shown for vanillic acid. As can be seen, there appears to be no significant differences in the C term for glycerol values below 3% but, as the values increase above 5%, the C term increases steadily as witnessed by an increase in the slopes of the plots. This trend is also observed with the other low-

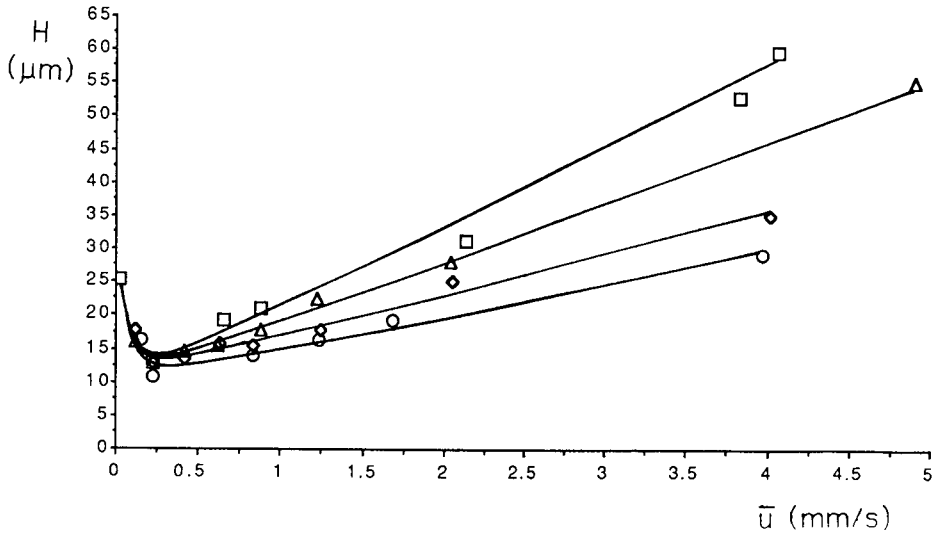

Fig. 2. Van Deemter plots obtained for met-enkephalin with increasing glycerol concentration (x)in the mobile phase: ○ = 0%; ◇ = 5%; △ = 10%; □ = 20%. Mobile phase: ACN–H_2O–GLY–TFA (30:70 − x:x:0.1).

molecular-weight compounds studied. Hence, the Van Deemter plots obtained indicate that there is a net decrease in system efficiency with an increase in the viscous matrix content in the mobile phase. As the C term of eqn. 4, which is affected by the change in glycerol concentration, depends on k' and D_m, it is possible to evaluate the relative importance of both of these factors.

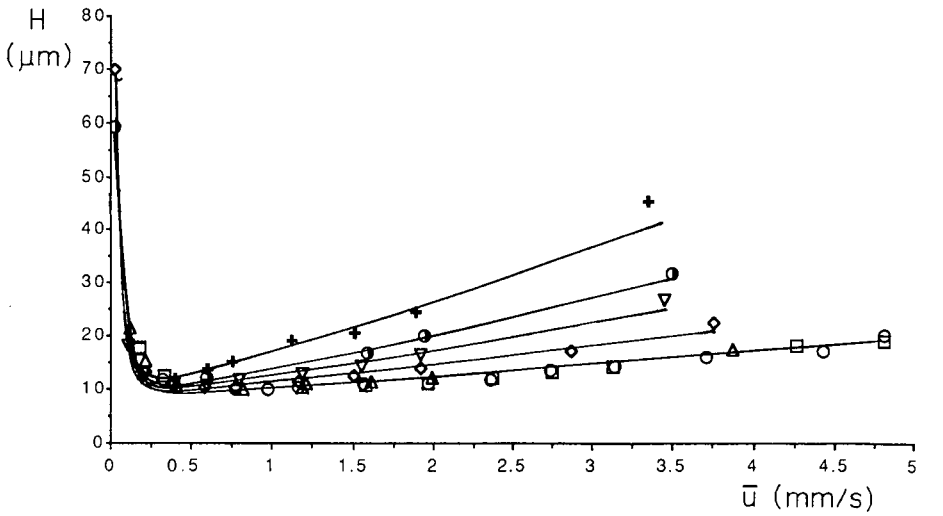

Fig. 3. Van Deemter plots obtained for vanillic acid with increasing glycerol concentration (x) in the mobile phase: ○ = 0%; □ = 1%; △ = 3%; ◇ = 5%; ▽ = 10%; ◑ = 20%; + = 30%. Mobile phase: ACN–H_2O–GLY–AcOH (10:90 − x:x:1).

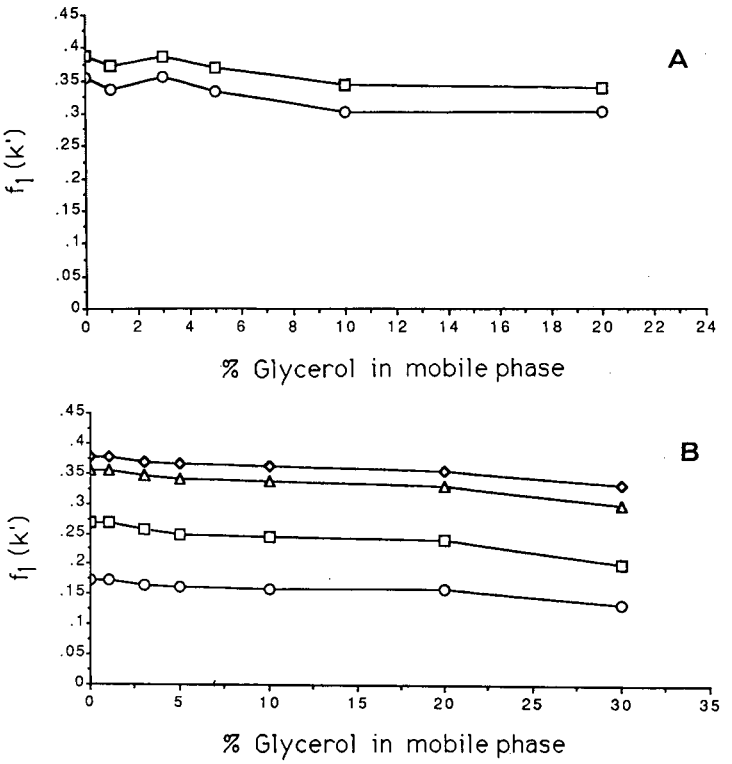

Fig. 4. Variation of $f_1(k')$ with glycerol content in the mobile phase. (A) □ = Bradykinin; ○ = met-enkephalin; (B) □ = *p*-hydroxybenzoic acid; △ = 3,5-dihydrobenzoic acid; ◇ = vanillic acid; ○ = phloroglucinol.

Results obtained in a previous study [14] concerning the effect on chromatographic behavior of the addition of a viscous matrix to the mobile phase have demonstrated that the capacity factors decrease when the content of glycerol is increased. This behavior is shown in Fig. 4A for the peptides met-enkephalin and bradykinin and in Fig. 4B for vanillic acid, 3,5-dihydrobenzoic acid, *p*-hydroxybenzoic acid and phloroglucinol, where the $f_1(k')$ functions, appearing in eqn. 4, are plotted against glycerol content in the mobile phase. The data can be rationalized by the fact that as the glycerol content increases the distribution of the analytes is changed. Glycerol is acting as an efficient organic modifier, the effect of which is to reduce the capacity factors. The isolated effect of the variation of the capacity factors should be to decrease the slopes of the Van Deemter plots, as the reduction in capacity factors induces a reduction in the $f(k')$ function as shown in Fig. 4.

The observed effect of glycerol content on the chromatographic system is not, however, what is predicted from the changes in the capacity factors. As the slopes of the Van Deemter plots increase with increasing concentrations of glycerol (Figs. 2 and 3), it appears that variations in the other factor involved, the diffusion coefficient (D_m), are significant. The data available for *p*-hydroxybenzoic acid allow an estimation of the variation in the diffusion coefficient using the Wilke–Chang equation [26],

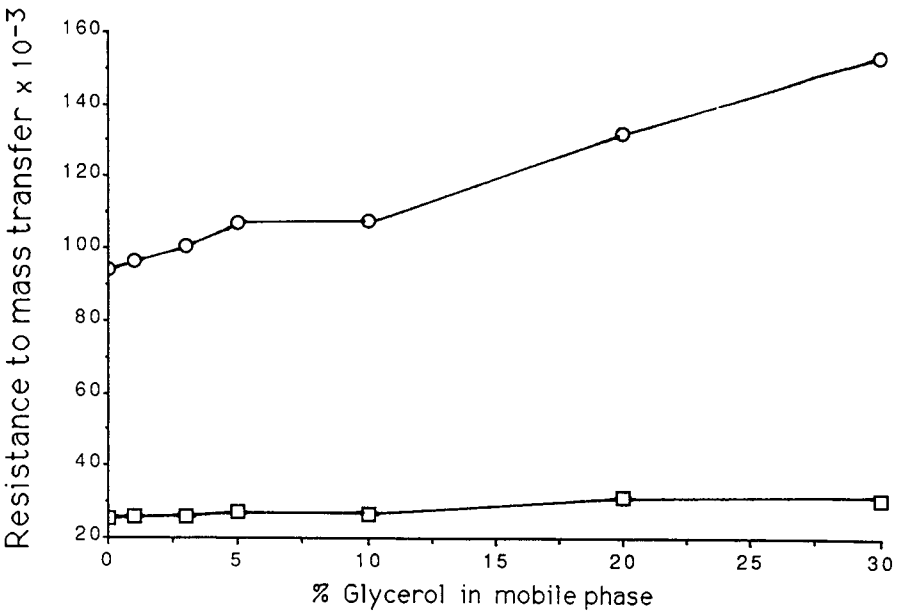

Fig. 5. Variation of the estimated diffusion coefficient, (○) $1/D_m$ and (□) $f_1(k')/D_m$, for *p*-hydroxybenzoic acid with glycerol concentration in the mobile phase. Units for *y*-axis are s.

and assuming that glycerol has an association constant comparable to that of methanol. Fig. 5 shows the variation that is expected in $1/D_m$ along with that of the C term in the Van Deemter plots. As observed, the variation of the C term is smaller than that of D_m owing to the opposite effects of $f(k')$ and D_m on the slope. However, the data obtained experimentally and by estimation of D_m clearly indicate that the variations observed experimentally are mainly due to variations in D_m which are caused by an increase in the viscosity of the mobile phase as the glycerol content increases. The variation of the viscosity of the mobile phase with the increase in the glycerol concentration was measured and the results are given in Table I. The data indicate

TABLE I

VARIATION OF THE VISCOSITY OF THE MOBILE PHASE WITH GLYCEROL CONTENT

Viscosity in cP.

Glycerol (%) (x)	ACN–H_2O–GLY–TFA (30:70 − x:x:0.1)	ACN–H_2O–GLY–AcOH (10:90 − x:x:1)
0	0.95	0.93
1	0.96	0.96
3	1.01	1.03
5	1.05	1.12
10	1.26	1.29
20	1.46	1.56
30	–	1.92

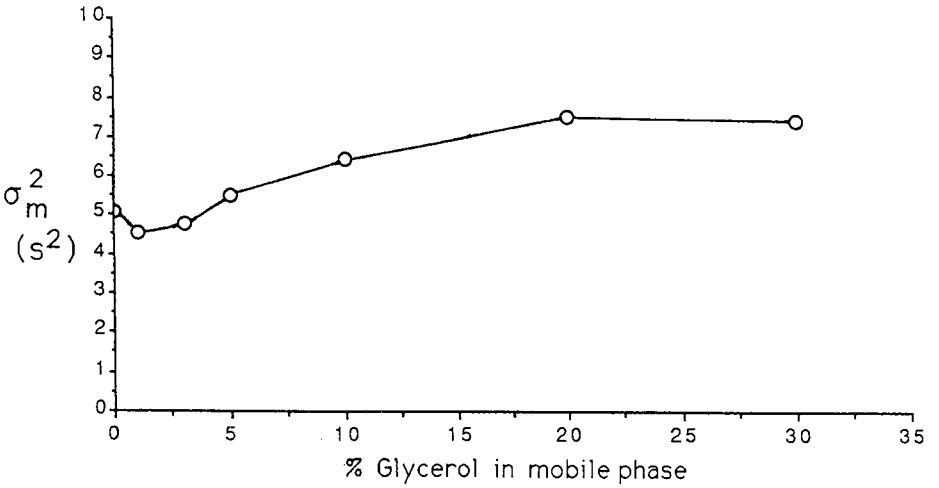

Fig. 6. Variation of the chromatographic variance, σ_m^2, associated with t_m (retention time of $NaNO_3$), with the concentration of glycerol in the mobile phase.

that the viscosity increases with the addition of glycerol and, therefore, D_m is reduced. For example, D_m as estimated for *p*-hydroxybenzoic acid decreases by 40% when the glycerol content increases from 0 to 30%. Therefore, the factor that is mainly responsible for the decrease in chromatographic efficiency of the system is the change in D_m which results from the increase in viscosity of the mobile phase. This increase in viscosity also produces an increase in the operating pressure of the system, therefore causing the separation impedance to be higher [14].

The findings that the addition of a viscous matrix such as glycerol affects the diffusion in the chromatographic system are also reflected in the variance σ_m^2 associated with a non-retained analyte. The variation of σ_m^2, which is associated with the increase in the viscous matrix content of the mobile phase, is shown in Fig. 6, which indicates that σ_m^2 is almost constant for glycerol contents below 3%, where changes in viscosity are small, and then increases with increasing concentration of glycerol. This demonstrates that convective diffusion processes become more important in the system and are responsible for a partial loss of chromatographic efficiency. The increase in the viscosity of the mobile phase modifies the flow dynamics in the system in accordance with eqn. 6.

$$\sigma_{tu}^2 = \frac{\pi r^4 LF}{24\, D_m} \tag{6}$$

The equation shows that the variance σ_{tu}^2 of the system varies inversely with D_m and this is reflected by the increase in σ_m^2 for a non-retained compound such as sodium nitrate. Hence, it would appear that the most important factor that influences the chromatographic broadening (σ_{chr}^2) in LC–FAB-MS systems using precolumn addition of glycerol are the changes in viscosity as shown by the increase in σ_m^2 and in the kinetics of mass transfer, as shown by the Van Deemter plots, that are induced by the increase in the viscosity of the mobile phase with glycerol content. The most

important contribution to broadening comes from the changes that occur in the mass transfer kinetics (σ_c^2) while broadening due to changes in flow dynamics (σ_{ex}^2) occurs but to a lesser extent.

In LC–FAB-MS systems, other components such as the interface and the mass spectrometer are also likely to act as dispersion operators. The interface that is used to couple the chromatographic system to the mass spectrometer consists essentially of a fused-silica capillary that is introduced in the hollow shaft of the CF-FAB probe between the column and the ion source. The capillary allows the transfer of the analytes to the heated surface of the FAB probe where fast atom bombardment occurs [2,4,5]. The dispersion operators in the interface will be the transfer capillary (fused silica, 1000 mm × 0.075 mm I.D.) and the liquid droplet which forms at the end of the probe tip (wetting). The total variance, σ_{int}^2, associated with the interface will be the sum of the variance of the transfer tube, σ_{tu}^2, and the variance σ_d^2 associated with the droplet formed on the probe tip, σ_d^2, as expressed by

$$\sigma_{int}^2 = \sigma_{tu}^2 + \sigma_d^2 \tag{7}$$

The contribution of the transfer capillary can be estimated using the Taylor–Golay relationship [16,22,27] when the linear velocity is sufficiently high. It can be seen from eqn. 6 that the variance σ_{tu}^2 is a function of the radius of the transfer tube (r), its length (L), the flow-rate (F) and the diffusion coefficient (D_m). In LC–FAB-MS systems, the volumetric dispersion caused by the transfer capillary is given in Table II, where σ_{tu} is shown as a function of capillary length, diameter and glycerol content for *p*-hydroxybenzoic acid. It is observed from Table II that a typical capillary of 75 μm, in the absence of glycerol, has a volumetric dispersion of 0.11 μl, and that this value can be reduced to 0.01 μl if the diameter of the tube is reduced to 25 μm. At 30% glycerol, the dispersion is only slightly increased to 0.14 and 0.02 for the same radii. Hence, the dispersion produced by the transfer capillary appears to be relatively small and its contribution should not significantly affect the total variance of the system unless the diameter of the transfer line is greater than 100 μm.

The other volumetric dispersion which occurs at the end of the probe and is referred to as a "memory effect" [8,20] is relatively difficult to evaluate as there are many phenomena occurring in the droplet that forms at the end of the probe tip (evaporation, diffusion, sputtering, mixing, etc.). One approach to estimate the dis-

TABLE II

DISPERSION CAUSED BY A CAPILLARY TRANSFER TUBE

Length × diameter (mm × μm)	Volume (μl)	σ_{tu} (0% glycerol) (μl)	σ_{tu} (30% glycerol) (μl)
1000 × 75	4.42	0.11	0.14
2250 × 50	4.42	0.08	0.09
1000 × 50	1.96	0.05	0.06
1000 × 25	0.49	0.01	0.02

TABLE III

EVALUATION OF VOLUMETRIC DISPERSIONS AT THE PROBE TIP

Dimensions		Volume (μl)	Dispersion (laminar)[a] (μl)	Dispersion (laminar)[b] (μl)	Dispersion (mixing) (μl)
Diameter (mm)	Thickness (mm)				
2	0.20	0.63	1.22	1.47	0.63
2	0.15	0.47	1.06	1.27	0.47
2	0.10	0.31	0.86	1.04	0.31
1	0.20	0.16	0.28	0.36	0.16
1	0.15	0.12	0.24	0.31	0.12
1	0.10	0.08	0.20	0.25	0.08

[a] Calculated at 0% glycerol.
[b] Calculated at 30% glycerol.

persion of the system is to concentrate on the droplet itself and consider it the major source of broadening. From this assumption, the droplet can be considered as a "connecting tube" and the variance associated with it can be obtained from the Taylor–Golay relationship [16,22,27]. Alternatively, the droplet can be considered as a mixing chamber, in which case the variance associated with it can be obtained from the equation [15,16,28,29]

$$\sigma_d^2 = \frac{V_d^2}{F^2} \tag{8}$$

If it is assumed that the composition of the liquid phase is constant within the droplet, the variance can be estimated. The values for the variance σ_d^2 that can be obtained using each of the models described are given in Table III.

The data in Table III show that the dispersions evaluated using the two approaches are within a factor of two of one another and that the laminar contribution is superior to the mixing effect. Further, it can be observed that the effect of the addition of glycerol increases the value of the laminar contribution. These two contributions allow the estimation of the magnitude of the dispersion caused by this operator. Hence, the dispersion created by the droplet at the tip of the FAB probe is between 0.63 and 1.47 μl when the concentration of glycerol is *ca.* 30%. These values appear as minimum values as other broadening phenomena are occurring at the tip. The differential vaporization of the components creates an enrichment of the less volatile components at the tip which produces an increase in the viscosity of the droplet [30]. This increase in viscosity reduces the diffusivity of the analyte, which results in a higher variance in the system, in agreement with eqn. 6. Therefore, a dispersion of the order of 1.47 μl appears probable under those circumstances.

The data in Tables II and III indicate that the contribution of the interface to the total broadening of the chromatographic band is mainly due to the formation of the liquid droplet at the end of the probe. This contribution is of the order of 1.5 μl for experimental conditions usually encountered in CF-FAB. Our experience with such

systems consisting of a 0.5-μl injector, a transfer capillary of 1000 mm × 75 mm I.D. and a tip 2 mm in diameter show that the elution volume under those experimental conditions is between 2 and 3 μl [4,5], depending on the amount of analyte injected on the content of glycerol and on the scanning speed of the mass spectrometer. These values are essentially the same as those reported by Caprioli *et al.* [2] using a similar system. The differences between the experimental and estimated values can be attributed to errors originating from the estimation of the thickness of the droplet or the diffusivity of the analyte. Alternatively, a small contribution of the mass spectrometer originating from the slow scanning speed used in these experiments can be considered. Thus, the measured dispersion implies that the interface can contribute significantly to the broadening of the chromatographic band, especially for narrow bands such as those found with capillary columns. These effects will be less important for conventional columns as the elution volume after splitting of the eluent can easily be of the order of 7–10 μl, which is much greater than extra-column contributions. With conventional columns, the broadening produced by the interface is comparable to that created by the decrease in efficiency observed with 30% of glycerol present in the mobile phase.

Finally, the signal can also be broadened by the mass spectrometer, σ^2_{spec}, which serves as the detector in the LC–FAB-MS system. The broadening that will be induced by the mass spectrometer is essentially related to the scanning speed of the instrument, which must be sufficiently rapid to reduce broadening of the signal. For compounds that elute in narrow bands, the cycle time should be of the order of 0.5–1 s [31,32] to maintain chromatographic integrity. This is well below the scan speeds usually used in LC–FAB-MS systems, which are of the order of 3–5 s and above.

CONCLUSIONS

The results presented clearly indicate that the precolumn addition of significant amounts of glycerol in LC–FAB-MS systems induces changes in the viscosity of the mobile phase and affects the distribution of the analytes between phases. Examination of the Van Deemter plots obtained for several analytes with different chemical structures shows that the C term in these plots increases with increasing glycerol content in the mobile phase. This increase is due to changes in the diffusivity of the analytes induced by an increase in the viscosity of the mobile phase. The reduction of the capacity factors with increasing glycerol content affects the system but to a much lesser extent. Hence, the source of chromatographic broadening in these systems can be attributed mainly to changes in diffusive processes and has been shown to increase the peak width by 30%. Other contributions, such as extra-column broadening, produce minor effects and can be neglected if dead volumes in the system are reduced.

The variances associated with other dispersion operators, such as the interface and the mass spectrometer, present in the LC–FAB-MS system have also been evaluated. The measured volumetric dispersion of 2.5 μl caused by the interface can be attributed mainly to effects occurring at the tip of the FAB probe, as the variance associated with the dead volume of the transfer capillary is found to be small. The dispersion at the tip of the probe will vary with glycerol content in the mobile phase, the thickness of the droplet on the tip, the temperature of the tip and the flow-rate in the system. The dispersion caused by the mass spectrometer is essentially related to

the scanning speed, which has to be sufficiently rapid to avoid broadening of the signal.

ACKNOWLEDGEMENTS

The authors acknowledge the financial contributions of the National Science and Engineering Research Council of Canada (NSERC) and Hydro-Québec that permitted this study. They are also grateful to Dr. G. Paul for editorial assistance.

REFERENCES

1 M. Barber, R. Bordolini, R. D. Sedgwick and A. N. J. Tyler, *J. Chem. Soc., Chem. Commun.*, (1981) 325.
2 R. M. Caprioli, T. Fan and J. S. Cottrell, *Anal. Chem.*, 58 (1986) 2949.
3 Y. Ito, T. Takeuchi, D. Ishii and M. Goto, *J. Chromatogr.*, 346 (1985) 161.
4 M. J. Bertrand, V. Benham, R. St-Louis and M. J. Evans, *Can. J. Chem.*, 67 (1989) 910.
5 M. J. Bertrand and V. Benham, in T. Theophanides (Editor), *Spectroscopy of inorganic Bioactivators, Theory and Applications*, Nato ASI Series, Kluwer, Dordrecht, 1989, pp. 349–377.
6 T. Takeuchi, S. Watanabe, N. Kondo, D. Ishii and M. Goto, *J. Chromatogr.*, 435 (1988) 482.
7 A. E. Ashcroft, *Org. Mass Spectrom.*, 22 (1987) 304.
8 S. Pleasance, P. Thibault, M. A. Moseley, L. J. Deterding, K. B. Tomer and J. W. Jorgenson, *J. Am. Soc. Mass Spectrom.*, 1 (1990) 312.
9 D. E. Games, S. Pleasance, E. D. Ramsey and M. A. Mc Dowall, *Biomed. Environ. Mass Spectrom.*, 15 (1988) 179.
10 M. A. Moseley, L. J. Deterding, J. S. M. de Wit, K. B. Tomer, R. T. Kennedy, N. Bragg and J. W. Jorgenson, *Anal. Chem.*, 61 (1989) 1577.
11 D. J. Bell, M. D. Brightwell, W. A. Neville and A. West, *Rapid Commun. Mass Spectrom.*, 4 (1990) 88.
12 M. A. Moseley, L. J. Deterding, J. S. M. de Wit and K. B. Tomer, R. T. Kennedy, N. Bragg and J. W. Jorgenson, *Anal. Chem.*, 61 (1989) 1577.
13 J. S. M. de Wit, L. J. Deterding, M. A. Moseley, K. B. Tomer and J. W. Jorgenson, *Rapid Commun. Mass Spectrom.*, 2 (1988) 100.
14 J.-P. Gagne, A. Carrier and M. J. Bertrand, *J. Chromatogr.*, 554 (1991) 61.
15 J. C. Sternberg, *Adv. Chromatogr.*, 2 (1966) 205.
16 M. Martin, C. Eon and G. Guiochon, *J. Chromatogr.*, 108 (1975) 229.
17 J. L. DiCesare, M. W. Dong and L. S. Ettre, *Introduction to High-Speed Liquid Chromatography*, Perkin-Elmer, Norwalk, CT, 1981.
18 J. J. Kirkland, W. W. Yau, H. J. Stoklosa and C. H. Dilks Jr., *J. Chromatogr. Sci.*, 15 (1977) 303.
19 H. H. Lauer and G. P. Rozing, *Chromatographia*, 14 (1981) 641.
20 D. Ishii, K. Asai, K. Hibi, T. Jonokuchi and M. Nagaya, *J. Chromatogr.*, 144 (1977) 157.
21 J. J. van Deemter, F. J. Zuiderweg and A. Klinkenberg, *Chem. Eng. Sci.*, 5 (1956) 271.
22 M. J. E. Golay, in D. H. Desty (Editor), *Gas Chromatography*, Butterworths, London, 1958, p. 36.
23 J. A. Jonsson, in J. A. Jonsson (Editor), *Chromatographic Theory and Basic Principles*, Marcel Dekker, New York, 1987, p. 27.
24 E. D. Katz, K. L. Ogan and R. P. W. Scott, *J. Chromatogr.*, 270 (1983) 51.
25 C. Gluckman, A. Hirose, V. L. McGffin and M. Novotny, *Chromatographia*, 17 (1983) 303.
26 C. R. Wilke and P. Chang, *AIChE J.*, 1 (1955) 264.
27 G. Taylor, *Proc. R. Soc. London, Ser. A*, 255 (1956) 67.
28 G. Guiochon and H. Colin, in P. Kucera (Editor), *Microcolumn High-Performance Liquid Chromatography*, Elsevier, Amsterdam, 1984, p. 1.
29 K.-P. Hupe, R. J. Jonker and G. Rozing, *J. Chromatogr.*, 285 (1984) 253.
30 M. J. Connoly and R. G. Orth, *Anal. Chem.*, 59 (1987) 903.
31 G. Guiochon and P. J. Arpino, *J. Chromatogr.*, 271 (1983) 13.
32 B. L. Karger and P. Vouros, *J. Chromatogr.*, 323 (1985) 13.

Journal of Chromatography, 554 (1991) 61–71
Elsevier Science Publishers B.V., Amsterdam

CHROMSYMP. 2344

Effect of the addition of viscous matrices to the mobile phase on chromatographic performance in liquid chromatography–fast atom bombardment mass spectrometry

JEAN-PIERRE GAGNÉ, ALAIN CARRIER and MICHEL J. BERTRAND*
Regional Center for Mass Spectrometry, Department of Chemistry, University of Montreal, P.O. Box 6128, Stn A, Montreal H3C 3J7 (Canada)

ABSTRACT

The effect of the pre-column addition of a viscous matrix to the mobile phase in liquid chromatographic–fast atom bombardment mass spectrometric experiments was studied with respect to the chromatographic process. A series of experiments, designed to discriminate against the mass spectral components, were conducted with six compounds, ranging in mass from 100 to 1100 daltons and distributed into three chemical classes. Several chromatographic indicators such as retention times, capacity ratios, number of theoretical plates, peak widths, resolution and separation impedance were monitored as a function of the glycerol content of the mobile phase. The results obtained indicate that the retention times and the capacity ratios decrease with increasing glycerol content of the mobile phase. Increasing concentrations of glycerol also reduce the number of theoretical plates in the chromatographic system and generally have a detrimental effect on peak widths for glycerol contents above 5%. However, lower glycerol contents produce negative effects on compounds with smaller capacity ratios but not on compounds with higher capacity ratios such as peptides. Furthermore, the increase in glycerol concentrations reduces the chromatographic resolution for all classes of compounds studied and creates a significant increase in the separation impedance of the system, resulting in higher operation pressures. The overall effect of a viscous matrix in the chromatographic system can be rationalized in terms of the modification of the analyte distribution between phases and changes in the kinetics of the system created by an increase in mobile phase viscosity.

INTRODUCTION

Since its introduction in 1981 [1], fast atom bombardment mass spectrometry (FABMS) has been confirmed as a powerful technique to provide mass spectral data on polar, thermally labile and non-volatile compounds. The major innovation in FAB resides in the solvation or dispersion of the analyte in a liquid matrix rather than in the use of a fast neutral beam to produce the ions, since the latter originates from secondary-ion mass spectrometry (SIMS), which has a long analytical tradition [2,3]. The use of a liquid matrix provides a mean by which the molecules on the surface can be replenished by molecular diffusion in the liquid, thus allowing for the presence of fresh material at the surface and partial elimination of secondary products issued from the radiation damage of the solution. Although exceptions have been reported [4–7], polar compounds will usually give rise, in the positive-ion mode, to intense

0021-9673/91/$03.50

parent molecular ions of the type $[M + H]^+$ under fast atom bombardment.

In recent years, the technique of FAB has evolved, and it is presently used in three types of analysis: static or conventional FAB [1,2], continuous-flow (CF)–FAB or dynamic FAB [8] and liquid chromatography (LC)–FAB-MS [9,10]. In static FAB, the analyte is first dissolved in glycerol or some other suitable viscous matrix and a few microliters are placed on the probe tip, which is made of brass or another material. In CF- or dynamic FAB, the analyte is continuously introduced into the ion source as an aqueous solution, typically containing glycerol. The solution flows to the probe tip through a fused-silica capillary which is introduced into the hollow shaft of the probe. The capillary is connected to the probe tip at one end, while the other end is connected to a solution reservoir or a pumping system. The solution reservoir or pumping system delivers the mobile phase through a loop injector into which the analytes can be introduced [8,11]. The flow-rates used in CF-FAB are typically below 10 μl/min, which is the maximum pumping capacity of most mass spectrometers [12], and the glycerol content in the mobile phase can vary from a few percent to as high as 25%. FAB-MS can also be used in conjunction with LC for the analysis of complex mixtures. Several investigators have reported work involving different LC–FAB-MS systems [9,10,13–21]. One approach involves the use of a moving belt, onto which fractions of the high-performance liquid chromatographic (HPLC) are deposited [13,14]. The belt is continuously cycled into the ion source of the mass spectrometer, where the sample spots are exposed to the fast atom beam. A second approach uses a capillary inlet device to connect a microbore HPLC column to a FAB source [9,15,16]. The interface comprises a porous stainless-steel filter onto which vaporization of the solvent and ionization of the analytes occur. Finally, LC–FAB-MS systems in which the CF-FAB probe is directly connected to the LC system have been reported [17–19]. In these systems, conventional [17,18] and microbore [19] columns have been used with split-flow devices. More recently, work with capillary LC columns coupled to FAB-MS has shown promising results [20-22].

The optimization of experimental conditions in LC–MS systems is usually dependent on two types of factors, *i.e.* those affecting the chromatographic separation and those affecting the mass spectral analysis. In LC–FAB-MS, it is necessary that a viscous matrix be used for ionization to occur. The addition of a viscous matrix to the mobile phase can significantly alter the chromatographic conditions depending on whether the addition occurs before (pre-column) or after (post-column) the chromatographic separation. The concentration of viscous matrix in the mobile phase that has been used for LC–FAB-MS experiments varies from 1 to 25%. The addition can be made before the separation [9,16,18,19] or after the separation using several post-column devices [17,21–23]. The pre-column addition of the viscous matrix can create substantial changes in the polarity and viscosity of the mobile phase, modifying the chromatographic conditions. Furthermore, it has been reported that the addition of a viscous matrix requires higher operating pressures in the chromatographic system. In order to eliminate these undesirable effects, it has been suggested that, using conventional LC columns [17,23], post-column addition of the FAB matrix can be a viable solution. With microbore and capillary columns, post-column addition of the matrix introduces peak broadening due to the presence of additional dead volumes. Coaxial addition of the matrix has been tried in order to limit the peak-broadening phenomenon in capillary systems [22–24]. However, preliminary results indicate that peak

broadening is still present as a result of dead volumes and special effects on the probe tip [21].

Some of the effects caused by the addition of glycerol to the mobile phase in LC–FAB-MS have been reported in several studies [9,17,21,22,24]. However, the effect of the addition of a viscous matrix on chromatographic performance has been the immediate object of only one study [21] in which results obtained by pre-column addition were compared with those obtained by coaxial post-column addition. In order to evaluate the overall influence of pre-column addition on chromatographic performance and other chromatographic indicators, a systematic study was undertaken in which the concentration of the matrix was varied from 0 to 30% and important chromatographic parameters were monitored for compounds of different chemical classes and molecular weights ranging from 100 to 1100 daltons. The conditions of the study were such that they allowed for discrimination against combined effects of the chromatographic system and the interface used in FAB-MS. Problems related to the integrated LC–FAB-MS system have been studied elsewhere [25].

EXPERIMENTAL

Instrumentation

The LC system used in this study consisted of a Perkin-Elmer Model 410 pump connected to a Rheodyne 7125 injector with a 6-μl sample loop. Detection was effected by a variable-wavelength (254 or 280 nm) Perkin-Elmer LC-90 detector. The chromatographic columns [Spherisorb ODS-2 particle diameter, (d_p) = 5 μm, 125 mm × 4.6 mm I.D. (CSC, Montreal, Canada); Perisorb RP-18, d_p = 40 μm, used as precolumn] used in this study were maintained at 25°C by a water jacket regulated by a Haake circulator (Haake, Berlin-Steglitz, Germany). Viscosity measurements of the mobile phases were performed with a capillary viscosimeter.

Chemicals

The peptides met-enkephalin and bradykinin used in this study were obtained from Sigma (St. Louis, MO, USA). Substituted phenolic compounds, such as phloroglucinol and *p*-hydroxybenzoic acid, and 3,5-dihydroxybenzoic acid, vanillic acid and trifluoroacetic acid (TFA) were purchased from Aldrich (Milwaukee, WI, USA). Glass-distilled glycerol (>99.0%) was obtained from BDH (Toronto, Canada). All compounds were used without further purification, and the mobile phases were prepared using HPLC-grade acetonitrile, acetic acid and distilled, deionized water (Milli-Q system, Millipore, Bedford, MA, USA).

Mobile phases

The chromatographic eluents used in this study were carefully prepared by mixing the appropriate volumes of distilled, deionized water and appropriate organic modifiers. The mobile phase used for the experiments with peptides contained fixed proportions of TFA (0.1%) and acetonitrile (ACN) (39%), and the proportion of water was adjusted to complement the volume of glycerol (GLY) in the solution (ACN–H_2O–GLY–TFA, 30:70 − *x*:*x*:0.1). A similar procedure was utilized for the mobile phases used in the analysis of low-molecular-weight phenolic compounds and organic acids. The ratio of acetic acid (AcOH) to acetonitrile was fixed at 1:10, and

water was used to complement the volume of glycerol in the solution ($ACN–H_2O–GLY–AcOH$, 10:90 − x:x:1). Sufficient quantities of each mixture were prepared to ensure that all experiments would be conducted with the same mobile phases. In all instances, the solvents were filtered (0.45 μm) and degassed prior to use.

Chromatographic measurements

All chromatographic experiments were carried out at a nominal flow-rate of 0.8 ml/min. Precise values for the volumetric flow were measured for each injection. Whenever the composition of the mobile phase was changed, the chromatographic system was purged and allowed to equilibrate for at least 90 min prior to subsequent sample injection. The retention of sodium nitrate was taken as dead volume, and the capacity ratios (k') were calculated from the retention of the solutes. The number of theoretical plates per meter (N/m) was estimated from the widths at half-height of the peaks, and the impedance of separation was estimated from the relationship of Bristow and Knox [26].

RESULTS AND DISCUSSION

The effect of the addition of a viscous matrix to the mobile phase can be examined by monitoring the changes that occur in the major chromatographic indicators as the matrix concentration is increased in the mobile phase. The quantification of the changes in chromatographic parameters such as retention time, void volume, peak width, capacity ratio, number of theoretical plates, resolution and separation impedance that occur upon addition of the viscous matrix should allow an assessment of its global effect on the chromatographic system. The trends observed in these parameters with increasing content of the matrix may enable one to characterize the modifications that occur, and to identify those which are most important. In order to analyze the effects of the added matrix on the chromatographic system, it was decided initially to study glycerol, the most commonly used matrix in FAB, because correlations could be made with other data that are available in the literature. Furthermore, it was decided to use compounds of different structures and molecular weights so that a general overview of the effects could be obtained without bias. The six compounds chosen for the study were bradykinin, met-enkephalin, *p*-hydroxybenzoic acid, 3,5-dihydroxybenzoid acid, vanillic acid and phloroglucinol. The chromatographic behavior of these compounds with respect to the variation of the concentration of glycerol was studied over the concentration range 0–30%, which is the range of values reported in the literature.

The first parameter studied was the retention time, and its variation for the six compounds with increase in the glycerol content is shown in Fig. 1. It can be seen from Fig. 1 that in all cases the retention times decrease steadily and significantly with increased glycerol content. The retention of the peptides bradykinin and met-enkephalin, shown in Fig. 1A, is decreased by 50% as the glycerol content is increased from 0 to 20%. The variation observed for the acidic compounds (Fig. 1B) is of the order of 40%, while that of the less retained phenolic compounds is somewhat less. It is interesting and noteworthy that these results are in disagreement with those reported by Pleasance *et al.* [21], which indicate a decrease in retention for glycerol concentrations below 2% and an increase in retention for higher values. The fact that a

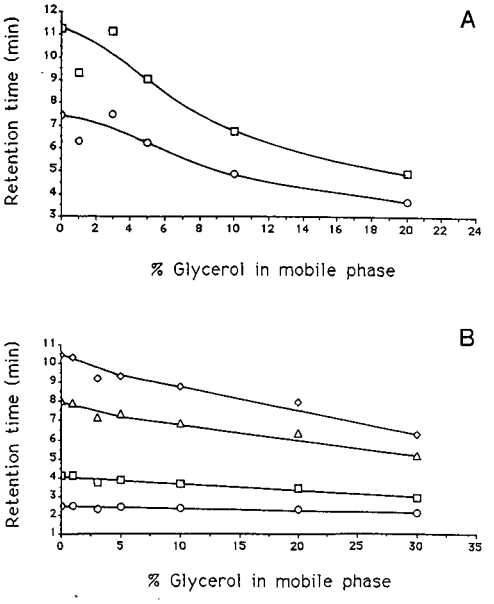

Fig. 1. Variation of the retention time with the glycerol content of the mobile phase. (A) □ = bradykinin; ○ = met-enkephalin in ACN–H_2O–GLY–AcOH (30:70-*x*:*x*:0.1). (B) ○ = phloroglucinol; □ = *p*-hydroxybenzoic acid; △ = 3,5-dihydroxybenzoic acid; ◇ = vanillic acid in ACN–H_2O–GLY–AcOH (10:90-*x*:*x*:1).

decrease in retention is observed for all the compounds in this study and that the decrease is related to the structure of the compounds [peptides (50%), acids (40%), phenols (20%)] strongly indicates that the presence of glycerol in the mobile phase affects the kinetics of the chromatographic process.

The changes in retention of the analytes can better be qualified by the variation of the capacity ratio (k') with the content of glycerol in the mobile phase. The variations in k' for the six compounds studied are shown in Fig. 2. In all cases it is observed that the capacity ratio (k') decreases with the increase in glycerol content of the mobile phase, contrary to the data published by Pleasance *et al.* [21], which indicate an increase in k' for glycerol values above 2%. The significant reduction observed in k' suggests that glycerol is acting as an efficient organic modifier in the mobile phase. As observed from Fig. 2A and B, compounds such as peptides which have important k' values are more affected by slight variations in the glycerol content, indicating changes in the eluotropic force of the mobile phase. The fluctuations observed occur mostly between values of 0 and 5%. Thus, the increase in the glycerol content of the mobile phase produces an effect similar to that which would be observed using an elution gradient.

The effect of the increase in glycerol on the number of theoretical plates per meter (N/m) and peak width can also provide information on the action of the viscous matrix on the chromatographic process. The results presented in Fig. 3 indicate that the chromatographic performance as measured by the number of theoretical plates decreases as the amount of glycerol in the mobile phase is increased. The data from

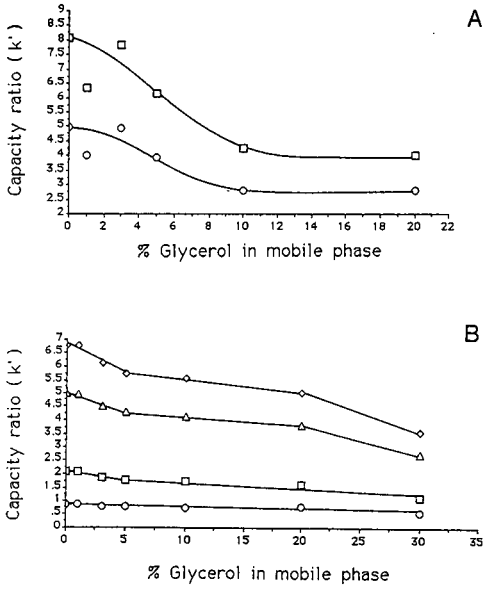

Fig. 2. Variation of the capacity ratio with the glycerol content of the mobile phase. (A) □ = bradykinin; ○ = met-enkephalin in ACN–H_2O–GLY–AcOH (30:70-*x*:*x*:0.1). (B) ○ = Phloroglucinol; □ = *p*-hydroxybenzoic acid; △ = 3,5-dihydroxybenzoic acid; ◇ = vanillic acid in ACN–H_2O–GLY–AcOH (10:90-*x*:*x*:1).

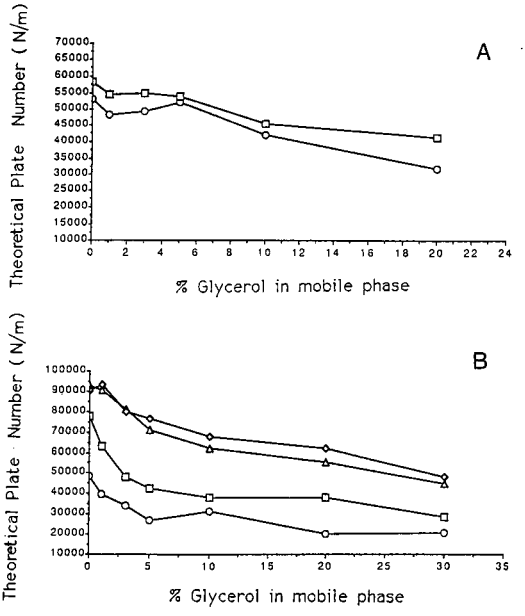

Fig. 3. Variation in the number of theoretical plates per meter with glycerol content in the mobile phase. (A) □ = bradykinin; ○ = met-enkephalin in ACN–H_2O–GLY–AcOH (30:70-*x*:*x*:0.1). (B) ○ = Phloroglucinol; □ = *p*-hydroxybenzoic acid; △ = 3,5-dihydroxybenzoic acid; ◇ = vanillic acid in ACN–H_2O–GLY–AcOH (10:90-*x*:*x*:1).

Fig. 3A indicate a 45% decrease in N/m for bradykinin as the glycerol content increases from 0 to 20%. The values are almost stable in the first 5% and then decrease as the content exceeds this value. This decrease is present for all compounds studied, and the maximum effect is observed with *p*-hydroxybenzoic acid where loss in efficiency is 64% when the glycerol content is 30%. As mentioned previously, changes are most evident in the initial 5% glycerol. For example, while an 8% reduction is seen for bradykinin at low content, an increase of 6% occurs for met-enkephalin. A similar situation can be observed for vanillic acid where a slight increase in efficiency is noticed in the first few percent of glycerol. Furthermore, the data from Fig. 3B indicate that compounds with a low capacity ratio are more readily affected by the presence of small amounts of glycerol. Phloroglucinol and *p*-hydroxybenzoic acid show a substantial reduction in efficiency (45%) when the content of glycerol varies from 0 to 5%, which suggests that the kinetic processes in the system are affected.

The variation in the efficiency of the chromatographic system can be caused by band broadening, but it appears that the effect is more subtle. The results shown in Fig. 4 represent the variation of the normalized widths at half height ($w_{1/2}$) with glycerol content for the compounds studied. Although the experimental peak widths are observed to decrease, the ratio $w_{1/2}/t_r$ (where t_r = retention time) is relatively stable for peptides when the glycerol content is below 5%, while the ratio is seen to increase at higher glycerol content, indicating that peak broadening is occurring. For the other compounds, the ratio increases rapidly with small glycerol contents and then less sharply at concentrations greater than 5%. The effect is greater for phenolic

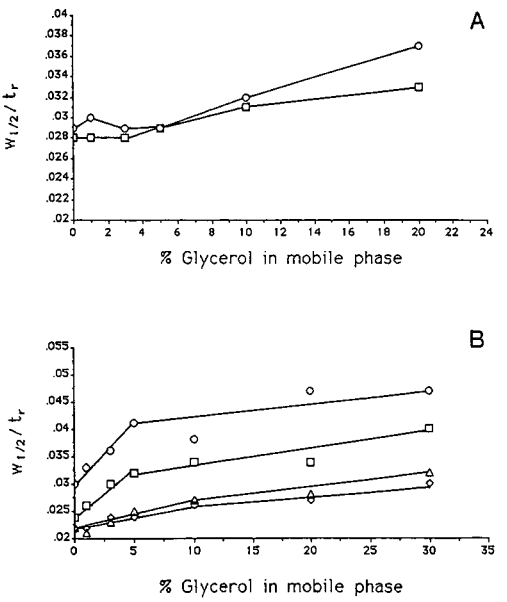

Fig. 4. Variation of the peak width with glycerol content in the mobile phase. (A) □ = bradykinin; ○ = met-enkephalin in ACN–H_2O–GLY–AcOH (30:70-*x*:*x*:0.1). (B) ○ = Phloroglucinol; □ = *p*-hydroxybenzoic acid; △ = 3,5-dihydroxybenzoic acid; ◇ = vanillic acid in ACN–H_2O–GLY–AcOH (10:90-*x*:*x*:1).

compounds having low k' values, which may suggest an increase in instrumental band width, since this contribution has a greater effect on analytes with shorter retentions [27].

This observation suggests that band broadening is related to the variation of the viscosity of the mobile phase. The viscosity of the mobile phase used for the analysis of peptides is given in Table I and is seen to vary from 0.95 to 1.05 as the glycerol content increases from 0 to 5%, while it varies from 0.93 to 1.12 over the same range for the mobile phase used for the other compounds. For content values above 5%, the relative variation in viscosity is similar for both systems and the band broadening is seen to increase in a similar fashion. A more specific study on the variation of the viscosity in this mixture has been conducted, and the results show that variations in the diffusion coefficient can explain most of the broadening observed in those systems [25]. Thus the reduction in efficiency that is observed for low-molecular-weight compounds at low glycerol content and for peptides at glycerol contents above 5% can be attributed to changes that are occurring in the kinetics of mass transfer in the chromatographic systems caused by a change in the diffusivity of the analyte upon change in the viscosity. For compounds with elevated k' values the variation in the retention almost compensates for the kinetic effects due to changes in viscosity below 5% and the efficiency appears stable in that region. For compounds with smaller k' the reduction in retention (Fig. 2) is not sufficient to compensate for the increase in diffusion processes with an increase in glycerol, and the system decreases in efficiency, as indicated by the substantial reduction in N/m.

In order to observe the net effect of an increase in the glycerol content of the mobile phase on chromatographic separation, the resolution has been calculated for two pairs of compounds, and the results are shown in Fig. 5. The variation of the resolution for the pair of peptides is seen to decrease in a similar way to the pair of acids when the glycerol content of the mobile phase is increased. In view of the effects that have already been observed on the retention times, the capacity ratios and the peak widths, the results obtained for the resolution reflect that the variations in those parameters produce an overall effect that results in a loss of the separation efficiency of the system. This reflects the modifications that are occurring in the distribution and kinetics of the system.

TABLE I

VARIATION OF THE VISCOSITY OF THE MOBILE PHASE WITH GLYCEROL CONTENT

Viscosity in cP.

Glycerol (%)	ACN–H_2O–GLY–TFA (30:70-x:x:0.1).	ACN–H_2O–GLY–AcOH (10:90 − x:x:1)
0	0.95	0.93
1	0.96	0.96
3	1.01	1.03
5	1.05	1.12
10	1.26	1.29
20	1.46	1.56
30	–	1.92

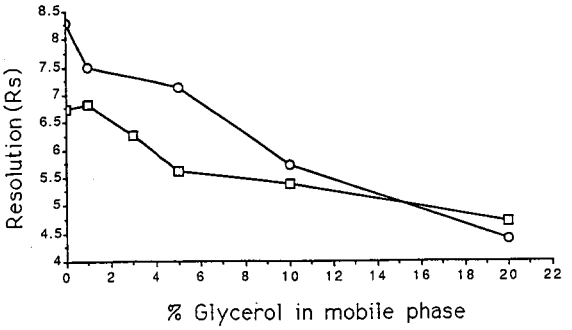

Fig. 5. Variation of the resolution with glycerol content of the mobile phase for two pairs: ○ = bradykinin–met-enkephalin; □ = 3,5-dihydroxybenzoic acid–vanillic acid.

The impedance of separation suggested by Bristow and Knox [26] is another way in which the variation of the overall performance of a chromatographic system can be evaluated. The impedance reveals the apparent viscosity which develops in a chromatographic system as a function of the viscosity of the mobile phase. The variation in the separation impedance of the chromatographic system with the glycerol content of the mobile phase is shown in Fig. 6. It is observed that the impedance is stable for concentrations of glycerol below 3% but increases rapidly as the glycerol content changes from 3 to 10%. This increase in the separation impedance reveals a general loss of performance by the system, which can be attributed to several phenomena caused by the increase in the viscosity of the mobile phase. The impedance demonstrates that the apparent viscosity of the system is increased by 2.5 by the addition of glycerol. This indicates that the presence of glycerol modifies significantly the initial characteristics of the system more than the two-fold variation in the mobile phase viscosity that it causes (Table I). The system is, thus, less efficient in the presence of a significant amount of glycerol (> 5%), and increases in the operation pressure are to be expected, as has been observed experimentally by several other investigators.

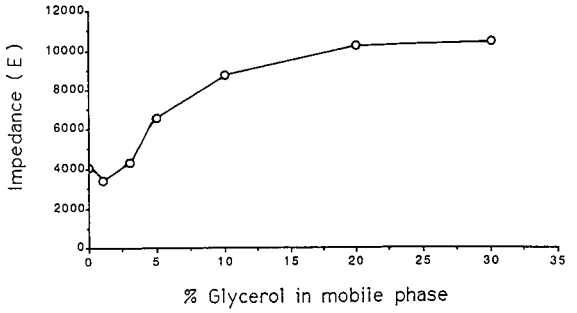

Fig. 6. Variation of the separation impedance with glycerol content of the mobile phase.

CONCLUSIONS

The pre-column addition of a viscous matrix such as glycerol can significantly alter the chromatographic conditions in systems used in LC–FAB-MS. The addition of glycerol shows effects on the retention times of the analytes, capacity ratios, number of theoretical plates, peak width, resolution and impedance of separation. In general terms, the trends are the same whether the compounds are peptides of high molecular weight or acids and phenols of lower molecular weight. The negative effects that the addition of glycerol has on the chromatographic system appear to be more important in compounds having smaller capacity ratios. The net effect of high glycerol contents on the chromatographic system is observed in terms of loss of efficiency and resolution and a significant increase in the separation impedance of the system, indicating a net deterioration in the chromatographic performance. At higher glycerol content, the main factor perturbing the system seems to be the increase in viscosity of the mobile phase that alters the mass transfer kinetics and the flow dynamics of the system. At lower concentrations of glycerol, even if the distribution is affected because glycerol is acting as an efficient organic modifier, the net effect on the chromatographic system, although not positive, is not necessarily detrimental. In fact, it would appear that below 3% glycerol in the mobile phase the chromatographic conditions are essentially stable and the presence of a viscous matrix does not appreciably interfere with the separation characteristics of the system. In those concentration values, although resolution is slightly decreased, the variation in retention induced by glycerol for compounds with a high capacity ratio tends to override the kinetic effects caused by the increase in the viscosity of the mobile phase. Thus optimization of LC–FAB-MS systems should require the minimal use of a viscous matrix or alternatively utilize a matrix with a lower viscosity inasmuch as it does not reduce mass spectral sensitivity.

ACKNOWLEDGEMENTS

The authors wish to acknowledge the financial contributions of the National Science and Engineering Research Council of Canada (NSERC) and Hydro-Québec that have permitted this study. The authors are also grateful to Dr. G. Paul for his editorial assistance.

REFERENCES

1 M. Barber, R. Bordoli, R. D. Segdwick and A. N. J. Tyler, *Chem. Soc., Chem. Commun.*, (1981) 325.
2 M. Barber, R. S. Bordoli, G. J. Elliot, R. D. Segdwick and A. N. Tyler, *Anal. Chem.*, 54 (1982) 645A.
3 C. Fenselau and R. J. Cotter, *Chem. Rev.*, 87 (1987) 501.
4 Q. Zha and M. J. Bertrand, *Org. Mass Spectrom.*, 25 (1990) 435.
5 Q. Zha and M. J. Bertrand, *Proceedings of the 37th ASMS Annual Conference on Mass Spectrometry and Allied Topics, Miami, FL, May 21–26, 1989*, ASMS, East Lansing, MI, 1989, pp. 792–794.
6 Q. Zha and M. J. Bertrand, *Can. J. Appl. Spectrosc.*, 35 (1990) 141.
7 M. A. Baldwin, K. J. Welham, I. Toth and W. A. Gibbons, *Org. Mass Spectrom.*, 23 (1988) 697.
8 R. M. Caprioli, T. Fan and J. S. Cottrell, *Anal. Chem.*, 58 (1986) 2949.
9 Y. Ito, T. Takeuchi, D. Ishii and M. Goto, *J. Chromatogr.*, 346 (1985) 161.
10 K. Tomer and C. E. Parker, *J. Chromatogr.*, 492 (1989) 189.
11 M. J. Bertrand and V. Benham, in T. Theophanides (Editor), *Spectroscopy of Inorganic Bioactivators, Theory and Applications*, Nato ASI Series, Kluwer, Dordrecht, 1989, pp. 349–377.

12 P. J. Arpino and G. Guiochon, *J. Chromatogr.*, 185 (1979) 529.
13 J. G. Stroh, J. Carter Cook, R. M. Milberg, L. Brayton, T. Kihara, Z. Huang, K. L. Rinehart, Jr. and I. A. S. Lewis, *Anal. Chem.*, 57 (1985) 985.
14 P. Dobberstein, E. Korte, G. Mererhoff and R. Pesch, *Int. J. Mass Spectrom. Ion Phys.*, 46 (1985) 985.
15 T. Takeuchi, S. Watanabe, N. Kondo, D. Ishii and M. Goto, *J. Chromatogr.*, 435 (1988) 482.
16 P. Kokkonen, J. van der Greef, W. M. A. Niessen, U. R. Tjaden, G. J. ten Hove and G. van de Werken, *Rapid Commun. Mass Spectrom.*, 3 (1989) 102.
17 D. E. Games, S. Pleasance, E. D. Ramsey and M. A. McDowall, *Biomed. Environ. Mass Spectrom.*, 15 (1988) 179.
18 D. W. Hutchinson, A. R. Woolfitt and A. E. Ashcroft, *Org. Mass Spectrom.*, 22 (1987) 304.
19 A. E. Ashcroft, *Org. Mass Spectrom.*, 22 (1987) 734.
20 P. Boulenguer, Y. Leroy, J. M. Alonso, J. Montreuil, G. Ricart, C. Colbert, D. Duquet, C. Dewaele and B. Fournet, *Anal. Biochem.*, 168 (1988) 164.
21 S. Pleasance, P. Thibault, M. A. Moseley, L. J. Deterding, K. B. Tomer and J. W. Jorgenson, *J. Am. Soc. Mass Spectrom.*, 1 (1990) 321.
22 M. A. Moseley, L. J. Deterding, J. S. M. de Wit, K. B. Tomer, R. T. Kennedy, N. Bragg and J. W. Jorgenson, *Anal. Chem.*, 61 (1989) 1577.
23 D. J. Bell, M. D. Brightwell, W. A. Neville and A. West, *Rapid Commun. Mass Spectrom.*, 4 (1990) 88.
24 J. S. M. de Wit, L. J. Deterding, M. A. Moseley, K. B. Tomer and J. W. Jorgenson, *Rapid Commun. Mass Spectrom.*, 2 (1988) 100.
25 J. P. Gagné, A. Carrier and M. J. Bertrand, *J. Chromatogr.*, 554 (1991) 47.
26 P. A. Bristow and J. H. Knox, *Chromatographia*, 10 (1977) 279.
27 J. L. DiCesare, M. W. Dong and L. S. Ettre, *Introduction to High Speed Liquid Chromatography*, Perkin-Elmer, Norwalk, CT, 1981.

Journal of Chromatography, 554 (1991) 73–82
Elsevier Science Publishers B.V., Amsterdam

CHROMSYMP. 2216

Nanoscale separations combined with tandem mass spectrometry

LEESA J. DETERDING*

Laboratory of Molecular Biophysics, National Institute of Environmental Health Sciences, P.O. Box 12233, Research Triangle Park, NC 27709 (USA)

M. ARTHUR MOSELEY

Laboratory of Molecular Biophysics, National Institute of Environmental Health Sciences, P.O. Box 12233, Research Triangle Park, NC 27709, and Department of Chemistry, University of North Carolina, C.B. 3290, Chapel Hill, NC 27514 (USA)

KENNETH B. TOMER

Laboratory of Molecular Biophysics, National Institute of Environmental Health Sciences, P.O. Box 12233, Research Triangle Park, NC 27709 (USA)

and

JAMES W. JORGENSON

Department of Chemistry, University of North Carolina, C.B. 3290, Chapel Hill, NC 27514 (USA)

ABSTRACT

High-efficiency separations of peptide mixtures, tryptic digests and other biological compounds have been achieved using nanoscale packed capillaries and capillary zone electrophoresis (CZE). The coaxial continuous-flow fast atom bombardment design is an excellent interface for coupling these separation techniques with mass spectrometry (MS). In addition, this interface is very useful for the acquisition of MS–MS data from compounds separated by nanoscale packed capillary liquid chromatography and CZE. Structurally informative daughter-ion spectra can be obtained at the low picomole to femtomole level.

INTRODUCTION

Fast atom bombardment mass spectrometry (FAB-MS), as first developed by Barber *et al.* [1], has become a widely used desorption technique for the analysis of polar, non-volatile, and/or thermally labile compounds such as biomolecules. Because both liquid chromatography (LC) and FAB-MS are suitable for the analysis of biomolecules, the coupling of LC with FAB-MS is currently an area of great interest. One of the most commonly used interfaces between flowing liquid streams and mass spectrometry for the analysis of polar molecules is continuous-flow fast atom bombardment (CF-FAB) [2,3]. Generally, LC–CF-FAB interfaces employ a single fused-silica capillary to deliver the column analytes to the probe tip in the mass spectrometer. These systems are designed to operate with conventional and microbore LC columns (typically 4.6–0.22 mm I.D.). Addition of the FAB matrix is accomplished

0021-9673/91/$03.50

by either adding the matrix to the mobile phase solvents or by postcolumn addition. The presence of the matrix in the mobile phase, however, can compromise the chromatography due to changes in the polarity and viscosity of the mobile phase. On the other hand, post-column addition of the matrix sometimes leads to chromatographic peak broadening, particularly with microbore LC columns.

Miniaturization of LC columns has also drawn a considerable amount of interest. Two approaches to this miniaturization that we have been developing are nanoscale packed capillary liquid chromatography (nCLC) and capillary zone electrophoresis (CZE). These techniques hold great promise in the analysis of biological mixtures, due to their high separation efficiencies (greater than $1 \cdot 10^6$ theoretical plates [4]). In addition, the low flow-rates associated with these methodologies (less than 100 nl/min, with injection and detection volumes of less than 20 nl/min) facilitates the coupling of these separation techniques with the high vacuums required by MS.

To avoid the problems associated with the addition of the FAB matrix in the mobile phase (which are especially severe with the nanoscale techniques), we have recently developed a coaxial CF-FAB interface [5–7] in which the analytes and matrix are delivered separately to the FAB probe tip. Briefly, this coaxial CF-FAB interface consists of a fused-silica capillary column or a nanoscale packed capillary column which is surrounded by a second fused-silica capillary column in which the matrix is introduced. In this manner, there is no mixing of the matrix with the LC analytes until both have reached the probe tip. This coaxial design is advantageous since (1) the chromatography is not affected by the matrix, and (2) both the LC flow-rate and composition and the FAB matrix flow-rate and composition can be independently optimized. A comparison of precolumn versus coaxial matrix delivery showed the coaxial CF-FAB interface offered higher separation efficiencies (by up to a factor of four) and lower detection limits than the precolumn addition of matrix [8]. Using the coaxial CF-FAB interface, full-scan mass spectra were acquired from 54 fmol of a tripeptide, and a detection limit of 1.8 fmol was achieved with a narrow scan range [6].

In addition, the coaxial CF-FAB design has been successfully applied as an interface between CZE and MS. While maintaining separation efficiencies of hundreds of thousands of theoretical plates, peptide mixtures can be separated and analyzed by MS. CZE–MS detection limits have been observed for peptides of less than 10 fmol [9–12].

We have also demonstrated the ability to obtain MS–MS spectra of analytes using the coaxial CF-FAB interface [7,9–13]. Structurally informative MS–MS spectra of a tripeptide have been acquired on-the-fly from 540 fmol. A 54-fmol injection resulted in an MS–MS spectrum of sufficient quality to confirm the identity of a compound. In addition, the MS–MS spectra of peptides can be obtained as they are electrophoretically separated by CZE. Because the peak widths of CZE peaks are so narrow (typically 1–5 s wide at half-height), the acquisition of on-the-fly MS–MS data from a CZE separation can be somewhat difficult. A compromise between the separation efficiencies and the CZE peak widths, however, can allow one to obtain good MS–MS spectra. As an extension of this work, we report here the MS–MS data acquired from the separation of tryptic digests and peptide mixtures acquired using nanoscale packed capillary columns and capillary zone electrophoresis.

EXPERIMENTAL

Nanoscale capillary LC system

The nanoscale packed capillary LC columns used in this work were fabricated by using a modification of the method of Kennedy and Jorgenson [14]. For the analysis of the tryptic digest of bovine growth hormone releasing factor (1–29) a 50 μm I.D. × 150 μm O.D. column packed with 10-μm Hypersil C_{18} particles (Shandon) was used. For the horse heart cytochrome *c* tryptic digest a 75 μm I.D. × 150 μm O.D. column packed with 10 μm AQ-C_{18} particles (YMC) was used. In both analyses, the column was fully packed for 2 m in length. For the analysis of adrenocorticotropic hormone (ACTH) (1–24) a 75-μm I.D. column with a 30-cm packing bed of 10-μm AQ-C_{18} particles was used. A stirred slurry of 30:1 (ml solvent:g particles) was used to pack the columns. Hexane was used as the slurry solvent and 2-propanol was used as the packing solvent. A syringe pump (μLC-500, Isco, Lincoln, NE, USA) was used to pressurize the packing slurry to 275 bar.

LC mobile phase gradients were generated using two reciprocating piston pumps (Waters Model 6000A, Waters Assoc., Milford, MA, USA) and a gradient-control system (Waters solvent programmer Model 660, Water Assoc.). HPLC-grade acetonitrile and methanol and 18 MΩ water (Milli-Q water system, Millipore, Bedford, MA, USA) were used for preparation of samples and mobile phases. All mobile phases and sample solutions contained 0.1% trifluoroacetic acid (TFA) and were filtered (0.45 μm) and degassed prior to use. Solvent delivery was accomplished by using a capillary liquid chromatography system that was modified for use with conventional LC gradient pumps [15,16]. Sample injections were made using a stainless-steel pressure vessel which contains a microvial of sample solution. The sample was injected onto the LC column by pressurizing the vessel to 1500 p.s.i. using helium gas. After the desired volume was injected, the vessel was depressurized and the LC capillary column was removed from the injection vessel and remounted in the capillary LC system.

The electrophoretic separations were performed using a CZE system which has been previously described [9]. The CZE columns were 12–15 μm I.D. × 150 μm O.D. fused-silica capillaries which terminate at the FAB probe tip. The CZE buffer was 0.005 *M* ammonium acetate. A 60-kV reversible power supply (Glassman High Voltage) was used. A safety interlock system incorporating a high-voltage relay (Kilovac High Voltage) was used for operator safety.

Mass spectrometry

The coaxial CF-FAB interface has been previously described [5]. A CZE or nanoscale packed capillary column is inserted into a sheath column (typically 160 μm I.D. × 350 μm O.D.). The separations take place in the inner column while the matrix simultaneously flows through the outer column. The mass spectrometer used to acquire the data for this work was a VG ZAB-4F of B_1E_1–E_2B_2 geometry [17]. The instrument is operated at 8 kV and is equipped with an Ion Tech atom gun and a standard VG CF-FAB source which was heated at 40–60°C. The samples were bombarded with 8-keV xenon atoms. The MS spectra were acquired by scanning MS-I (B_1E_1) with detection in the third field-free region. The MS–MS experiments were performed by focussing the parent through MS-I into the collision cell in the third

field-free region. Daughter-ion spectra were obtained by collisions at 8 keV with helium gas (50% beam reduction). The collisional activation decomposition (CAD) spectra were obtained by a linear E_2B_2 linked scan of MS-II. The data acquisition system used was a VG Analytical 11-250 data system.

Chemicals

The peptides were purchased from Sigma (St. Louis, USA). The L-(tosylamido-2-phenyl)ethyl chloromethyl ketone (TPCK) trypsin was purchased from Worthington Biochemical (Freehold, NJ, USA). The tryptic digests were carried out on bovine growth hormone releasing factor (1–29), horse heart cytochrome *c*, and adrenocorticotropic hormone (1–24) with a 1:100 ratio of enzyme to peptide in 0.2 *M* NH_4HCO_3 buffer. Digests were allowed to proceed for 1 h at 37°C. The enzymatic digestion was stopped by either freeze-drying or by the addition of TFA. All solvents were acquired from J. T. Baker, (Pittsburgh, NJ, USA).

RESULTS AND DISCUSSION

nCLC analysis

ACTH (1–24) was analyzed using a 75-μm I.D. nanoscale packed capillary column with a 30-cm packing bed. An injection corresponding to approximately 82 pmol of undigested protein was injected using the pressure injection vessel. All of the expected tryptic peptide fragments, fragment 16–17, 18–21, 17–21, 22–24, 9–15 and 1–8, were observed and separated in less than 60 min (Fig. 1). A gradient of 0%

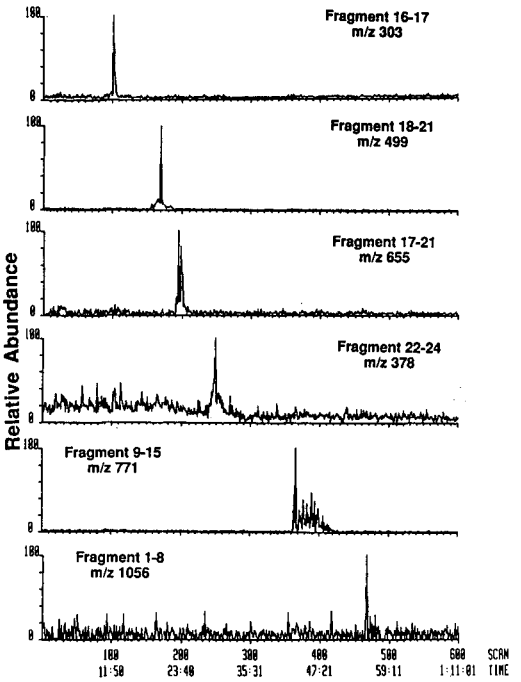

Fig. 1. Single-ion chromatograms of the tryptic fragments of ACTH (1–24) obtained from full-scan (2000–150 a.m.u.) data. Approximately 82 pmol of the protein was injected. Time in h:min:s.

acetonitrile for 5 min, then stepped to 10% and linearly programmed to 30% acetonitrile in water (0.1% TFA) was used to achieve this separation. The analysis was then repeated in order to obtain the corresponding MS–MS spectra of the tryptic fragments. An injection of approximately 250 pmol was used in order to obtain good daughter-ion information (Fig. 2). Fragments 16–17 and 18–21 (Fig. 2A and B, respectively) produce abundant side-chain cleavages as well as fragment ions corresponding to backbone cleavages of the tryptic peptide. Upon collisional activation fragment 17–21, 22–24 and 9–15 (Fig. 2C, D and E, respectively) decompose into structurally informative daughter ions including an *a*, *b* and/or *y* fragmentation at each peptide bond. Thus, information as to the identity of each amino acid in sequence is observed. The concentration of tryptic fragment 1–8 was insufficient to obtain a good MS–MS spectrum. Fragment ions corresponding to the backbone cleavages b_6 and a_7 were, however, observed for this tryptic peptide. Nomenclature for the peptide cleavages is that of Roepstorff and Fohlman [18] as modified by Biemann [19].

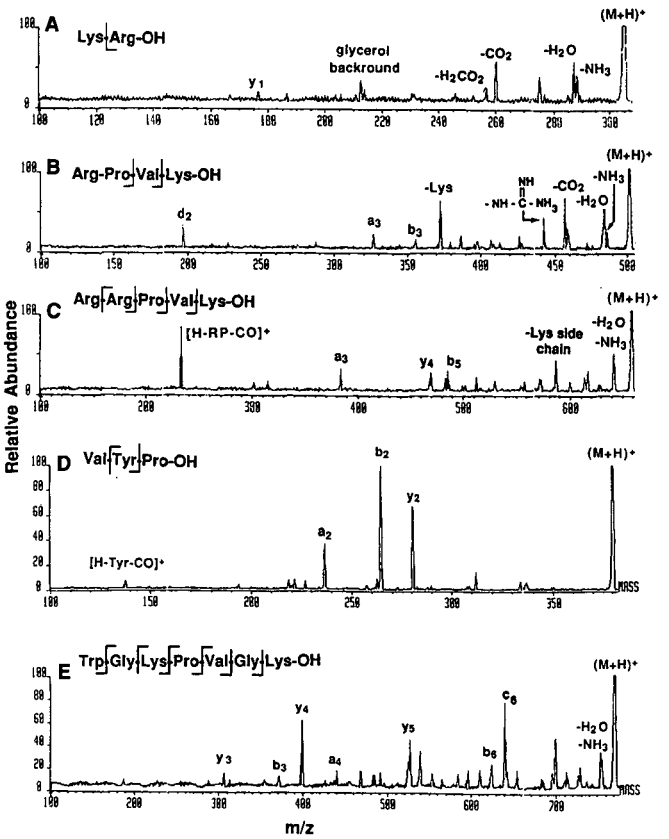

Fig. 2. MS–MS spectra of the $(M + H)^+$ ion of (A) fragment 16–17 (*m/z* 303); (B) fragment 18–21 (*m/z* 499); (C) fragment 17–21 (*m/z* 655); (D) fragment 22–24 (*m/z* 378); and (E) fragment 9–15 (*m/z* 771) of ACTH (1–24) acquired on-line from a nanoscale packed capillary column. Approximately 250 pmol of protein was injected.

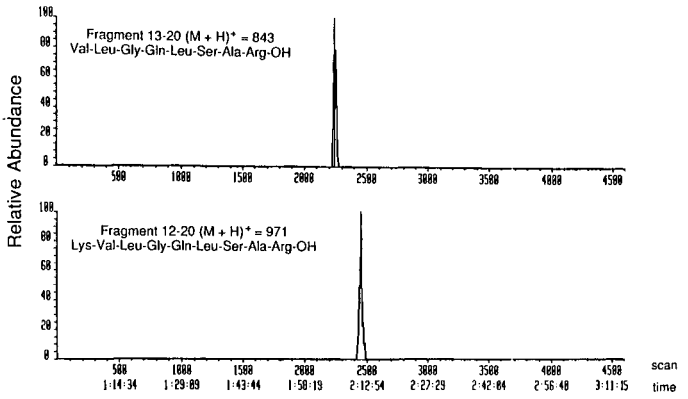

Fig. 3. Single-ion chromatograms of two tryptic fragments of bovine growth hormone releasing factor (1–29) analyzed by nanoscale LC–MS while scanning from 1160 to 800 a.m.u. The total amount of protein injected was approximately 0.8 pmol.

The tryptic digest of bovine growth hormone releasing factor was analyzed using a nanoscale packed capillary column. The total amount of protein injected was approximately 0.8 pmol in 2.5 nl of solution. At this low analyte level, a separation of four of the tryptic peptide fragments was obtained from a linear gradient of 5–70% methanol in water (0.1% TFA) over 180 min. These four peptide fragments correspond to fragments 13–20, 12–20, 22–29 and 21–29. The reconstructed-ion chromatograms of two of these tryptic fragments, fragments 13–20 Val–Leu–Gly–Gln–Leu–Ser–Ala–Arg and 12–20 Lys–Val–Leu–Gly–Gln–Leu–Ser–Ala–Arg, are shown, respectively, in Fig. 3. The MS–MS spectra of these two tryptic fragments were acquired and are shown in Fig. 4. Structurally informative daughter ions, including cleavages at five of the seven peptide bonds in fragment 13–20 (Fig. 4A) and five of the eight peptide bonds in fragment 12–20 (Fig. 4B), resulted from the collisional activation of the parent ions. Side-chain cleavages and *w* ions are the most abundant fragment ions observed. The other two tryptic fragments that were observed had a signal-to-noise ratio of approximately 3:1. At this level, the parent ions were too weak to obtain reasonable MS–MS spectra. Therefore, their reconstructed-ion chromatograms are not shown here.

The analysis of the tryptic digest of horse heart cytochrome *c* was acquired using an injection corresponding to 96 pmol of undigested protein. A large injection volume was used to insure detection of as many tryptic fragments as possible. Over 40 chromatographic peaks were found using a gradient of 0% acetonitrile for 10 min, then stepped up to 15% and linearly programmed to 35% acetonitrile in water (0.1% TFA) over 120 min. Analysis of the digest by electrospray ionization MS revealed that the horse heart cytochrome *c* had only partially digested (approximately 75% undigested protein remained); therefore, the MS–MS spectra of only three of the most abundant tryptic peptides were obtained. The reconstructed-ion chromatograms of these tryptic fragments, fragments 9–13, 28–38 and 80–86, are shown in Fig. 5, and their corresponding MS–MS spectra are shown in Fig. 6. The CAD spectrum of fragment 9–13 (Fig. 6A) reveals peptide backbone cleavages at all peptide bonds

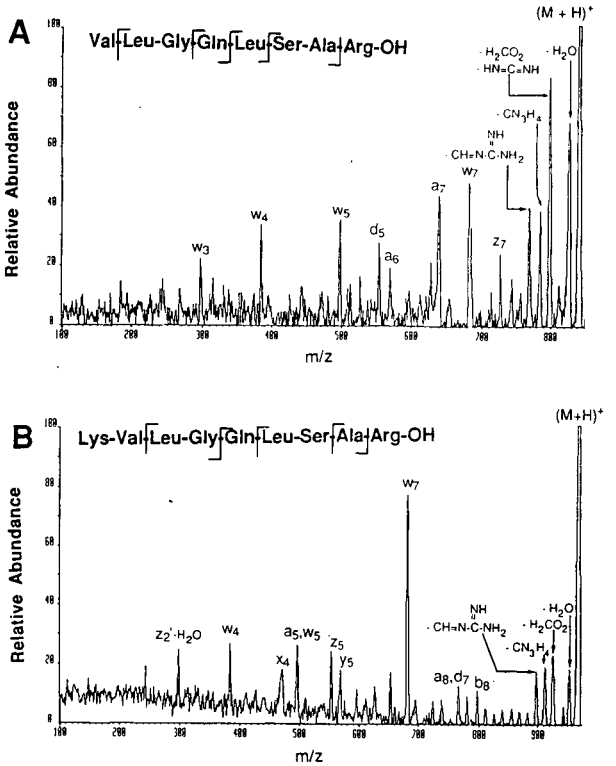

Fig. 4. MS–MS spectra of the $(M + H)^+$ ions of (A) tryptic peptide fragment 13–20 (m/z 843), and (B) tryptic peptide fragment 12–20 (m/z 971) of bovine growth hormone releasing factor (1–29).

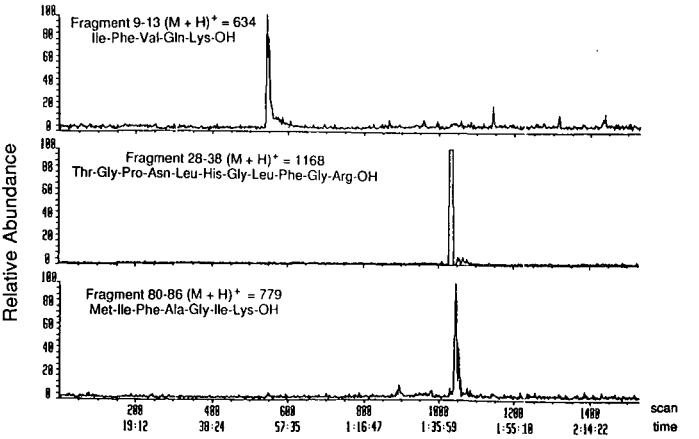

Fig. 5. Single-ion chromatograms of three tryptic fragments of horse heart cytochrome c analyzed by nanoscale LC—MS in the full-scan mode (1520– 200 a.m.u.). The total amount of protein injected was approximately 96 pmol.

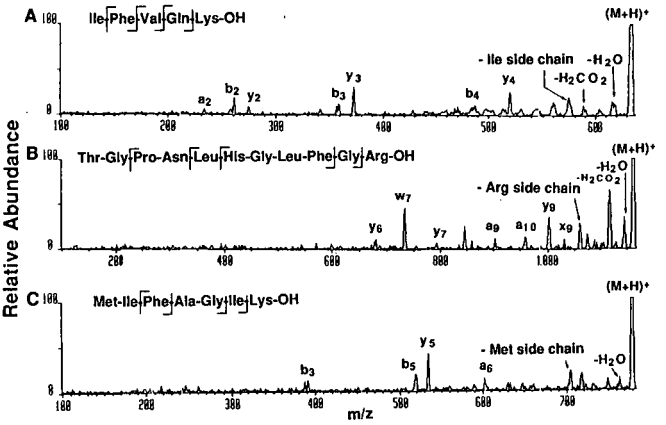

Fig. 6. MS–MS spectra of the $(M + H)^+$ ions of (A) tryptic peptide fragment 9–13 (*m/z* 634), (B) tryptic peptide fragment 28–38 (*m/z* 1168) and (C) tryptic peptide fragment 80–86 (*m/z* 779) of horse heart cytochrome *c*.

which can be used to determine the amino acid sequence of the peptide. The CAD spectra of the tryptic fragments 28–38 and 80–86 (Fig. 6B and C, respectively), while insufficient for complete sequence determination, provide a significant amount of structural information.

CZE analyses

The coaxial CF-FAB interface has proven to be useful for the analysis of peptide mixtures. The single-ion electropherograms of a separation of a mixture of met-enkephalinamide and met-enkephalin are shown in Fig. 7. The amount injected of each analyte is approximately 100 fmol. The CZE analysis was then repeated twice in order to acquire the MS–MS spectra of the two analytes as they migrated through the CZE column. Fig. 8 shows the MS–MS spectra of the $(M + H)^+$ ions of met-enkepha-

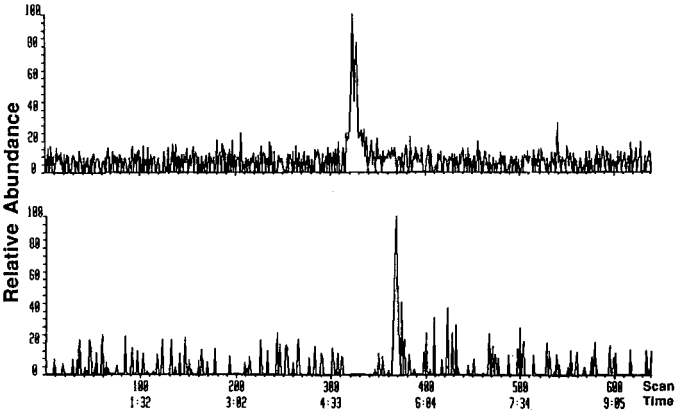

Fig. 7. Single-ion electropherograms of the $(M + H)^+$ ions of met-enkephalin-amide (*m/z* 573, top) and met-enkephalin (*m/z* 574, bottom) determined by CZE–MS (scanning from 590 to 545 a.m.u.).

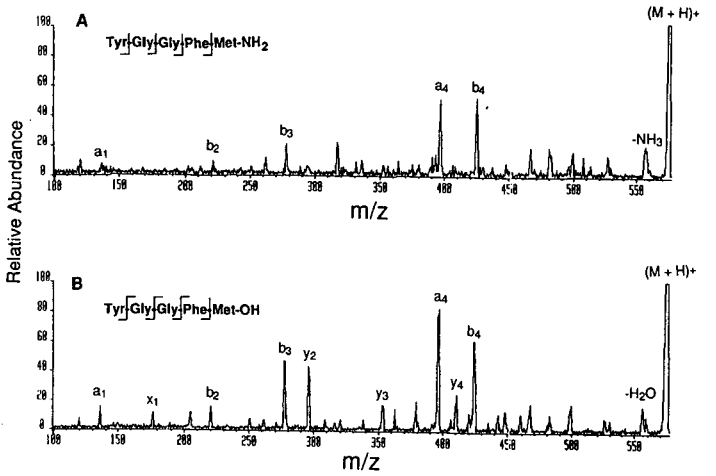

Fig. 8. MS–MS spectra of the $(M + H)^+$ ions of (A) met-enkephalinamide (*m/z* 573) and (B) met-enkephalin (*m/z* 574) electrophoretically separated by CZE.

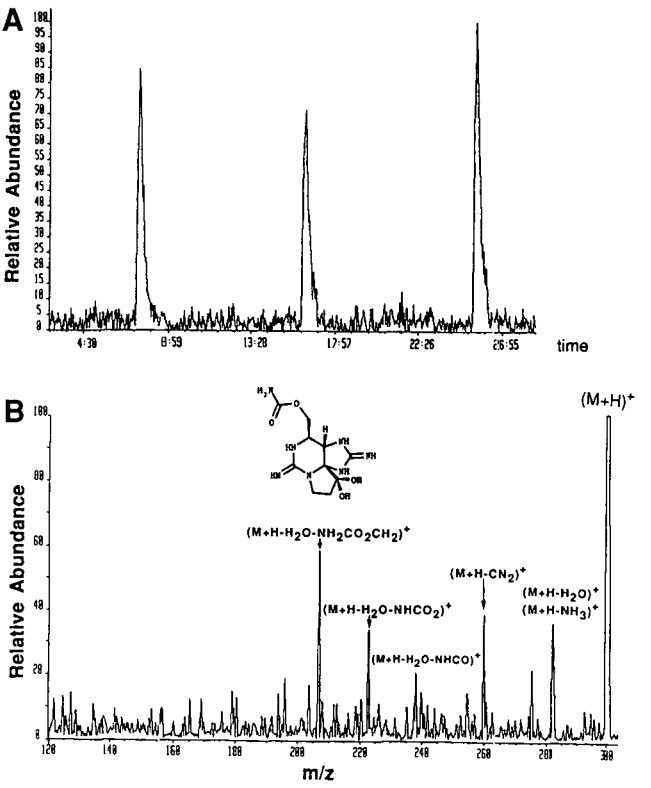

Fig. 9. (A) Single-ion chromatogram of the $(M + H)^+$ ion of saxitoxin acquired from triplicate injections of 260 fmol each while scanning from 305 to 285 a.m.u. (B) MS–MS spectrum of the $(M + H)^+$ ion of saxitoxin acquired by CZE in conjunction with coaxial CF-FAB.

linamide and met-enkephalin (approximately 400–800 fmol injected) acquired as the analytes migrated through the CZE column. Fragmentations at each peptide linkage as well as side-chain cleavages are observed in the CAD spectra. Sufficient fragmentation is observed to determine the amino acid sequence in the two peptides. In addition, the loss of NH_3 *vs.* the loss of H_2O clearly distinguishes the met-enkephalinamide from the met-enkephalin.

In addition to peptides, CZE–MS–MS is useful for the determination of other types of biological compounds. For example, saxitoxin, a paralytic shellfish toxin from the red-tide denoflagellate, can be analyzed by CZE in conjunction with coaxial CF-FAB. Excellent sensitivities can be obtained by this technique as demonstrated in Fig. 9A which shows triplicate injections of the marine toxin at the 260 fmol level while scanning the mass spectrometer over 20 a.m.u. Good reproducibility is observed at this low fmol level. The MS–MS spectrum of the $(M+H)^+$ ion of saxitoxin reveals structurally informative daughter ions (Fig. 9B). These ions compare with those which were obtained by FAB mass-analyzed ion kinetic energy spectroscopy [20] and ion spray [21].

ACKNOWLEDGEMENT

The saxitoxin sample was provided by Dr. C. J. Mirocha of the University of Minnesota.

REFERENCES

1 M. Barber, R. S. Bordoli, R. D. Sedwick and A. M. Tyler *J. Chem. Soc. Commun.*, (1981) 325.
2 Y. Ito, T. Takeuchi, D. Ishii and M. Goto, *J. Chromatogr.*, 346 (1985) 161.
3 R. M. Caprioli, T. Fan and J. S. Cottrell, *Anal. Chem.*, 58 (1986) 2949.
4 J. W. Jorgenson and E. J. Guthrie, *J. Chromatogr.*, 255 (1983) 335.
5 J. S. M. de Wit, L. J Deterding, M. A. Moseley, K. B. Tomer and J. W. Jorgenson, *Rapid Commun. Mass Spectrom.*, 2 (1988) 100.
6 M. A. Moseley, L. J. Deterding, J. S. M. de Wit, K. B. Tomer, R. T. Kennedy, N. Bragg and J. W. Jorgenson, *Anal. Chem.*, 61 (1989) 1577.
7 L. J. Deterding, M. A. Moseley, K. B. Tomer and J. W. Jorgenson, *Anal. Chem.*, 61 (1989) 2504.
8 S. Pleasance, P. Thibault, M. A. Moseley, L. J. Deterding, K. B. Tomer and J. W. Jorgenson, *J. Am. Soc. Mass Spectrom.*, 1 (1990) 312.
9 M. A. Moseley, L. J. Deterding, K. B. Tomer and J. W. Jorgenson, *Rapid Commun. Mass Spectrom.*, 3 (1989) 87.
10 M. A. Moseley, L. J. Deterding, K. B. Tomer and J. W. Jorgenson, *J. Chromatogr.*, 480 (1989) 247.
11 M. A. Moseley, L. J. Deterding, K. B. Tomer and J. W. Jorgenson, *J. Chromatogr.*, 516 (1990) 167.
12 M. A. Moseley, L. J. Deterding, K. B. Tomer and J. W. Jorgenson, *Anal. Chem.*, 63 (1991) 109–114.
13 L. J. Deterding and M. A. Moseley in R. M. Capridi (Editor), *Continuous Flow Fast Atom Bombardment Mass Spectrometry*, Wiley, New York, 1990, p. 181–185.
14 R. T. Kennedy and J. W. Jorgenson, *Anal. Chem.*, 61 (1989) 1128.
15 J. W. Jorgenson and E. J. Guthrie, *J. Chromatogr.*, 255 (1983) 335.
16 M. D. Oates and J. W. Jorgenson, *Anal. Chem.*, 61 (1989) 432.
17 J. R. Hass, B. N. Green, R. H. Bateman and P. A. Bott, *Proceedings of the 32nd Annual Conference on Mass Spectrometry and Allied Topics, San Antonio, TX, May 1984*, p. 380.
18 P. Roepstorff and J. Fohlman, *Biomed. Environ. Mass Spectrom.*, 11 (1984) 601.
19 K. Biemann, *Biomed. Environ. Mass Spectrom.*, 16 (1988) 99.
20 K. D. White, J. A. Sphon and S. Hall, *Anal. Chem.*, 58 (1986) 562.
21 M. A. Quilliam, B. A. Thomson, G. J. Scott and K. W. M. Siu, *Rapid Commun. Mass Spectrom.*, 3 (1989) 145.

Journal of Chromatography, 554 (1991) 83–90
Elsevier Science Publishers B.V., Amsterdam

CHROMSYMP. 2325

Approach to studying proteinase specificity by continuous-flow fast atom bombardment mass spectrometry and high-performance liquid chromatography combined with photodiode-array ultraviolet detection

JERZY SILBERRING, PETER BROSTEDT, MADELEINE THÖRNWALL and FRED NYBERG*
Department of Pharmacology, University of Uppsala, P.O. Box 591, S-751 24 Uppsala (Sweden)

ABSTRACT

Fast atom bombardment mass spectrometry (FAB-MS) and high-performance liquid chromatography using a photodiode-array ultraviolet detector were applied to study a dynorphin-converting endopeptidase from the human pituitary gland. The specificity of the enzyme was tested towards various opioid peptides derived from the prodynorphin precursor, *i.e.* dynorphin A, dynorphin B and α-neoendorphin. Peptide fragments were analysed directly by continuous-flow FAB-MS and those containing aromatic amino acids were detected independently by the photodiode-array ultraviolet detector. The results obtained suggest a similar processing of these structure-related substrates and it appears that the enzyme recognizes the dibasic stretch in their sequence. It is also clear from this study that the combination of the above techniques provides a powerful tool for studies of enzymatic conversion among the prodynorphin-derived peptides and it should be applicable to studies of similar mechanisms in other peptide systems.

INTRODUCTION

It is well known that many of the biological processes occurring in living systems are regulated by a variety of proteinases present in various tissues or body fluids [1]. In recent years a particular interest has been focused on proteolytic regulation in peptidergic pathways in the central nervous system (CNS). One important pathway concerns the conversion and degradation of the prodynorphin-derived neuropeptides (Table I) as they are reported to be involved in pain control [2]. Specific cleavage of these peptides may alter their receptor activation profile from κ- to δ-specific, *i.e.* the parent peptides exhibit an affinity for the so-called κ opioid receptors, whereas their products (Leu-enkephalin or Leu-enkephalin-Arg^6) preferentially bind to δ receptors [3].

The detailed and quantitative determination of the converted fragments by radioimmunoassay (RIA) is difficult because of the lack of all necessary antibodies and in such cases fast atom bombardment mass spectrometry (FAB-MS) and high performance liquid chromatography (HPLC) techniques are the methods of choice. The simultaneous analysis of several fragments by direct probe is limited, however,

0021-9673/91/$03.50

TABLE I

STRUCTURE OF PRODYNORPHIN-DERIVED PEPTIDES

Peptide	Structure	[M + H]$^+$
Dynorphin A	Tyr–Gly–Gly–Phe–Leu–Arg–Arg–Ile–Arg–Pro–Lys–Leu–Lys–Trp–Asp–Asn–Gln 1 5 10 15	2147
Dynorphin B	Tyr–Gly–Gly–Phe–Leu–Arg–Arg–Gln–Phe–Lys–Val–Val–Thr 1 5 10	1570
α-Neoendorphin	Tyr–Gly–Gly–Phe–Leu–Arg–Lys–Tyr–Pro–Lys 1 5 10	1229

due to the signal suppression of the more hydrophilic peptides in a matrix with a high glycerol concentration [4]. Continuous-flow (CF) FAB-MS analysis overcomes this problem and also allows the quantitation of the molar ratios of the released peptides [5]. The analysis can be further extended to a multispectral search for fragments containing aromatic amino acids. This latter technique allows the rapid, on-line verification of the separated products and can also serve to monitor the progress of the reaction.

The aim of this work was to apply CF-FAB-MS and HPLC combined with a photodiode-array UV detector for the identification of the cleavage sites of various prodynorphin-derived peptides converted by the same enzyme purified from the human pituitary gland.

EXPERIMENTAL

The peptides used in this study were purchased from Bachem (Bubendorf, Switzerland). They were analysed by FAB-MS and by reversed-phase HPLC for impurities that could interfere with the described techniques. All other chemicals were of analytical-reagent grade and were purchased from various commercial sources.

Frozen human pituitary glands were collected at autopsy and generously supplied by Kabi (Stockholm, Sweden). The dynorphin-converting enzyme (DCE) was purified to apparent homogeneity, essentially following the procedure outlined elsewhere [6]; the detailed isolation protocol will be published in a separate paper.

The enzyme assay was performed as described by Silberring and Nyberg [6], with minor modifications. Briefly, 0.5 μg of enzyme was incubated with the particular peptide (15 μg) and the reaction volume was adjusted to 60 μl with 0.1 *M* disodium hydrogenphosphate–hydrochloric acid buffer (pH 6.0). The reaction was terminated with 500 μl of 0.04% trifluoroacetic acid (TFA) and the samples were desalted on Sep-Pak C_{18} cartridges (Waters, Milford, MA, USA) and evaporated before analysis by FAB-MS. The instrument used was a Finnigan MAT 90 double-focusing mass spectrometer with reverse geometry (*B*, *E* where *B* = magnetic field and *E* = electric field). Xenon was used as a source beam operating at 7 kV and 2 mA. Positive mode magnetic scans were acquired at a full accelerating voltage of 5 kV. The samples were analysed by the CF-FAB-MS technique with the interface supplied by Finnigan MAT, as described by Caprioli *et al.* [7]. After desalting, the incubation mixture was

evaporated and then redissolved to the appropriate concentration in the mobile phase which consisted of 5% glycerol, 5% acetonitrile and 0.1% TFA. Elution was performed through a 0.075-mm fused-silica capillary column at a flow-rate of 5 μl/min, as described elsewhere [8].

An identical degradation experiment was performed in parallel where the samples were separated directly on the reversed-phase HPLC column (TSK ODS-120T; 250 × 4.6 mm; particle size 5 μm) and analysed on-line with a Model 2140 photodiode-array UV detector (Pharmacia, Uppsala, Sweden) as described previously [9]. The column was developed by a linear gradient of acetonitrile (15–45%) containing 0.04% TFA, maintaining a flow-rate of 0.5 ml/min.

The RIA for dynorphin A_{1-6} (DYN A_{1-6}) (or Leu-enkephalin-Arg^6) was based on the charcoal adsorption technique and conducted as described elsewhere [6].

RESULTS AND DISCUSSION

Fig. 1a shows the conversion pattern detected by CF-FAB-MS when DYN A was used as a substrate. The most abundant peak at *m/z* 713 was identified as DYN A_{1-6} (YGGFLR), suggesting that the heptadecapeptide is initially split into two fragments: DYN A_{1-6} and DYN A_{7-17} (RIRPKLKWDNQ, *m/z* 1455). The secondary cleavage was observed between Lys^{11}-Leu^{12}, which leads to the formation of two fragments: DYN A_{7-11} (RIRPK, *m/z* 669) and DYN A_{12-17} (LKWDNQ, *m/z* 804). The question remains open as to whether DCE recognized the Arg^6–Arg^7 stretch as a primary target or whether both events occur simultaneously. Detailed studies require time-dependent experiments which were not the aim of this work. DYN A itself was not observed in the mass spectrum as it was completely converted, nor was any signal recorded at *m/z* 555 belonging to DYN A_{1-5} (YGGFL), *i.e.* Leu-enkephalin, which is probably formed by the sequential action of DCE and a carboxypeptidase B-like enzyme [10]. The pituitary enzyme recognizes the C-terminal side of the basic amino acids, but its specificity seems to be limited to certain recognition sites as it does not process the bond between Arg^9-Pro^{10} and Lys^{13}-Trp^{14}. The signal at *m/z* 713 is ambiguous, as it can also be formed by the fragment DYN A_{5-9} (LRRIR), but the HPLC data and the specific RIA confirm that DYN A_{1-6} is, in fact, present in the incubation mixture.

The fragments obtained after degradation were also analysed on the reversed-phase HPLC combined with a photodiode-array UV detector. Using this technique, three fragments were resolved (data not shown) and the spectra of the two most intense peaks (eluting at retention times of 14 and 20 min) recorded in the range 190–320 nm (Fig. 1b). The peak, eluted at a retention time of 20 min, contains tyrosine, which gives a characteristic maximum around 276 nm, returning to the baseline at 290 nm [11]. Thus, this peak can be identified as the fragment. DYN A_{1-6}, and RIA measurement revealed that the peak eluting at 20 min belongs to Leu-enkephalin-Arg^6. The second component eluting at 14 min is probably identical to the fragment DYN A_{7-17}, as its second maximum returns to baseline at 310 nm (Fig. 1b), which is characteristic for tryptophan [11].

When a reaction mixture of DYN B incubated with the same proteinase was analysed by CF-FAB-MS, only two fragments, at *m/z* 712 and 876, respectively, were observed (Fig. 2a), supporting the indication that in this case the major conversion

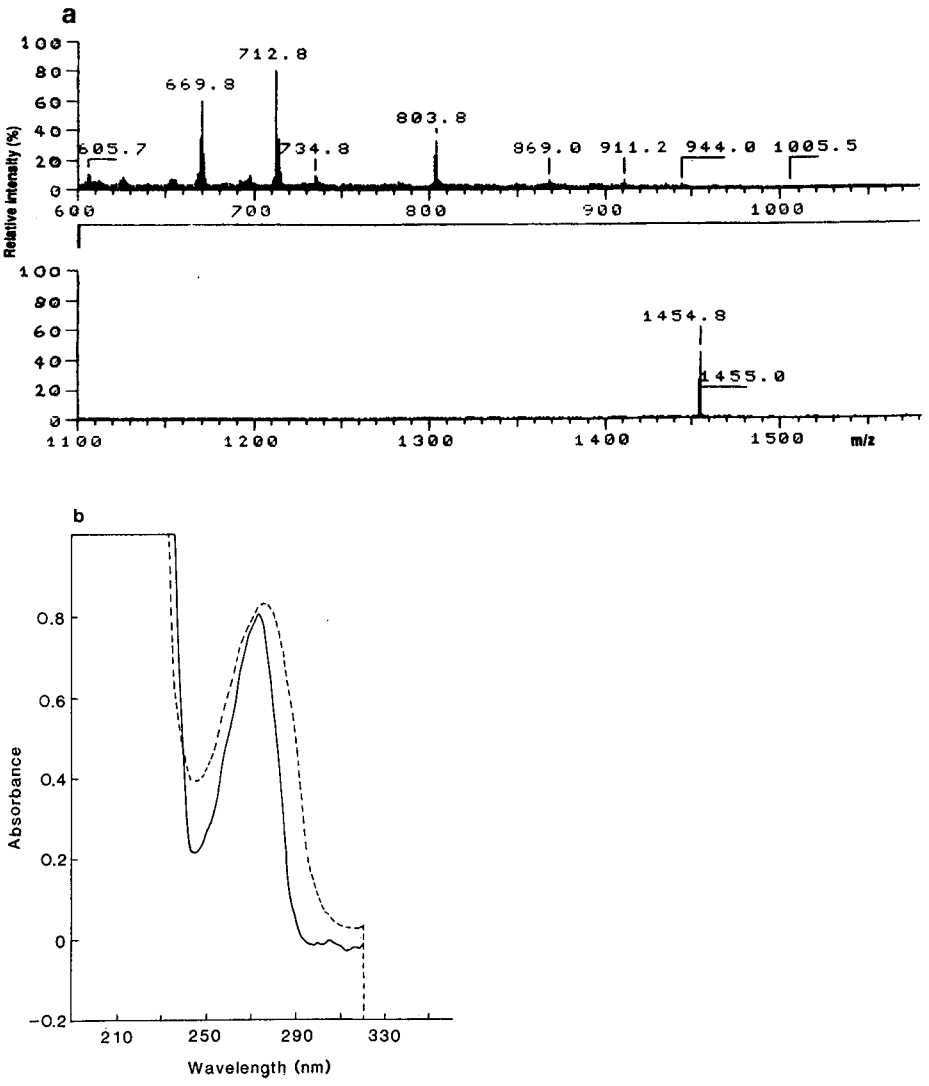

Fig. 1. Analysis of the dynorphin A fragments. (a) CF-FAB mass spectrum of the peptides obtained during conversion by pituitary DCE. DYN A itself was completely processed by the enzyme. (b) Enhanced spectra of the particular fragments containing tyrosine or tryptophan taken within the range 190–320 nm. The spectra were recorded during reversed-phase HPLC separation of the reaction mixture of DYN A and pituitary DCE. The solid line represents the peak containing tyrosine, eluting at a retention time of 20 min, whereas the broken line corresponds to the peak (containing tryptophan) eluting at 14 min. Separation conditions are given in the text.

product is DYN B_{1-6} (YGGFLR) without any secondary cleavage. This is in contrast to the findings when DYN A was served as a substrate. The other ion is formed by DYN B_{7-13} (RQFKVVT). These results were confirmed by HPLC studies (Fig. 2b), where three major peaks were found when the chromatogram was taken at 214

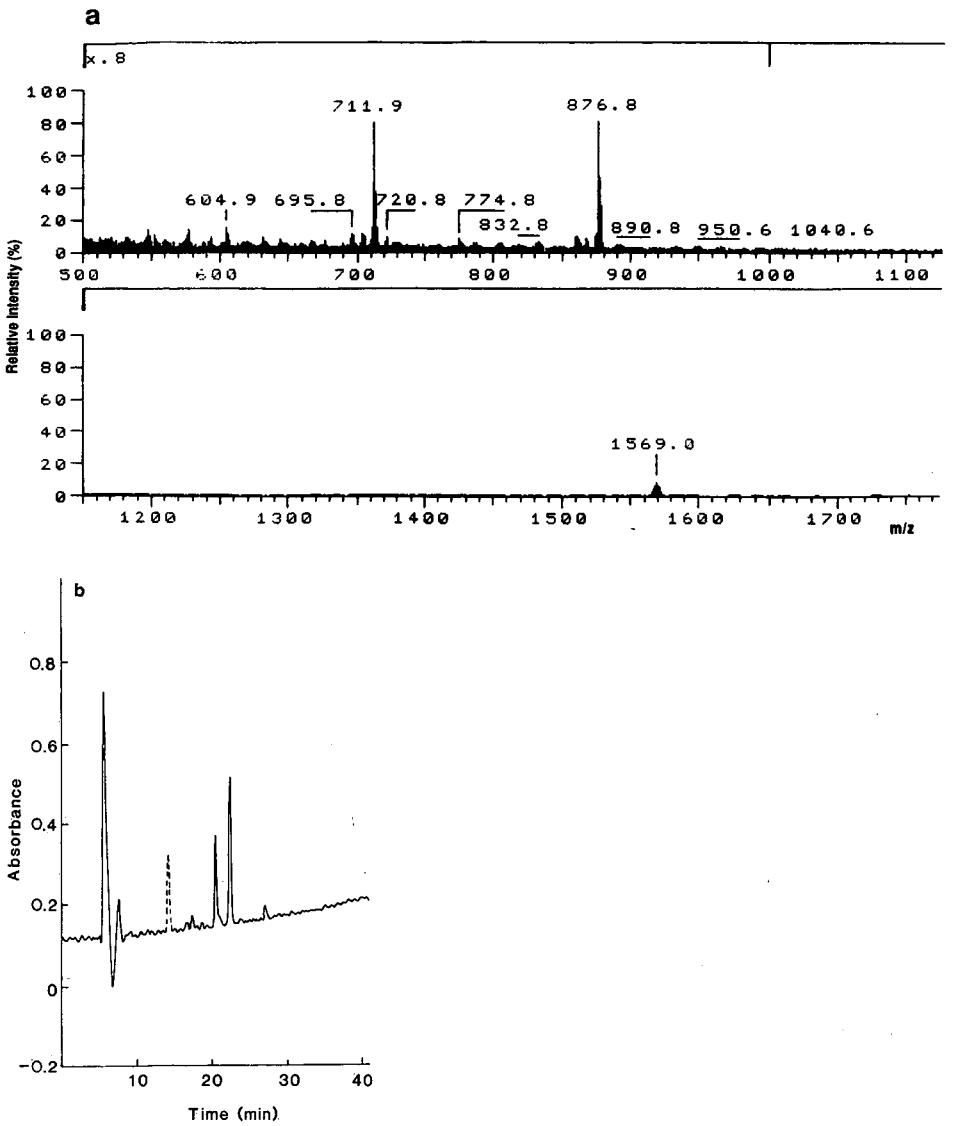

Fig. 2. Analysis of the dynorphin B fragments following conversion of the tridecapeptide by pituitary DCE. (a) CF-FAB mass spectrum of the converted fragments. (b) Reversed-phase HPLC chromatograms, taken at 214 (broken line) and 276 (solid line) nm. (Note that the peak eluted at 14 min belongs to DYN B_{7-13}, which does not contain tyrosine). For further details, see text.

nm. However, the same separation recorded at 276 nm (which is the wavelength characteristic for tyrosine) shows only two peaks, eluted at 20 and 22 min, respectively. The DYN B structure contains only one tyrosine located at the N-terminus and the peak with the retention time of 14 min thus belongs to DYN B_{7-13}, which also correlates with the FAB-MS data.

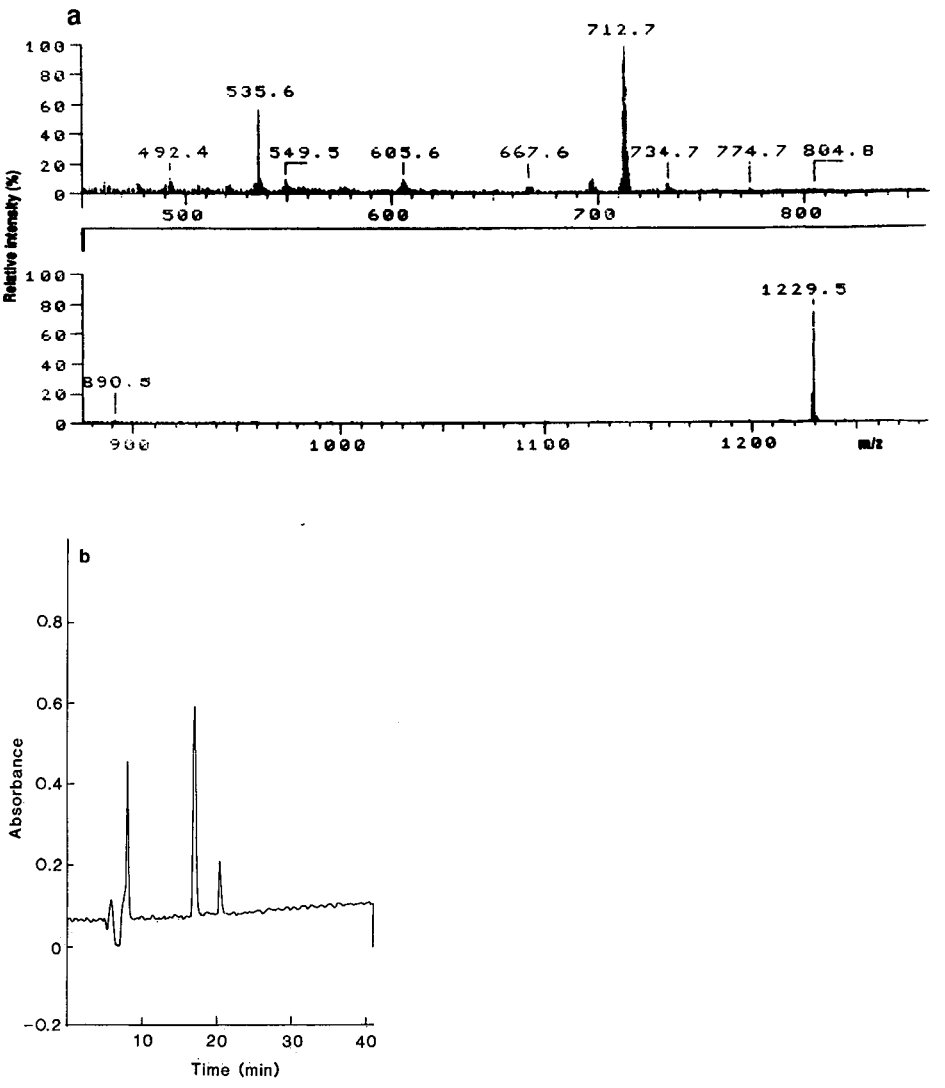

Fig. 3. Analysis of the α-neoendorphin fragments released by the pituitary DCE. (a) CF-FAB mass spectrum of the converted fragments. (b) Chromatogram taken at 276 nm following reversed-phase HPLC. A detailed description of the separation conditions is given in the text.

The data given in Fig. 3a indicate that α-neoendorphin (ANEO) is converted directly to YGGFLR (*m/z* 713) and KYPK (*m/z* 535). No other cleavage sites were recorded. It should be noted that in this study all the peptides were incubated with the pituitary DCE for the same time interval. Therefore, ANEO seems to be a poorer substrate than DYN A, as the molecular ion corresponding to unaltered ANEO (*m/z* 1229) is still present in the spectrum. This observation was corfirmed by the analysis of the reaction mixture by reversed-phase HPLC. Thus, the chromatogram, taken at 276 nm (Fig. 3b), also shows three peaks, eluting at 8, 17 and 20 min, respectively.

This result suggests that all fragments contain a tyrosine residue in their structure, which was confirmed by enhancing the spectral range around 276 nm (data not shown). The absorbance profiles were identical, returning to baseline at around 290 nm, thus indicating the same aromatic components in all structures. Retention data as well as the RIA for $ANEO_{1-6}$ (or Leu-enkephalin-Arg^6) revealed that the peak eluting at 8 min belongs to $ANEO_{7-10}$, which has the lowest hydrophobicity index, and the two others to the unconverted decapeptide (17 min) and $ANEO_{1-6}$ (20 min), respectively.

It can be seen from this study that the different techniques applied have been of great use for the identification of the peptide bonds hydrolysed by the pituitary enzyme. A common cleavage site of all the substrates seems to be located between their dibasic stretch, resulting in the release of Leu-enkephalin-Arg^6, which is the common N-terminal sequence of all the prodynorphin-derived opioid peptides. A secondary cleavage sites was only observed for dynorphin A.

Several converting and degrading enzymes from human cereborspinal fluid and spinal cord capable of cleaving prodynorphin-derived peptides to enkephalins have recently been reported [12]. In these studies, however, the completed fragmentation patterns could not be detected as the only quantitative and reliable method was simple HPLC and an RIA towards DYN A_{1-6}. The latter technique allows the measurement of one or two peptides with high precision, whereas no other fragments are detected and detailed studies on, for example, the ratio between various reaction products are difficult or even impossible. Investigations on the specificity of proteinases recovered from the CNS are also difficult as a result of the limited availablity of tissues or body fluids. The HPLC technique utilizes at least a ten-fold higher amount of the enzyme and at least 100 times more of the substrate than the RIA detection, which might influence the final results due to minor contaminants or the "non-physiological" concentrations of the reagents. This work has described the applications of CF-FAB-MS for the rapid and efficient screening of the cleavage sites of several neuropeptides converted by a pituirary proteinase. HPLC combined with photodiode-array UV detection was applied complementary to the FAB-MS technique. The enzyme action seems to be dependent on the applied substrate, regardless of the presence of a dibasic stretch in all structures, as well as the identical N-terminal fragment YGGFLR. This fact might be of physiological importance during maturation of the bioactive fragments. The samples were analysed directly without prior purification, which significantly simplifies the procedure.

An interesting application of FAB-MS to study peptide fragments directly on the probe after enzymatic cleavage was reported by Hafok-Peters *et al.* [13]. In that work the tryptic or chymotryptic fragments of genetically engineered interferon could be identified. The sensitivity of this technique can be comparable with the RIA method in certain cases, thus this procedure requires only minor amounts of all reagents, whereas spectral analysis with the aid of HPLC photodiode-array detectors which require much higher sample amounts, can be complementary to CF-FAB-MS for the determination of ambiguous fragments [8].

CONCLUDING REMARKS

In this work CF-FAB-MS and HPLC with diode-array UV detection were used

to study the cleavage pattern of a pituitary enzyme acting on prodynorphin-derived opioid peptides. In combination these techniques provide a rapid procedure with a high precision for the identification of peptide fragments with aromatic amino acid residues. It is therefore suggested that, when a sufficient amount of sample is available, the possible incorporation of a photodiode-array UV detector into the HPLC–MS system may give a powerful tool for the assessment of definite cleavage sites in substrate peptides containing these particular residues.

ACKNOWLEDGEMENTS

This work was supported by Göran Gustavssons Stiftelse, the Swedish Board for Technical Development, Ulf Lindahl's Foundation and the Swedish Medical Research Council Grant 03X-9459.

REFERENCES

1 A. J. Barrett (Editor), *Proteinases in Mammalian Cells and Tissues*, North-Holland, Amsterdam, 1977.
2 M. J. Millan, *Trends Pharmacol. Sci.*, 11 (1990) 70.
3 L. Terenius and F. Nyberg, *Int. Rev. Neurobiol.*, 30 (1988) 101.
4 S. Naylor, F. Findeis, B. W. Gibson and D. H. Williams, *J. Am. Chem. Soc.*, 108 (1986) 6359.
5 R. M. Caprioli, *Biochemistry*, 27 (1988) 513.
6 J. Silberring and F. Nybereg, *J. Biol. Chem.*, 264 (1989) 11082.
7 R. M. Caprioli, T. Fan and J. S. Cottrell, *Anal. Chem.*, 58 (1986) 2949.
8 J. Silberring and F. Nyberg, *J. Chromatogr.*, 562 (1990) 459.
9 F. Nyberg, Ch. Pernow, U. Moberg and R. B. Eriksson, *J. Chromatogr.*, 359 (1986) 541.
10 S. M. Strittmatter, D. R. Lynch and S. H. Snyder, *J. Biol. Chem.*, 259 (1984) 11812.
11 J. Escribano, M. Asuncion, J. Miguel, L. Lamas and E. Mendez, *J. Chromatogr.*, 512 (1990) 255.
12 F. Nyberg and J. Silberring, *Progr. Clin. Biol. Res.*, 20 (1990) 261.
13 Ch. Hafok-Peters, I. Maurer-Fogy and E. R. Schmid, *Biomed. Envrion. Mass Spectrom.*, 19 (1990) 159.

Journal of Chromatography, 554 (1991) 91–101
Elsevier Science Publishers B.V., Amsterdam

CHROMSYMP. 2182

Application of microcolumn liquid chromatography–continuous-flow fast atom bombardment mass spectrometry in environmental studies of sulfonylurea herbicides

R. W. REISER*, A. C. BAREFOOT, R. F. DIETRICH, A. J. FOGIEL, W. R. JOHNSON and M. T. SCOTT

E. I. du Pont de Nemours and Company, Agricultural products Department, Experimental Station, Wilmington, DE 19880-0402 (USA)

ABSTRACT

The use of 0.25-mm I.D. packed capillary liquid chromatography columns coupled with continuous-flow fast atom bombardment (FAB) mass spectrometry has proven to be a very valuable technique, especially for the identification of unknown sulfonylurea herbicide metabolites. Several new and unusual heterocycle ring-opened metabolites and hydrolysis products were identified, and metabolic pathways were proposed. Typical column flow-rates are 1–2 μl/min, which allows direct coupling with no sample splitting. This is important in our metabolite identification work, since we are usually sample-limited. Techniques for increasing injection volume to allow analyses of dilute solutions and the use of polymeric packing for separation of polar metabolites are discussed. The FAB mass spectra usually provide unequivocal molecular weights and structurally useful fragments ions, which often allows structure assignments on exceedingly small quantities of isolated metabolites.

INTRODUCTION

The environmental impact of crop protection chemicals is of growing concern, and DuPont is developing many new environmentally safe agricultural products. These new products are very specific to the target organisms, have very low use rates and break down rapidly in the environment. Prime examples of these new products are the sulfonylurea herbicides, which have use rates 100-fold less than earlier herbicides and are metabolized extensively in plants, animals and soil [1]. These herbicides were first introduced by DuPont in 1982, and we now have developed and introduced nine new sulfonylureas. These compounds act on an enzyme found only in plants [1], and have no significant toxicity to animals or other non-target organisms.

The low use rate and extentisive breakdown of the sulfonylurea herbicides requires very sensitive analytical techniques for identification of their environmental metabolites, since only very small quantities of metabolites are isolated. These compounds are extremely thermally labile, precluding their analysis by gas chromatography (GC)–mass spectrometry (MS). Attempts at derivatization prior to GC–MS have

0021-9673/91/$03.50

been unsuccessful due to chemical breakdown during derivatization or thermal instability of the derivative. The method of choice for identification of sulfonylurea herbicide metabolites is liquid chromatography (LC)–MS [2]. Since these compounds are very temperature-sensitive, their mass spectra typically show very weak or no molecular ions with electron ionization, chemical ionization and thermospray ionization when the thermospray vaporizer temperature is set for optimum sensitivity [2]. A low-temperature mass spectral ionization technique, such as fast atom bombardment (FAB) or electrospray–ion spray [3], is needed to obtain prominent molecular ions for unequivocal molecular-weight assignments.

Miniaturization of the LC column gives increased mass sensitivity, since the minimum amount detectable is directly proportional to the square of the column radius [4]. Use of a 0.25 mm I.D. packed capillary column will give a 300-fold increase in sensitivity over a conventional 4.6 mm I.D. column, and the low flow-rates facilitate MS interfacing. In previous work, the use of 0.25 mm I.D. packed fused-silica LC columns allowed us to obtain improved performance in reversed-phase LC–MS analyses with a moving belt interface [5–7]. The 1–2-μl/min flow-rates used with these columns are ideally suited to interfacing with continuous-flow FAB, since no effluent splitter or make-up flow are required [7–9].

A further advantage of micro- over conventional LC columns is that the 1000-fold reduction in solvent consumption greatly reduces costs and solvent waste.

In previous work [9], the utility of microcolumn LC interfaced with continuous-flow FAB-MS for the identification of microbial metabolites of sulfonylurea herbicides was demonstrated, using the soil bacterium *Streptomyces griseolus*. Crude broth extracts were injected directly. Identification of plant, animal or soil metabolites typically requires some cleanup, since these extracts are more complex mixtures.

This paper shows the utility of LC–FAB-MS for the identification of sulfonylurea herbicide metabolites obtained in environmental studies.

EXPERIMENTAL

A Beckman (Berkeley, CA, USA) Model 114M LC pump was used in the constant pressure mode. Column pressures were typically 100–200 bar to obtain flow-rates of 1–2 μl/min. A Valco (Houston, TX, USA) Model C14W submicroliter injection valve was used with a 0.1-μl rotor. Fused-silica columns (J&W Scientific, Folsom, CA, USA), 30 cm × 0.25 mm I.D. were slurry packed as described in ref. 5 with 3-μm Zorbax ODS (DuPont, Wilmington, DE, USA), Nucleosil ODS (Macherey-Nagel, Düren, Germany), Spherisorb ODS-2 (Phase Sep, Norwalk, CT, USA) or 10- and 5-μm PRP-1 (Hamilton, Reno, NV, USA). The transfer line (epoxy glued into the column prior to packing) was 0.025 mm I.D. 0.195 mm O.D. fused-silica tubing (Polymicro Technologies, Phoenix, AZ, USA). An Isco (Lincoln, NE, USA) Model CV4 ultraviolet (UV) detector was used on-line at 238 nm wavelength. A 1-cm length of the polyimide coating on the 0.025 mm I.D. fused-silica transfer line was burned off to serve as the UV detector cell. Teflon (polytetrafluoroethylene) tubing of 0.18 mm I.D., 1.6 mm O.D. (Alltech Stock No. 35676) was cut into 5-mm lengths to serve as unions in the transfer line before and after the UV detector. The Teflon tubes were reamed out with a short length of transfer line, then cleaned with solvent prior to use. The continuous-flow FAB probe was designed and fabricated in our laboratory and is

interchangeable with a moving-belt interface, as described in ref. 7. A Finnigan MAT Model 8230 magnetic-sector mass spectrometer was used with an Ion Tech FAB gun using xenon gas and 8-kV anode voltage. The ion source temperature was 200°C, which heats the FAB target by radiation to 45–50°C. Typical MS parameters were: resolution, 1000; source ion gauge reading, $4 \cdot 10^{-4}$ mm; scan rate, 10 s/decade; mass range, 95–650.

RESULTS AND DISCUSSION

System description

Incorporation of an on-line UV detector is especially important when working with low-molecular-weight (below 500) compounds. The glycerol matrix ions are more intense at lower mass, making detection of trace level LC peaks in the reconstructed ion current chromatogram difficult. The Isco CV4 UV detector was designed for capillary zone electrophoresis, but works well for micro-LC.

The lifetime of packed capillary LC columns in our laboratory is typically 2–6 months. Since we often inject biological extracts which leave material at the head of the column that can cause a loss in performance, we periodically cut off 0.5–1 cm from the head of the column to restore performance. All analyses were carried out using isocratic conditions, with acetonitrile (0–70%)–water (pH 3, formic acid)–10% or 5% glycerol (FAB matrix). In most cases, gradient elution was not essential since the samples were cleaned up by preparative LC or solid-phase extraction. Addition of glycerol to the mobile phase has caused no problems with the chromatography or LC pump. Initial work was carried out using 10% glycerol in the mobile phase. Reduction to 5% glycerol gave better stability and chromatographic performance, likely due to obtaining a thinner film of glycerol on the FAB target.

Injection techniques for dilute solutions

Although microcolumns increase mass sensitivity, there is no increase in concentration sensitivity [3] since the injection volume must be reduced in proportion to the column diameter to avoid band broadening. In conventional LC, increased concentration sensitivity is obtained by dissolving the analyte in a weak LC solvent (high percentage of water) which allows injection of a large volume, since the analytes concentrate at the head of the column if they are non-polar to moderately polar. We have used this same technique in micro-LC to allow injection of 1–2-μl volumes. Another technique we have developed for analyses of dilute solutions for identification of small quantities is to dissolve the sample in a volatile solvent, such as acetonitrile or methanol, and coat 1–5 μl onto the groove in the Valco 0.1-μl rotor [5–7]. The coated rotor is held in the "inject" position for 10 s. While this technique worked well with the moving-belt interface (*ca.* 80% recovery of analytes), we obtained low recoveries (*ca.* 5%) using the standard W rotor (Valcon S, polyphenylene sulfide) in the FAB mode, apparantly due to the 10% glycerol in the mobile phase preventing efficient removal of analytes from the rotor. We evaluated rotors obtained from Valco made from three other materials: WF (polyether–Teflon), WT (Vespel polyimide) and WP (polyphenylene sulfide cross-linked with Teflon), and obtained good recoveries (50–70%) only with the WP rotor. Recoveries were determined by injecting ^{14}C-labelled compounds, and collecting the peaks for liquid scintillation counting.

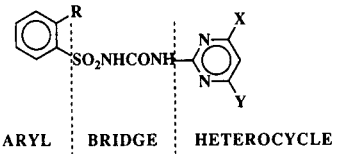

Fig. 1. General structure of sulfonylurea herbicides.

Polymeric column packings

We evaluated the use of PRP-1 (polysterene–divinylbenzene copolymer) column packing for separating polar metabolites. Initially we prepared a 30-cm column using 10-μm particles. Efficiency was poor (1800 theoretical plates), but peaks were symmetrical and selectivity was good. We were able to obtain on-column concentration of polar compounds by dissolving the sample in a weak LC solvent (90% water), allowing injection of 1–2-μl volumes. Addition of 5% glycerol to the sample solvent was necessary to maintain FAB stability during elution of the solvent. We recently obtained 5-μm PRP-1 packing, and prepared a 30-cm column which had 10 000 theoretical plates.

Chromatography of sulfonylurea herbicides

A general structure of sulfonylurea herbicides is shown in Fig. 1. The sulfonylurea bridge portion of the molecule is quite labile. The bridge cleaves thermally and hydrolytically on both sides of the carbonyl to give the aryl sulfonamide and heterocycle amine.

A separation of eight sulfonylurea herbicides is presented in Fig. 2. This sep-

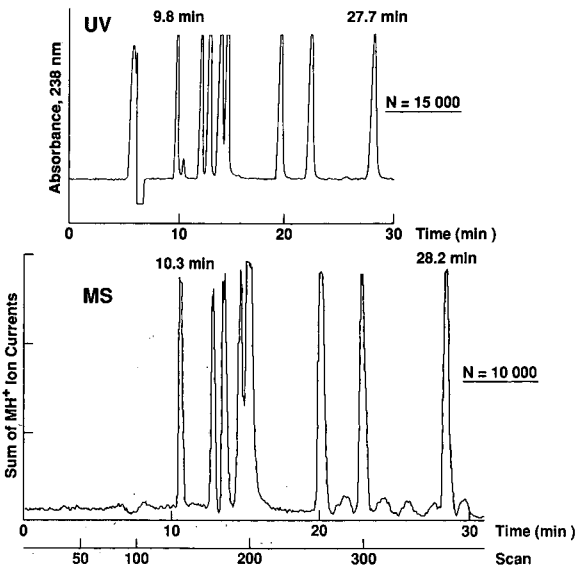

Fig. 2. Separation of eight sulfonylurea herbicides (50 ng/peak). In order of elution, the active ingredients in: Accent, Harmony, Ally, Glean, Oust, Londax, Express and Classic. Column: 27 cm × 0.25 mm I.D. Spherisorb ODS-2 (3 μm). Mobile phase: acetonitrile–water (pH 3, formic acid)–glycerol (50:40:10).

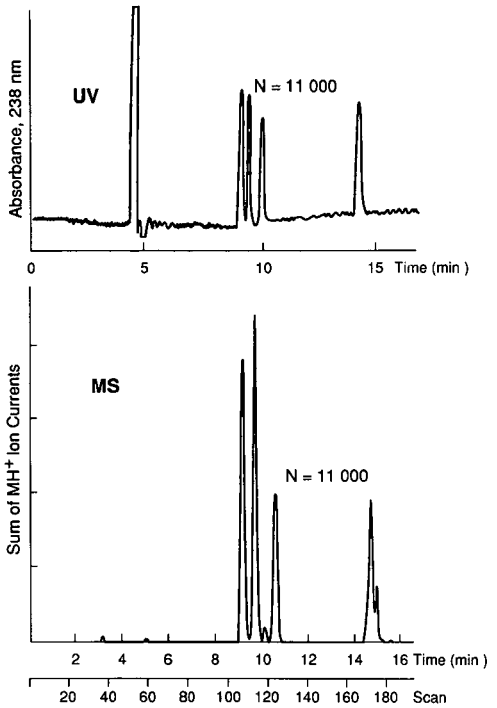

Fig. 3. Separation of four sulfonylurea herbicides (10 ng/peak). In order of elution, the active ingredients in: Harmony, Ally, Glean and Londax. Column: 20 cm × 0.25 mm I.D. Spherisorb ODS-2. Mobile phase: acetonitrile–water–glycerol (50:45:5).

aration was obtained by injection of 0.1 μl of a 0.5-μg/μl solution of each component in acetonitrile–water (50:50, 50 ng/peak), with the UV detector on-line. The LC retention times in the MS-extracted ion chromatogram (sum of protonated molecular ions) are 0.5 min later than those obtained with the UV detector, due to the 1-m length of 0.025 mm I.D. transfer line between the UV and MS (0.5-μl volume). The theoretical plate count (N) obtained on the last-eluting peak dropped from 15 000 with the UV detector to 10 000 with the MS. Most of the drop in plate count appears to be due to slow desorption off the FAB target, since when we reduced the glycerol level in the mobile phase from 10% to 5%, there was no difference in efficiency between the UV and MS chromatograms. This is illustrated in Fig. 3, a separation of four sulfonylurea herbicides at the 10 ng/peak level (we routinely obtain strong, good-quality FAB mass spectra on 10 ng/component injected into the LC) obtained using 5% glycerol in the mobile phase. N values of 11 000 were determined on the third-eluting peak on both the UV and MS chromatograms. These data also show there is no significant band spreading in the transfer line between the UV and MS.

As in GC–MS, plotting the individual mass chromatograms allows one to use the MS as a multiple-ion detector to effectively improve the chromatographic resolution.

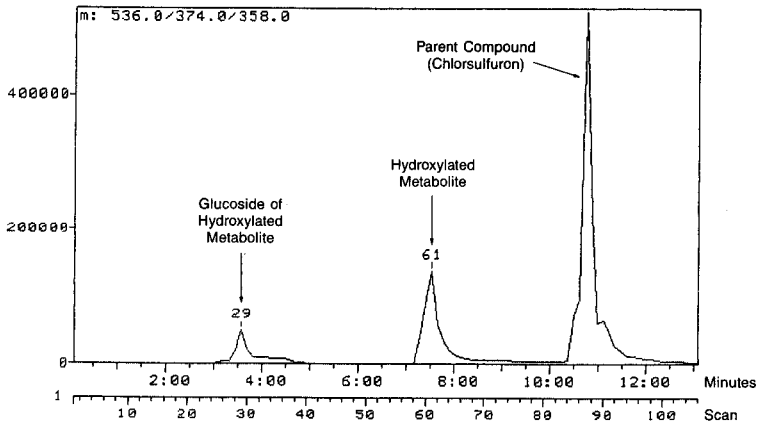

Fig. 4. Separation of chlorsulfuron and two wheat metabolites (extracted-ion current of the protonated molecular ions, *m/z* 536, 374, 358). Column as in Fig. 1. Mobile phase: acetonitrile–water–glycerol (40:50:10).

Chlorsulfuron wheat metabolites

Most sulfonylurea herbicides are selective for a particular crop, *i.e.*, they kill weeds but do not harm the crop. The basis of selectivity is mainly due to rapid conversion to inactive metabolites by the crop plant, but not by weeds [1]. For example, chlorsulfuron, the active ingredient in Glean herbicide, is used to control weeds in wheat and other cereal crops. It is rapidly metabolized in wheat plants by hydroxylation on the phenyl ring, followed by conjugation with glucose. Fig. 4 shows the extracted-ion chromatogram of the protonated molecular ions obained on a mixture of chlorsulfuron and the two wheat metabolites. Fig. 5 shows the background-subtracted FAB mass spectra obtained on chlorsulfuron and the wheat metabolites. The protonated molecular ion is the base peak in all three spectra, and all show prominent fragment ions, typical of sulfonylureas, due to the protonated triazine amine, isocyanate and urea. These fragments show there was no change in the triazine portion of the molecules, which helps elucidate their structures.

Chlorsulfuron hydrolysis products

In aqueous hydrolysis studies at pH 5 with [^{14}C]chlorsulfuron, five degradation products were formed. The products were separated and purified by preparative LC, and identified by LC–FAB-MS. Proposed hydrolysis pathways, given in Fig. 6, are based on chemically logical hydrolysis reactions involving cleavage of the sulfonylurea bridge or *O*-demethylation followed by hydrolytic cleavage of the triazine ring. Identification of the sulfonamide, triazine amine and O-desmethylchlorsulfuron products were confirmed by comparison of LC retention times and FAB mass spectra with synthetic standards, using a 27-cm Zorbax ODS column and an acetonitrile–water–glycerol (50:40:10) mobile phase. The FAB mass spectra of the triazine amine and sulfonamide showed only the protonated molecular ions and glycerol adduct ions with no significant fragment ions, while the spectrum of O-desmethylchlorsulfuron shows the fragment ions expected from demethylation on the triazine portion of the molecule.

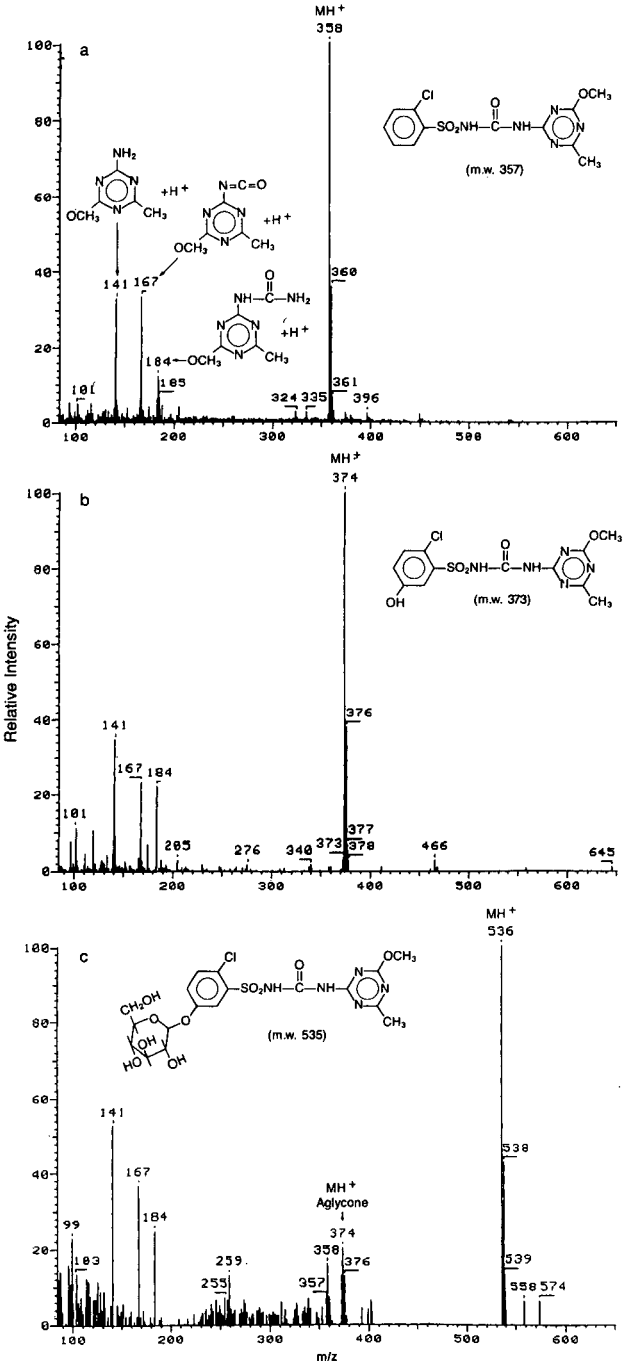

Fig. 5. FAB mass spectra of (a) chlorsulfuron; (b) hydroxylated chlorsulfuron wheat metabolite; and (c) glucoside wheat metabolite. m.w. = Molecular weight.

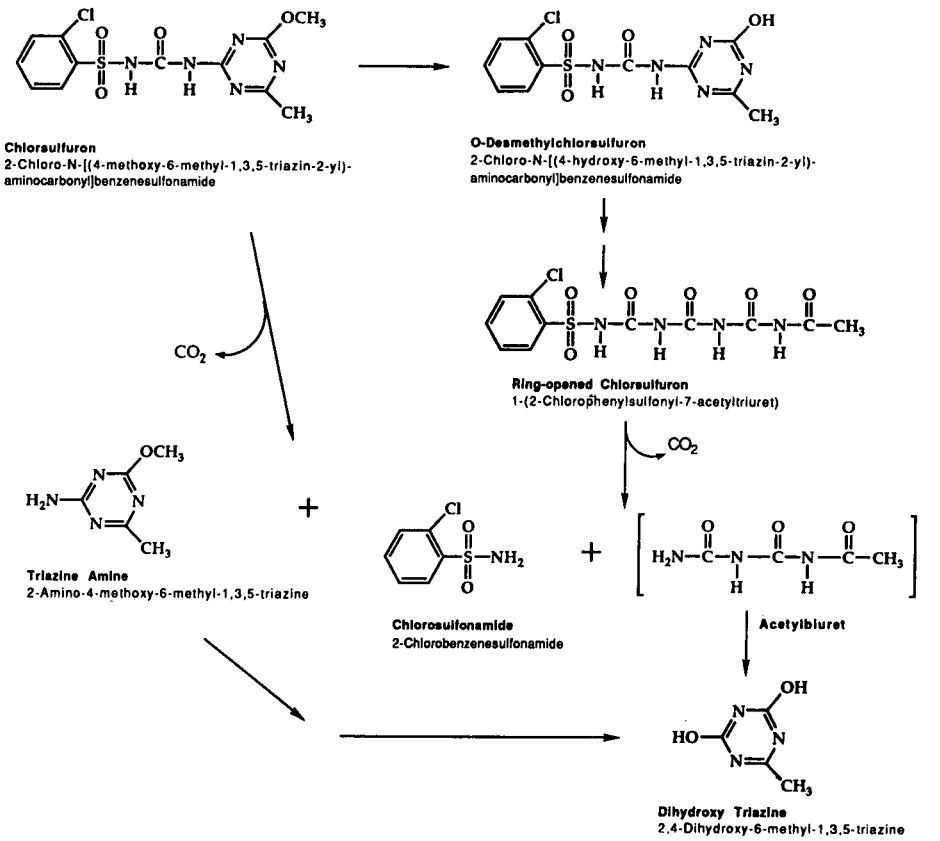

Fig. 6. Proposed hydrolytic degradation pathways for chlorsulfuron at pH 5.

The FAB mass spectrum of the triazine ring-opened product (Fig. 7) shows it is a monochloro compound of molecular weight 362, an unusual 5 mass units higher than the parent compound. Lack of heterocycle fragment ions indicates a major change in this portion of the molecule. NMR data showed four aromatic protons and an acetyl methyl, consistent with the proposed structure. This novel compound forms from O-desmethylchlorsulfuron by cleavage of the triazine ring in a two-step hydrolysis process.

Initial analyses of the most polar hydrolysis product, the dihydroxy methyl triazine, were unsuccessful since it eluted near the void volume of the ODS column and sample contaminants suppressed its ionization. Analysis of this sample on a PRP-1 column (30 cm × 0.25 mm I.D., 10 μm) resulted in a separation of the polar product from the contaminants, and its FAB mass spectrum showed a prominent protonated molecular ion at m/z 128. The structure was confirmed by electron impact probe/library search on a more purified sample.

Bensulfuron methyl poultry metabolites

Three unknown poultry metabolites of bensulfuron methyl, the active ingredient in Londax and Mariner rice herbicides, were purified by preparative LC and

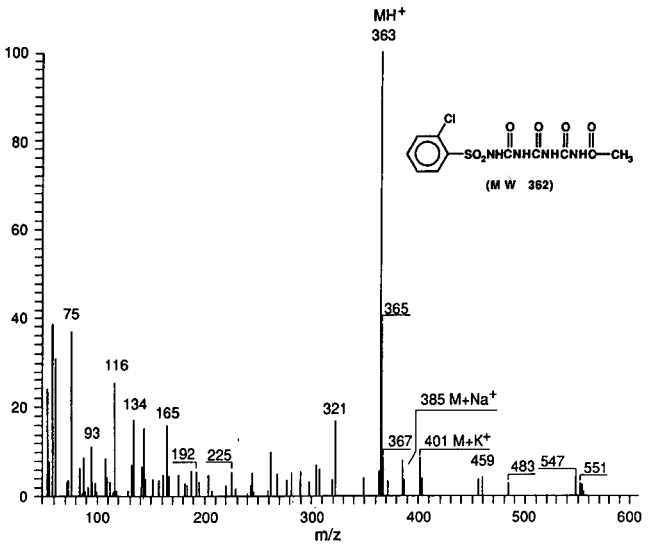

Fig. 7. FAB mass spectrum of triazine ring-opened chlorsulfuron hydrolysis product. MW = molecular weight.

identified by LC–FAB-MS. A proposed metabolic pathway is given in Fig. 8. These metabolites were obtained in separate studies using [^{14}C]phenyl-labelled bensulfuron methyl and pyrimidine-2-^{14}C-labelled bensulfuron methyl. A Spherisorb ODS-2 mi-

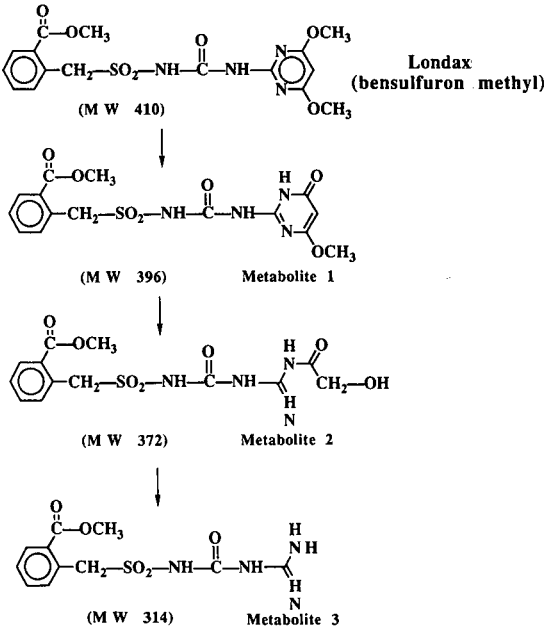

Fig. 8. Proposed metabolic pathway for bensulfuron methyl poultry metabolites.

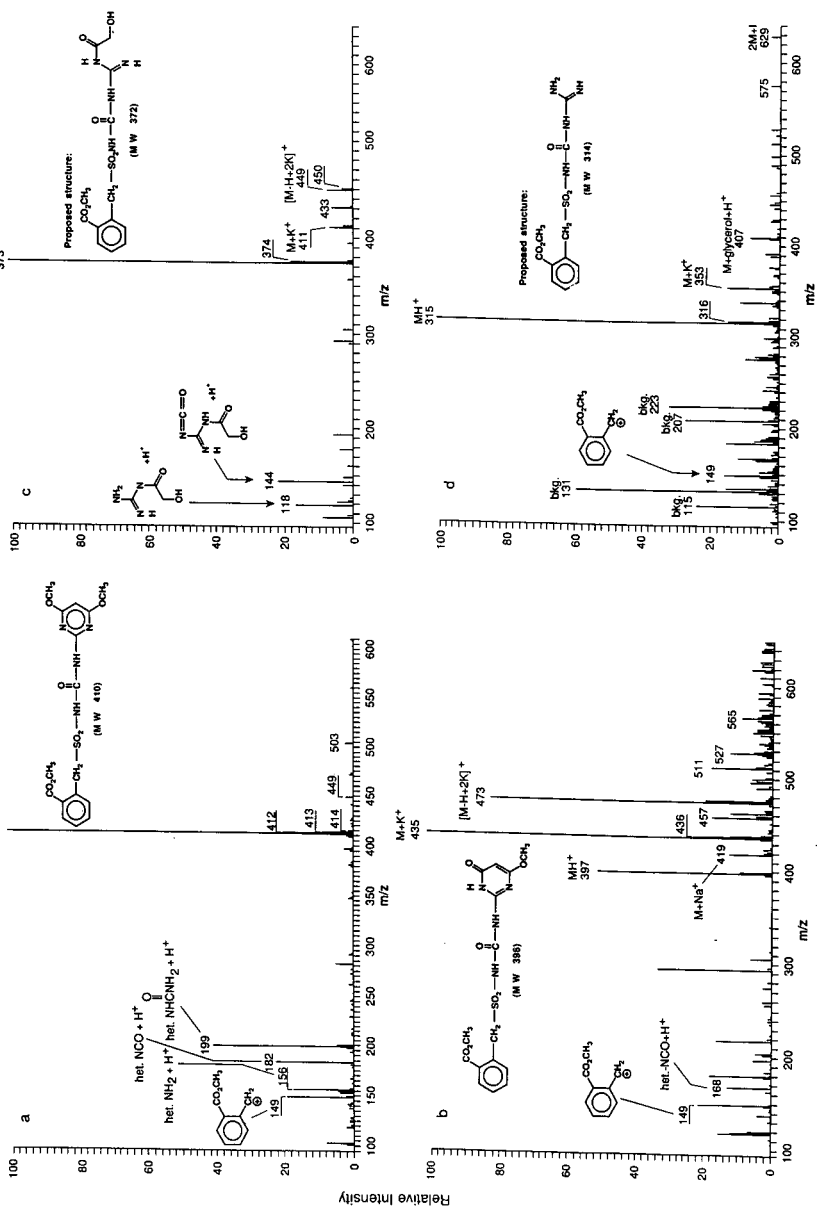

Fig. 9. FAB mass spectra of (a) bensulfuron methyl; (b) poultry metabolite **1**; (c) poultry metabolite **2**; and (d) poultry metabolite **3**.

crocolumn (27 cm × 0.25 mm I.D.) was used with an acetonitrile–water–glycerol (50:40:10) mobile phase. Bensulfuron methyl eluted at 24 min, metabolite **1** at 8.7 min and metabolite **2** at 9.2 min. Metabolite **3** eluted near the void volume (*ca.* 6 min) on the ODS columns, and did not give a spectrum due to suppression of ionization by coeluting impurities. Use of a PRP-1 column was again successful in separating the metabolite from contaminants and allowed us to obtain a FAB spectrum. The spectrum of the parent (Fig. 9a) shows the protonated molecular ion as base peak, the expected protonated heterocycle fragments and a significant aryl fragment at *m/z* 149. This aryl fragment, likely a tropylium ion, appears in the spectra of all three metabolites, showing there is no change in this portion of the molecule. The spectrum of metabolite **1** (Fig. 9b) shows a prominent MH^+ ion and atypically strong potassium ion adducts, indicating the sample contained potassium. The spectrum of metabolite **2** (Fig. 9c) shows the MH^+ as base peak, and protonated fragments of the ring-opened pyrimidine portion of the molecule in support of the proposed structure. The spectrum of metabolite **3** (Fig. 9d), obtained using the PRP-1 column, shows it has a molecular weight of 314. The proposed structure was confirmed by comparison of its FAB mass spectrum with that obtained on a synthetic sample.

The proposed metabolic pathway is based on a logical sequence of metabolic reactions, *i.e.*, demethylation (metabolite **1**), oxidation–hydrolytic ring-opening–decarboxylation (metabolite **2**) and hydrolysis (metabolite **3**).

CONCLUSIONS

Microcolumn LC coupled with continuous-flow FAB-MS has proven to be a practical technique for the identification of sulfonylurea herbicide metabolites and degradates. High-quality, strong-intensity FAB mass spectra are routinely obtained on 10 ng (25 Pmol) quantities injected into the LC system. Use of this technique has facilitated the identification of many intractable compounds, and has provided information that was previously impossible or very difficult to obtain.

REFERENCES

1 E. M. Beyer, M. J. Duffy, J. V. Hay and D. D. Schlueter, *Herbicides: Chemistry, Degradation and Mode of Action*, Vol. 3, Marcel Dekker, New York, 1987, Ch. 3.
2 L. M. Shalaby and R. W. Reiser, in C. N. McEwen and B. S. Larsen (Editors), *Mass Spectrometry of Biological Materials*, Marcel Dekker, New York, 1990, Ch. 11.
3 E. C. Huang, T. Wachs, J. J. Conboy and J. D. Henion, *Anal. Chem.*, 62 (1990) 713A.
4 R. P. W. Scott, *Small Bore Liquid Chromatography Columns: Their Properties and Uses*, Wiley-Interscience, New York, 1984, Ch. 1, pp. 17–19.
5 A. C. Barefoot and R. W. Reiser, *J. Chromatogr.*, 398 (1987) 217.
6 A. C. Barefoot and R. W. Reiser, *Biomed. Environ. Mass Spectrom*, 18 (1989) 77.
7 A. C. Barefoot, R. W. Reiser and S. A. Cousins, *J. Chromatogr.*, 474 (1989) 39.
8 R. W. Reiser, presented at the *37th ASMA Conference on Mass Spectrometry and Allied Topics, Miami Beach, FL, May 21–26, 1989.*
9 R. W. Reiser and B. Stieglitz, in R. M. Caprioli (Editor), *Continuous-Flow Fast Atom Bombardment Mass Spectrometry*, Wiley, Chichester, 1990, Ch. 8.3.

Journal of Chromatography, 554 (1991) 103–118
Elsevier Science Publishers B.V., Amsterdam

CHROMSYMP. 2354

Quantitation and linearity for particle-beam liquid chromatography–mass spectrometry

ALEX APFFEL*
Scientific Instruments Division, Hewlett-Packard Co., 1601 California Avenue, Palo Alto, CA 94304 (USA)
and
MARY LAURA PERRY
Department of Chemistry, Virginia Polytechnic Institute and State University, Blacksburg, VA 24061 (USA)

ABSTRACT

Quantitative performance for a particle-beam liquid chromatography–mass spectrometry system is evaluated with particular attention to non-linear behavior at low concentrations. A mathematical model for the non-linear behavior is proposed and shown to be in agreement with experimental data. The effects of 10 high-performance liquid chromatography mobile phase additives and 24 analytical probes on the linearity are shown. Although certain combinations of probes and additives show improved linear response, no single additive appears to completely alleviate the non-linear behavior as has been suggested by earlier work.

INTRODUCTION

Since the commercial introduction several years ago of particle-beam (PB) liquid chromatography (LC)–mass spectrometry (MS) systems, the technique has rapidly gained acceptance and popularity making it one of the most widely used techniques for combining the disparate techniques of LC and MS. This popularity is due to the technique's ability to yield either classical library-searchable electron impact (EI) spectra or solvent independent chemical ionization (CI) spectra and its ease of use relative to other LC–MS interfaces.

The technique has gone through a series of stages typical of all new analytical techniques. Initially describes as MAGIC LC–MS (monodispersed aerosol generation interface combining LC and MS) [1], the technique was met with some skepticism and largely overshadowed by thermospray LC–MS. Immediately following the introduction of the first commercial interface systems, a great deal of excitement was generated as the initial results in the analytical community indicated a great potential for the technique in a number of areas, such as environmental and pharmaceutical analysis requiring quantitative analysis of analytes coupled with sufficient qualitative information to ensure positive identification. Naturally, as the LC–PB-MS became more widely used, the limitations of the system became recognized. The primary

0021-9673/91/$03.50

limitations of the system were limited sensitivity, dependence of quantitative performance on high-performance LC (HPLC) conditions and limited linearity. The first two of these limitations prompted the introduction of a second generation of commercial instrumentation resulting in significantly improved sensitivity (5–10-fold for the current generation of instrumentation relative to its predecessor) and improved performance over a wider range of HPLC operating conditions (particularly for aqueous mobile phases). The non-linear behavior, however, is still to be addressed. The non-linear behavior was first described by Bellar *et al.* [2], and has since been described by McLaughlin *et al.* [3] and Kim *et al.* [4]. Bellar *et al.* [2] described the phenomenon as a "carrier effect" referring to the appearance of increased ion abundances for coeluting compounds. The described mechanism involves coeluting compounds or mobile phase additives "carrying" analyte particles through the PB momentum separator resulting in an increased transfer efficiency. The addition of mobile phase additives, such as ammonium acetate was shown to improve sensitivity and linearity with the implication that such an approach could alleviate the non-linear behavior. Similarly, Kim *et al.* [4] showed that the addition of 0.4 m*M* malic acid lead to significantly improved sensitivity and linearity in the analysis of Alar.

The purpose of the current work is to demonstrate that while the addition of mobile phase additives can have positive effects on both sensitivity and linearity for various analytes, the effect is both sample and additive dependent and there is currently no "magic bullet" additive which leads to linear behavior under all conditions.

EXPERIMENTAL

Instrumentation

An HP1090 HPLC system with ternary solvent delivery system, autosampler, column oven and filter photometric detector (Hewlett-Packard, Palo Alto, CA, USA) was used as a pumping system throughout this work. The flow was set at 0.2 ml/min of methanol–water (50:50) (with additives as noted below). Injections of 1–2 μl were made in a flow injection analysis (FIA) mode.

An HP 59980A PB interface coupled to an HP5988 quadrapole mass spectrometer with high mass option and high-energy dynode (HED) detector was used for all the MS work. The PB nebulizer was operated at 30–60 p.s.i. helium inlet pressure, as determined by a standard optimization procedure. The PB desolvation chamber was operated at 60°C. The MS source temperature was 250°C and the MS analyzer was held at 100°C. The MS electron multiplier was run at approximately 200 V above autotune values and the HED voltage was set at 7 kV. All data acquisition was done in selected ion monitoring (SIM) mode of 70 eV EI ionization, monitoring the ions of interest for selected analytical probes.

The HPLC and the PB interface were connected using approximately 50 cm of 0.12 mm I.D. × 0.50 mm O.D. flexible stainless-steel capillary and a 0.5-μm low-dead-volume precolumn filter (Upchurch Scientific, Oak Harbor, WA, USA).

The system was controlled using a custom prototype data system running under Microsoft Windows running on an HP Vectra QS16 computer. All data manipulation was performed using Statgraphics version 3.0 (STSC, Rockville, MD, USA). The theoretical modelling was performed using MathCad version 2.5 (Math Soft, Cambridge, MA, USA).

Chemicals

HPLC-grade methanol was obtained from Burdick & Jackson (Baxter Healthcare Corp., Muskegon, MI, USA). HPLC-grade water was prepared inhouse starting from distilled water and further processing the solvent with a Water-I (Barnstead, Boston, MA, USA) solvent-purification system until the resistivity was greater than 18 MΩs/cm.

The mobile phase additives studied are listed in Table I and were obtained from Aldrich (Milwaukee, WI, USA). The analytical probes were obtained from either Aldrich or from Sigma (St. Louis, MO, USA). The chemical structures of the probes are shown in Fig. 1.

Techniques

The bulk of this work is based on two separate series of experiments. The first examined the effect of sample type and mobile phase additives on linear behavior. The second experiment examined the so called "carrier effect" by injecting coeluting compounds and evaluating any increased ion abundances.

The linearity studies were conducted as follows. Serial dilutions of the analytical probe samples listed in Table II (and shown in Fig. 1) were made at twelve levels from stock solutions at the 1000 ng/μl level in methanol. The resulting concentrations were 1000, 750, 500, 250, 125, 62.5, 31.25, 15.625, 7.81, 3.90, 1.95 and 0.97 ng/μl. For each different mobile phase additive evaluated, new dilutions were prepared using the mobile phase as the diluent. Mobile phases were prepared using methanol–water (50:50) plus the additive at 0.1 *M* concentration. The mobile phase plus additive were premixed and used as a single HPLC mobile phase channel. The samples were then run in triplicate in SIM mode, monitoring the ions listed in Table II. The samples were run as 2-μl injections in order from lowest to highest concentration to avoid any cross-contamination or carry-over. The peak height data based on the integration were then subjected to least squares linear regression to evaluate the linear performance. For some combinations of mobile phase additive and analytical probe the poor sensitivity resulted in less than four concentration data points for the linear regression. These data were rejected from further consideration. Due to the large number of combinations of mobile phase additives and analytical probes, the entire experiment required several months to complete. In order to account for day-to-day variations in instrument performance, a 20-ng benzidine sample was run in SIM mode every morning and later used to normalize peak height data.

As a subset of the above experiment, a number of mobile phase additives were run at different concentrations and/or different pH values to estimate these effects.

TABLE I

MOBILE PHASE ADDITIVES

Ammonium acetate	Ammonium bicarbonate
Ammonium formate	Ammonium thiocyanate
Ammonium citrate	Trifluoracetic acid (TFA)
Ammonium oxalate	Triethylamine
Ammonium tartrate	Ethylamine

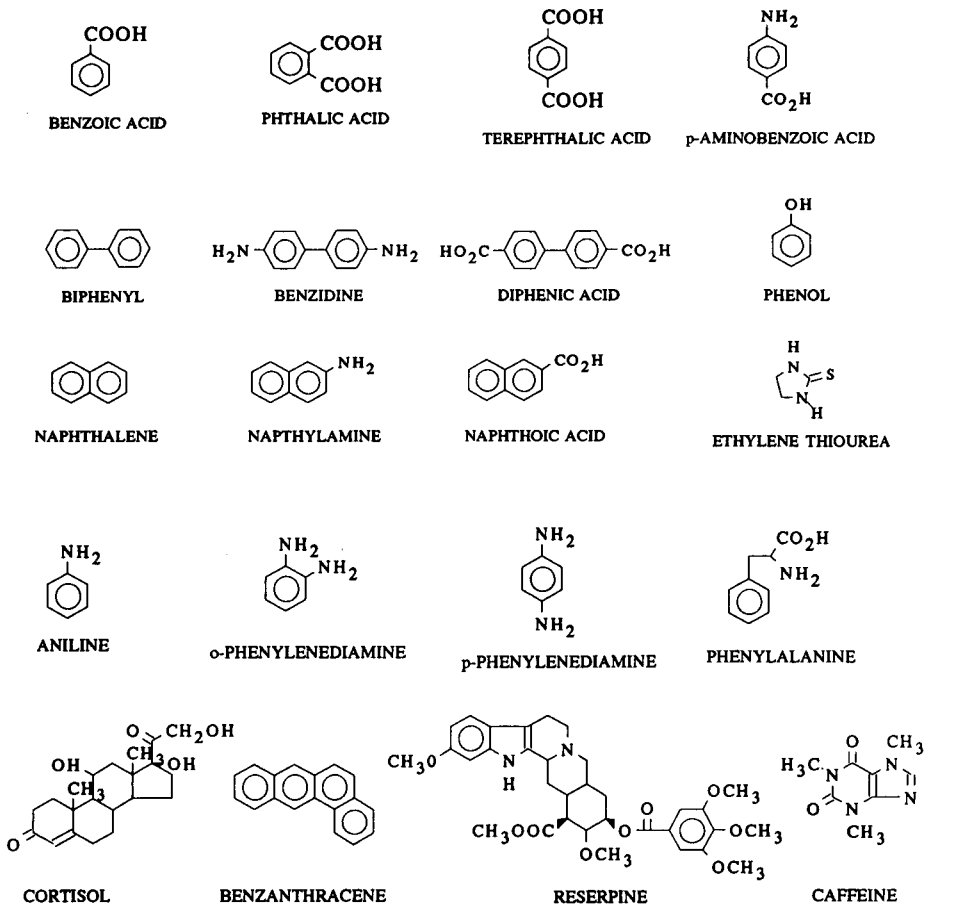

Fig. 1. Chemical structures of analytical probes used in linearity study.

TABLE II

LIST OF ANALYTICAL PROBES

Sample	Mol.wt.	Ions monitored	Sample	Mol.wt.	Ions monitored
Benzoic acid	122	105,122	Phenol	94	94
Aniline	93	93	*o*-Nitrophenol	139	109,139
p-Aminobenzoic acid	137	120,137	*p*-Nitrophenol	139	109,139
Phthalic acid	166	77,105	2,4-Dinitrophenol	184	124,184
p-Phenylenediamine	108	80,108	Picric acid	229	180,229
o-Phenylenediamine	108	80,108	Diphenic acid	242	197,242
Terephthalic acid	166	71,166	Benzidine	184	184
Phenylalanine	165	74,91,120	Biphenyl	154	154
Naphthoic acid	172	127,172	Reserpine	608	365,608
Naphthylamine	149	128,149	Caffeine	194	109,194
Naphthalene	128	128	Ethylenetiourea	102	73,102
2,3-Benzanthracene	228	71,228	Cortisol	363	163,302

For the carrier effect studies, samples were prepared at 20 and 50 ng/μl concentrations either alone in the mobile phase (plus additive) or in the presence of 1000 ng/μl cortisol as carrier in the mobile phase (plus additive). While monitoring the characteristic ions for the probe, the samples were run first injecting 1 μl five times without the carrier and then 1 μl five times with the carrier.

RESULTS AND DISCUSSION

The PB interface is shown schematically in Fig. 2 and operates as follows: the effluent from the HPLC enters the system through a coaxial pneumatic nebulizer which generates an aerosol. The aerosol passes through a desolvation chamber which is held at approximately 200 Torr and 60°C. As the droplets are desolvated the more volatile components (such as the HPLC solvent) evaporates leaving the less volatile components (*e.g.* analyte) to condense into desolvated particles. At the end of the desolvation chamber, a mixture of helium gas, solvent vapor and desolvated analyte particles enters a two-stage momentum separator. The momentum separator consists of three parts; a nozzle and two skimmers. The vapor, gas and particles exit the nozzle at supersonic velocities. The heavier particles have significantly higher momentum relative to the vapor and gas molecules and consequently pass through the momentum separator and into the mass spectrometer source volume. The lighter gas and vapor molecules have less momentum than the particles and can be pumped away to exhaust. This process results in analyte enrichment relative to the mobile phase and a pressure reduction from a pressure of approximately 200 Torr in the desolvation chamber to 5–10 Torr in the first momentum separator stage to <0.5 Torr in the second momentum separator stage to $1\text{–}2 \cdot 10^{-5}$ Torr in the mass spectrometer source manifold. After the particles in the particle beam enter the MS source, they strike the heated source wall, are vaporized and ionized by EI or CI. For the current work, all spectra were EI.

Theoretical model

In an attempt to more fully understand the phenomenon involved in the non-linear behavior, a mathematical model was proposed and evaluated to predict the characteristics of the response factors and linear performance. The model is based on hypothesizing that the PB interface has a particle size cutoff level below which small particles are pumped away in the momentum separator (or otherwise lost in the

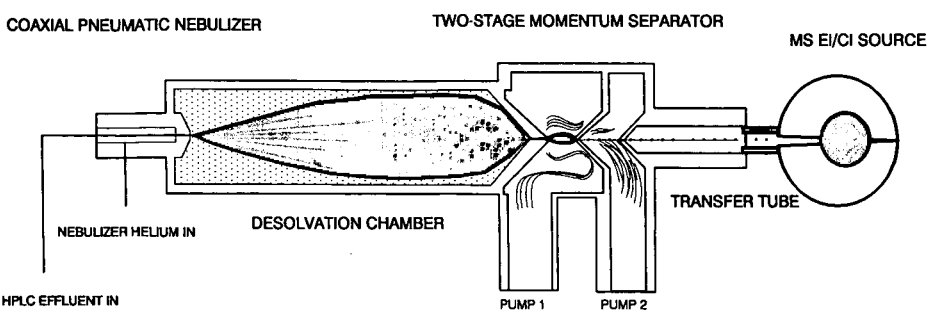

Fig. 2. Schematic of particle-beam LC–MS interface.

system) and above which the larger particles are transferred quantitatively into the MS source. Although the use of such an abrupt high pass filter analogy is an over simplification, the general concept is reasonable if one considers small particles in the limit of one molecule per particle. The entire purpose of the particle beam interface is to separate these vapor molecules from the larger particles.

Given an initial aerosol entering the PB desolvation chamber with a given droplet size distribution (assumed to be normal), it is possible to calculate the resulting desolvated particle diameter if the further assumptions of solid spherical particles with densities identical to their respective bulk materials are made. Again these assumptions are simplifications since it has been shown [5] that the particles may have a number of different non-spherical forms. However, for this model it is assumed that the size and mass of the resulting desolvated particle depend only on the initial droplet size, the sample concentration and the sample bulk density. As the sample concentration is reduced, the resulting particle size is reduced as well. At some point, the mean of the particle distribution begins to pass the hypothetical cutoff level. This results in a reduction in response factor going eventually to zero as shown in Fig. 3A. This, in turn, results in a calibration plot with a characteristic linear range at the

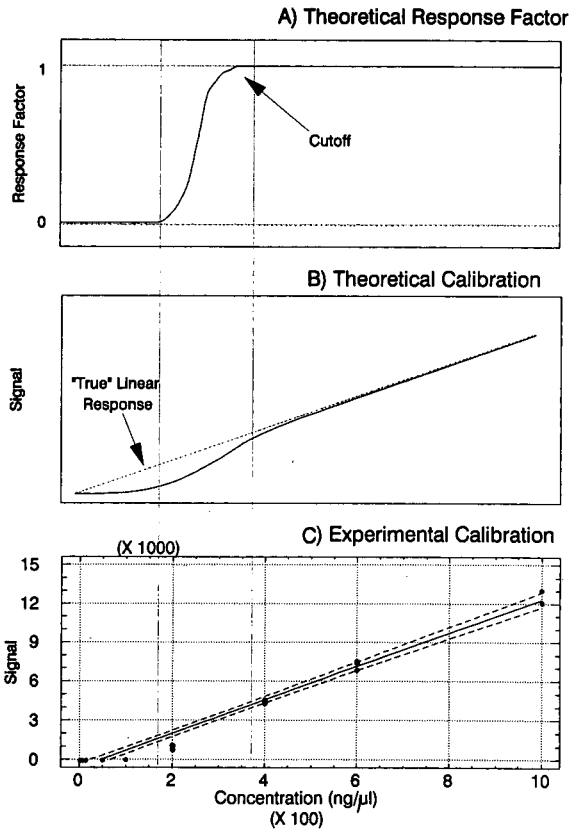

Fig. 3. Theoretical model for non-linear behavior in LC–PB-MS. (A) Calculated response factor, (B) calculated calibration plot, (C) example of experimental calibration plot for *p*-phenylenediamine.

higher concentrations and a deviation from linearity at the lower levels, as shown in Fig. 3B. Although it is not possible to get a direct comparison with real data without further information about the actual physical cutoff level, comparison with the data in Fig. 3C show that experimental data are consistent with the behavior proposed by this model.

Effect of mobile phase additives

As noted in the introduction, several researchers have suggested that the addition of semivolatile compounds to the mobile phase can show improvements in both linearity and sensitivity. In light of the model described above, it is clear that, in principle, this should be true. The addition of some mobile phase modifier will have the effect of increasing the overall concentration of material in each aerosol droplet, and consequently will increase the resulting desolvated particle size. This improvement, however, will depend on the ability of the probe and the additive to interact in such a way that neither is evaporated and pumped away in the system. It is demonstrated below, that although it is possible to make substantial gains in both linearity and sensitivity, it is not universally the case that addition of a modifier will lead to improvements.

The results of the least squares linear regression analysis, as expressed as the coefficient of variation (r^2), for the combinations of mobile phase additives and analytical probes, is shown in Table III. Table IV shows the Δr^2 values which are obtained by subtracting the r^2 value with mobile phase additive from the r^2 value with no additive. Brief examination of Table IV shows that there are both positive and negative values throughout the table indicating that in some cases (positive values) there is an improvement in linearity and in others (negative values) there is a degradation in performance. For none of the mobile phase additives is there an overall improvement in all sample cases.

This can be evaluated more systematically through analysis of regression (ANOVA) studies. The results of ANOVA for the effect of mobile phase additives are shown in Table V and depicted graphically in the "box and whisker" plot in Fig. 4. From the ANOVA table, we can conclude that at the 98 confidence limit, the mobile phase additives do have a statistically significant effect. The F value of 2.1 indicates the significance of this effect as the ratio of the "between additive" means square and the "within additive" mean square. In the "box and whisker" plot shown in Fig. 4, each box and whisker represents all of the analytical probes run for a given mobile phase additive, the center line in each box indicates the mean while the edges of the box are the 50 percentile and the whiskers are the range extremes. The additional points represent actual data points. Although the mean in each case is near 0 (no effect), there is a range of responses for different combinations of additive and probe. (Compare this plot to the similar discussion concerning the effect of analytical probes below.) Fig. 5 shows a similar box and whisker plot for the effect of additive on sensitivity.

As an example consider Fig. 6 in which the linearity for *p*-phenylenediamine is shown with no additive (A), 0.1 *M* ammonium acetate (B) and 0.1 *M* ammonium oxalate (C). In this case, the addition of the additives does result in a significant improvement in performance. Note the characteristic deviation from linearity at low levels in A which improves in B with acetate and almost disappears in C with oxalate.

TABLE III

COEFFICIENTS OF DETERMINATION (r^2) FOR ADDITIVE PROBE MATRIX

All additives at 0.1 *M* (except as noted in text) and adjusted to pH 7.0 if possible. Blank values represent insufficient data.

	No additive	Ammonium acetate	Ammonium formate	Ammonium citrate	Ammonium oxalate	Ammonium tartrate	Ammonium bicarbonate	Thio-cyanate	TFA	Triethyl-amine	Ethyl-amine
Benzoic acid	83.7				98.29					93.23	90.32
Aniline	99.25	99.48	99.95		99.57					76.62	99.74
p-Aminobenzoic acid	92.92	95.65	98.99	99.86	99.4	99.9	87.29	31.55	98.19	73.01	96.18
Phthalic acid	95	96.58	99.51		99.96		99.27	62.02	93.97	99.86	98.5
p-Phenylenediamine	75.17	72.01	90.71	98.72	99.93	99.84	94.48	99.5	99.74	98.59	93.5
o-Phenylenediamine	78.49			99.74	99.07	99.7	76.46	59.68	66.71	34.85	93.83
Terephthalic acid	98.5	98.59	99.93	99.75	99.92	84.84	99.8	99.44	99.25	98.57	97.6
Phenylalanine	87.05		89.14	73.84	99.51	99.21	98.57	96.85	86.05	91.11	92.4
β-Naphthoic acid	89.07	93.87		99.42	98.93	90.57	96.91		93.31	90.54	83.06
β-Naphthylamine	92.2	83.36	74.71	99.62	97.15	95.85			82.26	93.67	97.78
Naphthalene	99.9	94.75	99.95		99.92	97.39	98.78	99.7	99.77	99.33	99.62
2,3-Benzanthracene	98.86	99.63	99.87	99.88	99.84		99.76	93.76	98.36	98.05	98.75
Phenol	99.79	99.41	89.57		98.09		99.32	88.61	92.81	87.68	99.68
o-Nitrophenol	67.13				63.43		99.26		98.48	85.96	95.15
p-Nitrophenol	92.39	18.48	56.63	88.56	99.17	99.74	96.7			97.94	95.52
2,4-Dinitrophenol	48.5	93.23	94.91	91.25	96.49	75.25					97.25
Picric acid	99.09		91.83	99.2	93.52	99.78	99.75		97.7	99.35	98.37
Diphenic acid	95.58		97.83	83.54	95.06	98.79	95.13	95.01	94.92	94.14	95.81
Benzidine	99.57	76.02	99.31	94.21	99.88	99.53	99.6	93.61		99.65	98.33
Biphenyl	99.7	99.86			99.57	95.02	99.38	98.11	99.85	98.12	99.54
Reserpine	95.93	99.18	99.77	97.28			96.16	97.06	98.23	95.28	98.55
Caffeine	99.78	98.31	98.77	92.02		97.2	97.44	98.59	90.81	98.25	98.64
Ethylene thiourea	98.2	98.56	99.65		95.85		95.41	98.41	96.48	97.18	98.21
Cortisol	99.34	99.05	99.92		88.67	98.83	99.63	98.41	98.37	99.02	98.7

TABLE IV

DIFFERENCES IN COEFFICIENTS OF DETERMINATION (r^2) FOR ADDITIVE/PROBE MATRIX

All additives at 0.1 *M* (except as noted in text) and adjusted to pH 7.0 if possible. Blank values represent insufficient data.

	Ammonium acetate	Ammonium formate	Ammonium citrate	Ammonium oxalate	Ammonium tartrate	Ammonium bicarbonate	Thio-cyanate	TFA	Triethyl-amine	Ethyl-amine
Benzoic acid				14.59					9.53	6.62
Aniline	0.23	0.7		0.32					−22.63	0.49
p-Aminobenzoic acid	2.73	6.07	6.94	6.48	6.98	−5.63	−61.37	5.27	−19.91	3.26
Phthalic acid	1.58	4.51		4.96		4.27	−32.98	−1.03	4.86	3.5
p-Phenylenediamine	−3.16	15.54	23.55	24.76	24.67	19.31	24.33	24.57	23.42	18.33
o-Phenylenediamine			21.25	20.58	21.21	−2.03	−18.81	−11.78	−43.64	15.34
Terephthalic acid	0.09	1.43	1.25	1.42	−13.66	1.3	0.94	0.75	0.07	−0.9
Phenylalanine		2.09	−13.21	12.46	12.16	11.52	9.8	−1	4.06	5.35
β-Naphthoic acid	4.8		10.35	9.86	1.5	7.84		4.24	1.47	−6.01
β-Naphthylamine	−8.84	−17.49	7.42	4.95	3.65			−9.94	1.47	5.58
Naphthalene	−5.15	0.05		0.02	−2.51	−1.14	−0.2	−0.13	−0.57	−0.28
2,3-Benzanthracene	0.77	1.01	1.02	0.98		0.9	−5.1	−0.5	−0.81	−0.11
Phenol	−0.38	−10.22		−1.7		−0.47	−11.18	−6.98	−12.11	−0.11
o-Nitrophenol				−3.7		32.13		31.35	18.83	28.02
p-Nitrophenol	−73.91	−35.76	−3.83	6.78	7.35	4.31			5.55	3.13
2,4-Dinitrophenol	44.73	46.41	42.75	47.99	26.75					48.75
Picric acid		−7.26	0.11	−5.57	0.69	0.66		−1.39	0.26	−0.72
Diphenic acid		2.25	−12.04	−0.52	3.21	−0.45	−0.57	−0.66	−1.44	0.23
Benzidine	−23.55	−0.26	−5.36	0.31	−0.04	0.03	−5.96		0.08	−1.24
Biphenyl	0.16			−0.13	−4.68	−0.32	−1.59	0.15	−1.58	−0.16
Reserpine	3.25	3.84	1.35			0.23	1.13	2.3	−0.65	2.62
Caffeine	−1.47	−1.01	−7.76		−2.58	−2.34	−1.19	−8.97	−1.53	−1.14
Ethylene thiourea	0.36	1.45		−2.35		−2.79	0.21	−1.72	−1.02	0.01
Cortisol	−0.29	0.58		−10.67	−0.51	0.29	−0.93	−0.97	−0.32	−0.64

TABLE V

EFFECT OF ADDITIVES ON LINEARITY

D.F. = Degrees of freedom.

Source of variation	Analysis of variance			
	Sum of squares	D.F.	Mean square	*F*-ratio
Between additives	6237	10	623	2.1
Within additives	70 729	239	297	
Total (corr.)	76 966	249		

Fig. 7 shows the residuals for the linear regressions shown in Fig. 6. Although in Fig. 7A (no additive), Fig. 7B (0.1 *M* ammonium acetate) and Fig. 7C (0.1 *M* ammonium oxalate) there is a clearly discernable deviation from linear performance, note that the magnitudes of the deviations decrease more than 30-fold from no additive to oxalate.

Table VI shows the normalized peak heights for 600-ng injections for the combinations of mobile phase additives and analytical probes. By examining the ANOVA results (Table VII) and the corresponding box and whisker plot (Fig. 8), it can be seen that over the entire set of probes there is not a statistical difference in signal heights that can be attributed to the additive. However, in several specific cases, the sensitivity is improved by using a mobile phase additive, and in particular, the use of acetate and oxalate lead to significant improvements. This is further reinforced by examining the peak intensities shown in the calibration plot in Fig. 6 which show an approximately 6-fold increase comparing A (no additive) to C (0.1 *M* ammonium oxalate).

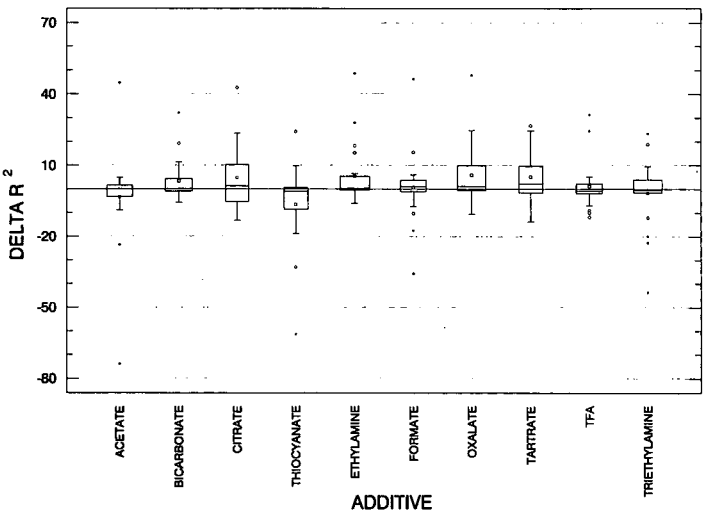

Fig. 4. Effect of additive on linearity; box and whisker plot. Delta R^2 = Differences in coefficient of determination (r^2) relative to a mobile phase with no additive.

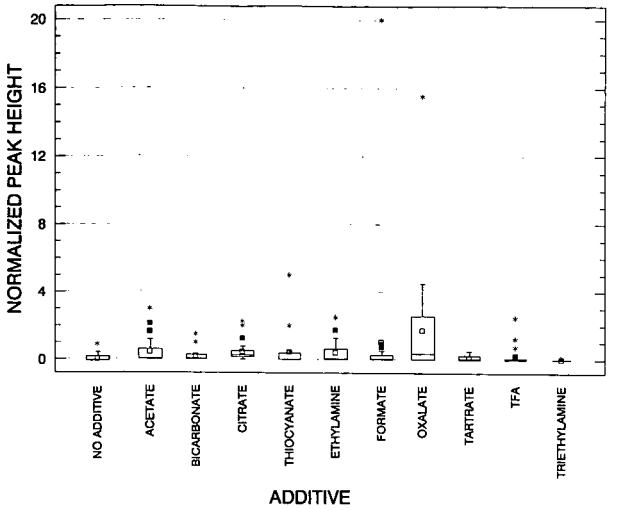

Fig. 5. Effect of additive on sensitivity; box and whisker plot. Normalized peak heights are normalized with respect to daily instrument response and benzidine run with no additive.

Effect of analytical probes

The effects of the analytical probes on linearity and sensitivity are similar to the effects of the mobile phase additives. Results of ANOVA on the Δr^2 values in Table IV are shown in Table VIII along with corresponding box and whisker plot in Fig. 8. Again, although the results are mixed, it is possible to say that at the 95% confidence limit, the character of the analytical probes does have a statistically significant effect. In fact, examining the F-value of 6.4 shows that this effect is more significant than that of the mobile phase additives.

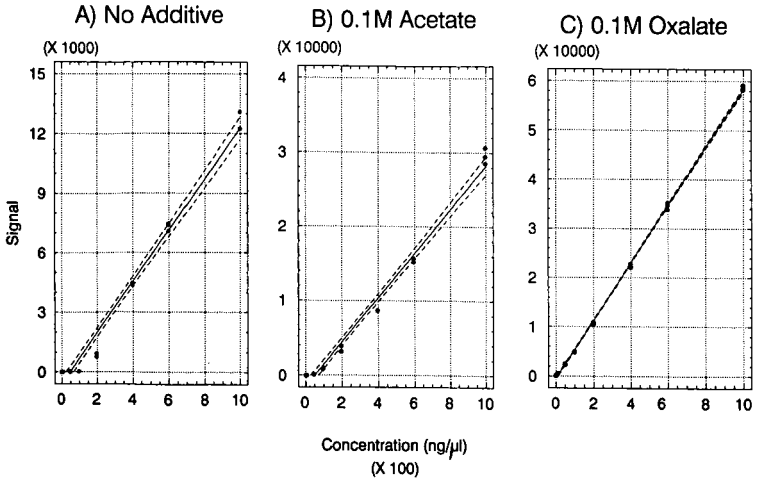

Fig. 6. *p*-Phenylenediamine calibration plot with (A) no additive, (B) 0.1 *M* ammonium acetate and (C) 0.1 *M* ammonium oxalate.

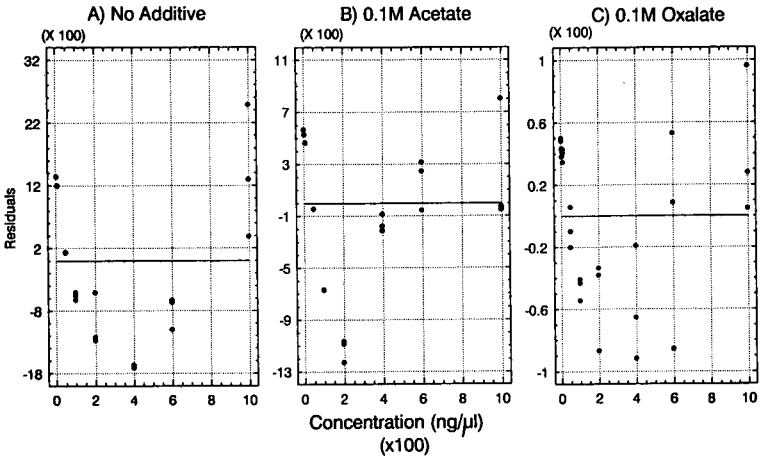

Fig. 7. Residuals for regression plots shown in Fig. 6 (A) No additive, (B) 0.1 *M* ammonium acetate and (C) 0.1 *M* ammonium oxalate.

Although comparisons between thermospray and particle-beam LC–MS [6,7] have suggested that the range of response factors is less for particle beam than thermospray resulting in a more uniform response, of course the response factors are not totally uniform. This is evident in the data shown in Table VI.

By comparing subsets of the analytical probes, it is possible to characterize some structural effects on a preliminary basis. It should be noted that this work is still in progress and the following analysis is not taking into account any other physical or thermodynamic characteristics of the probes or modifiers. In particular, by comparing three sets; (benzoic acid, aniline and *p*-aminobenzoic acid), (biphenyl, benzidine and diphenic acid), and (naphthalene, naphthylamine and naphthoic acid), it is possible to compare acids and bases. In general, for the acidic modifiers, the acids and neutral probes work better than the basic probes whereas the basic probes improve for basic modifiers. This is perhaps not surprising, but it does suggest more chemical interaction than simply physical. Similarly, by comparing the subsets (benzoic acid, phthalic acid and therephthalic acid), (aniline, *p*-phenylenediamine and *o*-phenylenediamine) and (phenol, *o*-nitrophenol, *p*-nitrophenol, 2,4-dinitrophenol and picric acid), one can compare the effect of 1, 2 or 3 polar substituents. To some extent this overlaps a comparison of relative positioning of aromatic substituents that can be obtained by comparing the subsets (*o*-nitrophenol and *p*-nitrophenol), (*o*-phenyl-

TABLE VII

EFFECT OF ADDITIVES ON SENSITIVITY

Source of variance	Analysis of variance			
	Sum of squares	D.F.	Mean square	*F*-ratio
Between additives	56	10	5.59	1.79
Within additives	698	223	3.13	
Total (corr.)	754	233		

TABLE VI

NORMALIZED PEAK HEIGHTS FOR ADDITIVE PROBE MATRIX

All additives at 0.1 *M* (except as notes in text) and adjusted to pH 7.0 if possible. Data normalized with respect to benzidine/no additive.

	No additive	Ammonium acetate	Ammonium formate	Ammonium citrate	Ammonium oxalate	Ammonium tartrate	Ammonium bicarbonate	Thio-cyanate	TFA	Triethyl-amine	Ethyl-amine
Benzoic acid	0.018	0.042	0.001	0.250	1.320				0.001		0.007
Aniline	0.001	0.001	0.007	0.002	0.007			0.001			0.002
p-Aminobenzoic acid	0.150	0.140	0.750	0.500	2.750	0.500	1.500	0.009	0.750	0.150	1.000
Phthalic acid	0.022	0.088	0.033	0.250	0.279		0.008	0.011	0.090	0.007	0.225
p-Phenylenediamine	0.250	0.306	20.000	0.248	2.750	0.235	0.039	2.000	1.250	0.017	0.225
o-Phenylenediamine	0.001	0.003	0.250	0.222	2.301	0.078	0.002	0.004	0.038		0.002
Terephthalic acid	0.250	0.787	1.000	1.250	4.500	0.250	0.217	5.000	0.750	0.025	1.250
Phenylalanine	0.175	0.800	0.182	0.750	4.000	0.163	0.239	0.500	0.063	0.009	0.750
β-Naphthoic acid	0.250	0.375	0.057	0.143	2.400	0.033	0.250	0.050	0.097	0.018	0.500
β-Naphthylamine	0.001	0.002	0.001	0.022	0.389	0.003		0.005	0.011		0.002
Naphthalene	0.003	0.009	0.010		0.020	0.002	0.002	0.003	0.004	0.001	0.006
2,3-Benzanthracene	0.250	1.165	0.500	2.250	15.545	0.250	0.250	0.150	0.250	0.018	0.500
Phenol	0.001	0.003	0.001	2.000	0.009	0.002	0.001	0.001	0.002		0.002
o-Nitrophenol		0.001			0.006	0.001					0.001
p-Nitrophenol	0.001	0.012	0.036	0.250	0.416	0.131	0.001		0.005	0.001	0.012
2,4-Dinitrophenol	0.001	0.034	0.004	0.171	0.332	0.024			0.000		0.007
Picric acid	0.001	0.011	0.001	0.204	0.064	0.072	0.008	0.001	0.004	0.001	0.014
Diphenic acid	0.002	0.030	0.002	0.500	0.351	0.249	0.005	0.004	0.035	0.006	0.050
Benzidine	1.000	2.127	0.750	0.500	4.250	0.500	1.000	0.250	2.500	0.125	2.500
Biphenyl	0.002	0.006	0.001	0.021	0.007	0.001	0.001	0.001	0.001		0.004
Reserpine	0.004	0.014	0.001	0.013	0.013		0.003	0.002	0.015		0.013
Caffeine	0.500	3.000	0.247	0.199	0.003	0.032	0.239	0.500	0.001	0.050	1.750
Ethylene thiourea	0.225	1.658	0.196	0.250	0.224	0.023	0.250	0.500		0.025	1.000
Cortisol	0.050	0.276	0.022	0.013	0.039	0.006	0.038	0.024	0.001		0.150

TABLE VIII

EFFECT OF PROBES ON LINEARITY

Source of variance	Analysis of variance			
	Sum of squares	D.F.	Mean square	*F*-ratio
Between probes	30 304	23	1317	6.4
Within probes	46 662	225	207	
Total (corr.)	76 966	248		

enediamine and *p*-phenylenediamine) and (phthalic acid and terephthalic acid). In terms of the number of substituents there is not a significant difference in linearity based on number of substituents (for these compounds). The substituted compounds do behave more linearly than their unsubstituted parents. In almost all cases the *para*-substituted examples behave more linearly than the *ortho* substitution. For the three pairs given as examples, the *para*-substituted compound also gives significantly larger signals.

Carrier effect experiments

The non-linear behavior observed for LC–PB-MS can also be seen as an increase in signal for coeluting peaks. In the presence of a coeluting, compound, an analyte may exhibit more efficient transport and therefore yield a larger signal than in the absence of the coeluting "carrier" compound. An example of this is shown in Figs. 9 and 10. In Fig. 9, 10 ng *p*-phenylenediamine is injected alone and then together with 1000 ng cortisol using mobile phases with (A) no additive, (B) 0.1 *M* ammonium acetate and (C) 0.1 *M* ammonium oxalate. It can be clearly seen that the 0.1 *M* oxalate reduces the magnitude of the "carrier effect" relative to the no additive case.

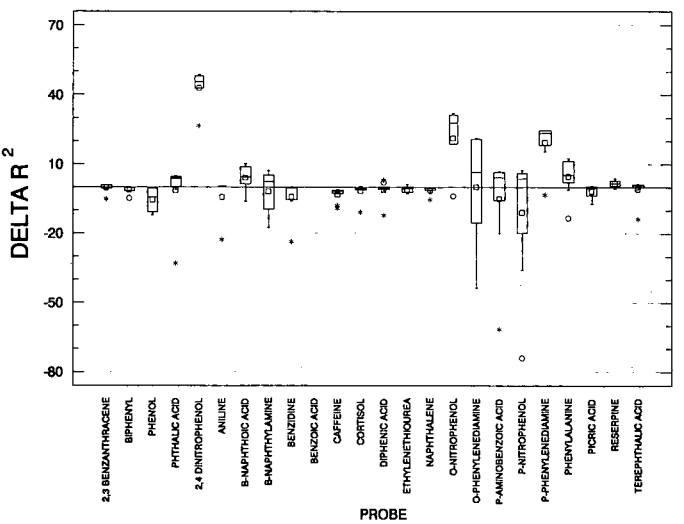

Fig. 8. Effect of probe on linearity box and whisker plot. Delta R^2 = Differences in coefficient of determination (r^2) relative to a mobile phase with no additive.

Fig. 10 represents an identical experiment except that the *p*-phenylenediamine is at 50 ng level. In this case, even in the absence of any additive, the increase in signal due to the "carrier effect" is relatively minor compared to the 10-ng case. This is because at 50 ng, *p*-phenylenediamine is just beginning to exhibit non-linear behavior. At levels above this, the non-linearity becomes less significant. In essence, at this level, *p*-phenylenediamine is its own carrier.

The effect of coeluting peaks on analyte signal intensities has raised questions concerning the use of isotopically labelled internal standards for quantitation. Although it has yet to be demonstrated, it seems clear that the use of such coeluting standards should be a viable approach to quantitation since the effect of coeluting compounds is to decrease the reduction in the response factor due to non-quantitative transfer processes. It should be noted that ion abundances can only increase to the point at which 100% of the analyte is being transferred into the ion source. Thus, depending on the level of the internal standard, the linear response of the analyte should be more or less improved. We hope to demonstrate this in future work.

CONCLUSIONS

In conclusion, it has been demonstrated that the so-called "carrier effect" and the non-linear behavior of LC–PB-MS are based on the same phenomenon which is consistent with a "high pass filter" model.

It has been shown that effect can be mitigated in some cases though the use of semivolatile mobile phase additives, but that this does not result in improvement in all cases. The effectiveness of this approach depends on the chemical characteristics of both the additive and of the analyte. This strongly suggests that the phenomenon involves a chemical interaction rather than a simple physical process.

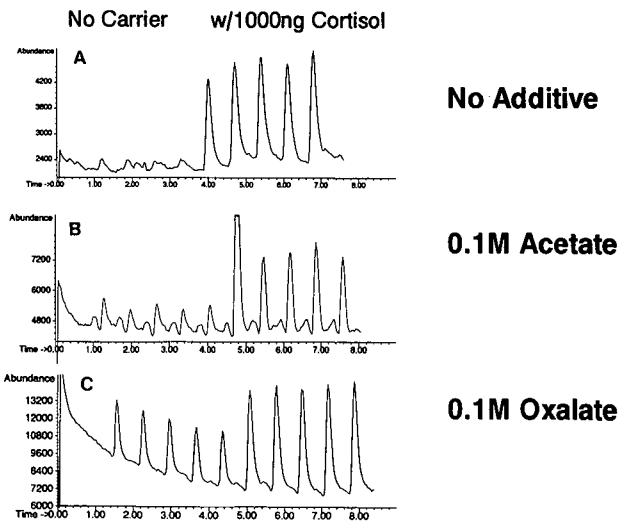

Fig. 9. Carrier effect for 10 ng *p*-phenylenediamine for (A) no additive, (B) 0.1 *M* ammonium acetate and (C) 0.1 *M* ammonium oxalate. The first five injections contain only 10 ng *p*-phenylenediamine, the second five contain 10 ng *p*-phenylenediamine coeluting with 1000 ng cortisol as carrier. Time in min.

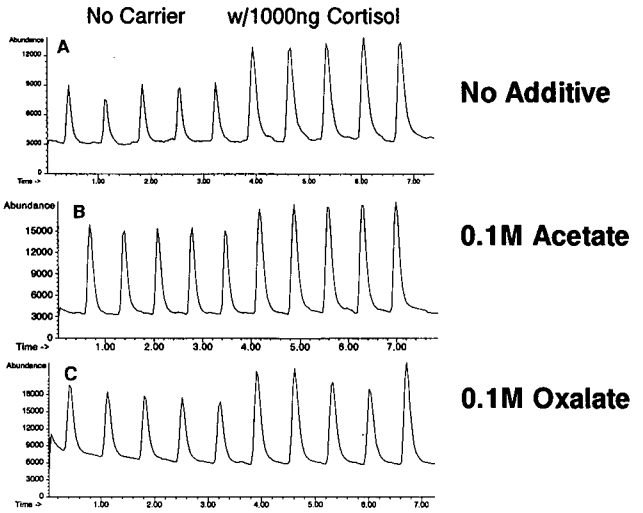

Fig. 10. Carrier effect for 50 ng *p*-phenylenediamine for (A) no additive, (B) 0.1 *M* ammonium acetate and (C) 0.1 *M* ammonium oxalate. The first five injections contain only 50 ng *p*-phenylenediamine, the second five contain 50 ng *p*-phenylenediamine coeluting with 1000 ng cortisol as carrier. Time in min.

In future work, we hope to further investigate and characterize the nature of the chemical interactions with the aim of providing useful criteria for choosing appropriate mobile phase additives for a given analysis.

ACKNOWLEDGEMENTS

In keeping with the spirit of the *7th Montreux Symposium on LC–MS*, we would like to acknowledge how we greatly miss the presence of Professor R. W. Frei both as a friend and as a colleague in the scientific community.

M.L.P. would like to acknowledge her gratitude to Hewlett-Packard for the support of this research.

REFERENCES

1 R. C. Willoughby and R. F. Browner, *Anal. Chem.*, 56 (1984) 2626–2631.
2 T. A. Bellar, T. D. Behymer and W. L. Budde, *J. Am. Soc. Mass Spectrom*, 1 (1990) 92–98.
3 L. McLaughlin, T. Wachs, R. Pavelka, G. Maylin and J. Henion, presented at the *6th (Montreux) Symposium on LC–MS, Cornell, NY 1989.*
4 I. S. Kim, F. I. Sasinos, R. D. Stephens and M. A. Brown, *J. Agric. Food Chem.*, 38 (1990) 1223–1226.
5 R. C. Willoughby, presented at the *6th (Montreux) Symposium on LC–MS, Cornell, NY, 1989.*
6 A. Apffel and P. C. Goodley, in D. Friedman (Editor), *Environmental Applications, Waste and Testing Quality Assurance*, Vol. 2, American Society for Testing and Materials, Philadelphia, PA, 1990, ASTM STP 1062.
7 R. D. Voyksner, C. S. Smith and P. C. Knox, *Biomed. Environ. Mass Spectrom.*, 19 (1990) 523–534.

Journal of Chromatography, 554 (1991) 119–124
Elsevier Science Publishers B.V., Amsterdam

CHROMSYMP. 2291

Some aspects of peak broadening in particle-beam liquid chromatography–mass spectrometry

A. P. TINKE, R. A. M. VAN DER HOEVEN, W. M. A. NIESSEN*, U. R. TJADEN and J. VAN DER GREEF

Division of Analytical Chemistry, Center for Bio-Pharmaceutical Sciences, P.O. Box 9502, 2300 RA Leiden (Netherlands)

ABSTRACT

The particle-beam interface has recently been introduced for coupling liquid chromatography and mass spectrometry. The coupling of a particle-beam interface to a Finnigan MAT TSQ-70 triple quadrupole instrument is described. A compound-dependent peak broadening in the interface has been observed. In this paper various experiments are described to investigate some of the sources of peak broadening. For this purpose, the transfer efficiency of the particle-beam interface has been measured, and the potential of volatility-enhancing derivatization procedures has been explored. The detection of 40 pg of the pentafluorobenzyl derivative of palmitic acid is demonstrated.

INTRODUCTION

The particle-beam (PB) interface is a relatively new interface for coupling liquid chromatography and mass spectrometry (LC–MS), which has been commercially available since 1988 [1–3]. In a PB interface the column effluent is pneumatically nebulized in a heated desolvation chamber at nearly atmospheric pressure. The analyte molecules in the solvent stream nucleate to form submicrometre particles, which are selectively separated from the solvent vapour molecules in a two-stage momentum separator and subsequently transported to the mass spectrometry ion source. The particles evaporate on collision at the heated ion source wall and the released molecules are ionized and mass analysed. The PB interface enables the on-line LC–MS acquisition of electron-impact (EI) and solvent-independent chemical ionization (CI) spectra as well as fast atom bombardment (FAB) [1–5] spectra, although the latter is not well documented. Compared to other successful LC–MS interfaces applicable to conventional LC splitless columns, the PB interface is easier to operate than the moving-belt interface [6], which can also yield EI and CI spectra, but its applicability range is limited compared to the thermospray interface [7], which cannot generate EI spectra.

During the evaluation of a PB interface in this laboratory it was found that significant peak broadening in the PB interface can be observed. The extent of peak

0021-9673/91/$03.50

broadening appeared to be compound-dependent. Various experiments were performed to determine the sources of peak broadening. The results of these experiments are reported here.

EXPERIMENTAL

Equipment

A Hewlett-Packard (Palo Alto, CA, USA) 59980A PB interface with a pneumatic nebulizer was coupled to a Finnigan MAT (San José, CA, USA) TSQ-70 mass spectrometer with a standard EI–CI source using a laboratory-made stainless-steel transfer tube, introduced into the vacuum through the gas chromatography (GC)–MS inlet flange. A schematic diagram of the interface is given in Fig. 1. A Busch (Virginia Beach, VA, USA) Model RA 0025 and an Edwards (Crawley, Sussex, UK) E2M18 mechanical pump were used at the first and second stage of the momentum separator, respectively.

An LKB (Bromma, Sweden) Model 2150 LC pump was used for the delivery of a mobile phase of 80% methanol in water at a flow-rate of 0.5 ml/min. The sample solutions were injected with a Rheodyne (Cotati, CA, USA) Model 7125 injection valve equipped with a 20-μl sample loop.

Chemicals

Methanol (p.a.) and acetonitrile (p.a.) were obtained from Baker (Deventer, Netherlands). Clobazam [7-chloro-1-methyl-5-phenyl-1H-1,5-benzodiazepine-2,4-(3H,5H)-dione] (Fig. 2) (Hoechst, Frankfurt, Germany), pentafluorobenzyl bromide (PFBBr) (Sigma, St. Louis, MO, USA) and 0.2 *M* of trimethylanilinium hydroxide in methanol (Pierce, Rockford, IL, USA) were stored at −20°C. All other solutes were purchased from various commercial sources and were used without further purification.

Determination of transfer efficiency

The skimmer set, transfer tube and a CI ion volume were cleaned thoroughly and washed with 5 ml of methanol (later used as blanks) before installation. The source pressure was adjusted to *ca.* 700 mPa of air and the temperature to 45°C (or to

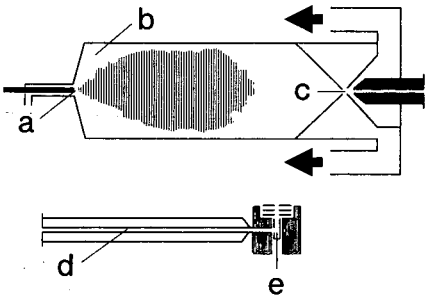

Fig. 1. Schematic diagram of the PB interface. a = Nebulizer; b = desolvation chamber; c = momentum separator; d = transfer tube; e = ion source with ion volume.

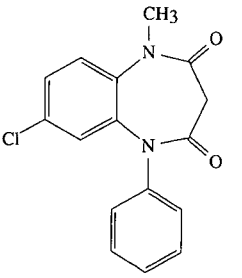

Fig. 2. Structure of clobazam.

250°C in some other experiments). Clobazam (10 μg) was injected in the column bypass mode. After 2 min, the transfer tube and the ion volume were washed separately with 5 ml of methanol. The amounts of clobazam collected in the two fractions were determined by high-performance liquid chromatography with ultraviolet (UV) detection against a series of standard solutions. The possibility of evaporative losses in the high vacuum during the procedure was excluded; a *ca.* 90% recovery was found for clobazam after storage of the ion volumes, at which clobazam was deposited, in the ion source for a similar time periode and under similar conditions.

Derivatization of fatty acids

Fatty acids were converted into the corresponding pentafluorobenzyl derivatives [8] by adding 2 ml of an aqueous solution of 0.1 mol/l tetrabutylammonium hydrogensulphate in 0.2 mol/l sodium hydroxide solution and 40 μl PFBBr to 0.5 mg of fatty acid in 2 ml of dichloromethane. After shaking for 20 min the water layer was discarded, the dichlotomethane layer was diluted with methanol and an aliquot was injected onto a 100 × 3 mm I.D. C_8 column for LC–MS detection in the negative-ion chemical ionization (NCI) mode.

RESULTS AND DISCUSSION

The PB interface was evaluated in this laboratory for various reasons. Previously, considerably effort has been put into the application of various LC–MS interfaces in both qualitative and quantitative bioanalysis. Other interfaces applied so far, *i.e.* thermospray, moving-belt and continuous-flow FAB, were successful in many applications, but also showed limitations in either the information content of the spectra for qualitative analysis or the determination limits for quantitative analysis. The PB interface is especially attractive with respect to qualitative analysis because of its ability to acquire on-line EI spectra, whereas its potential in quantitative analysis is at first sight less promising, but on the other hand has hardly been evaluated systematically. In addition, the PB interface would be most helpful for the automated acquisition of series of EI spectra from a variety of samples. In comparison with the moving-belt interface, which has similar potential, the PB interface is more robust.

From the first experiments, it appeared that with some analytes significant peak broadening is observed. As an example, the UV peak and the EI-MS peak after a column bypass injection of 2 μg of clobazam are given in Fig. 3. The peak width at the base is 4.8 s in the UV trace (asymmetry factor at 10% of the height of 1.3) and 23.2 s in the MS trace (asymmetry factor of 2.8). In principle, possible sources of peak broadening are the nebulizer, the desolvation chamber, the momentum separator, the transfer tube and the ion source. It was decided to study the effects of the transfer tube and the TSQ-70 ion source first, *i.e.* the parts differing from the Hewlett-Packard system. In this way, it would also be possible to evaluate the transfer efficiency of the PB interface. The transfer efficiency is defined here as the ratio of the amount of analyte collected in the ion source to the amount of analyse injected in the mobile phase. Transfer efficiencies between 0.05 and 0.70 have been claimed [9,10] for the various commercially available PB interfaces.

The transfer efficiency can be measured in the TSQ-70 system relatively easily, because the EI–CI ion source is equipped with replaceable ion volumes. By decreasing

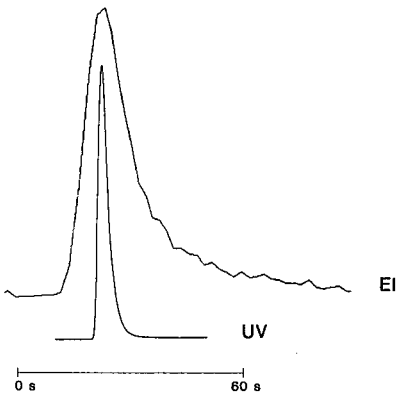

Fig. 3. Illustration of the peak broadening in the PB interface [2 μg column bypass injection of clobazam (mol. wt. = 300)].

the ion source temperature to avoid losses due to analyte evaporation, the amount of sample transferred to the ion source can be measured. For each experiment a thoroughly cleaned skimmer set, transfer and CI ion volume were installed. The sample, 0.5 mg/ml clobazam in methanol, was injected and after a pre-set period of time the ion volume was removed and the amount of clobazam collected in the ion volume was measured. Typical transfer efficiencies measured under these conditions were 2%. As this figure was unexpectedly low, it was decided to measure the amount of clobazam collected in the transfer tube as well, which was 19% of the injected amount. Apparently, the particle beam from the momentum separator does not behave as a narrow parallel beam of particles, as was stated by Winkler *et al.* [2], but significantly diverges, allowing the particles to collide with the transfer tube surface. It can also be concluded that for clobazam only 21% of the injected amount passes the momentum separator, *i.e.* significant sample losses take place in the PB interface.

Under normal operating conditions, the temperature of the transfer tube is higher due to thermal conductance from the ion source, which is typically at 250°C. Therefore, a more efficient evaporation of collided particles from the tube wall is anticipated at a higher temperature. It was decided to measure the amount of clobazam collected in the transfer tube while the ion source was kept at 250°C. This amount was 5% of the injected sample, which means that the effective transfer efficiency for clobazam to the ion source is *ca.* 16% under normal operating conditions.

From these data two conclusions were drawn. Firstly, the transfer tube must be as short as possible. Independent heating of the transfer tube might be helpful as well. The implementation of a short heated transfer tube in this experimental set-up is currently under investigation. Therefore, further studies on the transfer efficiency were postponed. Secondly, the divergence of the particle beam and the resulting collisions and subsequent sample evaporation at the transfer tube wall will lead to peak broadening, the extent of which depends on the sample volatility and the wall temperature. Similarly, the evaporation step in the ion source on particle collision prior to the ionization will lead to peak broadening, the extent to which also depends on the sample volatility and the wall temperature. At this stage, it was decided to

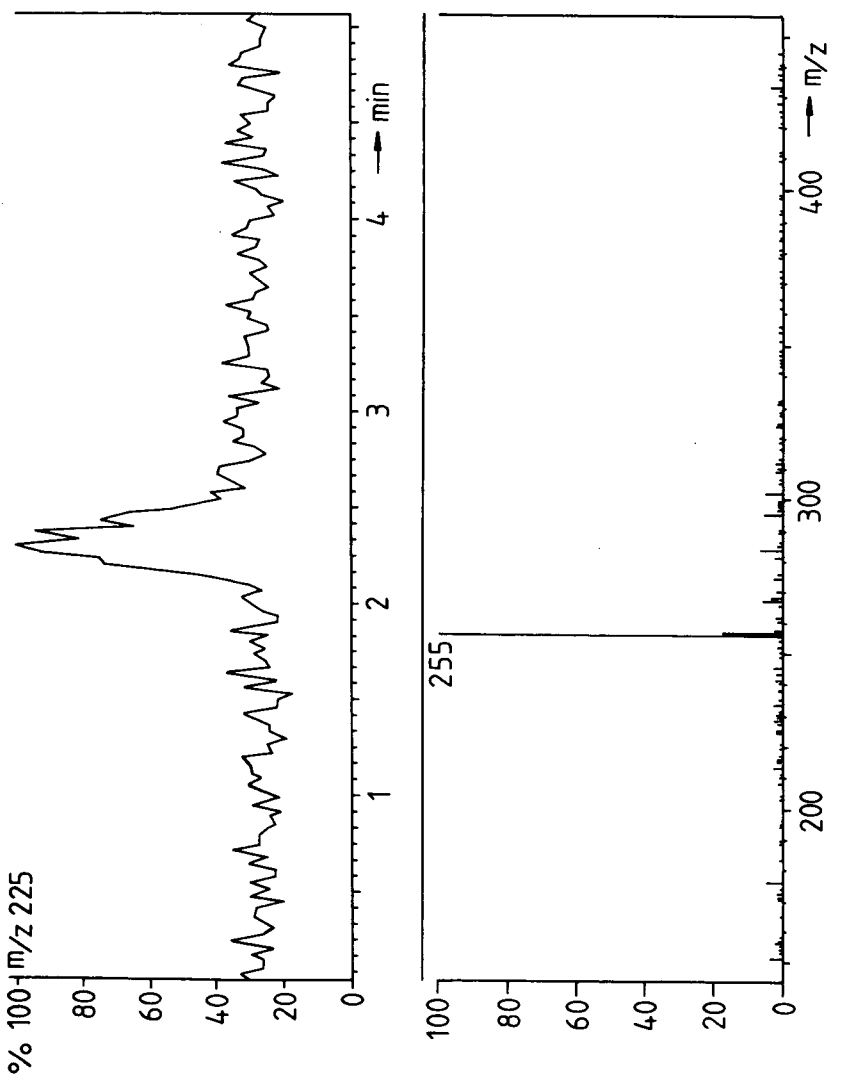

Fig. 4. (upper) Selected ion chromatogram of 40 pg of the pentafluorobenzyl derivative of palmitic acid (mol. wt. = 256) after injection of the reaction mixture on a 100 × 3 mm I.D. C_8 column and monitored under ammonia–NCI conditions. (lower) NCI spectrum of 400 pg of the pentafluorobenzyl derivative of palmitic acid.

evaluate the potential of volatility-enhancing derivatization reactions. Reactions for a wide variety of compounds are available from GC–MS practice [11].

To test the hypothesis of the influence of sample volatility in a more systematic way, the signals obtained from column bypass injections of a series of fatty acids and their methyl esters were compared. In general, the sensitivity for the fatty acids was not very good. Injections of *ca.* 100 μg of palmitic or stearic acid were necessary to achieve signals in scanning mode with a reasonable signal-to-noise ratio. The peak width at the base was 27.3 s (asymmetry factor at 10% of the height of 4.2). In contrast, for methyl palmitate and methyl stearate, 100 times higher signal-to-noise ratios were achieved on the injection of *ca.* 1 μg. Significantly less peak broadening and more symmetric peaks are observed; the peak width at the base is 12.0 s (asymmetry factor of 2.3) The methylation of carboxylic acids to enhance their volatility can also be readily performed on-line, as demonstrated by Vouros and co-workers [12,13] in a post-column ion-pair liquid–liquid extraction system, where the carboxylic acids are extracted as ion pairs with the trimethylanilinium (TMA) counter ion to the organic phase. The fatty acid–TMA ion pair decomposes on heating to form the methyl esters [12,13]. Preliminary experiments with this approach indicate significant improvements in signal-to-noise ratios and peak shape for some fatty acids.

The demonstrated potential of volatility enhancing derivatization procedures to improve the analyte detection in PB LC–MS also opens the possibility of a broad application of other potentially more sensitive ionization methods, such as electron-capture NCI. In Fig. 4, the NCI spectrum of 400 pg of the pentafluorobenzyl derivative of palmitic acid and the on-column chromatogram of 40 pg of the derivative are shown. The peak at m/z 255 is formed in a dissociative electron capture.

In conclusion, it can be stated that a more profound knowledge of the processes determining the operation of the PB interface will enable improvements of the interface performance. Further studies along this line are presently being performed in this laboratory to enhance the applicability of the PB interface.

REFERENCES

1 R. C. Willoughby and R. F. Browner, *Anal. Chem.*, 56 (1984) 2626.
2 P. C. Winkler, D. D. Perkins, W. K. Williams and R. F. Browner, *Anal. Chem.*, 60 (1988) 489.
3 J. A. Apffel, *Hewlett-Packard Particle-Beam LC–MS Book of Spectra, HP Publication No. 23-5959-7105*, Hewlett-Packard, Palo Alto, CA, 1988.
4 J. D. Kirk and R. F. Browner, *Biomed. Environ. Mass Spectrom.*, 18 (1989) 355.
5 P. E. Sanders, *Rapid Commun. Mass Spectrom.*, 4 (1990) 123.
6 P. J. Arpino, *Mass Spectrom. Rev.*, 8 (1989) 35.
7 P. J. Arpino, *Mass Spectrom. Rev.*, 9 (1990), 631.
8 O. Gylledhaal and H. Ehrsson, *J. Chromatogr.*, 107 (1975) 327.
9 K. R. Edman, J. D. Kirk and R. F. Browner, *Proceedings of the 37th ASMS Conference on Mass Spectrometry and Allied Topics, May 21–26, 1989, Miami Beach, FL*, ASMS, East Lansing, MI, 1989, p. 130.
10 M. L. Vestal, D. Winn, C. H. Vestal and J. G. Wilkes, *Proceedings of the 37th ASMS Conference on Mass Spectrometry and Allied Topics, May 21–26, 1989, Miami Beach, FL*, ASMS, East Lansing, MI, 1989, p. 939.
11 J. Drozd, *Chemical Derivatization in Gas Chromatography* (*Journal of Chromatographic Library*, Vol. 19), Elsevier, Amsterdam, 1981.
12 P. Vouros, E. P. Lankmayr, M. J. Hayes, B. L. Karger and J. M. McGuire, *J. Chromatogr.*, 251 (1986) 175.
13 C. P. Tsai, A. Sahil, J. M. McGuire, B. L. Karger and P. Vouros, *Anal. Chem.*, 58 (1986) 2.

Journal of Chromatography, 554 (1991) 125–140
Elsevier Science Publishers B.V., Amsterdam

CHROMSYMP. 2360

On-line derivatization of eluted substances in dynamic high-performance liquid chromatography–mass spectrometry through the particle-beam interface

VITTORIO RAVERDINO
Hewlett-Packard SA, 39 Rue de Veyrot, 1217 Meyrin (Switzerland)

ABSTRACT

Derivatization reagents were added through the particle beam high-performance liquid chromatograph–mass spectrometer interface in order to improve the detectability of polar compounds separated by high-performance liquid chromatography and detected by mass spectrometry by formation of the corresponding derivative. Mainly qualitative aspects are considered in this work. Dynamic derivatization in the gas phase of several substances containing carboxylic, sulphonic, hydroxy and other acidic or basic functional groups is described.

INTRODUCTION

Since the development of the first high-performance liquid chromatographic–mass spectrometric (HPLC–MS) interface based on the monodispersed areosol technique [1], a number of improvements have been achieved by modifying the geometry of the nebulizer and of the design of the momentum separator. Although the latest developments of the particle-beam HPLC–MS interface allow its use for a wide range of applications, *e.g.*, to compounds of higher polarity such as acids, bases and sulphonic acids, in principle derivatization may extend its applicability to a larger number of compounds by producing derivatives of higher volatility.

Another aspect of the applicability of the particle-beam HPLC–MS interface is the observation that high concentrations of water present in the mobile phase do not favour the detectability of the analytes. This seems to be related to the efficiency of both the nebulization and desolvation processes. This paper considers the possibility of dynamically derivatizing certain types of substances in the vapour or gas phase as they fly through the particle beam interface into the ion source of the mass spectrometer.

The objective of this work was the examination of the following aspects: to improve the volatility of some polar substances that are hardly brought into the vapour phase by the heat generated by the ion source; to provide additional qualitative information about the eluting compounds by examination of the spectra of the derivatized analytes; to improve the detectability of the sample by bringing the ions of

0021-9673/91/$03.50

interest into a higher mass range where the matrix does not interfere; to study the effect of transforming water as a mobile phase flowing through the nebulizer or at the outlet from the particle beam interface, in order to improve the operation of the particle-beam interface at high water concentrations of the mobile phase; and possibly to improve the detectability of a substance by the formation of a polyfluoro derivative and the use of chemical ionization and detection of negative ions.

A few common derivatization procedures were considered, as follows.

Silylation

This is one of the most widely used derivatization procedures in gas chromatography. Silyl derivatives are generally more volatile, less polar and more thermally stable than their parent compounds. Mass spectra obtained by electron impact and chemical ionization present intense ions in the higher mass range, often out of the region of the background.

Many compounds are completely derivatized as soon as they come into contact with the reagent. This is especially true for monofunctional molecules, where an active hydrogen is replaced with an alkylsilyl group, typically trimethylsilyl. Polyfunctional groups in terms of the number of active hydrogens or sterically hindered groups may react only partially. Silylation is a well known and common derivatization technique in the analysis of acids, alcohols, phenols, amines (primary and secondary), carbohydrates and some inorganic ions. The substances are derivatized in the liquid phase, and generally the reaction is complete rapidly under mild conditions. Less explored is derivatization into the vapour phase, as happens in an on-line configuration through the particle-beam HPLC–MS interface, as described.

Moreover, when the reagent is present in large excess, in the source of the mass spectrometer, additional ion–molecule reactions can occur in the gas phase inside the ion source.

Reagents used for this work are the well known trimethylchlorosilane (TMCS) and bis(trimethylsilyl)trifluoroacetamide (BSTFA) [molecular weight (MW) 257; b.p. 146°C or 40°C at 12 mmHg]. The reaction generates product ions and by-products following the general reaction scheme

$$\underset{\text{(MW 257)}}{CF_3CON[Si(CH_3)_3]_2} + HOR \rightarrow \underset{\text{(if R = H, MW 90)}}{(CH_3)_3SiOR} + \underset{\text{(MW 185)}}{CF_3CONHSi(CH_3)_3}$$

Acylation

Fluorinated anhydrides are widely used acylating reagents for alcohols, phenols and amines and produce stable, highly volatile derivatives. The presence of fluorine makes them particularly interesting for electron-capture detection and negative-ion detection in mass spectrometry. Trifluoroacetic anhydride (TFAA) is the most volatile, and it can be easily brought into the particle beam interface in the vapour phase. N-Methylbistrifluoroactamide (MBTFA) does not produce acidic by-products and can be more conveniently used for derivatizing phenols and alcohols [2]. The pentafluoropropionic (PFPAA) derivatives could provide more fluorine atoms for electron capture by chemical ionization and negative-ion detection [3].

There are several acylating procedures in the liquid phase, which usually involve heating at 60–100°C for 15–60 min and eventually washing the organic phase

with water [4] or methods specially designed for the derivatization of sugars [5] or catecholamines [6].

Less well known are acylation reactions in the gas phase, induced by heat and ionization. "On-line" combination in the gas phase through the particle beam interface allows these types of chemical reactions to be studied under particular conditions of vacuum and plasma. Hydrolysis of the anhydrides and the formation of derivatives and adducts can be observed in the mass spectra.

In this work, only TFAA and PFPAA were tested as acylating reagents.

Use of water scavangers and modifiers

2,2-Dimethoxypropane (DMP) is used as a water scavanger for some alkylation reactions as for the formation of butylboronate derivatives. DMP converts water into organic compounds. Some tests have been done using the particle-beam interface by adding a certain amount of DMP in the gas phase, together with the helium flow in the nebulizer section, with the objective of transforming water-rich effluents chemically into a more rich organic phase, and verifying changes in the detectability of the eluted substances.

EXPERIMENTAL

Reagents

TMCS and BSTFA were used for the experiments in which silylation was involved. Acylation was performed with TFAA and PFPAA. DMP was used as a water scavenger. All these reagents were supplied by Supelco (Bellefonte, PA, USA).

Acetonitrile, methanol and water, all of HPLC grade, were supplied by Merck, Darmstadt, Germany. Water was quartz distilled twice before use.

Addition of derivatization reagents through the PB interface

The addition of derivatization reagents into the particle beam interface was performed as follows (see Fig. 1): through a tee-piece before the nebulizer (modifier acetonitrile) at position (a); together with the helium flow at position (b) (modifier DMP); and at the inlet of the gas for chemical ionization at position (d), together or without the methane reactant gas. For some preliminary tests not reported here the reagent was placed in the bulb that is normally used for the calibrant (perfluorotributylamine) of the mass spectrometer when this is used in the HPLC–MS mode. The

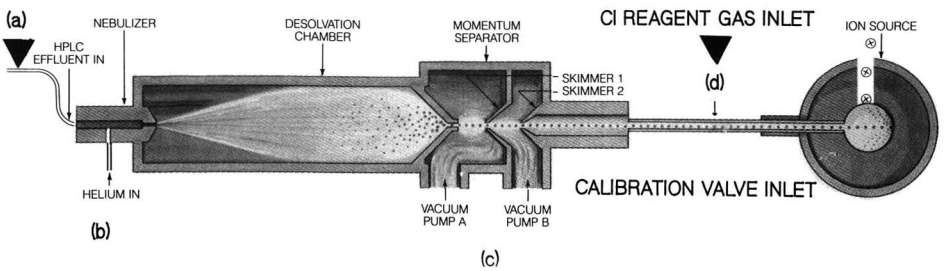

Fig. 1. Schematic representation of the particle beam HPLC–MS interface and locations (a–d) where derivatization reagents can be added.

point of addition is at position (d). The advantage is that these is no need for modification of the standard hardware, but the control of the amount of derivatization reagent flowing into the source is more critical.

The series of experiments performed are summarized in Table I.

TABLE I
DERIVATIZATION REAGENTS USED AND LOCATION OF ADDITION THROUGH THE PARTICLE BEAM INTERFACE

Derivatization method	Derivatization reagent	Location (see Fig. 1)	Remarks
Silylation	TMCS, BSTFA	(d)	Used for steroids, sugars, carboxylates, sulphonates, polyfunctional compounds. Chemical ionization has been used
Acylation	TFAA, PFPAA	(d)	Used for steroids. Chemical ionization has been used
Water scavenger	DMP	(b)	Experiments on nebulization process. Electron impact has been used
Mobile phase modifier	Acetonitrile	(a)	Increase percentage of organic solvent in the mobile phase for better detectability

On-line silylation and acylation

At the outlet of the particle-beam interface [position (d) in Fig. 1], a mixture of methane and silylating or acylating reagent was added. The total pressure into the ion source was 130 Pa with a ratio of methane to reagent of about 1:1. These are the conditions under which most of the actual work has been done and the majority of the results have been obtained. A necessary modification to the standard hardware is the addition of a tee-piece and a bulb containing the derivatization reagent with a flow regulator, on the line that is normally used for the chemical ionization reactant gas. This minor modification can be retained even for the usual HPLC–MS work, as the reactant can be isolated from the flow line by shutting off the flow regulator.

The analyte elutes from the HPLC column into the particle-beam interface and at position (d) (Fig. 1) comes into contact with the derivatization reagent. Note that, at this point, most of the mobile phase has been already removed by the nomentum separator.

The amount of analytes injected using this instrumental configuration ranged from 100 to 1000 ng. Separation through the HPLC column was performed for the analysis of steroids and, in some instances, for diuretics. For the other components flow injection was used.

Addition of a water scavanger at the nebulizer

In order to acquire a better knowledge of the nebulization process and consider the reasons why the presence of high concentrations of water in the mobile phase can decrease the performance of the transport process of substances through the interface, the helium flow that sustains the nebulization was doped with DMP as a water scavenger.

Modification is required to the standard hardware, *i.e.*, a Hewlett-Packard (Palo Alto, CA, USA) solvent-delivery system, part number 05985-60238, which is part of the kit of the previous direct liquid introduction HPLC–MS interface, is installed and connected to the line of the helium flow. The helium bubbles into the liquid DMP, or other modifier, and flows into the nebulizer. The helium flow-rate is about 2 l/min and the DMP flow-rate, vaporized into the helium, corresponds to about 2 ml/min of liquid unter these conditions.

The experiment consisted in injecting repeatedly 2 μl of a 50 ng/μl solution of benzidine in acetonitrile, bypassing the analytical column, and gradually changing the composition of the mobile phase from 100% acetonitrile to 100% water without readjusting the position of the fused-silica tubing of the nebulizer. Moreover, the helium flow for the nebulizer was bubbled through a bomb containing about 20 ml of water scavenger. During this test, the presence of DMP was monitored, in addition to the benzidine signal. In particular, the relative intensity of the signal of the molecular ion of benzidine at m/z 184 indicates how well this substance is transported through the interface by changing the composition of the mobile phase.

The experiment lasted about 20 min before all the water scavenger had been consumed. Hence it can be calculated that the flow of DMP into the nebulizer area was ca. 1 ml/min. The signal of benzidine was monitored under electron impact conditions, scanning from 45 to 220 u at 2 scans/s, and plotting the extracted ion chromatogram for the molecular ion at m/z 184.

HPLC–MS combination

An HP 1090L liquid chromatograph (Hewlett-Packard) equipped with a dual pumping system, variable-volume injector and diode-array detector was used for all tests. An additional HP 1050 pump (Hewlett-Packard) was occassionally used to add modifiers at the end of the HPLC column.

Model 59980B particle-beam interfaces (LC–PB-MS) from Hewlett-Packard were used. The experiments were conducted at a desolvation temperature of typically 50°C and a helium head pressure of 300 kPa.

Several experiments were repeated and reconfirmed using two different mass spectrometers: an HP 5988A and an HP 5989A (Hewlett-Packard). The ion source was maintained at 250°C and the quadrupole housing at 100°C.

Chemical ionization (CI) was used for all tests except those for which a modifier (acetonitrile or DMP) was added at the nebulizer (see Table I), when the electron impact mode was used. For the CI experiments methane was used both as reagent gas for chemical ionization and as a "carrier" of the derivatizing reagents. The total pressure into the ion source was 130 Pa.

Chromatographic conditions

For the separation of steroids, a stainless-steel column (100 × 2.1 mm I.D.) from Hewlett-Packard packed with 5-μm Hypersil ODS was used with a gradient of water–methanol from 40:60 to 1:99 (v/v) in 30 min at a flow-rate of 0.4 ml/min.

For the analysis of diuretics, the mobile phase was water–acetonitrile–formic acid (55:45:0.5, v/v/v). Flow-injection analysis bypassing the column was occasionally performed. Chromatographic analysis was done with a 25 × 2.1 mm I.D. stainless-steel column from Hewlett-Packard packed with 5-μm Hypersil ODS. The flow-rate was 0.4 ml/min.

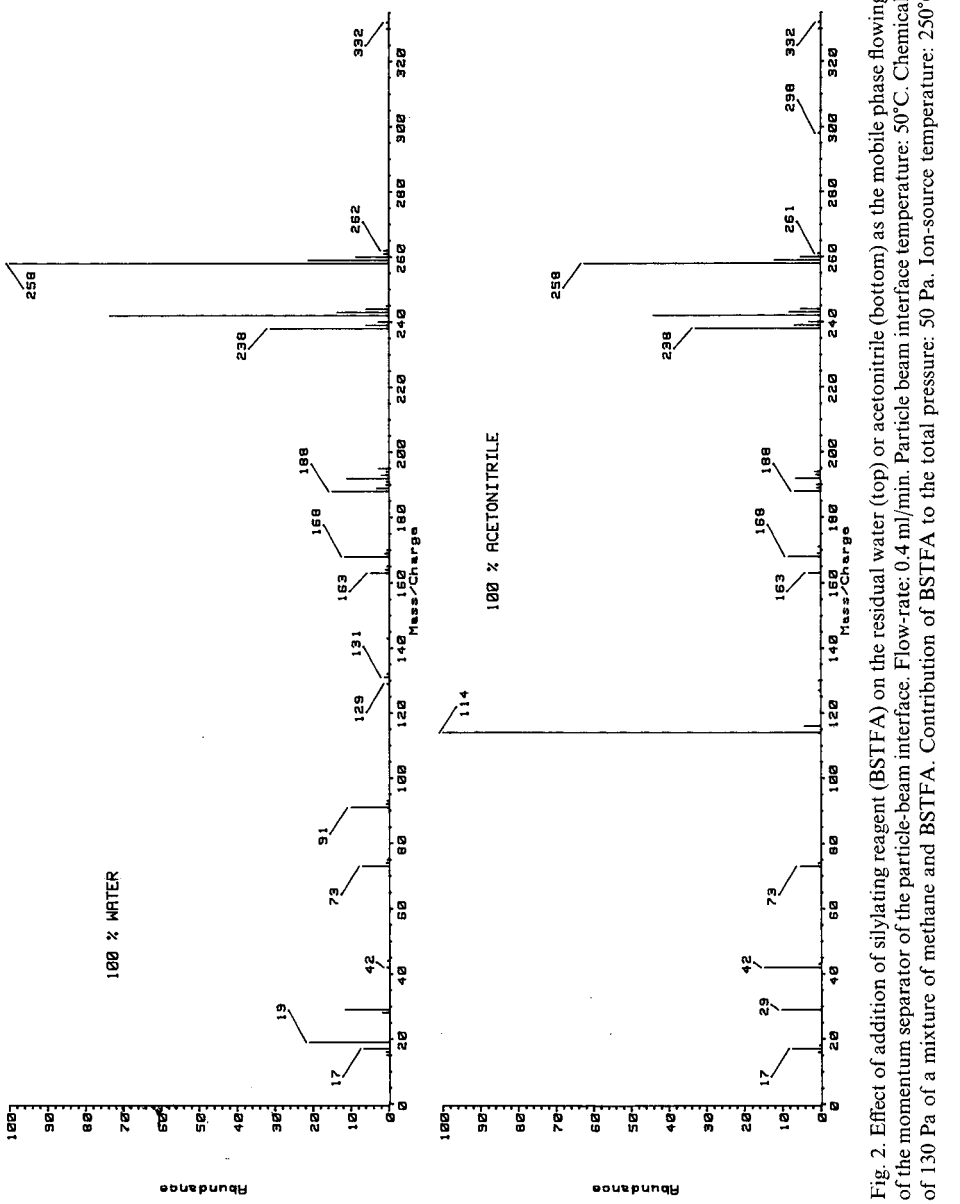

Fig. 2. Effect of addition of silylating reagent (BSTFA) on the residual water (top) or acetonitrile (bottom) as the mobile phase flowing from the HPLC column out of the momentum separator of the particle-beam interface. Flow-rate: 0.4 ml/min. Particle beam interface temperature: 50°C. Chemical ionization at a total pressure of 130 Pa of a mixture of methane and BSTFA. Contribution of BSTFA to the total pressure: 50 Pa. Ion-source temperature: 250°C.

Flow injection bypassing the column was used for the other substances analysed, using methanol as mobile phase at a flow-rate of 0.4 ml/min.

RESULTS

Derivatization with TMCS and BSTFA: effects on the mobile phase

In order to evaluate the effectiveness of derivatization, two parameters were changed initially: solvent composition, from 100% water to 100% acetonitrile; and the amount of derivatization reagent flowing into the mass spectrometer from position (d).

The spectra obtained by using a relatively small amount of BSTFA and water as mobile phase show that under chemical ionization conditions *m/z* 19 is still the base peak (protonated water), while *m/z* 91 appears at low intensity as protonated monohydroxytrimethylsilane. An ion at *m/z* 258 appears as protonated BSTFA.

In a similar manner, for acetonitrile as mobile phase, *m/z* 42 can be observed (protonated acetonitrile) as the base peak, with the presence of an ion at *m/z* 114 representing a charged species constituted by a trimethylsilyl group on the acetonitrile molecule.

By adding a relatively larger amount of BSTFA, the reaction can be brought almost to completion as shown in Fig. 2. The ratio between the abundances of the *m/z* 91 and *m/z* 19 ions changes in favour of the *m/z* 91 ion and anion of *m/z* 163 (two trimethylsilyl groups on the water molecule) is present. A similar behaviour is observed for the ions at *m/z* 114 and 42 when acetonitrile is used as the mobile phase. An abundant peak of protonated BSTFA at *m/z* 258 is present, of course. Derivatization with TMCS is also effective: no ion at *m/z* 19 is found with water flow as the mobile phase, *m/z* 91 and *m/z* 163 ions being present instead.

In Table II the relative abundances of some significant ions are related to the absolute pressure of BSTFA in the ion source as measured with a Pirani gauge, without taking into account any eventual response factor. It should be pointed out that the total pressure in the ion source was maintained the same in the different experiments by compensating with addition of more or less methane. It is not known at which point of the HPLC–MS interface the reaction with water actually takes place. Formation of adduct can be observed as the derivatization reagent also contributes to the chemical ionization process.

It should be pointed out that a similar behaviour has been reported [7] by using chemical ionization conditions with mixtures of methane and tetramethylsilane. The use of silylating reagents instead of tetramethylsilane shows an additional reactivity on the active sites of the molecules.

Derivatization of different analytes

The derivatization of analytes was performed by using an excess of derivatization reagent, in order possibly to bring the reaction to completion. A trial-and-error procedure with inspection of the resulting spectrum of the analyte generally allows a convenient pressure of the reagent to be established.

Using BSTFA pressures between 50 and 90 Pa, no important qualitative changes to the mass spectrum of the derivatized analyte can be observed. A practical advantage of this situation is that the response also is relatively constant.

TABLE II

RELATIVE ABUNDANCES OF SOME IONS IN THE MASS SPECTRUM OF THE MOBILE PHASE (WATER FLOWING AT 0.4 ml/min) IN RELATION TO THE AMOUNT OF BSTFA ADDED TO THE PARTICLE-BEAM INTERFACE

The total pressure in the ion source was constant at 130 Pa in all experiments, by compensation with methane.

Absolute BSTFA pressure (Pa)	Protonated water (*m/z* 19)	*m/z* 91	*m/z* 163	Protonated BSTFA (*m/z* 258)
13	100	16	7	20
45	20	17	19	100
70	–	35	45	100

TABLE III

MOST ABUNDANT IONS IN THE MASS SPECTRUM OF SOME POLYFUNCTIONAL SUBSTANCES WITH ON-LINE SILYLATION

Relative abundances of the most significant ions expressed in % are given and the corresponding mass units are reported in parentheses.

Substance	Functional groups[a]	MW	$[M+1]^+$	1 × Silyl	2 × Silyl	3 × Silyl	Remarks
Bumetanide	Sulphonamide, sec. amine, carboxylic acid	364	Abs.	18% (437)	100% (509)	10% (581)	
Probenecid (*m/z* 504)	Carboxylic acid, sulphonamide	285	8% (286)	89% (358)	100% (430)	8% (504)	Adducts
Furosemide	Aromatic amine, carboxylic acid, sulphonamide	330	Abs.	13% (403)	100% (475)	8% (547)	
Ethacrynic acid	Carboxylic acid, methylene, keto	303	Abs.	35% (375)	100% (447)	4% (519)	Adducts
Piretanide	Carboxylic acid, sulphonamide	362	Abs.	Abs.	72% (507)	Abs.	Base peak *m/z* 385
Testosterone	Hydroxy	288	Abs.	100% (361)			Adducts present
Androsterone	Hydroxy	290	Abs.	100% (363)			Adducts present
Cortisol	3 × Hydroxy	362	Abs.	100% (435)	4% (507)	Abs.	
Cortisone[b]	2 × Hydroxy	360	Abs.	100% (433)	8% (505)		
Glucose	5 × Hydroxy	180	Abs.	12% (253)	11% (325)	9% (397)	4 × Silyl present; base peak *m/z* 235
17-α-Hydroxy-progesterone	Hydroxy	330	Abs.	100% (403)			
Acid Red 88[c]	Hydroxy, sulphonate	378[d]	Abs.	–[e]			Base peak *m/z* 205

[a] Only functions containing active hydrogens are mentioned.
[b] See Figs. 3 and 4.
[c] No signal was observed on injecting this compound without on-line derivatization.
[d] Calculated as acid.
[e] Other ions present at *m/z* 481 (5%), 374 (12%), 368 (17%), 302 (32%), 132 (22%). All mentioned fragments show the effect of the presence of silicon in the isotopic pattern.

Qualitative similar spectra can be observed for different concentrations of an analyte. The consequence is that, for example, a linear calibration graph could constructed for testosterone injected in amounts between 20 and 1000 ng.

For most of the monofunctional substances (one active hydrogen atom) analysed here, the reaction is complete and no original $[M+1]^+$ is observed. Polyfunctional substances may be derivatized at all possible positions, but in some instances the reaction is not complete (see Table III).

In the chromatogram obtained under dynamic conditions where a mixture of testosterone, epitestosterone, andreosterone and etiocholanolone (3-α-hydroxy-5-β-androstan-17-one) was separated by reversed-phase HPLC (see Fig. 3) and silylated on-line with BSTFA, the spectra of the mono-functional components show a complete reaction, while cortisol and cortisone (Fig. 4) are not totally silylated at all possible active positions.

However, for the qualitative analysis of some polyfunctional substances such as diuretics [8], the mass spectra show that the silylation reaction is complete in some instances. Adducts produced by ion–molecule reactions under chemical ionization conditions may be present in the spectra (see Table III). For the analysis of furosemide, "one-line" derivatization with BSTFA increases the positive-ion detection in the chemical ionization mode by a factor of about 20, although the most sensitive method is still the detection of negative ions and chemical ionization with methane or ammonia. A similar behaviour can be found for diuretics of analogous molecular structure. For the electron impact response taken as a reference, the measured response ratios using different detection methods were as reported in Table IV.

The advantage of derivatization, in this instance, is that the measurement is made at higher mass values, hence an improvement in the signal-to-noise and repeatability (see R.S.D. values in Table IV) is observed.

On-line acylation with TFAA and PFTFA

These anhydrides were at the end of the particle beam interface at position (d) (see Fig. 1) together or without the reagent gas. Nitrogen, argon or methane were tested as additional "carriers" for these anhydrides, although the volatility of the anhydrides was sufficient to transfer them into the inlet line of the mass spectrometer. Methane was found to give the best performance.

Under chemical ionization conditions and with detection of the negative ions, the molecular ion of pentafluoropropionic anhydride is observed and the base peak is constituted by the corresponding acyl group at *m/z* 147.

As with silyl derivatization, water flowing from the HPLC column into the interface reacts with the acylating reagent to produce hydrolysis products.

The addition of TFAA "on-line" for the analysis of polyfunctional compounds produces a partial derivatization; this behaviour was observed on injecting cortisol or cortisone.

As shown in Fig. 5, the derivatization of cortisone "off-line", following the usual procedure, produces a spectrum that, under chemical ionization conditions and with flow injection of the mixture containing the reactant, corresponds to the reaction of three trifluoroacyl groups (indicated here as TFA). The ion at *m/z* 648 derives from MW (360) − 3 H (3) + 3TFA (97). An additional adduct of the trifluoroacetic acid anion is observed at *m/z* 761.

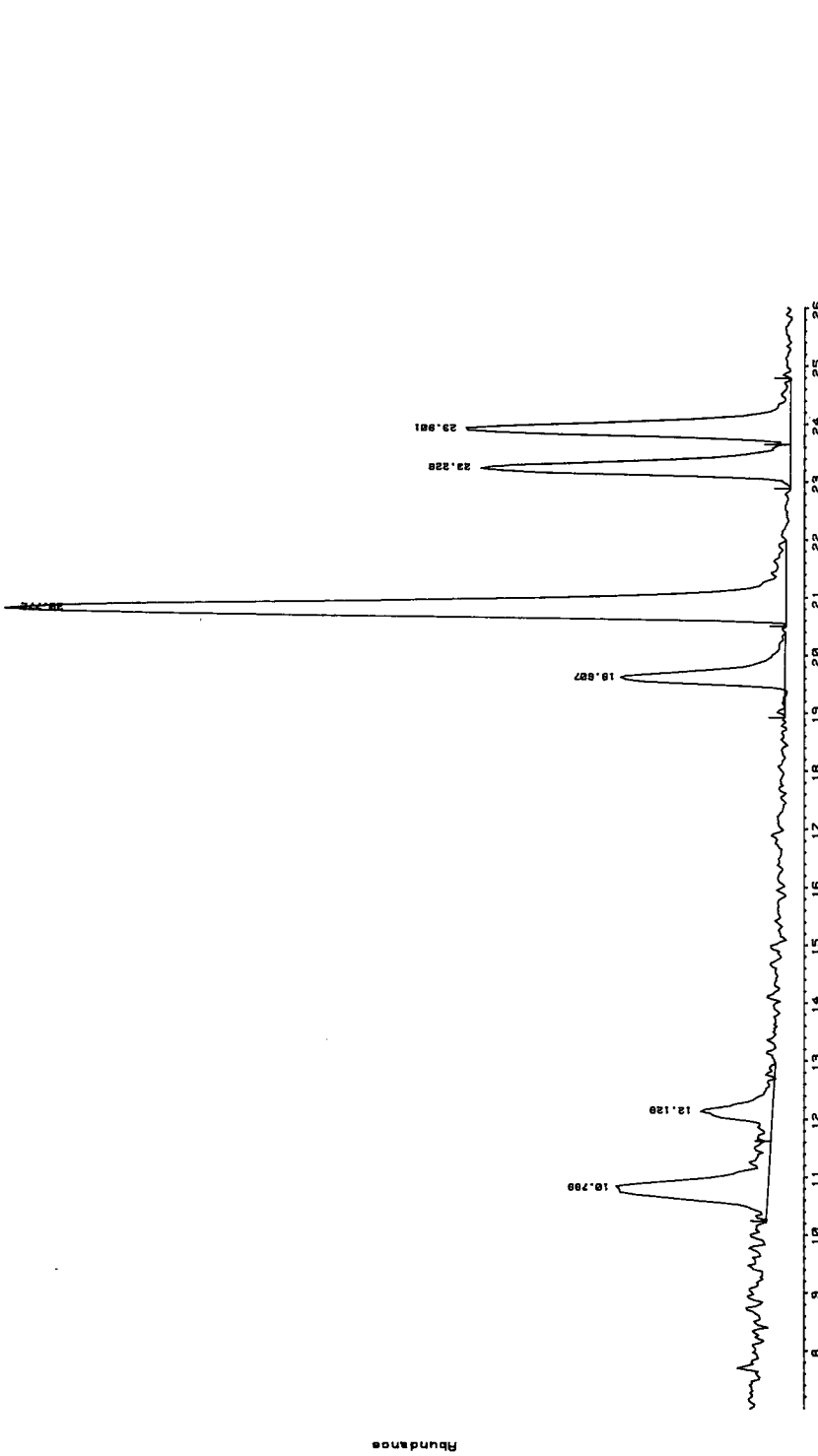

Fig. 3. Chromatogram of a mixture of hydro cortisone, cortisone, testosterone, epitestosterone, androsterone and epiandrosterone by on-line derivatization with BSTFA. Amount injected: 200 ng for all components except epitestosterone (600 ng). Column: 100 × 2.1 mm I.D. stainless steel (Hewlett-Packard) packed with 5-μm Hypersil ODS. Mobile phase: gradient of water–methanol from 40:60 to 1:99 (v/v) in 30 min. flow-rate: 0.4 ml/min. Desolvation chamber temperature: 50°C. Chemical ionization conditions and detection of positive ions. Source temperature: 250°C. Total pressure into the ion source: 130 Pa. Reactant gas: methane–BSTFA (*ca.* 2:1).

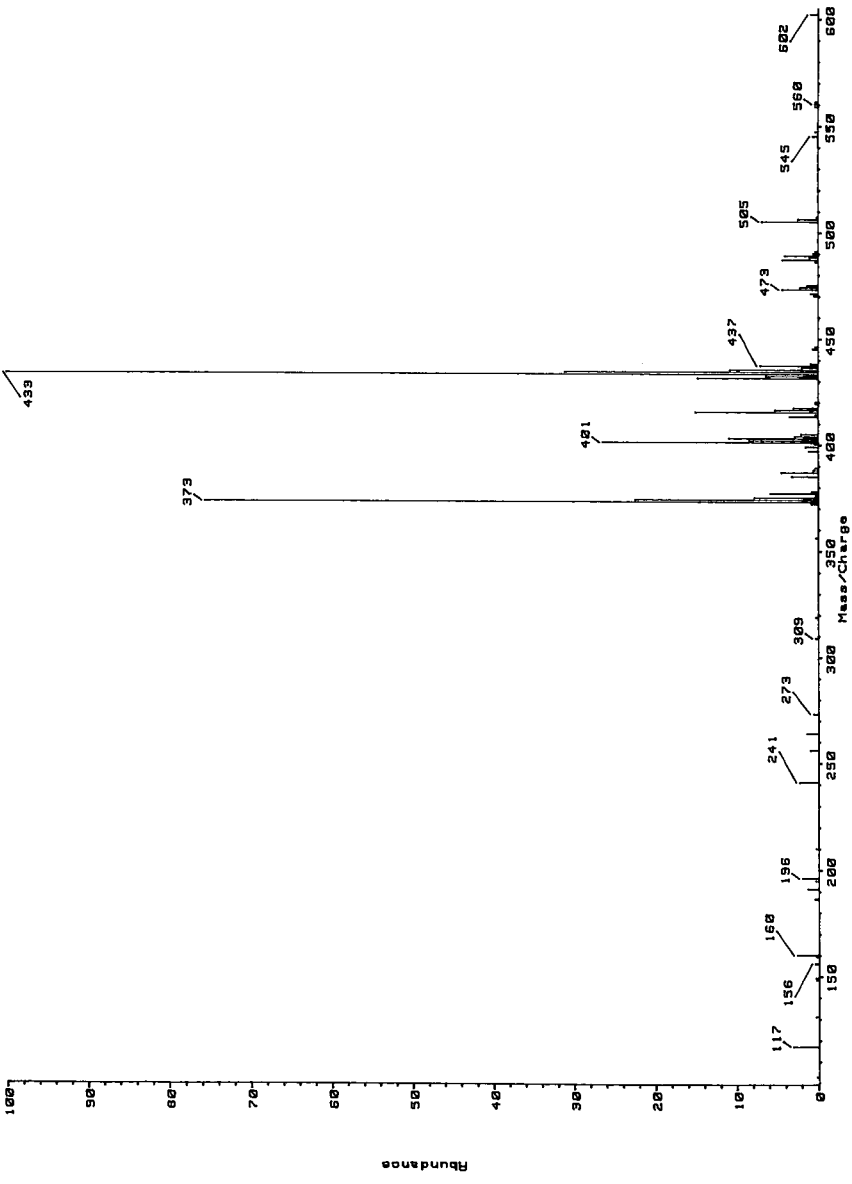

Fig. 4. Mass spectrum of cortisone by on-line derivatization with BSTFA. Conditions as in Fig. 3.

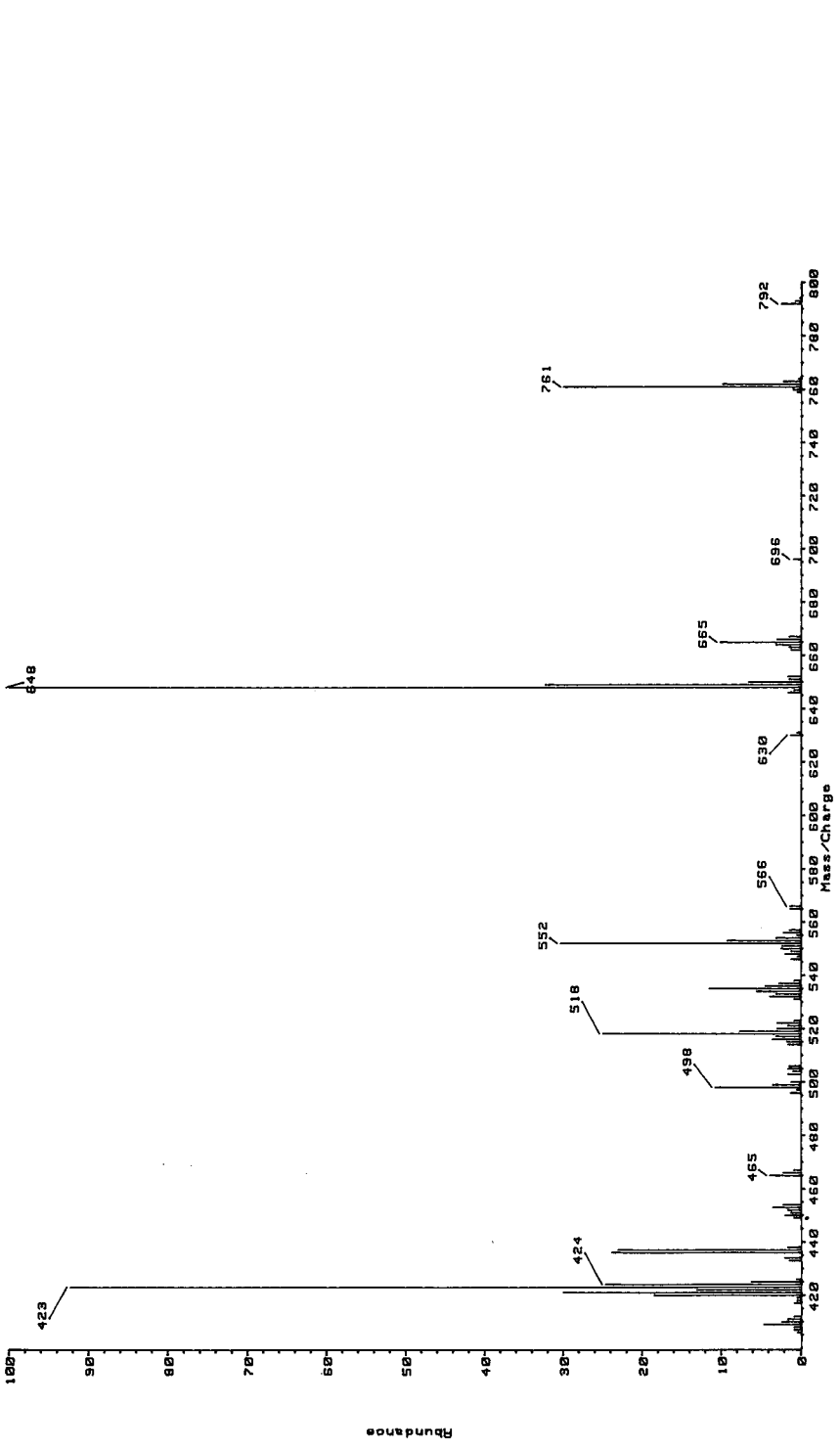

Fig. 5. Mass spectrum of cortisone after reaction with TFAA at 80°C for 1 h and injected bypassing the analytical column. Particle beam interface temperature: 50°C. Chemical ionization conditions with a pressure into the ion source of 130 Pa. Reagent gas: methane. Detection of negative ions. Mobile phase: acetonitrile at a flow-rate of 0.4 ml/min.

TABLE IV

RELATIVE RESPONSE OF FUROSEMIDE USING DIFFERENT DETECTION TECHNIQUES

Detection	R.S.D. (%)[a]	Response ratio[b]
Electron impact	3.5	1 (reference)
Negative ions (CI)	7.6	36.7
Positive ions (CI)	27.4	0.01[c]
Positive CI, on-line derivatization	3.2	0.2

[a] Relative standard derivation (n = 12).
[b] These data are based on absolute response (total ion current) under similar operating conditions.
[c] Methane was used as a chemical ionization reagent.

The "on-line" addition of TFAA (Fig. 6) in the gas phase to cortisone produces mainly the derivatization of one trifluoroacyl group with an addition of one TFAA anion (360 − 1 + 97 + 113) at m/z 569, and a smaller amount of the product of two trifluoroacyl substitutions with a resulting ion at m/z 665.

A similar behaviour was observed on using PFPAA as reactant, but the reaction seems to be less effective as only one group is reacted with the molecule. Ions are found at m/z 669 and 523. No traces of ions are found for the underivatized cortisone. It should be pointed out that the background signal of the derivatization reagent is relatively high with negative-ion detection and under chemical ionization conditions.

Effect of the addition of a water scavenger at the nebulizer

It is known that high water concentrations do not favour the transmission of substances through the particle-beam interface. The detectability of 100 ng of benzidine on changing mobile pahse composition from acetonitrile to pure water, without nebulizer readjustement, drops to about 15% (Table V). Note that if the nebulizer position is readjusted, the response for benzidine with water is about one third of the response obtained with acetonitrile as the mobile phase.

Addition of DMP to the helium used for the nebulization changes this behaviour to some extent by keeping the response less sensitive to changes in mobile phase composition. However, is should be pointed out that the absolute response of the benzidine signal is low.

Postcolumn addition of acetonitrile

It could be verified that the addition of acetonitrile at the outlet of the HPLC column [position (a)] to a water-rich mobile phase (95–100%) improves the detectability by an average factor of *ca.* 2–3, depending of the flow conditions (data not reported).

CONCLUSIONS

On-line derivatization through the particle-beam HPLC–MS interface can be performed in different ways, with a relatively wide selection of derivatization reagents. Criteria for the selection of the derivatization reagent are based on both

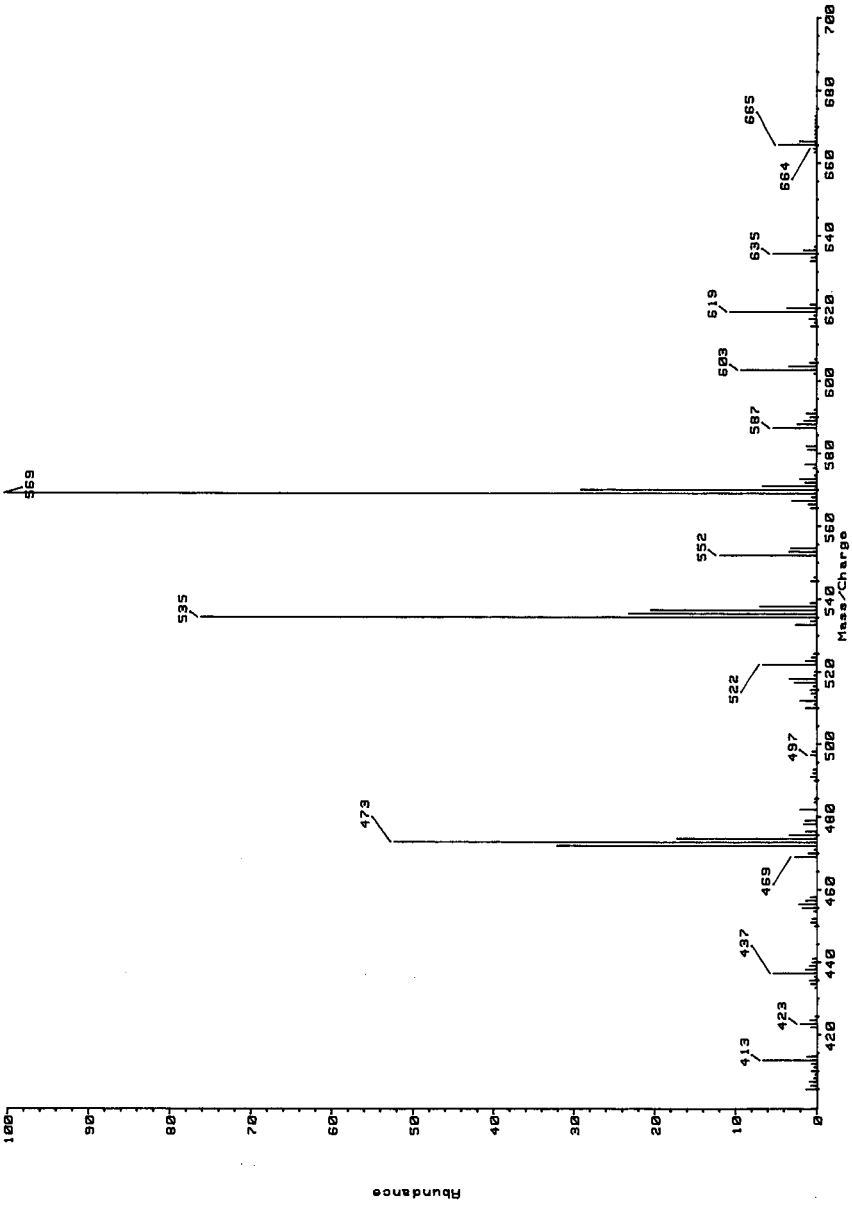

Fig. 6. Mass spectrum of cortisone injected bypassing the analytical column. Mobile phase: acetonitrile at a flow-rate of 0.4 ml/min. Particle-beam interface temperature: 50°C. Chemical ionization conditions. Reactant gas: TFAA. On-line derivatization conditions.

TABLE V

EFFECT OF THE ADDITION OF DMP TO HELIUM USED FOR NEBULIZATION ON THE RESPONSE FOR 100 ng OF INJECTED BENZIDINE

All data obtained without readjustment of the nebulizer position.

Conditions	Mobile phase composition (% of water in acetonitrile)					
	0	25	50	75	90	100
Without addition of DMP	100	88	73	41	20	15
With addition of DMP	18	9	8	8	8	7

volatility and functionality. Volatility is important to be able to bring the reagent into the mass spectrometer in the gas phase. Functionality depends on its activity and rate of reaction with the analyte.

Successful silylations and acylations of several substances have been obtained, and the results have been evaluated on the basis of the resulting mass spectra. On-line silylation reactions are complete for compounds containing one active functional group. For polyfunctional compounds the reaction may take place only for a limited number of functional groups or with all of them to a limited extent.

Some substances with relatively high polarity and low volatility have been derivatized using the described procedure.

Some aspects of the improvement of detectability of some of the substances without or with on-line derivatization, *e.g.*, Acid Red 88, furosemide, maltose and cortisol, are reported. These molecules contain, among others, sulphonate, carboxylic or hydroxy functions or their combinations. The detectability of furosemide with positive-ion detection and under chemical ionization conditions improved by a factor of 20. Reasons for the higher detectability are related to both a higher volatility and mass spectral behaviour of the derivative.

In order to obtain additional qualitative information about the nature of the analyte, the spectra of the derivatives are particularly useful and complementary to other mass spectral data obtained without derivatization.

Typical solvents used for reversed-phase HPLC separations have been used (water, acetonitrile, methanol). Derivatization of the residual solvent at the outlet of the momentum separator has been observed, and this happens even with water as the mobile phase.

Simple modifications to standard instruments were made in order to introduce the reagent into the particle-beam interface. As a general remark, BSTFA can be used more conveniently than TMCS for reliable long-term work, with a limited effect on the contamination of the ion source.

Other experiments involving the addition of a water scavenger to the nebulizer can only reconfirm that the water concentration is definitely an important parameter for the efficiency of both the nebulization process and the desolvation. No other conclusions have been drawn so far from those experiments. Therefore, these data

can be considered as a partial contribution to studies on the nebulization process, which can affect the performance of a particle-beam HPLC–MS interface.

REFERENCES

1 R. C. Willoughby and R. F. Browner, *Anal. Chem.* 56 (1984) 2626–2631.
2 M. Donike, *J. Chromatogr.*, 115 (1975) 591.
3 W. A. Joerne, *J. Anal. Toxicol.*, 11 (1987) 49–52.
4 M. Donike, *J. Chromatogr.*, 78 (1973) 273.
5 E. Sullivan and L. R. Schewe, *J. Chromatogr. Sci.*, 15 (1977) 196.
6 E. Gelpi, E. Peralta and J. Segura, *J. Chromatogr. Sci.*, 12 (1974) 701.
7 R. N. Stillwell, D. I. Carroll, J. G. Nowlin and E. C. Horning, *Anal. Chem.*, 55 (1983) 1313.
8 R. Ventura, D. Fraisse, M. Becchi, O. Paisse and J. Segura, *J. Chromatogr.*, 562 (1991) 723–736.

Journal of Chromatography, 554 (1991) 141–148
Elsevier Science Publishers B.V., Amsterdam

CHROMSYMP. 2230

Characterization of N-acyl-D-biotinols by particle-beam liquid chromatography–mass spectrometry

An alternative to probe mass spectrometry for thermally labile samples

GARY R. CHIPMAN*
Amoco Corporation, Amoco Research Center, P.O. Box 3011, Naperville, IL 60566 (USA)
and
KENNETH A. CRUICKSHANK
Amoco Technology Company, Amoco Research Center, P.O. Box 3011, Naperville, IL 60566 (USA)

ABSTRACT

In the course of preparing biotin-labeled nucleic acid probes, it was necessary to verify structures of intermediate N-acyl derivatives of biotinol. Characterization by mass spectrometry (MS) involved use of particle-beam liquid chromatography (LC)–mass spectrometry MS to supplement standard heated-solids probe techniques. The probe data for a sample of N-toluoylbiotinol indicated it to be a mixture of mono- and di-toluoylbiotinols which was inconsistent with other analytical information. Analysis of the same sample by LC–MS on a reversed-phase column with a water–acetonitrile gradient showed a single major peak with spectrum consistent with that for the monotoluoyl species. These results suggested that a thermal transacylation reaction might be occurring in the probe during heating prior to volatilization and ionization. This was confirmed by heating the sample to 200°C and then repeating the LC–MS analysis to find peaks now present for biotinol and ditoluoylbiotinol as well as the starting material. These results demonstrate the value of particle-beam LC–MS as a technique for obtaining electron-impact mass spectra of thermally sensitive compounds.

INTRODUCTION

The unusually strong and specific interaction between biotin and avidin has been used in a wide variety of applications in analytical biochemistry [1,2]. The basic approach involves labelling the analyte of interest with biotin and then allowing the biotinylated conjugate to bind to the corresponding target molecule. This divalent analyte–receptor complex can be detected by formation of a trivalent complex between the biotin ligand and an avidin derivative which has been conjugated to a signal-generating group such as an enzyme, antibody, fluorophore or chemiluminescent species.

0021-9673/91/$03.50

This approach has found great utility in nucleic acid probes [3,4]. Here biotin-labelled oligonucleotides are used to seek out specific target nucleic acid sequences within biological specimens. For example, the target may be derived from a bacterium or virus whose presence indicates the existence of an infectious disease etiological agent within the specimen. In the present work, biotinylated nucleid acid probes were prepared by the attachment of biotinol via the O-cyanoethyl phosphoramidite derivative to the 5'-terminus of synthetic oligonucleotides. During the course of this work, N-acyl biotinols were isolated as synthetic intermediates and characterized by several analytical techniques to verify the synthetic sequence. Standard heated-probe mass spectrometry (MS) results were found to be inconsistent with other analytical results and particle-beam liquid chromatography (LC)–MS was investigated as a supplemental method to verify purity.

EXPERIMENTAL

LC conditions

The LC system consisted of a multisolvent delivery system (Model 600-MS; Waters Assoc., Milford, MA, USA) and a Waters Model 484-MS absorbance detector. The separations were performed on a Waters Nova-Pak C_{18} (30 cm × 3.9 mm I.D.) reversed-phase column. The flow-rate of the water–acetonitrile mobile phase through the column was 0.6 ml/min. The initial gradient composition of 5% acetonitrile was linearly programmed to 95% in 30 min and then held at the latter condition for 20 min.

MS conditions

The LC–MS analyses were made on an ELQ-400 quadrupole mass spectrometer (Extrel Corp., Pittsburgh, PA, USA) equipped with a Thermabeam interface. A mass range of 70–700 a.m.u. was scanned at a rate of 500 a.m.u./s. The source temperature was 200°C. Helium was used for the nebulizing gas. The desolvation chamber (momentum separator) was held at 110°C and the nebulizer tip was at 150°C. High-resolution probe MS analyses were made on a ZAB-2F magnetic sector instrument (VG Analytical, Manchester, UK).

Chemicals and synthetic procedures

The N-acylbiotinols were prepared from biotin in several steps. D-Biotin (Sigma, St. Louis, MO, USA) was esterified with methanol in the presence of *p*-toluenesulfonic acid. The resulting ester was reduced with lithium aluminum hydride in tetrahydrofuran to D-biotinol [5]. The alcohol function was protected as the monomethoxytrityl ether during the acylation as described below.

N1-(p-Toluoyl)-D-biotinol. To a suspension of D-biotinol (0.860 g, 3.74 mmol) in anhydrous pyridine was added monomethoxytrityl chloride (1.501 g, 4.86 mmol) and the resulting mixture was stirred at room temperature for 16 h. Next, *p*-toluoyl chloride (0.751 g, 4.86 mmol) was added and stirring at room temperature continued for 24 h. After the pyridine was evaporated in vacuo, the residue was dissolved in ethyl acetate, extracted twice with saturated sodium bicarbonate solution and dried over magnesium sulfate. Evaporation of the ethyl acetate left a dark orange oil which was purified by flash chromatography on silica gel using gradient elution (ethyl ace-

tate–hexane, 1:4, v/v to 2:3, v/v and containing 2% triethylamine). The product was colorless foam (1.90 g, 82% yield). $C_{38}H_{24}N_2O_3S$ requires C, 73.52%; H, 6.49; N, 4.51. Found: C, 73.45; H, 6.55; N, 4.22.

A partial solution of the above product (1.5 g, 2.4 mmol) in 100 ml of acetic acid–water (4:1, v/v) was held at 40°C for 1 h while being rotated on a rotary evaporator. The pale yellow solution was evaporated in vacuo and then coevaporated with toluene. The resulting gum was dissolved in 50 ml of methanol, diluted with an equal volume of diethyl ether and allowed to crystallize. A total of 0.669 g (80% yield) of colorless crystalline product was recovered in two crops. M.p. 166–68°C. $C_{18}H_{24}N_2O_3S$ requires C, 62.04; H, 6.94; N, 8.04. Found: C, 61.95; H, 7.01; N, 7.67.

^{1}H NMR ([$^2H_6$]dimethyl sulfoxide (DMSO-d_6)): 7.91 (s, 1H, NH), 7.38–7.16 (m, 4H, phenyl), 5.05 (m,1 H, H_{6a}), 4.36 (t, J=4.8 Hz, ex, OH), 4.21 (m, 1H, H_{3a}), 3.40 (m, 2H, H_{11}), 3.25 (m, 1H, H_4), 3.04 (dd, J=5.1, 12.3 Hz, 1H, H_6'), 2.88 (d, J=12.3 Hz, 1H, H_6''), 2.34 (s, 3H, CH_3), 1.68 (m, 2H, H_7), 1.6–1.3 (m, 6H, $H_{8,9,10}$).

^{13}C NMR (DMSO-d_6): 168.89, 155.39, 140.56. 132.55, 128.41, 127.74, 61.60, 60.56, 57.21, 54.86, 37.34, 32.24, 28.49, 28.10, 25.42, 20.98.

IR (KBr disc): 3400(br), 2930, 1738(s), 1658, 1392, 1339, 1253, 829, 752 cm^{-1}. High-resolution MS: $C_{18}H_{24}N_2O_3S$ requires 348.1508; found 348.1497.

*N1-(p-phenylbenzoyl)-*D*-biotinol.* This compound was prepared from D-biotinol by a sequence of reactions similar to those decribed above, but *p*-phenylbenzoyl chloride was used in place of *p*-toluoyl chloride. The product, which was obtained as a colorless foam, could not be induced to crystallize.

^{1}H NMR (DMSO-d_6): 7.99 (s, 1H, NH), 7.76–7.38 (m, 9H, *p*-biphenyl), 5.08 (m, 1H, H_{6a}), 4.38 (t, J=4.8 Hz, ex, OH), 4.22 (m, 1H, H_{3a}), 3.40–3.20 (m, 3H, H_{11} & H_4 with HDO peak), 3.05 (dd, J=5.1, 12.3 Hz, 1H, H_6'), 2.92 (d, J=12.3 Hz, 1H, H_6''), 1.70 (m, 2H, H_7), 1.6–1.3 (m, 6H, $H_{8,9,10}$). High-resolution MS: $C_{23}H_{26}N_2O_3S$ requires 410.1666; found 410.1661.

RESULTS AND DISCUSSION

The acylated biotinols were isolated and purified as intermediates in a synthetic route to biotinylated nucleic acid probes. It was necessary to confirm their structures to verify that the synthesis was proceeding as planned. There are three possible mono acylbiotinols (Fig. 1). Two of these are acylated at nitrogen (structures I and II) and one is acylated at the hydroxyl oxygen (III). Protection of the hydroxyl group as the monomethoxytrityl ether during acylation should have prevented formation of III. Steric considerations should favor the formation of I over II.

Mass spectral characterization of monoacylbiotinols by standard heated-probe methods was undertaken to supplement and verify the structure and purity as determined by other techniques such as nuclear magnetic resonance. The probe MS data obtained for a monotoluoylbiotinol (Ia) sample suggested that is was not pure, but was mixed with significant amounts of the ditoluoyl species (IVa). Fig. 2 shows single-ion plots for m/z 348 and 466, the corresponding molecular ions of Ia and IVa, respectively, generated from the probe MS data. As can be seen, the plots do not maximize at the same place and clearly indicate the presence of two separate species. This was inconsistent with other analytical information which indicated this sample to be relatively pure.

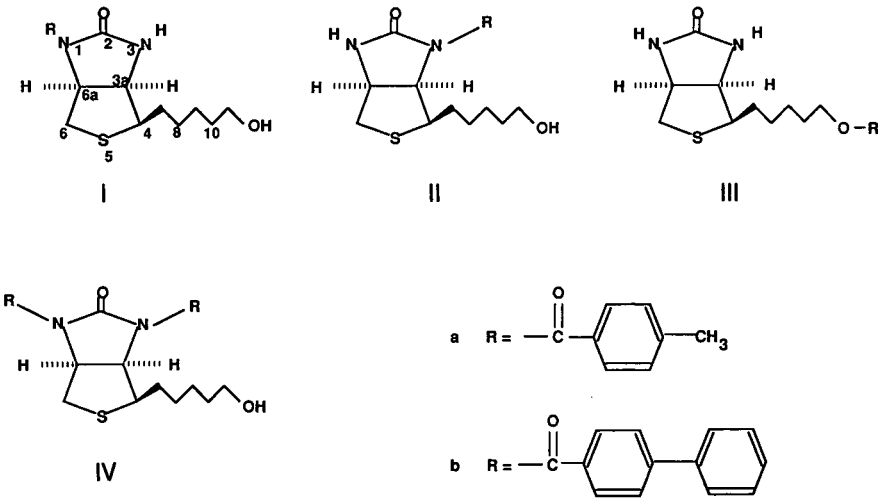

Fig. 1. Structures of acylbiotinols.

The sample was analyzed by particle-beam LC–MS to compare with the probe MS results. The reconstructed-ion chromatogram is shown in Fig. 3a. One major peak (C) was found, with two smaller impurity peaks (D and G) eluting later. The spectral data for peak C indicated a molecular weight of 348 with fragmentation consistent with that expected for Ia. Both D and G are toluoyl derivatives and have molecular weights 390 and 348, respectively. The molecular weight of the peak G species being the same as that of the main component suggests that it is an isomer.

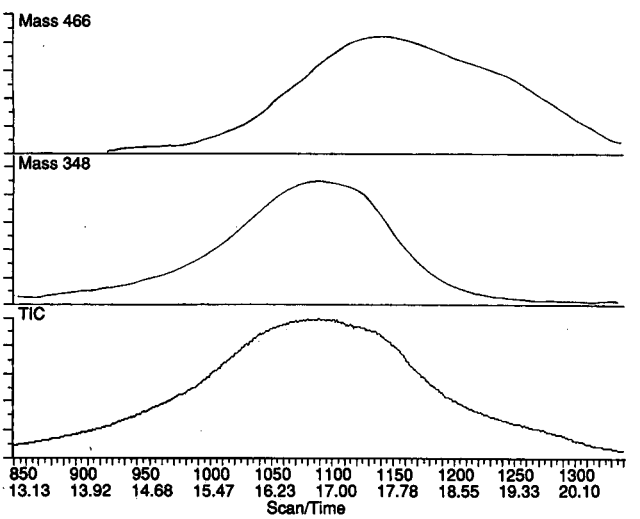

Fig. 2. Probe mass spectrum of mono-*p*-toluoylbiotinol (mol.wt. 348) showing thermal generation of di-*p*-toluoylbiotinol (mol.wt. 466). Time in min.

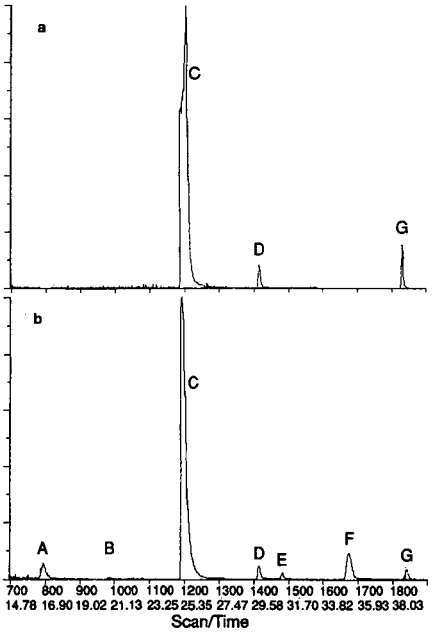

Fig. 3. Total-ion chromatograms of mono-*p*-toluoylbiotinol: (a) as received; (b) after heating to 200°C. Peaks: A = biotinol; B = sulfoxide of I_a (mol. wt. 364); C = I_a; D = acetyl derivative of I_a (mol.wt. 390); E = ring-opened form of peak D? (mol.wt. 392); F = IV_a; G = III_a. Time in min.

This is probably the oxygen-acylated product IIIa which formed in small amounts in spite of the protective monomethoxytrityl group. The long retention time would be consistent with the reduced polarity of the esterified hydroxyl. The impurity at peak D may be a mixed diacylated species having one toluoyl group and one acetyl group. The acetyl group may have been incorporated from contact with ethyl acetate during the synthesis. The LC–MS data show no evidence for the ditoluoyl species detected by probe MS.

The presence of the ditoluoyl species during the probe analysis, but not during LC–MS, suggested that it might be forming by a thermal process during the heat-up of the probe prior to volatilization and ionization. To verify this, a portion of the sample was heated in a small vial to 200–210°C and then analyzed by LC–MS. The reconstructed-ion chromatogram is shown in Fig. 3b and and several new peaks are evident. The spectral data for peak A indicate it has molecular weight 230 and is unsubstituted biotinol. This is consistent with a transacylation reaction, since forming the diacyl species from the monoacyl species requires formation of an equal amount of non-acylated species. The required complement to peak A is peak F which shows apparent molecular weight 466 and has a spectrum consistent with that for the ditoluoyl species IVa. The LC–MS spectrum of this matches that from probe data in showing a fragment at 433 for loss of hydrosulfide from the molecular ion and also toluoyl- and biotinyl-derived fragments analogous to those in the spectrum of Ia. An N,O-ditoluoyl species is also possible, but was ruled out based on observed LC reten-

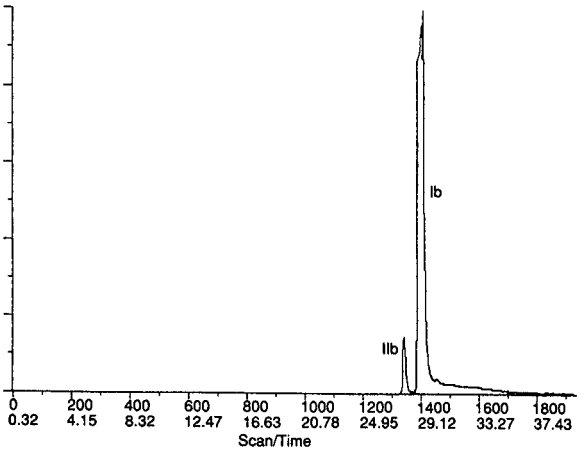

Fig. 4. Total-ion chromatogram of mono-*p*-phenylbenzoylbiotinol. Time in min.

tion time. If present, this species would be less polar than the mono-O-toluoyl compound IIIa (Peak G) and should elute after it on the reversed-phase column. The small peak at B has a molecular weight of 364 and is probably the sulfoxide derivative of Ia which formed during heating in the presence of air. Spectral data for peak E resemble that for peak D, but the molecular weight is 292. This is two units higher than D and may possibly indicate a ring-opened form of D.

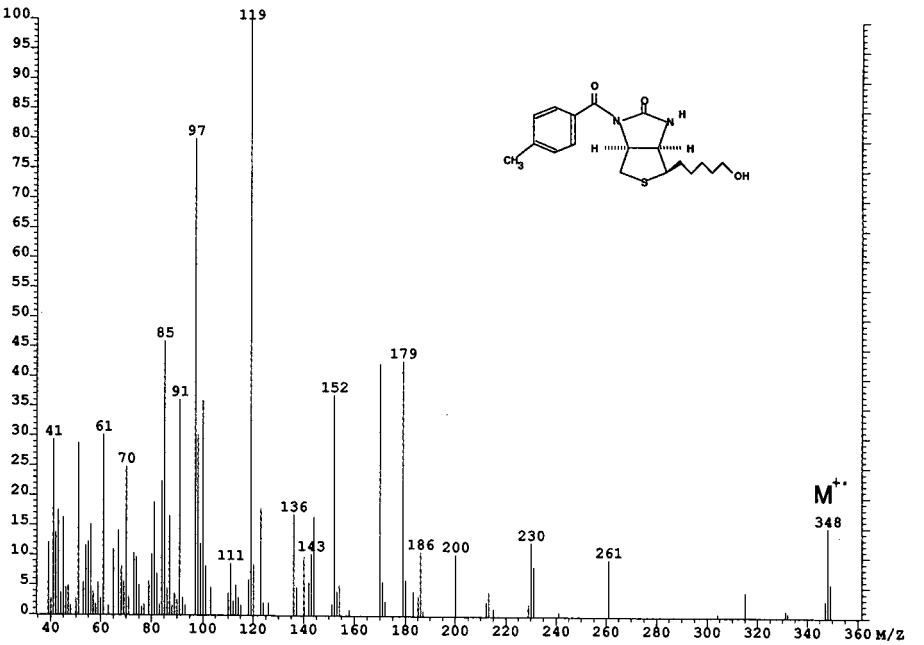

Fig. 5. Mass spectrum of mono-*p*-toluoylbiotinol.

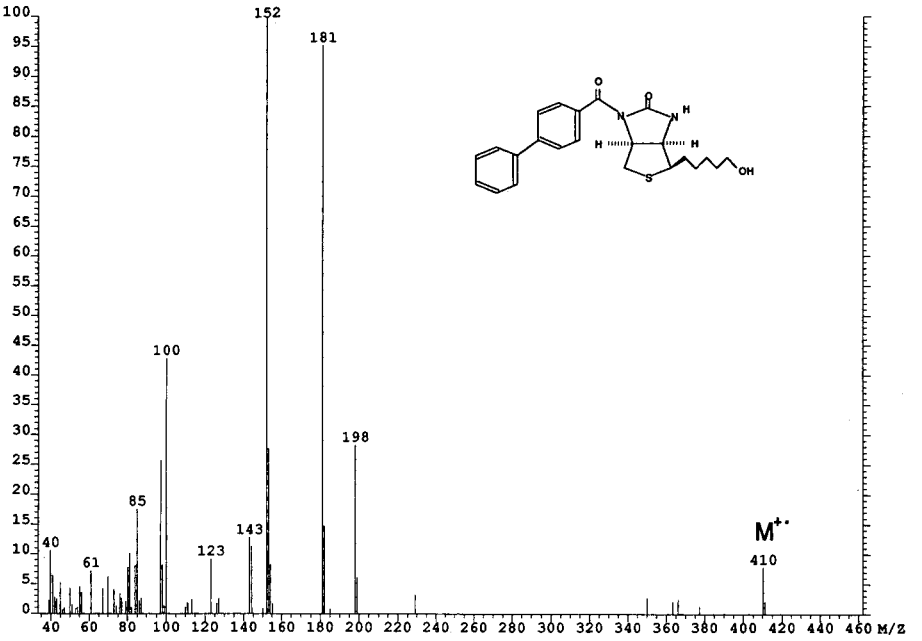

Fig. 6. Mass spectrum of mono-*p*-phenylbenzoylbiotinol.

The *p*-phenylbenzoyl derivative of biotinol (Ib) was also prepared and characterized. It was found to be far more thermally stable than the toluoyl derivative and no evidence for the corresponding diacyl species (IVb) was detected during probe MS analysis of samples of Ib. Fig. 4 shows the reconstructed-ion chromatogram from LC–MS analysis of a sample of Ib. The spectral data for the two peaks are virtually identical and indicate molecular weight 410. The larger peak is probably due to Ib and the smaller one to IIb. Having the less-hindered nitrogen uncovered should increase the polarity of IIb relative to Ib and would explain the shorter retention time.

Mass spectra of Ia and Ib from high-resolution solids probe data are shown in Fig.5 and 6, respectively. In both cases, the acyl ion and its fragments dominate the spectra. The molecular ions are detectable in both cases and lose 33 units (HS) to give their highest mass primary fragment. The lower mass region shows several major fragment peaks containing nitrogen or sulfur which may be stabilized as heterocyclic structures. Fragements such as *m/z* 179 ($C_9H_{11}N_2O_2$), 97 ($C_4H_5N_2O$) and 85 ($C_3H_5N_2O$) probably have imidazolidone-related structures, while 152 ($C_9H_{12}S$) and 100 (C_5H_8S) are thiophene derived. In the spectrum of Fig. 6, the *m/z* 152 peak would also be partly due to $C_{12}H_8$.

CONCLUSIONS

Particle-beam LC–MS has been successfully demonstrated to characterize acylbiotinols for purity and structure. A thermal transacylation reaction was suspected of occurring during probe MS of Ia and giving misleading results. This was verified by

obtaining similar results by heating the sample prior to LC–MS analysis. Particle-beam LC–MS offers a gentler method than probe MS for obtaining electron-impact mass spectra of thermally sensitive samples.

ACKNOWLEDGEMENTS

The assistance of A. J. Dalal, D. E. Reed and J. B. Schilling with data acquisition is gratefully acknowledged.

REFERENCES

1 E. A. Bayer and M. Wilchek, in D. Glick (Editor), *Methods of Biochemical Analysis*, Vol 25, Wiley, New York, 1980, pp. 1–45.
2 P. C. Weber, D. H. Ohlendorf, J. J. Wendoloski and R. F. Salemme, *Science (Washington, D.C.)*, 243 (1980) 85.
3 P. Langer, A. A. Waldrop and D. C. Ward, *Proc. Natl. Acad. Sci. U.S.A.*, 78 (1981) 6633.
4 A. Roget, H. Bazine and R. Theoule, *Nucl. Acids Res.*, 17 (1989) 7643.
5 H. Flaster and H. Kohn, *J. Heterocycl. Chem.*, 18 (1981) 1425.

Journal of Chromatography, 554 (1991) 149–154
Elsevier Science Publishers B.V., Amsterdam

CHROMSYMP. 2242

Increasing thermospray response for cortisol by derivatization

JAN PAULSON* and CLAES LINDBERG
Bioanalytical Chemistry, AB Draco (Subsidiary of AB Astra), P.O. Box 34, S-221 00 Lund (Sweden)

ABSTRACT

The 21-hydroxyl group of cortisol was selectively acetylated under mild conditions without affecting the more sterically hindered 11β- and 17α-hydroxyl groups. The reaction was performed with a mixture of acetic anhydride and triethylamine in acetonitrile and was complete in less than 15 min at room temperature. The thermospray mass spectrum of cortisol 21-acetate showed minimal fragmentation with the $[M + H]^+$ ion as the base peak. High sensitivity was achieved for acetylated cortisol during selected ion monitoring, the signal-to-noise ratio being increased by a factor of about 4, compared to underivatized cortisol. The limit of detection of cortisol 21-acetate was estimated at 0.24 pmol injected, making thermospray liquid chromatography–mass spectrometry competitive with gas chromatography–mass spectrometry for the determination of cortisol in biological fluids.

INTRODUCTION

Measurement of plasma, serum or urine cortisol concentration is useful in assessing adrenocortical function. Stable isotope dilution combined with gas chromatography (GC)–mass spectrometry (MS) offers the required sensitivity and selectivity and has been widely used for cortisol analysis [1–7]. These methods are based on electron ionization [1,2,4–7] or positive-ion chemical ionization [3] of the dimethoxime-tris(trimethylsilyl) derivative of cortisol. Recently, methods based on thermospray (TSP) liquid chromatography (LC)–MS have been used for serum cortisol determination [8,9], thereby obviating the lengthy, two-stage derivatization procedure required by GC–MS. Detection limits of 5 pmol [9] and 14 pmol (5 ng) [10] have been reported for cortisol by LC–TSP-MS. Gaskell *et al.* [8] found LC–MS inferior to GC–MS in terms of sensitivity and precision and concluded that the magnitude and stability of the LC–MS response for cortisol had to be improved to make this method competitive.

Detection-oriented derivatization, to increase analyte response, has been successfully applied to several areas of LC [11]. Thermospray response varies widely between different compounds [10,12,13], but although lack of response can be a serious drawback of the technique for certain applications derivatization has not been frequently used to overcome this problem. Voyksner and Bush [14] used post-column

0021-9673/91/$03.50

addition of trimethylanilinium hydroxide to achieve thermally induced methylation of carboxylic acids in the thermospray vaporizer. Voyksner *et al.* [15] also esterified carboxylic acids with diethylaminoethyl chloride, thereby increasing proton affinity by introducing a basic amino group in the derivative. Abián *et al.* [16] used diazomethane to form the carboxylic acid methyl esters of prostaglandins. They also tried methoximation of prostaglandin keto groups but obtained no improved sensitivity with this derivative [16]. We have found that acetylation of the 21-hydroxyl group of cortisol, by a simple and rapid derivatization procedure (see Fig. 1), increases thermospray response and decreases the detection limit of cortisol in biological samples.

EXPERIMENTAL

Chemicals

The structures of cortisol and cortisol 21-acetate are shown in Fig. 1. Cortisol (98%) was obtained from Sigma (St. Louis, MO, USA) and trideuterated cortisol ([9,12,12-$^2H_3$]cortisol) from KOR Isotopes (Cambridge, MA, USA). Acetic acid (Gold Label grade, 99+%), triethylamine (Gold Label grade, 99+%) and acetic anhydride (GC grade, 98–99%) were obtained from Aldrich-Chemie (Steinheim, Germany). Ammonium acetate (MicroSelect, >99%) was obtained from Fluka Chemie (Buchs, Switzerland) and acetonitrile and methanol (HPLC quality) from Fison (FSA Laboratory Supplies, Loughborough, UK). All water was purified in a Milli-Q system (Millipore, Molsheim, France).

Mobile phase preparation

The pH of a 1.0 *M* ammonium acetate solution was adjusted to 5.2 with 1.0 *M* acetic acid. To prepare 1 l of mobile phase, 100 ml of 1.0 *M* ammoium acetate buffer, pH 5.2, were mixed with 400 ml of water and 500 ml of methanol, giving a 0.1 *M* ammonium acetate buffer containing 50% methanol. [The pH of 0.1 *M* ammonium acetate buffer, prepared by diluting a 1.0 *M* solution (pH 5.2) with water, is approximately 5.0.]

Derivatization procedure

To mimic the eluate obtained after solid-phase extraction (the extraction will be described elsewhere), alcoholic standard solutions of cortisol were evaporated to dryness in polypropylene tubes. The residue was treated with 250 µl of a solution containing 12.5% acetic anhydride and 12.5% triethylamine in acetonitrile. After vortex-

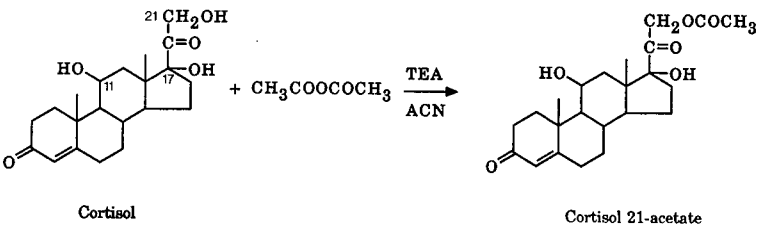

Cortisol Cortisol 21-acetate

Fig. 1. Reaction scheme for the derivatization of cortisol with acetic anhydride in the presence of triethylamine (TEA) and acetonitrile (ACN).

ing, the tubes were allowed to stand uncapped at room temperature for 15 min, and then evaporated to dryness. The residue was dissolved in 100 μl of 30% methanol in water and 40 μl of the solution were injected into the LC–MS system.

Liquid chromatography–mass spectrometry

A Finnigan TSQ70 mass spectrometer equipped with a Finnigan thermospray interface (TSP1) (Finnigan MAT, San José, CA, USA) was used in an automated LC–MS system [17]. Mass calibration was performed with a solution of polyethyleneglycol [17]. The instrument was tuned for maximum sensitivity by direct injection of a solution of cortisol 21-acetate. Cortisol and acetylated cortisol were chromatographed on a 33 × 4.6 mm I.D. Supelcosil LC-8-DB (3 μm) cartridge. The mobile phase was 0.1 *M* ammonium acetate buffer, pH 5, containing 50% methanol, pumped at a flow-rate of 1.9 ml/min. To investigate the thermally induced fragmentation of cortisol and cortisol 21-acetate the vaporizer temperature was varied between 80 and 90°C and the jet temperature between 160 and 220°C. The repeller potential was kept at 100 V. Mass spectra were obtained by scanning from *m/z* 200 to *m/z* 500 in 1 s. For quantitative analysis the vaporizer was kept at 90°C and the jet block at 172°C. The $[M + H]^+$ ions of cortisol (*m/z* 363), cortisol 21-acetate (*m/z* 405), and $[^2H_3]$cortisol 21-acetate (*m/z* 408) were recorded by selected ion monitoring by scanning over a 0.6-a.m.u. window in 400 ms for each mass.

RESULTS AND DISCUSSION

Cortisol, as well as various synthetic corticosteroids, are known to undergo facile eliminiation of the C-20–C-21 side-chain ($[M + H - 60]^+$) under thermospray ionization conditions [8–10, 18–21]. During development work on new corticosteroid drugs we have found that the C-20–C-21 side-chain can be stabilized during thermospray ionization by acetylation of the 21-hydroxyl group. This group can be selectively acetylated under mild conditions without affecting the more sterically hindered 11β- and 17α-hydroxyl groups in cortisol (*cf.* ref. 22). The reaction was complete in less than 15 min at room temperature, and the formation of di- or triacetyl derivatives was not observed even after extended reaction time. Acetylation of the corticosteroid 21-hydroxyl group has been used previously as a derivatization reaction in GC [23] and GC–MS [24]. Fig. 2 compares thermospray mass spectra of cortisol and cortisol 21-acetate, obtained at two different interface temperature combinations. The spectra were obtained from mixtures of unlabelled and deuterium-labelled compounds. Underivatized cortisol showed extensive fragmentation, which could not be significantly improved by lowering the vaporizer and ion source temperatures. Cortisol 21-acetate, on the other hand, produced the $[M + H]^+$ ion as the base peak with minimal fragmentation even at high temperature of the thermospray interface. The formation of the $[M + H - H_2O]^+$ ion and $[M + H - 60]^+$ ion in the thermospray mass spectrum of cortisol has been suggested to be promoted by the 17α-hydroxyl group [8]. Interestingly, the corresponding fragments in the spectrum of cortisol 21-acetate were small (*m/z* 387, 5%; *m/z* 345, 20%) in spite of the presence of a free 17α-hydroxyl group.

Fig. 3 compares selected ion current profiles of three consecutive injections of 1.0 pmol of cortisol and acetylated cortisol. The results show that derivatization of

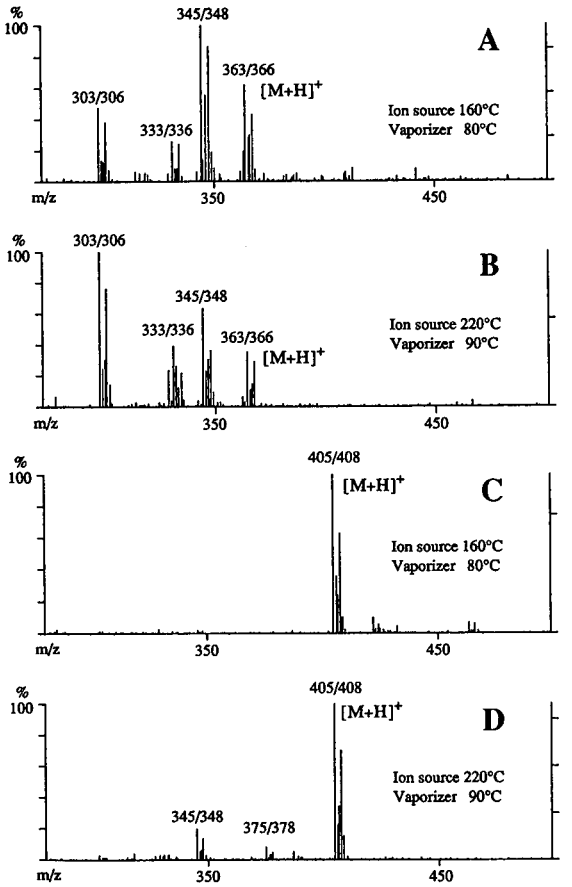

Fig. 2. Thermospray mass spectra of cortisol (A) and (B) and cortisol 21-acetate (C) and (D) at different temperatures of the thermospray interface. The spectra were obtained from mixtures of unlabelled and deuterium-labelled compounds.

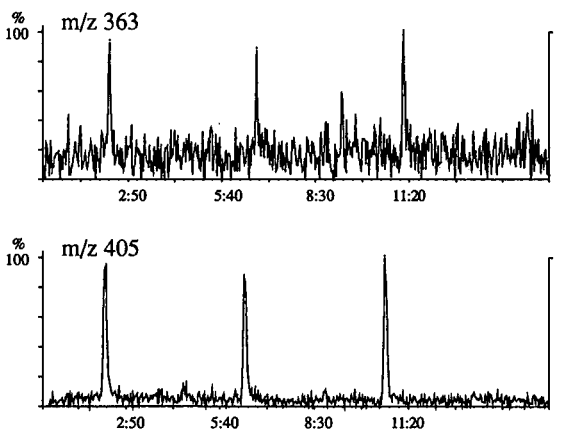

Fig. 3. Selected ion current profiles of three consecutive injections of 1.0 pmol of cortisol (*m/z* 363) and cortisol 21-acetate (*m/z* 405). Time in min.

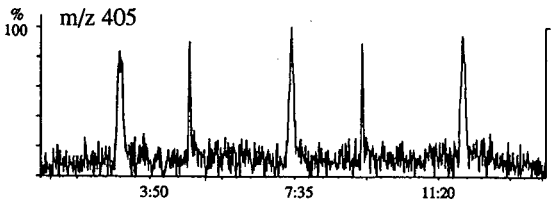

Fig. 4. Selected ion current profile of three injections of 0.24 pmol of cortisol 21-acetate. Time in min.

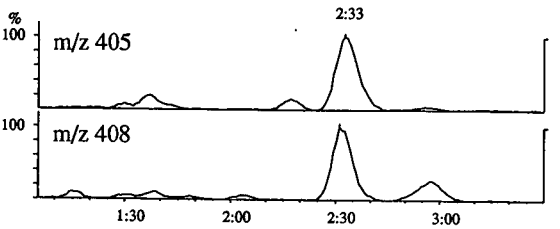

Fig. 5. Selected ion current profiles of cortisol 21-acetate (*m/z* 405) and [$^2H_3$]cortisol 21-acetate (*m/z* 408) (internal standard) obtained from a urine extract. The urine cortisol concentration was estimated at 24 nmol/l. Time in min.

cortisol increased the signal-to-noise ratio by a factor of about 4. Fig. 4 shows a selected ion current profile of three 0.24-pmol injections of cortisol 21-acetate, corresponding to the limit of detection. This limit of detection is twenty times lower than that reported by Esteban *et al.* [9], making LC–TSP-MS a viable alternative to GC–MS for the determination of cortisol in biological samples. Linear calibration curves for cortisol, analysed as the 21-acetate and by using [$^2H_3$]cortisol as internal standard, were obtained in the range 2–80 pmol injected. Fig. 5 shows a chromatogram obtained after solid-phase extraction of 1 ml of urine, with a cortisol concentration estimated at 24 nmol/l. A full report of the method will be published elsewhere.

CONCLUSIONS

Elimination of the need for derivatization is, as often stated, a great advantage of LC–TSP-MS. The present example, however, shows that derivatization can be worth considering as a means of increasing sensitivity. Acetylation of cortisol is a simple and rapid reaction making the LC–MS method less labour-intensive and less time-consuming than GC–MS.

REFERENCES

1 I. Björkhem, R. Blomstrand, O. Lantto, A. Löf and L. Svensson, *Clin. Chim. Acta*, 56 (1974) 241.
2 L. Siekmann and H. Breuer, *J. Clin. Chem. Clin. Biochem.*, 20 (1982) 883.
3 C. Lindberg, S. Jönsson, P. Hedner and Å. Gustafsson, *Clin. Chem.*, 28 (1982) 174.
4 J. A. Jonckheere and A. P. de Leenheer, *Biomed. Mass Spectrom.*, 10 (1983) 197.
5 S. J. Gaskell, C. J. Collins, C. G. Thorne and G. V. Groom, *Clin. Chem.*, 29 (1983) 862.

6 D. G. Patterson, M. B. Patterson, P. H. Culbreth, D. M. Fast, J. S. Holler, E. J. Sampson and D. D. Bayse, *Clin. Chem.*, 30 (1984) 619.
7 N. Hirota, T. Furuta and Y. Kasuya, *J. Chromatogr.*, 425 (1988) 237.
8 S. J. Gaskell, K. Rollins, R. W. Smith and C. E. Parker, *Biomed. Environ. Mass Spectrom.*, 14 (1987) 717.
9 N. V. Esteban, A. L. Yergey, D. J. Liberato, T. Loughlin and D. L. Loriaux, *Biomed. Environ. Mass Spectrom.*, 15 (1988) 603.
10 L. D. Bowers, *Clin. Chem.*, 35 (1989) 1282.
11 H. Lingeman and W. J. M. Underberg, *Detection-Oriented Derivatization Techniques in Liquid Chromatography*, Marcel Dekker, New York, 1990.
12 R. D. Voyksner and C. A. Haney, *Anal. Chem.*, 57 (1985) 991.
13 T. R. Covey, E. D. Lee, A. P. Bruins and J. D. Henion, *Anal. Chem.*, 58 (1986) 1451A.
14 R. D. Voyksner and E. D. Bush, *Biomed. Environ. Mass Spectrom.*, 14 (1987) 213.
15 R. D. Voyksner, E. D. Bush and D. Brent, *Biomed. Environ. Mass Spectrom.*, 14 (1987) 523.
16 J. Abián, O. Bulbena and E. Gelpí, *Biomed. Environ. Mass Spectrom.*, 16 (1988) 215.
17 C. Lindberg, J. Paulson and A. Blomqvist, *J. Chromatogr.*, 554 (1991) 215.
18 T. Covey and J. Henion, *Anal. Chem.*, 55 (1983) 2275.
19 D. J. Liberato, A. L. Yergey, N. Esteban, C. E. Gomez-Sanchez and C. H. L. Shackleton, *J. Steroid Biochem.*, 27 (1987) 61.
20 P. R. Das, B. N. Pramanik, R. D. Malchow and K. J. Ng, *Biomed. Environ, Mass Spectrom.*, 15 (1988) 253.
21 P. C. Goodley, *Compilation of Thermospray Mass Spectra*, Hewlett-Packard, Palo Alto, CA, 1986.
22 D. R. Knapp, *Handbook of Analytical Derivatization Reactions*, Wiley, New York, 1979, p. 449.
23 H. H. Wotiz, I. Naukkarinen and H. E. Carr, Sr., *Biochim. Biophys. Acta*, 53 (1961) 449.
24 D. G. Watson, J. M. Midgley and C. N. J. McGhee, *Rapid Commun. Mass Spectrom.*, 3 (1989) 8.

Journal of Chromatography, 554 (1991) 155–173
Elsevier Science Publishers B.V., Amsterdam

CHROMSYMP. 2339

Use of methyl oxime derivatives to enhance structural information in thermospray high-performance liquid chromatography–mass spectrometry

Analysis of linoleic acid lipoxygenase metabolites in maize embryos

J. ABIÁN

Department of Neurochemistry, Centro de Investigación y Desarrollo, CSIC, Jordi Girona 18–26, 08034 Barcelona (Spain)

M. PAGÈS

Department of Molecular Genetics, Centro de Investigación y Desarrollo, CSIC, Jordi Girona 18–26, 08034 Barcelona (Spain)

and

E. GELPÍ*

Department of Neurochemistry, Centro de Investigación y Desarrollo, CSIC, Jordi Girona 18–26, 08034 Barcelona (Spain)

ABSTRACT

Lipoxygenase derived metabolites of linoleic acid generated by incubation with protein extracts from maize embryos treated with abscisic acid have been analysed by thermospray high-performance liquid chromatography–mass spectrometry (HPLC–TSP-MS). TSP-MS data for various isomeric α- and γ-ketols, ketodiols and trihydroxyacids are reported. The molecular weight and the minimum number of oxygenated functions in the structures can be readily characterized from the TSP spectra obtained in the positive and negative ion modes of acquisition. TSP analysis of the methoximated compounds allows the characterization of ketone or aldehyde groups. Additionally, the methoximated derivatives show abundant ions derived from concomitant losses of methanol and the breakdown of the C–C bond α to the methoxime. These ions are the base peaks in the TSP spectra of compounds bearing an α-ketol moiety in their structures. The TSP data and fragment assignments are in agreement with the structures previously elucidated by gas chromatography (GC)–MS techniques. Furthermore, the characteristic fragmentation pattern of the methoxime derivatives allows the characterization of a pair of positional isomer α-ketols not detected previously by GC–MS. Some of these metabolites have not been described before in maize.

INTRODUCTION

Lipoxygenase (LOX) activity was initially discovered in the plant kingdom where the most common substrates are linoleic (LA) and linolenic acid. In general,

0021-9673/91/$03.50

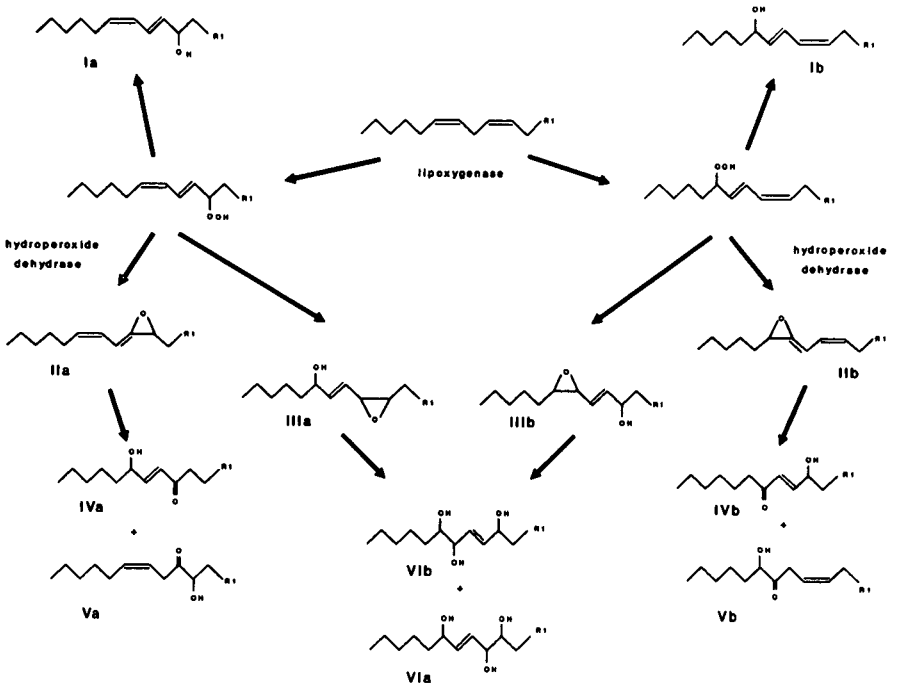

Fig. 1. LOX metabolic pathways of LA leading to linear chain C_{18} acids. R1 is $(CH_2)_6COOH$.

LOX in plants catalyses the addition of oxygen to positions *n*-6 or *n*-10 of the fatty acid, giving rise to conjugated hydroperoxyoctadecadienes (HPODEs) such as the 9- or 13-HPODEs. These HPODEs can either be reduced to their corresponding hydroxy acids (9- or 13-HODEs) or they can generate α- and γ-ketols, various short chain aldehydes and oxo acids and a group of compounds structurally similar to prostaglandins, with 12-oxo-phytodienoic acid as the parent compound [1]. Some of the LOX derived metabolites of LA detected to date in various plant sources are illustrated in Fig. 1. The physiological role of these compounds is for the most part still to be determined, although they seem to be implicated in growth and development, senescence and responses to physical or pest derived injuries [1,2].

Work has recently been completed on the identification of LOX metabolites of LA in maize embryos using gas chromatography–mass spectrometry (GC–MS) and on the effect of abscisic acid (ABA) on this metabolism during embriogenesis [3]. ABA is a plant hormone that regulates growth during seed maturation [4]. In the course of this work the role of thermospray high-performance liquid chromatography–mass spectrometry (HPLC–TSP-MS) in this type of application was evaluated. This paper shows how TSP can provide not only molecular but also structural information leading to the identification of individual metabolites, verified by GC–MS. Along these lines we illustrate the identification of new metabolites based only on the analysis of data from TSP-MS; to our knowledge this is a unique example of new compound identification by TSP-MS.

MATERIALS AND METHODS

Reagents

LA was obtained from Merck (Darmstadt, Germany) and [1-^{14}C] LA (59 mCi/mmol) from New England Nuclear (Du Pont de Nemours, Dreieich, Germany).

The scintillation liquid, Unisolve 1, was from Koch-Light (Colnbrook, UK). The derivatization reagents used were 1-methyl-3-nitro-1-nitrosoguanidine (Aldrich-Chemie, Steinheim, Germany) and methoxyamine hydrochloride (Eastman Kodak, Rochester, NY, USA).

The water used in the HPLC eluents was of Milli-Q grade (Waters Assoc., Milford, MA, USA) and was passed through a 0.45-μm filter. The other reagents and solvents were of analytical or spectroscopic grade.

Plant material

Isolated embryos of Zea maize L inbred line W-64 at different stages of development (from 15 days after pollination to dry embryos) were used. Incubation of embryos in the presence of ABA was performed by culturing the isolated embryos for 7 days in basal medium with 10 μM ABA, as described previously [5].

Enzyme extracts

Extracts from control and ABA incubated embryos were prepared by grinding the fresh material in a mortar with liquid nitrogen [6]. A 100–200-mg mass of powder was immediately sonicated in 1 ml of 0.05 *M* phosphate buffer (pH 7) (2% sodium metabisulphite). The samples were centrifuged and the supernatants were used for the incubation with LA.

Oxidation products of linoleic acid

A 100-μg mass of LA and 0.5 μCi of [1-^{14}C] LA were added to 4 ml of 0.05 *M* phosphate buffer (pH 6) with 500–800 μl of the enzyme extract. To avoid the presence of LA autooxidation products, both LA and [1-^{14}C] LA were previously purified and monitored by reversed-phase HPLC. The incubation was carried out at room temperature for 30 min with vigorous shaking and in the presence of air.

Residual hydroperoxides in the media were then reduced by the addition of 500 μl of tin(II) chloride (1 mg/ml in ethanol). After a 30 min reaction time the incubation media were saturated with sodium chloride and extracted at pH 3 with diethyl ether. The ethereal extracts were dried with anhydrous sodium sulphate and evaporated to dryness under a stream of helium. The residue was redisolved in acetonitrile (ACN) and stored at -80°C until analysis.

Liquid chromatography

The HPLC separations were carried out using a reversed-phase 10 μm (30 × 0.4 cm) Spherisorb ODS-2 column (Phase Separations, Queensferry, UK). The mobile phase was water (pH 3.5 with acetic acid) with a gradient of ACN from 30 to 95% in 30 min.

Radioactivity was detected using an on-line LS detector (Ramona, RAYTEST) or by the counting radioactivity of sequential 30 s fractions in a Beckman LS counter detector.

Derivatization

Methylation and methoximation were carried out by standard procedures (ethereal diazomethane and methoxyamine hydrochloride in pyridine as reagents, respectively) as described previously [7]. Derivatized fractions were redisolved in methanol and injected directly in the TSP system.

HPLC–TSP-MS

A Hewlett Packard 5988A quadrupole instrument with a Vestal type TSP source and interface was used.

The chromatography was accomplished using a 5 μm (15 × 0.4 cm) Spherisorb ODS-2 reversed-phase column. The mobile phase consisted of mixtures of 0.1 *M* ammonium acetate buffer (AMAC) and 0.05 *M* AMAC in methanol. The specific HPLC–TSP-MS conditions and gradient programmes are given in Tables I–VII.

The amount of LA metabolites injected for each TSP-MS analysis (full scan acquisition) was around 0.1–0.5 μg as measured by the total radioactivity counted in each HPLC fraction and for a theoretical 100% extraction recovery.

Metabolite characterization by GC–MS

Compounds in the major radioactive HPLC fractions were characterized by GC–MS techniques as described elsewhere [3].

RESULTS AND DISCUSSION

Radiochromatography profiles and TSP-MS analysis of selected HPLC fractions

The radiochromatographic profiles from extracts of 15-day-old maize embryos treated or untreated with ABA are shown in Fig. 2.

Under the described incubation conditions only minor amounts of unmetabolized LA could be detected. Various radioactive peaks were observed in these profiles and eight of these were amenable to analysis by MS, their individual abundances varying with ABA treatment and stage of development. All of theses peaks disappeared after the extracts were deactivated by heat at 100°C for 1 min prior to incubation.

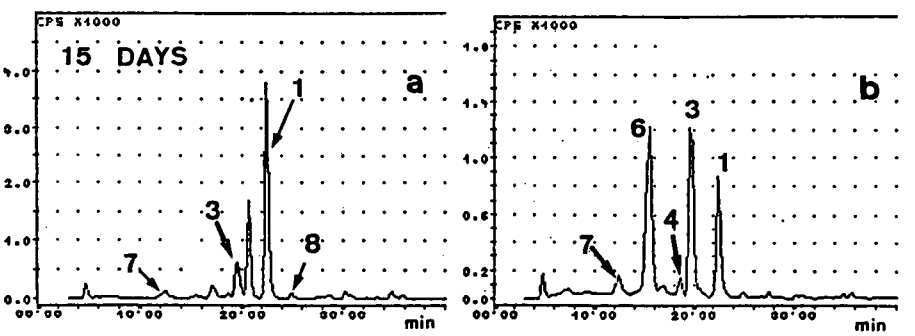

Fig. 2. HPLC radiochromatograms obtained from incubates of [1-14C]LA with maize embryo extracts 15 days after polinization. (a) Control; (b) sample treated with ABA as described under Experimental.

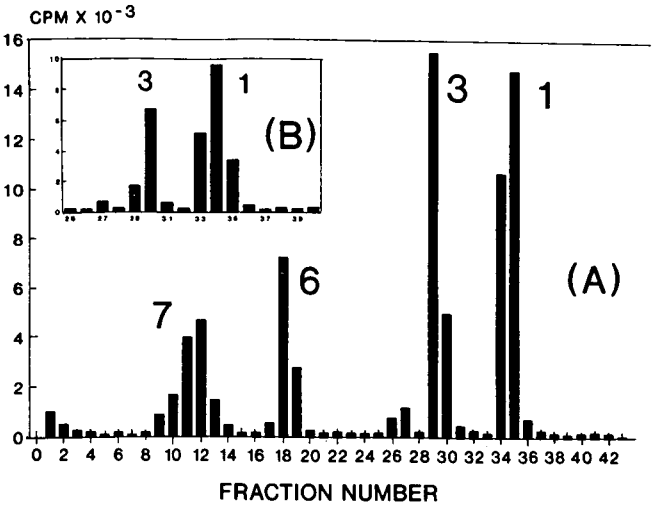

Fig. 3 (A) HPLC reconstructed radiochromatogram with indication of fraction numbers. Peaks 1, 3, 6 and 7 indicating the major radioactive fractions correspond to the same peaks shown in Fig. 2b. Partial profile from a different experiment. Fractions 33–35 in this profile were selected for a more accurate analysis of the composition of peak 1.

The most pronounced change in the profile is that observed in the appearance and high relative abundance of peak 6 when young embryos are exposed to ABA, especially in the earlier stages of development (Fig. 2b). The peak, which can hardly be detected at 15 days without ABA treatment (Fig. 2a), attains a height equivalent to that of peak 3 after ABA treatment. The induction of peak 6 gradually decreases with maturation and disappears in the dry embryos. During normal embryogenesis this

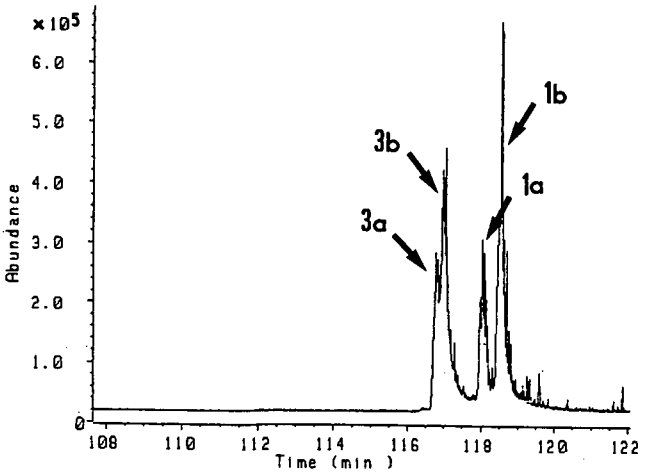

Fig. 4. Reversed-phase TSP-MS chromatogram of a 1:1 mixture of the central fractions obtained from peak 1 (peaks 1a and b) and peak 3 (peaks 3a and b) in Fig. 2.

peak can be detected during the period in which endogenous levels of ABA are at a maximum. Peak 1 also undergoes a significant ABA-induced change, decreasing by approximately four-fold.

The compounds labelled 1, 3, 6 and 7 in the radiochromatograms of Fig. 2 were analysed by HPLC–TSP-MS and the results were confirmed by GC–MS [3]. For this purpose the embryo incubates were fractionated by HPLC and 30 s fractions were individually collected. An example of the reconstructed radiochromatograms for two different extracts is shown in Fig. 3. Fig. 3b corresponds to part of the sample used for a more detailed study of the components in peak 1.

TSP-MS analysis of fractions from peak 1

The eluate fractions corresponding to peak 1 (fractions 33–35 in Fig. 3b) show the presence of two components with identical TSP-MS spectra, indicated as 1a and 1b in Fig. 4. Both can be assigned a molecular weight of 312 in accordance with the data in Table I. In the TSP-MS positive ion mode (Table Ia) the mass of the base peaks corresponds to that of an ammonium adduct and in the negative mode (Table Ib) the base peak corresponds to $[M-H]^-$, whereas abundant M^- ions can also be seen with the filament on. Ions arising from the loss of water are abundant both in the

TABLE I

HPLC–TSP-MS SPECTRA OF COMPOUNDS IN HPLC FRACTIONS CORRESPONDING TO PEAKS 1 AND 3

Positive ions: filament on; negative ions: filament on or off, as indicated. HPLC eluents: A = 0.1 *M* ammonium acetate buffer; B = 0.05 *M* ammonium acetate in methanol. HPLC gradient programme: 60–75% B in 10 min; Flow-rate, 1 ml/min; interface, 96°C; vaporizer exit, 181°C; ion source, 270°C. [ASSIGN] molecular assignment according to observed *m/z* value of ion; AcO = acetate. The corresponding relative abundances of ions are shown under 1a, 1b and 3a+3b. HPLC–TSP-MS retention times are shown in parentheses in Table Ia.

[ASSIGN]$^+$	*m/z*	1a (12.6)		1b (13.1)		3a+3b (11.3,11.6)	
(a) *Positive ions*							
$M+NH_4-2H_2O$	294	5		–		2	
$M+H-H_2O$	295	26		12		46	
$M+NH_4-H_2O$	312	8		–		16	
$M+H$	313	19		14		64	
$M+NH_4$	330	100		100		100	
		1a		1b		3a+3b	
		On	Off	On	Off	On	Off
(b) *Negative ions*							
$M-H-H_2O$	293	7	8	3	4	11	8
$M-H_2O$	294	8	2	4	1	42	2
$M-H$	311	100	100	100	100	100	100
M	312	50	14	64	20	42	16
$M+Cl$	347	12	2	14	2	14	2
$M+AcO-H_2O$	353	4	5	5	2	7	5
$M+AcO$	371	3	2	1	4	11	7

positive and in the negative ion mode, indicating the presence of at least one hydroxyl group in the molecule.

TSP–MS analysis of fractions from peak 3

The HPLC eluate fractions corresponding to the retention time of peak 3 (fractions 29–30 in Fig. 3) also show the presence of two components with TSP-MS features identical to those of the components found in peak 1 (Table I). These two compounds are indicated as 3a and 3b in Fig. 4.

The spectra obtained by TSP-MS across the peak band profiles of peak 1a, b and 3a, b (Fig. 4) show differences in the extent of dehydration processes as well as in the ion ratios $[M+H]^+/[M+NH_4]^+$ and $[M-H-H_2O]^-/[M-H_2O]^-$ (see Table I). The apparently higher relative proton affinity of this pair of isomers and the extent of water elimination, which is consistent with an additional oxygenated structural moiety leading to the elimination of water (hydroxyl, ketone or aldehyde function), together with the importance of electron capture ions due to water losses suggest a conjugated system in which conjugation is enhanced by dehydration processes.

TSP-MS analysis of fractions from peak 6

Fractions collected at the retention time of peak 6 (fractions 18–19 in Fig. 3) produce a wide but homogeneous peak on HPLC–TSP-MS analysis. The molecular weight deduced from the spectra obtained by TSP-MS is 328 a.m.u. (Table II). The mass spectrum is characterized by the abundance of signals arising from losses of up to two water molecules.

TSP-MS analysis of fractions from peak 7

The fraction collected across the elution pattern of peak 7 (fractions 10–13 in Fig. 3) also show an homogeneous peak in the HPLC–TSP-MS spectra with a molecular weight at 330 a.m.u. (Table III). The positive ion mode TSP-MS spectrum corresponds to that of a compound with a relatively lower proton affinity and thus more

TABLE II

HPLC–TSP-MS SPECTRA OF COMPOUNDS IN HPLC FRACTIONS CORRESPONDING TO PEAK 6

Eluent: 0.1 *M* AMAC–methanol (0.05 *M* ammonium acetate) (3:7). Flow-rate, 1 ml/min; interface, 104°C; vaporizer exit, 180°C; ion source, 270°C; filament on. RA = Relative abundances of ions. See also Table I.

Positive ions			Negative ions		
$[ASSIGN]^+$	*m/z*	RA	$[ASSIGN]^-$	*m/z*	RA
$M+H-2H_2O$	293	25	$M-H-2H_2O$	291	–
$M+NH_4-2H_2O$	310	17	$M-2H_2O$	292	12
$M+H-H_2O$	311	66	$M-H-H_2O$	309	13
$M+NH_4-H_2O$	328	76	$M-H_2O$	310	100
$M+H$	329	42	$M-H$	327	21
$M+NH_4$	346	100	M	328	14
			M+AcO	369	1
			M+AcOH	370	3

TABLE III

HPLC–TSP-MS SPECTRA OF COMPOUNDS IN HPLC FRACTIONS CORRESPONDING TO PEAK 7

HPLC eluent: 30% 0.1 *M* ammonium acetate buffer–70% 0.05 *M* ammonium acetate in methanol. Flow-rate, 1 ml/min; interface, 104°C; vaporizer exit, 180°C; ion source, 270°C; filament on. RA = Relative abundances of ions. See also Table I.

Positive ions			Negative ions		
$[ASSIGN]^+$	*m/z*	RA	$[ASSIGN]^-$	*m/z*	RA
$M+H-3H_2O$	277	7	$M-H-3H_2O$	275	3
$M+NH_4-3H_2O$	294	6	$M-3H_2O$	276	4
$M+H-2H_2O$	295	100	$M-H-2H_2O$	293	33
$M+NH_4-2H_2O$	312	50	$M-2H_2O$	294	96
$M+H-H_2O$	313	19	$M-H-H_2O$	311	12
$M+NH_4-H_2O$	330	17	$M-H_2O$	312	17
$M+H$	331	5	$M-H$	329	100
$M+NH_4$	348	67	M	330	19
			M+AcO	359	–
			M+AcOH	360	–

abundant $(M+NH_4]^+$ and $[M+NH_4-H_2O]^+$ ions. In this instance, ions generated by the loss of two water molecules can be readily observed and the base peak at $[M+H-2H_2O]^+$ is twice as high as the corresponding ammonium adduct. In the negative ion mode the base peak corresponds to the $[M-H]^-$ ion and the loss of two water molecules can also be observed. Electron capture processes are also apparent in the more dehydrated forms.

Methoxime derivatives of selected HPLC fractions

According to the TSP-MS data the components of HPLC peaks 1, 3, 6 and 7 (see Fig. 2) can be tentatively characterized as di- or trioxygenated derivatives of LA with various unsaturation centres as a result of the presence of double bonds, cyclic structures, epoxides and ketone or aldehyde groups. The last two groups can be readily determined by previous methoximation of the samples. Methoxime (MO) derivatives show molecular weight peaks at 29 a.m.u. greater than those of the original ketone or aldehyde groups present in the analyte molecule. It has recently been shown that the TSP spectrum of methoximated thromboxane B_2, a compound bearing an aldehyde group, is characterized by important signals due to losses of methanol [8]. In contrast, the methoximes of compounds with keto groups positioned in linear chains or cyclic structures, such as in prostaglandin (PG) 6-keto $PGF_{1\alpha}$ or prostaglandins PGE_2 and PGD_2, predominantly show ions derived from the hydrolysis or ammoniolysis of the methoxime group [7]. Low abundance ions derived from methanol losses in these prostaglandins seem to be related to fragmentation of the C–C bonds α to the methoxime group, giving rise to a nitrile structure. Accordingly, the TSP-MS spectra of methoximated 6-keto $PGF_{1\alpha}$ show ions derived from the combined losses of methanol and the C1–C5 carboxylic linear chain [9]. Methoxime formation is therefore able to differentiate between aldehydes and ketones and could therefore give useful structural information.

Methoxime derivatives of fractions from peak 1

After methoxime formation, the TSP-MS analysis of fractions collected at the retention time of HPLC peak 1 (Fig. 2) which, when underivatized, gave two isomers

TABLE IV

HPLC–TSP-MS SPECTRA OF METHOXIMATED COMPOUNDS IN HPLC FRACTIONS CORRESPONDING TO PEAK 1 (1MO)

HPLC eluents: A = 0.1 *M* ammonium acetate buffer; B = 0.05 *M* ammonium acetate in methanol. HPLC gradient programme, 75–85% B in 20 min; flow-rate, 1 ml/min; interface, 95°C; vaporizer exit, 184°C; ion source, 300°C; filament on. Retention times in TSP are shown in parentheses. MO = Methoxyamine; Na = sodium ion. See also caption to Table I and Fig. 5 for fragment assignments.

[ASSIGN]$^+$	*m/z*	1MO1 (12.1)	1MO2 (14.3)	1MO3 (12.2)	1MO4 (14.8)	1MO5 (13.3)	1MO6 (13.9)
	106	–	–	–	–	3	5
	108	–	–	–	–	1	1
	120	–	–	–	–	–	2
	126	–	–	–	–	1	2
	130	–	–	–	–	1	6
	131	–	–	–	–	–	2
	135	–	–	–	–	–	2
X9 + H − H_2O	155	–	–	1	2	–	–
X9 + NH_4 − H_2O	172	–	–	2	2	–	2
X9 + H	173	–	–	3	3	–	–
Y10 + H	184	–	–	–	–	7	2
	187	–	–	–	–	–	4
X9 + NH_4	190	–	–	100	100	4	24
Y12 + H − H_2O	192	2	2	2	2	–	1
	195	–	–	4	1	–	–
X11 + NH_4 − H_2O	198	–	–	–	–	–	4
X11 + H	199	–	–	1	–	–	20
	200	1	–	1	–	–	5
Y10 + NH_4	201	–	–	5	1	100	35
	204	–	–	1	2	–	–
	206	–	–	–	–	3	1
Y12 + H	210	9	8	–	–	–	1
	214	–	–	–	–	–	3
	215	–	–	–	–	–	2
X11 + NH_4	216	–	–	6	–	–	100
	217	–	–	2	–	–	14
	221	–	–	–	–	–	2
Y12 + NH_4	227	100	100	4	2	4	6
	232	1	1	–	–	–	1
	234	–	–	–	–	–	1
	241	1	1	–	–	–	–
	279	–	–	–	–	2	–
M + H − H_2O − 32	292	1	–	1	3	2	5
M + NH_4 − H_2O − MO	294	1	1	–	1	1	3
M + H − 32	310	1	5	1	10	2	7
M + NH_4 − MO	312	1	8	1	11	2	4
M + H − H_2O	324	–	3	2	5	18	40
M + H	342	21	34	35	48	6	17
M + 15	356	–	–	–	–	–	4
M + Na	364	4	3	9	9	7	23

in TSP-MS (peaks 1a and b in Fig. 4), shows a total of six peaks labelled as 1MO1–1MO6 (see Table IV). Peaks 1MO1, 1MO2 and 1MO5, 1MO6 are present in the fractions collected across the upward and downward slopes of HPLC peak 1, respectively, whereas peaks 1MO3 and 1MO4 dominate in the centre portion of HPLC peak 1.

All of these signals (1MO1–1MO6) show an apparent molecular weight of 341 a.m.u., that is 29 a.m.u. over the apparent molecular weight of the original products (312 in Table I) and with an $[M+H]^+$ ion dominating over the corresponding ammonium adducts. Methoxime formation can therefore be inferred, proving the presence of a ketone or aldehyde group in the original compound. The two pairs of peaks, 1MO1–1MO2 and 1MO3–1MO4 can be correlated with the expected *syn-* and *anti-*isomers of the methoximes of peaks 1a and 1b (Fig. 4), respectively.

Fragmentation processes are important, as is shown by the base peaks at *m/z* 227 (1MO1–2), 190 (1MO3–4), 201 (1MO5) and 216 (1MO6). In the latter two cases mass spectral differences (Table IV) indicate that these peaks are not due to the methoxime *syn-* and *anti-*isomers but to different products. Their corresponding methoxime isomers can be found coeluting with 1MO3 by a detailed study of the ion chromatograms at *m/z* 201 and 216 (not shown in Table IV).

Fig. 5 shows the structures proposed for fragments X9 and Y12 in methoxime derivatives 1MO1–4 (see Table IV). The adduct ions $[Y12+NH_4]^+$ and $[X9+NH_4]^+$ correspond to the base peaks observed in the TSP-MS spectra of derivatives 1MO1–2 and 1MO3–4, respectively. Their abundance can be accounted for by fragmentation favoured by the hydroxyl group being in a position α to the methoxime. These base peaks are characteristics of the position of the α-ketol group within the fatty acid chain. Thus, these ions are useful diagnostic tools in the interpretation of these TSP-MS spectra. Accordingly, the ions in 1MO1–2 arise from the methoxime isomers of 13-hydroxy,12-keto octadecenoic acid (base peak at $[Y12+NH_4]^+$ in Table IV) whereas ions in 1MO3–4 arise from the isomers of 9-hydroxy,10-keto-octadecenoic

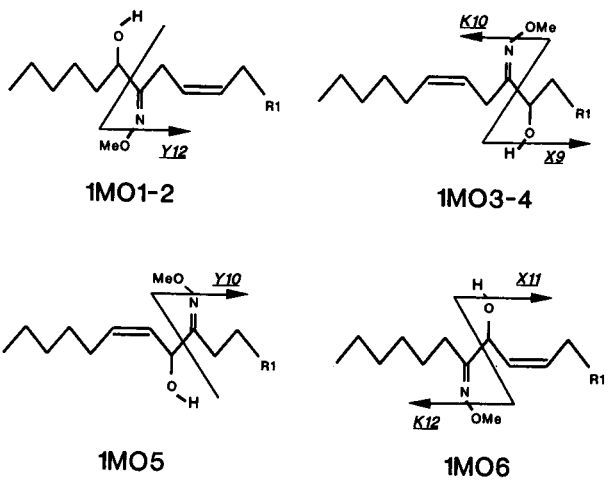

Fig. 5. Main fragmentation pathways observed in the spectra obtained by TSP-MS of methoxime derivatives 1MO1–6. R1 is $(CH_2)_6COOH$. Me = Methyl.

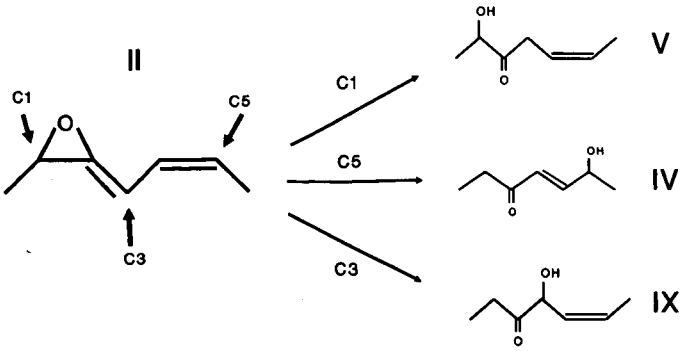

Fig. 6. Scheme illustrating the formation of metabolites IV and V (Fig. 1) through water attack on the C1 and C5 centre of the allene oxide precursor II. As attack on C3 leads to type IX structures detected in peak 1 of the HPLC profile of these incubates.

acid (base peak at $[X9 + NH_4]^+$ in Table IV). The MO derivatives 1MO5 and 1MO6 show mass spectra similar to those of derivatives 1MO1–4 (Table IV), although their corresponding base peaks at *m/z* 201 and 216 do not correlate with fragments for the derivatives 1MO1–4. These ions have been assigned to the ammonium adducts of two fragments identified as Y10 and X11 in Fig. 5, respectively, and their structure is consistent with the MO derivatives of 11-hydroxy,10-keto (Y10) and 11-hydroxy,12-keto-octadecenoic (X11) acids. The addition of water on carbons 1 or 5 of the 1-oxo-2,4-pentadiene system in allene oxides IIa and IIb in Fig. 1 generates metabolites Va and Vb (peaks 1a, b in Fig. 4) as well as IVa and IVb (peaks 3a, b in Fig. 4) [10]. In contrast, the addition of water on carbon 3 (Fig. 6) of this common precursor would lead to the formation of the 11-OH,10-keto and 11-OH,12-keto metabolites (IXa,b in Fig. 7). Neither of these two metabolites were detected in the previous GC–MS study [3] and they have not been reported before in products arising from LOX activity on LA.

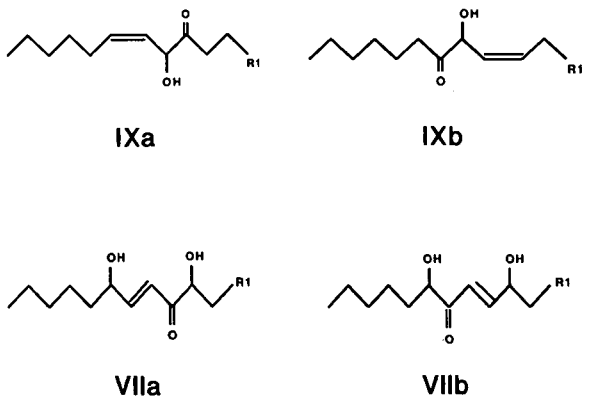

Fig. 7. Structures for the compounds found in HPLC peaks 1 (IXa and IXb) and 6 (VIIa and VIIb).

TABLE V

HPLC–TSP-MS SPECTRA OF METHOXIMATED COMPOUNDS IN HPLC FRACTIONS CORRESPONDING TO PEAK 3 (3MO)

HPLC eluents: A = 0.1 *M* ammonium acetate buffer; B = 0.05 *M* ammonium acetate in methanol. HPLC gradient programme, 75–85% B in 20 min; flow-rate, 1 ml/min; interface, 95°C; vaporizer exit, 184°C; ion source, 300°C; filament on. See also captions for Tables I and IV and Fig. 8 for fragment assignments.

[ASSIGN]$^+$	*m/z*	3MO1 (10.3)	3MO2 (12.0)	3MO3 (12.1)
	126	1	2	1
	130	1	–	1
S10+H	138	24	–	22
	140	1	–	1
Z10+NH_4	171	1	1	–
Y10+H	184	–	1	–
X9+NH_4	190	10	1	9
J11+H	199	2	–	2
Y10+NH_4	201	3	6	1
	202	1	2	–
X9+NH_4+14	204	1	–	2
	208	1	1	–
S12+H	210	3	4	–
J11+NH_4	216	7	–	6
	218	1	–	1
Z12+NH_4−H_2O	225	1	–	2
S12+NH_4	227	1	1	–
	236	–	2	–
Z12+NH_4	243	2	–	2
	290	3	3	2
M+H−H_2O−32	292	12	15	10
	293	6	5	3
M+NH_4−H_2O−MO	294	33	28	25
M+H−MO	295	10	10	11
M+NH_4−H_2O−MO+14	308	1	1	1
M+H−32	310	3	4	3
M+NH_4−MO	312	1	1	1
M+H−H_2O	324	17	100	21
M+H−2H	340	2	2	2
M+H	342	100	14	100
M+H+14	356	1	1	1
M+Na	364	12	11	7

Methoxime derivatives of fractions from peak 3

For the fractions corresponding to the elution time of HPLC peak 3 (Fig. 2), methoxime formation produces three distinct TSP-MS signals labelled 3MO1–3 in Table V and showing the mass spectral characteristics of the presence of a ketone group in the parent compound. The assigned molecular weight in this instance is also at 341 a.m.u., as expected from previous TSP data on the underivatized HPLC fraction (Fig. 4, compounds a, b). A detailed study of these spectra and of the selected ion chromatograms of major importance as diagnostic ions (*m/z* 190, 216, 225 and 243 for 3MO1 and 3MO3; *m/z* 201 and 210 for 3MO1 and 3MO2) indicates that the

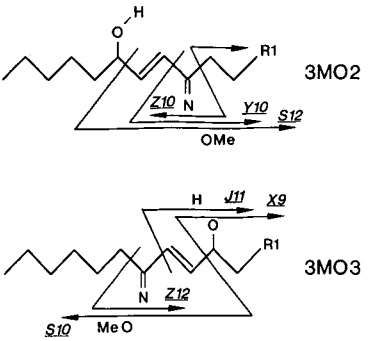

Fig. 8. Fragments observed in the spectra obtained by TSP-MS of derivatives 3MO2–3.

TSP-MS signal for 3MO1 is a mixture of derivatization isomers from components 3MO2 and 3MO3. Thus, as for HPLC peak 1, the two peaks arising from HPLC peak 3 fractions (peaks 3a and b in Fig. 4) produce four major peaks upon methoximation due to the respective methoxime *syn*- and *anti*-isomers of compounds IVa and IVb in Fig. 1.

The formation of ions arising from TSP-MS fragmentation is less favoured in this instance relative to the methoximes of α-ketol compounds. Nevertheless, the spectra of 3MO2 and 3MO3 can be differentiated by the presence of ions at *m/z* 201 and 210 ($[Y10+NH_4]^+$ and $[S12+H]^+$, respectively for 3MO2) and at *m/z* 138, 190,

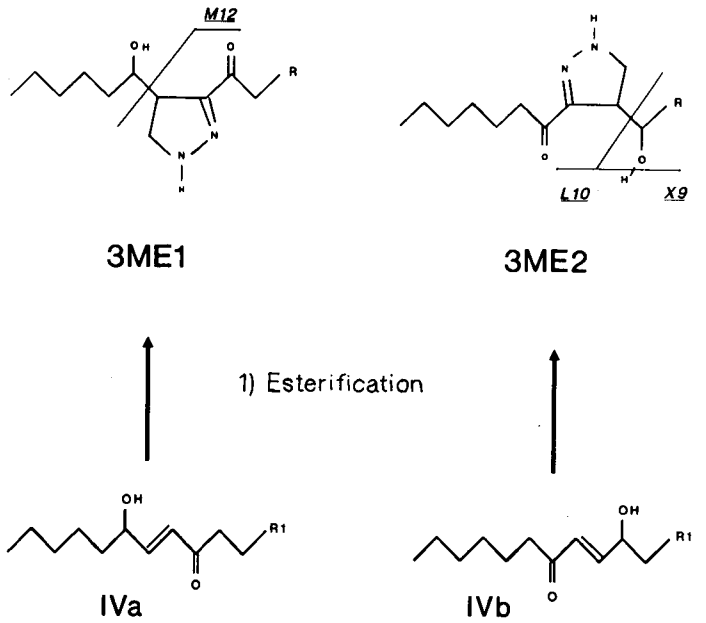

Fig. 9. Formation of diazomethane addition derivatives of compounds IVa and IVb upon methylation and fragments observed in their spectra obtained by TSP-MS.

216 and 243 ($[S10+H]^+$, $[X9+NH_4]^+$, $[J11+NH_4]^+$ and $[Z12+NH_4]^+$, respectively for 3MO3) (see Table V). These fragments are depicted schematically in Fig. 8.

It is interesting to note that in the course of a GC–MS study of the corresponding methyl ester–methoxime–trimethylsilyl ether (MEMOTMS) derivatives, the fractions collected from HPLC peak 3 showed a very peculiar behaviour which made attempts at MS identification difficult. In this instance, the resulting major GC peak shows a mass spectra with apparent molecular masses of 541 a.m.u., 114 a.m.u. higher than would correspond to the components of peak 1, even though, as indicated above, the TSP-MS spectra and HPLC retention characteristics suggest the presence of similar functional groups for HPLC peaks 1 and 3. However, the higher molecular mass could not be readily explained and, in addition, catalytic hydrogenation gave rise to two partially resolved peaks with an apparent molecular mass of 429 a.m.u. coincident with the corresponding hydrogenated derivatives of peak 1. Likewise, fully silylated and mixed methoxime–silyl derivatives produced electron impact mass spectra consistent with the structural features of hydroxy-keto octadecenoic acid type of compounds (IVa and IVb in Fig. 1).

The peculiar GC-MS mass spectra of MEMOTMS derivatives has been explained by the addition of a diazomethane molecule during the methylation reaction through 2+3 cyclo-addition of the diazomethane reagent to the activated double bond in the 4-hydroxy-2-alkenone system, as shown in Fig. 9 [3]. The addition of diazomethane to double bonds has been previously described for prostanoids [3,11,12]. The new chiral centre at C-10 or C-12 and/or the possible silylation of

TABLE VI

HPLC–TSP-MS SPECTRA OF METHYLATED COMPOUNDS IN HPLC FRACTIONS CORRESPONDING TO PEAK 3 (3ME)

HPLC eluents: A = 0.1 *M* ammonium acetate buffer; B = 0.05 *M* ammonium acetate in methanol. HPLC gradient programme, 70–85% B in 15 min; flow-rate, 1 ml/min; interface, 95°C; vaporizer exit, 186°C; ion source, 300°C. See also captions for Tables I and IV and Fig. 9 for fragment assignments.

$[ASSIGN]^+$	*m/z*	3ME1 (15.4)	3ME2 (16.1)
	151	1	–
L10+H−28	153	1	–
L10+H	181	4	5
L10+H+2	183	1	–
$L10+NH_4$	198	3	4
$X9+NH_4$	204	8	9
	237	1	–
M12+H−28	239	2	1
M12+H	267	4	6
$M12+NH_4$	284	1	1
$M+H-H_2O-28$	323	1	1
	324	1	1
M+H−28	341	1	–
$M+H-H_2O-2H$	349	1	2
M+H	369	100	100
M+Na	391	20	11

isomers explains the isomers found for this structure. In contrast, if the order of sequential derivatization is changed so that methoximation is carried out before methylation, no such addition is observed.

TABLE VII

HPLC–TSP-MS SPECTRA OF METHOXIMATED COMPOUNDS IN HPLC FRACTIONS CORRESPONDING TO PEAK 6 (6MO)

HPLC eluents: A = 0.1 *M* ammonium acetate buffer; B = 0.05 *M* ammonium acetate in methanol. HPLC gradient programme, 60–85% B in 25 min; flow-rate, 1 ml/min; interface, 95°C; vaporizer exit, 190°C; ion source, 300 °C; filament on. Fragments in parentheses indicate alternative structures for the observed ion. See also captions for Tables I and IV and Fig. 10 for fragment assignments.

[ASSIGN]$^+$	*m/z*	6MO1 (14.8)	6MO2 (15.2)	6MO3 (15.8)
	102	2	–	3
	104	–	1	9
	112	3	1	2
Z(R)10+H−H_2O	136	–	2	–
	146	–	–	3
	152	9	–	8
R(Z)10+H	154	7	2	8
X9+NH_4−H_2O	155	2	–	3
	156	6	–	3
Z(R)10+NH_4	171	9	5	4
X9+NH_4−H_2O	172	3	2	2
X9+H_4	173	3	3	–
X9+NH_4	190	97	100	39
	192	3	2	1
	195	2	4	–
J11+NH_4−H_2O	198	–	–	4
J11+H	199	7	–	18
T10+H	200	1	–	3
	202	1	–	2
	204	16	2	41
Z(R)12+H−H_2O	208	1	–	3
J11+NH_4	216	38	4	93
T10+NH_4	217	5	1	12
	221	–	–	6
Z(R)12+NH_4−H_2O	225	7	–	22
Z(R)12+H	226	3	–	8
	241	–	–	2
Z(R)12+NH_4	243	47	4	100
	248	2	–	5
	257	1	–	1
	290	1	1	2
	292	3	2	4
M+H−H_2O−32	308	4	3	6
M+NH_4−MO−H_2O	310	11	4	11
	311	2	1	2
	322	1	1	21
M+H−H_2O	340	11	33	87
M+H	358	100	8	76
M+Na	380	35	10	54
	396	3	–	5

TSP-MS analysis of the methylated fraction from peak 3

The TSP-MS analysis of methyl derivatives of the fractions obtained from peak 3 provides additional information about the formation of an dihydropyrazole ring by diazomethane addition, as postulated in the preceding section. The TSP chromatogram shows two major signals with very similar spectra. According to these data, the molecular mass of both components is 368 or 56 a.m.u. greater than that of the free compounds and 42 a.m.u. greater than in the expected methyl ester derivative (Table VI) which is indicative of diazomethane addition (42 a.m.u.).

Some useful fragmentation can also be observed. Diagnostic fragments are labelled L10 (at *m/z* 181 and 198, $[L10+H]^+$ and $[L10+NH_4]^+$, respectively), M12 (at *m/z* 267 and 284, $[M12+H]^+$ and $[M12+NH_4]^+$, respectively) and X9 (at *m/z* 204, $[X9+NH_4]^+$ (see Fig. 9). Thus the TSP-MS analysis of the methyl derivative facilitates the determination of the positions of the double bond and the hydroxyl and ketone groups. Fragments L10, X9 and M12 are characteristic of the 9 hydroxy- and 13-hydroxy-isomers, respectively.

An interesting ion which would be difficult to account for by solvent addition and/or water elimination is that observed at *m/z* 349 (Table IV). This ion could arise from a diazomethane loss from the $[M+Na]^+$ ion. However, ions due to Na^+ addition do not usually show signals from elimination or fragmentation processes [13] and furthermore, ions due to diazomethane loss from $[M+H]^+$ were not detected in this instance. Accordingly, the formation of this ion could be explained by the loss of a hydride ion involving redox processes. The same considerations apply to ions L10 and M12 with apparent molecular masses of 180 and 266 a.m.u., respectively. The formation of a highly stable aromatic pyrazole ring structure could be the factor behind the favoured loss of hydride ions in this spectra. Other ions in Table IV involving losses of 28 a.m.u. could be ascribed to the loss of an N_2 moiety.

Methoxime derivatives of fractions from peak 6

The TSP-MS analysis of the methoximated compounds in the HPLC eluate fraction collected at the retention time of peak 6 (Fig. 1) shows a group of three signals only partially resolved and labelled 6MO1–3 in Table VII. All of these ions show an apparent molecular weight of 357 a.m.u., also 29 a.m.u. over the apparent molecular weight of the underivatized peak 6 and indicative of a ketone moiety. The selected ion traces from *m/z* 190, 216 and 243 suggest the presence of at least four distinct products in this fraction. As for the HPLC peak 3 described in the preceding section, the TSP-MS spectrum for 6MO1 corresponds to a mixture of isomers from 6MO2 and 6MO3, whereas the latter can be characterized by their dominant ions at *m/z* 190 and at *m/z* 216 and 243, respectively. Thus, it seems that in this instance *syn*- and *anti*-isomers of the methoximes are present from two positional isomers.

The assignments of the TSP-MS fragments observed for the 6MO derivatives are illustrated in Fig. 10, corresponding to the methoximes of the 9,13-dihydroxy-10-keto,11-octadecenoic acid and the 9,13-dihydroxy-12-keto,10-octadecenoic acid (illustrated as 6MO2 and 6MO3, respectively, and as VIIa and VIIb in Fig. 5). These fragmentations are analogous to those observed for the 1MO1 and 3MO derivatives. As in these instances, the hydroxyl group α to the oxime moiety directs the ion profile. Thus, fragment Y12 in the 1MO1 and 1MO2 derivatives (Fig. 5) gives rise to fragment Z12 in 6MO3 (Fig. 10). This fragment is found at 16 a.m.u. higher because of the

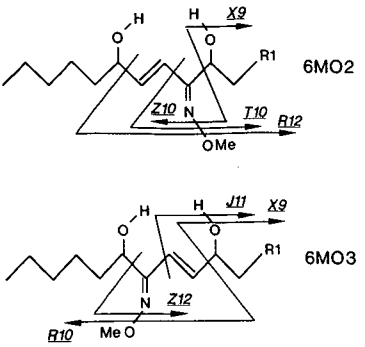

Fig. 10. Fragments observed in the spectra of derivatives 6MO2 and 6MO3 obtained by TSP-MS.

presence of an additional hydroxyl group and shows the expected adducts generated by the loss of water. The ions derived from fragments R12 and Z10 from 6MO2 are isobaric with the ions derived from fragments Z12 and R10 in 6MO3. Ions Z10 and Z12 are produced by fragmentations equivalent to those observed for the 1MO derivatives and thus are favoured relative to R10 and R12 (Table VII). However, the ion abundances for R10 and Z10 derived fragments in 6MO2 and 6MO3 do not distinguish between the two compounds. In all of the methoxime derivatives discussed in this paper, those adducts containing the carboxylic acid group are more abundant than the equivalent fragments containing the end part of the molecule. This indicates that ionization is driven by the carboxyl moiety and can be related to the low abundance of equivalent adduct fragments in the case of derivatized thromboxane [8]. Thus, fragment Z12 containing the carboxyl moiety is favoured relative to its isobare R12 and in this instance the relative abundance of the corresponding ions is important and allows for a differentiation between derivatives 6MO2 and 6MO3.

Finally, fragmentation at J11 gives very prominent ions in 6MO3 (*m/z* 216, RA 93% as shown in Table VII). This ion shows the same *m/z* ratio as the corresponding adduct arising from fragmentation X11 in 1MO6 (Table IV) and indicates the presence of a 11,12-ketol system. Nevertheless, the GC–MS data do not justify such an structure. Likewise, the ion at *m/z* 216 appears at a lower abundance in the TSP-MS spectrum of 3MO3 (Table V), together with the ion at *m/z* 243 corresponding in both instances to the fragment Z12 (Tables V and VII). The relative abundances of these two ions in both derivatives supports the formation of J11 from Z12 by nitrile elimination.

Methoxime derivatives of fractions from peak 7

The same approach applied to the eluate fractions from HPLC peak 7 (Fig. 2) did not result in any changes in the TSP-MS spectra, so that no ketone or aldehyde groups should be expected in its structure.

In summary, the information provided at this point by TSP indicates that the compounds present in the HPLC fractions collected from peaks 1 and 3 (Fig. 3) are positional isomers of hydroxy-keto-octadecenoic acids. The differences in the extent of fragmentation of components 1MO and 3MO could be ascribed to the different position of the hydroxyl and methoxime groups relative to the double bound.

Along these lines, an α-ketol type of structure justifies the extensive fragmentation observed on TSP-MS as well as the adduct ions observed for the compounds derived from HPLC peak 1. These fragments ions allow the assignment of the position of hydroxy and keto groups in the molecule and characterize the compounds found in fractions collected from HPLC peak 1 as the 9-hydroxy,10-keto-, 13-hydroxy,12-keto-, 11-hydroxy,10-keto- and 11-hydroxy,12-keto-octadecenoic acids and compounds in HPLC fractions from peak 3 as the 9-hydroxy,12-keto- and 13-hydroxy,10-keto-octadecenoic acid. The double bond position in these compounds cannot be determined from the TSP-MS data alone. However, fragments from the methoximes of peak 3 indicate that the double bond is in positions 10 (9-hydroxy,12-keto) and 11 (13-hydroxy,10-keto).

The derivative products from HPLC peak 6 could be ascribed to metabolites with the structural features of dihydroxyketo octadecenoic acids. Fragmentations, which are equivalent to those in the methoximes from peaks 1 and 3, indicate that at least one hydroxyl group is in a position α to the oxime. The second hydroxyl moiety and the double bond are possibly placed in positions which, relative to the oxime, are identical to those in the methoximes of peak 3. Overall, the observed TSP-MS fragments ions allow the identification of these compounds as 9,13-dihydroxy,10-keto, 11-octadecenoic and 9,13-dihydroxy,12-keto,10-octadecenoic acids (see VIIa and VIIb in Fig. 7).

Compounds in the HPLC fractions corresponding to peak 7 can be identified as trihydroxyoctadecenoic (or dihydroxyepoxyoctadecanoic) acids. However, the positions of the hydroxyl groups and double bonds cannot be pinpointed from the TSP-MS data alone. The necessary additional information leading to further identification of the structural features of these compounds was obtained from a parallel GC–MS study of the corresponding fractions, as reported elsewhere [3]. The GC–MS data allowed the identification of two positional trihydroxyoctadecenoic acid isomers with the structures of compounds VIa and VIb in Fig. 1.

CONCLUSIONS

Despite the supposedly greater amount of information that can be obtained by GC–MS techniques. HPLC–TSP-MS can provide molecular information much more rapidly which can be of critical importance for structural identification when giving rise to unexpected derivatization products, as shown for the metabolites IV and VII.

Positive and negative TSP-MS give additional information on the minimum number of groups which can lose water molecules and on the possible presence of conjugated systems in the intact molecular or in the dehydration products. It is also noteworthy that in an application such as that reported here, in which the precursor compound is known (LA) and where the number of double bonds due to oxo or acid groups can be determined through the analysis of methylated or methoxime derivatives, the TSP-MS information gives by itself a reliable approximation to the atomic composition and functional groups of the compound of interest.

Through the use of derivatization reactions is is possible to obtain products which are liable to undergo fragmentation reactions due to thermal degradation, ionization or collision processes in the ion source. Regardless of their mechanism of formation, these fragmentations provide a degree of structural information which, as

shown here, leads to easier interpretations and the same conclusions as obtained by the more elaborate GC–MS analyses.

This HPLC–TSP-MS assay has facilitated the detection of two new structures (IXa and IXb in Fig. 7) derived from LOX activity in maize embryos which were difficult to characterize by standard GC–MS techniques. The structure of the new metabolite VII, and those of metabolites IV and V, can be also readily established from the TSP-MS data for the free and oximated compounds.

ACKNOWLEDGEMENTS

This work was supported in part by grants 89/0386 from FIS and BIO88:0162 from CICYT (Spain).

REFERENCES

1 V. A. Vick and D. C. Zimmerman, in P. K. Stumpf and E. E. Conn (Editors), *The Biochemistry of Plants*, Vol. 9, Academic Press, London, 1987, pp. 53-90.
2 D. F. Hildebrand, *Physiol. Plant.*, 76 (1989) 249.
3 J. Abián, E. Gelpí and M. Pagès, *Plant Physiol.*, 95 (1991) 1277.
4 M. J. Davies and T. A. Mansfield, in F. T. Addicott (Editor), *Abscisic Acid*, Praeger, New York, 1983, pp. 237-268.
5 M. Pla, A. Goday, J. Vilardell, J. Gomez and M. Pagès, *Plant Mol. Biol.*, 13 (1989) 385.
6 A. Goday, D. Sanchez Martinez, J. Gomez, P. Puigdomenech and M. Pagès, *Plant Physiol.*, 88 (1988) 564.
7 J. Abián, J. Oriol Bulbena and E. Gelpí, *Biomed. Environ. Mass Spectrom.*, 16 (1988) 215.
8 J. Abián and E. Gelpí, *J. Chromatogr.*, 562 (1991) 153.
9 J. Abián and E. Gelpí, presented at the *39th ASMS Conference, Nashville, TN, May 19–24, 1991.*
10 M. Hamberg, *Biochim. Biophys. Acta*, 920 (1987) 76.
11 A. F. Cockerill, N. J. A. Gutteridge, D. N. B. Mallen, D. J. Osborne and D. M. Rackham, *Biomed. Mass Spectrom.*, 4 (1977) 187.
12 A. F. Cockerill, *Prostaglandins*, 13 (1966) 1036.
13 J. A. Yergey, H.-Y. Kim and N. Salem Jr., *Anal. Chem.*, 58 (1986) 1344.

Journal of Chromatography, 554 (1991) 175–180
Elsevier Science Publishers B.V., Amsterdam

CHROMSYMP. 2306

Thermospray liquid chromatography–mass spectrometry for the characterisation of sulphate ester conjugates

G. D. BOWERS, D. M. HIGTON, G. R. MANCHEE, J. OXFORD and D. A. SAYNOR
Department of Biochemical Pharmacology, Glaxo Group Research Limited, Park Road, Ware, Hertfordshire SG12 0DP (UK)

ABSTRACT

Formation of polar conjugates is a well documented metabolic pathway for xenobiotics containing phenolic hydroxyl groups. This paper describes the analysis of two sulphate ester conjugates by fast atom bombardment mass spectrometry and thermospray liquid chromatography–mass spectrometry. Thermospray liquid chromatography–mass spectrometry proved the more succesful technique for obtaining the molecular weight of the intact conjugate, but only by removal of the buffer from the high-performance liquid chromatography eluent.

INTRODUCTION

Sulphate conjugation of phenolic compounds is a well documented metabolic pathway [1]. Characterisation of sulphate conjugates has often involved acid or specific enzyme hydrolysis and subsequent analysis of the hydrolysed product. More recently both fast atom bombardment mass spectromy (FAB-MS) and thermospray liquid chromatography–mass spectrometry (LC–MS) have been used for sulphate ester analysis. At present FAB is the MS technique of choice, provided that the sample is sufficiently pure [2].

Thermospray LC–MS of these conjugates isolated from biological fluids have been reported [3,4], however, sensitivity, which is often an important factor in metabolism studies, has been limited. Evidence of the intact molecular species is an essential part of metabolite structure elucidation. Unfortunately, when ammonium acetate buffer is used in the mobile phase, the mass spectral data often shows little, if any, indication of this species. However, published data by Watson *et al.* [5] have shown the analysis of intact steroid conjugates by thermospray LC–MS with the absence of buffer in the mobile phase.

A series of metabolic studies were performed for two drugs, salbutamol (Fig. 1) a β_2-adrenoceptor agonist used in the treatment of asthma and ondansetron (Fig. 2) a $5HT_3$ receptor antagonist used as an anti-emetic in cancer chemotherapy. Following oral administration of salbutamol and ondansetron, suspected sulphate ester conjugates were isolated from marmoset urine and dog bile, respectively. Here we report

0021-9673/91/$03.50

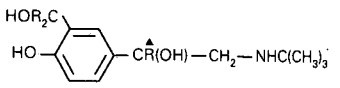

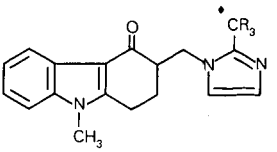

Fig. 1. The structure of salbutamol. R = H: Salbutamol; R = ^2H: [$^2H_3$]salbutamol; ▲ = Position of the tritium label.

Fig. 2. The structure of ondansetron. R = H: Ondansetron; R = ^2H: [$^2H_3$]ondansetron; ◆ = Position of the carbon-14 label.

the analysis of these intact sulphate conjugates by thermospray LC–MS following unsuccessful attempts by FAB-MS.

EXPERIMENTAL

Animal experiments

A male common marmoset received a single oral dose, 5 mg/kg, of a 1:1 mixture of salbutamol and its deuterated analogue with a trace amount of [^{3}H]salbutamol (40 μCi, 1.46 MBq), (Fig. 1). Urine was collected over the period 0–24 h and the major metabolite isolated by solid-phase extraction and semi-preparative high-performance liquid chromatography (HPLC) (Fig. 3).

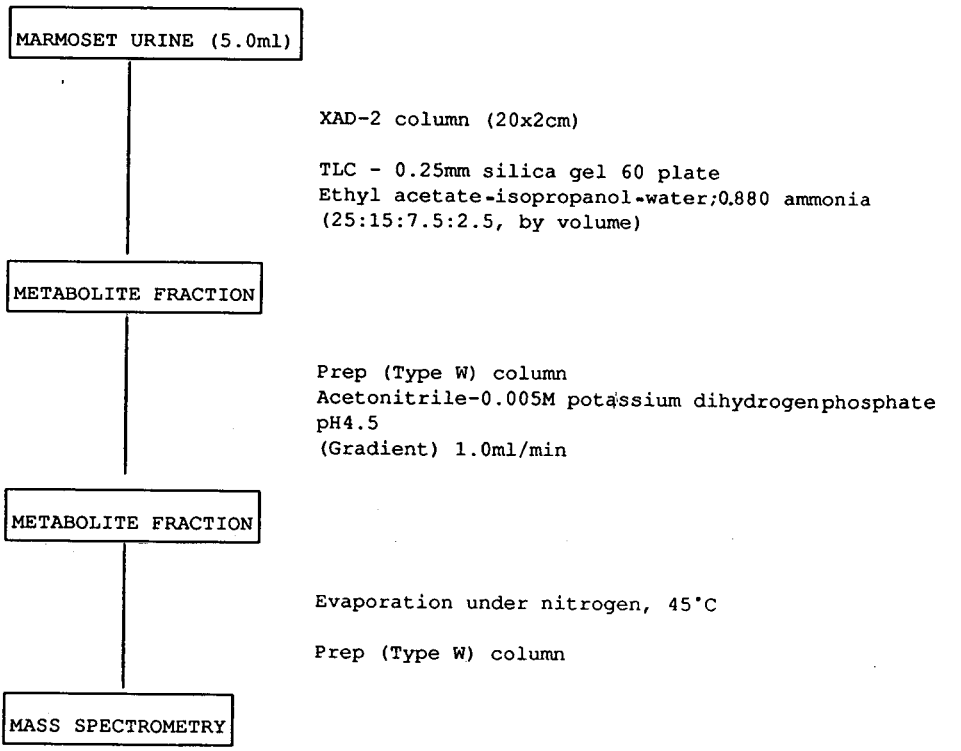

Fig. 3. Isolation of the salbutamol metabolite.

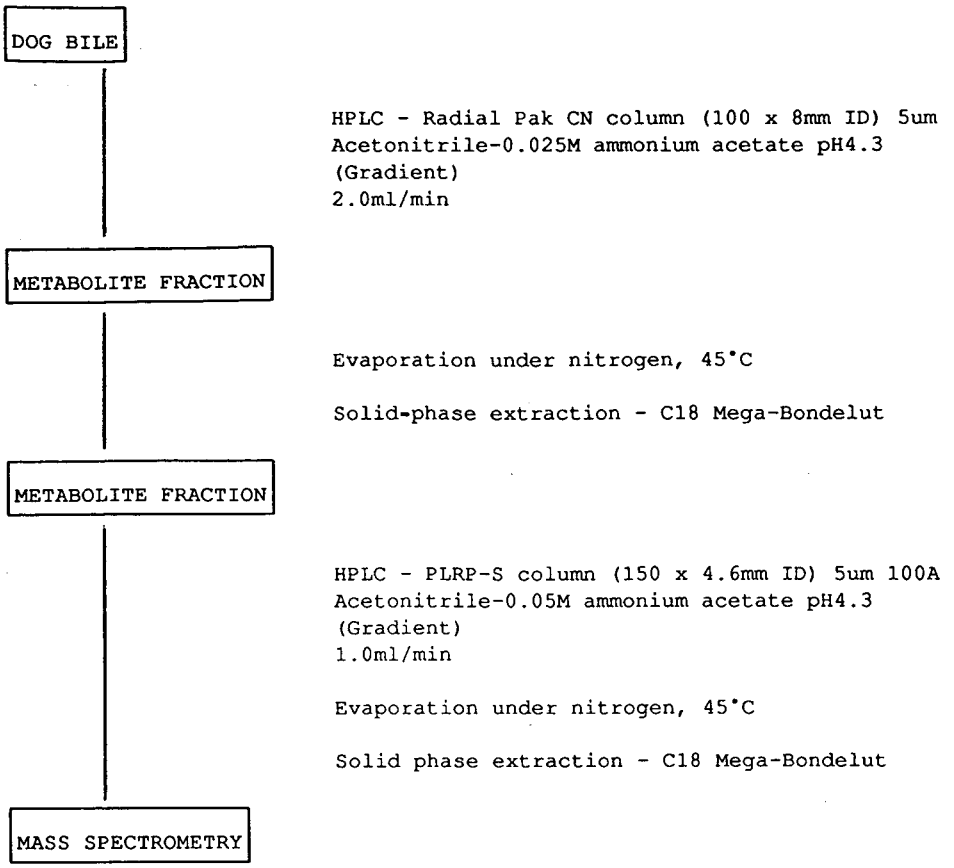

Fig. 4. Isolation of the ondansetron metabolite.

In the second experiment a male dog received a single oral dose, 1 mg/kg, of a mixture of ondansetron–[^{14}C]ondansetron–[$^{2}H_3$]ondansetron (0.85:0.15:1.0), (Fig. 2). Bile was collected over the period 0–6 h and a major metabolite was isolated by solid phase extraction and semi-preparative HPLC (Fig. 4).

HPLC

A Hewlett-Packard HP1090A liquid chromatograph (Hewlett Packard, Winnersh, UK) equipped with an auto-injector was used. The system was run at a flow-rate of 1.0 ml/min. The column used for the analysis of α-napthyl sulphate (Sigma, Dorset, UK) and the salbutamol metabolite was a Spherisorb ODS2 (100 × 4.6 mm I.D., 5 μm) (Phase Separations, Cheshire, UK) and was operated at room temperature. The ondansetron metabolite was introduced via a loop injection. The isocratic solvent system used for thermospray LC–MS analysis of α-napthyl sulphate was acetonitrile–water or acetonitrile–0.05 *M* ammonium acetate (2:98). For the analysis of the salbutanol and ondansetron metabolites the mobile phase comprised acetonitrile–water (8:92 or 50:50, respectively).

MS

FAB-MS was performed on a VG 7070E mass spectrometer (VG Analytical, Manchester, UK) equipped with a VG 11/250J data system. The instrument was operated at 6 kV accelerating voltage and a resolution of 1000. The saddle field ion gun (Ion Tech, Middlesex, UK) was operated at 8 keV and 100 μA current using xenon gas. An aliquot of the sample was added in methanol to the sample probe to which glycerol had been previously applied and spectra were recorded in negative ion mode.

Thermospray LC–MS was performed on a Hewlett-Packard HP5987A mass spectrometer equipped with an RTE-6 data system (Hewlett-Packard, Palo Alto, CA, USA) and a TSP interface (Vestec, Cheshire, UK). The TSP source block temperature was maintained at 250°C for all experiments and the vapouriser temperature in the range 209–211°C. All spectra were recorded in the negative ion mode. The TSP source was operated in the filament and discharge off mode. Approximately 10 μg of the salbutamol metabolite and 1.2 μg of the ondanestron metabolite were used for the analyses.

RESULTS AND DISCUSSION

FAB-MS analysis of the salbutamol metabolite produced a spectrum containing two weak ions at *m/z* 318 and 321 which could be assigned as $[M-H]^-$ for salbutamol and its deuterated analogue. However, these data proved inconclusive due to the amount of endogenous material present in the sample (Fig. 5). For similar reasons this technique also proved unsuccessful for analysis of the ondansetron metabolite. In this instance the presence of bile acids, including taurocholic acid, $[M-H]^-$ at *m/z* 514, dominated the spectrum (Fig. 6).

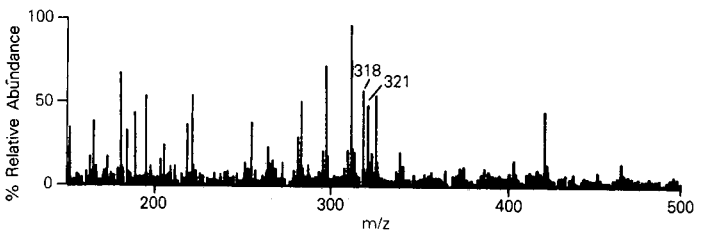

Fig. 5. FAB mass spectrum of the salbutamol metabolite.

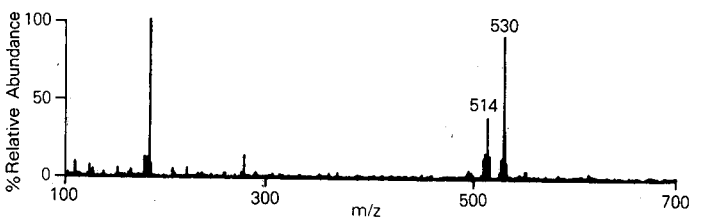

Fig. 6. FAB mass spectrum of the ondansetron metabolite.

Thermospray LC–MS was investigated an an alternative technique. However, because no authentic standards were available, conditions were optimised initially using α-napthyl sulphate. In the absence of ammonium acetate the molecular anion, *m/z* 223, is the base peak in the spectrum (Fig. 7). However, in the presence of buffer the base peak at *m/z* 203 is derived from [α-napthol + acetate]$^-$. The α-napthol is probably formed by buffer catalysed hydrolysis of the α-napthyl sulphate, similar processes have been reported previously for the thermospray of purine-6-sulfonate [6]. Thus, in the absence of buffer, an ion evaporation process predominates, whereas chemical degradation occurs in its presence.

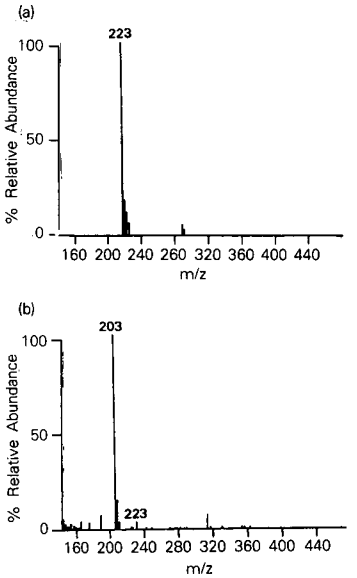

Fig. 7. Thermospray mass spectra of α-napthyl sulphate (a) in the absence and (b) in the presence of ammonium acetate buffer.

To minimuse hydrolysis and obtain important molecular weight information, thermospray LC–MS analysis of the metabolites of salbutamol and ondansetron were performed in the absence of buffer. Fig. 8 shows the total ion current (TIC) chromatogram and mass spectrum obtained for thermospray LC–MS analysis of the salbutamol metabolite. The ions at *m/z* 318 and 321 are assigned as $[M-H]^-$ for the salbutamol metabolite and its deuterated analogue. Confirmation of the position of sulphate conjugation has not been established for this metabolite, although evidence obtained from human studies have previously indicated phenolic conjugation [7].

Fig. 9 shows the TIC chromatogram and thermospray mass spectrum of the ondansetron metabolite. The ions at *m/z* 388 and *m/z* 391 are assigned as $[M-H]^-$ for the ondansetron metabolite and its deuterated analogue. The determined molecular weight of the metabolite, 389, is consistent with a sulphate ester conjugate of the mono-hydroxylated drug. Analysis by NMR has confirmed the structure of the metabolite as the 8-hydroxy sulphate ester of ondansetron.

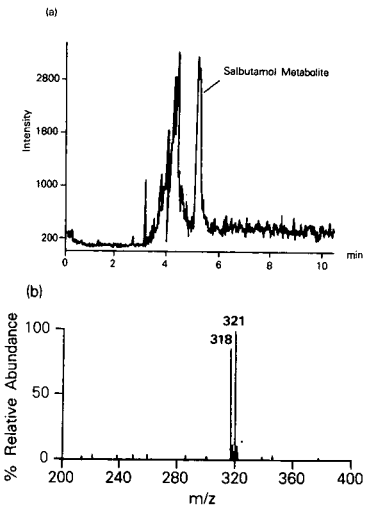

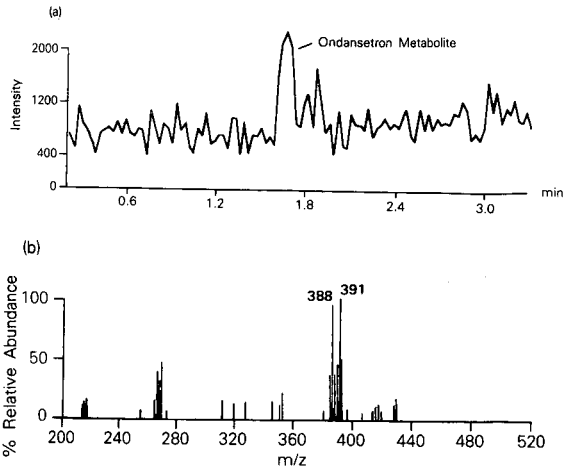

Fig. 8. Thermospray (a) TIC chromatogram and (b) mass spectrum from analysis of the salbutamol metabolite.

Fig. 9. Thermospray (a) TIC chromatogram and (b) mass spectrum from analysis of the ondansetron metabolite.

CONCLUSION

The metabolites of two drugs, ondansetron and salbutamol have been characterised by thermospray LC–MS. The results of our experiments have demonstrated that in the absence of ammonium acetate, ion evaporation of the molecular anions occurs. Use of this technique has allowed unambiguous determination of the molecular weights of intact conjugates which would not have been obtained from FAB-MS.

REFERENCES

1 G. J. Mulder, in W. M. Jackoby, J. R. Bend and J. Caldwell (Editors), *Metabolic Basis of Detoxication*, Academic Press, New York, 1982, p. 247.
2 K. M. Straub, in J. W. Bridges, L. L. Chasseaud and G. G. Gibson (Editors), *Progress in Drug Metabolism*, Taylor & Francis, London, 1988, Ch. 7, p. 267.
3 D. C. Mays, S. G. Hecht, S. E. Unger, C. M. Pacula, J. M. Climie, D. E. Sharpe and N. Gerber, *Drug Metab. Dispos.*, 15 (1987) 318.
4 L. A. Shipley, M. D. Coleman, T. G. Brewer, R. W. Ashmore and A. D. Theoharides, *Xenobiotica*, 20 (1990) 31.
5 D. Watson, G. W. Taylor and S. Murray, *Biomed. Mass Spectrom.*, 12 (1985) 610.
6 K. J. Volk, R. A. Yost and A. Brajter-Toth, *J. Chromatogr.*, 474 (1989) 231.
7 C. Lin, Y. Li, J. McGlotten, J. B. Morton and S. Symchowicz, *Drug Metab. Dispos.*, 5 (1977) 234.

Journal of Chromatography, 554 (1991) 181–189
Elsevier Science Publishers B.V., Amsterdam

CHROMSYMP. 2277

Use of thermospray liquid chromatography–mass spectrometry to aid in the identification of urinary metabolites of a novel antiepileptic drug, Lamotrigine

M. V. DOIG* and R. A. CLARE
Department of Bioanalytical Sciences, Wellcome Research Laboratories, Beckenham, Kent (UK)

ABSTRACT

The use of thermospray liquid chromatography–mass spectrometry allowed the structural elucidation of a number of urinary metabolites of Lamotrigine, 3,5-diamino-6-(2,3-dichlorophenyl)-1,2,4-triazine, formed after administering the drug to man, Cynomolgus monkey and rabbit. This data when combined with the data obtained from high-performance liquid chromatography with radiochemical detection enabled us to determine the types and amounts of unchanged drug and metabolites excreted in urine by man and a number of laboratory animal species. This technique was particularly useful as it highlighted a previously unknown fact that Lamotrigine is metabolised to form two different N-glucuronides, one of which is resistant to cleavage *in vitro* by a crude β-glucuronidase preparation from *Helix pomatia*.

INTRODUCTION

For the registration of any potential drug candidate it is essential to provide evidence that the drug's general metabolism in humans is similar to its metabolism in the animal species utilised for toxicological evaluation. To obtain this information a number of studies are performed using radiolabelled and unlabelled drug. This report shows how thermospray liquid chromatography–mass spectrometry (LC–TSP-MS) played an important role in obtaining this evidence for Lamotrigine, 3,5-diamino-6-(2,3-dichlorophenyl)-1,2,4-triazine, a novel antiepileptic drug chemically unrelated to existing therapies.

Drugs are generally metabolised by a diversity of enzymes to generate more polar compounds that can be eliminated from the body. Metabolism of drugs is normally divided into two phases: phase I, functionalization type reactions such as oxidation, reduction and hydrolysis; and phase II, conjugative reactions such as glucuronidation, methylation and acetylation [1]. As a result of the breadth of polarities that a drug and its metabolites cover, the most widely used method for their analysis is reversed-phase high-performance liquid chromatography (HPLC) utilising UV and radiochemical detectors. With the advent of LC–TSP-MS [2] it has become far easier to extend this analysis to acquire structural and molecular weight information without spending vast amounts of time and effort on sample pretreatment.

0021-9673/91/$03.50

Initial work in laboratory animals using radiolabelled Lamotrigine had shown that 95% of an orally administered dose was recovered in urine while the remaining 5% was found in the faeces. Metabolite profiling of the urine samples using HPLC with UV and radiochemical detection had suggested the following: significant interspecies variation with complex metabolite patterns; man excreted approximately 90% of the dose in urine as a polar metabolite; this polar metabolite was also excreted by Cynomolgus monkey, rat and rabbit and experiments with β-glucuronidase indicated this polar metabolite was a glucuronide of Lamotrigine. This report shows how LC–TSP-MS enabled the confirmation and extension of these findings.

MATERIALS AND METHODS

Sample pretreatment

All samples were stored at −20°C prior to analysis. Prior to examination by LC–TSP-MS all samples were filtered through 25 mm Millex 0.45-μl filters obtained from Millipore, UK.

Treatment of samples with β-glucuronidase

A 10-ml sample of urine was mixed with 700 μl of 1 *M* sodium acetate buffer, pH 5, and 500 μl of a crude solution of β-glucuronidase, *Helix pomatia* (G0876, Sigma). This mixture was incubated overnight (16 h) at 37°C.

Instrumentation

HPLC was performed on a Hewlett-Packard 1090L DR5 ternary pumping system with a Waters 490 programmable multiwavelength detector monitoring at 308, 304, 295 or 257 nm. The first ^{14}C human urine separations were carried out on a 5 μm Zorbax C_8 column (250 mm × 4.6 mm I.D.) protected by a 5-μm Zorbax C_8 guard column (12.5 mm × 4 mm I.D.) with a column temperature of 45°C. The mobile phase consisted of acetonitrile–aqueous 0.1 *M* ammonium acetate which was programmed from 5:95 to 95:5 (v/v) over 0.5 h with a flow of 1.5 or 2.0 ml/min. All subsequent work was performed on a 5-μm ChromSpher C_8 glass cartridge column (100 mm × 3 mm I.D.) protected by a 30–40 μm pellicular reversed-phase guard column (10 mm × 2.1 mm I.D.) with a column temperature of 40°C. The mobile phase was identical to that used with the Zorbax C_8 column except for the examination of component R, for which the mobile phase was acetonitrile–aqueous 0.1 *M* ammonium acetate (7.5:92.5). The flow-rate was 0.5 ml/min with a make-up solvent consisting of 0.05 *M* ammonium acetate in acetonitrile–water (30:70) at a flow-rate of 1.5 ml/min. The make-up solvent was added to the column effluent prior to UV detection.

The mass spectral data was acquired on a Finnigan MAT TSQ70 mass spectrometer equipped with a Finnigan MAT TSP 1 interface. The aerosol temperature varied from 250 to 300°C, the vaporiser temperature varied from 98 to 115°C and the repeller voltage varied from 60 to 80 V. Prior to use the system was optimised to solvent background ions, particularly an ion at *m/z* 433. Collisional dissociation experiments provided no additional data.

RESULTS

^{14}C labelled study in man

The first urine samples examined by LC–TSP-MS were from the oral administration to man of 240 mg (*ca.* 3.0 mg/kg) Lamotrigine. This dose administered as a gelatin capsule contained 15 μCi of ^{14}C material {3,5-diamino-6-(2,3-dichlorophenyl)-[5-^{14}C-]1,2,4-triazine} prepared by co-precipitation of [^{14}C]Lamotrigine (54.5 μCi/mg) and Lamotrigine from a methanolic solution. The urine samples analysed were pooled samples collected during the following time periods: 0–24 h and 24–48 h. Examples of the total and selected ion chromatograms obtained before and after incubation with β-glucuronidase are shown in Fig. 1. The mass spectra of com-

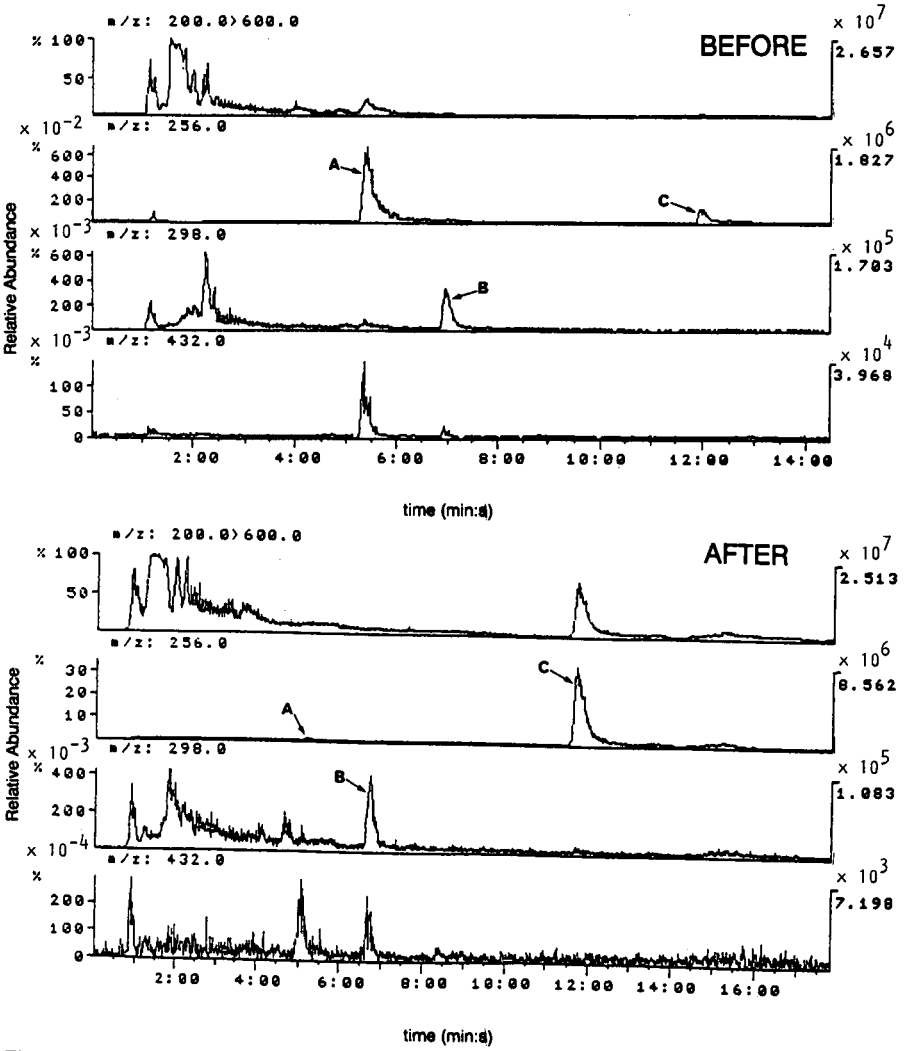

Fig. 1. Total and selected ion chromatograms obtained from LC–TSP-MS of 100-μl injections of human urine before and after treatment with β-glucuronidase.

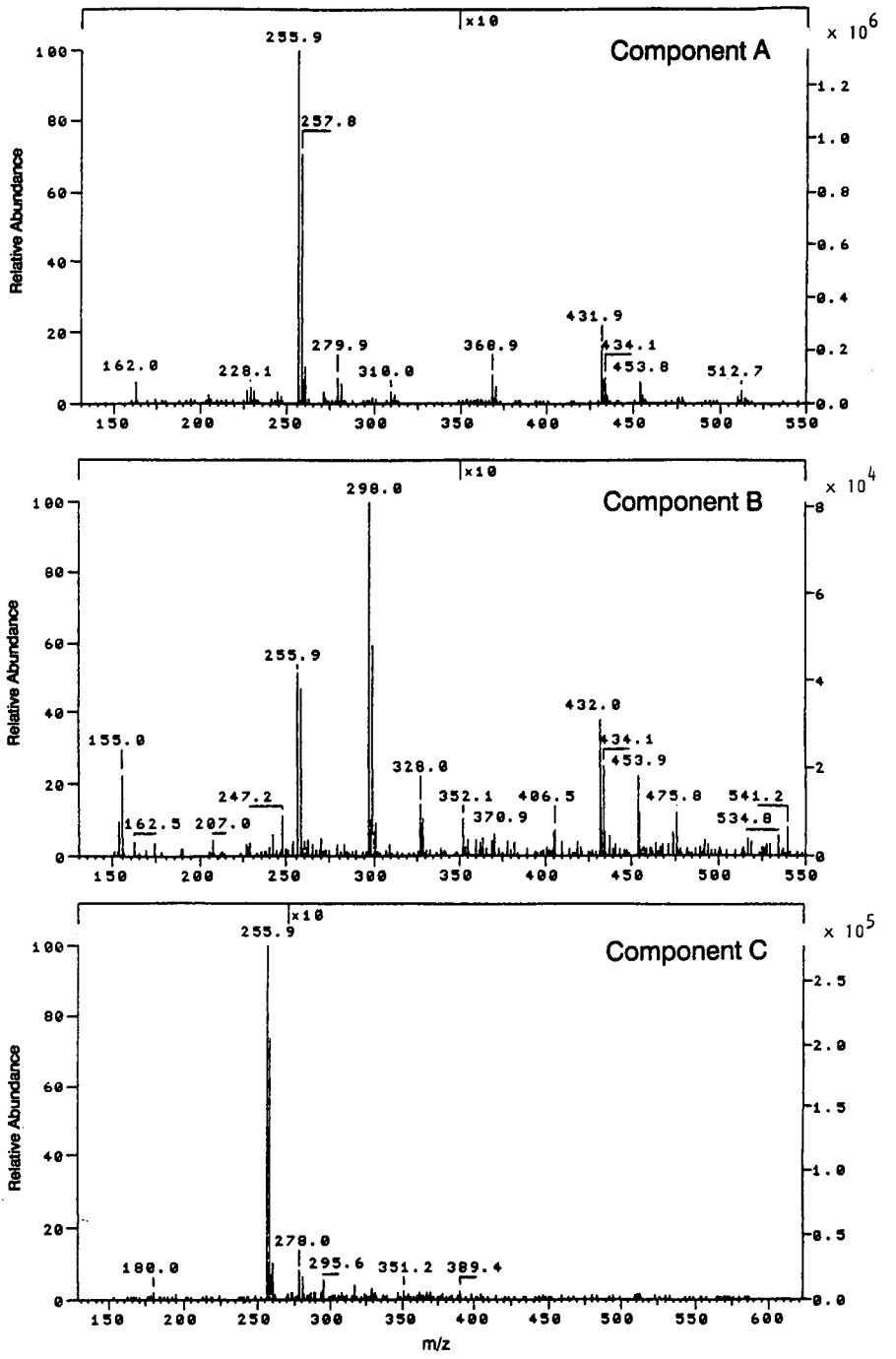

Fig. 2. Mass spectra of the components labelled A, B and C in Fig. 1 obtained by LC–TSP-MS after injection of 100 μl of human urine.

ponents A, B and C are shown in Fig. 2. The spectrum of component C consists essentially of a single ion at *m/z* 256 with the expected characteristic isotope pattern for a molecule containing two atoms of chlorine. The mass spectral data plus the results obtained after incubation with β-glucuronidase indicate that component C is the unchanged drug, Lamotrigine. The spectrum of component A has *m/z* 256 as the base peak and an ion at *m/z* 432, the expected protonated molecular ion for a glucuronide of Lamotrigine, and fragment ions at *m/z* 280 and 310 which are likely to be produced by cleavage across the glucuronic acid ring with concomitant loss of water. The spectrum of component B also contains a peak at *m/z* 432 but in this case the ion at *m/z* 256 due to the protonated aglycone is no longer the base peak. The base peak at *m/z* 298 and the ion at *m/z* 328 could again be formed by cleavage across the glucuronic acid ring but in this case without the loss of water. These results, together with the results obtained from the enzyme work with β-glucuronidase and radiochemical detection indicated that man produces two N-glucuronides of Lamotrigine of which only the major one is cleaved by the action of β-glucuronidase. Evidence of an N-oxide and a methylated metabolite were also observed in some of these urine samples but this represented less than 5% of the total radioactivity injected on to the liquid chromatograph and was only positively assigned when the results were compared with those obtained from the urines of laboratory animals.

^{14}C labelled studies in laboratory animals

Cynomolgus monkeys were dosed orally at 10 mg/kg and the 0–6-h, 6–24-h and 24–48-h urine samples were analysed.

The total and selected ion chromatograms obtained from a 100-μl injection from a 6–24-h urine sample are shown in Fig. 3. The spectra obtained for components A, B and C were the same as those obtained from human urine and represented the presence of two different N-glucoronides and unchanged Lamotrigine. The spectrum obtained for component D is shown in Fig. 4. Its HPLC retention time and LC–TSP-MS spectrum were identical to the data obtained from the chemically synthesized 2-N-oxide of Lamotrigine. Component E was only just detectable by the presence of an ion at *m/z* 270 and a large isotope peak at *m/z* 272. The presence of these ions and the comparison of its retention time with an authentic standard indicated that it was the 2-N-methyl analogue of Lamotrigine. Rabbits were orally dosed with 30 mg/kg of Lamotrigine. When 100 μl of a 0–24 h sample of urine was examined by LC–TSP-MS a large broad peak was observed in the *m/z* 256 selected ion chromatogram with a retention time equivalent to components A and B. Comparison of the *m/z* 272 and 274 ion chromatograms indicated the presence of a small amount of the 2-N-oxide of Lamotrigine. When 10 μl of rabbit urine was analysed using a chromatographic system in which the 0.05 *M* ammonium acetate was replaced by a 0.1-*M* solution a good chromatographic peak was obtained. The retention time and mass spectrum obtained from this peak indicated that the major drug related component excreted in urine by rabbits was the N-glucuronide of Lamotrigine that is resistant to hydrolysis by β-glucuronidase.

Further studies with human urine

Our American colleagues reported [3] that when certain clinical urine samples were kept at room temperature the major metabolite, component A, appeared to

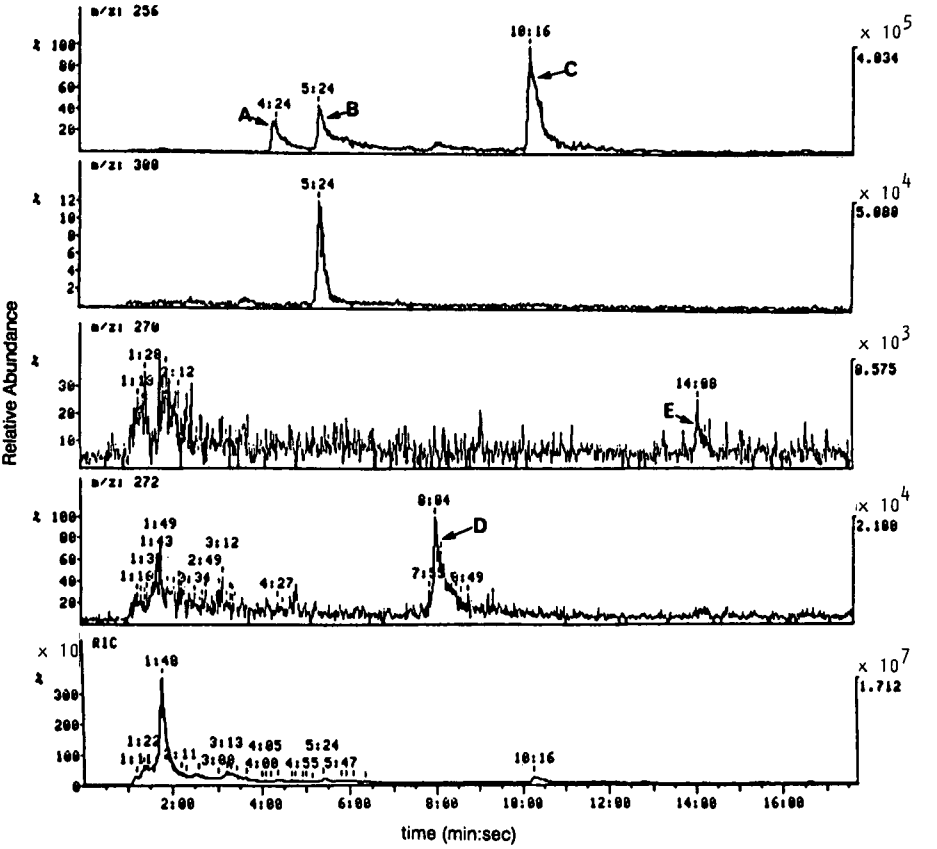

Fig. 3. Total and selected ion chromatograms obtained from an injection of 100 μl of Cynomolgus monkey urine.

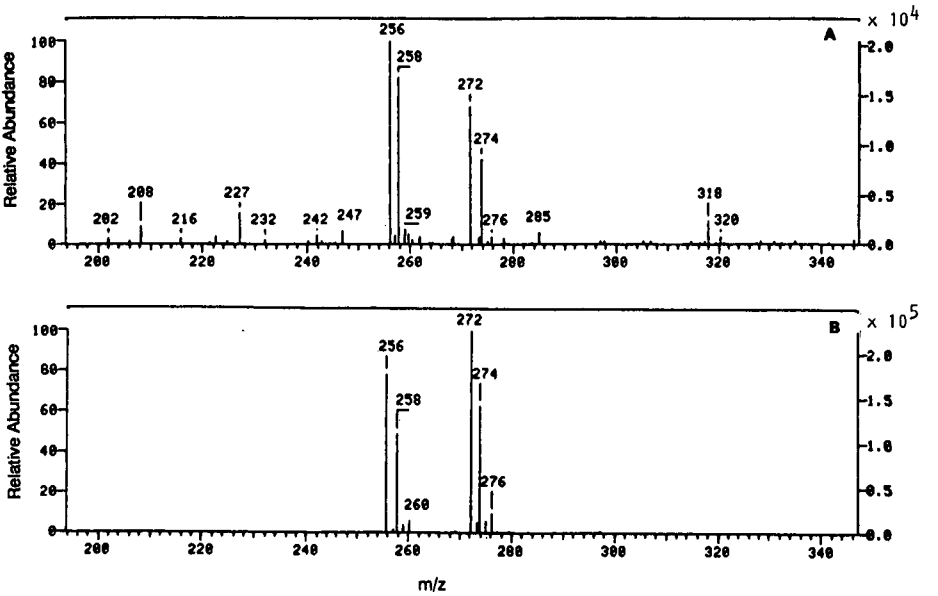

Fig. 4. Spectra obtained from (A) component D in Cynomolgus monkey urine and (B) authentic 2-N-oxide of Lamotrigine.

slowly convert to another component R, which was resistant to hydrolysis by β-glucuronidase. When we kept a sample of one of these urines (pH 7.6) at 37°C we also observed the formation of R. The spectrum of component R (Fig. 5) is consistent with a compound of molecular weight 432 formed by hydrolytic deamination of component A. The ions at *m/z* 433, 455 and 477 are $(M + H)^+$, $(M + Na)^+$ and $(M + 2Na - H)^+$, respectively. Two samples of urine obtained from volunteers dosed with Lamotrigine and shown to contain component A were also studied. When these urines, pH 5.5 and 6.5 respectively, were stored under identical conditions to the clinical samples no component R was formed.

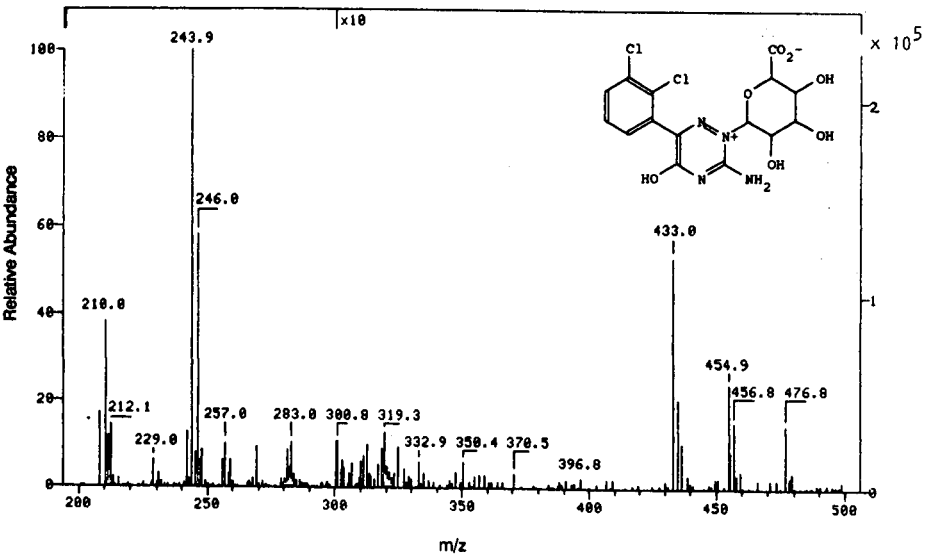

Fig. 5. The spectrum obtained from component R and its suggested structure. Component R was formed from component A when human urine with a pH 7.6 was left at room temperature.

CONCLUSIONS

The application of LC–TSP-MS allowed us to identify all the major Lamotrigine components in urine as well as many, if not all of the minor ones. Full mass spectra were obtained from samples containing approximately 100 ng of drug related material. This is important since the minor metabolites of a drug can be overlooked due to the limit on the radioactive dose that can be administered to humans and the lack of sensitivity of HPLC radiochemical detectors.

Our results, when correlated with the quantitative data obtained by reversed-phase HPLC with radiochemical detection enabled us to summarise the metabolism of Lamotrigine by man and laboratory animal species as shown in Fig. 6. Utilisation of these LC–TSP-MS conditions and facilities helped our colleagues in the Department of Physical Sciences [4] to optimise synthetic conditions for the chemical syn-

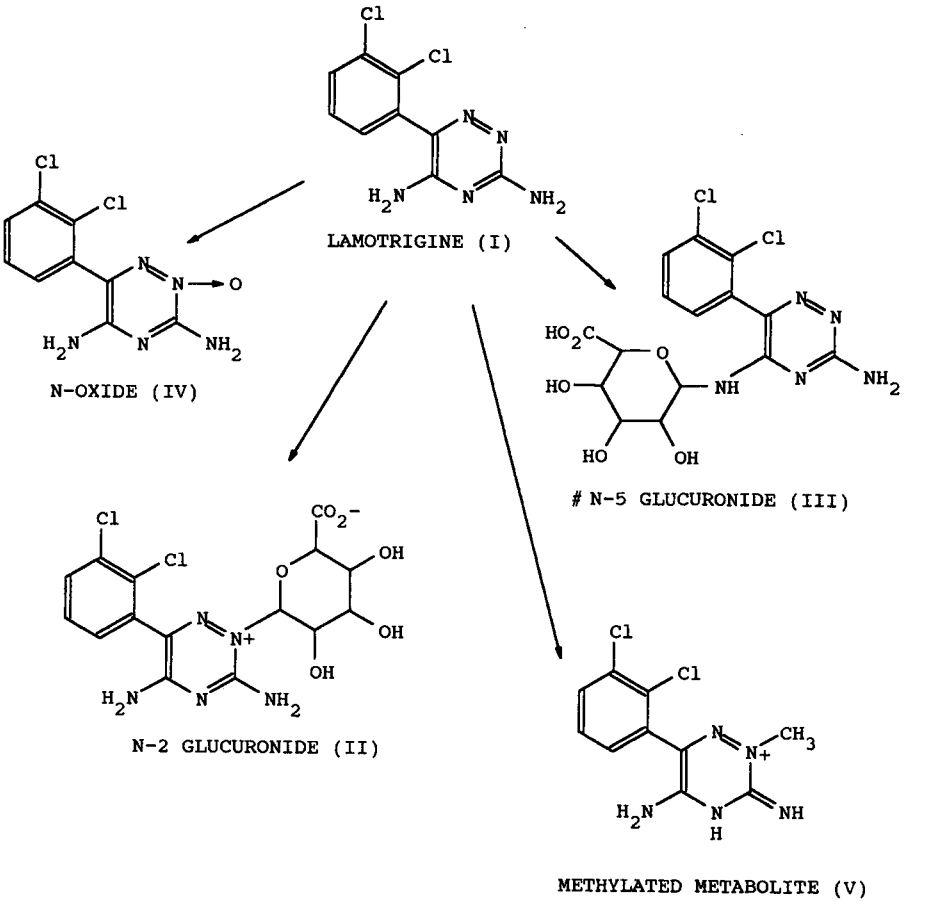

Fig. 6. A summary of the metabolism of Lamotrigine in man and laboratory animal species. Percentage of radioactivity in 0–24-h urine sample for (I) Lamotrigine: primates/man 7–30%, rabbit 3%, dog 2%, rat 50–60%; (II) N-2 glucuronide: man 80–90%, monkey 20–30%, rabbit 20–30%, rat 5–10%; (III) N-5 glucuronide: man 10%, monkey 30–40%, rabbit 40–70%, rat 5–10%; (IV) N-oxide: man 0–5%, monkey 5%, rat 10–25%; (V) methylated metabolite' dog 77%, other species 0–5%. # = Site of glucuronidation uncertain.

thesis of the N-2 glucuronide of Lamotrigine; to isolate, purify and characterise component A in human urine as the N-2 glucuronide of Lamotrigine; and to isolate, purify and tentatively conclude that the most likely structure of component B found in human and rabbit urine is an N-5 glucuronide of Lamotrigine. As we found with rabbit urine the chromatographic behaviour of component B greatly hampered its isolation, purification and characterisation and thus its absolute structural assignment is tentative rather than conclusive.

ACKNOWLEDGEMENTS

The authors wish to thank Dr. A. R. Buick, Ms. E. A. M. Neill and co-workers, from the Departments of Bioanalytical Sciences and Drug Safety Evaluation for the

preliminary profiling and quantitation of the urine samples using HPLC with radiochemical detection.

REFERENCES

1 G. G. Gibson and P. Skett, *Introduction to Drug Metabolism*, Chapman & Hall, London, New York, 1986.
2 C. R. Blakley and M. L. Vestal, *Anal. Chem.*, 55 (1983) 750.
3 J. Hubbell, T. Allsup and V. Otto, Burroughs Wellcome Co. US, personal communication, 1988.
4 A. M. Leone, P. L. Francis and M. J. Seddon, Wellcome Research Labs., Beckenham, UK, personal communication, 1990.

Journal of Chromatography, 554 (1991) 191–203
Elsevier Science Publishers B.V., Amsterdam

CHROMSYMP. 2357

Analysis of gentamicin sulfate by high-performance liquid chromatography combined with thermospray mass spectrometry

T. A. GETEK*,[a] and M. L. VESTAL
Department of Chemistry, University of Houston, Houston, TX 77004 (USA)
and
T. G. ALEXANDER
Food and Drug Administration, Center for Drug Evaluation and Research, Washington, DC 20204 (USA)

ABSTRACT

The quantitative analysis of gentamicin sulfate by high-performance liquid chromatography (HPLC) with mass spectrometry was performed on-line utilizing thermospray mass spectrometry (TSP-MS). Chromatographic reversed-phase separation utilizing trifluoroacetic acid as an ion pair reagent resulted in the observation by TSP-MS of the major components (C_{1a}, C_2 and C_1) of gentamicin sulfate as well as an additional minor component. This minor component had the identical $[M+H]^+$ ion and fragmentation pattern of the major fraction C_2 which indicated that the minor component may be the C_{2a} component. Method development and optimization of the mobile phase for HPLC–TSP-MS were accomplished with a variable simplex algorithm. HPLC with electrochemical detection was utilized in conjunction with the simplex algorithm to establish a mobile phase suitable for the HPLC–TSP-MS analysis of gentamicin sulfate. Bulk preparations of gentamicin sulfate were assayed by HPLC–TSP-MS for the major components by comparison with an external standard, and by a comparison of peak areas obtained for the individual components *vs.* the totaled peak areas.

INTRODUCTION

The aminoglycoside antibiotic gentamicin is produced from the fermentation of *Micromonospora purpurea*. The analysis of gentamicin sulfate is a difficult and challenging task for two particular reasons. Firstly, gentamicin is a multicomponent mixture primarily made of three major constituents, the C_{1a}, C_2, and C_1 fractions as shown in Fig. 1. The small substituent difference on the aminomethyl saccharide (F_3, Fig. 1) makes separation of these major constituents non-trivial. Furthermore, there exist minor constituents (C_{2a} and C_{2b}) which may represent a substantial percentage of the gentamicin antibiotic in newer formulations [1]. The second reason that makes the analysis of gentamicin difficult is the lack of chromophores in the gentamicin

[a] Present address: Battelle, 505 King Avenue, Columbus, OH 43201, USA.

0021-9673/91/$03.50

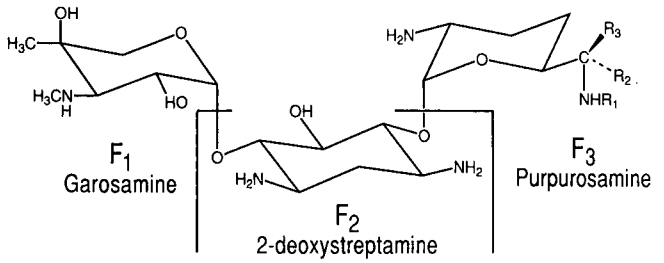

GENTAMICIN	R_1	R_2	R_3
C_1	Me	H	Me
C_2	H	H	Me
C_{1a}	H	H	H
C_{2a}	H	Me	H
C_{2b}	Me	H	H

Fig. 1. Structures of the components of the gentamicin complex.

moieties (Fig. 1). This lack of a chromophore does not readily allow the detection of gentamicin by conventional ultraviolet (UV) spectroscopic methods.

Gentamicin was first isolated by Weinstein *et al.* [2] in 1963. Numerous analytical methods have been applied to assay gentamicin. These methods initially employed paper chromatography to determine the C_1 and C_2 composition of gentamicin [3], and later the C_{1a} component was separated [4]. The paper chromatographic method followed by microbiological assay of the separated components was adopted as the official Food and Drug Administration (FDA) protocol [5]. Subsequently, additional investigations by paper and thin-layer chromatography established that several other minor components existed in gentamicin [6–8]. Detection with a conductivity bridge after ion-exchange chromatography separated and detected the major components of gentamicin [9]. Thomas and Tappin [10] employed ion-exchange column chromatography with optical rotation detection for gentamicin analysis. The first utilization of an ion pair reagent with a reversed-phase column for gentamicin analysis was reported by Anhalt [11]. Detection of gentamicin sulfate was accomplished with fluorescence after post-column derivatization with *o*-phthalaldehyde (OPA) [11,12]. Similar high-performance liquid chromatography (HPLC) with pre-column derivatization by OPA [13] and dansyl chloride [14] followed by fluorescence was performed for gentamicin analyses. Other workers examined gentamicin by HPLC followed by derivatization in plasma and urine samples analyzed in the range of 0.25 to 25 $\mu g\ ml^{-1}$ [15]. Freeman *et al.* [1] employed pre-column derivatization with an OPA–thioglycollic acid reagent followed by UV detection at 330 nm. They reported that the C_{2a} component represented a significant proportion of the gentamicin antibiotic. Later studies [16,17] confirmed the importance of monitoring the C_{2a} component. Claes *et al.* [18] utilized ion pair HPLC and pre-column derivatization with UV detection at 350 nm for analysis of the C_{2a} component. Other gentamicin analyses were accomplished with pre-column derivatization by 2,4,6-trinitrobenzenesulphonic acid [19]. Recently, the effect of inorganic cations on the separation of OPA derivatives of

gentamicin by HPLC was examined [20]. The concentration of these inorganic cations affected the separation order of the gentamicin components. Seidl and Nerad [21] used isocratic ion-exchange chromatography with post-column OPA reaction followed by fluorescence to detect the C_1, C_{1a}, C_2, C_{2a}, and C_{2b} components. The separation order for this ion-exchange chromatography [21] was C_{1a}, C_2, and C_1 which supported the observed effect of potassium iodide concentration on the elution order of OPA derivatives by reversed-phase HPLC [20]. Inchauspé and Samain [22] were able to separate several aminoglycoside antibiotics by utilizing perfluorinated carboxylic acids as ion pair reagents in reversed-phase HPLC with refractive index (RI) detection. The separation of gentamicin sulfate was in the elution order of C_{1a}, C_2, and C_1 with an unidentified gentamicin peak labeled "X".

All the ion pair reversed-phase HPLC analyses cited using UV or fluorescence detection required derivatization prior to assay. RI detection was used after the perfluorinated carboxylic acid separations without derivatization [22,23]. Previous studies have shown that HPLC with electrochemical detection (ED) is useful for detecting gentamicin sulfate without the need for derivatization [24].

Mass spectrometry (MS) of gentamicin sulfate has been reported by chemical ionization (CI), and the type of ions formed evaluated [25]. Parfitt *et al.* [26] discussed the electron impact (EI), CI by isobutane, and field desorption (FD) mass spectrometry of gentamicins. The EI-MS of gentamicin was reported to have no diagnostic value for evaluating commercial mixtures, and FD-MS was used to obtain the $[M + H]^+$ ions with little glycosidic cleavage for the various gentamicin components at optimum conditions. FD-MS with emitter CI was also discussed by Takeda *et al.* [27]. Inchauspé *et al.* [28] examined gentamicin sulfate by FD-MS after off-line separation by HPLC using perfluorinated carboxylic acids as ion pair reagents. Plasma desorption MS was applied for analysis of several aminoglucoside antibiotics, including gentamicin sulfate [29]. Atmospheric pressure ionization MS with corona discharge has been employed successfully for a wide variety of aminoglycoside antibiotics [30]. The applicability of thermospray mass spectrometry (TSP-MS) utilizing trifluoroacetic acid (TFA) as an ion pair reagent for on-line reversed-phase HPLC for separating and detecting the components of gentamicin sulfate has been discussed [31]. Fast atom bombardment MS of aminoglycoside antibiotics has also been accomplished [32].

This study reports the details for the on-line HPLC–TSP-MS determination of gentamicin sulfate. Before performing on-line HPLC–TSP-MS, the mobile phase was optimized using a simplex algorithm and LC–ED. Several bulk preparations of gentamicin sulfate were examined for C_{1a}, C_2, and C_1 content and for possible characterization of previously unidentified components by HPLC–TSP-MS.

EXPERIMENTAL

For the HPLC–TSP-MS analysis, a Hewlett-Packard (HP) 5988A mass spectrometer with HP Chemstation data handling system (version 3) was utilized. A Vestec (Houston, TX, USA) Thermospray source and controller were used. The HPLC pump was an SSI, Model GS400 (College Station, PA, USA). The conditions for TSP-MS were control, 110°C and block, 308°C with filament and discharge off. Scan range was approximately m/z 100 to 500. Selected ion currents (SIC) were

plotted after a full scan measurement. For the HPLC with ED analysis, a Brinkmann/Metrohm EA-1096 cell (Westbury, NY, USA) with Ag/AgCl reference electrode and glassy carbon working and auxiliary electrodes was employed. A BAS (West Lafayette, IN, USA) CV-1B was used as the potentiostat in conjunction with this cell. The HPLC pump for HPLC–ED was a Spectra-Physics (San Jose, CA, USA) SP-8700 with ternary solvent capability. The potential of the electrochemical cell was set to approximatgely +1.2 V.

In both cases, HPLC–TSP-MS and HPLC–ED, the flow-rate was 1.0 ml min^{-1} and a 3-μm ODS-II reversed-phase column (100 × 4.6 mm I.D.; LC Custom, Houston, TX, USA) was employed. A Rheodyne (Cocati, CA, USA) 7125 injector with 20-μl loop was utilized.

Prior to the HPLC–TSP-MS analysis of gentamicin, the mobile phase was optimized employing a variable simplex algorithm software program compatible with a PC based computer (Statistical Products, Houston, TX, USA) and HPLC–ED. Only mobile phase composition was considered in the optimization and three factors were selected. These factors consisted of solvent A which contained 0.22 *M* trifluoroacetic acid (TFA) raised to a pH of 3.6 with ammonium hydroxide in deionized water, solvent B was deionized water only, and solvent C was methanol. The simplex program normalized the percent composition of each solvent (factor) to 100%. These percentages were then selected for each solvent on the SP-8700 HPLC pump which was capable of handling a three-solvent system for the mobile phase. This set-up allowed for rapid change of the mobile phase based on the response of the simplex calculation for every new experimental point designated. The final mobile phase utilized for HPLC–TSP-MS consisted of 0.11 *M* aqueous TFA–methanol (94:6) where the aqueous TFA was adjusted to pH 3.6 with ammonium hydroxide.

Gentamicin sulfate samples were bulk preparations. The standard was a USP standard, Lot H, rated at a potency of 663 μg/mg. The percent components as stated for Lot H were C_{1a} = 31.5%; C_2 = 31.6%; C_1 = 36.9%. Analysis by paper chromatography followed by microbiological assay [5] gave C_{1a} = 31.33%; C_2 = 30.31%; C_1 = 38.37% for Lot H (see Table III). The HPLC–TSP-MS percentages are compared directly with the microbiological assay after taking into account the activities of the three major gentamicin components [5]. Samples and standards for HPLC–TSP-MS were diluted in deionized water at a nomial concentration of 1 mg ml^{-1}.

RESULTS AND DISCUSSION

The TSP-MS of the gentamicin sulfate components in the positive ion mode produced low ion intensity for the $[M + H]^+$ ions, but high ion intensity for the fragments resulting from the cleaving of the glycosidic bonds [31,32]. The resultant reduction in ion intensity for the $[M + H]^+$ ions is probably due to the thermal lability of the compound via TSP-MS. A distinct fragment ion corresponding to each of the major components of gentamicin sulfate (Fig. 1) was observed. These distinct ions arose from the differences in the number of methyl groups bonded to a terminal aminomethyl substituent on the F_3 fragment. The distinctive F_3 fragment and $[M + H]^+$ ions are listed in Table I for each gentamicin sulfate component. Two fragments (F_1 and F_2) were identical in all components (Fig. 1) and their corresponding ions were also identical (Table 1). The ion indicative of the F_2 fragment resulted from the

TABLE I

DISTINCTIVE FRAGMENT AND $[M + H]^+$ IONS FOR EACH COMPONENT OF GENTAMICIN SULFATE BY TSP-MS

Component	*m/z*			
	$[F_1]^{+a}$	$[F_2 + 3H]^{+b}$	$[F_3]^{+c}$	$[M + H]^+$
C_{1a}	160	163	129	450
C_2	160	163	143	464
C_1	160	163	157	478
C_{2a}	160	163	143	464
C_{2b}	160	163	143	464

[a] Terminal saccharide without aminomethyl substituent (Fig. 1).
[b] Central fragment ion resulting from addition of three hydrogens.
[c] Distinctive terminal saccharide with aminomethyl substituent (Fig. 1).

retention of the two glycosidic oxygens to this fragment after cleavage followed by addition of three hydrogens to this fragment. This generated the $[F_2 + 3H]^+$ ion at *m/z* 163 as listed in Table I. The nature of the $[F_1]^+$ and $[F_3]^+$ ions has not been clearly defined. The ion indicative of fragment F_1 gave a *m/z* of 160, as indicated in Table I. For fragment F_1, the removal of the glycosidic oxygen leaves a total mass of 160 a.m.u. One possibility that may produce an ion at *m/z* 160 for F_1 is a proton abstraction to form a double bond, which makes the F_1 fragment 159 a.m.u., followed by addition of a proton to generate the observed ion fragment at *m/z* 160. This ion at *m/z* 160 may also be due to the formation of a cation on the ethereal oxygen to produce a $[F_1]^+$ ion. The same possibilities exist for the nature of the ion indicative of the distinctive F_3 fragment. Fragmentation of gentamicin sulfate observed in FD-MS [27] resulted in ions corresponding to the F_1 and F_3 fragments identical to those indicated in Table I. These fragment ions were considered to have a positive charge on the ethereal oxygen [27]. A similar ion was suggested for the F_1 fragment by EI-MS, and identical ions appeared in the isobutane CI mass spectra [26]. At this time, it is not clear what the true nature of the formation of the $[F_1]^+$ and $[F_3]^+$ ions in TSP-MS is; however, it is definite that the ions indicated in Table I are correlated to the particular fragments from studies dealing with analogues of gentamicin sulfate [32].

As stated earlier, the separation and detection of the components of gentamicin sulfate is not a trivial task. The reversed-phase separation by HPLC usually required some ion-pair reagent to exaggerate the small differences in the gentamicin components. Anhalt and co-workers [11,12] used a mobile phase containing sodium pentanesulfonate (SPS) and sodium sulfate to achieve separation of the C_{1a}, C_2, and C_1 components followed by post-column derivatization with OPA and fluorescence detection. Initial attempts to use a similar mobile phase containing SPS for HPLC–TSP-MS were unsuccessful due to the non-volatility of the salts used. Ion exchange of protons for sodium in SPS and substitution of ammonium sulfate for sodium sulfate in the mobile phase were also unproductive due to the incompatibility of this mobile phase with the thermospray (TSP) source. A volatile ion pair reagent was needed to accomplish the separation of the gentamicin sulfate components and be compatible

with the TSP source. Inschauspé and Samain [22] utilized trifluoracetic acid (TFA) as an ion-pair reagent to separate the gentamicin sulfate components. Using a TFA mobile phase with reversed-phase HPLC, the on-line separation and detection of gentamicin sulfate by TSP-MS was successful [31].

In order to improve the TFA mobile phase for gentamicin sulfate analysis by HPLC–TSP-MS, the separation of the various components was optimized with respect to the mobile phase composition. A variable simplex algorithm with three factors was used. These three factors represented three solvents which were incorporated into the mobile phase. The response factor (R) involved two goals: (1) to minimize the analysis time, and (2) to achieve good separation of the various components by comparing the capacity factors (k') of each neighboring chromatographic peak to some ideal predetermined difference in capacity factors of neighboring chromatographic peaks. Based on these goals, an equation for R was generated. As R approached zero, this was considered to be the best separation.

$$R = \frac{(k'_1 - k'_0) - I_0}{2} + \ldots + \frac{(k'_{n+1} - k'_n) - I_n}{2} \quad (1)$$

where k'_0 is the capacity factor of the solvent front ($k'_0 = 0$); k'_1 is the capacity factor of the first chromatographic peak, in this case, component C_{1a}; I_0 is the ideal predetermined difference in $k'_1 - k'_0$, in the first instance, $I_0 = 1$. For $n + 1$ number of chromatographic peaks, a summation is carried out for all of the peaks. One change is that I_n is greater than I_0 for late eluting peaks. The increase in I for late eluting peaks is due to band broadening over chromatographic time. This aids in maintaining good separation between late eluting components. The value for I should be chosen with respect to the particular HPLC column size, column type and flow-rate. Of the two goals stated above, good separation was considered a higher priority than length of analysis time. For this reason, when $[k_{n+1} - k_n) - I_n] < 0$, there was no division by two for that particular difference in eqn. 1. In cases where no separation occurred between neighboring peaks, $(k_{n+1} - k_n) = 0$, a value of ten was arbitrarily given to this separation.

Using the simplex algorithm and HPLC–ED, a suitable mobile phase was achieved after 13 vertices, three of which were beyond value limits. This final mobile phase is described in the Experimental section. A chromatogram of gentamicin sulfate by HPLC–ED is shown in Fig. 2. For analytical purposes, the chromatographic

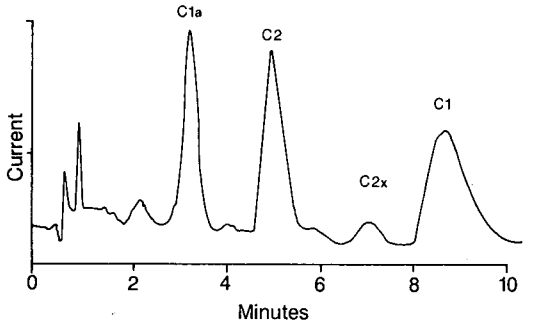

Fig. 2. HPLC–ED of gentamicin sulfate using the trifluoroacetic acid ion pair mobile phase. Peak C_{2x} is considered as component C_{2a} as described in text. Approximately 15 μg injected on-column.

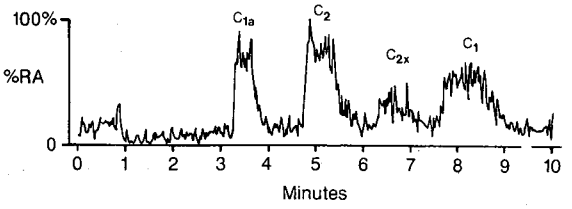

Fig. 3. HPLC–TSP-MS of gentamicin sulfate as a function of percent relative abundance (RA) *vs.* chromatographic time. Peak C_{2x} is considered as component C_{2a}, and the mobile phase is identical to the one used for HPLC–ED (Fig. 2). Approximately 15 μg injected on-column.

peak C_{2x} represents the C_{2a} and C_{2b} components of gentamicin sulfate. The occurrence of C_{2x} in Fig. 2 between the C_2 and C_1 chromatographic peaks has the identical location to peak "X" employing a TFA containing mobile phase [22].

The HPLC–TSP-MS of gentamicin sulfate using the same mobile phase employed for HPLC–ED is seen in Fig. 3. The total ion current (TIC) trace is identical to the HPLC–ED. In Fig. 4, the selected ion current (SIC) is plotted for the $[F_3]^+$ ions indicated in Table I. As shown in Fig. 4, these fragment ions are distinctive for each component of gentamicin sulfate. It is also seen that the peak labeled C_{2x} is related to C_2 in that the $[F_3]^+$ ion is identical.

The mass spectrum for each chromatographic peak in Fig. 3 was examined after background subtraction. The ions listed in Table 1 were observed in the mass spectra of the various components (Fig. 5a–d). In comparing Fig. 5b for the C_2 component with Fig. 5d, it is clearly indicated that C_{2x} is related to the C_2 component. Because the amount of component C_{2b}, also known as sagamicin, is expected to be very low [21], the C_{2x} will be considered to be the C_{2a} component of gentamicin sulfate. For analytical purposes, the peak area contributed by C_{2a} (C_{2x}) will be totaled with the C_2

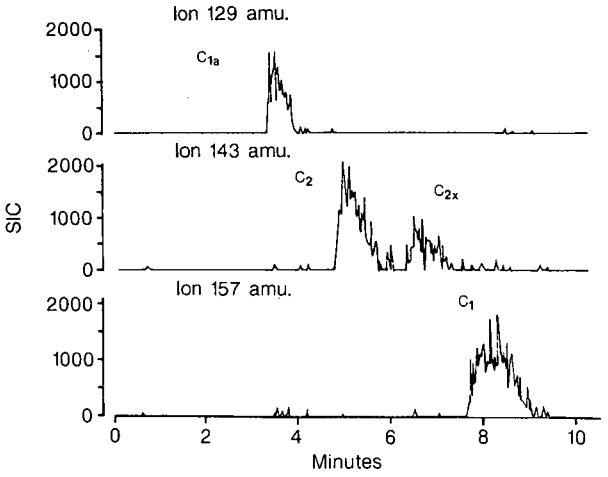

Fig. 4. Selected ion current (SIC) for the individual distinctive ions representing the F_3 part of the gentamicin sulfate complex as described in Table I.

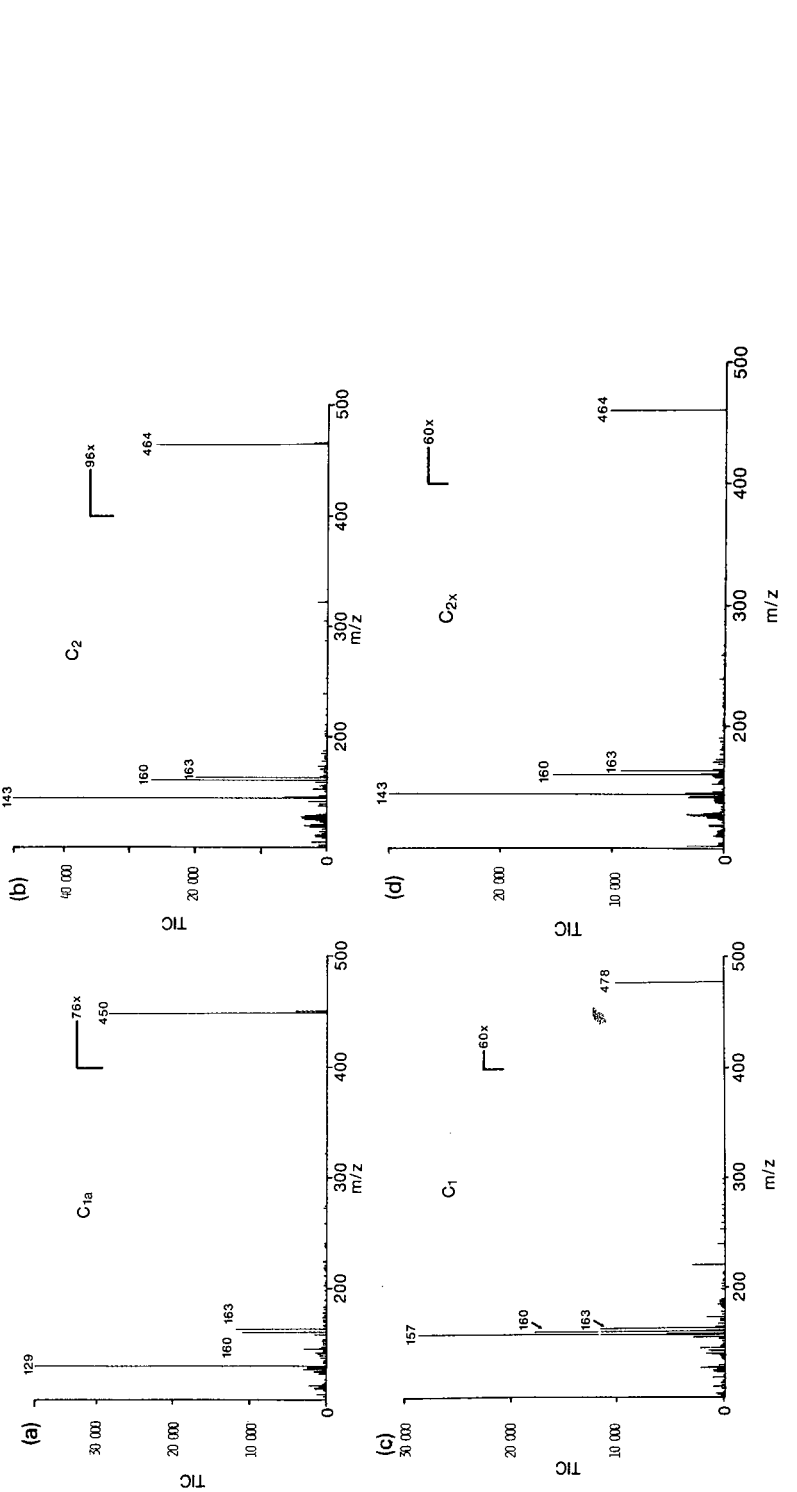

Fig. 5. (a) Thermospray mass spectrum of the gentamicin sulfate C_{1a} component. (b) Thermospray mass spectrum of the gentamicin sulfate C_2 component. (c) Thermospray mass spectrum of the gentamicin sulfate C_1 component. (d) Thermospray mass spectrum of the C_{2x} fraction considered to be the gentamicin sulfate C_{2a} component.

peak area. Finally, two additional points should be made clear with respect to the HPLC–TSP-MS of gentamicin sulfate. Firstly, the ion intensity for the $[M + H]^+$ ions is close to zero for low concentrations of the gentamicin sulfate injected on-column, thus the need to monitor the distinct ion produced from the F_3 fragment (Fig. 1). Secondly, an ion is sometimes observed at *m/z* 322 for all components of gentamicin sulfate. It was concluded that this ion was representative of the combined $F_1 + F_2$ (Fig. 1) fragments producing a $[F_1 + F_2 + 2H]^+$ ion. The corresponding $[F_2 + F_3 + 2H]^+$ ions were not observed suggesting that the first glycosidic bond breakage was between the F_2 and F_3 segments. This behavior was noted for analogues of gentamicin sulfate [32]. The FD-MS of gentamicin [27] did detect the $[F_2 + F_3 + 2H]^+$ ion.

The linearity of the signal *vs.* solute injected on-column by HPLC–TSP-MS for gentamicin was evaluated. The correlation coefficient (*r*) for each of the components is shown in Table II. The sample used for this linearity study was a bulk preparation. The USP standard for gentamicin sulfate was observed to have a very low amount of C_{2a}, thus the utilization of a bulk preparation so that a signal *vs.* concentration curve could be generated for C_{2a}. The *r* for all components was 0.98 or better. The amount injected on-column is the total amount of the gentamicin complex injected. The actual amount for each component is unknown, but the approximated amount is indicated in Table II. Because the exact amount are unknown for this bulk preparation, a detection limit could only be approximated to be 0.4 μg injected for the total gentamicin sulfate complex. In order to assay the bulk preparation, it was necessary to compare the composition of the gentamicin sulfate USP standard to the peak area obtained by HPLC–TSP-MS. The stated composition of the USP standard does not take into account any C_{2a} component. For assay purposes, the peak area obtained for C_{2a} was added to the C_2 peak area. Three standards were weighed out and each standard was analyzed in triplicate. A signal *vs.* μg injected on-column response was calculated using the percent composition of the gentamicin sulfate USP standard. It is important to note the μg injected represents microbiological activity and takes in account the relative activity for each component [5]. The results of HPLC–TSP-MS analysis of the standard are shown in Table III.

Three bulk preparations of gentamicin sulfate were assayed. One noticeable difference was that the peak area associated with the C_{2a} component in the bulk

TABLE II

LINEARITY OF GENTAMICIN SULFATE COMPONENTS AS DETERMINED BY THE CHROMATOGRAPHIC PEAK AREA *VS.* THE AMOUNT OF BULK GENTAMICIN SULFATE INJECTED ON-COLUMN

Component	Range of μg injected[a]	Correlation coefficient (*r*)
C_{1a}	0.3–6.0	0.985
C_2	0.3–6.0	0.994
C_{2a}[b]	0.1–2.0	0.9996
C_1	0.3–6.0	0.996

[a] This range was based on 30% of the total amount of the gentamicin sulfate complex injected for the three major components, and 10% for C_{2a}. It represents only approximate amounts.

[b] The component C_{2x} was considered to be C_{2a} with no major contribution from C_{2b}.

TABLE III

RESPONSES OF GENTAMICIN SULFATE STANDARD BY HPLC–TSP-MS COMPARED TO QUANTITIES INJECTED

μg Injected on-column[a]				Signal[c]/μg Injected		
Total[b]	C_{1a}	C_2	C_1	C_{1a}	C_2	C_1
7.20	2.26	2.18	2.76	2.10	2.99	2.80
9.92	3.10	3.00	3.80	1.97	3.11	2.84
8.00	2.50	2.42	3.06	1.98	3.26	2.76
Mean				2.02	3.12	2.80
R.S.D.[d]				3.6%	4.3%	1.4%

[a] The μg injected for each component was based on percentage obtained from microbiological assay as noted in Experimental and represents a relative amount related to the activity of the individual components.
[b] Amount of C_{2a} was observed to be negligible in standard.
[c] (Signal from integrated peak area) · 10^{-5}.
[d] R.S.D. = Relative standard deviation, $n = 3$.

preparations was substantially higher than the USP standard. Table IV shows the results of the HPLC–TSP-MS assay using an external standard compared to the official paper chromatographic method. As can be seen from Table IV, the values obtained by paper chromatography *vs.* HPLC–TSP-MS do not agree exactly. Several points should be considered when comparing these two methods. The paper chromatography method does not take into account the C_{2a} component. For HPLC–TSP-MS, the peak area from the C_{2a} was summed with the C_2 peak area. This may not represent the situation in paper chromatography. The C_{2a} component may be summed with either the C_1 or C_{1a} components, thus affecting the percentages obtained by paper chromatography. Weigand and Coombes [33] considered the problems with the analysis of the C_{2a} component by HPLC compared to the paper chromatographic assay. They reported that for the two methods to agree, C_{2a} must coelute with C_2. From HPLC–TSP-MS, the peak area corresponding to C_{2a} repre-

TABLE IV

ASSAY OF GENTAMICIN SULFATE BULK PREPARATIONS BY HPLC–TSP-MS COMPARED TO PAPER CHROMATOGRAPHIC METHOD AS CALCULATED BY EXTERNAL STANDARD METHOD

Sample	Paper chromatography (%)			HPLC–TSP-MS[a] (%)		
	C_{1a}	C_2	C_1	C_{1a}	C_2[b]	C_1
A	28.10	32.96	38.94	29.3	41.8	28.9
B	20.60	36.78	42.65	20.2	45.8	34.0
C	17.59	35.18	47.22	22.5	40.9	36.5

[a] These percentages compare directly with paper chromatography values after accounting for the microbiological activities for each component as indicated in ref. 5.
[b] Component C_{2a} combined with C_2.

TABLE V

PERCENT COMPOSITION OF THE MAJOR COMPONENTS FOR GENTAMICIN AS CALCULATED BY USP PROCEDURE (REF. 35) VIA TOTALING PEAK AREAS *VS.* COMPONENT PEAK AREA

Sample	C_{1a}[a] (%)	C_2 (%)	C_{2a} (%)	C_1[b] (%)	$C_2 + C_{2a}$[c] (%)
A	21.9	35.6	12.6	29.9	48.2
B	14.6	31.8	19.4	34.1	51.2
C	16.5	34.8	11.6	37.1	46.4

[a] USP limits 10–35%.
[b] USP limits 25–50%.
[c] USP limits 25–55%.

sented 12 to 19% of the total peak area, as seen in Table V, for the bulk preparations. Another point to consider is that the paper chromatography percentages were based on microbiological methods and the potency of the various components. This percent potency does not correlate directly with percent composition since the microbiological activity of the various components differ.

Although the percentages do not agree completely in Table IV for the two methods, trends are noted in the percentages. Comparing sample A with sample B, it is seen that C_{1a} is less in sample B (28.10% to 20.60%) as measured by the paper chromatography method. A similar decrease is observed for C_{1a} in sample B in the HPLC–TSP-MS method (29.3% to 20.2%). Likewise, an approximate 4% increase in both methods is noted for the C_2 component going from A to sample B, and an approximate 3 to 5% increase for the C_1 component. The trend is not as clear with sample C; however, this may be due to the effect of the C_{2a} composition.

The difficulties in comparing analyses by HPLC to microbiological assay for gentamicin sulfate [33] and other antibiotics have been discussed by Thomas [34]. Because of the question of C_{2a} composition and other difficulties, USP has established guidelines for approving bulk preparations of gentamicin sulfate by HPLC assay [35] without an external standard. The HPLC assay established by USP is similar to the method of Freeman *et al.* [1] and employs UV detection at 330 nm with pre-column derivatization with OPA. The procedure consists of totaling the chromatographic peak areas for C_{1a}, C_2, C_{2a}, and C_1 and calculating the percent peak areas contributed by the fractions. The C_{2a} peak area is incorporated with the C_2 peak area [35]. Using this procedure for HPLC–TSP-MS, the percentages for the major components for the gentamicin sulfate bulk preparations are given in Table V. As seen from Table V, the gentamicin sulfate components are within USP limits for all samples.

Finally, the elution order of the major components of gentamicin should be considered. The elution order for the USP method [1,35] is C_1, C_{1a}, and then C_2 for the OPA derivatized components. Modifying the mobile phase may affect the elution order [12]. With the HPLC–TSP-MS method reported in this study, any change in elution order will be detected immediately by monitoring the distinctive ions for each component. Furthermore, there is no need to derivatize the gentamicin components, although it may be a point of interest to observe what effects derivatization may have on detection limits.

CONCLUSIONS

The analysis of the major components of gentamicin sulfate by on-line HPLC–TSP-MS was achieved using volatile TFA as an ion pair reagent with reversed-phase HPLC, and required no derivatization. The utilization of simplex optimization with HPLC–ED permitted a rapid and simple means by which a compatible mobile phase for TSP-MS was selected. The technique of HPLC–ED detected the major components of gentamicin sulfate without derivatization. An advantage of using an alternate detection method, such as HPLC–ED, for optimization before performing HPLC–TSP-MS is that valuable and expensive instrumental time is not consumed on a mass spectrometer. Adjustment of thermospray vaporizer and block temperatures are ususally necessary after altering the mobile phase composition. With the mobile phase optimized and selected by HPLC–ED, an advantage is that only one set of temperature conditions for HPLC–TSP-MS required optimizing instead of adjusting the temperature conditions for each new mobile phase.

The quantitative analysis of gentamicin sulfate was accomplished by an external standard method, and by the USP procedure of comparing individual peak areas to the totaled peak area [35]. Few studies have discussed quantification by HPLC–TSP-MS. The degree of reproducibility for this HPLC–TSP-MS analysis was indicated by a 1 to 4% relative standard deviation for triplicate assays of the standard. For the assay of gentamicin sulfate, the advantage of TSP-MS is demonstrated by the ability to characterize the C_{2a} component. Other detection schemes, such as HPLC–ED, could not definitively ascertain that a particular chromatographic peak was due to a fraction without a comparison of retention times with an authentic standard of the individual components. The distinctive fragmentation pattern and observation of the $[M + H]^+$ ion for C_2 and C_{2a} allowed for a confident summation of these two chromatographic peak areas for analytical purposes.

One drawback of TSP-MS is the incompatibility of non-volatile salts in the ion source. The incorporation of TFA as an ion pair reagent in the mobile phase for on-line HPLC–TSP-MS, as exemplified by this analysis of gentamicin sulfate, may be applied to other aminoglycoside antibiotics and similar compounds that are difficult to separate by reversed-phase HPLC.

The detection limits for gentamicin sulfate via HPLC–TSP-MS was approximately 400 ng injected on-column compared to 16 μg for HPLC–ED [24]. The UV detection method with derivatization was estimated to be 10 μg on-column [1]. Fluorescence detection after derivatization is very sensitive giving an estimated detection limit of 10 ng [15]. For routine assay procedures, the UV and fluorescence methods would be adequate provided that standards are available to assure the identity of the components by retention times. The HPLC–TSP-MS technique has the advantage for characterizing the components without standards, and changes in retention times due to column degradation or contamination would not affect the HPLC–TSP-MS identification. It should be noted that the mass spectra were full scan measurements; selective ion monitoring (SIM) modes may give detection limits similar to the fluorescence methods.

The nature of the ions observed for the F_1 and F_3 fragments (Fig. 1) has not been defined; however, this unique fragmentation as exemplified for gentamicin sulfate at the glycosidic bond will make characterization of similar unknown aminogly-

coside antibiotics possible. Further studies will be needed to confidently identify the type of ions indicative of the F_1 and F_3 fragments produced by thermospray ionization.

ACKNOWLEDGEMENTS

The authors thank S. West and M. Hayden of the FDA, Washington, DC, USA for their assistance. We would also like the acknowledge the kind gift of PC-based simplex program by Dr. S. N. Deming, and C. Hartwick for typing the manuscript. This work was supported by the Robert A. Welch Foundation.

REFERENCES

1 M. Freeman, P. Hawkins, J. Loran and J. Stead, *J. Liq. Chromatogr.*, 2 (1979) 1305–1317.
2 M. Weinstein, G. Luedemann, E. Oden and G. Wagman, *Antimicrob. Agents Chemother.*, 1 (1963) 1–13.
3 J. Rosselet, J. Marquez, E. Meseck, A. Murawski, A. Hanndan, C. Joyner, R. Schmidt, D. Migliore and H. Herzog, *Antimicrob. Agents Chemother.*, 1 (1963) 14–16.
4 N. Kantor and G. Selzer, *J. Pharm. Sci.*, 57 (1968) 2170–2171.
5 *Code of Federal Regulations*, 1981, Title 2, Part 444.20a.
6 G. Wagman, J. Marquez, J. Bailey, D. Cooper, J. Weinstein, R. Tkach and P. Daniels, *J. Chromatogr.*, 70 (1972) 171–173.
7 W. Wilson, G. Richard and D. Hughes, *J. Pharm. Sci.*, 62 (1973) 282–284.
8 W. Wilson, G. Richard and D. Hughes, *J. Chromatogr.*, 78 (1973) 442–444.
9 H. Maehr and C. Shaffner, *J. Chromatogr.*, 30 (1967) 572–578.
10 A. Thomas and S. Tappin, *J. Chromatogr.*, 97 (1974) 280–283.
11 J. Anhalt, *Antimicrob. Agents Chemother.*, 11 (1977) 651–655.
12 J. Anhalt, F. Sancilio and T. McCorkle, *J. Chromatogr.*, 153 (1978) 489–493.
13 S. Maitra, T. Yoshikawa, J. Hansen, I. Nilsson-Ehle, W. Palin, M. Schotz and L. Guze, *Clin. Chem.*, 23 (1977) 2275–2278.
14 G. Peng, M. Gadalla, A. Peng, V. Smith and W. Chiou, *Clin. Chem.*, 23 (1977) 1838–1844.
15 J. D'Souza and R. Ogilvie, *J. Chromatogr.*, 232 (1982) 212–218.
16 J. Marples and M.Oates, *J. Antimicrob. Chemother.*, 10 (1982) 311–318.
17 L. White, A. Lovering and D. Reeves, *Ther. Drug Monit.*, 5 (1983) 123–126.
18 P. Claes, R. Busson and H. Vanderhaeghe, *J. Chromatogr.*, 298 (1984) 445–457.
19 P. Gambardella, R. Punziano, M. Gionti, C. Guadalupi, G. Mancini and A. Mangia, *J. Chromatogr.*, 348 (1985) 229–240.
20 J. Lacy, R. Parfitt and M. Rowan, *Int. J. Pharm.*, 43 (1988) 111–117.
21 G. Seidl and H. Nerad, *Chromatographia*, 25 (1988) 169–171.
22 G., Inchauspé and D. Samain, *J. Chromatogr.*, 303 (1984) 277–282.
23 D. Samain, P. Dupin, P. Debrieu and G. Inchauspé, *Chromatographia*, 24 (1978) 748–752.
24 T. Getek, A. Haneke and G. Selzer, *J. Assoc. Off. Anal. Chem.*, 66 (1983) 172.
25 B. Rosenkranz, J. Greco, J. Hoogerheide and E. Oden, *Analytical Profiles of Drug Substances*, Vol. 9, Academic Press, New York, 1980, p. 295.
26 R. Parfitt, D. Games, M. Rossiter, M. Rogers and A. Weston, *Biomed. Environ. Mass Spec.*, 3 (1976) 232.
27 N. Takeda, K. Harada, M. Suzuki, A. Tatematsu and T. Kubodera, *Org. Mass Spectrom.*, 17 (1982) 247.
28 G. Inchauspé, C. Deshayes and D. Samain, *J. Antibiotics*, 38 (1985) 1526–1535.
29 A. Khan, S. Badar, E. Allen and E. Sokoloski, *Biomed. Environ. Mass Spectrom.*, 17 (1988) 3209.
30 M. Sakairi and H. Kambara, *Anal. Chem.*, 60 (1988) 774.
31 T. Getek and T. Alexander, presented at the *34th Annual Conference on Mass Spectrometry and Allied Topics, Cincinnati, OH, June 8–13, 1986.*
32 T. Getek, W. Korfmacher and J. Freeman, presented at the *36th Annual Conference on Mass Spectrometry and Allied Topics, San Francisco, CA, June 5–10, 1988.*
33 R. Weigand and R. Coombes, *J. Chromatogr.*, 281 (1983) 381–385.
34 A. Thomas, *J. Pharm. Biomed. Anal.*, 5 (1987) 319.
35 *United States Pharmacopeia*, Supplement 4 United States Pharmacopeial Convention, Rockville, MD, 1986, p. 2169.

Journal of Chromatography, 554 (1991) 205–214
Elsevier Science Publishers B.V., Amsterdam

CHROMSYMP. 2350

Liquid chromatography–thermospray tandem mass spectrometry for identification of a heptabarbital metabolite and sample work-up artefacts

C. E. M. HEEREMANS

Division of Analytical Chemistry, Center for Bio-Pharmaceutical Sciences, University of Leiden, P.O. Box 9502, 2300 RA Leiden (Netherlands)

A. M. STIJNEN

Division of Pharmacology, Center for Bio-Pharmaceutical Sciences, University of Leiden, P.O. Box 9503, 2300 RA Leiden (Netherlands)

R. A. M. VAN DER HOEVEN and W. M. A. NIESSEN*

Division of Analytical Chemistry, Center for Bio-Pharmaceutical Sciences, University of Leiden, P.O. Box 9502, 2300 RA Leiden (Netherlands)

M. DANHOF

Division of Pharmacology, Center for Bio-Pharmaceutical Sciences, University of Leiden, P.O. Box 9503, 2300 RA Leiden (Netherlands)

and

J. VAN DER GREEF

Division of Analytical Chemistry, Center for Bio-Pharmaceutical Sciences, University of Leiden, P.O. Box 9502, 2300 RA Leiden (Netherlands)

ABSTRACT

An unknown heptabarbital metabolite, observed in the liquid chromatogram of rat plasma and urine samples after administration of heptabarbital, was identified by liquid chromatography–thermospray tandem mass spectrometry. By applying the parent scan mode for screening and the daughter scan mode for structure elucidation, the metabolite was determined to be 5-ethyl-5-(1′-, 3′- or 6′-cycloheptadienyl)barbituric acid. It was demonstrated that artefact formation occurred when hydrochloric acid was used for conjugate hydrolysis in the sample clean-up. Identification of the artefacts was achieved by the same method. Confirmation of the structures of the metabolite and the artefacts was obtained by gas chromatography–electron impact mass spectrometry.

INTRODUCTION

Sensitivity to various drugs is dependent on the (patho)physiological status of the individual (*e.g.*, diseases, age, pregnancy). Owing to alterations in the physiological status, the pharmacokinetics or the pharmacodynamics of drugs can be influenced. In our Centre, heptabarbital [5-ethyl-5-(1′-cycloheptenyl)barbituric acid] is used as a model substrate for the investigation of these effects [1–5].

0021-9673/91/$03.50

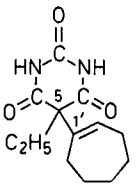

Heptabarbital (mol.wt. 250)

During pharmacological studies, a peak was observed on liquid chromatography (LC) with UV detection of a rat plasma sample after administration of heptabarbital [5], which followed the concentration–time profile of a metabolite but did not correspond to one of the known metabolites. Gilbert *et al.* [6] studied the metabolism of heptabarbital in humans and found three possible metabolites: 3′-hydroxyheptabarbital, 3′-ketoheptabarbital and 7′-hydroxyheptabarbital. Vermeulen [7] investigated the metabolic pathway of heptabarbital in male Wistar rats and identified 5-ethylbarbituric acid in the urine, which was suggested to be formed via an epoxide–diol pathway.

This paper describes the elucidation of the structure of the unknown metabolite in rat urine and plasma, employing coupled liquid chromatography (LC)–tandem mass spectrometry (MS–MS) with thermospray (TSP) ionization. The parent scan mode was used as a specific screening method for heptabarbital-related compounds, both metabolites and artefacts of hydrochloric acid hydrolysis, whereas structural information of the protonated compounds was obtained in the daughter scan mode.

The results from the LC–TSP-MS–MS experiments are compared with those obtained by gas chromatography–electron impact (EI) mass spectrometry (GC–MS) and solid-probe high-resolution (HR) measurements, which are techniques commonly used in the analysis of barbiturates.

EXPERIMENTAL

Sample clean-up and fraction collection

Urine: clean-up method 1. After addition of 1 ml of 36% hydrochloric acid to 1 ml of urine sample, the mixture was heated on a water-bath at 100°C for 30 min in order to hydrolyse possible conjugates. After cooling the mixture, 1.5 ml of saturated sodium chloride solution and 1 ml of distilled water were added. The mixture was extracted twice with 5 ml of diethyl ether. The combined ether extracts were evaporated to dryness under a stream of nitrogen.

Urine: clean-up method 2. A 7.5-ml volume of distilled water, 12.5 ml of saturated sodium chloride solution and 2.5 ml of 1.6 *M* phosphate buffer (pH 5.5) were added to a 5-ml urine sample and the mixture was extracted twice with 50 ml of diethyl ether. The combined ether extracts were evaporated to dryness under a stream of nitrogen.

Plasma. To 1 ml of plasma, 5 ml of acetonitrile were added to precipitate proteins. After thorough mixing and centrifugation, the supernatant was evaporated to dryness.

Fraction collection of the peak of interest. The dried samples were dissolved in 400 μl of mobile phase and 200 μl were injected into the LC system as described by

Danhof and Levy [8]. The metabolite fraction was collected and evaporated to dryness. The collected fractions from several animals were combined in order to obtain high concentrations of the compound. The total procedure was also applied to urine samples collected before the administration of heptabarbital, providing the blanks.

Liquid chromatography–mass spectrometry and tandem mass spectrometry

The LC system used for the LC–TSP-MS–MS experiments consisted of a Model 2150 high-pressure pump (LKB, Bromma, Sweden), a Model 7125 injection valve equipped with a 20-μl loop (Rheodyne, Berkeley, CA, USA) and a 150 × 3 mm I.D. Nucleosil C_{18} (5 μm) column (Macherey-Nagel, Düren, Germany).

LC–MS and LC–MS–MS experiments were performed using a Finnigan MAT (San José, CA, USA) TSQ 70 triple quadrupole MS–MS system equipped with a Finnigan MAT TSP interface.

In the buffer ionization mode the mobile phase consisted of 50 mmol/l ammonium acetate in methanol–water (50:50, v/v), whereas in the discharge-on mode methanol–water (50:50, v/v) was used, at a flow-rate of 1.2 ml/min. The discharge potential was 1000 V. The vaporizer temperature and the repeller potential were optimized [9], while the block temperature was kept at 200°C. In the daughter and parent scan MS–MS experiments the collision energy and pressure were optimized; air was used as the collision gas.

Gas chromatography–mass spectrometry

GC–MS was performed on a Finnigan MAT Model 700 ion trap detector, combined with a Model 438A gas chromatograph (Chrompack Packard, Middelburg, Netherlands) equipped with a split injector (splitting ratio 1:40) and a 10 m × 0.25 mm I.D. CP-Sil-5 column (Chrompack). The oven temperature was kept at 50°C for 5 min and subsequently increased linearly to 250°C at 15°C/min. EI mass spectra were obtained at 1 s per scan.

High-resolution electron impact mass spectrometry

Solid-probe high-resolution (R = 15000) EI-MS was performed on a Varian MAT 711 double-focusing mass spectrometer (Varian, Bremen, Germany).

RESULTS AND DISCUSSION

Because the concentration of the compound of interest is much higher in urine, identification is performed on rat urine samples. Acidic hydrolysis using 36% hydrochloric acid is applied, because the metabolite is expected to be a hydroxyheptabarbital, which will be conjugated before excretion into urine. GC–MS with EI ionization is a commonly used technique for the analysis of barbiturates. However, because an LC peak has to be identified, LC–MS is preferred, with direct coupling of the LC system to the mass spectrometer by a TSP interface. Moreover, urine samples contain too many involatile compounds for GC–MS analysis, necessitating extensive sample pretreatment.

Optimization of the thermospray (tandem) mass spectrometry conditions

In TSP-MS three different ionization modes, namely buffer ionization, dis-

charge-on and filament-on ionization, can be used. As the sensitivity for various classes of compounds can differ dramatically between these modes, a careful choice is important. In this study, buffer and discharge-on ionization were compared. Other experimental parameters that have to be optimized are the vaporizer temperature and the repeller potential [9,10]. This optimization is performed by injecting heptabarbital (mol.wt. 250) in the column bypass mode, assuming that heptabarbital metabolites will be ionized in the same way as the parent compound owing to structural similarities. The vaporizer temperature appears not to be critical for heptabarbital because no thermal degradation is observed in the normally used temperature range of 80–120°C.

The repeller potential not only can be used to improve sensitivity in TSP-MS, but can also induce useful fragmentation reactions in the discharge-on mode [9–12]. In the buffer ionization mode for heptabarbital an intense ammoniated molecule, $[M + NH_4]^+$, at m/z 268 and a weak protonated molecule, $[M + H]^+$, at $m/z = 251$ are observed at low repeller potentials. With increasing repeller potential the intensity of the ammoniated molecule (m/z 268) decreases, whereas the intensity of the protonated molecule (m/z 251) increases. However, the overall sensitivity decreases with increasing repeller potential, as is usually observed in the buffer ionization mode. Surprisingly, a fragment peak at m/z 157, due to the loss of cycloheptadiene, also appears with increasing intensity at higher repeller potentials. Fragmentation is not often observed in the buffer ionization mode [9,10]. In the discharge-on mode, fragmentation of the protonated molecule is induced at high repeller potentials without a loss of sensitivity [11,12]. Two fragment ion peaks are observed at m/z 157 and 221, explained as the result of the loss of either cycloheptadiene or ethane.

When these two ionization modes are compared, a tenfold higher signal for the protonated molecule is observed in the discharge-on mode at low repeller potentials compared with the buffer ionization mode. Because a high intensity of the protonated molecule is preferred for the detection of unknown compounds and for MS–MS analysis, further experiments were performed in the discharge-on mode at low repeller potentials. Further, the formation of ammoniated species with buffer ionization is a disadvantage, because molecular weight determinations of unknown compounds can be ambiguous when it is not clear whether only protonated species or ammoniated species also are present in the spectrum.

The possibilities of applying MS–MS in combination with LC–TSP-MS were also investigated, because of the higher selectivities that can be achieved. Further, in the daughter scan mode, structural information can be obtained from the protonated molecules observed in LC–TSP-MS.

In the daughter scan mode the protonated molecule of heptabarbital (m/z 251) is dissociated to a fragment at m/z 157, due to the loss of cycloheptadiene (Fig. 1). The fragment at m/z 95 corresponds to protonated cycloheptadiene.

LC–TSP-MS of urine samples (clean-up method 1)

LC–MS of a pretreated urine sample does not give any useful information, as no distinct differences between the urine sample and the blank sample are observed. This is probably due to the presence of non-UV-absorbing interfering compounds from the urine.

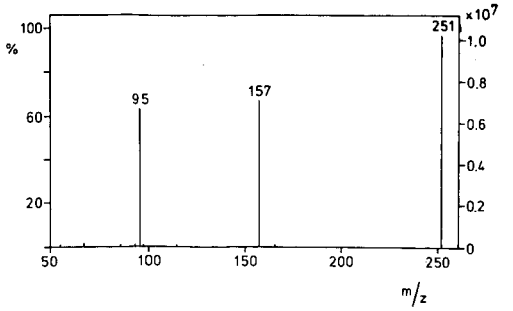

Fig. 1. Daughter-ion mass spectrum of the protonated molecule of heptabarbital (mol.wt. 250).

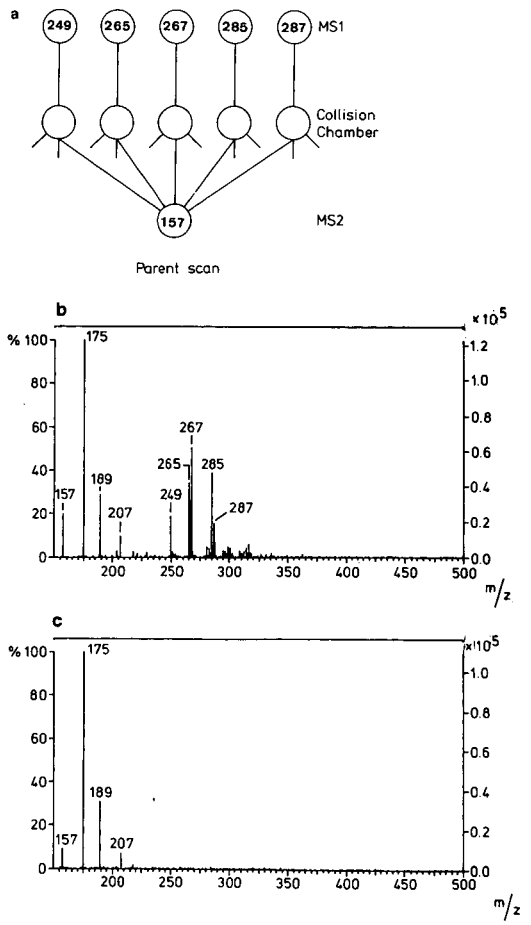

Fig. 2. (a) Parent m/z 157 scan mode; (b) parent m/z 157 mass spectrum of the collected fraction of the rat urine sample (clean-up method 1); (c) parent m/z 157 mass spectrum of a blank urine sample (clean-up method 1).

LC–TSP-MS of the collected fraction (clean-up method 1)

Off-line fraction collection of the chromatographic peak of interest, corresponding to the unknown metabolite, from the urine sample and the blank was performed using the LC system developed by Danhof and Levy [8]. The TSP mass spectrum of the collected fraction from the urine sample contains several peaks, *e.g.*, at *m/z* 249, 265, 267, 283 and 301, that are not present in the TSP mass spectrum of blank urine. It appears that the peak of interest probably consists of a number of compounds.

TSP-MS–MS of collected fraction of urine samples (clean-up method 1)

Because the metabolic reactions are expected to occur in the cycloheptenyl group [6,7], a daughter ion at *m/z* 157, obtained by loss of a cycloheptadiene from heptabarbital, is also expected to be formed by collision-induced dissociation (CID) in the MS–MS mode for heptabarbital metabolites. In order to screen for heptabarbital metabolites in the collected fraction of the rat urine, a parent *m/z* 157 scan (Fig. 2a) was performed in the column bypass mode. Peaks at *m/z* 249, 265, 267, 285 and 287 are observed in the parent *m/z* 157 mass spectrum of the urine sample that are not observed for the blank (Fig. 2b and c). These peaks are expected to be protonated molecules of heptabarbital-related compounds.

Subsequently, daughter-ion spectra of the above mentioned peaks were obtained and identification of the compounds was achieved (Table I). The compound with a molecular weight of 248 has an additional double bond in the cycloheptenyl group (see R_2 in Table I). The daughter-ion spectrum (Fig. 3a) shows a fragment at

TABLE I

STRUCTURES OF THE SAMPLE WORK-UP ARTEFACTS OF HEPTABARBITAL OBSERVED IN THE PARENT *m/z* 157 MASS SPECTRUM OF A RAT URINE SAMPLE AFTER CLEAN-UP METHOD 1

$[M+H]^+$ *m/z*	Structure
251 heptabarbital	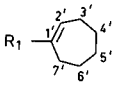
249	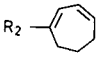
265	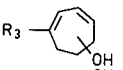
267	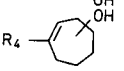
285	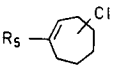
301	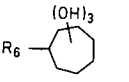

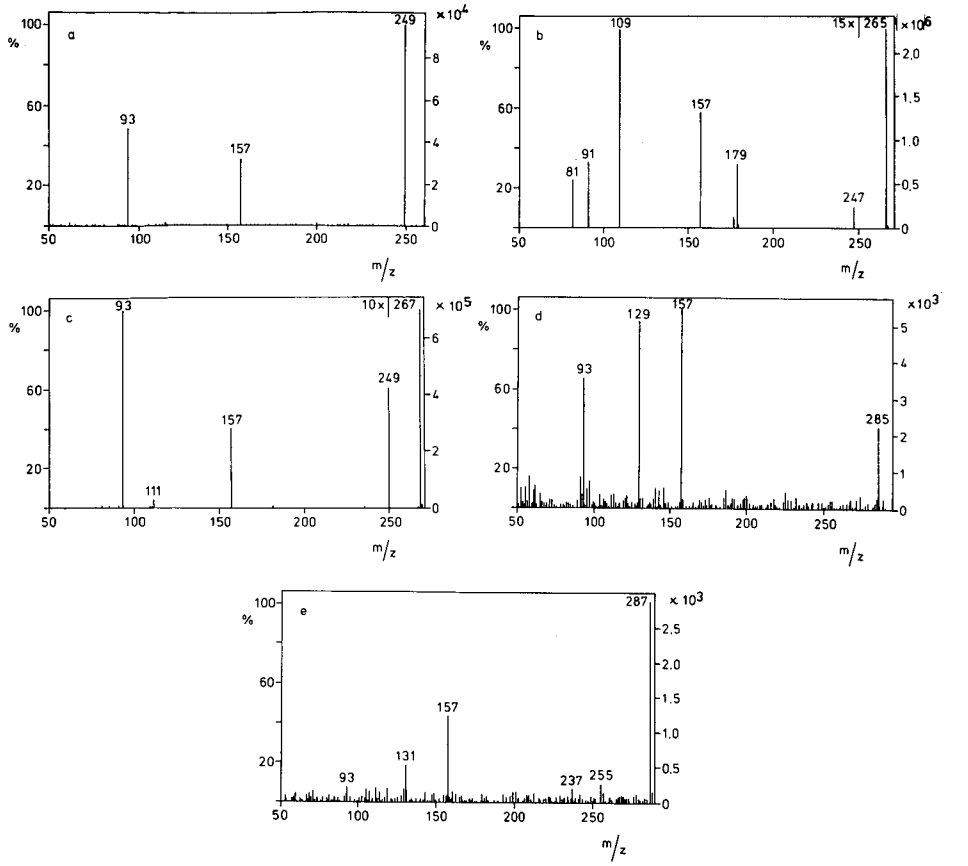

Fig. 3. Daughter-ion mass spectrum of the various protonated molecules observed in the parent *m/z* 157 mass spectrum of the urine sample. (a) *m/z* 249; (b) *m/z* 265; (c) *m/z* 267; (d) *m/z* 285; (e) *m/z* 287.

m/z 93 for protonated cycloheptatriene, while the daughter-ion spectrum of heptabarbital (mol.wt. 250) shows a fragment at *m/z* 95 for protonated cycloheptadiene (R_1).

The daugther-ion spectra of *m/z* = 265 and 267 (Fig. 3b and c, respectively) show similarities.

The compound corresponding to a protonated molecule at *m/z* 267 has a hydroxy group in the cycloheptenyl moiety (R_4). Loss of water from the protonated molecule and the abstracted protonated ring at *m/z* 111 results in fragments at *m/z* 249 and 93, respectively.

The compound corresponding to a protonated molecule at *m/z* 265 has an additional double bond and a hydroxy group in the cycloheptenyl group (R_3). Loss of water from the protonated molecule and the abstracted protonated ring (*m/z* 109) results in similar fragments at *m/z* 247 and 91. The daughter at *m/z* 179 is probably formed by loss of 2 HNCO.

The daughter-ion spectrum of *m/z* 285 (Fig. 3d) is not easily interpreted. Fragments are observed at *m/z* 129 and 93. The fragment at *m/z* 93 is likely to be protonat-

ed cycloheptatriene, as observed for the compounds corresponding with the protonated molecules at *m/z* 249 and 265. The ions at *m/z* 129 and 93 show a mass difference of 36 u, which might correspond to the loss of HCl from *m/z* 129. In the parent *m/z* 157 spectrum an isotope peak of *m/z* 285 is observed at *m/z* 287 with a 3:1 ratio, respectively, suggesting the presence of chlorine.

The daughter-ion spectrum of *m/z* 287 (Fig. 3e) proves the presence of a chlorine in the cycloheptenyl group. Fragments are observed at *m/z* 131 and 93 with a mass difference of 38 u, corresponding to the loss of $H^{37}Cl$.

In addition, the compounds with molecular weights of 282 and 300, observed in LC–MS, can be explained by the addition of one and two water molecules, respectively, at the double bonds in the cycloheptadienyl group of the compound with a molecular weight of 264 u. However, these compounds are not intensely observed in the parent *m/z* 157 scan, although a daughter-ion spectrum of *m/z* 301 shows a fragment at *m/z* 157.

It is not likely that the identified compounds given in Table I are eluted in the same region of the liquid chromatogram. Probably the hydroxy-containing components are formed in the ion source by addition of water to the double bonds (see below).

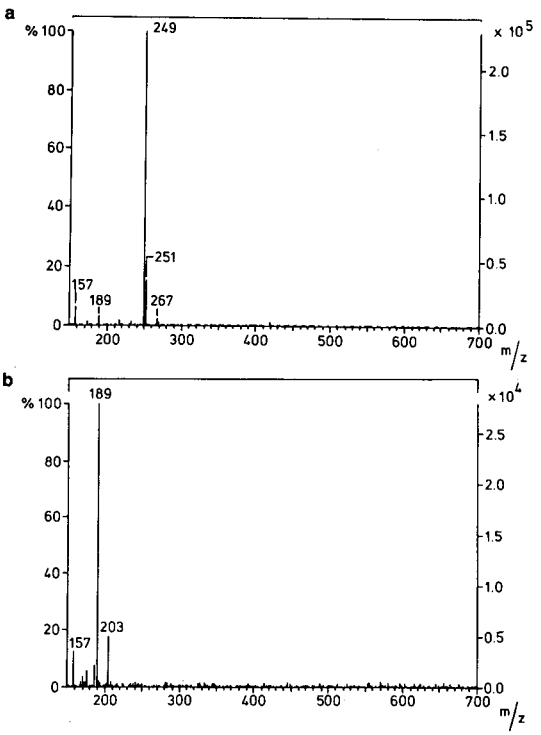

Fig. 4. (a) Parent *m/z* 157 mass spectrum of the collected fraction of the rat urine sample (clean-up method 2); (b) parent *m/z* 157 mass spectrum of a blank urine sample (clean-up method 2).

TSP-MS–MS of collected fraction (clean-up method 2)

Chlorinated compounds are not expected to be formed in metabolic reactions. Therefore, the sample clean-up (method 1), using hydrochloric acid for the hydrolysis of conjugated metabolites, was changed. Boiling with hydrochloric acid apparently introduces artefacts. When sample clean-up method 2 was used, the unknown peak was still observed in the liquid chromatogram obtained with UV detection. After fraction collection of the peak of interest, a parent *m/z* 157 scan was performed on the urine sample and also on a blank in the column bypass mode (Fig. 4). The peak at *m/z* 249 is the base peak of the spectrum of the urine sample. The structure of this protonated molecule is confirmed in the daughter scan mode to be heptabarbital with an additional double bond, probably conjugated (at the 3′- or 6′-position) with the other double bond at the 1′-position [5-ethyl-5-(1′-, 3′- or 6′-cycloheptadienyl)barbturic acid].

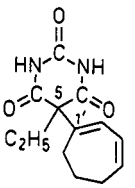

5-ethyl-5-(1′-, 3′- or 6′-cycloheptadienyl)barbituric acid (mol.wt. 248)

The daughter-ion spectrum of *m/z* 249 is in agreement with the former experiments, showing fragments at *m/z* 93 and 157. The small peak in the parent *m/z* 157 spectrum at *m/z* 267 might be due to the addition of water to a double bond in the cycloheptadienyl group of the metabolite, probably occurring in the ion source. The daughter-ion spectrum of *m/z* 267 also corresponds with the previously obtained spectrum, showing daughter-ions at *m/z* 111 and 93.

TSP-MS–MS of collected fraction of plasma samples (clean-up method 2)

A parent *m/z* 157 scan was also performed on the collected fraction of a plasma sample in which the concentration of the unknown compound was much lower, and on a blank. The plasma sample contained the metabolite (mol.wt. 248) with the additional double bond in the cycloheptenyl group [5-ethyl-5-[1′-, 3′- or 6′-cycloheptadienyl)barbituric acid].

Metabolic pathway

A possible mechanism for the formation of the metabolite is a hydroxylation to 3′-, 4′-, 6′- or 7′-hydroxyheptabarbital, followed by a dehydration step. The pharmacological behaviour of this metabolite is discussed elsewhere [13].

GC–MS of collected fractions combined with high-resolution MS

GC–EI-MS is generally used in the analysis of barbiturates. The EI fragmentation is relatively well understood [14]. After fraction collection the samples are much cleaner and the amount of non-volatile materials is greatly reduced. For these reasons, GC–MS analysis of the collected fractions was performed.

The GC–MS data confirmed the results from the LC–TSP-MS and -MS–MS studies. However, the identification was hampered by the absence of molecular ions in barbiturate EI mass spectra. After clean-up method 1 the compounds with R_2 and R_5 were observed. These data confirm that the hydroxy-containing compounds (R_3, R_4 and R_6 in Table I) are artefacts from the TSP ionization process. The presence of the chlorine atom in R_5 was confirmed by solid-probe HR-MS. After clean-up method 2, the compound with R_2 was observed, which is in agreement with the TSP-MS–MS data. The clean-up method with hydrochloric acid hydrolysis is responsible for the presence of the compound with the chlorinated cycloheptenyl group (R_5).

CONCLUSIONS

Using a combination of TSP-MS–MS in the parent and daughter scan modes, the unknown metabolite observed in rat plasma and urine samples after administration of heptabarbital was determined to be 5-ethyl-5-(1′-, 3′- or 6′-cycloheptadienyl)barbituric acid. It has been demonstrated that acidic hydrolysis with 36% hydrochloric acid can introduce artefacts. The identity of the metabolite and the sample work-up artefacts was confirmed by GC–EI-MS, but not as straightforwardly as with TSP-MS–MS.

REFERENCES

1 J. Dingemanse, M. Polhuijs and M. Danhof, *J. Pharmacol. Exp. Ther.*, 246 (1988) 371.
2 J. W. Mandema and M. Danhof, *J. Pharmacokinet. Biopharm.*, 18 (1990) 459.
3 A. M. Stijnen, S. H. van der Voort, C. F. A. van Bezooijen and M. Danhof, in K. W. Woodhouse, C. Yelland and O. F. W. James (Editors), *The Liver Metabolism and Ageing*, Eurage, Rijswijk, 1989, p. 57.
4 A. M. Stijnen, A. M. Bergveld, J. W. Mandema, C. F. A. van Bezooijen and M. Danhof, in preparation.
5 J. Dingemanse, D. Thomassen, B. H. Mentink and M. Danhof, *J. Pharm. Pharmacol.*, 40 (1988) 522.
6 J. N. T. Gilbert, B. J. Millard, J. W. Powell and W. B. Whalley, *J. Pharm. Pharmacol.*, 26 (1974) 123.
7 N. P. E. Vermeulen, *Ph.D. Thesis*, University of Leiden, Leiden, 1980, pp. 103–109.
8 M. Danhof and G. Levy, *J. Pharmacol. Exp. Ther.*, 232 (1985) 430.
9 C. E. M. Heeremans, R. A. M. van der Hoeven, W. M. A. Niessen, U. R. Tjaden and J. van der Greef, *J. Chromatogr.*, 474 (1989) 149.
10 C. Lindberg and J. Paulson, *J. Chromatogr.*, 349 (1987) 117.
11 W. H. McFadden and S. A. Lammert, *J. Chromatogr.*, 385 (1987) 201.
12 W. M. A. Niessen, R. A. M. van der Hoeven, M. A. G. de Kraa, C. E. M. Heeremans, U. R. Tjaden and J. van der Greef, *J. Chromatogr.*, 478 (1989) 325.
13 A. M. Stijnen, C. E. M. Heeremans, C. F. A. van Bezooijen, W. M. A. Niessen and M. Danhof, in preparation.
14 B. J. Gudzinowicz and M. J. Gudzinowicz, *Analysis of Drugs and Metabolites by GC/MS*, Vol. 2, Marcel Dekker, New York, 1977, pp. 1–184.

Journal of Chromatography, 554 (1991) 215–226
Elsevier Science Publishers B.V., Amsterdam

CHROMSYMP. 2243

Evaluation of an automated thermospray liquid chromatography–mass spectrometry system for quantitative use in bioanalytical chemistry

CLAES LINDBERG*, JAN PAULSON and ANN BLOMQVIST
Bioanalytical Chemistry, AB Draco (Subsidiary of AB Astra), P.O. Box 34, S-22100 Lund (Sweden)

ABSTRACT

An automated thermospray liquid chromatography–mass spectrometry system is described, including an autosampler and a gradient liquid chromatography system controlled from the mass spectrometer data system. The performance and reliability of the equipment during unattended operation were evaluated by repeated injections of standard solutions of some antiasthmatic drugs, using deuterium-labelled analogues as internal standards. High sensitivity and reproducibility were achieved during a 19-hour run, incorporating gradient elution and a total of 54 injections. The relative standard deviation of the peak area measurement of the internal standards was in the range of 6.5–8.2%. The corticosteroid budesonide can be routinely measured in plasma down to 0.1 nmol/l. Direct injection of a small plasma volume into the thermospray liquid chromatography–mass spectrometry system could be used to monitor drug plasma levels during a toxicity study in dogs.

INTRODUCTION

During the last few years liquid chromatography (LC) combined with thermospray (TSP) mass spectrometry (MS) has been extensively used for the identification of polar and thermally labile compounds of biomedical interest [1–5]. The technique has been less widely used for quantitative analysis, possibly because careful optimization of thermospray conditions is necessary to obtain high sensitivity and reproducibility [1,6–10]. Early applications of LC–TSP-MS demonstrated it to be potentially useful as a quantitative technique [11], and during recent years a number of quantitative or semi quantitative bioanalytical methods of various degrees of sophistication have been published [12–34]. Reports on more thoroughly validated methods, however, are scarce, and LC–TSP-MS does not seem to have found wide acceptance as a routine technique for the determination of drugs in biological fluids.

There are several attractive features of LC–TSP-MS which make it an interesting bioanalytical technique. The sensitivity, although widely varying for different compounds, is in many cases excellent, permitting measurement in the low nmol/l range. LC affords mild conditions for the separation of polar compounds, thereby reducing the risk of artefact formation. The high selectivity of the mass spectrometer generally allows simple sample clean-up procedures to be used. In addition, short

0021-9673/91/$03.50

chromatographic columns often give adequate separation, leading to short analysis time. LC–TSP-MS is a reliable and robust technique which has been shown to be useful for routine drug analysis using automated procedures [18,23,31,34].

This paper describes an automated LC–TSP-MS system, including an autosampler and a gradient LC system controlled from the mass spectrometer data system. The performance and reliability of the equipment during unattended operation were evaluated by repeated injections of standard solutions of some antiasthmatic drugs. Examples of the quantification of drugs in plasma are also given. Deuterium-labelled analogues were used as internal standards in all cases.

EXPERIMENTAL

Chemicals

The prodrug bambuterol and its metabolic hydrolysis products D2439 and terbutaline [35–37], from Draco (Lund, Sweden), were used to test the performance of the LC–MS system. The chemical structures of the compounds are shown in Fig. 3. [$^2H_6$] Terbutaline, [$^2H_6$]D2439, and [$^2H_6$]bambuterol, labelled with deuterium in the *tert.*-butyl group, were used as internal standards. The corticosteroid budesonide [38,39], also from Draco, and its internal standard [$^2H_8$]budesonide were analysed by LC–TSP-MS as the 21-acetyl esters (Fig. 3) after derivatization with a mixture of acetic anhydride and triethylamine [34,40]. Ammonium acetate and acetic acid (Gold Marke quality) were purchased from Aldrich Chemie (Steinheim, Germany) and methanol (HPLC grade) from Rathburn (Walkerburn, UK). Water was purified in a Milli-Q system (Millipore, Molsheim, France).

Instrumentation

A schematic view of the LC–MS instrumentation is given in Fig. 1. Pieces of equipment are identified by letters (A–M) which are referred to in the text. The LC equipment included two LKB 2150 pumps for eluent pumping (B) (Pharmacia LKB, Uppsala, Sweden) controlled by a VAX-based Autochrom M340 program (version 1.13) via a CIM 114 interface (A) (Autochrom, Milford, MA, USA). The solvents were pumped through two SSI Model LP-21 pulse dampers (C) (Scientific Systems, State College, PA, USA) and joined in an LKB mixer (D). The system included three injectors. A Rheodyne Model 7125 injector (E) with a 5-ml loop was used to inject a tuning solution into the mass spectrometer, a Valco Model C6W (F) with a Model A60 air actuator and a 100-μl loop was used for manual sample injection, and a CMA 200 autosampler (G) (Carnegie Medicin, Stockholm, Sweden) was used for automatic sample injection. The LC column was connected to a Rheodyne Model 7000 valve (H), acting as a column-bypass valve, to allow direct injection of samples into the mass spectrometer. A third LKB 2150 pump (I) was included to allow pumping of a make-up solvent, which was added post-column through a 10-μl Lee Visco mixer (J) (The Lee Company, Westbrook, CT, USA). A Waters Model 440 UV detector (K), connected in-line with the mass spectrometer, was used to check the performance of the chromatographic system. Besides the standard safety vent valve (L) (Rheodyne Model 7001) controlled by the mass spectrometer vacuum system, the automated LC–MS system was fitted with a Valco Model C6W valve (M) with a Model A60 air actuator, which allowed switching of the chromatographic front to waste. The MS

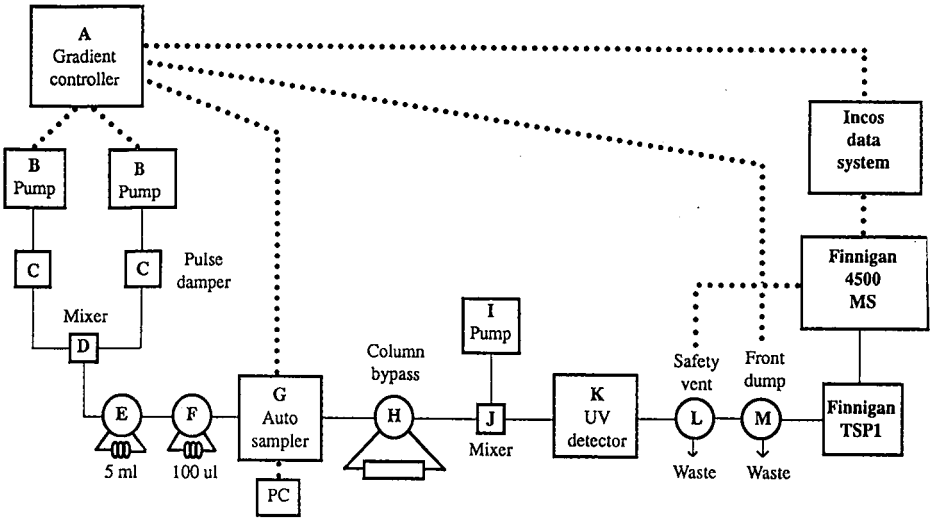

Fig. 1. Schematic view of the automated LC–TSP-MS system. Pieces of equipment labelled with letters A–M are described in the text. Dotted lines: control lines; solid lines: fluid lines.

equipment consisted of a Finnigan 4500 quadrupole instrument (Finnigan MAT, San José, CA, USA) equipped with a Finnigan thermospray interface (TSP1) and an Incos data system (SuperIncos revision 6.5 software). User-defined Incos procedures were used to start the acquisition, each sample being acquired into a separate file, and to send a start pulse to the gradient controller (A). Besides control of the LC pumps, the gradient controller was used to control the autosampler (G) and the front dump valve (M). The work described in this paper was performed with vaporizers, the tips of which had to be manually crimped to achieve satisfactory spray performance.

To delay contamination of the repeller surface and to ensure reproducible positioning in the source block, the thermospray ion source repeller was modified as shown in Fig. 2. The stainless-steel electrode, insulated with a polyimide sleeve, was

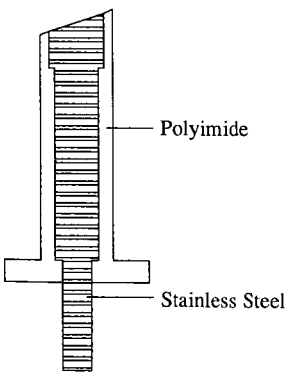

Fig. 2. Thermospray repeller electrode.

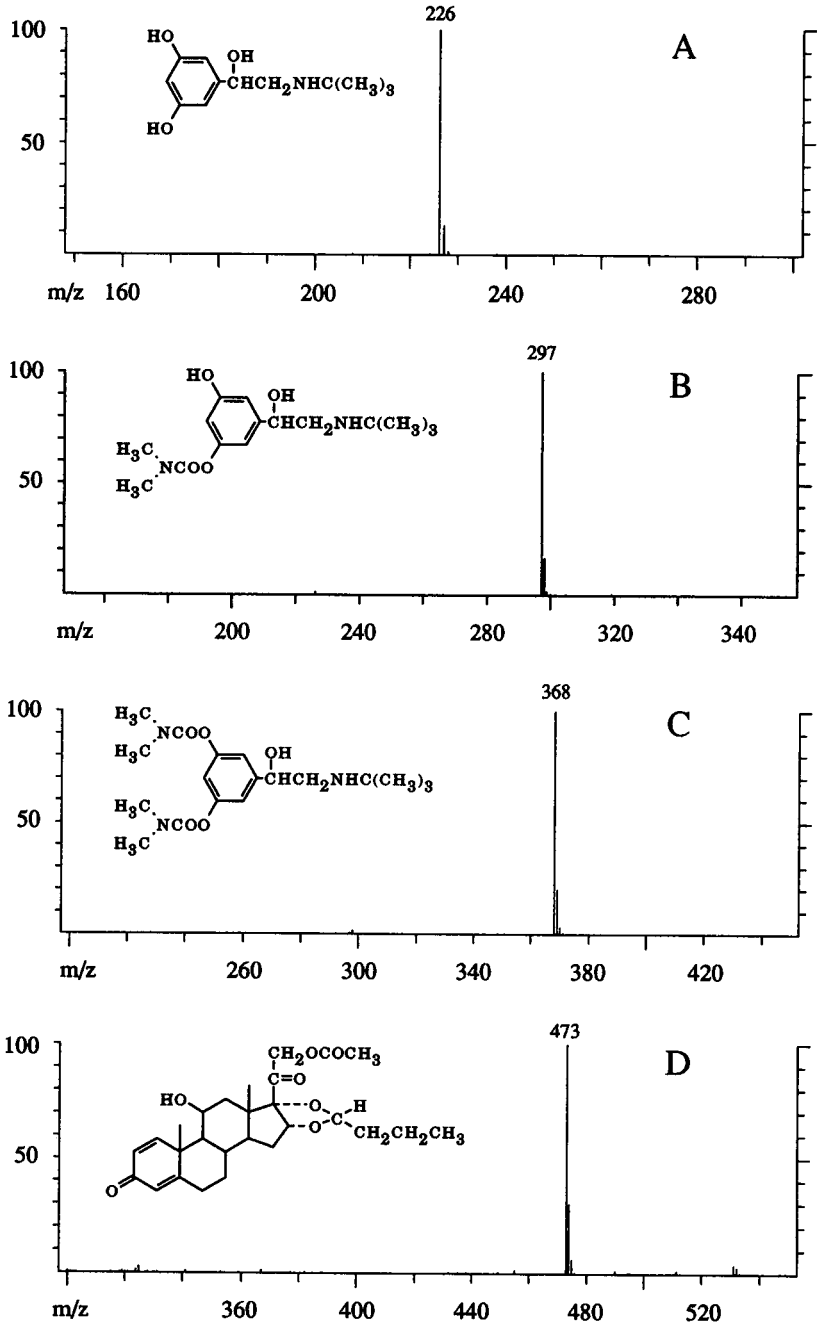

Fig. 3. Thermospray mass spectra and chemical structures of (A) terbutaline, (B) D2439, (C) bambuterol and (D) budesonide 21-acetate.

placed in the source block with the tip of the repeller facing the incoming vapor stream at an angle of about 30°. The exhaust line of the thermospray source was evacuated with a Rietschle CLF26 mechanical pump. Solvent vapor was trapped in a Savant RT490 refrigerated trap (Savant Instruments, Farmingdale, NY, USA), equipped with a 4-l flask kept at −90°C. To provide prolonged LC–MS operation, the inlet tube of the flask was shortened, allowing *ca.* 2000 ml of solvent to be trapped. During thermospray operation the analyzer pressure was $3.5 \cdot 10^{-5}$ Torr, the manifold forepressure 0.20 Torr, and the exhaust line pressure 1.1 Torr. Thermospray mass spectra of terbutaline, D2439, bambuterol, and budesonide 21-acetate are shown in Fig. 3. For quantitative analysis the $[M+H]^+$ ions of the compounds studied plus their deuterated internal standards were monitored, one pair at a time. The instrument was scanned in the selected-ion monitoring mode over a 0.5-a.m.u. window for each mass. The scan time was 400 ms for budesonide 21-acetate and 200 ms for the other compounds.

Liquid chromatography

Terbutaline, D2439 and bambuterol were chromatographed on a 50 × 4 mm LiChrospher RP-select B (5 μm) cartridge (E. Merck, Darmstadt, Germany) fitted with a 4 × 4 mm LiChrosorb RP-select B precolumn. The compounds were eluted during a 13-min gradient running from 3% up to 38% methanol in 0.1 *M* ammonium acetate buffer, pH 5, at a flow-rate of 1.40 ml/min. Budesonide 21-acetate was chromatographed on a 33 × 4.6 mm Supelcosil LC-8-DB (3 μm) cartridge fitted with a 10 × 3 mm Chromguard R precolumn. The mobile phase was 64% methanol in 0.1 *M* ammonium acetate buffer, pH 5, pumped at a flow-rate of 1.40 ml/min. Since it was difficult to crimp the vaporizer tip in a perfectly reproducible manner, the flow-rate of the make-up solvent (0.1 *M* ammonium acetate buffer, pH 5) was adjusted (0–0.20 ml/min) for each vaporizer to achieve optimum flow conditions. The mobile phases were filtered through a 0.22-μm Durapore filter (Millipore) before use and continuously degassed with helium during LC–MS operation.

Calibration and optimization

Mass calibration was performed with a polyethylene glycol (PEG) mixture (PEG200, PEG300, and PEG600, 2:1:1) dissolved in 30% methanol in 0.1 *M* ammonium acetate buffer, pH 5, at a concentration of about 0.1%. At a source block temperature of 220°C and a repeller voltage of 45 V this mixture produced $[M+NH_4]^+$ ions of PEG oligomers of relatively equal intensity over the mass range 150–1000. To achieve maximum sensitivity for target compound analysis the mass spectrometer was tuned by injecting 2–5 ml (from valve E) of a drug solution (1–5 μmol/l in mobile phase) with valve H in the column-bypass mode. In this way a stable flow of analyte into the ion source was achieved for a couple of minutes. Besides the "normal" adjustment of the lenses and the quadrupole parameters it was essential to optimize the vaporizer temperature, the time constant for the vaporizer temperature controller, and the repeller potential. Optimization of the last two parameters was facilitated by modifications of the wiring so that the potentiometers could be adjusted from outside the TSP1 electronics control module. The optimum repeller potential was found in the range 20–60 V, depending on the contamination of the repeller. Terbutaline, D2439 and bambuterol were analyzed at a vaporizer temperature of

115°C and a jet temperature of 200°C, giving an indicated aerosol temperature of about 270°C. Budesonide 21-acetate was analyzed with the vaporizer at 105°C and the jet block at 180°C, giving an aerosol temperature of about 220°C.

RESULTS AND DISCUSSION

Band-broadening effects

The equipment connected between the injector and the mass spectrometer may cause significant extracolumn effects, seriously affecting the chromatographic efficiency, unless the system is well-plumbed and the dead volumes kept to a minimum. The number of theoretical plates, measured from the UV response of terbutaline with the UV detector connected directly to the analytical column, was 2000. This figure decreased to 1900 when the UV detector was connected in the system as shown in Fig. 1. A further decrease to 1800 theoretical plates was noted when the chromatographic efficiency was determined for terbutaline by LC–TSP-MS. A similar investigation with budesonide 21-acetate gave an estimate of 2000 theoretical plates when the mass spectrometer was used as the detector compared with 2200 plates using the UV detector. The mass chromatograms showed somewhat increased tailing, possibly as a result of adsorption of the compounds onto the walls of the ion source [18]. The results obtained for both terbutaline and budesonide, using columns with 2000 theoretical plates, showed that only about 10% of the chromatographic efficiency was lost in the thermospray interface.

Optimization

Optimization of operating conditions is important to obtain high sensitivity in LC–TSP-MS and should be performed with the target compound for quantitative analysis [7]. As observed by others [18] the vaporizer temperature and the repeller potential could not be set for maximum signal intensity, because this resulted in a flickering response. A compromise between intensity and stability had to be found, giving the best signal-to-noise ratio for the chromatographic peak. Trimming of the time constant for the vaporizer temperature controller also had a profound effect on signal stability. Once optimal conditions had been established the system proved to be very stable and did not require retuning over a period of several weeks. Efficient pulse dampers were used, and essentially no pump pulsation could be measured after the LC column. We feel that imperfections in the heating of the vaporizer [9] are the major source of signal instability in the system described, rather than pump pulsation. During high-pressure gradient mixing the built-in pulse compensation of the LKB 2150 pumps cannot be used.

Reliability test of the LC–MS system

The stability and reliability of the automated LC–TSP-MS system was tested by repeated injections of aqueous standard solutions containing a mixture of terbutaline, D2439 and bambuterol at equal concentrations, together with their deuterated internal standards. The standard curve comprised six standard concentrations, covering the range 1–32 pmol expressed as amount injected. The amount injected of each of the internal standards was 10 pmol. Fig. 4 shows a chromatogram of a 4-pmol sample together with a profile of the methanol content of the gradient used. The six

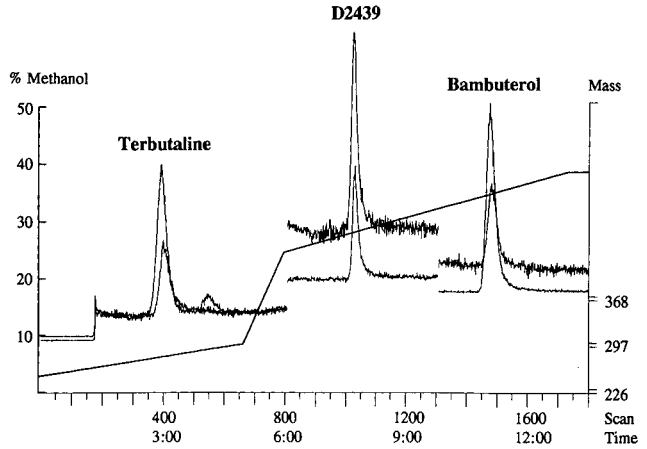

Fig. 4. Thermospray mass chromatogram of a 4-pmol standard solution containing terbutaline, D2439, and bambuterol. The amount of each of the internal standards was 10 pmol. The solid line shows the methanol content of the mobile phase during the gradient elution. Time in min.

standard samples were injected from low to high concentration, the series being repeated nine times, giving a total of 54 injections and a total run time of 19 h. Fig. 5 shows a plot of the measured peak areas of the internal standards *versus* injection number. The slopes of the regression lines were positive for all three compounds, indicating an increase in mass spectrometer response during the experimental period. Contamination of the ion source, leading to decreased thermospray response, occurred only slowly and, even if high sensitivity was required, the system could be operated daily for a couple of weeks before it was necessary to clean the repeller electrode. The coefficient of variation (C.V.) of the internal standard peak area, calculated on all 54 injections, was 7.9% for [$^2H_6$]terbutaline, 8.2% for [$^2H_6$]D2439, and 6.5 for [$^2H_6$]bambuterol. Calculation of the response factors showed that the internal standards compensated for the drift in mass spectrometer response. The variation of the response factor was 6.6% (C.V.) for terbutaline, 8.5% for D2439, and 9.1% for bambuterol. The calibration curves showed excellent linearity for all three compounds. The correlation coefficient was 0.9986 for terbutaline, 0.9971 for D2439, and 0.9993 for bambuterol. Table I shows the precision of the method at each of the six standard concentrations. The C.V. ranged from 10–14% at the low end of the standard curve to 2–4% at the high end.

In the study described above the vaporizer temperature was optimized for a mobile phase containing 6% methanol, corresponding to optimal conditions for terbutaline. Ramping of the vaporizer temperature during gradient elution, to compensate for the changing methanol content, could not be accomplished during unattended operation, because the TSP1 controle module does not allow automatic reset and restart of the temperature program. The results, however, show that acceptable sensitivity and reproducibility could be achieved for D2439 and bambuterol as well, in spite of suboptimal conditions for these compounds.

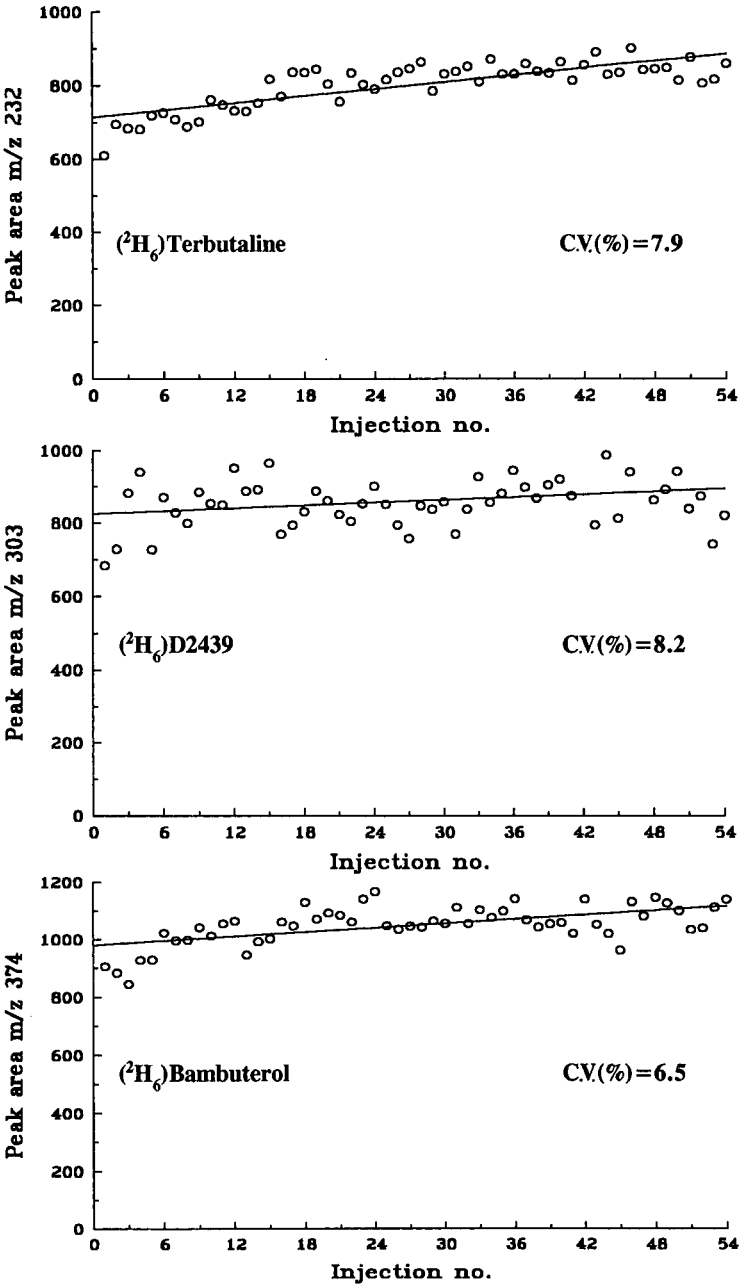

Fig. 5. Measured peak area of the internal standards for terbutaline, D2439, and bambuterol plotted *versus* injection number during the 19-h reliability test of the automated LC–TSP-MS system.

TABLE I

ANALYTICAL PRECISION FOR TERBUTALINE, D2439, AND BAMBUTEROL DURING LONG-TERM (19 h) LC–TSP-MS OPERATION

Compound	Amount injected (pmol)	Area ratio		C.V. (%)	*n*
		Mean	S.D.		
Terbutaline	1	0.1178	0.0114	9.67	9
	2	0.2390	0.0135	5.65	9
	4	0.4843	0.0402	8.30	9
	8	0.9429	0.0576	6.11	9
	16	1.8556	0.0740	3.99	9
	32	3.6781	0.1306	3.55	9
D2439	1	0.1172	0.0117	10.03	9
	2	0.2457	0.0173	7.04	9
	4	0.4977	0.0539	10.83	9
	8	1.0054	0.0753	7.49	9
	16	2.0481	0.1881	9.18	9
	32	4.0747	0.1762	4.32	9
Bambuterol	1	0.0966	0.0138	14.32	9
	2	0.2047	0.0181	8.83	9
	4	0.4360	0.0293	6.72	9
	8	0.8977	0.0281	3.13	9
	16	1.8251	0.0681	3.73	9
	32	3.6201	0.0824	2.28	9

Application to biological samples

LC–TSP-MS can afford elegant solutions to many bioanalytical problems encountered within the pharmaceutical industry. Selected-ion monitoring affords a detection system with high selectivity, making the sample extraction procedure less critical. This will generally facilitate rapid method development, which is important during the early tests of new drug candidates. Later, if the drug candidate is found safe and taken into extended clinical studies, the LC–MS method may be replaced by a simpler and less expensive method. The high selectivity of the mass spectrometer together with the compatibility of the thermospray interface with reversed-phase chromatography, opens the possibility of direct injection of biological samples onto the LC column.

We have used automated LC–TSP-MS for about one year for the determination of budesonide in plasma [34]. The plasma sample is mixed with the internal standard solution ([$^2H_8$]budesonide) and transferred to a conditioned Bond Elut C_{18} column. The column is rinsed in three steps with aqueous ethanol, water, and heptane, and finally eluted with a mixture of ethyl acetate in heptane. The eluate is evaporated to dryness and the residue treated with a mixture of acetic anhydride and triethylamine in acetonitrile to give the 21-acetyl derivative of budesonide. After evaporation of the derivatization reagent the extract is dissolved in mobile phase and injected into the LC–MS system by the CMA 200 autosampler. Batches of about 50 samples are routinely loaded into the autosampler and analyzed overnight. The drug can be measured down to 0.1 nmol/l with a relative standard deviation of less than

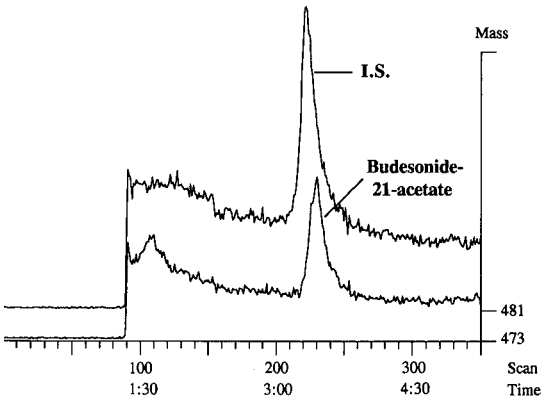

Fig. 6. Chromatogram of budesonide 21-acetate obtained by LC–TSP-MS after extraction and derivatization of a plasma sample containing 1.5 pmol of budesonide. [$^2H_8$]Budesonide (3 pmol) was added as internal standard (I.S.). Time in min.

20%. Fig. 6 shows a chromatogram of a plasma sample containing 1.5 pmol of budesonide. The example illustrates that high sensitivity can be achieved in spite of the use of a mobile phase with high (64%) methanol content. The details of the method will be reported elsewhere.

We have also used LC–TSP-MS to monitor the plasma levels of bambuterol during a toxicity study in dogs, in which high doses of bambuterol were administered, resulting in high plasma concentrations. A small plasma sample was diluted with buffer, containing the internal standard, and an aliquot of the solution, corresponding to 0.5 μl of dog plasma, was directly injected into the LC–MS system. Fig. 7 shows a chromatogram of such a sample containing 32 pmol of bambuterol, equivalent to a plasma concentration of 64 μmol/l. In spite of the absence of any sample clean-up the chromatographic baseline was free from interfering peaks. We do not recommend direct injection of crude plasma samples on a routine basis, because the efficiency of

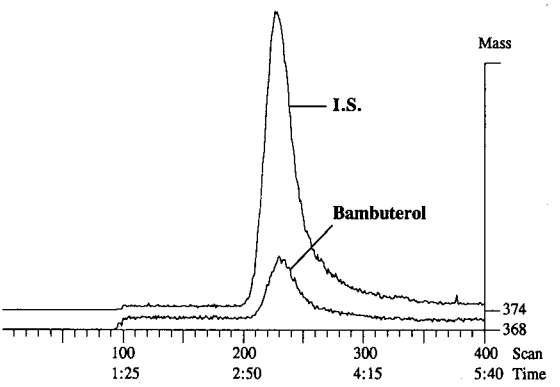

Fig. 7. Chromatogram of bambuterol (32 pmol) obtained by LC–TSP-MS after direct injection of 0.5 μl of dog plasma. [$^2H_6$]Bambuterol (160 pmol) was added as internal standard (I.S.). Time in min.

the chromatographic column will deteriorate relatively quickly. To preserve acceptable peak shape in the bambuterol study mentioned above the guard column had to be changed after less than 100 injections. Raw urine samples, on the other hand, can be injected over extended periods without deleterious effects. Direct injection of biological samples without any purification, or after only minimal sample pretreatment, reduces the risk of artefact formation and makes LC–TSP-MS an almost ideal reference method for the validation of other bioanalytical methods.

REFERENCES

1 M. L. Vestal and G. J. Fergusson, *Anal. Chem.*, 57 (1985) 2373.
2 H.-Y. Kim and N. Salem, Jr., *Anal. Chem.*, 59 (1987) 722.
3 I. G. Beattie and T. J. A. Blake, *Biomed. Environ. Mass Spectrom.*, 18 (1989) 872.
4 M. F. Bean, S. L. Pallante-Morell, D. M. Dulik and C. Feneslau, *Anal. Chem.*, 62 (1990) 121.
5 A. L. Yergey, C. G. Edmonds, I. A. S. Lewis and M. L. Vestal, *Liquid Chromatography/Mass Spectrometry —Techniques and Applications*, Plenum Press, New York, 1990.
6 R. D. Voyksner and C. A. Haney, *Anal. Chem.*, 57 (1985) 991.
7 C. Lindberg and J. Paulson, *J. Chromatogr.*, 394 (1987) 117.
8 R. H. Robins and F. W. Crow, *Rapid Comm. Mass Spectrom.*, 2 (1988) 30.
9 W. Genuit and H. van Binsbergen, *J. Chromatogr.*, 474 (1989) 145.
10 C. E. M. Heeremans, R. A. M. van der Hoeven, W. M. A. Niessen, U. R. Tjaden and J. van der Greef, *J. Chromatogr.*, 474 (1989) 149.
11 A. L. Yergey, D. J. Liberato and D. S. Millington, *Anal. Biochem.*, 139 (1984) 278.
12 D. J. Liberato, A. L. Yergey and S. T. Weintraub, *Biomed. Environ. Mass Spectrom.*, 13 (1986) 171.
13 A. I. Mallet and K. Rollins, *Biomed. Environ. Mass Spectrom.*, 13 (1986) 541.
14 Z. Yamaizumi, H. Kasai, S. Nishimura, C. G. Edmonds and J. A. McCloskey, *Mut. Res.*, 173 (1986) 1.
15 N. V. Esteban, D. J. Liberato, J. B. Sidbury and A. L. Yergey, *Anal. Chem.*, 59 (1987) 1674.
16 F. Artigas and E. Gelpi, *J. Chromatogr.*, 394 (1987) 123.
17 H. Milon, H. Bur and R. Turesky, *J. Chromatogr.*, 394 (1987) 201.
18 M. S. Lant, J. Oxford and L. E. Martin, *J. Chromatogr.*, 394 (1987) 223.
19 A. L. Yergey, N. V. Esteban and D. J. Liberato, *Biomed. Environ. Mass Spectrom.*, 14 (1987) 623.
20 S. J. Gaskell, K. Rollins, R. W. Smith and C. E. Parker, *Biomed. Environ. Mass Spectrom.*, 14 (1987) 717.
21 N. V. Esteban, A. L. Yergey, D. J. Liberato, T. Loughlin and D. L. Loriaux, *Biomed. Environ. Mass Spectrom.*, 15 (1988) 603.
22 L.-E. Edholm, C. Lindberg, J. Paulson and A. Walhagen, *J. Chromatogr.*, 424 (1988) 61.
23 C. Lindberg and J. Paulson, *Proceedings of the 36th ASMS Conference on Mass Spectrometry and Allied Topics, San Francisco, CA, June 5–10, 1988*, p. 1067.
24 R. D. Voyksner and T. W. Pack, *Biomed. Environ. Mass Spectrom.*, 18 (1989) 897.
25 W. J. Blanchflower and D. G. Kennedy, *Biomed. Environ. Mass Spectrom.*, 18 (1989) 935.
26 W. J. Blanchflower and D. G. Kennedy, *Analyst (London)*, 114 (1989) 1013.
27 T.-M. Chen and J. E. Coutant, *J. Chromatogr.*, 463 (1989) 95.
28 M. J. Moor, M. S. Rashed, T. F. Kalhorn, R. H. Levy and W. N. Howald, *J. Chromatogr.*, 474 (1989) 223.
29 K. Tyczkowska, R. D. Voyksner and A. L. Aronson, *J. Chromatogr.*, 490 (1989) 101.
30 H. J. Pieniaszek, Jr., H.-S. L. Shen, D. M. Garner, G. O. Page, L. M. Shalaby, R. K. Isensee and C. C. Whitney, Jr., *J. Chromatogr.*, 493 (1989) 79.
31 J. Oxford and M. S. Lant, *J. Chromatogr.*, 496 (1989) 137.
32 S. Reid, C. Shackleton, K. Wu, S. Kaempfer and M. Hellerstein, *Biomed. Environ. Mass Spectrom.*, 19 (1990) 535.
33 S. Auriola, T. Naaranlahti, R. Kostiainen and S. P. Lapinjoki, *Biomed. Environ. Mass Spectrom.*, 19 (1990) 609.
34 C. Lindberg, J. Paulson and A. Blomqvist, *Proceedings of the 38th ASMS Conference on Mass Spectrometry and Allied Topics, Tucson, AZ, June 3–8, 1990*, p. 1041.
35 L.-Å. Svensson and A. Tunek, *Drug Metab. Rev.*, 19 (1988) 165.

36 C. Lindberg, C. Roos, A. Tunek and L.-Å. Svensson, *Drug Metab. Dispos.*, 17 (1989) 311.
37 C. Lindberg, S. Jönsson, J. Paulson and A. Tunek, *Biomed. Environ. Mass Spectrom.*, 19 (1990) 218.
38 S. P. Clissold and R. C. Heel, *Drugs*, 28 (1984) 485.
39 C. Lindberg, J. Paulson and S. Edsbäcker, *Biomed. Environ. Mass Spectrom.*, 14 (1987) 535.
40 J. Paulson and C. Lindberg, *J. Chromatogr.*, 554 (1991) 149.

Journal of Chromatography, 554 (1991) 227–231
Elsevier Science Publishers B.V., Amsterdam

CHROMSYMP. 2214

Determination of *Catharanthus roseus* alkaloids by high-performance liquid chromatography–isotope dilution thermospray-mass spectrometry

S. AURIOLA* and T. NAARANLAHTI
Department of Pharmaceutical Chemistry, University of Kuopio, P.O. Box 6, SF-70211 Kuopio (Finland)
and
S. P. LAPINJOKI
VTT-Biotechnology, Technological Research Centre of Finland, SF-70211 Kuopio (Finland)

ABSTRACT

This paper describes a high-performance liquid chromatography–isotope dilution thermospray-mass spectrometry method for the determination of catharanthine, tabersonine, yohimbine and ajmalicine in cell culture samples of *Catharanthus roseus*. The use of deuterated analogues of the alkaloids as internal standards remarkably improved the precision of the analysis. The standard deviation between six repeated assays was close to or below 10% when the reference compounds were analysed, but was about 10% higher, in most instances, when vincamine was used as the internal standard. The precision of this method was about 20% for biological extracts.

INTRODUCTION

The Madagascan periwinkle *Catharanthus roseus* produces a wide range of medicinally active alkaloids [1]. Thermospray high-performance liquid chromatography–mass spectrometry (HPLC–TSP-MS) has been effectively used in the determination of these alkaloids in plant and plant cell culture samples [2–4]. Careful optimization of the TSP conditions is always necessary to obtain a good sensitivity and reproducibility [5]. In spite of this, the precision of the methods tends to be rather poor. The precision in the quantitation of several compounds with HPLC–TSP-MS has been improved by using internal standards labelled with stable isotopes [6–9]. For example in the HPLC–MS analysis of sumatriptan in plasma, the accuracy and precision were reduced to less than 10% with stable isotopes, whereas they exceeded 20% when a homologue was used as the internal standard [9]. In this study the same approach was used and ajmalicine, yohimbine, catharanthine and tabersonine were determined using HPLC–TSP-MS with trideuterated analogues as the internal standards.

0021-9673/91/$03.50

EXPERIMENTAL

Chemicals and sample preparation

Catharantine was purified from *C. roseus* leaves and identified as described previously [10]. Tabersonine hydrochloride was generously provided by Professor W. G. W. Kurz (Plant Biotechnology Institute, National Research Council, Saskatoon, Canada). Ajmalicine hydrochloride was purchased from Sigma (St. Louis, MO, USA) and yohimbine was a gift from Torkel Berglund (Tekniska Högskolan, Stockholm, Sweden). The [methyl-^{2}H]-labelled internal standards were synthesized by trans esterification in perdeuterated methanol and the labelled analogues were determined to contain less than 2% of the original compound [11].

The cultured plant cells were freeze-dried and samples of about 30 mg were pre-purified with Bond-Elut C_{18} cartridges (Analytichem, Harbor City, CA, USA) as described by Morris *et al.* [12]; the method was modifed by using ethanol as the solvent instead of methanol, and deuterated internal standards were added prior to extraction.

High-performance liquid chromatographic conditions

The HPLC system consisted of a Spectra-Physics SP8810 pump and a Rheodyne 7125 injector (Rheodyne, Cotati, CA, USA) with a 20-μl loop. The HPLC column was a μBondapak C_{18} (Waters Assoc. Milford, MA, USA, 300 × 3.9 mm, 10 μm). The isocratic eluent system consisted of 0.1 *M* ammonium acetate (pH 7.2)–acetonitrile (45:55). The flow-rate was 1.1 ml/min.

Mass spectrometry

The HPLC–MS system used was a VG thermospray–plasmaspray probe coupled to a VG Trio-2 quadrupole mass spectrometer (VG Masslab, Manchester, UK). The measurements were carried out using the thermospray mode. The ion source temperature was 150°C, the vaporizer tip temperature 200°C and the repeller potential 180 V. The thermospray spectra were recorded by injecting 2–10 μg of the alkaloids chromatographed as described in the preceding section. Selected ion recording was based on the protonated molecular ions: *m/z* 337 for catharanthine and tabersonine, *m/z* 353 for ajmalicine and *m/z* 355 for yohimbine (*m/z* 340, 356 and 358 for the trideuterated internal standards, respectively).

Calibration and quality control

Quantitation of the alkaloids was based on the internal standard method. Four-point calibration graphs (triplicate injections) were created for the range 2–200 ng per injection (10–200 ng for catharanthine) by plotting the ratios of analyte and internal standard *versus* the amounts of analyte. The amount of labelled standard was 10 ng per injection (50 ng for catharanthine). Linear regression analysis was used to calculate the curve parameters. Relative standard deviations were determined using 2 and 200 ng of the alkaloids (10 and 200 ng for catharanthine). The precision of the whole analytical procedure was tested by adding deuterated internal standards to six replicate plant cell culture samples that were extracted and analysed as described.

RESULTS AND DISCUSSION

The TSP mass spectra of the [methyl^{2}H]-labelled compounds (Fig. 1) are comparable to the mass spectra of non-labelled indole alkaloids which also show protonated molecular ions as the base peaks [4]. The mass spectrum of trideuterated catharanthine shows a fragment ion at m/z 338, which is formed by the loss of two protons. The corresponding ion at m/z 335 is also present in the spectrum of the original compound [4].

Selected ion recording of the protonated molecular ions of ajmalicine, yohimbine, tabersonine, catharanthine and the corresponding trideuterated standards was used for the quantitation of the compounds. Good linearity was observed ($r > 0.982$ in all instances) for the range 2–200 ng per injection (10–200 ng for catharanthine) when the analyte and internal standard peak-area ratios were plotted against the amount of analyte. The relative standard deviation (R.S.D.) for parallel samples (Table I) were markedly better at low sample concentrations than those (around 20%) of the method using vincamine as the internal standard [4].

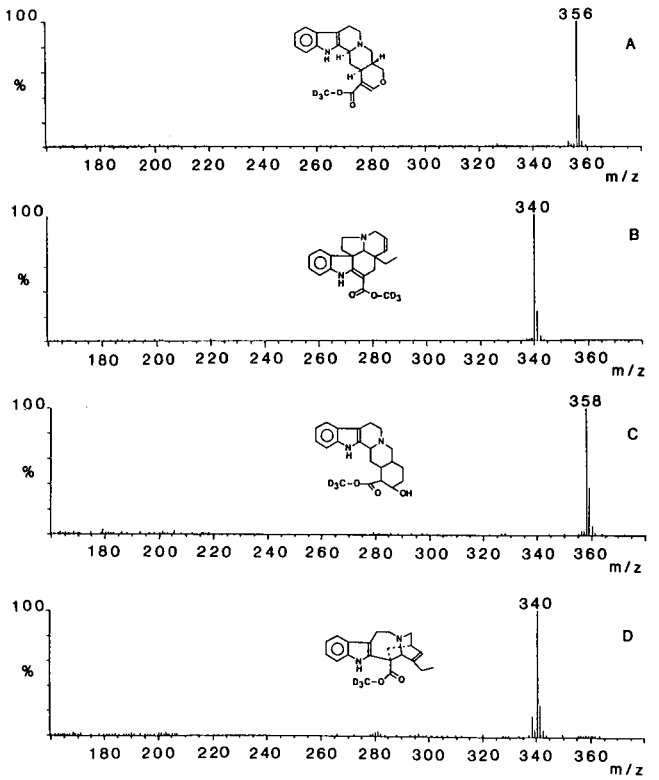

Fig. 1. Thermospray mass spectra of (A) [$^2H_3$]ajmalicine, (B) [$^2H_3$]tabersonine, (C) [$^2H_3$]yohimbine and (D) [$^2H_3$]catharanthine. Conditions: 0.1 *M* ammonium acetate–actonitrile (45 + 55); flow-rate, 1.1 ml/min; source temperature, 150°C; vaporizer temperature, 200°C; repeller 180 V. A 2–10 μg mass of the compounds was injected via a μBondapak C_{18} column (300 × 3.9 mm, 10 μm). No discharge or filament were used.

TABLE I

QUALITY PARAMETERS OF THE HPLC–TSP-MS ASSAY OF INDOLE ALKALOIDS

r = coefficient of correlation; R.S.D. = relative standard deviation (n = 6); x = amount of analyte in ng; y = peak-area ratio of analyte and internal standard.

Compound	Curve equation	r	R.S.D. (%)	
			2 ng	200 ng
Ajmalicine	$y=3.0052x+0.5291$	0.992	5.7	9.9
Yohimbine	$y=2.8181x+1.0528$	0.989	5.6	7.5
Tabersonine	$y=3.1732x+0.8321$	0.993	11.5	6.4
Catharanthine	$y=5.0974x+0.8508$	0.982	13.9 (10 ng)	10.8

The plant cell culture samples were chromatographed in 18 min using the isocratic solvent system. The trideuterated internal standards eluted a few seconds earlier than the non-labelled compounds. As a result of the complex matrix, baseline separation was not achieved for all of the compounds (Fig. 2).

The precision of the whole assay method was determined by analysing six replicate cell culture samples. The labelled standards were added before the extraction procedure. The precision is dependent on the varying chromatographic separation of the analytes and the amount of the compounds present in the cell samples. The R.S.D. values were 9.5% for yohimbine (approximately 18 ng per injection), 16% for

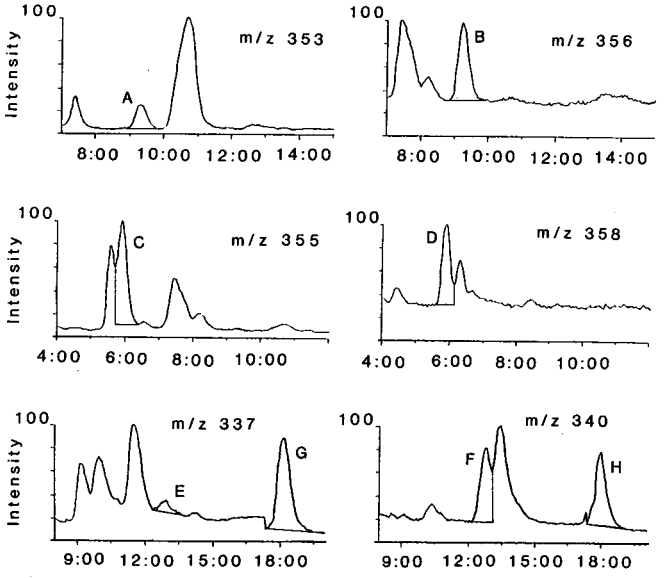

Fig. 2. Selected ion chromatograms of a cell culture sample of *C. roseus*. The intensities of the chromatograms were independently normalized. Compounds monitored: (A) ajmalicine, *m/z* 353; (B) [$^2H_3$]ajmalicine, *m/z* 356; (C) yohimbine, *m/z* 355; (D) [$^2H_3$]yohimbine, *m/z* 358; (E) catharanthine and (G) tabersonine *m/z* 337; (F) [$^2H_3$]catharanthine and (H) [$^2H_3$]tabersonine, *m/z* 340. Conditions as in Fig. 1.

tabersonine (14 ng), 21% for ajmalicine (3 ng) and 24% for catharanthine (less than 10 ng).

As seen in Fig. 2, the chromatograms for the ions at *m/z* 337 and *m/z* 340 show a sudden drop in the baseline at 17 min. This indicates some undefined change in the TSP source or probe conditions. The general and inevitable risk of this type of change in TSP analyses with the instruments currently available emphasizes the usefulness of stable isotope labelled internal standards.

CONCLUSIONS

HPLC–TSP-MS and selected ion monitoring of the MH^+ ions is a suitable method for the determination of various indole alkaloids in cell culture samples of *C. roseus*. The wide linear range of the assay is useful as the concentration of alkaloids varies greatly between different cell lines. The use of deuterium-labelled standards markedly improves the precision and general reliability of the analytical procedure.

ACKNOWLEDGEMENTS

This study was financially supported by the Provincial Government of Kuopio, the Orion Corporation Research Foundation and the Emil Aaltonen Foundation. The skilful technical assistance of Ms. Sari Ukkonen and Mr. J. Knuutinen is gratefully acknowledged.

REFERENCES

1 W. I. Taylor and N. R. Farnsworth, *The Catharanthus Alkaloids: Botany, Chemistry, Pharmacology and Clinical Use*, Marcel Dekker, New York, 1975.
2 J. Balsevich, L. R. Hodge, A. J. Berry, D. E. Games and I. C. Mylchreest, *J. Nat. Prod.*, 51 (1988) 1173.
3 F. A. Mellon, in R. J. Robbins and M. J. C. Rhodes (Editors), *Manipulating Secondary Metabolism in Cell Culture*, Cambridge University Press, Cambridge, 1988, p. 291.
4 S. Auriola, T. Naaranlahti, R. Kostiainen and S. P. Lapinjoki, *Biomed. Environ. Mass Spectrom.*, 19 (1990) 609.
5 C. Lindberg and J. Paulson, *J. Chromatogr.*, 394 (1987) 117.
6 A. L. Yergey, N. V. Esteban and D. J. Liberato, *Biomed. Environ. Mass Spectrom.*, 14 (1987) 623.
7 J. Maltas, J. Ayrton, G. D. Bowers, G. L. Evans and A. J. Harker, presented at *2nd International Symposium on Applied Mass Spectrometry in the Health Sciences, Barcelona, April 17–20, 1990.*
8 J. Paulson and C. Lindberg, presented at the *5th (Montreux) Symposium on Liquid Chromatography–Mass Spectroscopy, Freiburg, November 2–4, 1988.*
9 J. Oxford and M. S. Lant, *J. Chromatogr.*, 496 (1989) 137.
10 T. Naaranlahti, M. Nordström, S. P. Lapinjoki, A. Huhtikangas and M. Lounasmaa, *J. Chromatogr. Sci.*, 28 (1990) 173.
11 S. Auriola, T. Naaranlahti and S. P. Lapinjoki, *J. Labelled Compd. Radiopharm*, 29 (1991) 117.
12 P. Morris, A. H. Schragg, N. J. Smart and R. Stafford, in R. A. Dixon (Editor), *Plant Cell Culture: a Practical Approach*, IRL Press, Oxford, 1985, p. 127.

Journal of Chromatography, 554 (1991) 233–250
Elsevier Science Publishers B.V., Amsterdam

CHROMSYMP. 2362

Applications of thermospray liquid chromatography–mass spectrometry in photochemical studies of pesticides in water

G. DURAND, N. DE BERTRAND and D. BARCELÓ*
Environmental Chemistry Department, CID–CSIC, c/ Jordi Girona 18, 08034 Barcelona (Spain)

ABSTRACT

Thermospray liquid chromatography–mass spectrometry (TSP-LC–MS) in the positive- and negative-ion modes (PI and NI, respectively) was used for the characterization of the pesticides aldicarb, carbaryl, cyanazine, fenitrothion, linuron and parathion-methyl, including the corresponding photodegradation products. The LC analyses were performed on RP-18 columns using methanol–water (70:30 or 50:50) + 0.05 *M* ammonium acetate or 0.05 *M* ammonium formate. Photodegradation studies of pesticides in distilled water were performed using a suntest apparatus, except for fenitrothion, for which a high-pressure mercury lamp was used because of slow photodegradation. The main photodegradation pathways corresponded to dealkylation, deamination, dehalogenation and hydroxylation. Photodegradation experiments were carried out using solutions of the different pesticides at 10–200 ppm in distilled water. For carbaryl photolysis is very slow in distilled water, so 5% of acetone was needed as photosensitizer. When PI-mode TSP-LC–MS was employed, aldicarb sulphoxide, monolinuron, hydroxysimazine and fenitrooxon could be identified as breakdown products of aldicarb, linuron, cyanazine and fenitrothion, respectively. In NI-mode TSP-LC–MS aldicarb sulphoxide, 1-naphthol and *p*-nitrophenol could be identified as the main degradation products of aldicarb, carbaryl and parathion-methyl, respectively. As all the pesticides were dissolved in methanol for solubility reasons, methoxy analogues of the degradation products of cyanazine were also identified. In the PI mode of operation the base peak generally corresponded to $[M+H]^+$ for cyanazine and its photodegradation products and to $[M+NH_4]^+$ for linuron, aldicarb and fenitrothion and their corresponding degradation products. For carbaryl $[M+NH_4]^+$ was also the base peak, but its main photodegradation product, 1-naphthol, could only be identified under NI conditions. In the NI mode of operation different processes such as proton abstraction, (dissociative) electron capture and anion attachment, take place. Fragment ions such as $[M]^{\cdot-}$ for aldicarb sulphoxide, the main photodegradation product of aldicarb, $[M-H]^-$ for 1-naphthol and $[M-CONHCH_3]^-$ for carbaryl and anion attachment ions corresponding to $[M+CH_3COO]^-$ for aldicarb sulphoxide and 1-naphthol and to $[M-CONHCH_3+CH_3COOH]^-$ for carbaryl were formed. A tentative photodegradation pathway for the different pesticides in water is postulated.

INTRODUCTION

Polar pesticides such as carbamates, chlorotriazines, phenylureas and organophosphorus compounds are being used in many agricultural applications [1–3] and residue levels varying between 7 ng/l and 5 μg/l have been detected in different types of water [4–6]. After application, their environmental fate is poorly understood, depending upon several degradation pathways such as hydrolysis, photolysis and mi-

0021-9673/91/$03.50

crobial transformation. In this respect, *e.g.*, atrazine is degraded by soil microorganisms by mechanisms involving dealkylation, deamination, dehalogenation and hydroxylation [5]. As a consequence, atrazine, carbaryl and aldicarb and their corresponding degradation products such as dealkylated atrazines, 1-naphthol and aldicarb sulphoxide, respectively, have also been detected in soil and water samples [2,4,7,8].

For establishing the aquatic photolysis processes under field conditions, prior identification of the different photodegradation products formed in laboratory experiments is needed. Previous photolysis experiments under laboratory conditions have been reported for a variety of pesticides, including carbamates [9–11], phenylureas [12,13], organophosphorus compounds [12,14] and triazines [12,15]. The formation of photolysis products such as oxo derivatives of organophosphorus pesticides [16], hydroxyatrazine [17], 1-naphthol [10,11] and aldicarb sulphoxide [18] is of concern because of their toxicity. Difficulties are often compounded because most of these breakdown products are involatile and/or polar and so not readily amenable to direct gas chromatography (GC) and GC–mass spectrometric (MS) determinations and as a consequence isolation of the reaction products is required [10,11,13,14]. Thermospray liquid chromatography–mass spectrometry (TSP-LC–MS) has been demonstrated to be a valuable technique for the identification of several pesticides and their polar metabolites, such as the oxo derivatives of organophosphates [19], *p*-nitrophenol [20], hydroxytriazines [12,15] and 1-naphthol, metabolite of carbaryl [21], and aldicarb sulphoxide and sulphone [22,23]. TSP-LC–MS–MS has also been employed for the identification of triazine [24] and aldicarb and its metabolites [23,25].

This paper presents results on aquatic photodegradation studies of pesticides of four different groups, carbamates, chlorotriazines, organophosphorus compounds and phenylureas, *viz.*, aldicarb, carbaryl, cyanazine, fenitrothion, linuron and parathion-methyl. TSP-LC–MS in the positive-ion (PI) and negative-ion (NI) modes of operation together with co-elution using authentic photodegradation standards, when available, were used for the unequivocal identification of the different photodegradation products. This work is a sequel to previous research using TSP-LC–MS for the characterization of the photolysis products of atrazine and simazine [12,15] and diuron [12] in water.

EXPERIMENTAL

Chemicals

HPLC-grade water from Riedel-de Haën (Seelze-Hannover, Germany) and methanol and acetonitrile from Merck (Darmstadt, Germany) were passed through a 0.45-μm filter (Scharlau, Barcelona, Spain) before use. Ammonium acetate and ammonium formate were obtained from Merck (Darmstadt, Germany) and Fluka (Buchs, Switzerland), respectively. Analytical-reagent grade aldicarb, carbaryl and cyanazine were from Polyscience (Niles, IL, USA), 1-naphthol from Merck, linuron from Riedel-de Haën and parathion-methyl, fenitrothion and monolinuron from Promochem (Wesel, Germany). Fenitrooxon and aldicarb sulphoxide were gifts from Sumitomo Chemical (Osaka, Japan) and Rhône-Poulenc (Research Triangle Park, NC, USA), respectively, and hydroxysimazine (HSIM) and deisopropylhydroxyatrazine (DIHA) were gifts from Ciba-Geigy (Basle, Switzerland).

Chromatographic conditions

Eluent delivery was provided by two Model 510 high-pressure pumps coupled with a Model 680 automated gradient controller (Waters Chromatography Division, Millipore, Bedford, MA, USA) and a Model 7125 injection valve with a 20-μl loop from Rheodyne (Cotati, CA, USA). Cartridge columns of 12.5 cm × 4.0 mm I.D. from Merck and of 22 cm × 4.6 mm I.D. from Brownlee, Applied Biosystems (Santa Clara, CA, USA) were packed with 5-μm LiChrospher 100 RP-18 and 5-μm Spherisorb ODS, respectively, from Merck. A Polyglosil 500-7 C_{18} semi-preparative column (40 × 0.7 cm I.D.) from Macherey, Nagel & Co. (Düren, Germany) was employed for fractionation of UV-irradiated fenitrothion solutions.

The LC mobile phase compositions were methanol–water (50:50) + 0.05 *M* ammonium acetate for the analysis of aldicarb, carbaryl and linuron photodegraded solutions and methanol–water (70:30) + 0.05 *M* ammonium formate for the analysis of cyanazine and fenitrothion photodegraded solutions. Parathion-methyl photodegraded solution was analysed using acetonitrile–water (50:50) + 0.05 *M* ammonium acetate during 5 min with gradient elution up to 90% of acetonitrile in 20 min. The flow-rate was 1 ml/min.

Mass spectrometric analysis

A Hewlett-Packard (Palo Alto, CA, USA) Model 5988A quadrupole mass spectrometer and a Hewlett-Packard Model 59970C instrument for data acquisition and processing were employed. The temperatures of the TSP were stem 100°C, tip 188°C and vapour and ion source 270°C; the electron multiplier voltage was 2700 V and the electron energy was 255 eV. Full-scan spectra from m/z values of 150 and 180 in the PI and NI mode, respectively, were obtained. For parathion-methyl photodegradation products, the vapour and ion source temperatures were 200°C. In all the experiments the filament-on mode (ionization by an electron beam) was used. In the PI mode under full-scan conditions the sensitivity for the carbamates and organophosphorus compounds, chlorotriazines and phenylureas and their photolysis products was in the range 1–20 ng. The NI mode was used for the identification of *p*-nitrophenol, paraoxon-methyl and carbamate photolysis products as the sensitivity varied from 5 to 50 ng under full-scan conditions [12,15,19–21].

Photolysis experiments

In order to obtain stable and reproducible results in the photodegradation studies, a suntest apparatus from Heraeus (Hanau, Germany) equipped with a xenon lamp was used. This xenon arc lamp has been demonstrated to be equivalent to natural sunlight for conducting aqueous photolysis studies of several compounds, *e.g.*, carbaryl [26]. The wavelength range varies from 300 to 800 nm, which represents radiation very close to natural sunlight, and the temperature was set at 44°C. Distilled water samples, previously spiked at 0.1 ppm with aldicarb, carbaryl, cyanazine, linuron and parathion-methyl in methanolic solution and kept in a quartz reaction reservoir, were subsequently introduced into the suntest apparatus. At different periods of time, 20 μl of the solution were analysed by TSP-LC–MS. The identification of the different photolysis products was confirmed from retention index and spectral data using PI and NI modes of operation (when feasible, depending on the response of the compound) and matching with authentic standards (when available). For carbaryl,

5% of acetone was added as a photosensitizer, as done previously for organophosphorus and carbamate pesticides [12,27,28].

Fenitrothion showed slow photodegradation in distilled water when using the suntest apparatus and without the use of a photosensitizer [12]. As a consequence, in order to identify the possible photodegradation products, fenitrothion solution was irradiated in an HPK 125-W high-pressure mercury lamp fitted with a quartz filter (a gift from M. Mansour, GSF, Munich, Germany). A water–methanol (5:1) solution of 200 ppm of fenitrothion was kept in a 600 ml round-bottomed Quartz flask, attached to the high-pressure mercury lamp. In order to eliminate any effects from the heat which the mercury lamp emitted, the vessel was cooled with circulating distilled water provided by a cooling machine. The temperature of the test solution was kept at 25°C in a water-bath. After 7 h of irradiation, fenitrothion solution was injected onto a semi-preparative reversed-phase LC columns, from which six fractions were obtained by elution with methanol–water (60:40) at a flow-rate of 2 ml/min and UV detection at 254 nm. The collection times for each fraction were 0–12 min (fraction 1), 12–20 min (fraction 2) , 20–24 min (fraction 3), 24–27 min (fraction 4), 27–30 min (fraction 5) and 30–40 min (fraction 6). Fraction 1, the most polar, corresponded to fenitrooxon, and dimethylphosphoric acid and the last fraction, fraction 6, which is the least polar, corresponded to fenitrothion.

RESULTS AND DISCUSSION

Carbamates

Fig. 1 shows the amount of aldicarb and carbaryl degraded in distilled water after different periods of UV irradiation. Owing to the slower photodegradation of carbaryl than aldicarb, 5% of acetone was added to the carbaryl solutions as photosensitizer. A half-life of 50 min for carbaryl (without acetone) was obtained, 1-naphthol being the main breakdown product [11]. Previous results on the photodegradation of carbaryl using lake water and a medium-pressure mercury lamp showed a

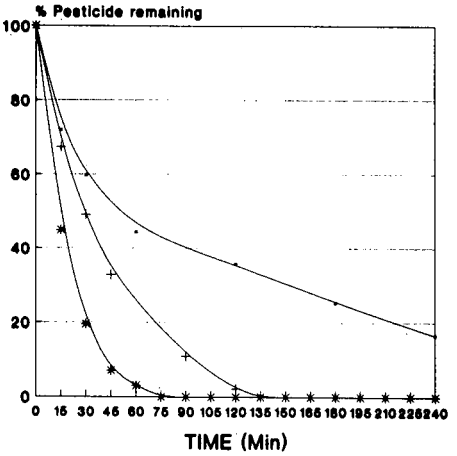

Fig. 1. Percentage of remaining pesticides aldicarb and carbaryl after UV irradiation as a function of time. ● = Carbaryl + 2% methanol; + = carbaryl + 5% of acetone; * = aldicarb + 4% of methanol.

half-life of 60 min. In general, when N-methylcarbamates are subjected to UV irradiation, the carbamate group is preserved after photolysis, although carbaryl is one of the exceptions to this rule, giving 1-naphthol [10,11]. When carbaryl is irradiated with a xenon arc lamp in an aqueous buffer solution at pH 5.5, which stabilizes the carbaryl, the photodegradation is much slower, giving a half-life of 200 h [26]. Also, when other types of water, *e.g.*, lake and sea water, were employed, quenching effects have been observed for carbaryl, thus retarding the photodegradation [11], similarly to what was observed with diuron [12].

A solution of carbaryl +5% acetone after 30 min of UV irradiation was injected directly into the TSP-LC–MS system and the total ion currents (TIC) obtained in the PI and NI modes are shown in Fig. 2. Of the different chromatographic peaks, only carbaryl (peak 1) and 1-naphthol (peak 2) could be unequivocally confirmed by TSP-LC–MS. Here carbaryl ions $[M + H]^+$ and $[M + NH_4]^+$ corresponded to *m/z* 202 and 219 with relative intensities of 10 and 100%, respectively [21]. Other workers have reported similar intensities [25,29]. As 1-naphthol does not give any signal under PI conditions [21], NI conditions were used. The $[M - H]^-$ and $[M + CH_3COO]^-$ ions, at *m/z* 143 and 203, for 1-naphthol and $[M - CONHCH_3 + CH_3COOH]^-$, at *m/z* 203, for carbaryl were obtained. The ion formation in the PI and NI modes in TSP-LC–MS and the differences in sensitivity between the PI and NI mode of operation for carbaryl and 1-naphthol were reported in previous papers [21,30].

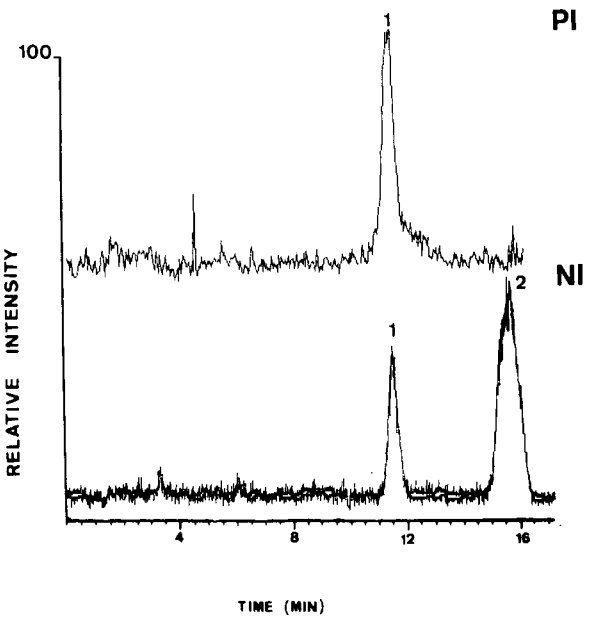

Fig. 2. TIC chromatogram obtained by TSP-LC–MS in PI and NI modes of a 9 ppm degraded solution of carbaryl (+ 5% acetone) after 30 min of photodegradation with the suntest apparatus. For carbaryl (peak 1), the ions identified corresponded to $[M + H]^+$ and $[M + NH_4]^+$ and $[M - CONHCH_3]^-$ in the PI and NI modes, respectively, whereas those for 1-naphthol (peak 2) corresponded to $[M - H]^-$ and $[M + CH_3COO]^-$ in the NI mode. The structures of both compounds are given in Fig. 3. LC mobile phase: methanol–water (50:50) + 0.05 *M* ammonium acetate at 1 ml/min. LC packing: 5-μm LiChrospher 100 RP-18.

The use of the NI mode for carbamate identification is not a common practice in MS, as indicated previously [31], as it gave poor sensitivities, close to 4–5 orders of magnitude lower than the PI mode [29]. The good sensitivity for carbaryl under NI conditions was attributed to its 1-naphthol structure, which can easily stabilize the negative charge under NI conditions [21]. The structures of carbaryl and its photodegradation product 1-naphthol are shown in Fig. 3.

Concerning the degradation of aldicarb, it has been reported that aldicarb sulphoxide and sulphone are the main degradation products of aldicarb under microbial degradation [32], hydrolysis [9] and chlorination of water at pH in the neutral to alkaline range [33]. Sulphoxide and sulphone metabolites are obtained when photooxidation is applied to a variety of organophosphates [14] and this was also expected to occur with aldicarb [10], but so far no data are available. Selected-ion monitoring (SIM) chromatograms obtained in the PI and NI modes for aldicarb sulphoxide are shown in Fig. 4, corresponding to an aldicarb solution after 180 min of UV irradiation. Fig. 3 shows the structures of aldicarb and aldicarb sulphoxide. Other

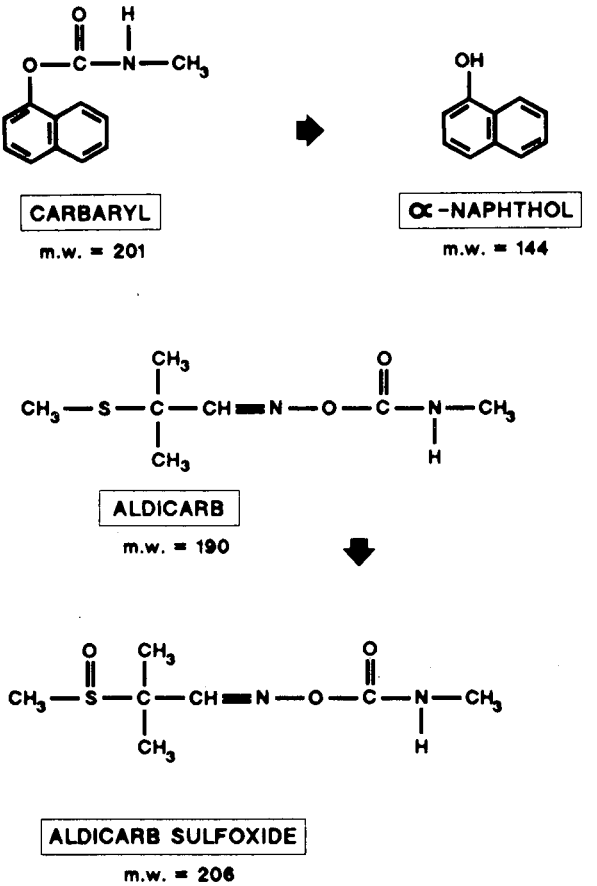

Fig. 3. Main photodegradation products of carbaryl and aldicarb in water. m.w. = Molecular weight.

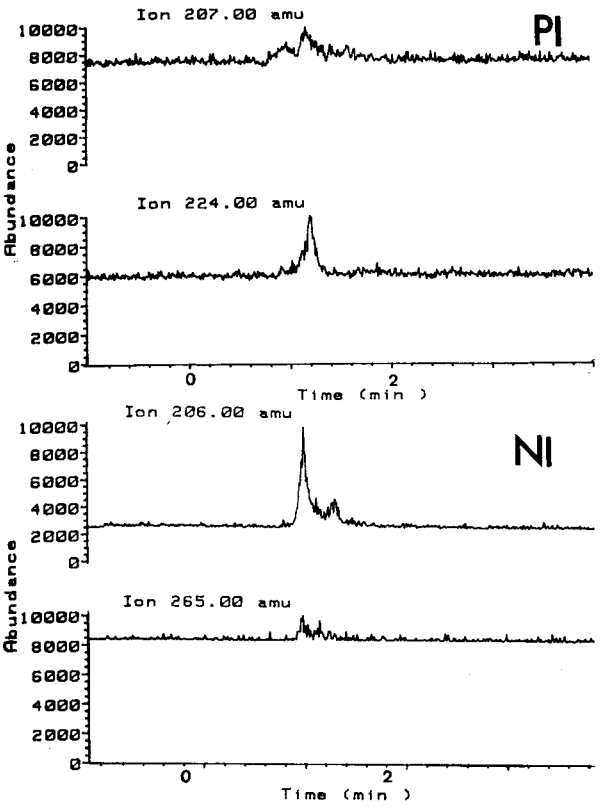

Fig. 4. SIM chromatograms obtained by TSP-LC–MS in PI and NI modes of a 15 ppm μg/l degraded solution of aldicarb after 180 min of photodegradation with the suntest apparatus. Aldicarb sulphoxide was identified by the $[M + H]^+$ and $[M + NH_4]^+$ ions and $[M]^-$ and $[M + CH_3COO]^-$ ion in PI and NI modes, respectivey. The structure of aldicarb sulphoxide is given in Fig. 3. Other experimental conditions as in Fig. 2.

peaks were observed in the chromatographic traces, but only aldicarb sulphoxide could be positively identified. In the PI mode of operation, aldicarb sulphoxide $[M + H]^+$ and $[M + NH_4]^+$ ions corresponded to *m/z* 207 and 224 whereas in the NI mode $[M]^{\cdot -}$ and $[M + CH_3COO]^-$ ions corresponded to *m/z* 206 and 265. The PI mode showed $[M + NH_4]^+$ as the base peak, as reported for aldicarb sulphoxide [22,23,25], whereas the NI TSP-LC–MS results are reported here for the first time. The different adduct ions obtained in the PI and NI modes of operation for the carbamate insecticides and their photolysis products are indicated in Table I.

Aldicarb sulphoxide and sulphone showed a 1.5 order of magnitude lower sensitivity in the NI than in the PI mode. Aldicarb sulphone was not detected in all the experiments performed, even with the use of SIM. This could be attributed to the fact that the formation of aldicarb sulphone may need the addition of a photosensitizer, such as acetone. In this respect, it has been reported that for the detection of aldicarb sulphone acetone is needed as a photosensitizer in postcolumn indirect photolysis [28].

TABLE I

IMPORTANT FRAGMENTS AND RELATIVE INTENSITIES OBSERVED IN TSP-LC–MS IN PI AND NI MODES AND FILAMENT-ON MODE OF OPERATION

Mol. wt.	Compounds and ions (m/z and tentative identification)		PI mode	NI mode
Carbamate pesticides + photolysis products				
144	Naphthol			
	143	$[M - H]^-$		100
	203	$[M + CH_3COO]^-$		50
201	Carbaryl			
	202	$[M + H]^+$	10	
	203	$[M - CONHCH_3 + CH_3COOH]^-$		100
	219	$[M + NH_4]^+$	100	
206	Aldicarb sulphoxide			
	206	$[M]^{\cdot -}$		100
	207	$[M + H]^+$	40	
	224	$[M + NH_4]^+$	100	
	265	$[M + CH_3COO]^-$		50
Chlorotriazine herbicides + photolysis products				
155	Deisopropylhydroxyatrazine			
	156	$[M + H]^+$	100	
	215	$[M + CH_3COONH_4 + H - H_2O]^+$	10	
183	Hydroxysimazine			
	184	$[M + H]^+$	100	
	243	$[M + CH_3COONH_4 + H - H_2O]^+$	10	
240	Cyanazine			
	241	$[M + H]^+$	100	
	300	$[M + CH_3COONH_4 + H - H_2O]^+$	10	
Organophosphorus pesticides + photolysis products				
126	Dimethylphosphoric acid			
	144	$[M + NH_4]^+$	100	
139	*p*-Nitrophenol			
	198	$[M + CH_3COO]^-$		100
247	Paraoxon-methyl			
	232	$[M - CH_3]^-$		100
261	Fenitrooxon			
	262	$[M + H]^+$	20	
	279	$[M + NH_4]^+$	100	
277	Fenitrothion			
	278	$[M + H]^+$	30	
	295	$[M + NH_4]^+$	100	
Phenylurea herbicides + photolysis products				
214	Monolinuron			
	215	$[M + H]^+$	20	
	232	$[M + NH_4]^+$	100	
248	Linuron			
	249	$[M + H]^+$	20	
	266	$[M + NH_4]^+$	100	

Chlorotriazines

Photodegradation studies carried out with the chlorotriazine atrazine have shown that hydroxyatrazine is one of the main degradation products formed in various water samples [12,27]. Further photolysis breakdown products such as 2-H, 2-H-deisopropylhydroxyatrazine and 2-methoxydeisopropyl analogues have been reported for atrazine and simazine in distilled water solution [15] and using particulate titania as a photocatalyst [34]. A solution of cyanazine degraded after 4.5 h was injected into the TSP-LC–MS system and the selected ion chromatograms obtained in the PI mode are shown in Fig. 5. By using this mode of operation, $[M + H]^+$ is obtained as base peak with no adduct formed with NH_4^+, which was attributed to a higher proton affinity of the chlorotriazines than ammonia [4,15,21]. As the second most abundant ion $[M + CH_3COONH_4 + H - H_2O]^+$ was formed with a relative abundance between 5 and 10%, which is not indicated in the Fig. 5 owing to its poor signal but it has been reported elsewhere [21].

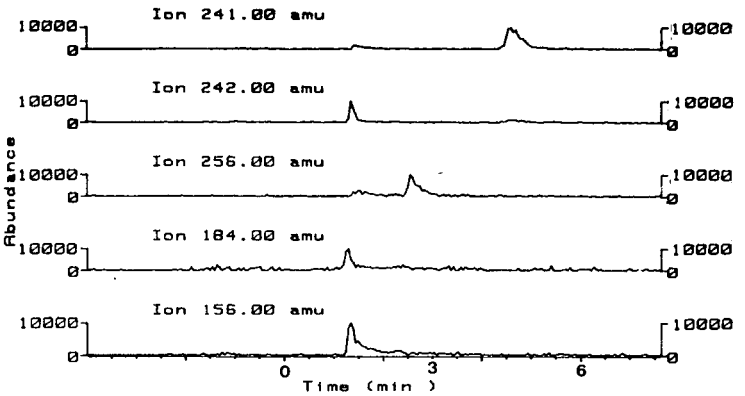

Fig. 5. Selected ion chromatograms obtained by TSP-LC–MS in the PI mode of a 200 ppm degraded solution of cyanazine after 300 min of photodegradation with the suntest apparatus. The ions identified correspond to $[M + H]^+$ and their structures are given in Fig. 6.

The tentative identification of the different photodegradation products is shown in Fig. 6. Hydroxysimazine (HSIM) (mol. wt. 183) and deisopropylhydroxyatrazine (DIHA) (mol. wt. 155) were positively identified and correspond to the degradation of the 2-chloro position of the triazines to its corresponding 2-hydroxy analogues together with a dealkylation process. These two breakdown products were previously identified for simazine [15] and are expected to be formed when chlorotriazines are subjected to UV irradiation [35].The formation of the methoxy analogue (mol. wt. 255) due to the photolysis in the presence of a small amount of methanol and the transformation of the cyano group into a carboxylic group (mol. wt. 241) are also expected behaviour in the degradation of chlorotriazines and it has been described elsewhere [35]. The ions and relative intensities of the main photolysis products are given in Table I.

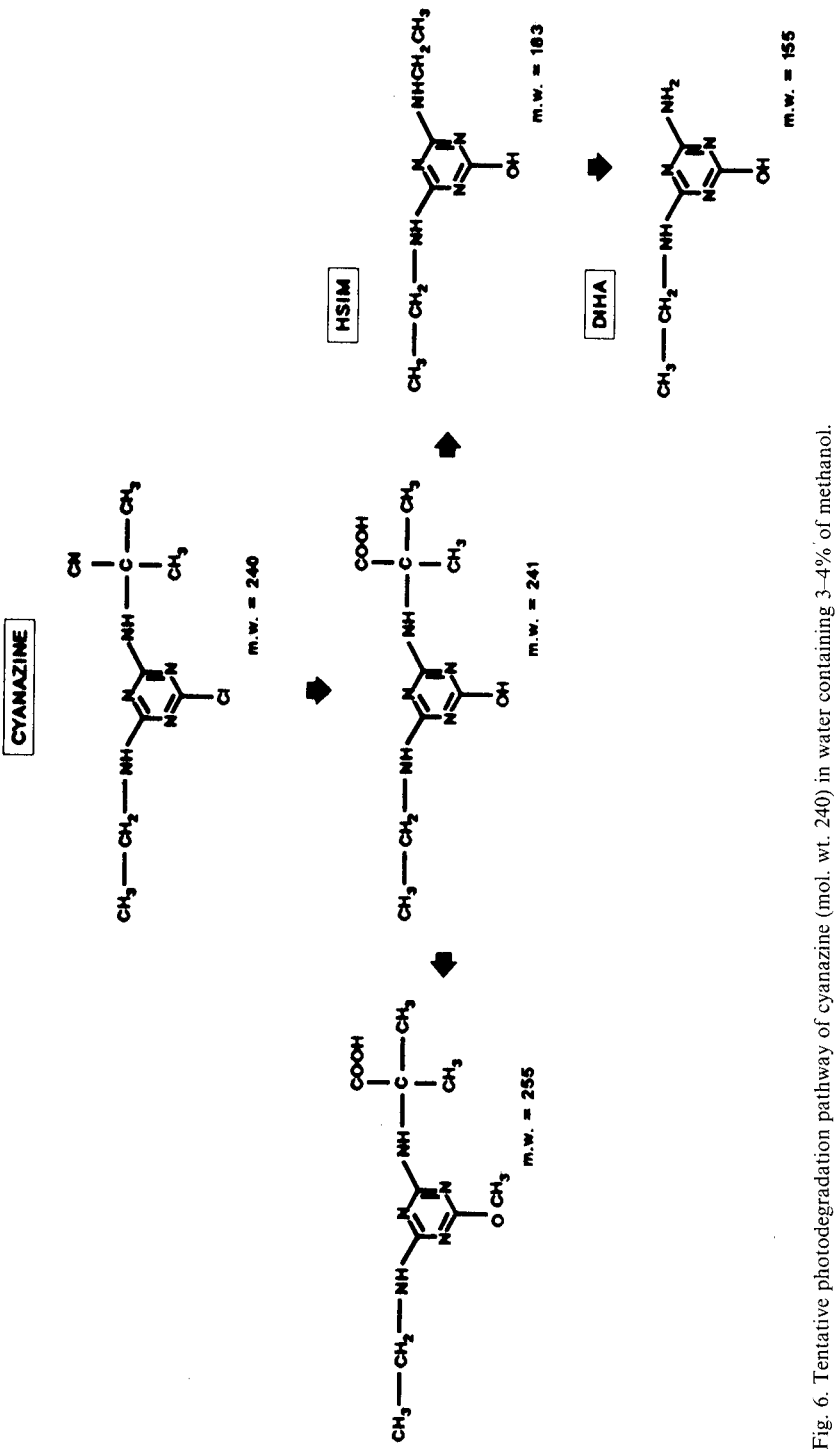

Fig. 6. Tentative photodegradation pathway of cyanazine (mol. wt. 240) in water containing 3–4% of methanol.

Organophosphorus compounds

Photodegradation studies in water using either sunlight [14] or UV irradiation [14,27,36] have shown a variety of photoalteration products, *e.g* oxo derivatives and different phenols. When solutions of fenitrothion in water were irradiated with a xenon lamp using the suntest apparatus [12], it has been shown that after 3 h of irradiation virtually no breakdown product was observed with 50% degradation of the parent compound. As a consequence, in the present experiments a solution of fenitrothion in water was irradiated with a high-pressure mercury lamp, which provides stronger UV irradiation than the xenon lamp. In this way, we still were able to identify some of the breakdown products formed. Fenitrothion solutions were irradiated for 7 h and subsequently the irradiated solution was injected onto a semi-preparative LC column from which six fractions were collected and analysed directly by

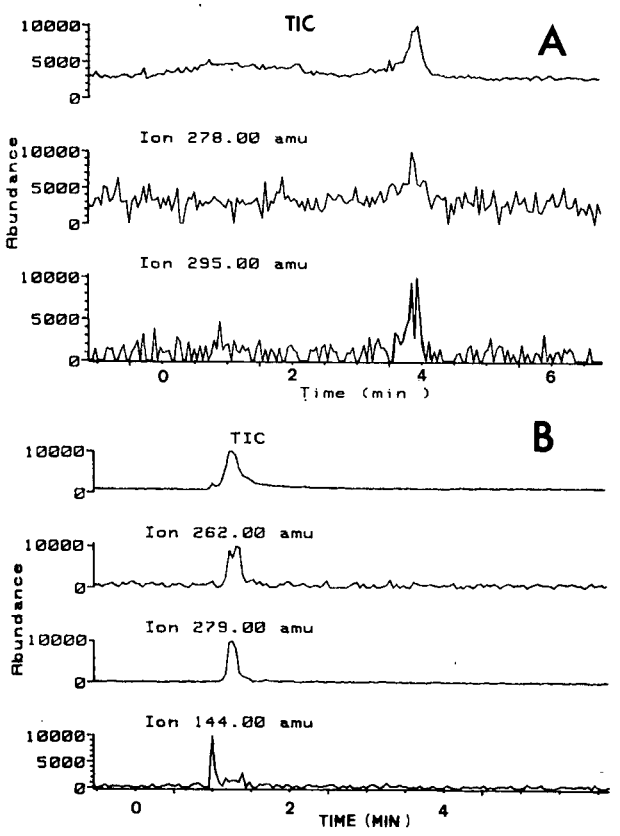

Fig. 7. TIC and selected ion chromatograms obtained by TSP-LC–MS in the PI mode of a 200 ppm degraded solution of fenitrothion after 420 min of irradiation with a high-pressure mercury lamp. Fractions 1 and 6 of the fenitrothion degraded solution were separated in a semi-preparative Polyglosil 500-7 C_{18} HPLC column and injected into the TSP-LC–MS system. In fraction 6 the ions of fenitrothion identified corresponded to $[M + H]^+$ and $[M + NH_4]^+$. In fraction 1 fenitrooxon was identified also by the $[M + H]^+$ and $[M + NH_4]^+$ ions, whereas dimethylphosphoric acid could be identified only by its $[M + NH_4]^+$ ion. The photodegradation scheme of fenitrothion is given in Fig. 8. LC mobile phase: methanol–water (70:30) + 0.05 *M* ammonium formate at 1 ml/min. LC packing: 5-μm LiChrospher 100 RP-18.

TSP-LC–MS. In the most polar fraction, fraction 1, fenitrooxon and dimethylphosphoric acid, could be identified, whereas fenitrothion was identified in the least polar fraction, fraction 6. Other compounds have been detected in the other fractions that may correspond to different photolysis products of fenitrothion, *e.g.*, carbometoxyfenitrothion [36]. Such fractions are still under investigation and future work will consider the identification of the different photolysis products of fenitrothion.

Fig. 7 shows the TIC and selected ion chromatograms obtained by TSP-LC–MS in the PI mode. Fenitrothion and fenitrooxon gave $[M + H]^+$ and $[M + NH_4]^+$ corresponding to *m/z* values of 278 and 295 for fenitrothion and *m/z* 262 and 279 for fenitrooxon. As the scan started at *m/z* 140 the $[M + H]^+$ ion could not be obtained for dimethylphosphoric acid and it was identified only by its $[M + NH_4]^+$ ion, corresponding to *m/z* 144. In all instances $[M + NH_4]^+$ was the base peak [19,37] and the identification of the two breakdown products was matched with authentic standards.

The identification of dimethylphosphoric acid was feasible as this compound was obtained during the synthesis of fenitrooxon and it is formed by hydrolysis [19] and matches the results obtained for this compound in TSP-LC–MS [38]. The tentative photodegradation pathway of fenitrothion is indicated in Fig. 8. The formation of the photoalteration products identified by us agrees with the photodegradation products which are expected to be formed for fenitrothion when using a low-pressure mercury lamp [36].

The photodegradation of parathion-methyl was carried out in aqueous solution and using the suntest apparatus. Fig. 9 shows the TIC chromatogram corresponding to a solution containing 0.1 ppm of parathion-methyl after 2 h of irradiation. In Fig. 9 the selected ions at *m/z* values of 198 and 232 corresponded to $[M + CH_3COO]^-$ and $[M - CH_3]^-$ of *p*-nitrophenol and paraoxon-methyl, respectively. Both metabolites have already been reported in photolysis experiments with parathion-methyl [14,27].

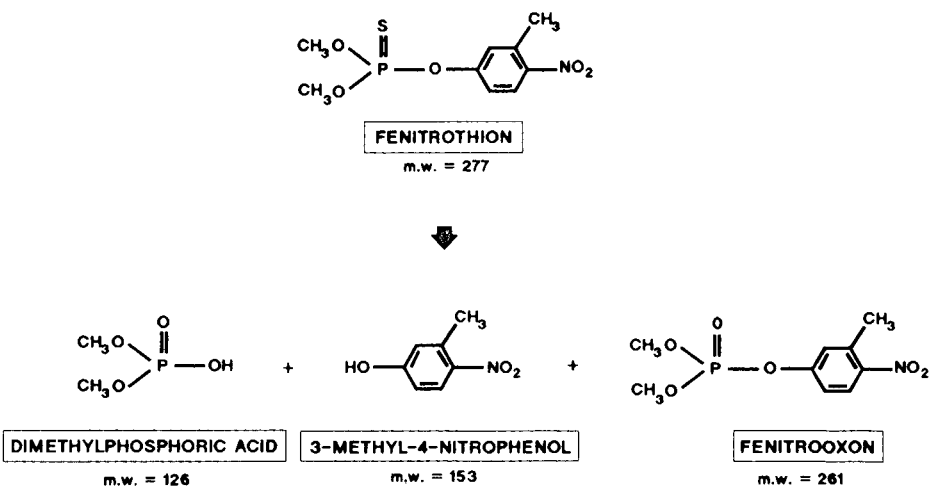

Fig. 8. Tentative photodegradation pathway of fenitrothion (mol. wt. 277) in water containing 3–4% of methanol.

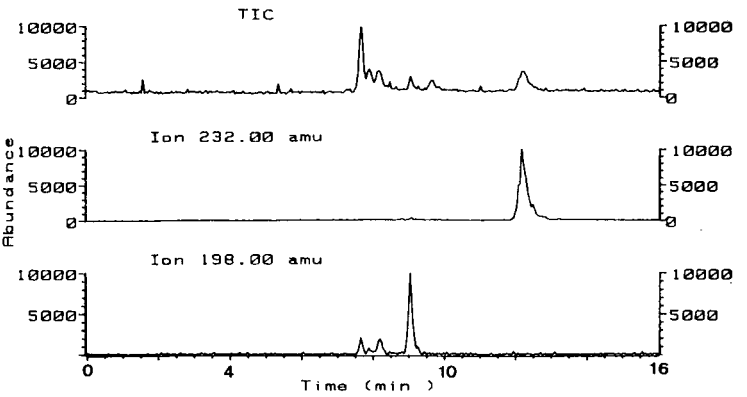

Fig. 9. TIC and selected ion chromatograms obtained by TSP-LC–MS in the NI mode of a 50 ppm degraded solution of parathion-methyl after 120 min of photodegradation with the suntest apparatus. The ions identified correspond to $[M + CH_3COO]^-$ and $[M - R]^-$ for *p*-nitrophenol and paraoxon-methyl, respectively. The photodegradation pathway is given in Fig. 10. LC mobile phase: acetonitrile–water (50:50) + 0.05 *M* ammonium acetate for 5 min with a gradient elution up to 90% of acetonitrile in 20 min. LC packing: 5-μm LiChrospher 100 RP-18. Flow-rate, 1 ml/min.

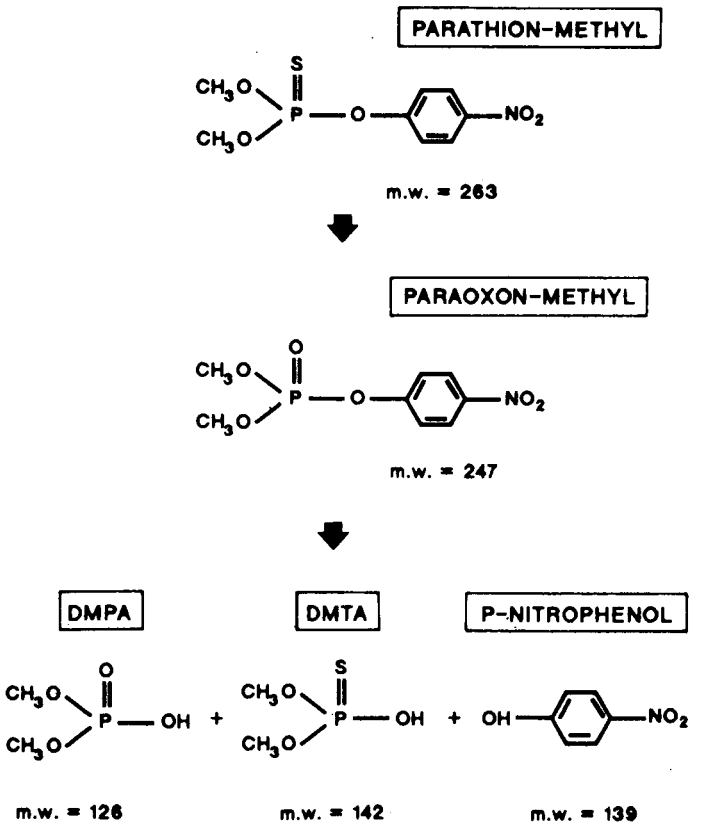

Fig. 10. Tentative photodegradation pathway of parathion-methyl (mol. wt. 263) in water containing 3–4% of methanol.

Identification of *p*-nitrophenol was reported previously under NI conditions [20] when hydrolysis experiments on parathion-methyl were carried out. As *p*-nitrophenol can only be detected under NI conditions but parathion-methyl in both modes of operation [19,37], the NI mode was preferred for the simultaneous identification of both compounds. The $[M - CH_3]^-$ ion was monitored instead of $[M]^{\cdot -}$ for parathion-methyl, because during these experiments we were working at lower vapour and source temperatures (200°C) instead of 270°C. At lower temperatures the $[M - CH_3]^-$ peak decreases whereas at higher temperatures $[M]^-$ is the base peak as a consequence of the better electron-capture mechanisms at these higher temperatures [19]. The tentative photodegradation pathway of parathion-methyl is indicated in Fig. 10. The ions and relative abundances of the different photolysis products of organophosphorus pesticides are given in Table I.

Under the experimental conditions used, parathion-methyl was not detected after 2 h of irradiation, which indicates a much stronger photodegradation than fenitrothion. This corresponds to a much shorter half-life than that reported [27], where degradation of 80% of the pesticide occurred after 5 h of irradiation. Such a

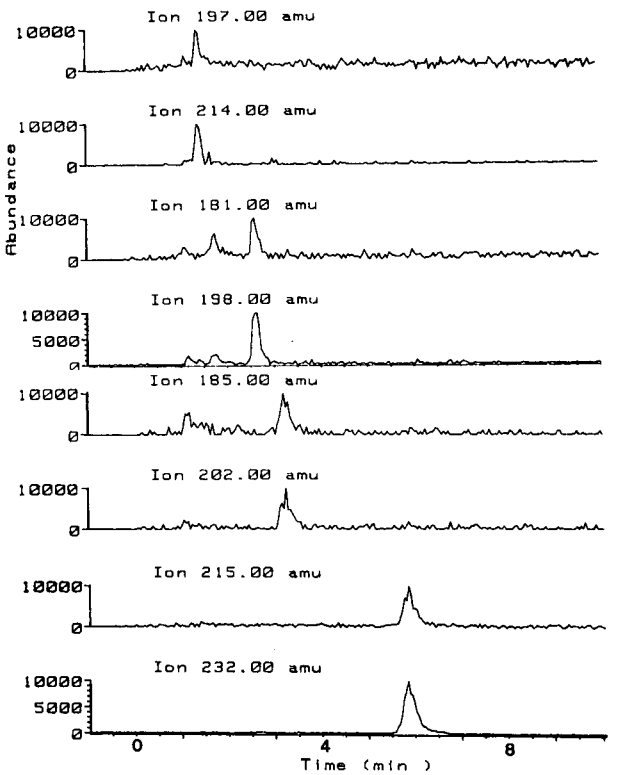

Fig. 11. Selected ion chromatograms obtained by TSP-LC–MS in the PI mode of a 100 ppm degraded solution of linuron after 300 min of photodegradation with the suntest apparatus. Each breakdown product was identified by $[M + H]^+$ and $[M + NH_4]^+$ ions and the corresponding photodegradation pathway is given in Fig. 12. LC mobile phase: methanol–water (50:50) + 0.05 *M* ammonium acetate. LC column, Brownlee. Flow-rate, 1 ml/min.

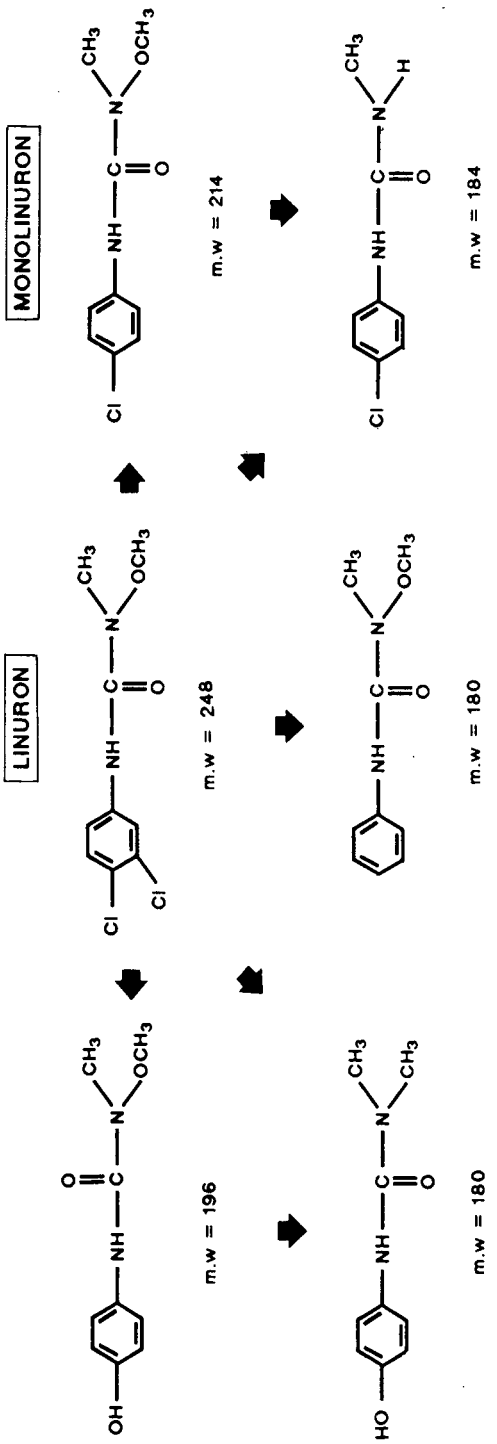

Fig. 12. Tentative photodegradation pathway of linuron (mol. wt. 248) in water containing 3–4% of methanol.

discrepancy can be explained by the different suntest photolysis temperature (44°C in our experiments *versus* 20°C).

Phenylureas

Previous photodegradation studies carried out with phenylurea herbicides showed that dechlorination is one of the main degradation pathways of diuron [12], linuron [13], buturon and monolinuron [39]. Further photodegradation products reported corresponded to OH, CHO and H derivatives [13,39]. In most of the examples cited [13,39], identification of the different photoproducts was carried out off-line, after isolation of the different reaction products and injection into a gas chromatograph.

Linuron solutions in distilled water were irradiated in the suntest apparatus and subsequently injected directly into the TSP-LC–MS system. A half-life of 2 h has been found for this compound. This is much shorter than the photodegradation under sunlight conditions, which has been reported to be very slow, 69% of the compound remaining after 2 months [13]. A solution of linuron after 4.5 h of irradiation was injected into the TSP-LC–MS system in the PI mode and the selected ion chromatograms obtained are shown in Fig. 11. The PI mode of operation was preferred to the NI mode [40] as the sensitivities are 30% better and the information obtained corresponds to $[M + NH_4]^+$ as the base peak and the second most abundant ion, varying from 10 to 25%, corresponds to $[M + H]^+$. In Fig. 11 each of the metabolites identified was monitored using both ions. Linuron could only be identified in the SIM mode, because after 4.5 h of irradiation of a linuron solution only 6% of the parent compound remained. The tentative degradation pathway of linuron is shown in Fig. 12, monolinuron being one of the main breakdown products. The ions and relative abundances of monolinuron and linuron are indicated in Table I.

At a molecular weight of 180 two possible photoproducts of linuron are indicated in Fig. 12. These two compounds are likely to be formed [13] but at present we do not know which one predominates in photolysis experiments. However, considering the retention times and structures of these two metabolites, it is feasible to consider that the dehydroxylated metabolite has been identified as it elutes later than the compound of mol. wt. 196, as can be observed in Fig. 11.

CONCLUSIONS

The combination of PI and NI modes of TSP-LC–MS has allowed the identification of different photolysis products of carbamate, chlorotriazine, organophosphorus and phenylurea pesticides in water by direct injection of the photodegradation solutions into the LC system. The method is much simpler than those currently used, which require various steps prior to the MS characterization of the breakdown products. By using PI and NI modes of operation and co-elution with authentic standards, different polar photodegradation products were identified, such as 1-naphthol and aldicarb sulphoxide for carbaryl and aldicarb, respectively, hydroxysimazine and deisopropylhydroxyatrazine for cyanazine, fenitrooxon and dimethylphosphoric acid for fenitrothion, paraoxon-methyl and *p*-nitrophenol for parathion-methyl and monolinuron for linuron.

Although aldicarb does not give any signal when 1 μg is injected into the TSP-

LC–MS, system in the NI mode, aldicarb sulphoxide could be unequivocally identified in this mode of operation for the first time, thus indicating the usefulness of utilizing both modes of operation in the detection of polar pesticide metabolites.

ACKNOWLEDGEMENTS

G. D. has a grant from the Commission of the European Communities (CEC) (ST2*-0488). N. de B. is the recipient of a fellowship from the Community Bureau of Reference (BCR) of the CEC. R. Alonso is thanked for laboratory assistance. M. C. Abril and K. Tanaka of Sumitomo Chemical (Barcelona, Spain, and Osaka, Japan, respectively) are thanked for kindly providing fenitrooxon. P. Adrian and D. Scarborough of Rhone-Poulenc (Lyon, France, and Research Triangle Park, NC, USA, respectively) are thanked for providing aldicarb sulphoxide. Dr. W. D. Hörmann and M. K. Huber (Ciba-Geigy, Basle) are thanked for kindly providing hydroxysimazine and deisopropylhydroxyatrazine.

REFERENCES

1 D. Barceló, C. Porte, J. Cid and J. Albaigés, *Int. J. Environ. Anal. Chem.*, 38 (1990) 199.
2 G. Durand, R. Forteza and D. Barceló, *Chromatographia*, 28 (1989) 597.
3 N. de Bertrand, G. Durand and D. Barceló, *J. Environ. Sci. Health*, A26(4) (1991) 575.
4 W. E. Pereira and C. E. Rostad, *Environ. Sci. Technol.*, 24 (1990) 1400.
5 *Agricultural Chemicals in Ground Water: Proposed Pesticide Strategy*, Environmental Protection Agency, Washington, DC, 1987, pp. 21–27.
6 C. D. Watts, L. Clark, S. Hennings, K. Moore and C. Parker, in *Pesticides: Analytical Requirements for Compliance with EEC Directives* (*Water Research Pollution Report*, 11), Commission of the European Communities, Brussels, 1989, pp. 16–34.
7 C. J. Miles, M. L. Treehy and R. A. Yost, *Bull. Environ. Contam. Toxicol.*, 41 (1988) 838.
8 G. Durand and D. Barceló, *Anal. Chim. Acta*, 243 (1991) 259.
9 L. Marcheterre, G. G. Choudhry and G. R. B. Webster, *Rev. Environ. Contam. Toxicol.*, 103 (1988) 61.
10 N. L. Wolfe, R. G. Zepp and D. F. Paris, *Water Res.*, 12 (1978) 565.
11 V. Samanidou, F. Fytianos, G. Pfister and M. Bahadir, *Sci. Total Environ.*, 76 (1988) 85.
12 G. Durand, D. Barceló, J. Albaigés and M. Mansour, *Chromatographia*, 29 (1990) 120.
13 J. D. Rosen, R. F. Strusz and C. C. Still, *J. Agric. Food Chem.*, 17 (1969) 206.
14 A. Chuckwudebe, R. B. March, M. Othman and T. R. Fukuto, *J. Agric. Food Chem.*, 37 (1989) 539.
15 G. Durand and D. Barceló, *J. Chromatogr.*, 502 (1990) 275.
16 M. Eto, *Organophosphorus Pesticides: Organic and Biological Chemistry*, CRC Press, Cleveland, OH, 1974, pp. 287–294.
17 E. M. Thurman, M. Meyer, M. Pomes, Ch. A. Perry and P. Schwab, *Anal. Chem.*, 62 (1990) 2043.
18 *Aldicarb Sylfoxide: Material Safety Data Sheet*, Rhone-Poulenc, Research Triangle Park, NC, 1990, pp. 1–8.
19 G. Durand, F. Sanchez Baeza, A. Messeguer and D. Barceló, *Biomed. Environ. Mass Spectrom.*, 20 (1991) 3.
20 A. Farran, J. De Pablo and D. Barceló, *J. Chromatogr.*, 455 (1988) 163.
21 G. Durand, N. de Bertrand and D. Barceló, *J. Chromatogr.*, 562 (1991) 507.
22 Th. Cairns, E. G. Siegmund and J. J. Stamp, *Rapid Commun. Mass Spectrom.*, 1 (1987) 89.
23 R. Voyksner, T. Pack, C. Smith, H. Swaisgood and D. Chen, in M. A. Brown (Editor), *Liquid Chromatography/Mass Spectrometry. Applications in Agricultural, Pharmaceutical and Environmental Chemistry* (*ACS Symposium Series*, No. 420), American Chemical Society, Washington, DC, 1990, pp. 14–39.
24 R. D. Voyksner, W. H. McFadden and S. A. Lammert, in J. D. Rosen (Editor) *Application of New Mass Spectrometric Techniques in Pesticide Chemistry*, Wiley, New York, 1987, pp. 247–258.
25 K. S. Chiu, A. Van Langenhove and C. Tanaka, *Biomed. Environ. Mass Spectrom*, 18 (1989) 200.

26 J. E. Yager and Ch. D. Yue, *Environ. Toxicol. Chem.*, 7 (1988) 1003.
27 M. Mansour, E. Feicht and P. Méallier, *Toxicol. Environ. Chem.*, 20–21 (1989) 139.
28 C. J. Miles and H. Anson Moye, *Chromatographia*, 24 (1987) 628.
29 R. D. Voyksner, J. T. Bursey and E. D. Pellizzari, *Anal. Chem.*, 56 (1984) 1507.
30 W. M. Draper, F. R. Brown, R. Bethem and M. J. Miille, *Biomed. Environ. Mass Spectrom.*, 18 (1989) 767.
31 S. V. Hummel and R. A. Yost, *Org. Mass Spectrom.*, 21 (1986) 785.
32 K. D. Racke and J. R. Coats, *J. Agric. Food Chem.*, 36 (1988) 1067.
33 Y. Manson, E. Choshen and Ch. Rav-Acha, *Water Res.*, 24 (1990) 11.
34 E. Pellizzetti, V. Maurino, C. Minero, V. Carlin, E. Pramauro, O. Zerbinati and M. L. Tosato, *Environ. Sci. Technol.*, 24 (1990) 1559.
35 H. O. Esser, G. Dupuis, E. Ebert, C. Vogel and G. J. Marco, in P. C. Kearney and D. D. Kauffman (Editors), *Herbicides, Chemistry, Degradation and Mode of Action*, Vol. I, Marcel Dekker, New York, 1975, Ch. 2.
36 Associate Committee on Scientific Criteria for Environmental Quality (Editor), *Fenitrothion: the Effects of Its Use on Environmental Quality and Its Chemistry*, National Research Council of Canada, Publication No. NRCC 14104 of the Environmental Secretariat, 1975, pp. 83–85.
37 D. Barceló, *Biomed. Environ. Mass Spectrom.*, 17 (1988) 363.
38 E. R. Wils and A. G. Hulst, *J. Chromatogr.*, 454 (1988) 261.
39 D. Kotzias, W. Klein and F. Korte, *Chemosphere*, 4 (1974) 161.
40 D. Barceló and J. Albaigés, *J. Chromatogr.*, 474 (1989) 163.

Journal of Chromatography, 554 (1991) 251–266
Elsevier Science Publishers B.V., Amsterdam

CHROMSYMP. 2365

Polar, hydrophilic compounds in drinking water produced from surface water

Determination by liquid chromatography–mass spectrometry

H. Fr. SCHRÖDER
Institut für Siedlungswasserwirtschaft, Technical University of Aachen, Templergraben 55, W-5100 Aachen (Germany)

ABSTRACT

Drinking water produced from surface water may contain many polar, hydrophilic compounds in spite of different treatment steps such as soil filtration, ozone treatment and activated carbon filtration. Little is known about these compounds. The objectives of this work were the detection and identification by means of tandem mass spectrometry (MS–MS) coupled on-line by a thermospray interface with liquid chromatography. Quantification is possible if standard compounds are available. The different compounds in the water extracts were not only separated by means of an analytical column but also using MS–MS after loop injection bypassing the analytical column. Molecular weight information in the loop spectra (overview spectra) and collisionally induced dissociation (CID) made possible the identification of some of these compounds which cannot be eliminated in the drinking water treatment process. Identification was not only done by interpretation of the recorded daughter- and parent-ion spectra but also by comparing them with a laboratory-made daughter-ion library of polar, hydrophilic pollutants. Direct mixture analysis using MS–MS allows the detection and identification of some of the pollutants if they reach the drinking water in the course of the surface water treatment process because of their biochemical and chemical persistence and/or non-sorbability during the soil or activated carbon filtration process. The proposed method for the analysis of water for polar, non-volatile and/or thermolabile organic substances is a quick, specific and powerful technique which makes it possible to detect and identify these substances without any chromatographic separation or derivatization.

INTRODUCTION

Effluents from municipal and industrial biological waste water treatment plants contain plenty of non-biodegradable compounds when they reach rivers and streams used as receiving waters. These surface waters may serve not only for shipping and cooling purposes but also for drinking water preparation before they reach the ocean. Drinking water preparation requires various treatment steps such as biochemical, chemical and physico-chemical treatment to make this water, polluted by waste water treatment plant effluents, potable. However, in spite of all treatment steps, many non-biodegradable polar compounds cannot be eliminated completely by soil filtration [1], ozone treatment or activated carbon filtration processes because of their resistance against microbial attack and ozone treatment or non-adsorbability on acti-

0021-9673/91/$03.50

vated carbon.Therefore, these compounds reach the drinking water nearly unchecked where they can be detected by specific and/or sensitive analytical methods. Complete enrichment from water for analytical purposes seems possible only by using special techniques such as solid-phase extraction combined with lyophilization or partitioning in aqueous two-phase systems.

Most of the organic compounds in effluents from waste water treatment plants are polar [2] and/or thermolabile because of their metabolic or anthropogenic origin. Assessments of the proportion of volatile compounds in the effluents from waste water treatment plants range from 10 to 30% [3–5]. Some of these pollutants are medium- to high-molecular weight substances such as fulvic and humic acids. However, size-exclusion chromatographic studies on river Rhine samples have shown [6], nearly 40% of these polar substances are low-molecular-weight substances. Analytical methods that require volatility for the separation and detection of polar water pollutants fail [2] in this instance, *i.e.*, detector systems that work well when coupled with gas chromatographic separation systems should not be used.

Nevertheless, so far mainly gas chromatography (GC) has been used in water and waste water analysis, combined with conventional detector systems such as the flame ionization detector (FID), electron-capture detector (ECD) and photoionization detector (PID). A mass spectrometer has also been used. For the reasons mentioned above, methods that require volatility for separation and detection are useful only for non-polar compounds but unsuitable for the mainly polar pollutants occurring in water.

Liquid chromatography coupled with a specific detector such as mass or tandem mass spectrometer would help to overcome some of these problems with polar, hydrophilic pollutants. Sample pretreatment is very important here. However, high-performance liquid chromatographic (HPLC) separation of waste and surface water extracts, even after selective desorption by varying eluents with increasing polarity and selective collection of the eluates from solid-phase extraction cartridges, is hardly successful because of matrix and co-elution effects [1,7]. Normally used detector systems such as UV–VIS, fluorescence, refraction and conductivity types are unsuitable because of insufficient specificity. Even selective detectors such as the mass spectrometer are only suitable if soft ionization techniques are used. Generation of fragments in the course of the ionization process cannot be tolerated because differentiation of molecular and cluster ions and also fragment ions is not possible and leads to misinterpretation of the recorded spectra.

Coupling of HPLC on-line with thermospray ionization and mass spectrometry ensures soft ionization and the generation of mainly molecular or cluster ions. The cluster ions produced were ammonia adduct ions when ammonium acetate was used for ionization purpose.

Only few results exist from comparable analytical studies of waste waters [1,2,7–9]. A little work on surface waters has been done using grab samples [1,7,10–14]. Rivera and co-workers [10–14] analysed in detail activated carbon extracts from filters of a drinking water treatment plant in Barcelona. They used off-line fast atom bombardment mass spectrometry (FAB-MS) and collisionally induced dissociation mass-analysed ion kinetic energy spectrometry (CID-MIKE). The examinations carried out so far confirm the observation that results obtained with detection methods such as FID, ECD and PID after GC separation only pretend clean water, drinking,

surface and waste water, and polar compounds could not be detected.

The aim of this work was to use on-line coupling of LC with tandem mass spectrometry by thermospray (LC–TSP-MS–MS) for the analysis of surface water being used for drinking water preparation. The pollutants dissolved in this water should be detected and identified as completely as possible during surface water treatment by soil filtration, ozone treatment and activated carbon filtration.

EXPERIMENTAL

Materials

Water pollutants were extracted using solid-phase extraction cartridges from Baker (Deventer, Netherlands). Solid-phase extraction materials were conditioned as prescribed by the manufacturer. Glass-fibre and membrane filters used for the pre-treatment of the water samples were obtained from Schleicher & Schüll (Dassel, Germany). Before use the glass-fibre and membrane filters were heated to 400°C or were treated with ultra-pure water obtained with a Milli-Q system (Waters Assoc., Milford, MA, USA) for 24 h and then washed with 100 ml of the same water. Hexane, diethyl ether, methanol and dichloromethane used for the desorption of water pollutants from the solid-phase material were Nanograde solvents from Promochem (Wesel, Germany). Nitrogen for drying of solid-phase cartridges was of 99.999% purity (Linde, Germany). All surfactant standards were gifts from the producers (Hüls, Marl; Hoechst, Frankfurt; BASF, Ludwigshafen; and Rewo, Steinau, Germany) and were of technical grade.

GC analyses were done on a DB-17 fused-silica column (J&W Scientific, Folsom, CA, USA) and helium (Linde) was used as the carrier gas. HPLC separations were done on a μBondapak C_{18} (5 μm) column (30 cm × 3.9 mm I.D.) (Waters). The mobile phase was methanol (HPLC grade) from Promochem and Milli-Q purified water. The ammonium acetate for thermospray ionization was of analytical-reagent grade from Merck (Darmstadt, Germany).

Sampling and sample preparation

All samples from the waste water treatment plant, surface waters and the drinking water treatment plant were taken as grab samples in glass bottles. The bottles were rinsed carefully with several portions of the same water that was subsequently stored in them. The storage temperature was 4°C.

Depending on the degree of pollution, different amounts of water were used for solid-phase extraction. Water samples were forced through the solid-phase extraction cartridges after passage through a glass-fibre filter. To ensure complete adsorption, the water samples were forced through two cartridges in series. The adsorbed pollutants were desorbed separately. Solvents of different polarities (hexane, hexane–diethyl ether, diethyl ether, water–methanol, methanol and dichloromethane) were used for this purpose. All eluates except those with methanol and methanol–water were evaporated to dryness with a stream of nitrogen and the residue was dissolved in methanol. The samples were rinsed into glass bottles after solid-phase extraction, and freeze-drying was applied to enrich non-C_{18}-adsorbable compounds. Samples containing high chloride concentration were mixed with silver ions to precipitate and separate the silver chloride before lyophilization. After freeze-drying, the samples

were dissolved in methanol and used for MS investigations. Loaded activated carbon from filters from the waste water treatment plant was dried by lyophilization and extracted with methanol.

Quantification

A 19-l volume of drinking water was enriched on a C_{18} solid-phase extraction column. Elution was effected with different eluents of increasing polarity. The combined eluates were evaporated to dryness under a stream of nitrogen and the residue was dissolved in a known volume of methanol.

Flow-injection analysis (FIA) for quantification was applied, recording mass spectra beginning at *m/z* 350 and ending at *m/z* 800 for quantification of nonanol polypropylene glycol ether. The compositions of the mobile phases for FIA were as follows: mobile phase I, methanol–water (60:40); mobile phase II, 0.1 *M* ammonium acetate in water. The overall flow-rate was 1.5 ml/min with a ratio of 0.8 ml/min of mobile phase I and 0.7 ml/min of mobile phase II.

Areas under the peaks of the mass traces of the cluster ions of *m/z* 394, 452, 510 and 568 from water extracts were determined and compared with a calibration graph obtained with standard solutions of 0.1, 0.5 and 1.0 mg/l of the surfactant mixture Degressal in methanol.

Gas chromatographic system

A Varian (Darmstadt, Germany) Model 3400 GC system with a fused-silica capillary column was used. The conditions were as follows: carrier gas, helium; linear gas velocity, 15 cm/s; injector temperature, 250°C; transfer line temperature, 250°C; column, DB-17, film thickness 0.25 μm, 30 m × 0.25 mm I.D.

Combined with GC, electron impact (EI) ionization was applied with an ionization energy of 70 eV. Under these conditions the pressure in the ion source was 8×10^{-6} Torr and in the manifold 3×10^{-2} Torr. The electron multiplier was operated at 1200 V with a dynode voltage of 5 kV. The temperature in the ion source was 150°C.

Liquid chromatographic system

LC separations coupled with MS, MS–MS and UV detection were achieved with a Waters Assoc. (Milford, MA, USA) Model 600 MS system. A Waters Model 510 pump was used for post-column addition of 0.1 *M* ammonium acetate solution in the TSP mode. A Waters Model 490 MS UV detector was connected in-line with the TSP interface. The conditions in FIA bypassing the analytical column were as given above. The chromatographic conditions for separations on the analytical column varied and are specified in the legends of the figures.

Direct chemical ionization (DCI)

For DCI spectra a triple-stage quadrupole mass spectrometer (TSQ 70) from Finnigan MAT (San Jose, CA, USA) was used. The temperature at the beginning of the DCI experiments was 50°C and at the end 450°C, with a gradient of 800°C/min.

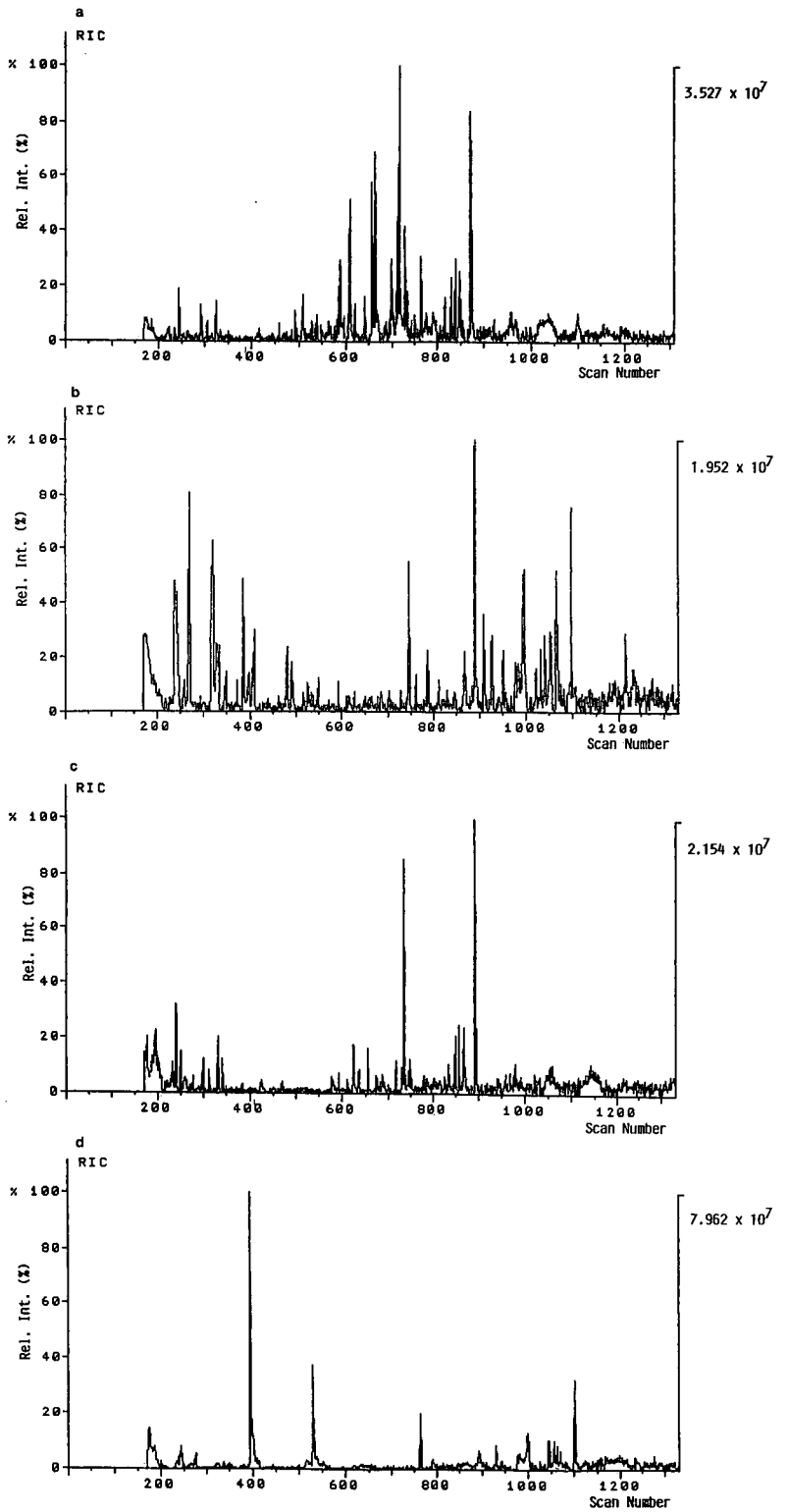

Fig. 1. GC–MS total ion current traces for (a) river Rhine water, (b) soil filtrate, (c) ozone-treated soil filtrate, (d) activated carbon filtrate drinking water. C_{18} solid-phase extract; eluent, methanol.

MS and MS–MS systems

The mass spectrometer was a TSQ 70 combined with a PDP 11/73 data station. The TSP interface was obtained from Finnigan MAT. For coupling the HPLC system with the mass spectrometer, the following conditions were chosen: vaporizer temperature, 90°C; jet block temperature, 200°C; aerosol temperature, 190°C. The conditions varied during the analytical separations. Under the above conditions the ion source pressure was 0.5 Torr and the pressure in the manifold was $2 \cdot 10^{-5}$ Torr.

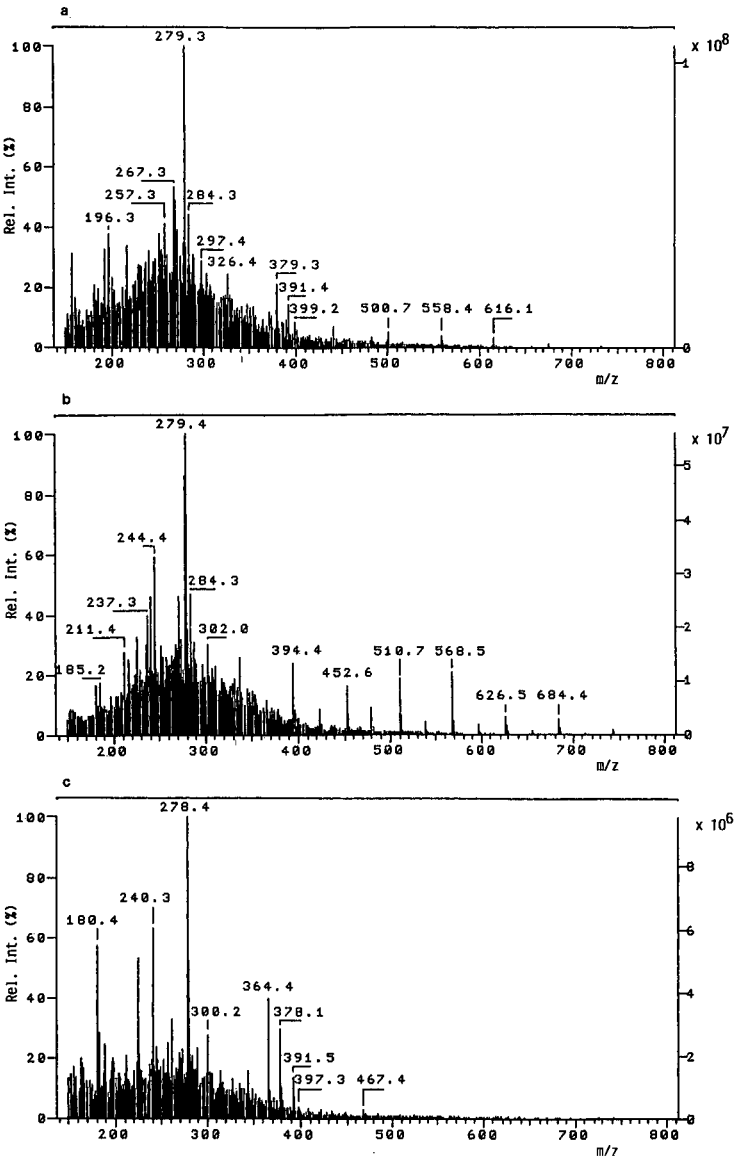

Fig. 2.

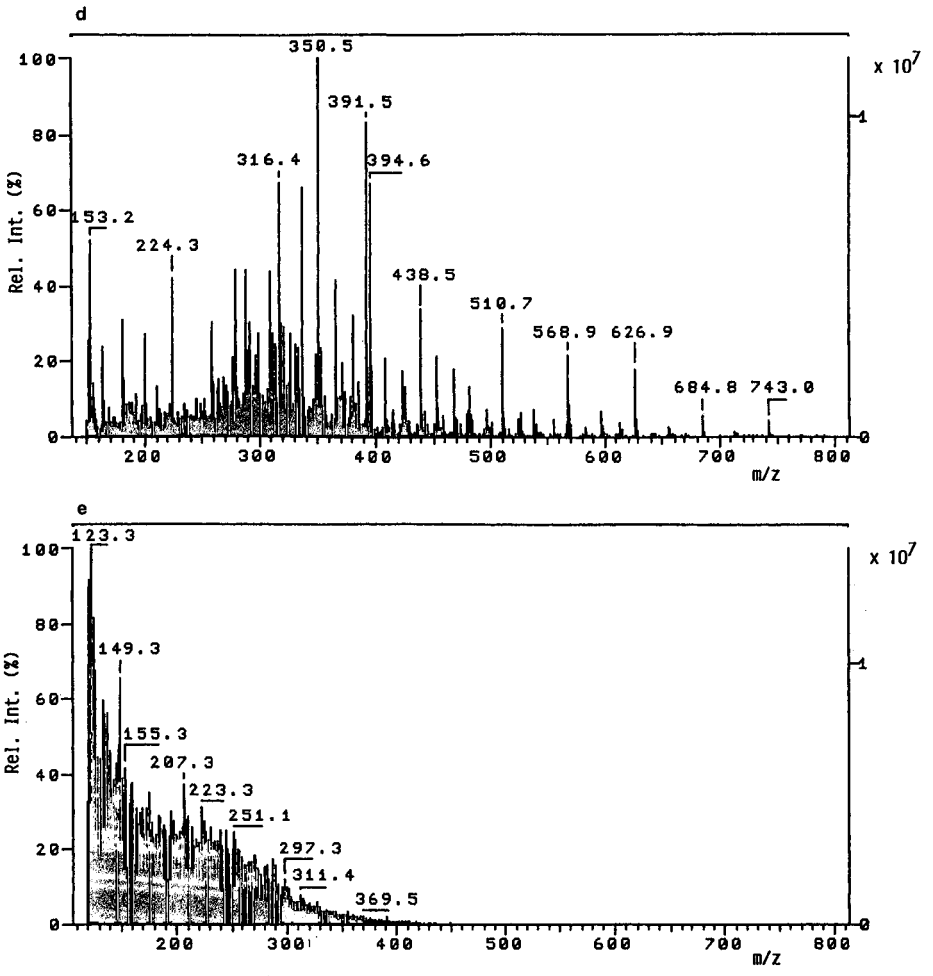

Fig. 2. LC–TSP-MS loop injection spectra (bypassing the analytical column) of solid-phase extracts of (a) river Rhine water, (b) soil filtration, (c) ozone-treated soil filtrate and (d) activated carbon filtrate (drinking water). (e) DCI spectrum of a drinking water extract. Compare Figs. 1d and 2d.

The electron multiplier was operated at 1200 V and the dynode at 5 kV. In the MS–MS mode the ion source pressure was also 0.5 Torr. Under CID conditions the pressure in quadrupole 2 (collision cell) was 1.3 mTorr. The electron multiplier voltage in quadrupole 3 was 1500 V with a dynode voltage of 5 kV.

RESULTS AND DISCUSSION

Water samples were taken from a drinking water treatment plant of a German city located on the river Rhine. During the drinking water preparation process, grab samples taken from the river Rhine, soil-filtered water, soil-filtered and ozone-treated water and drinking water after activated carbon filtration were analysed.

The Rhine is polluted by numerous voltatile and non-volatile organic compounds. Fig. 1a, the GC–MS total ion current profile of a river Rhine extract, shows the volatile compounds. Many of these pollutants can be identified by a library search using the NBS library of electron impact spectra.

Many more compounds appear if a LC–MS overview spectrum of this extract is generated, bypassing the analytical column (Fig. 2a). The TSP soft ionization process generates mainly molecular and cluster ions of defined chemical substances differing from each other only in their ratio of mass to charge (m/z).

To obtain molecular weight information, the pollutants occurring in the drinking water preparation process were detected by LC–TSP-MS. Identification was achieved by LC–TSP-MS–MS, generating the daughter ions essential for structural information. For comparison purposes the same extracts were also analysed by direct chemical ionization (DCI-MS).

A library of daughter-ion spectra for LC–MS research work comparable to the NBS EI mass spectral library of volatile compounds was not available. Therefore, identification has to be achieved by standard retention time comparisons after chromatographic separation and/or by the difficult process of interpreting the daughter-ion spectra.

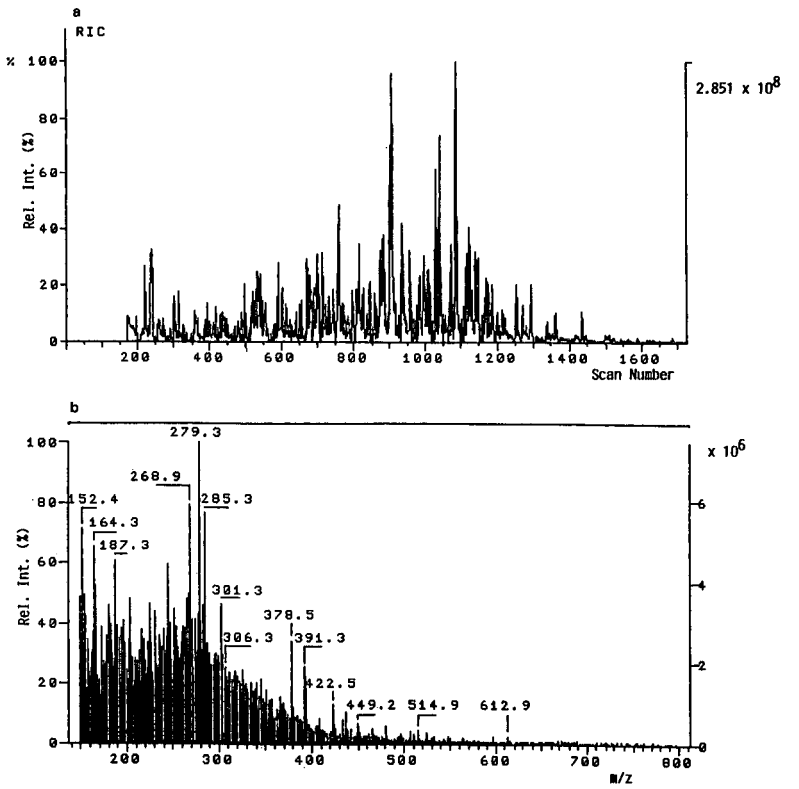

Fig. 3. (a) GC–MS total ion current trace and (b) LC–MS loop injection spectrum (bypassing the analytical column) of activated carbon filter extract. Solvent, methanol.

LC–TSP-MS is a selective ionization technique especially for polar molecules. Therefore, not all compounds in the extracts will be ionized, but as polar molecules are the dominant compounds in waste and surface waters, this ionization technique seemed to be very appropriate to the present research. Estimates of concentrations can only be made after calibration with standard compounds.

Phthalate esters can be recognized in Fig. 2a, the LC–MS overview spectrum of a river Rhine extract, at m/z 279 and 391. Compounds at m/z 442, 500, 558 and 616 can be identified as polypropylene oxide-containing pollutants because of their equidistant masses of $\Delta m/z = 58$.

The concentrations and number of the TSP-active pollutants decrease from one step to the next in the treatment process, *i.e.*, soil filtration, ozone treatment and activated carbon filtration (Fig. 2a–d). This applies to the volatile substances, the GC–MS profiles of which are shown in Fig. 1a–d. In the LC–MS overview spectra only the concentration decreases but the actual number of compounds does not change obviously.

Unfortunately, it was impossible to take time-successive samples, beginning with the river Rhine via the different stages of water treatment, and ending with drinking water. So the advance of the pollutants in the different stages of water treatment in relation to the retention time could not be followed.

As mentioned before, the number of slightly polar and non-polar compounds decreases whereas the number of polar compounds does not change (see Fig. 2a–d). Therefore, the signals of the polar compounds now arise from the background after the disappearance of those for slightly polar and non-polar compounds and then dominate the appearance of the overview spectra.

Comparison of DCI-MS with LC–TSP-MS analysis using ammonia gas or ammonium acetate, respectively, to generate the same ions from the same extract showed that TSP ionization is a softer ionization technique than DCI. More undesirable fragmentations and none of the higher molecular weight compounds could be observed in the DCI spectrum (Fig. 2e). Therefore, LC–TSP-MS was to be preferred for solving our problems with polar, thermolabile compounds.

As GC–MS and LC–MS demonstrate (compare Fig. 1a with 1b and Fig. 2a with 2b), adsorption effects and biochemical degradation seem to be the dominating effects in soil filtration. In this way many non-polar compounds were retained and/or metabolized by bacteria and became more polar. Activated carbon filtration eliminates many non-polar volatile compounds, as the GC profile of the activated carbon extracts shows (Fig. 3a). The LC–MS overview spectrum of the same extract (Fig 3b) is also crowded by many signals.

Phthalate esters can be identified immediately in this activated carbon filter at m/z 279 and 391. Polar compounds containing ethoxylate or propoxylate chains such as non-ionic surfactants cannot be observed in the full-scan spectra because these hydrophilic compounds were hardly adsorbed on activated carbon. Although they were adsorbed at low concentrations, the signals in the overview spectra were suppressed by the strong signals of non-polar and slightly polar compounds that were well adsorbed by the activated carbon. Normally these very hydrophilic compounds pass through activated carbon filters unchecked.

As it was difficult to identify the compounds in the LC–MS overview spectra in Fig. 2a–d, we tried to separate these mixtures of pollutants on an analytical column.

In this way it might perhaps be possible to concentrate some of these compounds by focusing and to make identification by CID easier.

Although the chromatographic conditions were varied systematically by changing the analytical columns from C_2 via C_8 to C_{18} and the composition of the mobile phases (gradient elution with 5, 10 and 20% of acetonitrile), the separation compared with the GC–MS profiles remained poor. As an example, Fig. 4a shows one of these LC–MS profiles for the different water treatment stages (extract of soil filtrate) recorded after time-consuming optimization efforts.

The appearance of the LC–MS profile shown is bad, but the UV trace at 220 nm (Fig. 4b), recorded parallel to LC–MS total ion current measurement, is worse. It is notable, however, that many of the TSP-active compounds show only little absorbance at 220 nm and the drinking water extract does not show any absorbance in the UV region at 254 nm. None of these polar and hydrophilic pollutants has any chro-

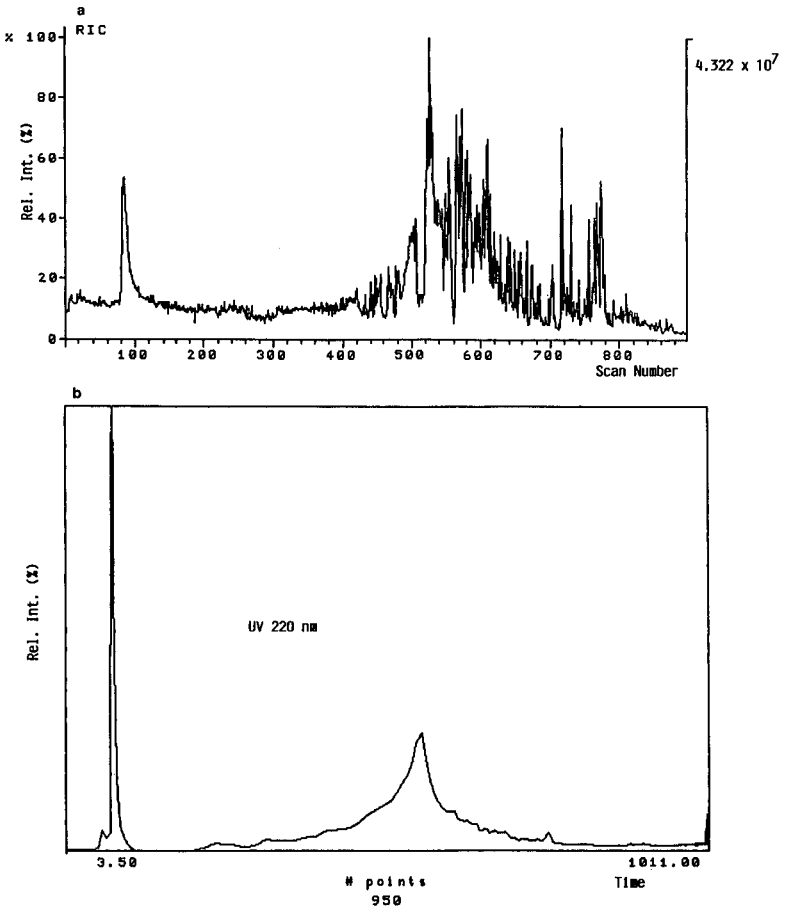

Fig. 4. (a) LC–TSP-MS total ion current trace from extract of Fig. 1b. Soil filtration; C_{18} column; mobile phase, methanol–water, gradient from 100% water to 100% methanol in 30 min. (b) UV (220 nm) trace of soil filtration extract; compare with (a). LC conditions as in (a).

mophore active in the higher UV ranges, which is essential for absorbance. This makes LC–TSP-MS analysis very useful for the detection of polar pollutants in water. On the other hand, non-polar but volatile compounds are sensitive to UV radiation but cannot be ionized by TSP. Therefore, the method of choice for volatile compounds is GC–MS, whereas LC–TSP-MS or electrospray (ESP) is very specific to polar and slightly polar compounds. Using these ionization techniques is often the only way to detect these substances.

A well established and useful method for the analysis of pollutants separated and detected by GC–MS or LC–MS may be analysis by mass chromatograms. In our investigations this seemed to be the only way to follow pollutants in river Rhine water or after soil filtration, up to the stage of drinking-water after activated carbon filtration. In this way mixtures of poorly separated compounds may be analysed more easily.

The ineffectiveness of the different treatment steps with some of these pollutants is notable. In LC–MS overview spectra of soil filtration and drinking water extracts (Fig. 2a and d), ions at m/z 394 and 452 are present, *i.e.*, ozone treatment and activated carbon filtration of the raw water are inefficient in eliminating these pollutants. Owing to this behaviour, in Germany these compounds are called "drinking water relevant compounds", which resist all purification efforts. Even the non-specific but strong oxidizing agent ozone fails to destroy these molecules.

This behaviour was also observed when waste water containing non-ionic surfactants was treated with ozone [7]. Further, the 44 a.m.u. spaced ion series pointed to widely used non-ionic surfactants with poly(ethylene oxide) chains which are non-biodegradable and, as shown here, poorly degradable by ozone. The oxidation in this type of anthropogenic molecule has proceeded to the maximum extent and seems to prevent further oxidation.

After the detection of the pollutants and tentative identification of these polar, hydrophilic compounds which cannot be eliminated in the drinking water treatment process, the possibilities for identification will now be discussed.

To identify these pollutants with the proposed LC–TSP-MS–MS system, different approaches were possible:

(1) Separation of the mixture of pollutants on an analytical column and comparison of retention times with those of standards, if available. Not only MS but also UV detection could be employed. However, a lack of standards and perhaps missing chromophores in the pollutants, respectively, would prevent these identification methods from being used.

(2) If this separation were successful, we should obtain information about retention times and, as the TSP soft ionization technique is used, about molecular weight. Generation of daughter ions by CID from column-separated pollutants would have given structural information for the identification of unknown compounds.

(3) The most promising alternative with regard to time and manpower was the analysis of mixture using MS–MS. Samples with complex matrices [15,16] and/or environmental samples [1,2,7,9,17] have been analysed using CID and series of neutral loss and parent-ion scans under data system control on a triple-stage quadrupole instrument. The mixtures were volatilized directly into the ion source of the MS–MS instrument, whereas we used a TSP interface between the liquid chromatograph and

the triple-stage quadrupole mass spectrometer. To solve the problems of polar pollutants in this work we used the mass filter in quadrupole 1 to separate the ions after loop injection bypassing the analytical column. CID was done in quadrupole 2. In quadrupole 3 daughter and parent ions and neutral loss scans could be recorded to obtain structural information.

As mentioned before, lack of standards would prevent the first approach to identification. However, even if standards were available, a complex matrix in these mixtures could also prevent separation, as observed with a polyethylene glycol (PEG)-containing sample. Although the more sensitive and selective procedure of generating mass traces was applied, no separation could be observed. Co-elution effects disturbed the chromatographic separation of PEG on a C_{18} column, as shown in Fig. 5a. In contrast, Fig. 5b shows a very good LC–MS profile of PEG separation under the same chromatographic conditions.

If the time-consuming separation of pollutants was successful and could be verified by mass chromatograms, CID of focused pollutants should be carried out to obtain daughter-ion spectra of unknown compounds. Comparing one of the CID spectra from the column separation (Fig. 6a) with library spectra in our laboratory-made library on the Finnigan TSQ 70 generated from hydrophilic, polar compounds, the identification was successful. The plot of the library search gives three alternatives

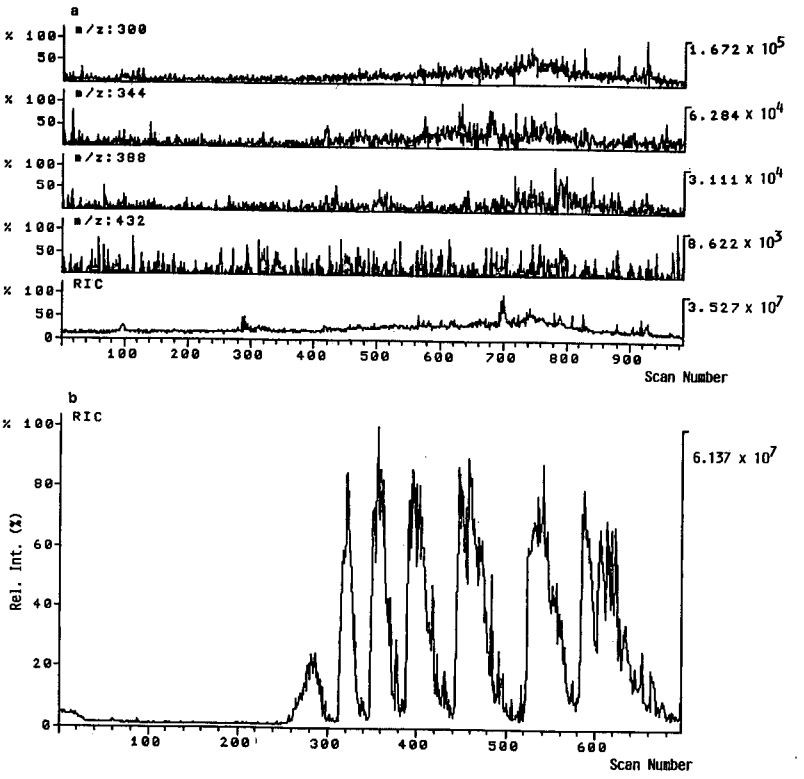

Fig. 5. LC–TSP-MS mass traces and total ion currents of (a) drinking water extract (C_{18}) and (b) polyethylene glycol standard. LC conditions as in Fig. 4a.

a

```
SPEC: THD ver 5 on UIC 2 4              25-JAN-90 DERIVED SPECTRUM      9
Samp: 3 E I                                       Start : 13:39:00     10
Comm: COLUMN / DAU 1.3
Mode: TSP +DAU 394.5 @ -30eV LMR SYNTH GAS UP LR
Oper: RS                                          Inlet :
Base: 377.0                Inten : 892985         Masses: 30 > 420
Norm: 377.0                RIC   : 14666139      # peaks: 487
Peak: 1000.00 mmu
Data: +  653 > 662
```

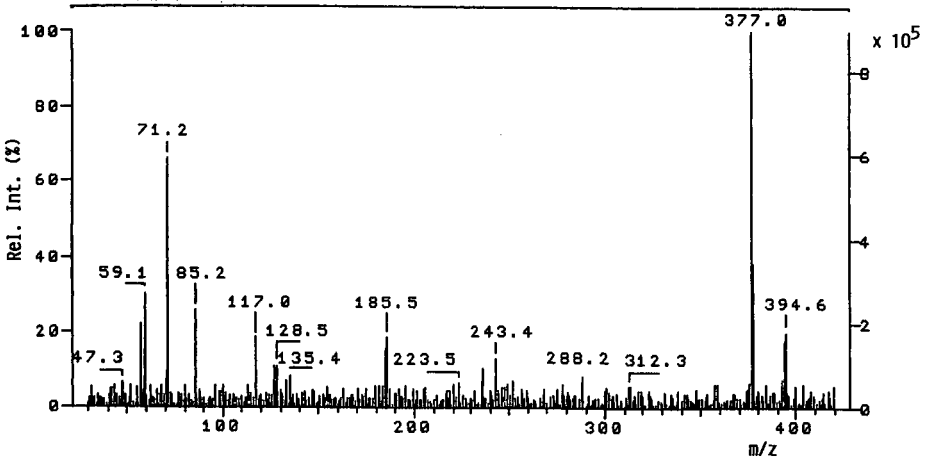

b

```
LIBR: THD ver 5 on UIC 2 4              25-JAN-90 DERIVED SPECTRUM      9
Samp: 3 E I                                       Start : 13:39:00     10
Comm: COLUMN / DAU 1.3
Mode: TSP +DAU 394.5 @ -30eV LMR SYNTH GAS UP LR
Oper: RS                                          Inlet :
Base: 377.0                Inten : 892985         Masses: 30 > 420
Srch: purity          Samp mass: all              Libr wt: all
Libr: ABC                          Defect: 0 @ 1, 300 @ 1000
Data: +  653 > 662

1      8 DEGRESSAL                                              SD 20
   Purity: 312  FiT: 844  Rfit: 343  mw:   394 bp:  377.0
   CAS#:

2     87 PLURAFAC                                               LF 120
   Purity: 189  FiT: 701  Rfit: 223  mw:   394 bp:  377.0
   CAS#:

3    110 TRITON                                                 DF 20
   Purity: 121  FiT: 416  Rfit: 272  mw:   378 bp:  378.0
   CAS#:
```

Fig. 6. Results of library search in laboratory-made library. (a) Daughter-ion spectrum from water extract; (b) proposed list for identification.

(Fig. 6b) for the compound which had to be identified. The pollutant, an anthropogenic, non-ionic surfactant, was a mixture of nonanol polypropylene glycol ethers. This could additionally be proved using the standard for generating the daughter ions and comparing them with the daughter ions of the unknown compound.

In contrast to this time- and manpower-consuming method of separation on an analytical column, direct mixture analysis [18,19] of the same extracts was done using MS–MS function. In this way ions of *m/z* 394 in the extract of soil-filtered water and *m/z* 452 in drinking water were separated by mass filtration. Daughter-ion spectra of *m/z* 394 (Fig. 7a) and *m/z* 452 (Fig. 7b) generated by CID do not show a very clean

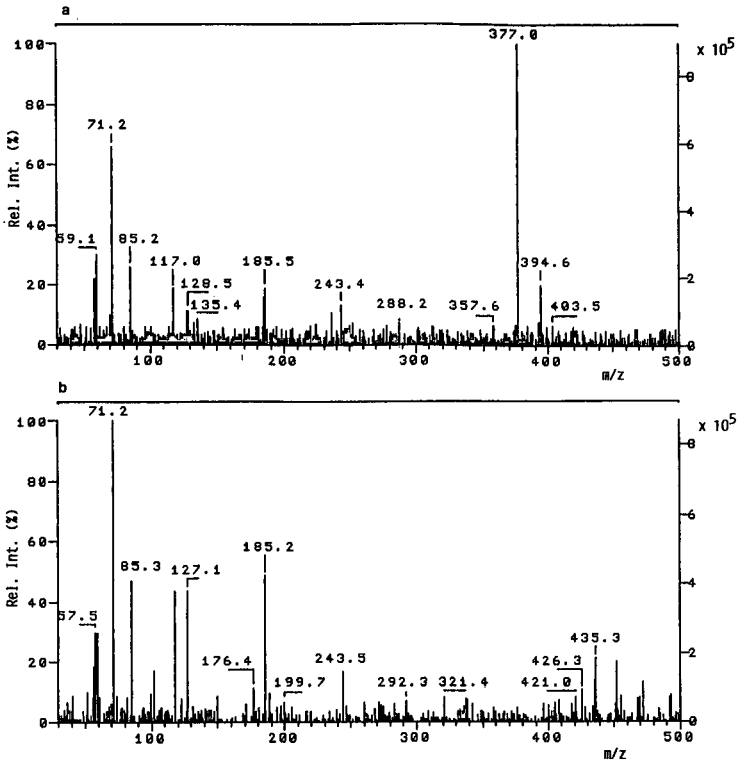

Fig. 7. TSP–MS–MS (daughter-ion spectrum bypassing the analytical column) of (a) *m/z* 394 (soil filtration extract) and (b) *m/z* 452 (drinking water extract).

background, although both spectra correspond well with the daughter-ion spectra of the standard in our laboratory-made library. The fragmentation behaviour under CID conditions and the safety data sheet of the producer confirmed the result of the interpretation of the daughter-ion spectrum, as shown in Fig. 8. The identification of this nonanol polypropylene glycol ether by mixture analysis was done in 10 min using the MS–MS function of the tandem mass spectrometer for daughter-ion generation and comparison of the recorded daughter-ion spectra with the library spectra.

In contrast, chromatographic separation before fixing the conditions for daughter-ion generation and the subsequent separation with simultaneous CID of the selected ions took 3.5 h.

FIA, bypassing the analytical column, allows the quantification of the identified mixture of nonanol polypropylene glycol ethers in drinking water. Peak areas under the mass traces of the cluster ions of *m/z* 394, 452, 510 and 568 from the drinking water extract were compared with the results for the same ions of a standard (Degressal) using a calibration graph. In this way we found 5 μg/l of the above ether in the mixed eluates (diethyl ether–hexane, diethyl ether and methanol) after C_{18} enrichment. Calculations relating to the dissolved organic carbon (DOC) content of the drinking water showed that about 0.1% DOC is induced by this polypropylene glycol ether mixture.

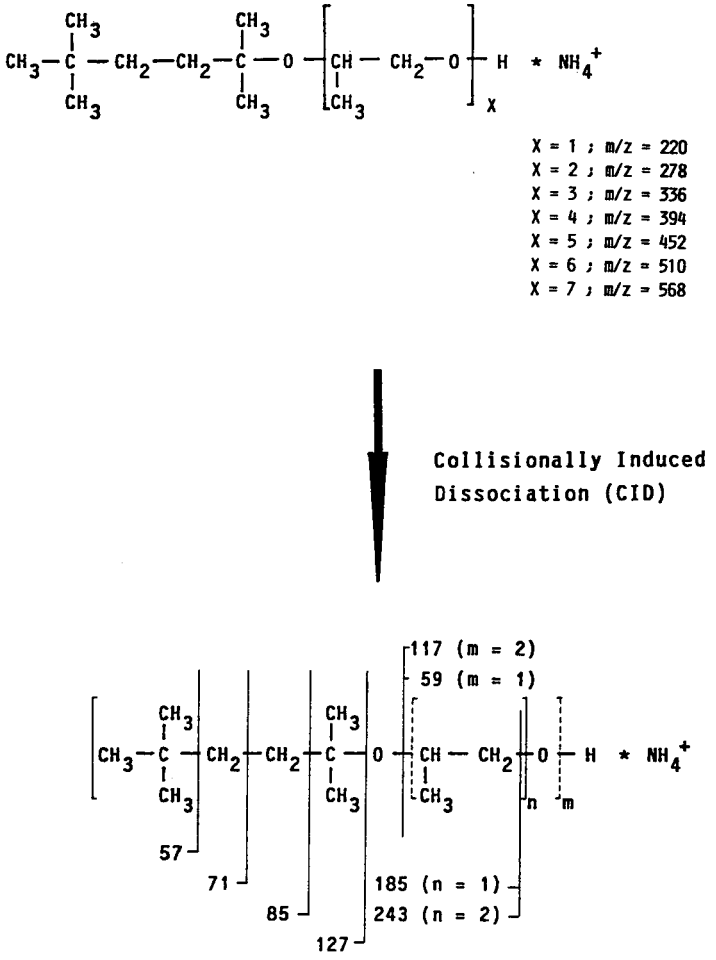

Fig. 8. Molecular ion (cluster ion) and fragmentation pattern of nonanol polypropylene glycol ether under CID conditions. Argon pressure, 1.3 mTorr.

CONCLUSIONS

LC separations of polar, hydrophilic water pollutants can be very difficult because of the complex matrix in these samples. Direct mixture analysis by LC–MS–MS for unknown polar, thermolabile compounds is an excellent and powerful method that is able to detect and identify many compounds from complex matrices without time-consuming derivatization and separation. Soft ionization of the compounds is essential for identification in order to obtain mainly molecular or cluster ions. After identification, quantification by mixture analysis is easy if standards for calibration are available.

Working in the MS–MS mode, daughter ions of the parent ions which have been selected by mass filtration give structural information because of their fragmentation behaviour under CID conditions. On the other hand, DCI is not suitable

for these problems because of extensive fragment generation. Soft ionization interfaces such as TSP can be used to suppress this fragmentation in the ionization process. Even slight fragmentation in this process can make chromatographic separation necessary or may lead to misinterpretation of the spectra.

The use of GC–MS for waste-, surface- and drinking water examinations is successful only with volatile compounds. In GC–MS analysis derivatization is essential for the chromatographic separation of the polar compounds, but this procedure discriminates non-reactive molecules.

Many compounds could still be detected in drinking water samples in spite of all previous efforts to eliminate them. So far only a few could be identified and recognized as anthropogenic substances. Their toxicological and ecotoxicological potential under chronic use must be checked.

ACKNOWLEDGEMENTS

The author acknowledges financial support by the German Minister for Research and Technology in project 02 WT-87332. The author thanks Mr. Scheding, Mr. Lohoff and Mr.Gschwendtner for their support in recording spectra and preparing numerous samples.

REFERENCES

1 H. Fr. Schröder, in DVGW Deutscher Verein des Gas- und Wasserfaches e.V. (Editor), *DVGW-Schriftenreihe Wasser*, No. 108, Wirtschafts- und Verlagsgesellschaft Gas und Wasser mbH, Bonn, 1990, pp. 121–144.
2 H. Fr. Schröder, *Vom Wasser*, 73 (1989) 111.
3 M. Sonneborn, in B. Böhnke (Editor), *Gewässerschutz, Wasser, Abwasser*, GWA 67, Gesellschaft zur Förderung der Siedlungswasserwirtschaft an der RWTH Aachen e.V., Aachen, 1983, pp. 123–142.
4 C. D. Watts, B. Crathorne, R. I. Crane and M. Fielding, in L. H. Keith (Editor), *Advances in the Identification and Analysis of Organic Pollutants in Water*, Vol. 1, Ann Arbor Sci. Publ., Ann Arbor, MI, 1981, pp. 383–398.
5 K. Levsen, in Commission of the European Communities, *Analysis of Organic Micropollutants in Water*, Reidel, Dordrecht, 1981, pp. 149–158.
6 R. Gimbel and H. Sontheimer (Editors), *Abschlussbericht Forschungsvorhaben 02-WT 86290, Erprobung und Weiterentwicklung eines Testfilters zur frühzeitigen Erkennung von unerwünschten Qualitätsbeeinträchtigungen bei Uferfiltratwasserwerken*, Bundesminister für Forschung und Technologie, Bonn, 1988.
7 H. Fr. Schröder, *Water Sci. Technol.*, 23 (1991) 339.
8 H. Fr. Schröder, in B. Böhnke (Editor), *Gewässerschutz, Wasser, Abwasser*, GWA 95, Gesellschaft zur Förderung der Siedlungswasserwirtschaft an der RWTH Aachen e.V., Aachen, 1987, pp. 347–365.
9 H. Fr. Schröder, in B. Böhnke (Editor), *Gewässerschutz, Wasser, Abwasser*, GWA 112, Gesellschaft zur Förderung der Siedlungswasserwirtschaft an der RWTH Aachen e.V., Aachen, 1990, pp. 351–384.
10 J. Rivera, J. Caixach, F. Ventura, D. Fraisse and G. Dessalces, presented at the *10th International Mass Spectrometry Conference, Swansea, September 1985*.
11 J.Rivera, F.Ventura, J. Caixach, D. Fraisse and G. Dessalces, in J. F. J. Todd (Editor), *Advances in Mass Spectrometry*, Wiley, Chichester, 1986, pp. 1453–1454.
12 J. Rivera, F. Ventura, J. Caixach, A. Figueras, D. Fraisse and V. Blondot, in A. Bjorseth and G. Angeletti (Editors), *Organic Micropollutants in the Aquatic Environment*, Reidel, Dordrecht, 1986, pp. 77–88.
13 J. Rivera, F. Ventura, J. Caixach, M. de Torres, A. Figueras and J. Guardiola, *Int. J. Environ. Anal. Chem.*, 29 (1987) 15.
14 F. Ventura, A. Figueras, J. Ciaxach, I. Espadaler, J. Romero, J. Guardiola and I. Rivera, *Water Res.*, 22 (1988) 1211.
15 K. V. Wood, C. E. Schmidt, R. G. Cooks and B. D. Batts, *Anal. Chem.*, 56 (1984) 1335.
16 D. F. Hunt, A. B. Giordani, G. Rhodes and D. A. Herold, *Clin. Chem.*, 28 (1982) 2387.
17 D. F. Hunt, J. Shabanowitz, T. M. Harvey and M. Coates, *Anal. Chem.*, 57 (1985) 525.
18 H. Schwarz, *Nachr. Chem. Tech. Lab.*, 29 (1981) 687.
19 J. Johnson and R. Yost, *Anal. Chem.*, 57 (1985) 758A.

Journal of Chromatography, 544 (1991) 267–280
Elsevier Science Publishers B.V., Amsterdam

CHROMSYMP. 2192

Liquid chromatography–mass spectrometry in metabolic research

I. Metabolites of benzbromarone in human plasma and urine

P. J. ARNOLD, R. GUSERLE and V. LUCKOW*
Pharmakin GmbH, Graf-Arco-Strasse 3, 7900 Ulm (Germany)
R. HEMMER
Center for Solar Energy and Hydrogen Research, 7900 Ulm (Germany)
and
H. GROTE
Schwarz Pharma AG, 4019 Monheim (Germany)

ABSTRACT

Seven benzbromarone metabolites were identified in human plasma and urine by electron-impact mass spectrometry after semipreparative high-performance liquid chromatographic fractionation and/or by liquid chromatography–mass spectrometry using a thermospray interface. The major metabolite in plasma and urine was a hydroxybenzofuranoyl species; the 1-hydroxyethyl entity was identified as a minor metabolite. Five urinary metabolites occurred in trace amounts, all of them carrying OH and/or C=O groups in different positions. The hydroxybenzofuranoyl metabolite has often been mistaken for benzarone in previous studies.

INTRODUCTION

Benzbromarone, 3,5-dibromo-4-hydroxyphenyl-2-ethyl-3-benzofuranyl ketone (BzB), is a uricosuric drug whose metabolism was first investigated by Broekhuysen *et al.* [1] using ^{3}H-labelled BzB in patients. They concluded that it is debrominated successively to form bromobenzarone (BBz) and benzarone (Bz) in phase I followed by appreciable glucuronidation in phase II. However, these authors failed to provide any information whatsoever about identification of the metabolites. Later, Vergin and Bishop [2], who developed a high-performance liquid chromatographic (HPLC) procedure to determine BzB and its putative metabolites in plasma and urine, partly corroborated these results by investigating BzB and Bz pharmacokinetics after oral application of 100 mg BzB in seven subjects [3]. These authors did not detect any BBz. Their only means of identifying analytes was HPLC retention times.

In a pharmacokinetic study using oral doses of 100 mg BzB in ten humans, we detected two plasma metabolites, one of which differed from Bz in its HPLC retention

0021-9673/91/$03.50

time by only 9 s. The retention time of the other metabolite did not coincide with any of the putative metabolites. BBz was below the limit of detection (20 ng/ml) in 240 plasma samples. Meanwhile, one of these metabolites has independently been identified as the 1-hydroxyethyl derivative of BzB by De Vries *et al.* [4] using gas chromatography–mass spectrometry (GC–MS) techniques after trimethylsilylation.

The work described in this paper was undertaken to identify this and six more BzB metabolites in human plasma and urine after the administration of therapeutic doses by applying HPLC and liquid chromatography–mass spectrometry (LC–MS) methods.

EXPERIMENTAL

Sample preparation

One male human subject received 100 mg BzB once daily for 4 days. Two hours after the first dose, a 60-ml blood sample was withdrawn. Plasma was obtained by centrifugation. The total urinary output was collected in 24-h fractions. The fractions were lyophilized and redissolved in 100 ml of 0.1 *M* acetate buffer (pH 5). Glucuronic acid conjugates in plasma and urine were hydrolyzed by digestion with β-glucuronidase from *Escherichia coli* (Boehringer Mannheim, Mannheim, Germany). A 50-μl sample of enzyme solution (200 U/ml at 37°C) was added to 1-ml samples of plasma or concentrated urine and kept at 37°C overnight.

Since only minor traces of free metabolites were found in urine and the highest concentration of conjugates proved to be in the fraction after the third dose, this fraction was treated entirely with β-glucuronidase for further investigations.

For clean-up, plasma and concentrated urine were acidified by addition of 0.25 ml of 0.1 *M* HCl per mililiter of sample and then extracted with 6 ml cyclohexane–*tert.*-butyl methyl ether (1:2, v/v) per mililiter of sample. The organic layers were centrifuged, evaporated to dryness in a gentle stream of nitrogen and redissolved in methanol for HPLC analysis.

High-performance liquid chromatography

Extracts of plasma and urine before and after digestion with β-glucuronidase were chromatographed on a Hewlett-Packard HP 1090M HPLC system using direct injection and precolumn enrichment techniques, respectively. Analytical separation was achieved by isocratic elution from a Nucleosil C_8 5-μm column (125 × 4.6 mm I.D.) at a flow-rate of 0.5 ml/min. The eluent consisted of acetonitrile and a 5 m*M* sodium dihydrogenphosphate buffer adjusted to pH 3.5 with phosphoric acid (60:40, v/v). Column temperature was maintained at 45°C. Detection was by UV absorption at 280 nm. UV spectra of unknown compounds were recorded on-line using an HP 1040 diode-array detector (Hewlett-Packard, Böblingen, Germany).

Extracts were fractionated by semi-preparative HPLC on a 250 × 8 mm I.D. column at a flow-rate of 3 ml/min, all other conditions being unchanged.

Fractions of urinary extracts were cut as follows: front cut, in 0.4-min steps; heart cut, one fraction per constituent of interest (controlled by UV detection); end cut, one fraction (including any BzB). Heart-cut and end-cut fractions were checked for purity by analytical HPLC as described above.

All fractions were further investigated by thermospray LC–MS and direct inlet probe electron-impact mass spectrometry (EI-MS) as follows.

Mass spectrometry

An HP 1090M high-performance liquid chromatograph was fitted to an HP5988A mass spectrometer (Hewlett-Packard, Palo Alto, CA, U.S.A.) by a Vestal-type thermospray interface. Using negative-ion mode, optimum signal-to-noise ratio was obtained with a 0.1 *M* ammonium acetate buffer adjusted to pH 3.5 with acetic acid, a source temperature of 230°C and a stem temperature of 110°C. In the positive-ion mode, optimum signal-to-noise ratio was obtained with a 1 *M* ammonium acetate buffer (pH 3.5) and a source temperature of 266°C. The analytical column was the same as above. Eluent (acetonitrile–ammonium acetate buffer) composition ranged from 43:57 to 58:42 depending on the polarity of the metabolites. Flow-rate was 0.7 ml/min. 'Filament-on' mode (1000 eV) was used throughout.

For EI and chemical ionization (CI) MS a direct inlet probe (DIP) technique was used. For EI-MS, source temperature was 200°C and DIP temperature programme was from 40 to 250°C at a rate of 30°C/min. Methane was used as a reagent gas for CI-MS at a source pressure of 1 Torr, an ionization potential of 200 eV and a multiplier voltage of 2000 V. Source temperature was 200°C for positive ion CI and 120°C for negative-ion CI.

Chemical synthesis

In analogy with benzarone metabolism, it was assumed that one of the metabolites was the 1-hydroxyethyl moiety [5], so this molecule was synthesized according to the procedure outlined by Grote and Sandrock [6]. The purity of the product was determined by GC and HPLC. Elemental analysis as well as ^{1}H and ^{13}C nuclear magnetic resonance (NMR) spectra were in accordance with the assumption of the 1-hydroxyethylbenzbromarone structure.

RESULTS

The most significant results were obtained using LC–MS fragmentation in the positive-ion mode and EI fragmentation. Negative-ion mode and CI proved to be less suitable because of lack of sensitivity and a lack of information on mass fragments.

In what follows the investigated metabolites are ranked according to conclusiveness of experimental findings.

Most reliable evidence is provided by chemical synthesis of the supposed molecule followed by comparison of HPLC retention times, UV spectra, mass fragments obtained by thermospray LC–MS and EI-MS of pure fractions. This was achieved for unchanged BzB and the 1-ethylhydroxylated metabolite (metabolite 1) in extracts of deconjugated urine.

HPLC retention times and diode-array UV spectra were identical for proposed and authentic BzB and metabolite 1. Thermospray and EI mass spectra of authentic BzB are depicted in Figs. 1 and 2. They are characterized by signals at *m/z* 425 ($[M + 1]^+$) and 424 (M^+) respectively, and by significant mass fragments (see Table I).

The corresponding results for authentic 1-hydroxyethylbenzbromarone are given in Figs. 3 and 4. Characteristic mass numbers are *m/z* 441 ($[M + 1]^+$) and 440 (M^+). LC and EI mass spectra of proposed and authentic substances were again identical. The position of the OH substituent of metabolite 1 in C-1 of the ethyl side-chain (as opposed to C-2) is proven by fragments of 173 and 145 a.m.u. (see Table II).

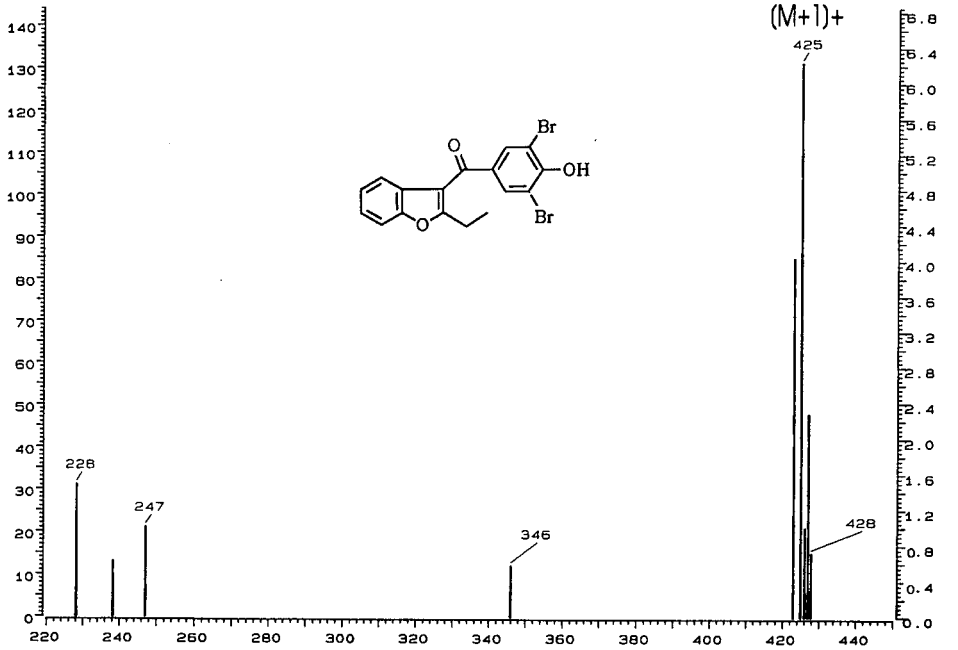

Fig. 1. LC–thermospray mass spectrum of authentic benzbromarone (BzB).

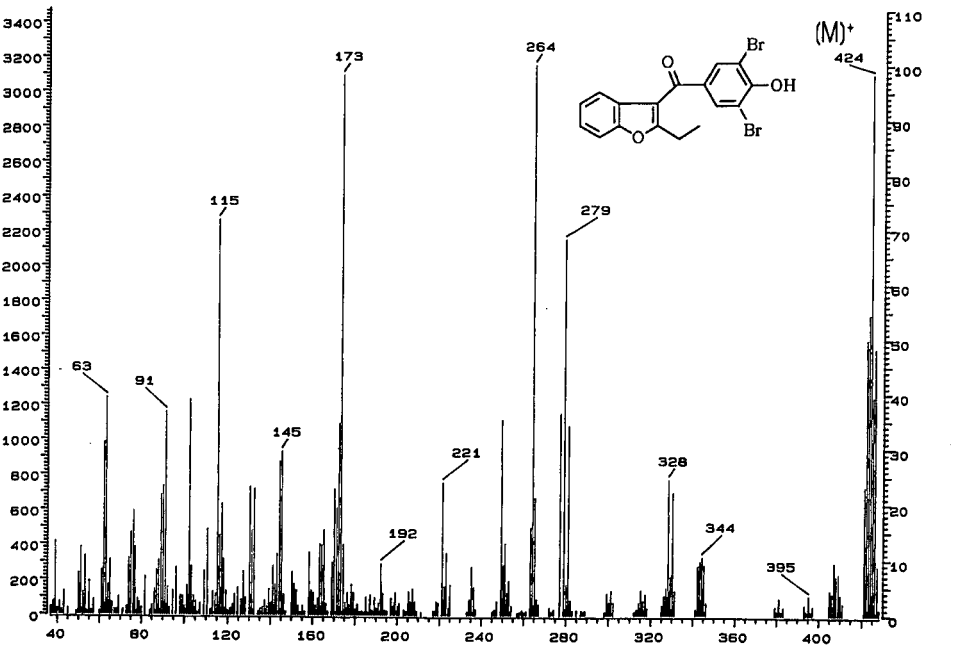

Fig. 2. DIP EI mass spectrum of authentic benzbromarone (BzB).

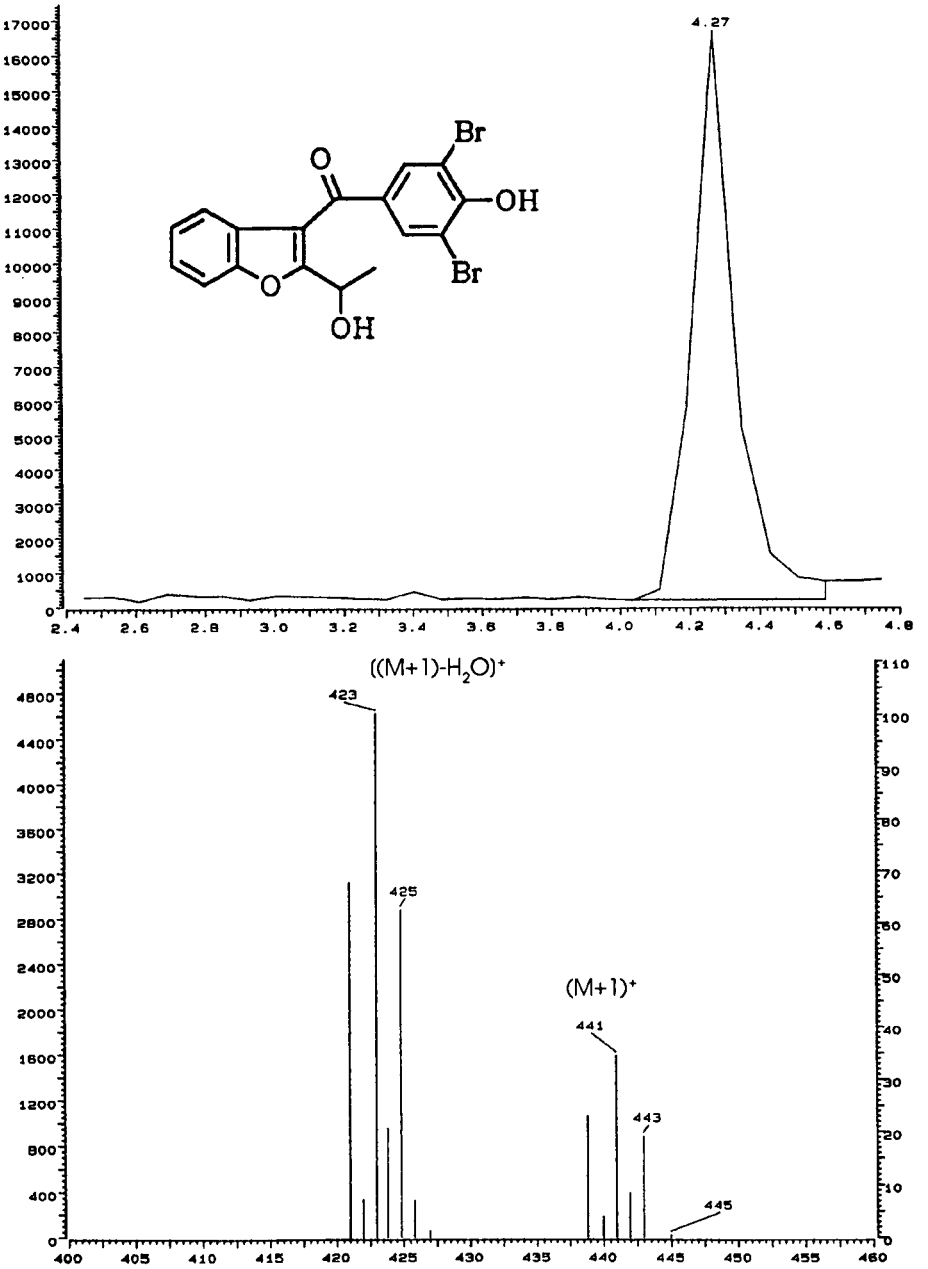

Fig. 3. Thermospray total ion current (top) and mass spectrum (bottom) of authentic 1-hydroxyethylbenzbromarone (metabolite 1).

TABLE I

EI MASS FRAGMENTS OF BENZBROMARONE (BzB)

m/z	Fragment	Relative intensity (%)
424	M^+	90
422		50
426		48
409	$[M-CH_3]^+$	8
411		
407		
344	$[M-Br]^+$	11
	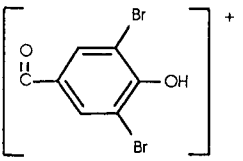	
279		68
281		34
277		38
264	$[M-2Br]^+$	100
	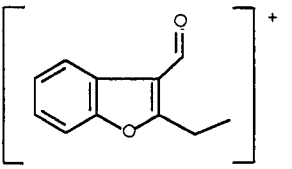	
173		98

Using HPLC retention times, UV spectra and LC mass spectra recorded on-line, these two substances were also identified in plasma extract. By interpretation of LC and EI mass fragmentograms, the major metabolite (metabolite 2) in purified fractions of urinary extracts could be identified as benzofuran ring-hydroxylated BzB. Its EI-MS is depicted in Fig. 5. The molecular peak appears at 440 a.m.u. as in metabolite 1; however, the fragment at 422 a.m.u. in Fig. 4, which is formed by elimination of water, is missing here. This result is also confirmed by LC–MS. The position of the OH substituent in the benzofuran system (as opposed to the phenolic ring) is proven by fragments at 161 and 189 a.m.u. (see Table III).

Again, using retention times, UV spectra and on-line LC–MS, metabolite 2 was also identified in plasma. It is this metabolite that has been mistaken for Bz (mol. wt. = 266) in previous studies because of their almost identical HPLC retention times.

On reversed-phase HPLC the more polar metabolites frequently elute with (polar) interfering substances, which often prevent or at least hinder their detection by UV absorption. For this reason front eluates were cut "blindly" into 0.4-min fractions, which were further assayed by LC–MS. In this way three more metabolites were detected. DIP EI-MS was impossible with these samples because of low amounts of analytes and the need for pure fractions.

The LC–mass spectrum of metabolite 3 is depicted in Fig. 6. The $[M + 1]^+$ peak at 457 a.m.u. provides evidence of two hydroxyl substituents. Loss of H_2O

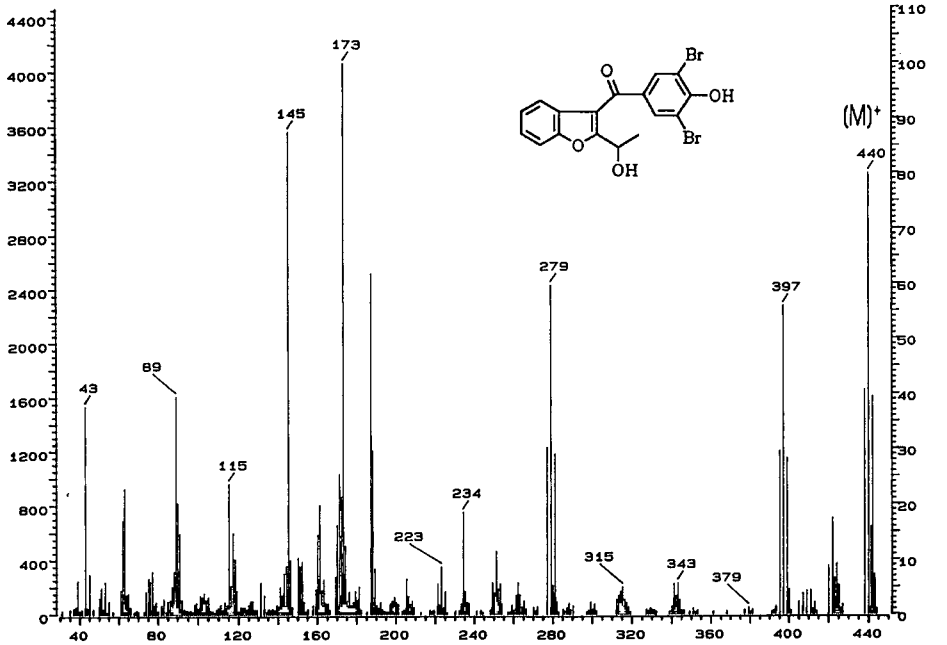

Fig. 4. DIP EI mass spectrum of authentic 1-hydroxyethylbenzbromarone (metabolite 1).

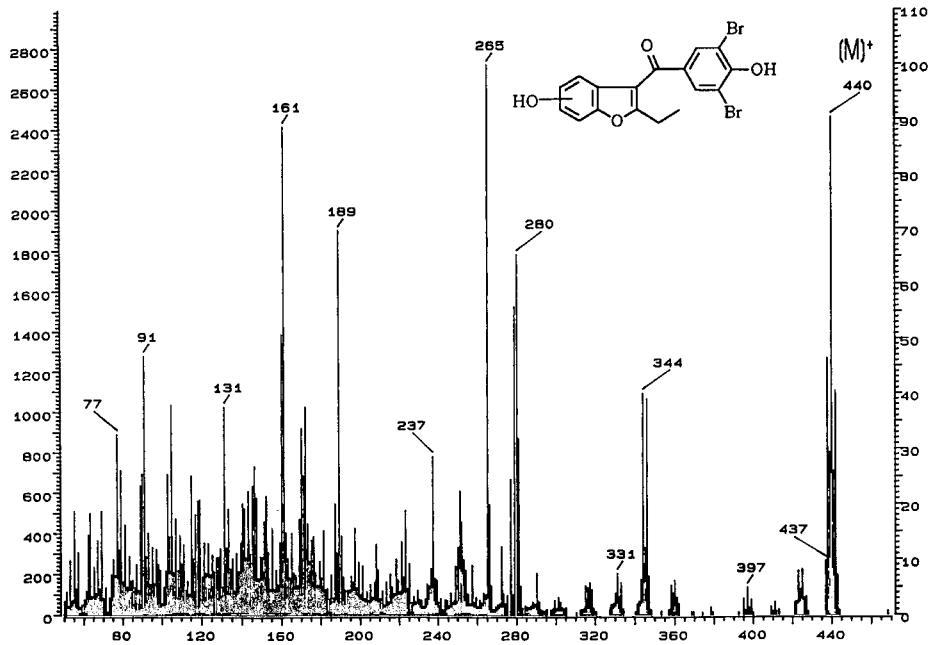

Fig. 5. DIP EI mass spectrum of hydroxyarylbenzbromarone (metabolite 2).

TABLE II

EI MASS FRAGMENTS OF 1-HYDROXYETHYLBENZBROMARONE (METABOLITE 1)

m/z	Fragment	Relative intensity (%)
440	M^+	80
442		36
438		37
422	$[M-H_2O]^+$	18
424		9
420		10
397	$[M-CH_3-CO]^+$	56
399		29
395		30
279	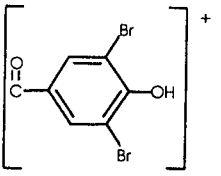	60
281		30
277		31
173	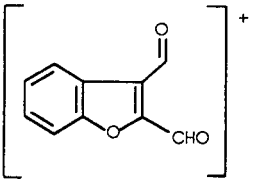	100
145	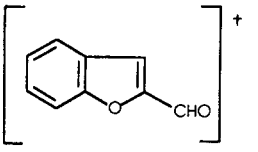	88

(fragment at 439) demonstrates that at least one OH group is located in the ethyl side-chain. In analogy with metabolite 1, it is assumed that it will be in position C-1. Because of the lack of fragmentation, the position of the other OH group cannot be determined exactly, however it will most probably be in the benzofuran system, since ring hydroxylation is the major metabolic pathway for BzB.

The LC–MS of metabolite 4 is shown in Fig. 7.

The $[M + 1]^+$ peak at 439 a.m.u. and the absence of water loss are consistent with a keto group in position 1 of the ethyl side-chain. A mass number of 439 a.m.u. could also be interpreted as water loss from metabolite 3. However, the $[M + 1]^+$ peak at 457 a.m.u. is missing in the LC–MS of metabolite 4. Moreover, metabolites 3 and 4 differ in HPLC retention times by 0.4 min.

Metabolite 5 ($[M + 1]^+$ at 455 a.m.u.) nearly coelutes with metabolite 3 ($[M + 1]^+$ at 457 a.m.u.). Its discovery was additionally complicated by the isotope distribu-

TABLE III

EI MASS FRAGMENTS OF METABOLITE 2 (ARYLHYDROXYBENZBROMARONE)

m/z	Fragment	Relative intensity (%)
440	M^+	91
442		41
438		47
280	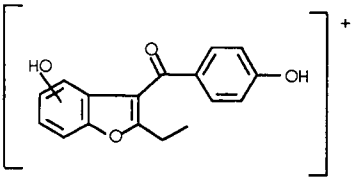	66
279	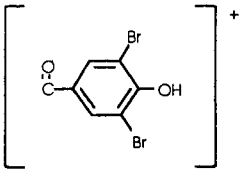	57
277		
281		
265	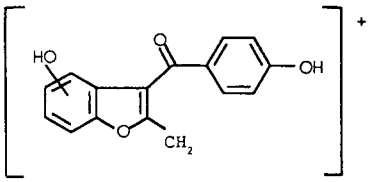	100
189	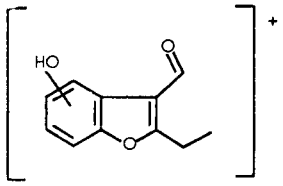	71
161	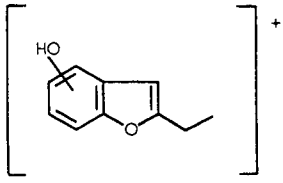	90

tion of the two bromine atoms, giving rise to two more signals at $[M + 1]^+ \pm 2$ a.m.u. In spite of this impairment, metabolite 5 could be detected by stepwise display of mass spectra which were recorded repeatedly over the entire peak (Fig. 8).

Metabolite 5 is a hydroxy derivative of metabolite 4, with the OH group again most probably in the benzofuran system.

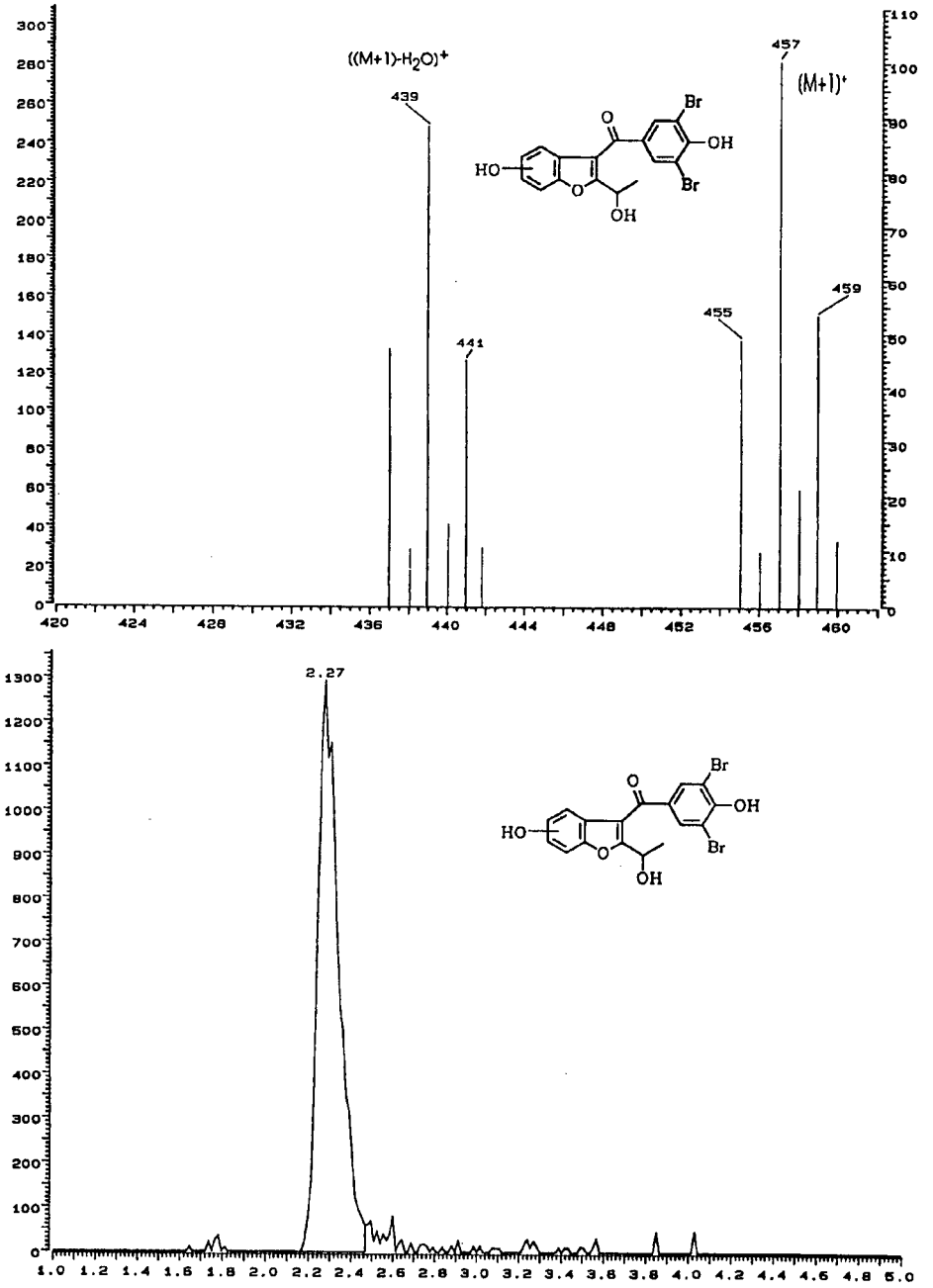

Fig. 6. LC–thermospray total ion current (bottom) and mass spectrum (top) of hydroxyarylhydroxyethylbenzbromarone (metabolite 3).

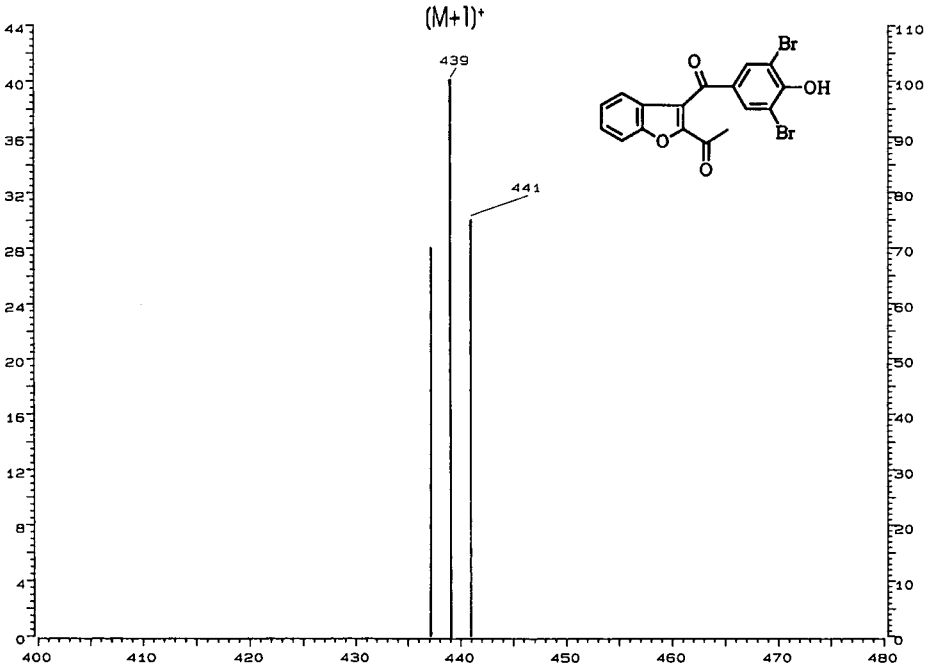

Fig. 7 LC–thermospray mass spectrum of oxoethylbenzbromarone (metabolite 4).

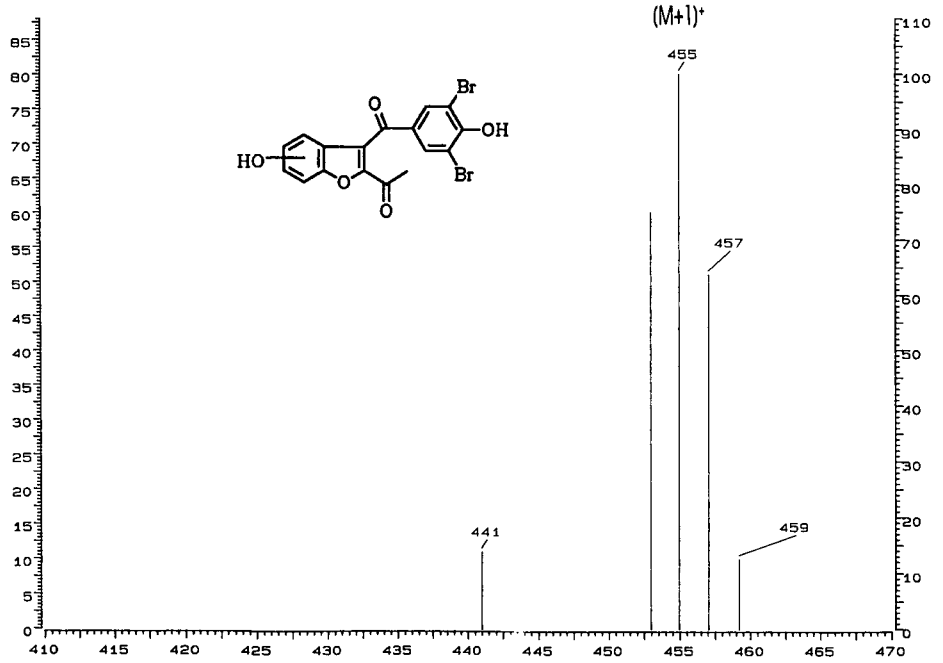

Fig. 8. LC–thermospray mass spectrum of hydroxyaryloxoethylbenzbromarone (metabolite 5).

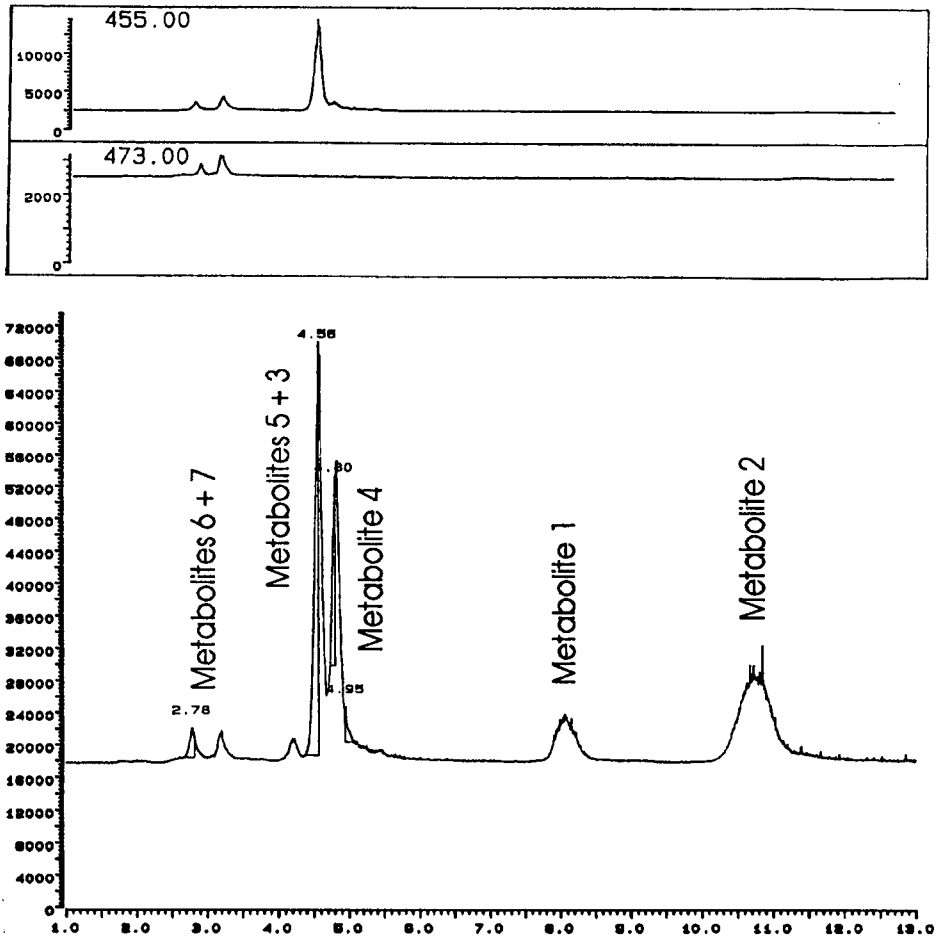

Fig. 9. SIM LC–MS chromatograms, *m/z* 473 and 455 (top) and total ion current (bottom) of deconjugated urinary extract.

Some metabolites occurred in such small concentrations that even on-line LC mass spectra were impossible to obtain. To search for any trihydroxylated metabolites, selected-ion monitoring (SIM) LC–MS runs on mass numbers 473 and 455 were recorded from the total urinary extract. The results are shown in Fig. 9. Evidently, two more species at $[M + 1]^+ = 473$ exist, both of them consistent with one OH group at C-1 of the ethyl side-chain with two more OH substituents at different positions whose locations could not be determined (metabolites 6 and 7).

Finally, the entire metabolic pathway of benzbromarone is depicted in Fig. 10.

Metabolite 2 proved to be the major metabolite, while metabolite 1 occurred in minor amounts in plasma and urine. Metabolites 3–7 were not detected in plasma. In urine they appeared in trace amounts only. All metabolites underwent Phase II conjugation with glucuronic acid. Only small amounts of free metabolites 1 and 2 were

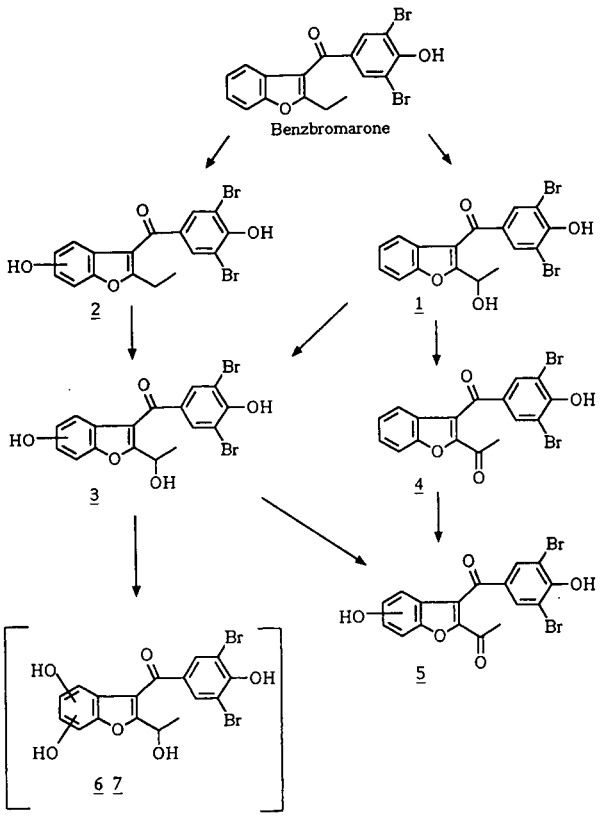

Fig. 10. Metabolic pathways of benzbromarone in man.

found in urine. In contrast, in plasma, metabolites 1 and 2 occurred in the free form and no conjugates could be detected.

DISCUSSION

Since most drug molecules can be analyzed in biological material by HPLC, this is also a suitable separation technique for metabolic research. However, structural identification of unknown substances remained difficult as long as no fully developed interfaces to mass spectrometers were available.

In our work we used EI ionization with a DIP as an off-line technique and thermospray for on-line interfacing.

Comparing these techniques, one can conclude that EI is suitable for identification of major metabolites which can be isolated by semi-preparative means. It requires relatively large amounts of analytes but supplies a large amount of mass spectral information. Identification of minor constituents is the domain of direct LC–MS coupling, which can work with smaller amounts and does not require additional clean-up but provides very little structural information.

Very recently, Maurer and Wollenberg [7] investigated BzB metabolites by GC–MS after derivatization in the urine of suicide victims who had ingested high doses of the drug. Our finding of unchanged BzB and metabolites 1, 2 and 4 in urine, mainly in conjugated form, corresponds with their results. However, unlike them we could not separate two different ring-hydroxylated metabolites nor could we detect any methoxylated entities. In addition we found metabolites 3 and 5–7. These differences may have been caused by the toxicity of the high doses taken by Maurer and Wollenberg's patients.

REFERENCES

1 I. Broekhuysen, M. Pacco, R. Sion, L. Demeulenaere and M. van Hee, *Eur. J. Clin. Pharmacol.*, 4 (1972) 125.
2 H. Vergin and G. Bishop, *J. Chromatogr.*, 183 (1980) 383.
3 H. Ferber, H. Vergin and G. Hitzenberger, *Eur. J. Clin. Pharmacol.*, 19 (1981) 431.
4 J. X. de Vries, I. Walter-Sack, A. Ittensohn and E. Weber, *Xenobiotica*, 19 (1989) 1461.
5 S. G. Wood, B. A. John, L. F. Casseaud, R. Bonn, H. Grote, K. Sandrock, A. Darragh and R. F. Lambe, *Xenobiotica*, 17 (1987) 881.
6 H. Grote and K. Sandrock, *Ger. Offen.*, DE 3 342 624 (1984); *C. A.*, 101 (1984) 54904v.
7 H. Maurer and P. Wollenberg, *Arzneim.-Forsch.*, 40 (1990) 460.

Journal of Chromatography, 554 (1991) 281–292
Elsevier Science Publishers B.V., Amsterdam

CHROMSYMP. 2340

Use of non-volatile ion-pairing agents for liquid chromatographic–mass spectrometric analyses with a moving-belt interface

R. E. A. ESCOTT*, P. G. McDOWELL and N. P. PORTER
BP Research, Analytical Division, Chertsey Road, Sunbury-on-Thames, Middlesex TW16 7LN (UK)

ABSTRACT

Micro-membrane suppressor systems were employed to allow non-volatile ion-pairing agents to be used with combined liquid chromatography–mass spectrometry (LC–MS). This enabled the technique to be used with reversed-phase gradient chromatography for the determination of both anionic and cationic species from a range of compounds. The membrane suppressors remove the ion-pairing agent by counter-current flow regeneration. The determination of cationic species is demonstrated with the use of pyridinium and imidazolium iodides. Hexanesulphonic acid was used as the chromatographic ion-pairing agent and tetrabutylammonium hydroxide as the regenerant. The determination of anionic species is demonstrated with carboxylic and sulphonic acids, which were chromatographed as the tetrabutylammonium hydroxide ion pair using sulphuric acid as the regenerant. The system described has been used successfully with a moving-belt interface, enabling spectra to be acquired in both electron impact (EI) and chemical ionization (CI) modes, with a magnetic sector instrument. The system is in essence compatible with any LC–MS interface, although some modification may be required if the interface generates a significant back-pressure, *e.g.*, thermospray.

INTRODUCTION

Liquid chromatography (LC) is often used, in preference to other analytical techniques, for the determination of polar compounds such as acids and amines. However, in order to obtain a chromatographic separation of these compounds, it is necessary to reduce their polarity. This is usually achieved with the addition of ion-pairing agents to the LC solvent system.

Careful choice of the ion-pairing agent can enhance difficult separations by providing additional selectivity. However, many ion-pairing agents are non-volatile, and the majority of LC–mass spectrometry (MS) interfaces are not designed for use with these types of reagents. This then precludes the advantages of ion-pair chromatography from many LC–MS applications, if non-volatile ion-pairs are required.

The use of volatile buffer systems has been investigated and shown to be readily used, particularly with thermospray (TSP) interfaces [1,2]. There is, however, a very limited range of volatile ion-pairing agents. The use of non-volatile ion-pairing agents

0021-9673/91/$03.50

requires post-column removal systems, which can allow the use of other types of LC–MS interfaces, *e.g.*, moving belt, ion spray–atmospheric pressure ionization (API) and particle beam. Ion-pairing agents have previously been removed with the use of a column-switching technique [3] and a two-phase extraction system [4]. Column switching can enable high sensitivities and selectivities to be obtained, but the system is discontinuous and therefore more suited to target analyte analysis, rather than routine LC–MS applications. Post-column ion-pair extraction will remove the "excess" of reagent, but it will also allow analyte/ion-pair species to enter the ion source, which can result in contamination and a poor MS response. The sensitivity achieved is determined by the extraction and phase separation efficiencies obtained.

The use of a counter-current membrane system permits complete removal of the ion pairs. In the work described here, the use of Dionex micro-membrane systems was investigated. These are available in two forms, anionic (AMMS) and cationic (CMMS), which remove cations and anions, respectively, when used with a suitable regenerant. These systems are designed for use in ion chromatography (IC) to remove background buffer ions and enhance the conductimetric detection of inorganic ions. They have been used with IC–API-MS for the determination of quaternary ammonium compounds [5] and IC–TSP-MS for carbohydrate determinations [6]. The work reported here illustrates that their use can be extended to reversed-phase ion-pair chromatographic systems, allowing LC–MS analysis of a wide range of cationic and anionic organic compounds.

EXPERIMENTAL

Reagents

Solvents and ion-pairing agents. The following were used: Acetonitrile, far-UV grade (Romil Chemicals), hexane sulphonic acid, 40% (Dionex), Tetrabutylammonium hydroxide, 40% (Dionex) and Sulphuric acid, 20 m*M* (FSA Laboratory Supplies). Water was purified with a Millipore Milli-Q system.

Standard materials. Phthalic acid, *p*-methoxybenzoic acid, *p*-chlorobenzoic acid and *p*-toluenesulphonic acid were obtained from BDH, *p*-chlorophenoxyacetic acid and N-methylimidazole from Aldrich and alkylated imidazolium iodides from BP Chemicals.

Equipment

A schematic diagram of the apparatus used is shown in Fig. 1.

Chromatography. The liquid chromatograph consisted of two Gilson Model 303 pumps with an Apple II microcomputer for gradient elution control. UV detection was achieved with Philips LC–UV and Kontron 720LC detectors. Injection volumes of 50 μl were made with a Valco C6W injection valve. The separations were achieved with 250 × 4.6 mm I.D. columns, packed with 5-μm BDS octadecylsilane material (Shandon Southern) and 5-μm PLRP-S, 100Å polystyrene–divinylbenzene polymeric reversed-phase material (Polymer Labs).

The micro-membrane suppressors used were the CMMS and AMMS obtained from Dionex. These were used with $^1/_{16}$ in O.D. × 0.010 in I.D. and $^1/_{16}$ in O.D. × 0.020 in I.D. PTFE tubing for the column eluent and regenerant streams, respectively. The sulphuric acid and tetrabutylammonium hydroxide regenerants were prepared as aqueous solutions as shown in Table I.

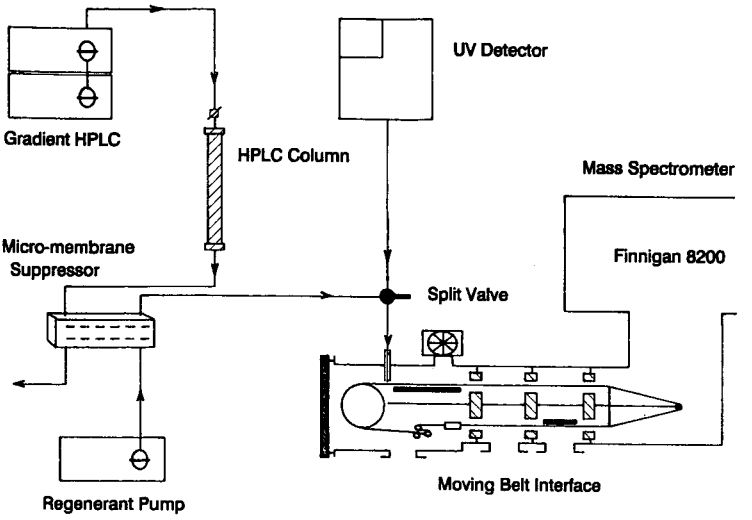

Fig. 1. Schematic diagram of the non-volatile ion-pair removal system for LC–MS.

Mass spectrometry. The analyses were performed on a Finnigan Model 8200 magnetic sector instrument operating in a low resolution/high intensity mode. Data were acquired using both electron impact (EI) ionization at 70 eV and chemical ionization (CI) with either ammonia or isobutane as the reagent gas. The instrument was scanned over the mass range m/z 50–800 at the rate of 2 s per scan.

The LC eluent was divided by a stainless-steel stream splitter with *ca.* 80% being passed to the UV detector and 20% to the mass spectrometer via a Finnigan moving-belt interface. The interface was operated with belt speed 3.5 cm/s, solvent evaporator temperature 180°C, sample tip heater power 8 W and clean-up heater 75%. The ion source of the spectrometer was maintained at 230°C.

Analysis conditions

The chromatographic conditions used are summarised in Table I.

RESULTS AND DISCUSSION

The basis of the suppressors is an ion-exchange resin membrane, which can be used with buffer concentrations of up to 100 m*M*. This concentration range encompasses that required for effective ion-pair chromatography, which is normally of the order of 3–10 m*M*. Within this concentration range, a combination of ion-pair adsorption (with ion exchange) and ion-pair partition mechanisms effects the separation [7]. However, the choice of the ion pair and the regenerant is critical for compatibility with LC–MS analyses, and as such the acid and hydroxide counter ions should be used.

The choices of reagents cited here have ensured that the ion-pair counter ion, which is replaced by the regenerant, produces water in the eluent stream. The pyridi-

TABLE I

LC CONDITIONS

Analyte	Separation conditions[a]	Regenerant[a]
Carboxylic acids	A = 5 m*M* aqueous tBAH B = ACN–H_2O (80:20) containing 5 m*M* tBAH 1 ml/min 10–100% B in 30 min BDS and PLRP-S columns	20 m*M* H_2SO_4 2 ml/min
Imidazolium iodides	A = ACN–H_2O (5:95) containing 5 m*M* HSA 1 ml/min B = ACN–H_2O (80:20) containing 5 m*M* HSA 0% B for 10 min 0–60% B in 30 min PLRP-S column	0.1% (v/v) tBAH 2 ml/min
Pyridinium iodides	ACN–H_2O (10:90) containing 5 m*M* HSA 1 ml/min	0.1% (v/v) tBAH 2 ml/min

[a] ACN = acetonitrile; H_2O = deionized water; HSA = hexanesulphonic acid; tBAH = tetrabutylammonium hydroxide.

nium and imidazolium sulphonate ion pairs are converted to the hydroxides, whilst the carboxylic acid tetrabutylammonium ion pairs become the free acids. Thus the processes result in column eluent streams which are totally compatible with the MS interface.

The extraction efficiency of the Dionex membranes has been shown to be >99.9% [5]. Fig. 2. shows the effectiveness of removing an ion pair (*e.g.* the tetrabutylammonium cation, *m/z* 242) by monitoring the 242 ion in the eluent with and

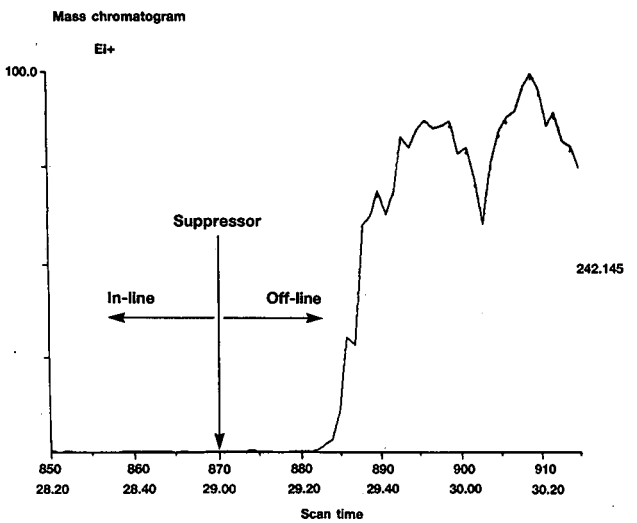

Fig. 2. Single ion chromatogram of *m/z* 242 (tetrabutylammonium ion) with and without the membrane suppressor in-line. Time in min.s.

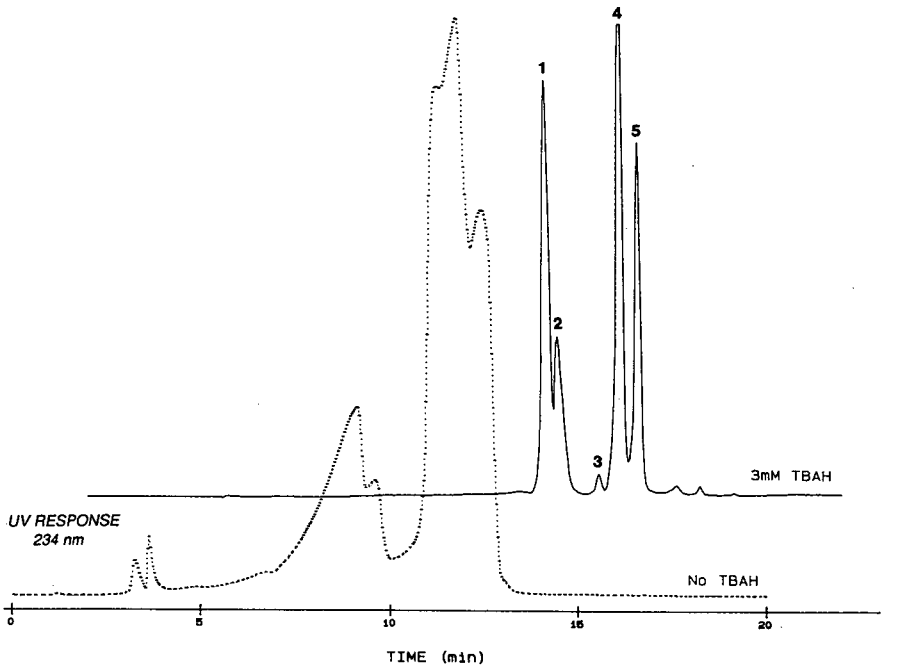

Fig. 3. Effect of the ion pair on the separation of carboxylic acids. Peaks: 1 = phthalic acid (96 mg/l); 2 = *p*-methoxybenzoic acid (432 mg/l); 3 = *p*-chlorobenzoic acid (746 mg/ml); 4 = *p*-toluene sulphonic acid (502 mg/l); 5 = *p*-chlorophenoxyacetic acid (502 mg/l).

without the membrane in-line. With the membrane in place, the ion current obtained is equivalent to that of the baseline without the ion pair in the solvents. The minimum concentration for the regenerant solutions was found to be 0.1%. Below this level the extraction efficiency was decreased, particularly with mobile phases containing high (>50%) concentrations of organic modifier.

The chromatographic separation of polar compounds and ionic compounds (both acidic and basic) by reversed-phase LC without the use of an ion pair or a buffer system, results in poor component resolution and peak shapes. This is due to polar interactions with the residual silanol groups on the column, which is in competition with the non-polar interactions with the bonded-phase ligands. The formation of the ion pair effectively decreases the analyte polarity and hence the interactions with the silanol groups. This greatly increases the chromatographic integrity of the separation, and this is clearly illustrated in Fig. 3. The upper trace was obtained with a solvent system containing 3 m*M* tetrabutylammonium hydroxide and the lower trace without the ion-paring agent. The use of the BDS column provided a more efficient separation, with better resolution of the acids, than the PLRP-S column. However, the apparent pH of the mobile phase, which as measured at 9.4, is above the working range of these columns (quoted by Shandon Southern to be pH 2–8). The column could therefore only be used continuously for 1 week before dissolution of the silica base caused significant deterioration of the peak shapes. The PLRP-S column, whilst

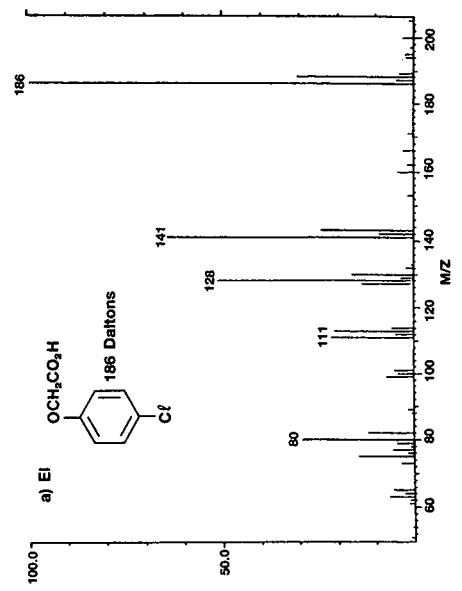

Fig. 4. (a) EI and (b) CI mass spectra of *p*-chlorobenzoic acid (peak 3, Fig. 3).

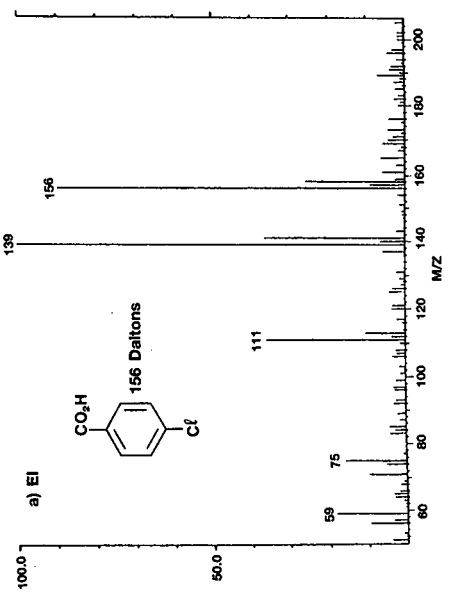

Fig. 5. (a) EI and (b) CI mass spectra of *p*-chlorophenoxyacetic acid (peak 5, Fig. 3).

being resistant to high pH values, does not provide an equivalent separation efficiency. The efficiency of these polymeric reversed-phase materials has been shown to be very dependant on the solvent system [8], but alternative mobile phases were not investigated in this study.

Examples of the EI and isobutane CI mass spectra of the acidic components are shown if Figs. 4 and 5. Mass spectral library searches identified these components correctly as *p*-chlorobenzoic acid and *p*-chlorophenoxyacetic acid. The CI spectrum of *p*-chlorophenoxyacetic acid (Fig. 5) shows only very weak pseudo-molecular ions, *m/z* 187/189, and it is dominated by fragment ions (*m/z* 141/143) corresponding to loss of H_2CO_2 from the protonated molecule. *p*-Toluenesulphonic acid gave an extremely poor response in both ionization modes, which appears to be due to decomposition of the compounds on the belt, and phthalic acid was observed only in the CI mode as the 149 dalton ion.

Fig. 6. shows the total ion current (TIC) and UV traces for the isocratic separation of a mixture containing 1-methyl-4-ethylpyridinium iodide (peak 1) and 4-

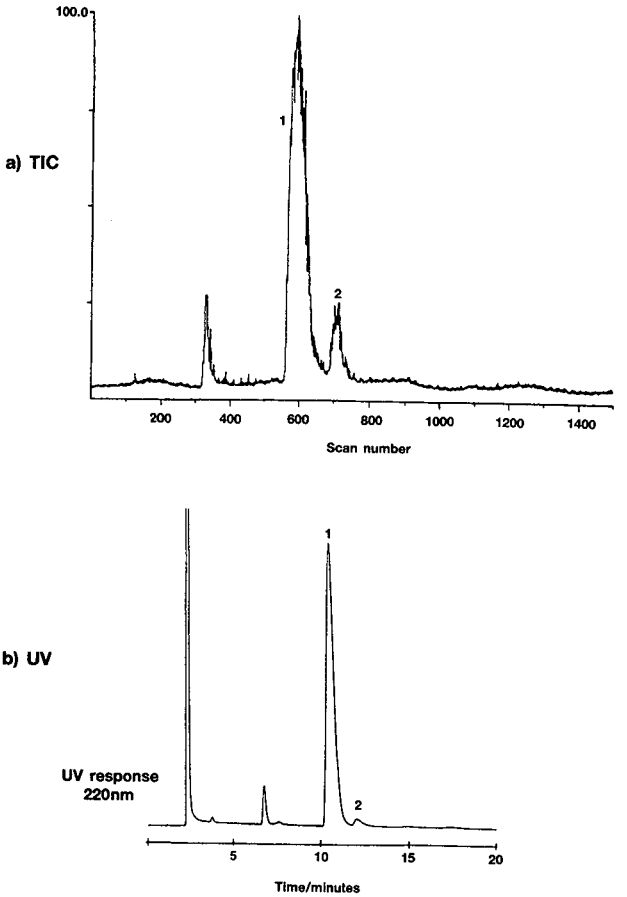

Fig. 6. TIC and UV traces from the LC–MS analysis of the pyridine–pyridinium iodide mixture.

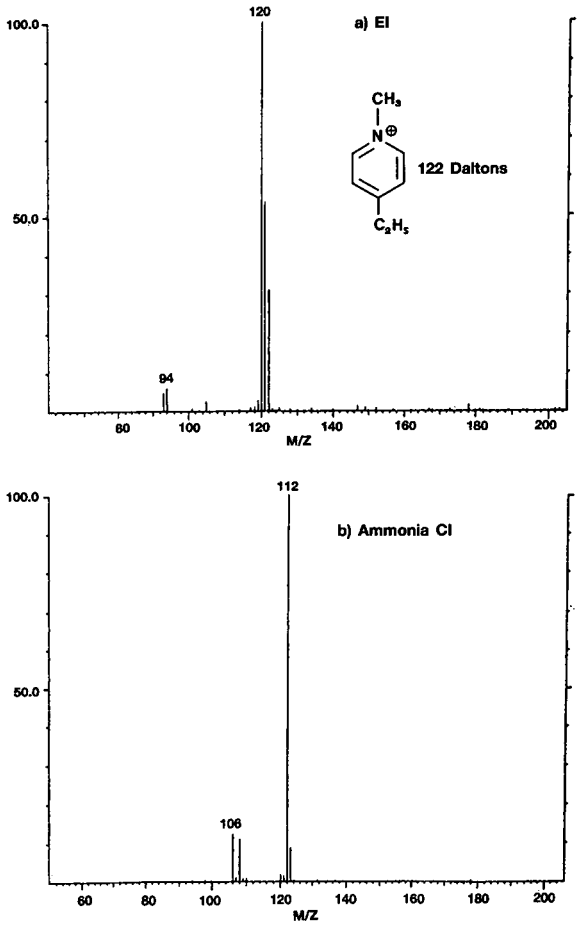

Fig. 7. (a) EI and (b) CI mass spectra of the ethylmethylpyridinium cation (peak 2, Fig. 6).

ethylpyridine (peak 2). The EI and CI mass spectra of the 1-methyl-4-ethyl pyridinium cation are shown in Fig. 7. The spectra obtained show no evidence for the presence of the hexanesulphonate ion pair (*m/z* M + 165), with prominent molecular ions for the cations evident in both EI and CI modes.

The ion-pair separation, obtained with gradient elution, for alkylimidazolium iodides is shown in Fig. 8. The AMMS micromembrane suppressor was again completely effective in removing the hexanesulphonate ion pair. When octanesulphonic acid was used as the ion-pairing agent, some breakthrough was observed with increasing acetonitrile content in the mobile phase, but this system was not studied further or optimized.

Typical spectra obtained from this separation are shown in Figs. 9 and 10. The major CI ions observed correspond to the imidazolium ions (*m/z* 97, 111 and 139) and ions at 14 mass units lower. These undoubtedly arise from thermal dequaternization

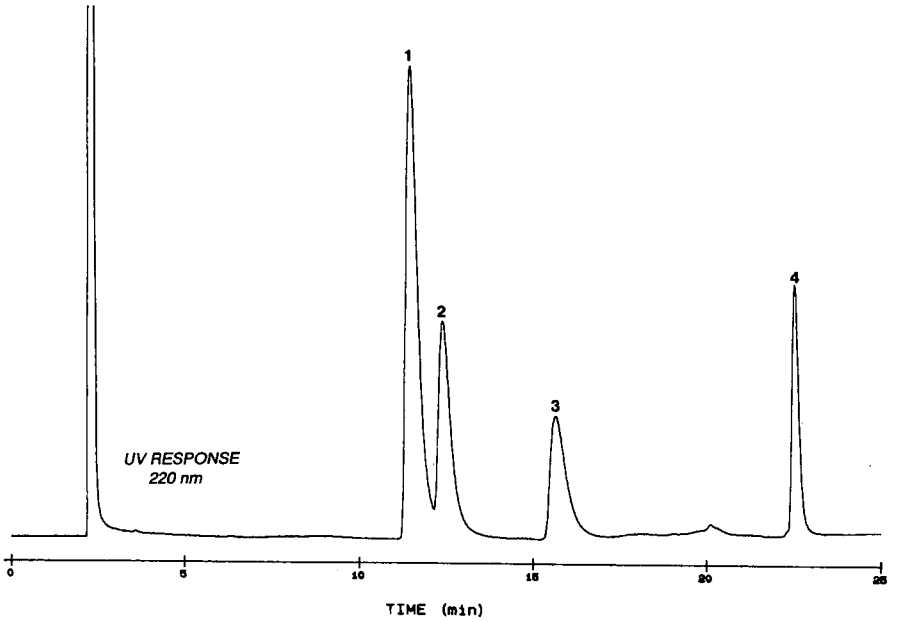

Fig. 8. Reversed-phase separation of methylimidazole and methylated imidazolium iodides. Peaks: 1 = N-methylimidazole (503 mg/l); 2 = N,N-dimethylimidazolium iodide (456 mg/l); 3 = 1,2,3-trimethylimidazolium iodide (301 mg/l); 4 = pentamethylimidazolium iodide (205 mg/l).

followed by re-protonation of the neutral imidazole. Such thermal degradation is well known, *e.g.*, with alkylpyridinium halides [9] and pyridinium N-oxides, which show variable intensity [M–O] ions depending on the thermal conditions employed [10–12]. Whereas quaternary salts are considered to be involatile, lower molecular weight compounds do volatilize directly (both with and without rearrangement), such as N-methyl-3-pyridinium oxide [13–15]. The "volatility" of these compounds is likely to be affected by the counter ion involved, which, after passage through the micromembrane suppressor, is effectively OH^-. It has certainly been shown that the counter ion is important in establishing the fragmentation pathway of quaternary species, *e.g.*, pyridinium salts [16].

Imidazolium compounds not substituted in the 2-position show adduct ions at M + 15 (*e.g.* *m/z* 112 for dimethyl imidazolium), which is postulated to be the result of replacement of H with NH_2 for in the 2-position to give the ion shown. Imidazolium compounds with alkyl substitution in the 2-position did not produce these adduct ions. Adduct ions derived from C-alkylation have been observed in the methane CI spectra of pyrroles, where M + C_2H_5 result from substitution at the C-3 position [17].

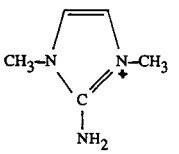

m/z 112

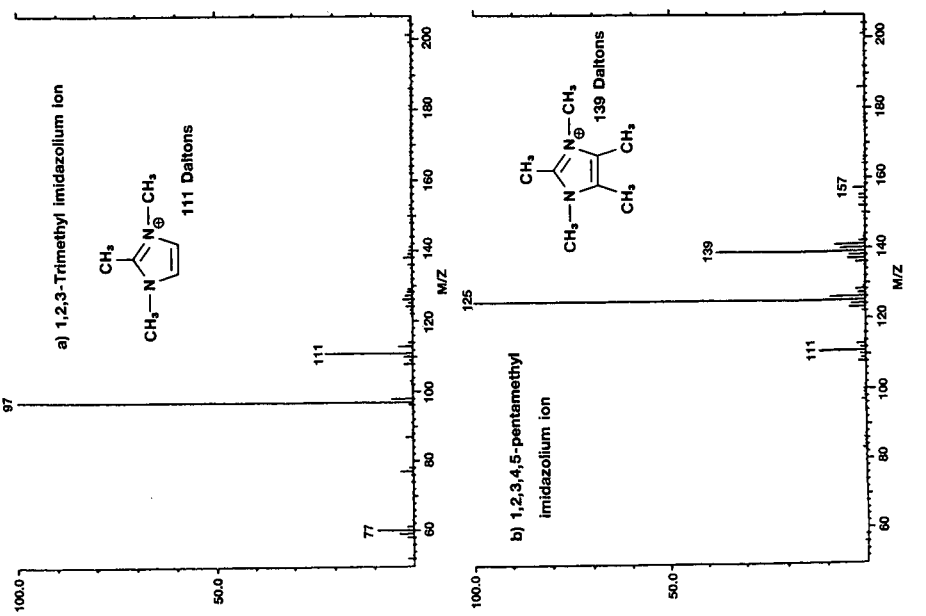

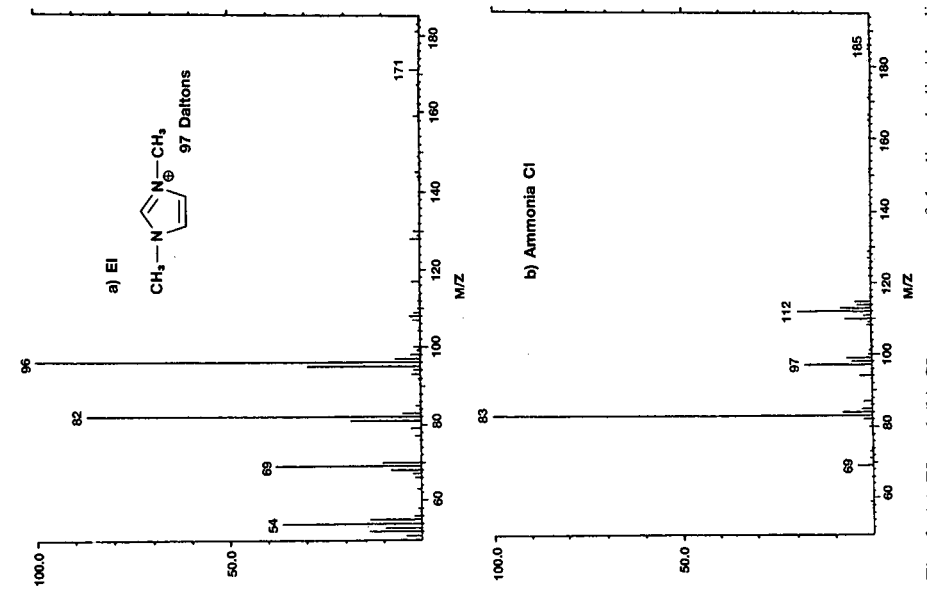

Fig. 9. (a) EI and (b) CI mass spectra of the dimethylimidazolium cation (peak 2, Fig. 8).

Fig. 10. Ammonium CI mass spectra of (a) the trimethyl- and (b) the pentamethylimidazolium ions (peaks 3 and 4, Fig. 8).

As would be expected, a degree of variability in both the EI and CI mass spectra of these quaternary compounds was observed, arising from thermal degradation. This might reduce the scope of the technique for these types of compounds, particularly for more complex mixtures with higher molecular weight quaternary species. The range of applications for the technique might be usefully extended with the use of fast atom bombardment (FAB) ionization combined with the moving-belt interface [18], but this has not yet been studied.

The use of the micromembrane suppressor has, however, considerable potential for the analysis of polar compounds, both acidic (as in the example detailed here) and basic which require ion-pairing agents to effect good separations and where the low volatility of such agents rapidly interferes with the operation of the MS interface. The use of the micromembrane suppressor should also be easily adaptable to other LC–MS interfaces.

CONCLUSIONS

The Dionex micromembrane suppressors can be readily used with a moving-belt interface, thus enabling polar organic acidic and basic compounds to be characterized by LC–MS. The system described is suitable for reversed-phase ion-pair chromatography with gradient elution. This provides a much wider range of ion-pairing agents, from which a suitable one can be chosen for a particular application. The ion-pairing agent and the regenerant can be chosen such that the composition of the solvent stream is compatible with the MS interface. The range of analytes and ion-pairing agents which can be used with the suppressors are currently being studied. A limitation of the current suppressor design is their low back-pressure tolerance, *ca.* < 300 p.s.i. Thus, without any modifications, this limits their applicability to LC–MS interfaces that do not generate any significant back-pressure.

It is apparent that no single LC–MS interface is universal in its application; *e.g.*, thermal degradation of analytes is one disadvantage of the moving-belt system. The use of FAB ionization with the moving-belt interface may overcome some of the thermal degradation problems, but recent developments in capillary zone electrophoresis –MS may provide a more suitable system, particularly for the analysis of higher molecular weight ionic compounds. Also, if the limitations of the membrane suppressors are established and overcome, then other modes of liquid chromatography (*e.g.*, ion-suppression, ion-exclusion and ion-exchange) can be used routinely with many LC–MS systems.

ACKNOWLEDGEMENTS

The authors thank Dr. D. Mealor for initiating and promoting this work and BP Research for allowing publication.

REFERENCES

1 R. E. A. Escott and D. W. Chandler, *J. Chromatogr. Sci.*, 27 1989 134.
2 A. L. L. Duchateau, B. H. M. Munsters, G. T. C. Kwakkenbos and R. G. J. van Leuken, *J. Chromatogr.*, 552 (1991) 605.
3 R. J. Vreeken, G. Bakker, J. Brakenhoff, G. J. de Jong, R. W. Frei and U. A. Th. Brinkman, presented at the *18th International Symposium on Chromatography, Amsterdam, september 23–28, 1990.*

4 D. Barceló, G. Durand, R. J. Vreeken, G. J. de Jong and U. A. Th. Brinkman, *Anal. Chem.*, 62 (1990) 1696.
5 J. J. Conboy, J. D. Henion, M. W. Martin and J. A. Zweigenbaum, *Anal. Chem.*, 62 (1990) 800.
6 R. C. Simpson, C. C. Fenselau, M. R. Hardy, R. R. Townsend and Y. C. Lee, *Anal. Chem.*, 62 (1990) 248.
7 J. H. Knox and G. R. Laird, *J. Chromatogr.*, 122 (1976) 17.
8 B. Gawdzik, J. Gawdzik and Y. Czerwinska-Bil, *Chromatographia*, 26 (1988) 399.
9 E. Larsen, H. Egsgaard and H. Holmen, *Org. Mass Spectrom.*, 13 (1978) 417.
10 R. Grigg and B. G. Odell, *J. Chem. Soc. B.*, (1966) 218.
11 N. Bild and M. Hesse, *Helv. Chim. Acta*, 50 (1967) 1885.
12 A. M. Duffield and O. Buchhardt, *Acta Chem. Scand.*, 26 (1972) 2423.
13 T. Gronneberg and K. Undheim, *Org. Mass Spectrom.*, 6 (1972) 823.
14 T. Gronneberg and K. Undheim, *Org. Mass Spectrom.*, 6 (1972) 225.
15 T. Gronneberg and K. Undheim, *Acta Chem. Scand.*, 25 (1971) 2807.
16 R. Salsmans and G. Van Binst, *Org. Mass Spectrom.*, 8 (1974) 357.
17 H. El Khadam, L. A. Kemler, Z. M. El-Shafei, M. M. A. Abdel Rahman and S. El Sadany, *J. Heterocycl. Chem.*, 9 (1972) 1413.
18 P. Dobberstein, E. Korte, G. Meyerhoff and R. Pesch, *Int. J. Mass Spectrom. Ion Phys.*, 46 (1983) 185.

Journal of Chromatography, 554 (1991) 293–304
Elsevier Science Publishers B.V., Amsterdam

CHROMSYMP. 2336

Simple direct liquid introduction system usable as an interface for liquid chromatography–mass spectrometry on quadrupole and magnetic-sector mass spectrometers

JEAN-PIERRE GAGNÉ, S. G. ROUSSIS and MICHEL J. BERTRAND*
Regional Center for Mass Spectrometry, Department of Chemistry, University of Montreal, P.O. Box 6128, Stn A, Montreal H3C 3J7 (Canada)

ABSTRACT

A simple and inexpensive direct liquid introduction system that can be used for tandem mass spectral analysis and for interfacing liquid chromatography on quadrupole and magnetic-sector mass spectrometers is described. The interface consists of a transfer fused-silica capillary that is introduced directly into the chemical ionization source of the mass spectrometer through the conventional gas chromatography–mass spectrometry interface, replacing the capillary column. The coupling uses no desolvation chamber and the transfer capillary is heated over the whole length of the interface. Experiments on the effect of interface temperature and flow-rate demonstrate that the system is extremely stable under optimal operating conditions, which are similar on different spectrometers. The chemical ionization plasma generated by the mobile phase under typical operation consists mainly of protonated monomers, and its composition is similar on different spectrometers, as shown by the comparison of spectra obtained. The system can be used with a series of mobile phases, and the ionization features that they produce are comparable. The system is stable, reproducible and allows picogram range sensitivity to be achieved in mass spectrometric, tandem mass spectrometric or liquid chromatographic–mass spectrometric experiments.

INTRODUCTION

The development of techniques allowing the introduction of liquid samples into the ion source of a mass spectrometer has considerably increased the range of compounds that can be analysed by mass spectrometry (MS). Although substantial efforts have been devoted to developing interfaces in order to couple liquid chromatography (LC) to MS, there are several other applications that can benefit from such liquid introduction techniques. Mass spectral applications that require the introduction of liquid samples can be classified into three general classes and theses are (i) the identification of organic compounds by techniques of MS or MS–MS, (ii) real-time monitoring of chemical reactions occurring in solution and (iii) interfacing of liquid chromatography to mass spectrometry.

Since the initial experiments reported by Tal'roze *et al.* [1] and by Baldwin and McLafferty [2] in the early 1970s, many reports describing liquid introduction techniques or LC interfaces have appeared in the literature, and these techniques have

0021-9673/91/$03.50

been the subject of periodic reviews over the last ten years [3–8]. Several approaches can be used to conduct experiments that require the introduction of a liquid into the ion source of a mass spectrometer, and these include direct liquid introduction (DLI) systems [1–3,8–10], moving belts [11], thermospray [12,13], electrospray [14], ion spray [15,16], fast atom bombardment [17], monodisperse aerosol interfaces [6] and many others. For example, fast atom bombardment (FAB) MS has been used successfully in its conventional form as an introduction system for MS and MS–MS analysis [18] and in the continuous-flow (CF) mode for real-time reaction monitoring (peptide hydrolysis) [19] and interfacing LC to MS (LC–FAB-MS) [20]. The use of FAB as an introduction system is advantageous since it allows an ion beam to persist for a long period of time (10–15 min), during which mass spectral techniques such as exact mass measurements or collision-induced dissociation experiments (MS–MS) can be performed.

A survey of the existing liquid introduction systems shows that the DLI systems using a simple metal or fused-silica capillary [9,10,21–26] to transfer the solvent or an analyte in solution into the ion source of the mass spectrometer are the most appealing. They are inexpensive and can be adapted easily to any type of mass spectrometer whether it be a quadrupole or a magnetic-sector instrument. This simple type of interface uses flow-rates in the range of 1–10 μl/min, which are within the pumping capacity of most mass spectrometers that use an electron ionization (EI) or a chemical ionization (CI) ion source, as shown by Tal'roze *et al.* [1] and by Baldwin and McLafferty almost twenty years ago. The simplicity of this interface has permitted the construction of home-built devices for the analysis of thermally labile or polar compounds [22] or high-molecular-weight materials (CF-FAB) [18].

The use of a DLI interface can lead to three conditions of stability that are interesting for mass spectral analysis. These interfaces can produce a stable liquid surface under vacuum as in FAB, a stable stream of liquid droplets, that can further be desolvated [21], as produced by pneumatic nebulizers [14,15] with or without electrical assistance, or alternatively a steady stream of gas as obtained with capillary thermal nebulizers [27].

Examination of the actual configuration of most gas chromatography (GC)–MS systems, using direct coupling of the capillary GC column into the ion source, immediately leads to the conclusion that these systems could be used as the basis for capillary DLI interfaces using thermal nebulization. It is in that perspective that the present work was untertaken in order to evaluate the feasibility of using conventional GC–MS interfaces for the introduction of liquid samples into quadrupole and magnetic-sector mass spectrometers. Experiments have been conducted in order to characterize the optimal operating conditions of such an interface coupled with a CI source and to use it as a liquid sample introduction system for MS and MS–MS analyses as well as a simple interface to perform LC–MS experiments on specific analytical systems.

EXPERIMENTAL

Instrumentation

The instruments used in this study were a VG-TRIO-1 quadrupole mass spectrometer equipped with differential pumping (240 L/s source, 50 L/s analyser) and a

LAB BASE data system, and a VG-AutoSpec-Q magnetic-sector hybrid mass spectrometer of EBEqQ geometry. Both instruments were interfaced to Hewlett-Packard 5890 gas chromatographs equipped with capillary GC columns. The TRIO-1 was slightly modified by the addition of a Penning CP25EK high-vacuum gauge (Edwards Vacuum) on the pumping circuit leading to the CI source, which was slightly altered to increase its pumping speed and sensitivity. The VG-AutoSpec-Q was used without modification. The combined EI–CI source was used for DLI-MS experiments. In DLI-MS–MS experiments, kinetic energy spectra (MIKES/CA) were obtained by isolating the ion of interest with the two sectors E_1 and B and by scanning the voltage on the second electric sector E_2 over the whole range of energies. The collision energy in the FF3 cell was 8 KeV, and helium was used as a collision gas at a pressure corresponding to a beam attenuation of 50%. Single- or multiple-scan experiments were performed with the SIOS interface using the VAX-based OPUS data system in the MCA mode.

DLI experiments

The DLI experiments performed in this study were done by directly introducing a 50 or 75 μm I.D. fused-silica transfer capillary into the ion source of either mass spectrometer. On both instruments, the transfer capillary was introduced by the GC oven through the conventional GC–MS interface where it replaced the GC capillary column and was adjusted into the ion source exactly like the GC column. The capillary was directly connected at the other end (in or outside GC oven) to a 60-nl Valco C14W manual injector valve through which the solution containing the sample was introduced. The mobile phase of variable composition was supplied to the DLI system by a Harvard Model 22 low-pressure syringe pump as shown in Fig. 1. All solvents were HPLC grade and degassed in an ultrasonic bath for 15 min before use. Typical flow-rates used were between 0.5 and 3 μl/min. For LC–MS experiments, the Harvard pump was replaced by a high-pressure syringe pump. The transfer capillary was heated over the length of the interface and maintained at the optimal temperature on both spectrometers using the standard GC–MS interface heaters and controls on the respective instruments. The CI ion source was operated using the DLI mobile

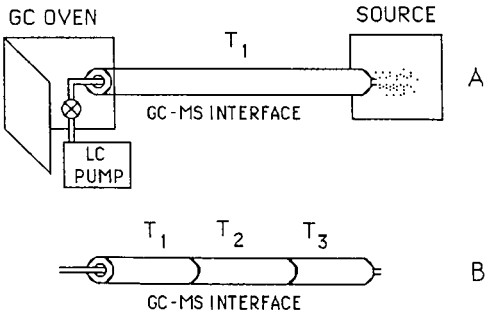

Fig. 1. Typical GC–MS interfaces that exist on mass spectrometers. (A) GC–MS interface on VG-TRIO-1 quadrupole mass spectrometer. (B) GC–MS interface on VG-AutoSpec magnetic-sector mass spectrometer. T_1, T_2 and T_3 represent thermal zones in the interface.

phase as a reagent gas with or without a make-up CI gas. Return to the GC–MS mode was done by simply replacing the DLI capillary with the GC capillary column. Essentially no time was wasted in resetting the interface temperature when changing the operating mode since temperatures were very similar in both types of experiments.

RESULTS AND DISCUSSION

The DLI system used in this study, which resembles several systems that have been reported in the literature [10,22,26], consists of a fused-silica capillary which is introduced directly into a CI source through a standard GC–MS interface. This capillary replaces the GC column in the interface and is connected to an injector and a pumping system as shown in Fig. 1. The characteristics of the system are (i) the absence of a desolvation chamber which is often used in DLI systems [7,9,12,21,25] and (ii) the fused-silica transfer capillary is heated over the whole length of the interface, which is of the order of 60 cm. The interface can have one temperature zone, as in Fig. 1A (TRIO-1), or several, as in Fig. 1B (AutoSpec-Q).

The main factors that influence the performance of DLI systems using capillary thermal nebulizers are the temperature of the capillary and the flow of the mobile phase into the ion source of the mass spectrometer. The temperature of the interface governs the rate of evaporation of the mobile phase, whereas the flow-rate affects the pressure within the ion source and thus the composition of the CI plasma. It is, therefore, essential for the optimization of the DLI system that the optimal interface temperature and flow-rate be determined in order to operate under stable experimental conditions [8,28,29].

The effect of the interface temperature on the stability of the DLI systems was studied in initial experiments on the quadrupole spectrometer that has a single thermal zone (Fig. 1A). The results obtained when the temperature was varied at constant flow-rate (*ca.* 1 μl/min) of the mobile phase indicated that the stability of the system, as measured by the ratio of the standard deviation of the total ion current (TIC) (σ) over the TIC, varied as a parabolic function of the interface temperature. Typically the ratio σ/TIC was of the order of a few percent between 150 and 180° (3% at 170°C [27]), where source conditions were found to be extremely stable. Partial to severe instability was encountered on both sides of this temperature range. These observations can be rationalized by the fact that at lower temperatures the evaporation of the mobile phase is too slow compared with the flow in the system, creating erratic evaporation in the ion source [10]. At temperature values well above 170°C, the evaporation rate is too high and the vaporization zone resides well within the capillary, creating instability in the flow.

The temperature effect observed when the DLI system was used on the AutoSpec-Q mass spectrometer showed similar behavior, but the results obtained for the stability of the system with the interface temperature were slightly different. This can be explained by the fact that the GC–MS interface on this particular mass spectrometer is constructed in three segments that can be maintained at different temperatures (Fig. 1). With this instrument a stability region also exists for a range of temperature between 180 and 240°C for segment T_3, when the temperatures of fragments T_2 and T_1 are maintained at 210 and 220°C, respectively. Temperature T_3 appears to be most critical, and if it is set outside this range instability in the operating conditions is observed, as with the other interface.

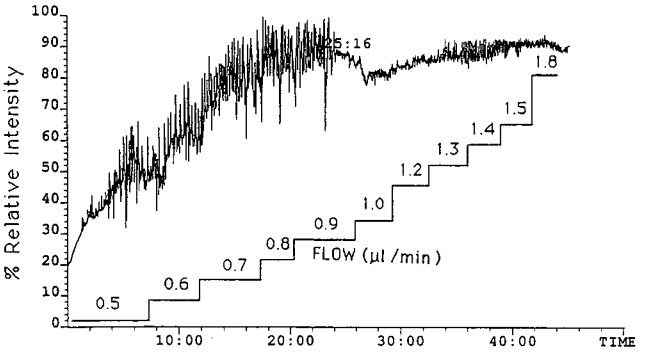

Fig. 2. Stability of the TIC in the ion source of the AutoSpec-Q with the flow-rate in the DLI interface. Time in min.

Another factor that affects the stability and the operating conditions is the flow-rate. Its value has to be such that the thermal input through the interface is sufficient to vaporize the mobile phase while the pressure within the CI source is adequate to maintain ionization and sensitivity. The pressure in the ion source depends on the flow-rate and the pumping capacity, and it must stay within a given range in order to produce a stable and reproducible plasma composition. If LC–MS experiments are to be conducted, additional constraints will be imposed on the flow-rate, since it will have to be such that the chromatographic conditions are also optimized.

The effect of the flow-rate was investigated on the AutoSpec-Q mass spectrometer at optimum temperature of the interface (T_1 = 220°C, T_2 = 210°C, T_3 = 190°C). The fluctuation of the TIC, including the mobile phase components, observed with flow-rate is shown in Fig. 2. For values of the flow-rate below 1.0 µl/min the system is quite unstable, as witnessed by the important variation in the signal. As the flow approaches the value of 1.1 µl/min, the noise on the TIC rapidly disappears and the standard deviation becomes of the order of a few percent, indicating that the overall operating conditions have stabilized. If the flow is increased above 1.3 µl/min, the noise reappears but to a much lesser extent, indicating that the system is slightly perturbed but still relatively stable. The range of flows corresponding to stable operating conditions is found to be 1.0–1.6 µl/min on the AutoSpec-Q mass spectrometer and 0.8–2.0 µl/min on the TRIO-1, corresponding, dependent on solvent, to indicated source pressures of $1 \cdot 10^{-5}$ to $6 \cdot 10^{-5}$ and $2 \cdot 10^{-5}$ to $2 \cdot 10^{-4}$ Torr, respectively, which indicates that flow conditions are probably similar on most instruments. This flow is compatible with the use of 0.25 mm I.D. packed capillary columns that operate at optimum flow-rates between 1 and 2 µl/min.

The flow-rate in a DLI system using CI also determines the pressure in the ion source and consequently the composition of the plasma. In order to assess the influence of the flow on ionization, the composition of the plasma was measured at varying source pressures corresponding to different flow-rates. In these experiments, several mobile phase compositions were studied, and typical results obtained with the binary mixture acetonitrile–water (75:25) are shown in Fig. 3. The figure gives the ion profiles on the TRIO-1 (Fig. 3A) and on the AutoSpec-Q (Fig. 3B) as a function of the

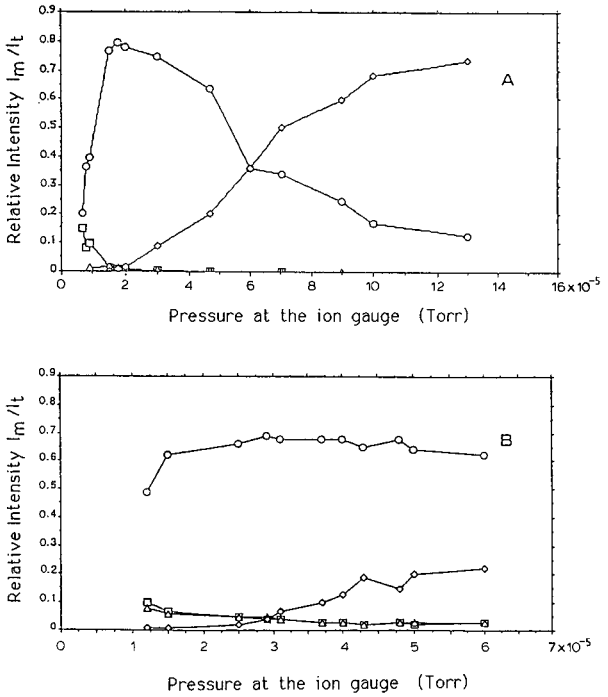

Fig. 3. Variation of the composition of the CI plasma with pressure (flow-rate) in the ion source. (A) TRIO-1: ○ = CH_3CNH^+ = *m/z* 42; ◇ = $(CH_3CN)_2H^+$ = *m/z* 83; □ = H_3O^+ = *m/z* 19; △ = H_2O^+ = *m/z* 18. (B) AutoSpec: ○ = CH_3CNH^+; ◇ = $(CH_3CN)_2H^+$; □ = H_3O^+; △ = H_2O^+. I_m represents the current of the individual mass and I_t the total ion current.

pressure in the source. It can be observed from Fig. 3A that the major ion in the plasma at the lower pressures ($<4 \cdot 10^{-5}$ Torr) corresponds to protonated acetonitrile at *m/z* 42, and that for pressures below this value the intensity of the protonated dimer of acetonitrile at *m/z* 83 is small. As the pressure is increased above that value, the intensity of the dimer increases and it becomes the most important ion. Ions at *m/z* 18 and 19 corresponding to H_2O^+ and H_3O^+ have much weaker intensities than those related to acetonitrile.

The distribution of ions in the source of the AutoSpec-Q is shown in Fig. 3B and is similar to that observed on the TRIO-1. The figures appear different because the pressure range shown in Fig. 3B ($1 \cdot 10^{-5}$ to $6 \cdot 10^{-5}$ Torr) is narrower than that in Fig. 3A ($2 \cdot 10^{-5}$ to $1.6 \cdot 10^{-4}$ Torr). The upper limit for pressure on the magnetic-sector spectrometer is lower than on the quadrupole because of the high voltage. The ion profiles in the source of this magnetic-sector mass spectrometer compare well with the ion intensities found at a pressure of $2 \cdot 10^{-5}$ on the quadrupole instrument, and it can be seen that the protonated dimer starts to increase while the protonated monomer starts to decrease as the pressure increases. The ions generated by water at *m/z* 18 and 19 are again weak as observed in the other source. The pressures indicated in the figures are not actual source pressures but those corresponding to readings on the vacuum gauges and are not exactly matched since the gauges are located at different positions on each spectrometer.

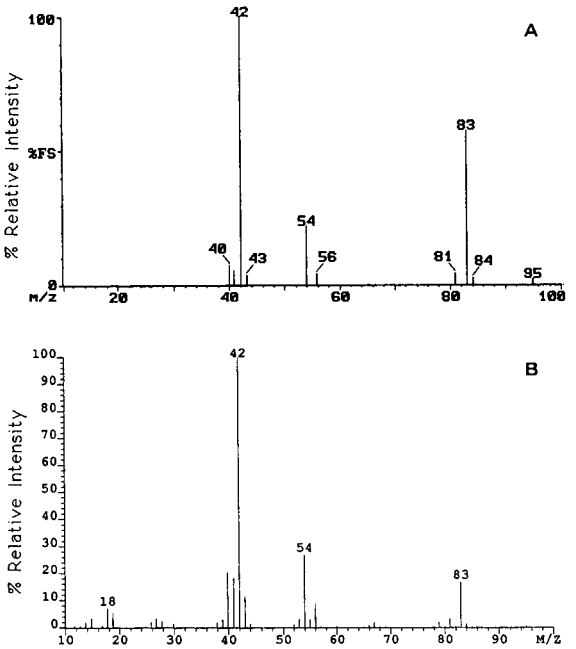

Fig. 4. Composition of the CI plasma obtained with a mobile phase acetonitrile–water (75:25) under typical operating conditions of the DLI system. (A) Composition on the VG-TRIO-1 mass spectrometer. (B) Composition on the AutoSpec-Q; CH_3CNH^+ = m/z 42.

The ionization conditions should be similar on both instruments since the operating conditions of the DLI systems are close. The mass spectrum corresponding to the plasma generated in both systems by the binary mobile phase, under optimized conditions, is given in Fig. 4A and B. Examination of the figures reveals that the ion populations are identical, which suggests that the DLI system will probably yield similar results on almost any mass spectrometer with a direct GC–MS capillary interface. For the acetonitrile–water (75:25) mixture the most important ionic species is CH_3CNH^+, but this ion is also quite important in other phases that we have analyzed, including ternary mixtures containing acetonitrile (acetonitrile–water–acetic acid). Thus, the qualitative results that can be obtained using these systems with different mobile phases containing acetonitrile should be similar. It is noteworthy that the presence of important ionic species higher than the dimer is not observed in our DLI-MS system even in the absence of a desolvation chamber. This observation is contrary to other reports using DLI interfaces in which the protonated dimer is by far the most important ionic species [30,31]. This disparity can be rationalized by the fact that our capillary is heated over a considerable length, and this causes higher clusters to dissociate before they enter the ion source.

In order to investigate qualitatively the variability of the ionization conditions in the DLI system, several compounds were analyzed using mobile phases of varying compositions. Typical spectra obtained in these experiments are shown in Fig. 5. The figure shows the mass spectra of *p*-hydroxybenzoic acid and vanillic acid obtained

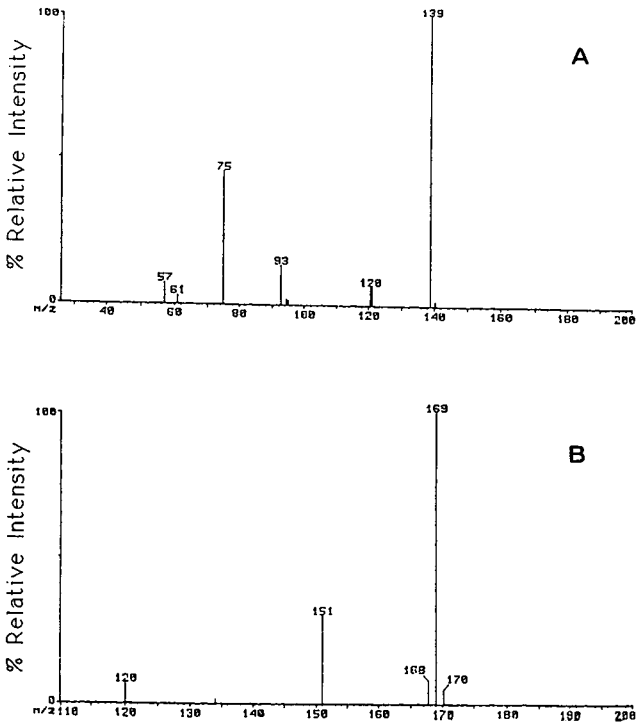

Fig. 5. Mass spectrum of (A) *p*-hydroxybenzoic acid obtained with pure water as mobile phase and (B) vanillic acid obtained with pure acetonitrile.

using pure water (Fig. 5A) and pure acetonitrile (Fig. 5B), respectively. It can be concluded from the data that, although the extent of fragmentation can vary slightly from one composition to another because of different proton affinities, the general features of the spectrum, presence of $[M+H]^+$ and $[M+H-H_2O]^+$, are generally the same. The mass spectra obtained with the same mobile phase but on different instruments can be compared. The spectra of ibuprofen obtained using the DLI interface (acetonitrile–water, 75:25) on the TRIO-1 (80 ng) and the AutoSpec-Q (6 ng) are shown in Fig. 6A and B, respectively. It is noteworthy that the relative intensity of the $[M+H]^+$ ion is considerably greater than that reported in the literature in similar systems using concentrations ten times greater [32]. Furthermore, the data reveal that the patterns obtained on different instruments are extremely similar, which suggests that the DLI system can be transported between instruments without noticing major changes. This supports the assumption made previously from the comparison of the plasma compositions.

The operating conditions having been determined, the DLI interface can be used for several types of applications. Beside its obvious use as an LC–MS interface as already shown [27], it can be used for real-time monitoring of reactions in solution and as a liquid introduction system for MS and MS–MS analysis.The latter application is interesting since, as is done with FAB, the DLI system can be helpful in mass

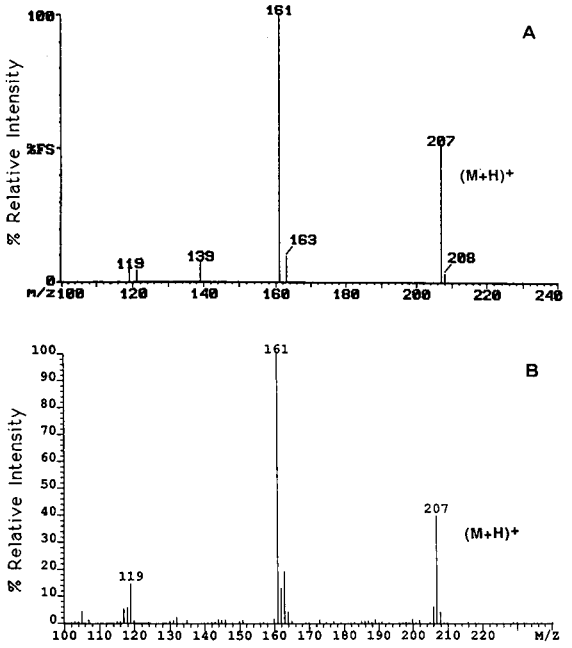

Fig. 6. Mass spectrum of ibuprofen obtained with acetonitrile–water (75:25). (A) Spectrum on TRIO-1; (B) spectrum on AutoSpec-Q.

spectral experiments that need a stable ion beam that can persist for a resonable period of time. In mass spectral techniques such as accurate mass measurement or mass-analyzed ion kinetic energy spectroscopy experiments, it is extremely useful to be able to maintain a steady ion beam of good intensity. Use of a direct insertion probe or a heated batch inlet system is not always desirable. Some compounds are too volatile for probe work and only give a transient signal, and others are too labile to be heated in a batch reservoir. Thus, the DLI inlet can be used with success in these types of analyses.

In order for the DLI interface to be useful for these applications it is necessary

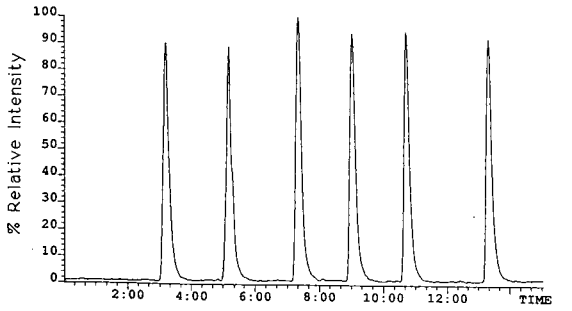

Fig. 7. TIC on AutoSpec-Q for repetitive injections of 60 nl of ibuprofen (100 pg/nl). Time in min.

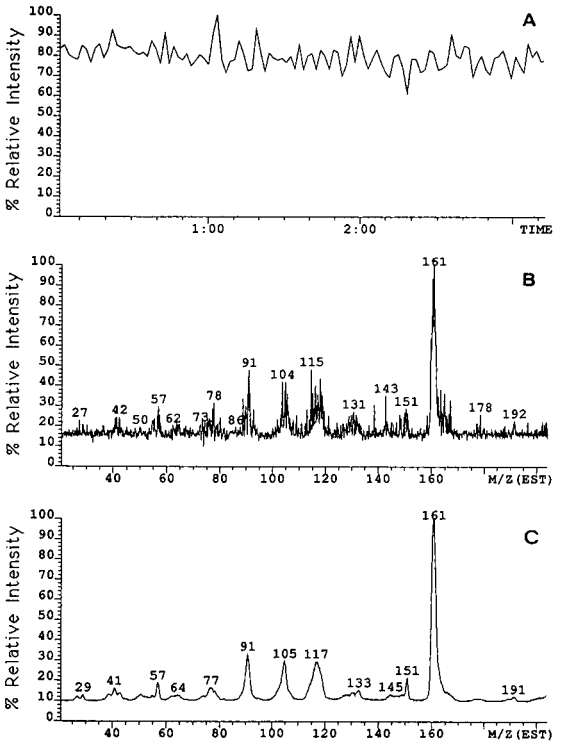

Fig. 8. MS–MS analysis of a solution of ibuprofen (100 pg/nl) in the DLI mode. (A) Mass chromatogram of $[M+H]^+$ at m/z 207. Time in min. (B) Collisionally activated spectrum of $[M+H]^+$ at m/z 207, single scan. (C) Average of ten scans.

that its operation be stable and reproducible. The reproducibility of sample injection has been studied with injections of ibuprofen. Fig. 7 gives the single-ion chromatogram of m/z 207 ($[M+H]^+$) reproduced from the TIC for several consecutive 60-nl injections of a solution of ibuprofen (100 ng/μl). As is observed from the figure, the reproducibility of the system is excellent considering that the peaks are reproduced from scanning data. An example of the use of the DLI system for MS–MS analysis is presented in Fig. 8. The figure shows the results of experiments in which MS–MS data were obtained when a solution of ibuprofen was continuously introduced into the ion source using the DLI interface. Fig. 8A shows the TIC of the primary ion current at m/z 207 ($[M+H]^+$), Fig. 8B a single scan of a MIKES/CA spectrum of m/z 207, and Fig. 8C gives the spectrum obtained by averaging ten scans of the electric sector. The data of Fig. 8A demonstrate that the stability of the system is very good since the TIC was reproduced from MIKES/CA spectra and the relative concentration of the $[M+H]^+$ ion in the plasma was extremely low. The results also indicate that the liquid introduction system allows MS–MS spectra to be easily obtained from very small amounts of material (*ca.* 1 ng) and that it is possible to integrate the signal to increase signal-to-noise ratio bacause of the persistence of the signal. Thus the DLI system represents an excellent introduction system for mass spectral analysis of compounds in solution or in mixtures.

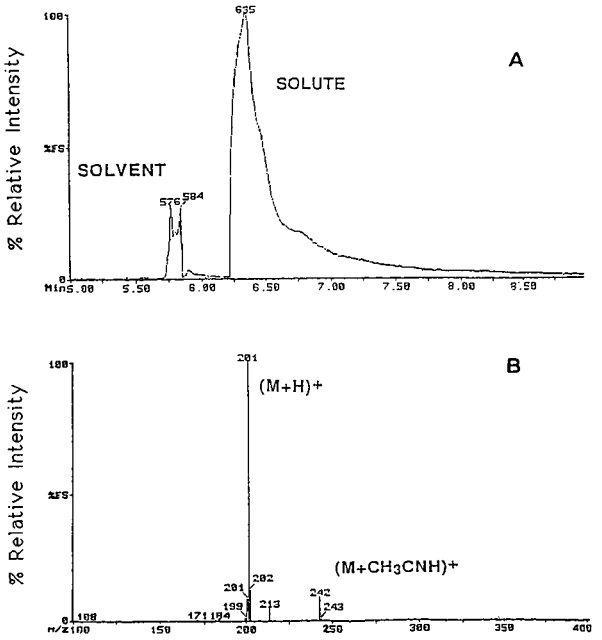

Fig. 9. Analysis of solution of 1,12-diaminododecane in hexane injected in acetonitrile–water (75:25). (A) TIC of DLI injection. (B) Mass spectrum of 1,12-diaminododecane.

The thermal nebulizer capillary DLI interface offers other advantages for the routine analysis of volatile compounds present in solutions. This can be seen from the data presented in Fig. 9, which shows the injection of a liquid solution of 1,12-diaminododecane in hexane. The TIC trace represented in Fig. 9A shows that the interface separates the solute from the solvent and that both compounds are analyzed separately in the mass spectrometer. The spectrum given in Fig. 9B corresponds to the spectrum of 1,12-diaminododecane in the mixture. Examination of the spectrum reveals that it is relatively pure and that interference from the solvent is almost absent. Several samples contained in solvents have been analyzed by direct liquid injection, and the phenomenon shown in Fig. 9 is almost always observed because of some activity in the transfer capillary. However, this phenomenon is not observed when the sample is continuously admitted into the ion source.

CONCLUSIONS

The simple DLI system using a conventional GC–MS interface that has been described in this work can be very useful to interface LC to MS and also as a stand-alone system that can be used for mass spectral analyses by MS or MS–MS. The system is easy to operate, offers very good stability when operated under optimum conditions and is transportable from one instrument to another. As has been shown in this study, the performance is equally good on the magnetic-sector or quadrupole mass spectrometers and the data obtained using both systems compare well. The mass

spectra obtained with several mixtures commonly used as mobile phases in LC are qualitatively similar. The system, although similar to other systems that have been reported, presents particular features since the plasma generated contains mostly protonated monomers. The system is reproducible and allows picogram sensitivity to be achieved in the MS–MS or LC–MS mode, using 0.25-mm packed capillary columns [27]. Over the period of 16 months that we have used the system, the capillary has never blocked with our analytical applications.

ACKNOWLEDGEMENTS

The authors wish to acknowledge the financial contributions of the National Science and Engineering Research Council of Canada (NSERC) and Hydro-Québec that have permitted this study. The authors are also grateful to Dr. G. Paul for his editorial assistance.

REFERENCES

1 V. L. Tal'roze, G. V. Karpov, I. G. Gorodetskii and V. E. Skurat, *J. Phys. Chem.*, 42 (1968) 1658.
2 M. A. Baldwin and F. W. McLafferty, *Org. Mass Spectrom.*, 7 (1973) 1111.
3 P. Arpino, *Mass Spectrom. Rev.*, 8 (1989) 35.
4 T. R. Covey, E. D. Lee, A. P. Bruins and J. D. Henion, *Anal. Chem.*, 58 (1986) 1451A.
5 D. E. Games, *Adv. Chromatogr.*, 21 (1983) 1.
6 K. B. Tomer and C. E. Parker, *J. Chromatogr.*, 492 (1989) 189.
7 W. M. A. Niessen, *Chromatographia*, 21 (1986) 277.
8 W. M. A. Niessen, *Chromatographia*, 21 (1986) 342.
9 P. J. Arpino and C. Beaugrand, *Int. J. Mass Spectrom. Ion Process.*, 64 (1985) 275.
10 A. P. Bruins and B. F. H. Drenth, *J. Chromatogr.*, 271 (1983) 71.
11 N. J. Alcock, C. Eckers, D. E. Games, M. P. L. Games, M. S. Lant, M. A. McDowall, M. Rossiter, R. W. Smith, S. A. Westwood and H.-Y. Wong, *J. Chromatogr.*, 251 (1982) 165.
12 M. L. Vestal and G. J. Fergusson, *Anal. Chem.*, 57 (1985) 2373.
13 C. R. Blakley and M. L. Vestal, *Anal.Chem.*, 55 (1983) 750.
14 J. B. Fenn, M. Mann, C. K. Meng, S. F. Wang and C. M. Whitehouse, *Mass Spectrom. Rev.*, 9 (1990) 37.
15 A. P. Bruins, T. R. Covey and J. Henion, *Anal. Chem.*, 59 (1987) 2642.
16 E. C. Huang, T. Wachs, J. J. Conboy and J. D. Henion, *Anal. Chem.*, 62 (1990) 731A.
17 R. M. Caprioli, T. Fan and J. S. Cottrell, *Anal. Chem.*, 58 (1986) 2949.
18 M. Barber, R. S. Bordoli, G. J. Elliott, R. D. Sedgwick and A. N. Tyler, *Anal. Chem.*, 54 (1982) 645A.
19 S.-N. Lin and R. M. Caprioli, *Proceedings of the 36th Annual Conference on Mass Spectrometry and Allied Topics, San Francisco, CA, June 5–10, 1988*, p. 1000.
20 S. Pleasance, P. Thibault, M. A. Mosely, L. J. Deterding, K. B. Tomer and J. N. Jorgenson, *J. Am. Soc. Mass Spectrom.*, 1 (1990) 312.
21 P. J. Arpino, P. Krien, S. Vajta and G. Devant, *J. Chromatogr.*, 203 (1981) 117.
22 H. Alborn and G. Stenhagen, *J. Chromatogr.*, 394 (1987) 35.
23 N. Evans and J. E. Williamson, *Biomed. Mass Spectrom.*, 8 (1981) 316.
24 J. D. Henion, *J. Chromatogr. Sci.*, 19 (1981) 57.
25 P. Hirter, H. J. Walter and P. Datwyler, *J. Chromatogr.*, 323 (1985) 89.
26 K. H. Schafer and K. Levsen, *J. Chromatogr.*, 206 (1981) 245.
27 J. P. Gagné and M. J. Bertrand, *Proceeding of the 38th Annual ASMS Conference on Mass Spectrometry and Allied Topics, Tucson, AZ, June 3–8, 1990*, p. 1214.
28 R. D. Voyksner, C. E. Parker, J. R. Hass and M. M. Bursey, *Anal. Chem.*, 54 (1982) 2583.
29 J. Yinon and A. Cohen, *Org. Mass Spectrom.*, 18 (1983) 47.
30 J. Yinon and D.-G. H. Wang, *J. Chromatogr.*, 268 (1983) 45.
31 A. B. Bruins and B. F. H. Drenth, *Int. J. Mass Spectrom. Ion Phys.*, 46 (1983) 213.

Journal of Chromatography, 554 (1991) 305–309
Elsevier Science Publishers B.V., Amsterdam

CHROM. 23 422

Short Communication

Identification of poly(ethylene terephthalate) cyclic oligomers by liquid chromatography–mass spectrometry

H. MILON
Nestec Ltd., Research Centre, Vers-chez-les-Blanc, P.O. Box 44, CH-1000 Lausanne 26 (Switzerland)

ABSTRACT

Plasmaspray liquid chromatography–mass spectrometry has been used to detect and identify cyclic oligomers, $(\overline{GT})_n$, in samples of poly(ethylene terephthalate). Operating the mass spectrometer at unusually high temperatures (370°C for the tip), the identity of the two main peaks, which were attributed to $(\overline{GT})_3$ and $(\overline{GT})_4$ on the masis of their UV absorption, could be confirmed by the *m/z* value of their molecular anions. The very poor results observed at lower temperatures exemplify the difficulty of vaporizing and ionizing these molecules.

INTRODUCTION

Poly(ethylene terephthalate) (PET) packaging materials may contain several monomers and low-molecular-weight polymers (oligomers) which are formed during the polymerization process. The use of PET as a food packaging material is expanding rapidly, especially for conventional or microwave heating and cooking, where PET is metallized with aluminium and bonded to a board surface to produce so-called 'active' packaging or 'susceptors'. Under these conditions temperatures over 200°C are reached, which may facilitate the migration of these chemicals into the packed food [1].

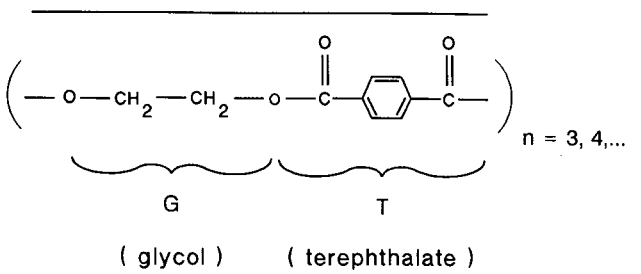

Fig. 1. General structure of the cyclic oligomers $(\overline{GT})_n$.

0021-9673/91/$03.50

Quantitatively, the most important compounds are a homologous series of cyclic oligomers, $(\overline{GT})_n$ (Fig. 1), which have been isolated and characterized [2]. They can be easily separated by high-performance or thin-layer chromatography [3] but are difficult to synthesize. The migration of the oligomers has been analysed by determining dimethyl terephthalate by stable isotope dilution gas chromatography-mass spectrometry after hydrolysis to terephthalic acid and methylation, thus avoiding the need to ionize the oligomers themselves [1]. The formation of cyclic oligomers from PET has been studied by direct mass spectrometry either by heating the polymer in the ion source [4] or by pyrolysis [5]. However, a direct identification technique would be useful and liquid chromatography–mass spectrometry (LC–MS) should be the method of choice in spite of the difficulty of vaporizing and ionizing the molecules. In this study, LC–plasmaspray MS (LC–PSP-MS) was used to confirm the identity of the chromatographic peaks attributed to some of these compounds by providing information on their molecular weight.

EXPERIMENTAL

Extraction

A 300-mg amount of PET (obtained by delamination of a sample of Susceptor; Waddingtons Cartons, Leeds, UK) was dissolved in 30 ml of 1,1,1,3,3,3-hexafluoro-2-propanol (HFIP) (Sigma, St. Louis, MO, USA)–dichloromethane (3:7). After precipitation of the polymer with 25 ml of acetone and centrifugation, the supernatant was evaporated and the pellet dissolved in 5 ml of N,N-dimethylacetamide (Eastman Chemical Products, Kingsport, TN, USA). Aliquots of 20 μl of this solution were used for chromatographic separations.

Liquid chromatography

The LC system consisted of a Waters Assoc. (Milford, MA, USA) Model 600-MS pump, a U6K injector and a Nova-Pak C_{18} column (15 cm × 4.6 mm I.D.) packed with 4-μm particles. The mobile phase was water–acetonitrile (2:1) adjusted to pH 3.5 with formic acid. The flow-rate was 2 ml/min.

Mass spectrometry

A Delsi Nermag (Argenteuil, France) Model R 10-10C quadrupole instrument was coupled to the LC system via a thermospray interface (Vestec, Houston, TX, USA) used in the plasmaspray (PSP) mode, *i.e.*, a discharge electrode (900 V, 10 kHz) was used to ionize the solutes and no salt was added to the mobile phase as in conventional thermospray operation.

The working temperatures were 370°C for the probe tip and 270°C for the ion-source block. A repeller electrode was set at −250 V. The mass spectrometer was operated in the negative-ion mode, scanning masses 100–800 u in 0.5 s. In some analyses, a UV detector (Spectroflow 773; Kratos, Manchester, UK) operated at 254 nm was used in place of the mass spectrometer.

RESULTS AND DISCUSSION

The UV trace obtained under the separation conditions used (Fig. 2A) is in full agreement with those usually obtained with this type of sample. By comparison with

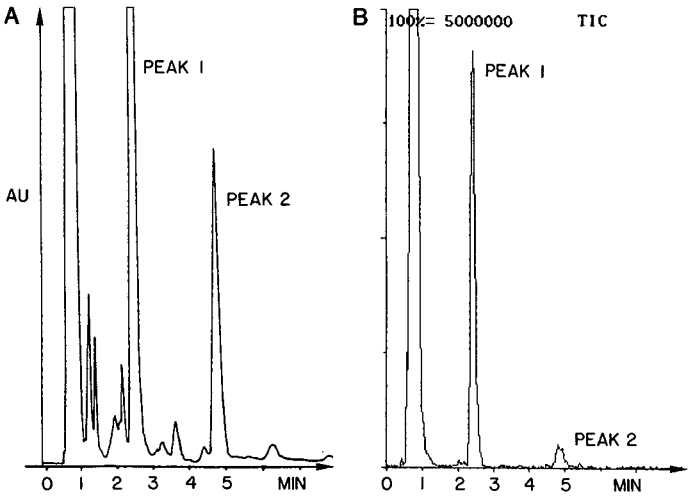

Fig. 2. (A) UV trace (254 nm) of a PET extract sample. (B) LC–PSP-MS TIC recording of the same sample under the same conditions (see text). Peaks 1 and 2 were identified by their retention times.

the published literature, peaks 1 and 2 can be tentatively attributed to $(\overline{GT})_3$ and $(\overline{GT})_4$, respectively. Fig. 2B shows the reconstructed total ion current (TIC) trace of an aliquot of the same sample.

The mass spectra for peaks 1 and 2 are shown in Fig. 3. In each spectrum, only one main ion is observable, probably the molecular anion. In fact their m/z values, 576 and 768, respectively, correspond to the molecular weight of each oligomer and the chromatographic peaks can be attributed to $(\overline{GT})_3$ and $(\overline{GT})_4$ with high probability.

The full UV trace of the sample (not shown) shows a series of at least five compounds. They all have identical UV absorption spectra, indicating high structural similarity and that they probably belong to the series $(\overline{GT})_n$ where $n = 3$–7. At the time these experiments were done, the calibrated mass range of the mass spectrometer did not allow the detection of masses higher than 800. In spite of this, the tip and source tenperatures necessary to observe oligomers higher than $n = 4$ would have been very difficult to reach.

The probe tip temperature used here was 370°C, which is unusually high for LC–thermospray MS operation. At a lower temperature of 290°C, which is already in the upper range of those commonly used, the analysis was much worse. This is shown in Fig. 4, which presents the TLC trace and the m/z 576 and 768 ion current recordings. There, the presence of peak 2 can only be guessed and the shape of the peaks and the abundance of the fragments are really unsatisfactory. Evidently, this type of cyclic molecule with no polar function is difficult to vaporize and ionize. In fact, preliminary experiments showed that by using conventional thermospray conditions (no discharge and 0.1 M ammonium acetate added to the mobile phase) no signal corresponding to the oligomers could be observed.

Mass spectra of these oligomers have been obtained by heating PET in the ion

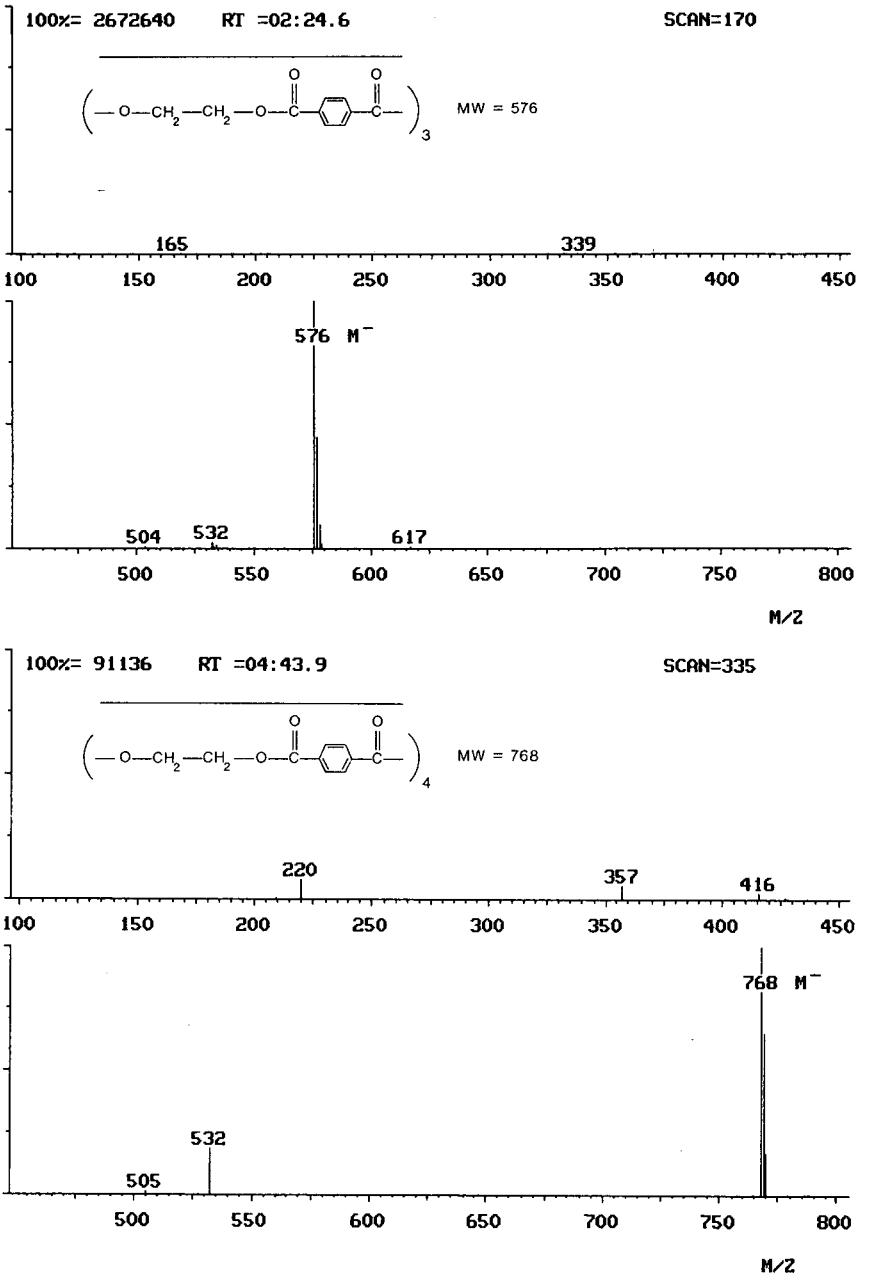

Fig. 3. Mass spectra for peaks 1 and 2 and probable structure of the main fragments. RT = Retention time in min:s; MW = molecular weight.

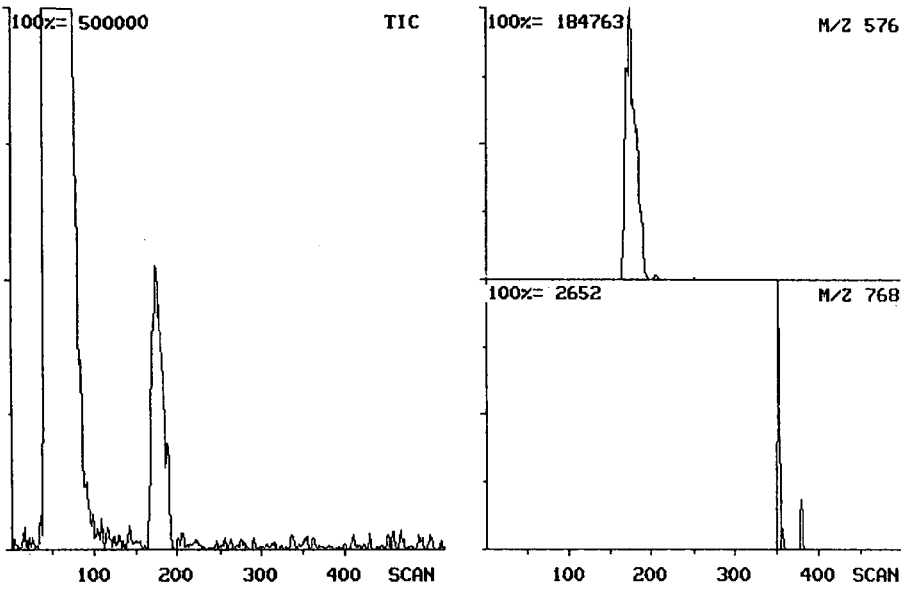

Fig. 4. LC–PSP-MS TIC and *m/z* 576 and 768 recordings of the same sample at a tip temperature of 290°C. Note the poor shape of the peaks and the very low abundance of *m/z* 768.

source [4] or in a pyrolysis probe [5]. The aim of these studies was to investigate the formation of oligomers by thermal degradation and temperatures up to 400°C were used. The electron impact mass spectrum of $(\overline{GT})_3$ contains an intense fragment ion at *m/z* 533 [4] and the negative-ion chemical ionization mass spectrum of a mixture of the cyclic oligomers contains intense ions at *m/z* 768, 576 and 532 [5], thus providing further support that peaks 1 and 2 in our study do correspond to $(\overline{GT})_3$ and $(\overline{GT})_4$.

ACKNOWLEDGEMENTS

The author acknowledges the contribution of J. Ruiz to the chromatographic separations and his skillful technical assistance and also the help of E. Castella.

REFERENCES

1 L. Castle, A. Mayo, C. Crews and J. Gilbert, *J. Food Protec.*, 52 (1989) 337.
2 T. H. Begley and H. C. Hollifield, *J. Assoc. Off. Anal. Chem.*, 72 (1989) 468.
3 W. R. Hudgins, K. Theurer and T. Mariani, *J. Appl. Polym. Sci. Appl. Polym. Symp.*, 34 (1978) 145.
4 J. C. Gilland, Jr., and J. S. Lewis, *Angew. Makromol. Chem.*, 54 (1976) 49.
5 R. E. Adams, *J. Polym. Sci. Polym. Chem. Ed.*, 20 (1982) 119.

Journal of Chromatography, 554 (1991) 311–327
Elsevier Science Publishers B.V., Amsterdam

CHROMSYMP. 2194

Capillary electrophoresis–atmospheric pressure ionization mass spectrometry for the characterization of peptides

Instrumental considerations for mass spectrometric detection

I. MONIKA JOHANSSON[a], ERIC C. HUANG[b] and JACK D. HENION*
Drug Testing and Toxicology, Cornell University, 925 Warren Drive, Ithaca, NY 14850 (USA)
and
JERRY ZWEIGENBAUM
Analytical Technology Division, Eastman Kodak Company, Rochester, NY 14652-3712 (USA)

ABSTRACT

On-line capillary electrophoresis (CE) separations are shown for a synthetic peptide mixture and a tryptic digest of human hemoglobin in an uncoated fused-silica capillary with detection using atmospheric pressure ionization mass spectrometry (API-MS). The CE system utilized a 1-m capillary column of either 75- or 100-μm I.D. These somewhat larger inside diameters allow higher sample capacities for MS detection, and the 1-m length facilitates connecting the CE column to the liquid junction–ion spray interface and MS system. Low volatile buffer concentrations (15–20 m*M*) of ammonium acetate or ammonium formate, and high organic modifier content (5–50%) of methanol or acetonitrile facilitates ionization under electrospray conditions.

This study shows that peptides separated by CE may be transferred to the API-MS system through a liquid junction coupling to the pneumatically assisted electrospray (ion spray) interface at low buffer pH when the electroosmotic flow is low (0–0.04 μl/min). CE–MS as described herein is facilitated by features in modern CE instrumentation including robotic cleaning and pressurization of the capillary inlet. The latter is particularly useful for repetitive rinsing and conditioning of the capillary column between analyses in addition to continuous 'infusion' of sample to the mass spectrometer for tuning purposes.

In addition to facile molecular weight determination, amino acid sequence information for peptides may be obtained by utilizing on-line tandem MS. After the tryptic digest sample components enter the API-MS system, the molecular ion species of individual peptides may be focussed and transmitted into the collision cell of the tandem triple quadrupole mass spectrometer. Collision-induced dissociation of protonated peptide molecules yielded structural information for their characterization following injection of 10 pmol of a tryptic digest from human hemoglobin.

INTRODUCTION

The interest and use of capillary electrophoresis (CE) as a separation technique has expanded considerably in recent years. Separations are based on the principles of

[a] Present address: University of Uppsala, Equine Drug Research Laboratory, Ulleråker, S-750 17 Uppsala, Sweden.
[b] Present address: Merck Sharp & Dohme Research Laboratories, West Point, PA 19486, USA.

0021-9673/91/$03.50

the electrically driven flow of ions in free solution. High separation efficiency, short analysis times and a low amount of sample consumed makes CE a very attractive separation technique. On-column detection with UV absorbance or fluorescence is commonly used. The technique has recently been reviewed [1].

Peptides belong to a group of compounds where CE may be very useful both to separate bioactive peptides when the sequences differ by only one amino acid and for peptide mapping from proteolytic digests of proteins [2]. At low pH the uncoated fused-silica capillary wall carries few negative charges, so the electroosmotic flow is low. Positively charged peptides migrate towards the negatively charged cathode at the capillary exit. A decrease in electroosmotic flow observed under low pH conditions provides a wider separation window for the positively charged peptides. Good separations have been obtained for dipeptides in low-pH phosphate buffer [3] and for the protease V8 digest of β-lactoglobulin in citric acid pH 2.5 [4] in uncoated fused-silica capillaries with UV detection.

It is desirable to obtain high-quality electropherograms with mass spectrometry (MS) as the detection system. An advantage for MS detection is that molecular weight information may be obtained in addition to the migration time for each component peak in a mixture. It is also possible to obtain structural information of the mixture components by tandem mass spectrometry (MS–MS). In fact, the mixture analysis capability of the latter may even provide structural information from co-eluting components (see below). Sodium citrate, phosphate and borate buffers that are commonly used in CE separations are, however, not generally suitable for CE in combination with MS. The production of gas-phase ions during the electrospray process is facilitated by using volatile buffers at low concentration to obtain a high analyte ion current response. In addition, organic solvents such as methanol and acetonitrile, which reduce the surface tension of electrospray droplets, are desirable and facilitate the formation of gas-phase ions in the ion spray process [5]. In this work we discuss factors that pertain to the CE system when a mass spectrometer equipped with an atmospheric-pressure ionization source is used as the detector (API-MS). A review of the API-MS instrumentation used in this work has been reported by Huang *et al.* [6].

CE–MS with ionization at atmospheric pressure has previously been demonstrated for a variety of compounds [7–15]. Developments in CE–MS interfacing are based either on the electrospray–ion spray process where gas-phase ions are formed at atmospheric pressure (API) or continuous-flow fast atom bombardment (CF-FAB) [16–18]. For the latter the CE–MS interface must accommodate very low flow-rates and differing buffers used in CE in addition to the introduction of 10–25% glycerol for the CF-FAB process. The make-up liquid is introduced either by a liquid junction [8,12–14,17,18] or as a sheath-flow arrangement [9–11,15,16]. The use of a liquid junction or a sheath flow has provided preliminary results for CE–MS characterization of peptides. Here we have used a pneumatically assisted electrospray (ion spray) interface with the liquid junction coupling described previously by Lee *et al.* [14]. The buffer in the liquid junction is typically but not necessarily the same as the separation buffer for CE, and provides suitable make-up buffer flow to sustain a stable spray to the API mass spectrometer.

Earlier investigations with the ion spray interface have shown that CE–MS performs well with buffers of pH 4.8–6.9 and 50–90% acetonitrile in the running

buffer which produces a bulk electroosmotic flow between 0.4–1.8 μl/min [8,12–14]. In this work we demonstrate that analyte ions are transferred from the CE capillary via the liquid junction to the ion spray interface and the API-MS system under conditions where the electroosmotic flow is very low.

Increased interest in CE is also reflected by the rapid development of commercial CE instrumentation. We present the advantages of interfacing a commercially available CE instrument to API-MS and show the utility of CE–MS and CE–MS–MS techniques for the determination of peptides for characterizing protein tryptic digests. Several CE–MS experimental parameters are assessed as they relate to MS detection using the described system.

EXPERIMENTAL

Chemicals

Fused-silica capillary tubes with dimensions of 50, 75 and 100 μm I.D. and 365 μm O.D. were obtained from Polymicro Technologies (Phoenix, AZ, USA). HPE calibrators were obtained from Bio-Rad Labs. (Richmond, CA, USA). The HPE calibrator consists of the following nine peptides: (1) bradykinin; (2) angiotensin II; (3) α-melanocyte stimulating hormone (α-MSH); (4) thyrotropin releasing hormone (TRH); (5) luteinizing hormone-releasing hormone (LHRH); (6) oxytocin; (7) leucine enkephalin; (8) methionine enkephalin and (9) bombesin. The individual proteins, human hemoglobin and trypsin, were obtained from Sigma (St. Louis, MO, USA). The enzyme that was used to digest hemoglobin was trypsin treated with L-tosylamide-2-phenylethyl chloromethyl ketone (TPCK). The electroosmotic flow marker used in the study with UV detection was a heptapeptide (Arg–Lys–Arg–Ser–Arg–Lys–Glu) obtained from Applied Biosystems (Santa Clara, CA, USA). Sequencing-grade trifluoroacetic acid (TFA) was obtained from Aldrich (Milwaukee, WI, USA). Optima-grade acetonitrile and methanol were obtained from Fisher Scientific (Flair Lawn, NJ, USA). Water was purified in-house with a Barnstead Nanopure system. All other chemicals were of analytical or reagent grade and used without further purification.

Capillary electrophoresis instrumentation

Two commercial CE systems were used in this work. System A was an Applied Biosystems (Foster City, CA, USA) Model 270A while system B was a Beckman (Palo Alto, CA, USA) Model P/ACE 2000. Most of the off-line work with UV detection at 210 nm was performed with system A. In system A the total length of the capillary was 72 cm with a length of 50 cm between the inlet end and the UV detector. All CE–MS experiments in this report were performed with system B. For CE–MS work the total length of the capillary was 100–104 cm with the UV detector located 20 cm from the inlet end. Two modifications were made on the commercial Beckman instrumentation (System B) to facilitate CE–MS operation. The first was installation of a switch to bypass the safety lock between the capillary ends. Measurement of the current across the capillary by system B could not be made during CE–MS operation with this modification. The current through the system was measured by an external meter. The second modification involved bypassing the capillary cartridge temperature control system during CE–MS operation. Since most of the CE capillary ex-

tended through ambient air between the CE system and the mass spectrometer, the normal temperature control system would have been ineffective.

In system B, the first 20 cm of the capillary were housed in a cartridge holder. This device was also used in the CE–MS work, but the capillary extended beyond the UV detector to reach the mass spectrometer. A slit was made in the upper portion of the cartridge holder to allow extension and connection of the capillary end to the liquid junction coupling and the ion spray interface. Of the 100 cm total length, 36 cm of the capillary were inside the cartridge holder while 64 cm were held in air outside this device. The temperature in system B is usually regulated by a circulating liquid inside the cartridge holder during CE operation. This liquid, a mixture of C_{5-18} perfluorocompounds containing sodium, had a very high response in the API-MS such that a small leakage of the liquid from the cartridge holder into the running buffer vial was sufficient to interfere with the analyte signal. Considerable difficulty was experienced rebuilding the cartridge holder, so it was more convenient to bypass the circulating liquid and thereby the temperature control of the capillary. Part of the capillary (64 cm) was positioned in air so there was no temperature control for that part of the capillary. Therefore, removal of the temperature control fluid from the first portion of the capillary had little effect on the separation. Both CE systems A and B employ a high-voltage power supply with a maximum of 30 kV.

Mass spectrometry

A Sciex TAGA 6000E triple quadrupole mass spectrometer equipped with an API source was used in this work (Sciex, Thornhill, Canada). The capillary exit end from the CE system was coupled to the API-MS via a liquid junction and a pneumatically assisted electrospray (ion spray) interface [5]. The same liquid junction and ion spray interface have been described by Henion and co-workers [8,12–14]. The only modification in this work was that the inner capillary in the ion spray interface consisted of uncoated fused silica instead of stainless steel. The I.D. of the fused-silica capillary in the ion spray interface was either 75 or 100 μm while the corresponding I.D. was used in the separation capillary. In the present study the liquid junction along with the ion spray interface were floated at +3.5–4.2 kV while the mass spectrometer was operated in the positive-ion mode of detection. When the high voltage required for the CE separation was maintained at 30 kV, the overall potential difference across the separation capillary was actually 26 kV.

Gas-phase ions generated from the ion spray interface via the ion evaporation mechanism [19] were sampled into the mass spectrometer by a potential difference of about 3 kV set between the ion spray interface and the ion sampling orifice. The sampling orifice was a 100-μm-diameter hole in the end of a conical skimmer extended towards atmosphere. To minimize solvent cluster formation a curtain of ultrapure nitrogen was applied at the atmospheric side of the skimmer. For full-scan CE–MS work the first quadrupole (Q1) was scanned from either m/z 250 or m/z 350 to m/z 850 in about 5 s with a mass scan step of 1 dalton. For CE–MS–MS work, ultrapure argon (AIRCO, The BOC Group, Murray Hill, NJ, USA) was used as the collision gas and was introduced into the collision cell (Q2) at a target gas thickness of $200 \cdot 10^{12}$ atoms/cm^2. The collision energy used for all MS–MS experiments described was 70 V.

Methods

Rinsing or conditioning of the capillary was performed by pressurizing the inlet vial to 20 p.s.i. in system B or by the built-in vacuum system at 10 in.Hg in system A. The latter was not deemed practical for connection to the ion spray interface due to the need to disconnect the capillary end from the ion spray interface during the capillary rinsing and sample injection process. New capillaries were flushed with 15 column volumes of 1 *M* sodium hydroxide, 5 column volumes of distilled water, 5 column volumes of 0.1 *M* hydrochloric acid, 5 column volumes of distilled water and finally with 10 column volumes of electrophoretic buffer. Between analyses the capillaries were usually either rinsed with 2–5 column volumes of 0.1 *M* sodium hydroxide followed by 8–10 column volumes of buffer or only with buffer. In some experiments the sodium hydroxide solution was replaced by 1 *M* NH_4OH.

The buffers were prepared from an aqueous solution of ammonium acetate. The pH of these solutions was adjusted to pH 5.0 with acetic acid or to pH 2.5 with trifluoroacetic acid (TFA). The final concentrations in this work were related to the total concentration of ammonium acetate. The electrophoretic running solutions were filtered through a 0.45-μm Miller-HV filter unit prior to use (Millipore, Bedford, MA, USA).

For CE–MS work one bottle of the synthetic peptide test mixture was dissolved in 50 μl of 1 m*M* ammonium acetate buffer to give a concentration of 500 μg/ml of each peptide. For CE–UV work one bottle of the synthetic peptide mixture was dissolved in 500 μl of 1 m*M* ammonium acetate buffer. Sample volumes ranging from 6 to 32 nl were introduced into the column using the automatic injection system. In system B the injection was made by pressurizing the inlet side of the capillary to 0.5 p.s.i. while a vacuum of 5.0 in.Hg applied at the capillary exit end was used to make the injection in system A.

Human hemoglobin was digested with TPCK-treated trypsin for 18 h at 37°C. A substrate-to-enzyme ratio of 50:1 (w/w) was used in 50 m*M* ammonium bicarbonate buffer solution where the pH had been adjusted to pH 8.5 with 1 *M* ammonium hydroxide. The digestion was stopped by adding acetic acid to the solution and the sample solution was kept at −20°C until CE–MS analysis was performed. The concentration of the hemoglobin tryptic digest was 2.5 mg/ml (154 pmol/μl). The injection was made by means of electromigration with a voltage of 10 kV and an injection time of 20–25 s.

The electroosmotic flow, v_{eo}, was calculated by measuring the migration time, t_0, from an electropherogram containing a neutral marker which was either benzyl alcohol or mesityloxide where $t_0 = V/v_{eo}$ and V is the volume of the capillary [20]. V was calculated where the capillary length (l) was the distance between the inlet end of the capillary and the UV detector; l = 20 cm in the CE–MS mode and l = 50 cm for the off-line work with the UV detector only. The calculation for column efficiency was based on $N = 5.54\ (t/w_{0.5})^2$, where N is the number of theoretical plates, t is the migration time for the compound and $w_{0.5}$ is the peak width at half peak height.

The extent of bulk flow generated by a deliberate "siphon" effect was investigated by elevating the capillary inlet (anode) relative to the buffer surface level in the liquid junction reservoir. The bulk flow was measured by moving the capillary inlet to an aqueous solution of benzyl alcohol while monotoring the "breakthrough" curve with UV detection at 210 nm and with the ion spray interface in operation. When the

surface of the electrode solution at the anode was at the same level as the surface of the makeup liquid in the liquid junction at the cathode, no "breakthrough" curve was observed over a period of 15 h. These conditions were normally used during CE–MS work reported herein.

The ion spray interface was positioned within 1 cm of the conical ion sampling orifice of the atmospheric pressure ionization mass spectrometer. The position of the spray from the ion spray interface relative to the ion sampling orifice of the API-MS system in addition to mass spectrometric tuning parameters were optimized by pressurized delivery ("infusion") of a bradykinin solution ($2 \cdot 10^{-4}$ *M* dissolved in the electrophoretic buffer) through the capillary using the 0.5 p.s.i. pressurized injection feature of system B. The doubly charged ion at *m/z* 531 for bradykinin was monitored while these parameters were adjusted to give optimal ion current signal from the API-MS system. The mass resolution for both Q1 and Q3 was maintained such that the ion peak width at half height was 1 dalton throughout this work.

RESULTS AND DISCUSSION

CE with UV detection

A synthetic mixture of nine model peptides was selected for the investigation of changes in electrophoresis conditions needed to connect a commercial CE instrument originally designed for UV detection to our liquid junction coupling ion spray API-MS system. Buffer compositions were studied which contained additives known to be favorable for good ion spray API-MS performance. The peptide mixture could be separated using 20 m*M* ammonium formate buffer adjusted to pH 2.5 with TFA. The UV electropherogram is shown in Fig. 1A. The first peak in the electropherogram in Fig. 1A–D is the positively charged heptapeptide marker used in system A to relate migration times to the electroosmotic flow at low pH. This was done by determining the electrophoretic mobility of the peptide standard in the buffer system used compared against a neutral marker [21]. The separation was made in an uncoated 50-μm I.D. fused-silica capillary with UV detection at 200 nm using system A. Although the peptide solution contained 50 μg/ml, only 6 nl were injected into the CE column corresponding to a sample loading of 0.3 ng or 0.18–0.97 pmol of each peptide.

The electropherogram in Fig. 1A is comparable to that obtained for the same peptide mixture using sodium citrate buffer at pH 2.5 [22]. We have used ammonium formate because this buffer is volatile and more compatible with ionization under electrospray conditions. The separation may be maintained with an increased percentage of methanol while holding the buffer concentration constant. The UV electropherograms resulting from using 5, 15 and 25% methanol in the electrophoresis buffer are shown in Fig. 1B–D. The ammonium formate concentration in the buffer was maintained at 20 m*M* in this experiment. The migration times increased for the peptides with increased methanol composition in the buffer. The applied voltage was 0.375 kV/cm capillary. The current dropped from 36 μA without methanol (Fig. 1A) to 21 μA with 25% methanol (Fig. 1D) in the buffer. No change in migration order for the peptides was observed. The additional methanol favors an increase in the ion current response in the API-MS system (*vide infra*). An electroosmotic flow of 0.02 μl/min was measured under conditions shown in Fig. 1A. When the content of methanol in the buffer increased, the electroosmotic flow decreased. The same observation

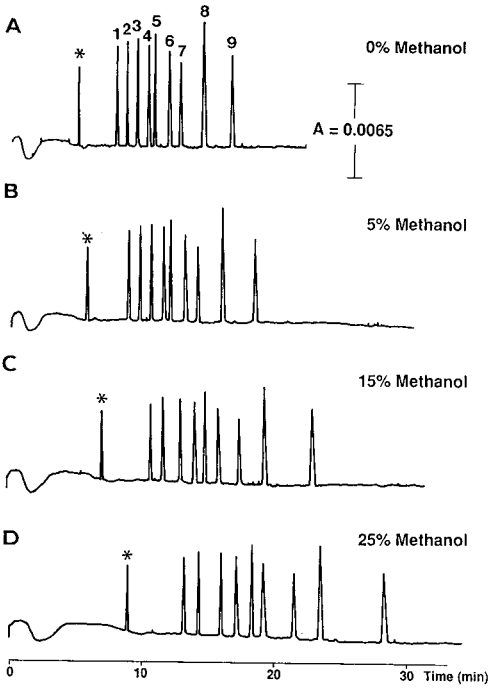

Fig. 1. CE–UV electropherogram of a synthetic peptide mixture. Capillary: uncoated fused-silica 72 cm × 50 μm I.D., 50 cm to the UV detector; detection: 200 nm; temperature: 30°C; voltage: 27 kV; buffer: 20 m*M* ammonium formate with TFA to pH 2.5 with 0–25% methanol; injection: 6 nl of a 50-μg/ml solution (0.3 ng or 0.18–0.97 pmol) of each peptide. Peaks: * = peptide standard; 1 = bradykinin; 2 = angiotensin II; 3 = α-MSH; 4 = TRH; 5 = LHRH; 6 = oxytocin; 7 = leucine enkephalin; 8 = methionine enkephalin and 9 = bombesin.

has been described by Altria and Simpson [23]. They also found that a methanol content higher than 25% reduced the buffer heat capacity enough to cause the methanol to boil within the CE capillary whereupon an electrical current breakdown in the system occurred. We observed the same phenomenon.

Changes for API-MS detection

There were some other changes required in the CE system which must be considered to integrate the CE system successfully with the present API-MS instrumentation. The overall capillary length must extend beyond the UV detector to facilitate connection to the API-MS system. The capillaries used for API-MS in this work were 100–104 cm long. Mass spectrometric detection of the substances was made at the exit end of the capillary via the liquid junction–ion spray interface so the migration distance for the substances was at least twice that with UV detection (50 cm in Fig. 1A–D). Another change implemented for CE–MS was the use of a wider-bore capillary. Thus, a 75-μm I.D. CE capillary was used in contrast to earlier reports using UV or fluorescent detection [1,21]. A wider-bore capillary increases the sample capacity of

the separation column which facilitates API-MS detection of mixture components. The increased capillary column diameter also reduced the separation efficiency as would be expected.

CE–MS analysis of the standard nine-component peptide mixture using 15% methanol in 15 m*M* ammonium acetate buffer, pH 2.5, with 15% methanol is shown in Fig. 2A with the API-MS system operated under selected-ion monitoring (SIM) conditions. The amounts injected were 3–16 pmol for each compound while the most abundant protonated molecule ion for each of the nine peptides was monitored. The applied voltage was 0.26 kV/cm when the maximum applied voltage was 30 kV and the interface was maintained at a potential of +4 kV. The potential drop across the length of the CE capillary was thus 26 kV. There are, however, only seven peaks in the electropherogram. Oxytocin, *m/z* 504 (5-pmol sample) and leucin enkephalin, *m/z* 556 (8 pmol injected) are below the detection limits for this experiment. For reasons not yet entirely understood, ammonium acetate used in this experiment provided greater sensitivity than ammonium formate under our ion spray conditions, and was used in place of the latter. A decrease in the ionic strength of the buffer from 20 m*M* to 15 m*M* gave a two-fold increase in the response from the API-MS system. The separation deteriorated to an unacceptable condition with a further decrease to 10 m*M* buffer ionic strength.

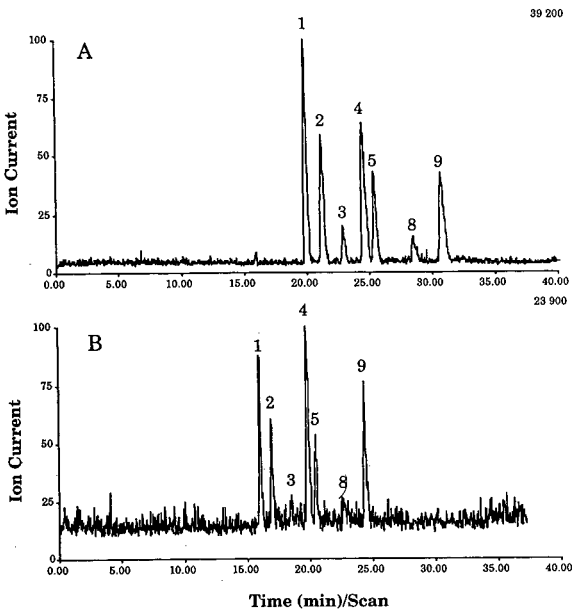

Fig. 2. SIM CE–MS total selected ion electropherogram of a synthetic peptide mixture. Capillary: uncoated fused-silica 100 cm × 75 μm I.D.; buffer: 15 m*M* ammonium acetate and TFA to pH 2.5 with (A) 15% methanol and (B) 15% acetonitrile; voltage: 26 kV; injection 10 nl of a 500-μg/ml solution of each peptide (3–16 pmol). Peaks: 1 = bradykinin, *m/z* 531 $[M + 2H]^{2+}$; 2 = angiotensin II, *m/z* 524 $[M + 2H]^{2+}$; 3 = α-MSH, *m/z* 556 $[M + 3H]^{3+}$; 4 = TRH, *m/z* 363 $[M + H]^{+}$; 5 = LHRH, *m/z* 592 $[M + 2H]^{2+}$; 8 = methionine enkephalin, *m/z* 574 $[M + H]^{+}$; and 9 = bombesin, *m/z* 811 $[M + 2H]^{2+}$.

Organic modifier

Acetonitrile as organic modifier in the separation buffer described for Fig. 2A resulted in a 25% reduction in migration times for the peptides compared to methanol-containing buffers. The comparison is shown in Fig. 2A and B with 15% methanol and acetonitrile, respectively. Peak identification is facilitated by CE–MS due to the ease of distinguishing the individual peptide components by, for example, their molecular weights. No change in selectivity was observed by varying the organic solvent in the 15 m*M* ammonium acetate buffer in Fig. 2A en B. Slightly higher electroosmotic flow was obtained with acetonitrile in the system; v_{eo} = 0.042 μl/min for acetonitrile compared to v_{eo} = 0.036 μl/min for methanol. The shorter analysis time using acetonitrile could be an advantage in certain circumstances where sample throughput is important. Acetonitrile gave sharper component peaks; *e.g.*, theoretical plates, N = 46 000–83 000, compared to N = 27 700–43 600 for methanol in the 100-cm capillary. The response, however, was about 20% lower for acetonitrile compared to methanol, and gave a poorer signal-to-noise ratio as observed in Fig. 2B. This change in response was confirmed using the pressurized injection of system B to "infuse" the sample through the capillary using bradykinin as the test analyte. The shorter analysis time for acetonitrile compared to methanol was also observed by Fujiwara and Honda [24] when they studied addition of organic solvent for the separation of positional isomers of substituted benzoic acids. They preferred acetonitrile because of the shorter analysis time and sharper peaks leading to higher sensitivity in the UV detector. The shorter analysis time is likewise a benefit for CE–MS. VanOrman *et al.* [25] studied the effect of methanol and acetonitrile on the electroosmotic flow and found that approximately 25% acetonitrile could be used in the buffer without significant decrease in electroosmotic flow. An additional advantage for using acetonitrile for CE–API-MS is that higher concentrations of acetonitrile may be used while still maintaining a stable electrophoresis system; 90% acetonitrile has been reported for the separation of acidic pesticides [14], for example.

Elevation of the capillary inlet

Migration times for the peptides could also be shortened by elevating the capillary inlet to induce a "siphon" effect for those instances of low or zero v_{eo}. This is illustrated in Fig. 3 where the same sample and buffer conditions as described in Fig. 2B were employed but the capillary inlet was elevated 8 cm. Thus the surface of the electrode solution at the anode was 8 cm higher than the surface of the makeup liquid in the liquid junction reservoir at the cathode. This created a bulk flow of 0.05 μl/min by siphoning through the capillary. The increased bulk flow "compresses" the electropherogram resulting in migration times for the peptides which are about 15% faster. Under these conditions the total-ion electropherogram in Fig. 3 was obtained for 4.5–25 pmol per component with a mass spectrometer scan range from m/z 250 to m/z 850. The buffer composition in Fig. 3 was the same as in Fig. 2B; *i.e.*, 15 m*M* ammonium acetate adjusted with TFA to pH 2.5 and 15% acetonitrile. The first peak in the electropherogram, bradykinin, was 22 s wide, so there were only 3–4 scans over the peak which makes calculation of N impractical. In this instance the "siphon" effect may be used to some degree to decrease analyses times under low electroosmotic flow conditions by increasing the bulk flow of buffer. The latter is practical provided there is adequate separation of the individual components, and the mass spectrom-

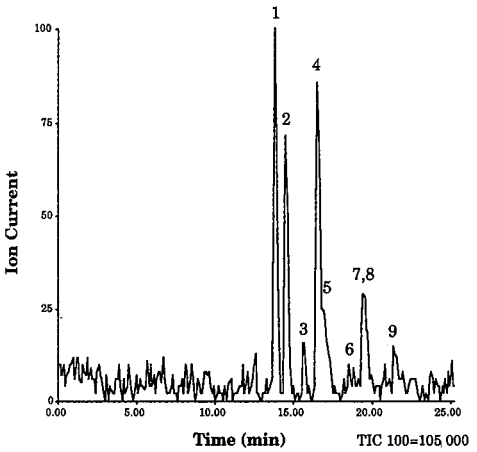

Fig. 3. TIC CE–MS reconstructed full-scan electropherogram of a synthetic peptide mixture. Capillary: uncoated fused-silica 100 cm × 75 μm I.D.; buffer: 15 m*M* ammonium acetate and TFA to pH 2.5 with 15% acetonitrile; the capillary inlet was elevated 8 cm; full-scan acquisition from *m/z* 250 to *m/z* 850, 6 s per scan; voltage: 26 kV; injection: 15 nl of a 500-μg/ml solution of each peptide (5–24 pmol). Peaks same as in Fig. 2, and 6 = oxytocin; 7 = leucine enkephalin.

eter scan rate is sufficient to provide several (8–10) scans across the CE component peaks. The data acquisition rate should be increased to accommodate the faster-eluting CE peaks, but there may be some compromise in sensitivity resulting from the increased mass spectrometric scan rate.

Separation of peptides at pH 5.0

An increase in CE sample loading may be achieved by using larger-I.D. capillaries. An experiment using a wider-bore capillary was performed at pH 5.0 because the pH 2.5 buffer gave excessively high current at the same applied voltage resulting in a breakdown in the electrophoretic process due to the heat generated inside the capillary. Fig. 4A–E shows the CE–MS ion current profile obtained from the analysis of the nine-component synthetic peptide mixture using a 100-μm I.D. capillary containing a buffer of 15 m*M* ammonium acetate–acetic acid, pH 5.0 with 50% acetonitrile. The injected amount was 9.6–52 pmol of each peptide.

The peptides possess a net positive charge at pH 5.0, but the net number of charges are different than at pH 2.5. For example, α-MSH has +3.3 charges at pH 2.5 and +2.1 charges at pH 5.0, resulting in a different migration order. The last two peptides, leucin enkephalin and methionine enkephalin, carry only +0.002 net charges at pH 5.0 as calculated with a computer program based on the aqueous acid dissociation constants for the individual amino acids [26]. Therefore, these two compounds have migration times comparable to a neutral compound. The mass spectrometric scan was from *m/z* 350 to *m/z* 850 because prior infusion experiments with these peptides have shown that their most abundant ions occur within this mass region. Fig. 4A–D shows the extracted ion current profile for the doubly charged ions at *m/z* 592, 811, 833 and 504 for LHRH, bombesin, α-MSH and oxytocin. The extracted ion electropherograms in Fig. 4A–D show that the peptides elute in bands

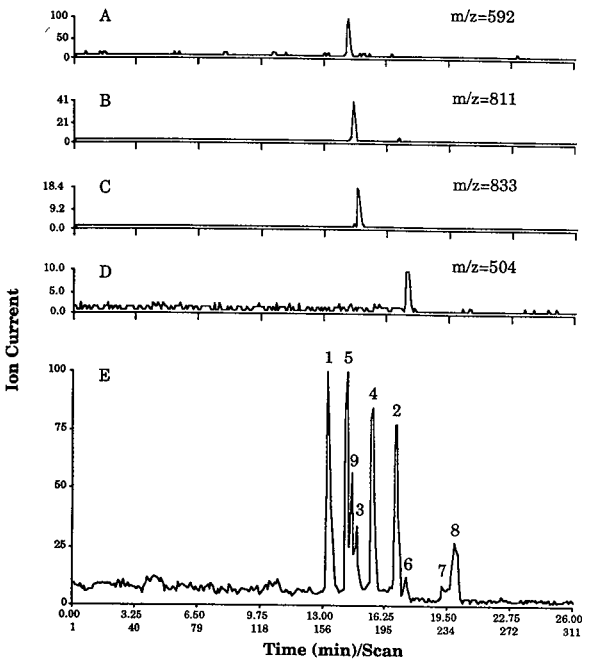

Fig. 4. Reconstructed full-scan CE–MS TIC profile (E) and extracted ion current profiles (A–D) from the analysis of a synthetic peptide mixture. Capillary: uncoated fused-silica 100 cm × 100 μm I.D.; buffer: 15 m*M* ammonium acetate and acetic acid to pH 5.0 with 50% acetonitrile; voltage: 26 kV; injection: 32 nl of a 500-μg/ml solution of each peptide (9.6–52 pmol). (A) LHRH, *m/z* 592 $[M + 2H]^{2+}$; (B) bombesin, *m/z* 811 $[M + 2H]^{2+}$; (C) α-MSH, *m/z* 833 $[M + 2H]^{2+}$ and (D) oxytocin, *m/z* 504 $[+ 2H]^{2+}$; (E) full-scan acquisition from *m/z* 350 to *m/z* 850, 5s per scan. Peaks same as in Fig. 1.

which are 17–22 s wide. The electroosmotic flow in this system was 0.4 μl/min. The smooth, stable total ion current (TIC) profile shown in Fig. 4D demonstrated the performance characteristics which may be expected from this system.

Mass spectra for the peptides at pH 5.0 and pH 2.5

The mass spectrum obtained at pH 2.5 for α-MSH shows the triply charged ion at *m/z* 556 to be the most abundant (Fig. 5A). However, at pH 5.0 the doubly charged ion at *m/z* 833 is the most abundant ion in the mass spectrum (Fig. 5B). A similar observation was made for bradykinin and angiotensin II which suggests that ions with a higher charge state may be preferred in this system under lower pH conditions. The doubly charged ions for bradykinin were the most abundant at both pH 5.0 and 2.5, but a triply charged ion with a relative abundance of 50% was also observed at pH 2.5. This is illustrated in Fig. 6A and B for bradykinin. This change in charge state could not be correlated with any particular structural feature for this peptide.

The peptides form adducts with sodium ions (Na^+) if the latter are present in the system as is illustrated in Fig. 6C for bradykinin. Since sodium hydroxide was used in the capillary rinsing procedure, it was important to change the buffer in the liquid junction before each injection. Fig. 6C shows that some residual sodium ions remained in the system after one rinsing procedure. Some attempts were made to

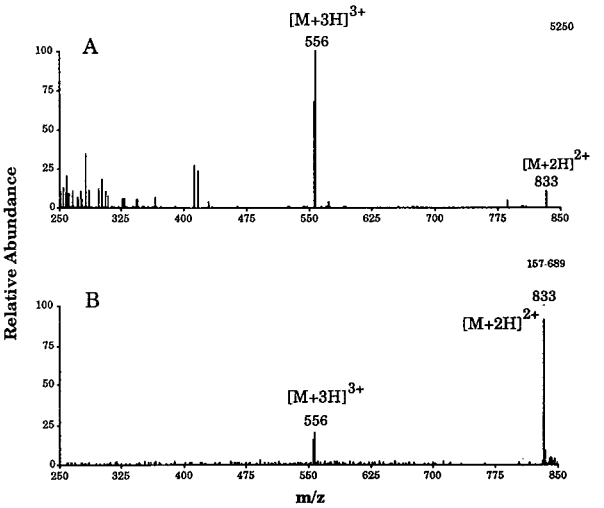

Fig. 5. Mass spectra of α-MSH. (A) pH 2.5 (conditions as in Fig. 3); (B) pH 5.0 (conditions as in Fig. 4).

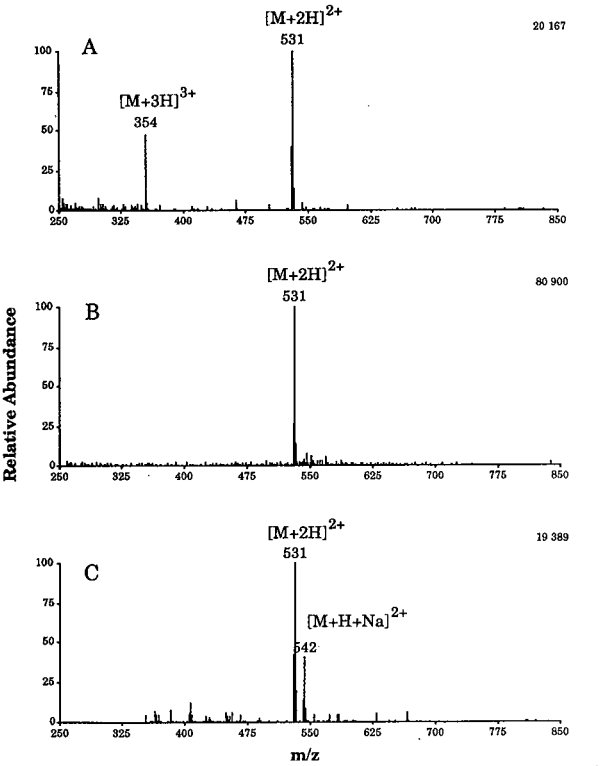

Fig. 6. Mass spectra of bradykinin. (A) pH 2.5 (conditions as in Fig. 4); (B) and (C) pH 5.0 (conditions as in Fig. 5). In (C) the buffer in the interface was not properly changed and bradykinin formed adducts with residual sodium ions remaining from the capillary rinsing solution.

rinse the capillary with 1 *M* ammonium hydroxide instead of sodium hydroxide, but ammonium hydroxide appeared to change the capillary wall to give an increase in ν_{eo} while the separation was lost after repeated rinsing with ammonium hydroxide.

Tandem mass spectrometry

Samples ranging from 10–52 pmol loaded onto the capillary at pH 5.0 contained sufficient material to obtain on-line MS–MS spectra to provide structural information for the peptides studied in this work. This is illustrated in Fig. 7 for TRH. By mass selecting the $(M+H)^+$ ion at *m/z* 363 for TRH with the first quadrupole (Q_1), performing collision-induced dissociation (CID) in the second quadrupole (Q_2), and scanning the third quadrupole (Q_3) from *m/z* 10 to 400 in 5 s, one obtains the full-scan total ion electropherogram (Fig. 7A) and its corresponding daughter-ion mass spectrum (Fig. 7B) obtained from 52 pmol of TRH. Daughter ions at *m/z* 84 and 221 are consistent with the sequence of this peptide. The immonium ions at *m/z* 70 for proline and *m/z* 110 for histidine are also observed in Fig. 7B [27]. These results demonstrate that structurally informative peptide mass spectra may be obtained by on-line CE–MS–MS using the described system. Sample loading for the capillary was 52 pmol in this experiment which is half the concentration used in earlier investiga-

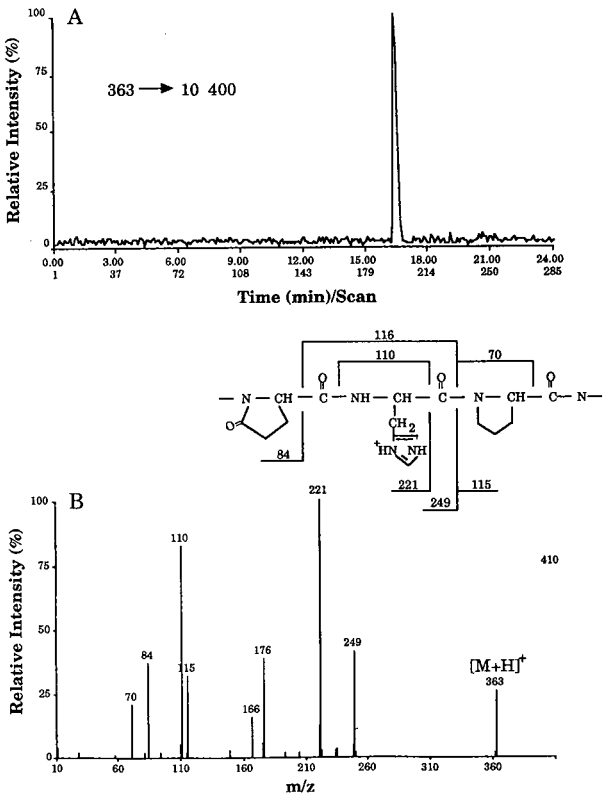

Fig. 7. CE–MS–MS total ion electropherogram (A) and daughter-ion mass spectrum (B) for 52 pmol TRH. Conditions as in Fig. 4.

tions to obtain daughter-ion mass spectra for peptides, *e.g.*, dynorphin 1–9, using microbore liquid chromatography (LC)–MS [28].

Hemoglobin tryptic digest

A total ion current electropherogram obtained from the injection of 10 pmol human hemoglobin tryptic digest is shown in Fig. 8A using a buffer consisting of acetonitrile–15 m*M* ammonium acetate 50:50 (v/v) adjusted to a pH of 5.0 with acetic acid. The sample contained both the α and β chain of hemoglobin which yields a total of 28 different peptides in the digest sample [29]. The injection was made by electromigration, 25 s at 10 kV, from a solution containing 154 pmol/μl hemoglobin tryptic digest. The mass of two tryptic fragments was too small to be detected in the scan range (m/z 250–850 u) used. The CE–MS total ion current electropherogram shown in Fig. 8A results from a buffer compromise imposed by the mass spectrometer. The electrospray conditions used in this work were optimized by using relatively low concentrations (less than 20 m*M*) volatile buffers and acids in addition to higher percentages of organic solvents such as methanol or acetonitrile than is customary for capillary electrophoresis conditions with UV or other detection. Several regions of the electropherogram show evidence for coelution of different peptides. It is, however, possible to obtain mass spectra of the different peaks. Since tryptic peptides typically yield abundant multiply protonated molecules in the scan range measured [30], we can determine their molecular weights. Extracted ion electropherograms may be obtained for individual peptides as is illustrated in Fig. 8B for tryptic fragment T-3

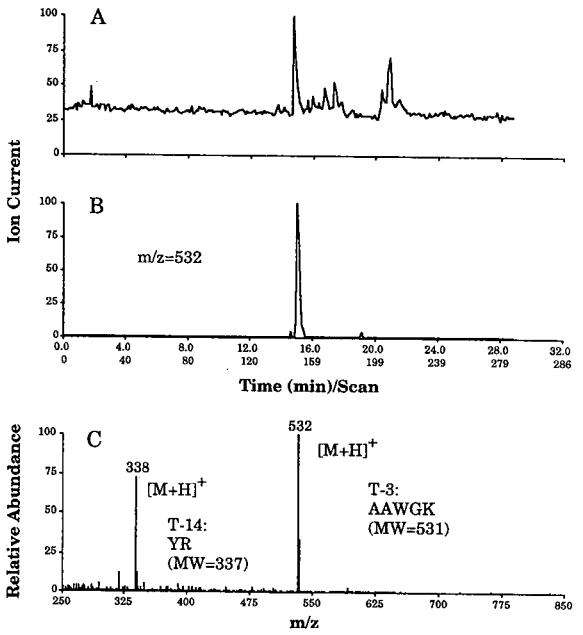

Fig. 8. Full-scan CE–MS TIC profile (A), extracted ion profile for m/z 532 (B) and mixed mass spectrum of T-3 and T-14 (C) from the analysis of 10 pmol human hemoglobin tryptic digest. Injection: 25 s at 10 kV of a 154 pmol/μl solution. Conditions as in Fig. 4. One-letter amino acid codes; MW = molecular weight.

at m/z 532. The appearance of an additional protonated molecule observed in Fig. 8C suggests the T-3 fragment migrates together with another fragment which was later determined to be T-14 by its molecular weight and CID mass spectrum (not shown). The mass spectrum shown in Fig. 8C reveals both peptides which appear as a shoulder in the 15-min peak observed in Fig. 8A. This ability to detect and identify coeluting components by CE–MS demonstrates the considerable analytical advantage of this technique. Comparison of the corresponding mass spectra and extracted ion profiles for particular peaks in the TIC electropherogram allows the detection and molecular-weight determination for all expected tryptic fragments in the hemoglobin tryptic digest. The two largest fragments of the α chain, T-12 with a mass of 2965 dalton and T-9 with a mass of 2996 dalton, appeared as $(M + 5H)^{5+}$ at m/z 594 and 600, respectively.

By monitoring the $(M + H)^+$ ion at m/z 532 for T-3 with the first quadrupole, performing CID in the second quadrupole, and scanning the third quadrupole from m/z 10 to 560 in 5 s, the full-scan total ion electropherogram (Fig. 9A) and the daughter-ion mass spectrum (Fig. 9B) for the T-3 fragment in 10 pmol of injected human hemoglobin tryptic digest were acquired. The daughter-ion mass spectrum shown in Fig. 9B reveals fragments corresponding to A, B and Y″ series ions [31]. In this case, less sample (10 pmol compared to 50 pmol) was used to obtain sequence information for tryptic fragments than was reported previously by microbore LC–MS [31]. However, LC–MS will typically allow injection of larger sample volumes and quantities of sample than is possible with CE–MS.

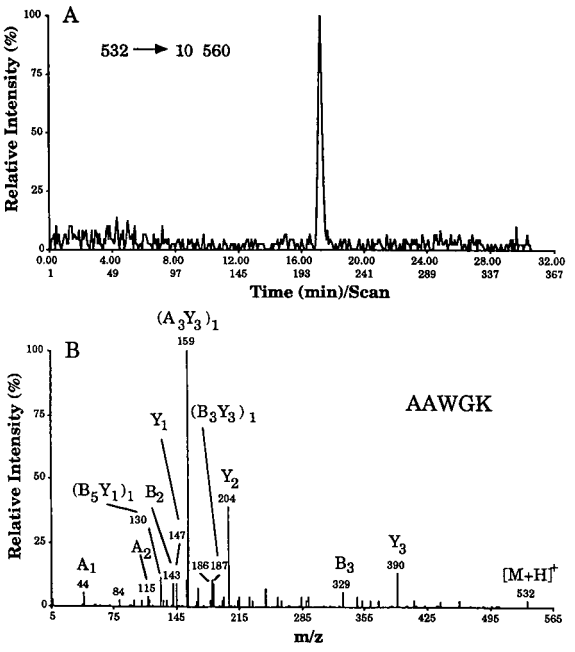

Fig. 9. Full-scan CE–MS–MS (m/z 10–560) product ion TIC electropherogram from the analysis of a human hemoglobin tryptic digest. (A) CE–MS–MS total ion electropherogram and (B) daughter-ion mass spectrum from m/z 532, T-3. Conditions as in Fig. 8.

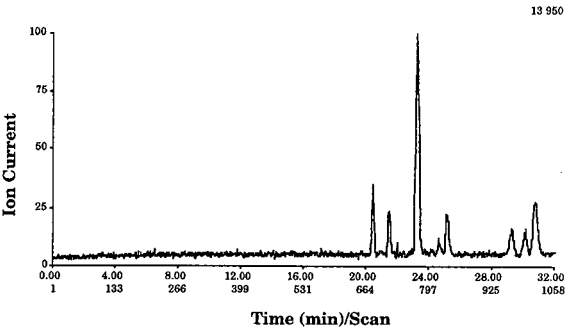

Fig. 10. SIM CE–MS total selected ion electropherogram for eight components in a human hemoglobin tryptic digest. Injection: 20 s at 10 kV of a 154 pmol/μl solution (8 pmol). Conditions as in Fig. 2A.

A SIM CE–MS analysis of the tryptic digest of normal β-chain hemoglobin was made at low pH with a 75-μm I.D. capillary and a buffer of 15 m*M* ammonium acetate adjusted with TFA to pH 2.5 and 15% methanol (Fig. 10). Eight different ions were monitored following an injection of about 8 pmol of sample. The peptides whose characteristic ions were not monitored in this SIM CE–MS experiment are of course not observed in Fig. 10. These data show acceptable separation efficiency, N = 85 000–135 000, from the on-line CE–MS analysis of a relatively low level of sample. The signal-to-noise level is good with excellent ion current stability and a minimum of peak broadening.

SUMMARY AND CONCLUSIONS

The changes which benefit MS detection with on-line CE include using a larger-I.D. capillary to increase the capillary column sample capacity, increased capillary length to connect the CE and MS instrumentation, volatile buffers with lower buffer salt concentration (less than 20 m*M*), and higher content of organic solvent than normally used for CE–UV. This study shows that it is possible to obtain useful CE–MS data for low pmol levels of peptides and a protein tryptic digest including the determination of their molecular weight and characteristic amino acid sequence information. These results also show the convenience of interfacing a commercial CE system equipped with a pressurized injection feature inlet to MS. The latter feature is particularly helpful for rinsing the capillary between analyses and for tuning the mass spectrometer using the entire CE–MS hardware.

The ion spray interface and its associated liquid junction decouples the CE capillary exit from the ion spray interface described in this report. Because the API-MS system does not require introduction of the CE capillary exit into the mass spectrometer vacuum system, both the inlet and exit of the capillary are maintained at atmospheric pressure. This arrangement avoids the extra-column band broadening and suction on the capillary exit which may be associated with the CF-FAB approach [16–18]. However, the ion evaporation ionization which takes place in the approach reported herein imposes some restrictions on the CE buffer which can compromise optimum CE separations. Future developments are needed which provide more flex-

ibility for CE buffers and more sensitive mass spectrometric detection before we may enjoy the full potential of CE–MS.

ACKNOWLEDGEMENTS

We thank Applied Biosystems and Beckman Instruments for providing the capillary electrophoresis instruments. We also thank the Eastman Kodak Company and Sciex for partial financial support of this work.

This work was supported financially by grants to one of us (M. J.) from the Swedish Medical Research Council, the Swedish Academy of Pharmaceutical Sciences and The Royal Swedish Academy of Sciences which are gratefully acknowledged.

REFERENCES

1 W. G. Kuhr, *Anal. Chem*, 62 (1990) 403R.
2 P. D. Grossman, J. C. Colburn, H. H. Lauer, R. G. Nielsen, R. M. Riggin, G. S. Sittampalam and E. C. Rickard, *Anal. Chem.*, 61 (1989) 1186.
3 R. M. McCormick, *Anal. Chem.*, 60 (1988) 2322.
4 P. D. Grossman, K. J. Wilson, G. Petrie and H. H. Lauer, *Anal. Biochem.*, 173 (1988) 265.
5 A. P. Bruins, T. R. Covey and J. D. Henion, *Anal. Chem.*, 59 (1987) 2642.
6 E. C. Huang, T. Wachs, J. J. Conboy and J. D. Henion, *Anal. Chem.*, 62 (1990) 713A.
7 J. A. Olivares, N. T. Nguyen, C. R. Yonker and R. D. Smith, *Anal. Chem.*, 59 (1987) 1232.
8 E. D. Lee, W. Mück, J. D. Henion and T. R. Covey, *J. Chromatogr.*, 458 (1988) 313.
9 R. D. Smith, J. A. Olivares, N. T. Nguyen and H. R. Udseth, *Anal. Chem.*, 60 (1988) 436.
10 R. D. Smith, C. J. Barinaga and H. R. Udseth, *Anal. Chem.*, 60 (1988) 1948.
11 R. D. Smith, J. A. Loo, C. J. Barinaga, C. G. Edmonds and H. R. Udseth, *J. Chromatogr.*, 480 (1989) 211.
12 E. D. Lee, W. Mück, J. D. Henion and T. R. Covey, *Biomed. Environ. Mass Spectrom.*, 18 (1989) 253.
13 W. M. Mück and J. D. Henion, *J. Chromatogr.*, 495 (1989) 41.
14 E. D. Lee, W. Mück, J. D. Henion and T. R. Covey, *Biomed. Environ. Mass Spectrom.*, 18 (1989) 844.
15 J. A. Loo, H. K. Jones, H. R. Udseth and R. D. Smith, *J. Microcol. Sep.*, 1 (1989) 223.
16 M. A. Moseley, J. L. Deterding, K. B. Tomer and J. W. Jorgenson, *J. Chromatogr.*, 480 (1989) 197.
17 N. J. Reinhoud, W. M. A. Niessen, U. R. Tjaden, L. G. Gramberg, E. R. Verheij and J. van der Greef, *Rapid Commun. Mass Spectrom.*, 3 (1989) 348.
18 R. M. Caprioli, W. T. Moore, M. Martin, B. B. DaGue, K. Wilson and S. Moring, *J. Chromatogr.*, 480 (1989) 247.
19 B. A. Thomson and J. V. Iribarne, *J. Chem. Phys.*, 71 (1979) 4451.
20 J. W. Jorgenson and K. D. Lukacs, *Anal. Chem*, 53 (1981) 1298.
21 P. D. Grossman, H. H. Lauer, S. E. Moring, D. E. Mead, M. F. Oldham, J. H. Nickel, J. R. P. Goudberg, A. Krever, D. H. Ransom and J. C. Colburn, *Am. Biotech. Lab.*, Feb. (1990) 35.
22 *Application Note Issue No. 16*, Applied Biosystems, Foster City, CA, 1989.
23 K. D. Altria and C. F. Simpson, *Anal. Proceed.*, 23 (1986) 453.
24 S. Fujiwara and S. Honda, *Anal. Chem.*, 59 (1987) 487.
25 B. B. VanOrman, G. G. Liverside, G. L. McIntire, T. M. Olefirowicz and A. G. Ewing, *J. Microcol. Sep.*, 2 (1990) 176.
26 D. J. Pennino, *Biopharm.*, 8 (1989) 41.
27 K. Eckart, H. Schwarz, K. B. Tomer and M. L. Gross, *J. Am. Chem. Soc.*, 107 (1985) 6765.
28 E. D. Lee, J. D. Henion and T. R. Covey, *J. Microcol. Sep.*, 1 (1990) 14.
29 T. Matsuo, H. Matsuda, I. Katakuse, Y. Wada, T. Fujita and A. Hayashi, *Biomed. Mass Spectrom.*, 8 (1981) 25.
30 E. C. Huang and J. D. Henion, *J. Am. Soc. Mass Spectrom.*, 1 (1990) 158.
31 P. Roepstorff and J. Fohlman, *J. Biomed. Mass Spectrom.*, 11 (1984) 601.

Journal of Chromatography, 554 (1991) 329–338
Elsevier Science Publishers B.V., Amsterdam

CHROMSYMP. 2208

Nanoscale separations

Capillary liquid chromatography–mass spectrometry and capillary zone electrophoresis–mass spectrometry for the determination of peptides and proteins

LEESA J. DETERDING, CAROL E. PARKER and JOHN R. PERKINS

Laboratory of Molecular Biophysics, National Institute of Environmental Health Sciences, P.O. Box 12233, Research Triangle Park, NC 27709 (USA)

M. ARTHUR MOSELEY

Laboratory of Molecular Biophysics, National Institute of Environmental Health Sciences, P.O. Box 12233, Research Triangle Park, NC 27709 (USA) and Department of Chemistry, University of North Carolina, C.B. 3290, Chapel Hill, NC 27514 (USA)

J. W. JORGENSON

Department of Chemistry, University of North Carolina, C.B. 3290, Chapel Hill, NC 27514 (USA)

and

KENNETH B. TOMER*

Laboratory of Molecular Biophysics, National Institute of Environmental Health Sciences, P.O. Box 12233, Research Triangle Park, NC 27709 (USA)

ABSTRACT

Nanoscale separation techniques, such as packed capillary liquid chromatography and capillary zone electrophoresis in which the column effluent flow-rates are in the nanoliter per minute range rather than microliter per minute range, have been successfully interfaced with continuous-flow fast atom bombardment and electrospray ionization. Applications of these techniques to the separation and determination of peptide mixtures, protein digests and protein mixtures are presented.

INTRODUCTION

The trend towards miniaturization has had a major, beneficial impact on separation science methodologies. The best known example is the impact that the development of open tubular capillary columns has had on gas chromatographic separations. The significantly better separation efficiencies, shorter analysis time and ease of coupling with mass spectrometry (MS) has made the use of capillary gas chromatography (GC) columns the standard GC technique.

Similar advantages have been found in liquid chromatography (LC). Smaller inner diameter columns provide greater separation efficiencies, reduced solvent con-

0021-9673/91/$03.50

sumption and increased ease in interfacing with mass spectrometers and other detector systems, such as laser-based detectors [1]. At the forefront of these developments are the nanoscale separation techniques, including packed nanoscale capillary columns and capillary zone electrophoresis (CZE).

Packed nanoscale capillary LC columns are columns with flow-rates in the nl/min range. Typically, these columns have inner diameters of 50 to 75 μm and are packed with 5–10-μm particles. Karlsson and Novotny [2] reported in 1988 on the evaluation of packed capillary columns with inner diameters as low as 44 μm and observed improved separation efficiency. This was attributed to a homogenous packing bed structure, in which the influence of the wall is felt by the entire packing bed. Kennedy and Jorgenson [3] then reported a comprehensive study on the effect of column diameter and particle size and observed that a column inner diameter to particle size ratio of $<10{:}1$ offered increased column performance due to decreased flow dispersion and a decrease in resistance to mass transfer in the mobile phase. This was also attributed to a more uniform packing bed density due to the wall effect being operative across the entire packing bed.

CZE separations are based on the differential migration of ionic species in an electric field [4]. Separation efficiencies of greater than $1{\cdot}10^6$ theoretical plates are possible in under 20 min using the technique [5]. Typical flow-rates associated with CZE are in the range of 500 nl/min and lower. Thus, CZE flow-rates are compatible with MS.

Two MS techniques have generally been considered to be most compatible with the flow-rates identified with nanoscale separations, continuous-flow fast atom bombardment (CF-FAB) [6] and electrospray ionization (ESI) [7]. In CF-FAB, the FAB matrix and carrier solvent flow directly onto the FAB probe tip. The analyte is introduced either by flow injection or as the effluent from an LC column. The low flow-rates required to maintain the high separation efficiencies of nanoscale LC are imcompatible with the typical CF-FAB flow-rates (5 μl/min). To circumvent this problem, we have designed a coaxial approach to CF-FAB in which the analyte and matrix streams do not meet until they reach the probe tip [8]. This coaxial design has been used successfully to interface both nanoscale capillary LC and CZE with CF-FAB with retention of the high separation efficiencies associated with the nanoscale techniques and has demonstrated high sensitivities [9–14]. CZE has also been interfaced wth CF-FAB by Caprioli *et al.* [15] and Reinhoud *et al.* [16] using a liquid junction interface.

In ESI-MS, a spray of fine droplets is formed at atmosperic pressure in the presence of a high voltage potential. The ions formed in this technique are often multiply charged which permits the molecular mass determination of relatively large molecules, such as proteins, on a low mass range quadrupole instrument. Flow-rates of 5–10 μl/min are usually optimal with ESI sources. As with CF-FAB, additional fluid must be delivered to the source for stable operation. CZE has been interfaced with ESI (and the related technique, ionspray) using either coaxial delivery [17] or liquid junction [18], and has been applied to the determination of peptides and proteins [19–21].

In this paper, we report on the application of nanoscale capillary LC and CZE combined with both coaxial CF-FAB and ESI for the determination of compounds of biological interest.

EXPERIMENTAL

MS

The CF-FAB experiments were performed on a VG ZAB 4F mass spectrometer (VG Analytical, Altrincham, UK) equipped with an Ion Tech FAB gun. Xenon was used as the FAB gas (8 kV at 1 mA).

The electrospray experiments were performed on a VG 12-250 quadropole (VG Masslabs, Altrincham, UK) equipped with a Vestec electrospray source Model 611B (Vestec, Houston, TX, USA). This source differs from other commercially available ESI sources in that the block is heated. Declustering and, possibly, ionization occurs in the electrospray chamber which is heated conductively to *ca.* 50°C. The electrospray needle voltage is 2–3 kV and the spray current is between 0.08 to 0.18 μA.

Data analysis was performed on a VG 11-250 data system with supplementary data analysis performed on a Sun 3/60 workstation (Mountain View, CA, USA) running Kratos (Ramsey, NJ, USA) Mach 3 software.

Coaxial CF-FAB

The coaxial FAB interface and probe used for the nanoscale capillary LC and CZE were fabricated in-house and have been described previously [8–14]. The CZE apparatus was built in-house and is described in detail elsewhere [8,11,13]. The packed nanoscale capillary LC columns were slurry packed using AQ-C18 (YMC, Morris Plains, NJ, USA) particles. Experimental conditions for the nanoscale capillary LC and CZE experiments are given in Table I. The linear gradients of acetonitrile–water (0.1% trifluoroacetic acid) were formed and delivered using a pair of Waters 6000A pumps and a Waters 660 gradient controller (Milford, MA, USA). The mobile phase flow was split prior to the column to produce the desired rate of flow through the column. Sample injections were performed using a pressurized injection vessel. A microvial of solution is placed in the vessel and the nanoscale capillary LC column was inserted through the lid into the vial. The vessel was then pressurized with helium to inject the sample onto the column. After the sample was injected, the column was removed from the injection vessel and reinserted into the LC system.

ESI-MS

The nanoscale capillary LC and CZE systems described for use with coaxial CF-FAB [8–14] are also used for ESI except for the probe design. The ESI probe is a standard Vestec electrospray probe that, using the main design features of our coaxial CF-FAB probe, has been modified to provide a coaxial delivery of the sheath fluid. The operating parameters are given in Table I.

RESULTS AND DISCUSSION

Nanoscale capillary LC–CF-FAB-MS

Our initial experiments investigating the performance and utility of packed nanoscale capillary columns were done with columns the entire lengths of which were filled with packing material. This prevents loss of resolution that might occur due to the large dead volume that will be present if the columns are only partially filled. (The total column length of *ca.* 1.2–2 m is dictated by the length of the CF-FAB probe and

TABLE I

NANOSCALE SEPARATION–MS PARAMETERS

Parameter	Nanoscale capillary CF-FAB	CZE–CF-FAB	Nanoscale capillary ESI	CZE–ESI
Column	50–75 μm I.D./ 150 μm O.D.	13 μm I.D. untreated or coated with aminopropylsilane	75 μm I.D. × 150 μm O.D.	75 μm I.D. × 150 μm O.D., untreated or coated with aminopropylsilane
Column packing	10 μ C_{18}	–	10 μm C_{18}	–
Column flow-rates (nl/min)	50–350	±30	50–500	500
Sample injection volumes (nl)	0.5 to 10	0.25 to 5	0.5 to 10	0.1 to 6
Sheath column	160 μm I.D. × 350 μm O.D.	160 μm I.D. × 365 μm O.D.	600 μm I.D. stainless steel	600 μm I.D. stainless steel
Sheath composition	(Glycerol–water 25–75)	Glycerol–0.5 m*M* aqueous heptafluorobutyric acid (25:75)	Methanol–3% aqueous acetic acid (50:50)	Methanol–3% aqueous acetic acid (50:50)
Sheath flow-rate (μl/min)	0.5	0.5	5–10	5–10
Voltage drop (kV)	–	± 30	–	± 30
Buffer composition	–	5 m*M* Ammonium acetate adjusted to pH 8.5 with ammonium hydroxide or 0.01 *M* acetic acid adjusted to pH 3.4–3.5 with ammonium hydroxide	–	10 m*M* Ammonium acetate adjusted to pH 8.5 with ammonium hydroxide or 0.01 *M* acetic acid adjusted to pH 3.4 with ammonium hydroxide

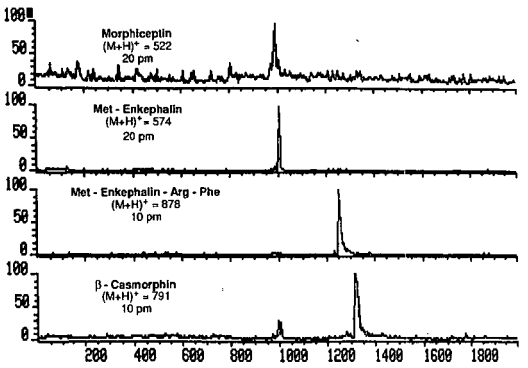

Fig. 1. Packed nanoscale capillary LC–MS separation and analysis of morphiceptin, met-enkephalin, met-enkepahlin-Arg-Phe and β-casmorphin. Selected ion chromatograms of $(M + H)^+$ from full scan data. The capillary column was 75 μm I.D. 2 m long capillary packed with 10 μm C_{18} particles. Gradient conditions were: 0% (10 min) stepped to 25%, followed by a linear gradient to 50% acetonitrile in water (0.1% TFA) over 120 min. pm = pmol.

sufficient length for maneuvering the column). For most purposes, however, optimum resolution is not necessary.

The separation of four opioid peptides is shown in Fig. 1. The flow-rate was 350 nl/min and 10–20 pmol of each component was injected. From the signal-to-noise ratio, it is apparent that the limits of detection under full scan conditions for the two enkephalins is less than 1 pmol injected. Under isocratic conditions this column exhibited a separation efficiency of 59 000 theoretical plates which compares favorably with a theoretical prediction of 66 000 plates.

A more complex example (which has previously been analyzed by microbore LC–ESI-MS [22]), a partial (*ca.* 80% of the protein remained undigested) tryptic digest corresponding to 96 pmol of undigested horse heart cytochrome *c*, was also investigated using a 2.2-m long column packed to a depth of 25 cm with 5 μm C_{18} particles. Selected ion chromatograms of major components eluting over the entire chromatograms as well as a selection of ions across the mass range scanned are shown in Fig. 2. All ions show very good signal-to-noise ratios and peak shape except for the fragment corresponding to residues 14–22 plus the iron containing heme group. The broad peak shape may be at least partially attributable to the presence of the heme moiety.

CZE–coaxial CF-FAB-MS

The CZE–coaxial CF-FAB-MS separation of a mixture of neuropeptides is shown in Fig. 3. The sensitivity of this technique can be seen from the levels of neuropeptides analyzed, ranging from 114 fmol to 172 fmol. Good resolution is observed with the number of theoretical plates ranging from 18 000 to 58 000. The separation was complete within 7 min. It should be noted that leu-enkephalin and met-enkephalin are barely separated. Given their structural similarity and that separations are based on charge, this is not surprising.

Three of these components in Fig. 3 are identical to three of the components separated by nanoscale capillary LC as shown in Fig. 1, morphiceptin, met-enkepha-

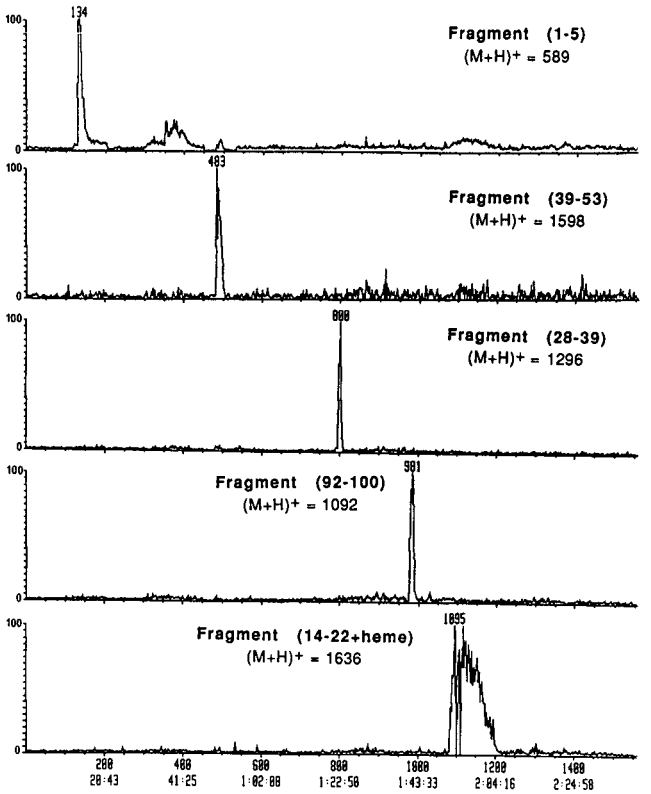

Fig. 2. Packed nanoscale capillary LC–MS separation and analysis of horse heart cytochrome *c* tryptic digest. Selected ion chromatograms of $(M + H)^+$ of selected tryptic peptides from full scan data. The capillary column was a 2 m column packed with 25 cm of 5 μm C_{18} particles. Gradient conditions were: 0% (10 min) stepped to 15% followed by a linear gradient to 35% acetonitrile in water (0.1% TFA) over 150 min. Time in h:min:s.

lin and β-casmorphin. Several observations can be made from a comparison of these two separations. The first is that the analysis time is significantly shorter for CZE than it is for nanoscale capillary LC. The second is that sensitivity by CZE is significantly better than for nanoscale capillary LC. For example, the signal-to-noise ratio for all three components is approximately the same, while the amount analyzed by CZE is approximately two orders of magnitude less than that analysed by nanoscale capillary LC. This is due to the significantly narrower peak widths observed in CZE, approximately 7 s. wide at half-height, than in nanoscale capillary LC, approximately 1 min, wide at half height, which results in a significantly greater flux of analyte into the ion source. The third observation can be made from a comparison of the elution order of the three identical components. Met-enkephalin is the second component to elute in the nanoscale capillary LC analysis while it is the last peak in the CZE analysis. As CZE separations are based on different molecular parameters than are nanoscale capillary LC separations, the separations are orthogonal and represent a valid confirmation technique.

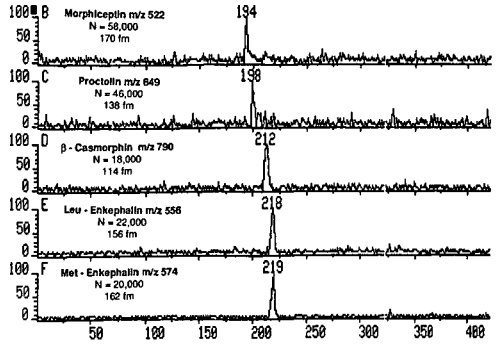

Fig. 3. CZE–CF-FAB-MS separation and analysis of neuropeptides. Selected ion chromatograms of $(M + H)^+$ from full scan data. The CZE capillary was 1 m long, 13 μm I.D. The buffer was 5 m*M* ammonium acetate (pH 8.5) containing 1% 2-propanol. The voltage drop across the column was 38 kV. *N* = Plate number.

A fourth feature that differentiates the two techniques is the loading factor. Although it is not obvious in Fig. 3, overloading of CZE–coaxial CF-FAB-MS occurs at significantly lower levels than for nanoscale capillary LC. The analysis in Fig. 3 is, in fact, close to the upper concentration limit.

Nanoscale capillary LC–ESI-MS

The analysis of the tryptic digest adrenocorticotropic hormone (ACTH) 1–24 (corresponding to 200 pmol of undigested protein) is presented as an example of the application of a packed nanoscale capillary LC–MS analysis using ESI (Fig. 4). The

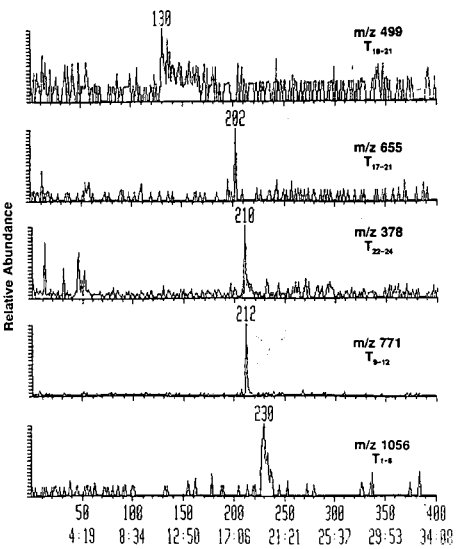

Fig. 4. Nanoscale capillary LC–ESI-MS separation and analysis of the tryptic digest of ACTH 1–24. Selected ion chromatograms of the most abundant molecular ion species from full scan data. The capillary column was 2 m × 75 μm I.D. packed to a depth of 25 cm with 10-μm AQ-C18 particles. Gradient conditions were: 0% (10 min) stepped to 15% followed by a linear gradient to 35% acetonitrile in water (0.1% TFA) over 120 min.

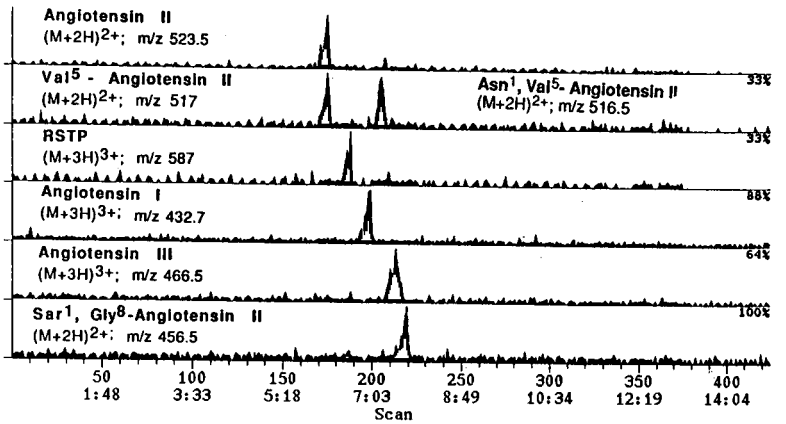

Fig. 5. CZE–ESI-MS separation and analysis of angiotensin-related peptides. Selected ion chromatograms of most abundant ion from full scan data. The CZE column was 1.1 m × 75 μm modified with aminopropylsilane. The buffer was 0.01 *M* acetic acid at pH 3.4. The voltage drop across the column was 30 kV.

column used in this separation is 2 m × 75 μm I.D. packed to a depth of 25 cm with 10-μm AQ-C18 particles. The significantly shorter column results in a greatly reduced analysis time compared to the 2.2 m long column. The analysis is complete within 21 min in comparison to the dead time of approximately 30 min observed with the 2.2 m columns. Peak shape, except for *m/z* 499 tryptic peptide T_{18-29} is still quite reasonable. The sensitivity observed here is similar to that observed with FAB detection [23].

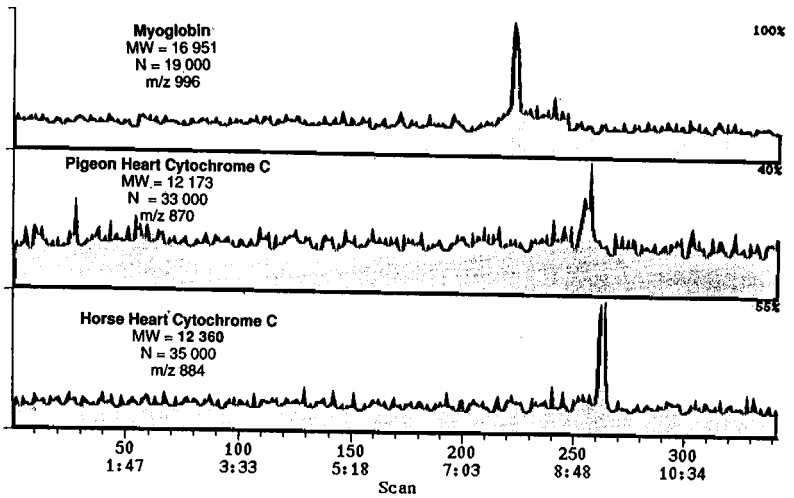

Fig. 6. CZE–ESI-MS separation and analysis of three proteins. Selected ion chromatograms of the most abundant molecular ion species from full scan data. The CZE column was 1.1 m × 75 μm I.D. modified with aminopropylsilane. The buffer was 0.01 *M* acetic acid at pH 3.4. The voltage drop across the column was 30 kV. MW = Molecular weight.

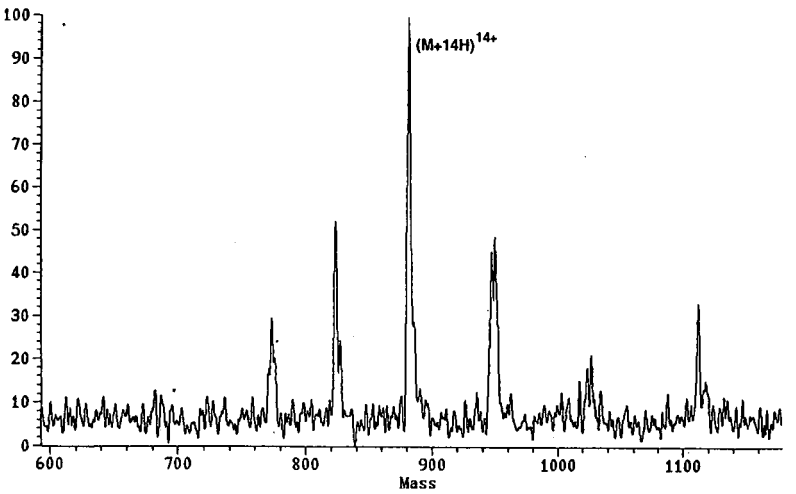

Fig. 7. CZE–ESI-MS spectrum of horse heart cytochrome *c* obtained from the separation shown in Fig. 6.

CZE–ESI-MS

There are several features of the combination of CZE with ESI-MS that make it attractive. As can be noted by comparing the column size used in the CF-FAB approach, 13 μm I.D., with that used in ESI, 75 μm I.D., the loading capacity of CZE–ESI analyses should be significantly greater. Thus, overloading the column does not present such a severe problem. The second factor is the observation of multiply charged species permits the separation and analysis of proteins. These two features are demonstrated below.

The separation and analysis of seven angiotensins are presented in Fig. 5. Each component was injected at the 2.5-pmol level. This level would cause severe overloading on a 13 μm I.D. column. Although the peaks are broader than that observed for low fmol analyses, the components are still separated.

A separation of three proteins, myoglobin, pigeon heart cytochrome *c* and horse heart cytochrome *c* is presented in Fig. 6. The amount of each protein injected was 400 fmol. Good separation (19 000 to 35 000 theoretical plates) and sensitivity is demonstrated in this analysis. As indicated above, ESI-MS spectra are dominated by multiply charged species and the spectrum of the horse heart cytochrome *c* obtained from the separation in Fig. 6 is shown in Fig. 7. The major peak is due to the $(M + 14H)^{14+}$.

REFERENCES

1 P.R. Brown, *Anal. Chem.*, 62 (1990) 995A.
2 K. E. Karlsson and M. Novotny, *Anal. Chem.*, 60 (1988) 1662.
3 R. T. Kennedy and J. W. Jorgenson, *Anal. Chem.*, 61 (1989) 1128.
4 J. W. Jorgenson and K. D. Lukacs, *Science (Washington, D.C.)*, 222 (1984) 266.
5 J. W. Jorgenson, *Anal. Chem.*, 58 (1986) 754A.
6 R. M. Caprioli, *Anal. Chem.*, 62 (1990) 477A.

7 J. B. Fenn, M. Mann, C. K. Meng, S. F. Wong and C. Whitehouse, *Science (Washington, D.C.)*, 246 (1989) 64.
8 M. A. Moseley, L. J. Deterding, K. B. Tomer, R. T. Kennedy, N. L. Bragg and J. W. Jorgenson, *Anal. Chem.*, 61 (1989) 1577.
9 J. S. M. de Wit, L. J. Deterding, M. A. Moseley, K. B. Tomer and J. W. Jorgenson, *Rapid Commun. Mass Spectrom.*, 2 (1988) 100.
10 M. A. Moseley, L. J. Deterding, K. B. Tomer and J. W. Jorgenson, *J. Chromatogr.*, 480 (1989) 197.
11 M. A. Moseley, L. J. Deterding, K. B. Tomer and J. W. Jorgenson, *Rapid Commun. Mass Spectrom.*, 3 (1989) 87.
12 R. M. Caprioli and K. B. Tomer, in R. M. Caprioli (Editor), *Continuous-Flow Fast Atom Bombardment Mass Sepctrometry*, Wiley, New York, 1990, p. 93.
13 K. B. Tomer and M. A. Moseley, in R. M. Caprioli (Editor), *Continuous-Flow Fast Atom Bombardment Mass Spectrometry*, Wiley, New York, 1990, p. 121.
14 M. A. Moseley, L. J. Deterding, K. B. Tomer and J. W. Jorgenson, *Anal. Chem.*, 63 (1991) 109.
15 R. M. Caprioli, W. T. Moore, M. Martin, B. B. DaGue, K. Wilson and S. Moring, *J. Chromatogr.*, 480 (1989) 247.
16 N. J. Reinhoud, W. M. A. Niessen, V. R. Tjaden, L. G. Gramberg, C. R. Verheij and J. v.d. Greef, *Rapid Commun. Mass Spectrom.*, 3 (1989) 348.
17 J. A. Olivares, N. T. Nguyen, C. R. Yonker and R. D. Smith, *Anal. Chem.*, 59 (1987) 1230.
18 E. D. Lee, W. Mueck, J. D. Henion and T. R. Covey, *J. Chromatogr.*, 458 (1988) 313.
19 R. D. Smith, J. A. Loo, C. J. Barinaga, C. G. Edmonds and H. R. Udseth, *J. Chromatogr.*, 480 (1989) 211.
20 J. A. Loo, H. R. Udseth and R. D. Smith, *Anal. Biochem.*, 179 (1989) 404.
21 E. D. Lee, W. Mueck, J. D. Henion and T. R. Covey, *Biomed. Environ. Mass Spectrom.*, 18 (1989) 844.
22 E. C. Huang and J. D. Henion, *J. Am. Soc. Mass Spectrom.*, 1, (1990) 158.
23 L. J. Deterding, M. A. Moseley, K. B. Tomer and J. W. Jorgenson, *J. Chromatogr.*, 554 (1991) 73.

Journal of Chromatography, 554 (1991) 339–349
Elsevier Science Publishers B.V., Amsterdam

CHROMSYMP. 2364

Pseudo-electrochromatography–mass spectrometry: a new alternative[a]

E. R. VERHEIJ

Division of Analytical Chemistry, Center for Bio-Pharmaceutical Sciences, University of Leiden, P.O. Box 9502, 2300 RA Leiden, and TNO–CIVO Institutes, P.O. Box 360, 3700 AJ Zeist (Netherlands)

U. R. TJADEN* and W. M. A. NIESSEN

Division of Analytical Chemistry, Center for Bio-Pharmaceutical Sciences, University of Leiden, P.O. Box 9502, 2300 RA Leiden (Netherlands)

and

J. VAN DER GREEF

Division of Analytical Chemistry, Center for Bio-Pharmaceutical Sciences, University of Leiden, P.O. Box 9502, 2300 RA Leiden, and TNO–CIVO Institutes, P.O. Box 360, 3700 AJ Zeist (Netherlands)

ABSTRACT

Pseudo-electrochromatography (pEC) is a separation method that is based on the combination of the chromatographic and electrophoretic behaviour of compounds. This combination enables tuning of the selectivity without changing the composition of the mobile phase. The loadability of pEC is considerably higher than for capillary electrophoresis, which makes the coupling to mass spectrometry very attractive. The applicability of the method was examined for some nucleotides, alkaloids and an antiviral drug as model compounds. The method appeared to be able to replace a modifier gradient elution in reversed-phase systems, thus circumventing the use of an expensive gradient system. pEC has been combined with continuous-flow fast atom bombardment mass spectrometry, as is demonstrated with some examples showing the improvement in the performance of the total system.

INTRODUCTION

Continuous-flow fast atom bombardment (CF-FAB) has become a valuable technique for interfacing different separation techniques with mass spectrometry (MS) [1]. This is due to the good performance of this type of interface, permitting FAB ionization in mass spectrometry combined with liquid chromatography (LC–MS) and capillary electrophoresis (CE–MS) [2]. With growing interest in the analysis of compounds of high molecular weight such as peptides, (glyco)proteins and (oligo)-nucleotides, separation techniques that permit the analysis of these polar and often charged compounds are needed.

[a] Part of this paper was presented at the *2nd International Symposium on Microcolumn Separation Methods, Stockholm, Sweden, August 20–22, 1990.*

0021-9673/91/$03.50

Typical flow-rates allowable in CF-FAB-MS are in the range 5–15 μl/min, implying that conventionally dimensioned high-performance LC (HPLC) is not directly compatible with this type of interface. Two approaches are often applied *i.e.*, the postcolumn splitting of the effluent stream in order to achieve the required flow-rate reduction and the application of miniaturized separation systems. In principle, both approaches result in similar analyte mass flows, meaning that the detection limits obtained will not differ significanlty. A third approach is the so-called phase system switching (PSS) [3]. In this technique, the compound of interest is trapped on a small column, and is subsequently eluted with an appropriate solvent. PSS allows the use of LC systems that are not compatible with (CF-FAB-)MS [4]. Although PSS offers detection limits superior to those given by the other approaches, *i.e.*, post-column splitting and miniaturized chromatography), the technique has the severe limitation that PSS is a target compound analysis approach, which means that the whole procedure has to be focused on one particular compound.

Another separation technique that shows promising results in combination with MS is CE. CE is a miniaturized separation technique that is based on the differences in the electrophoretic mobilities of charged compounds. The compounds are separated in a capillary filled with the electrophoresis buffer by the application of a high voltage over the length of the capillary. Charged compounds will migrate towards the electrode with opposite charge. The electrophoretic migration rate is determined by the charge and the size of the molecules and is proportional to the electrical field strength. In practice, mainly fused-silica capillaries are used, in which a so-called electroosmotic flow (EOF) is generated. This EOF results in a migration of all compounds in the direction of the cathode irrespective of their charge. Owing to the presence of the EOF, negatively and positively charged compounds can be separated in the same run. On the other hand, the length of the capillary needed for a certain separation has to be increased when high EOFs are used.

The efficiencies obtained in CE are far superior to those in other separation methods. Theoretical plate numbers range from 10^5 to $5 \cdot 10^6$ in comparison with 10^4 in chromatography. The use of narrow-bore fused-silica capillaries results in peak volumes that are of the order of only tens of nanolitres. As a consequence of the high efficiencies and the speed of the separation process, mass fluxes are relatively high, which, in principle, is favourable for a mass flow-sensitive detector as a mass spectrometer. Unfortunately, a high mass flux does not always mean a high mass flow. Especially in CE the resulting mass flow is limited owing to the small dimensions of the separation capillary applied. Typical inside diameters are in the range 25–100 μm, and the lengths are commonly between 25 and 100 cm. The flow-rate caused by electroosmosis is only a few hundred nanolitres per minute, which is too low for direct coupling with the CF-FAB interface. By adding a so-called make-up flow to the CE effluent, the final flow-rate can be adjusted to the desired 5–15 μl/min. In addition, this make-up flow can also be used for providing a suitable FAB matrix.

A technique that combines the features of HPLC and CE should overcome the limitations with respect to the flow-rate in CE and the efficiency in HPLC. Therefore, the potential of the combination of (miniaturized) LC and CE and its combination with CF-FAB-MS have been investigated. In fact, electrically driven chromatography or electrochromatography (EC), as described by Knox and Grant [5], is a similar approach, but as the flow in EC is only based on electroosmosis, the resulting flow-

rate is comparable to those obtained in CE. The selectivity in EC is based on the difference in the distribution of the compounds between the stationary and the mobile phases. The driving force is the EOF, which replaces the hydrodynamic flow caused by pressurizing the column in conventional chromatography. In so-called pseudo-EC (pEC), the flow is the combination of a hydrodynamic flow and the electroosmotic flow. The overall migration of the analytes in pEC is the resultant of the chromatographic migration and the electrophoretic migration, as described by Tsuda [6].

The aim of this study was to explore the potential of pEC as an alternative to miniaturized HPLC and to CE as a separation method, offering an additional tuning of the selectivity and suitable for combination with MS detection. Some examples are given to demonstrate the potential of pEC.

EXPERIMENTAL

Chromatography

An outline of the chromatographic system is shown in Fig. 1. The solvent-delivery system consisted of a Model 2150 HPLC pump in combination with a Model 2152 HPLC controller and a low-pressure gradient mixer (all from LKB, Bromma, Sweden). The capillary column was a laboratory-packed 200 mm × 220 μm I.D. fused-silica column packed with Nucleosil 100-5C_{18} (Macherey, Nagel & Co., Düren, Germany). The column effluent was monitored at 260 nm using a Spectroflow 757 variable-wavelength UV detector (ABI Kratos, Ramsey, NJ, USA) equipped with a laboratory-made capillary flowcell using 50-μm fused silica with a volume of about 4 nl. The signal was registered on a Model BD8 multirange recorder (Kipp & Zonen, Delft, Netherlands).

A pre-injector split was applied, as the generation of reproducible and smooth flow-rates appeared possible only at flow-rates above 250 μl/min. The flow was split in the desired ratio using a Swagelok tee (Crawford Fittin, Solon, OH, USA) fitted with a 100 × 3 mm I.D. stainless-steel column manually packed with 8–9-μm XAD-2 packing material as a dummy column. A 100 μm I.D. fused-silica capillary from the gradient system was passed through the splitting tee and the stainless-steel tubing and ended 5 mm short of the injector. Samples were injected with a Model 7413 injector (Rheodyne, Berkeley, CA, USA) fitted with a 0.5-μl sample loop.

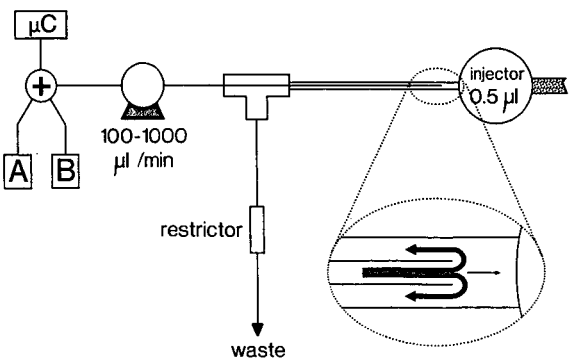

Fig. 1. Scheme of the micro-LC (gradient) system.

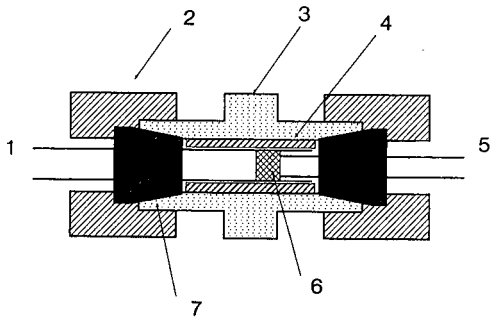

Fig. 2. End-fitting for packed fused-silica column in pseudo-electrochromatography. 1 = 220 μm I.D. packed fused-silica capillary; 2 = 1/16 in female nut; 3 = drilled-through union; 4 = PTFE insert; 5 = 50 μm I.D. fused-silica outlet capillary; 6 = silanized quartz-wool plus; 7 = Vespel ferrule.

For pEC experiments a Model VCS 303-1 reversible-polarity high-voltage power supply (Wallis, Worthing, UK) was used. The injector was connected grounded to earth in order to allow injections during high-voltage operation, while the high voltage was applied to the end of the packed fused-silica column by means of the device depicted in Fig. 2.

Micro-LC–CF-FAB interface

A coaxial [7] and a liquid junction [8] type of interface were employed. For the coaxial interface a 220 μm I.D. fused-silica capillary is inserted into the CF-FAB probe (Finnigan Mat, Bremen, Germany). The 50 μm I.D. detection capillary is run through this sheath capillary 5–50 mm short of the target. This distance was found to be of little importance.

The liquid junction type of interface (Fig. 3) is in principle based on the liquid junction interface used in previous work for the coupling of CE and CF-FAB-MS [9]. The 75-μm fused-silca capillary used in the CF-FAB probe is polished and inserted 10 mm into a 100 mm × 350 μm I.D. fused-silica capillary, and is fixed with epoxy. The 350-μm capillary is connected to a tee with a Vespel ferrule. The 50-μm capillary coming from the micro-LC system (see above) is passed through the tee and inserted

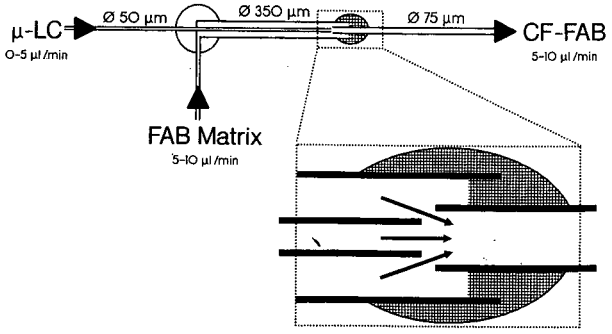

Fig. 3. Schematic diagram of the liquid junction micro-LC–CF-FAB interface for postcolumn FAB matrix addition. Ø = Diameter.

in the 350-μm capillary until positioned to the 75-μm capillary. Delivery of the FAB matrix is performed with a dual syringe pump (Model System 2; ABI Kratos) capable of precise pumping of flow-rates of 1–1000 μl/min. The make-up flow containing 15% of glycerol was applied at flow-rates between 5 and 10 μl/min. The total flow-rate going to the mass spectrometer was in the range 7–14 μl/min.

Mass spectrometry

The CF-FAB probe was mounted on a Finnigan MAT 90 doubly-focusing mass spectrometer equipped with a cryogenic pump at the ion-source housing. A saddle field gun (Ion Tech, Teddington, UK) was used to generate 7-kV xenon atoms. A gold-plated target was used in combination with a wick of pressed paper at the bottom of the ion volume to ascertain stable ionization conditions. Scans from m/z 100 up to 1200 were made at 3 s per decade (cycle time *ca.* 3.5 s) at a resolution of slightly more than 1000. The mass spectrometer was operated in both negative and positive ion mode.

Materials

Analytical-reagent grade methanol (Merck, Darmstadt, Germany) was used. Water was prepared from demineralized water with a GFL Bi-Dest 2108 distillation apparatus (GFL, Hamburg, Germany). Nucleotides were purchased from Boehringer (Mannheim, Germany), 98% chemically pure glycerol from Lamers & Pleuger ('s Hertogenbosch, Netherlands) and trifluoroacetic acid (TFA), dibutylamine (DBA) and ammonia (25%) from Merck.

Preparation of micro-columns

Pieces of 220-μm fused-silica capillary (SGE, Melbourne, Australia) of the desired length were cut and both ends were polished. One end of the capillary was connected to a male union (Swagelok) containing a metal frit (Alltech, Deerfield, IL, USA). Methanol was used as the packing solvent, and was delivered by an air-actuated pump (DSHF-302; Haskell, Burbank, CA, USA). The slurry reservoir was a 2-ml magnetically stirred high-pressure mixing chamber. In order to prevent the fused-silica capillary from exploding activation of the packing pump, a needle valve was installed between the slurry reservoir and the pump.

The packing procedure is as follows. Air is removed by flushing the system with methanol. The needle-valve is closed and a pressure of 50 bar is built up. Slurries are prepared by dispersing 250 mg of the packing material in 25 ml of methanol. This slurry is ultrasonically homogenized for 5 min and 2 ml are introduced into the slurry reservoir by means of a syringe. After connecting the fused-silica capillary to the slurry reservoir, the stirrer is activated, the needle valve is opened and the pressure is rapidly increased to 400 bar. Pressure is applied for 1 h, after which the needle valve is closed. The system is left to depressurize for 30 min and the column is disconnected. After packing, the column is primed with water and the column ends are sealed with septa.

Prior to use of the micro-column, 5 mm of the packing at the column end is removed, a 1-mm plug of silanized quartz-wool is introduced and a 50 μm I.D. fused-silica capillary is inserted in the micro-column. A piece of PTFE tubing (10 mm × 1/16 in. O.D. × 0.35 mm I.D.) is slid over this connection and inserted in a

drilled-through Swagelok male union and fixed with two Vespel ferrules, as shown in Fig. 2. The advantage of this type of connector over glueing is that columns can be changed without reinstalling the 50-μm detection capillary. Severe deterioration of plate numbers has not been observed with this construction.

The top of the column is connected to the injection valve by means of a Rheodyne nut, a Vespel ferrule and a PTFE liner (4 mm × 1/16 in O.D. × 0.35 mm I.D. tubing) to fill up the void space [10]. The described packing procedure is reproducible, and results in plate numbers for polycyclic aromatic hydrocarbons of about 12 000 for a 200-mm column. Further optimization of the procedure should improve this.

RESULTS AND DISCUSSION

Chromatographic phase systems that are applied for the separation of charged compounds are mainly based on the use of a counter ion either for ion-pair formation or as a competing ion in an ion-exchange system. As the coupling with MS requires that additives to the mobile phase are volatile, the number of applicable counter ions is drastically decreased. Commonly, strong acids are used to provide an anionic counter ion and quaternary amines to provide cationic counter ions. Volatile secondary and tertiary amines appear to be a good alternative to the non-volatile quanternary ammonium compounds. This study was limited to compounds that can be chromatograped in ion-pair reversed-phase systems. Several test mixtures have been used for the investigation of pEC.

Fig. 4a shows the chromatogram of a test mixture of some alkaloids run under isocratic conditions. Alkaloids are basic compounds that are neutral at high pH

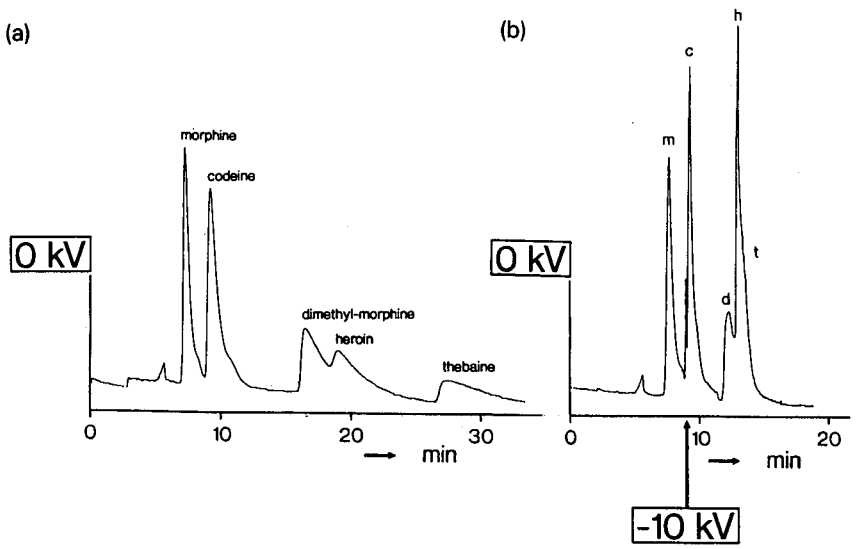

Fig. 4. Chromatograms of a test mixture of some morphine alkaloids. Column, 150 mm × 220 μm I.D. packed with 5-μm Nucleosil 100 C_{18}; mobile phase, acetonitrile–2 mmol/l ammonium acetate (2:3, v/v); applied voltage, 10 kV starting at time t = 9 min; UV detection at 220 nm, 0.01 a.u.f.s.; amounts injected, *ca.* 50 ng of each compound.

values ($pK_a > 9$). Although good efficiencies were obtained for neutral compounds, the charged alkaloids showed severe tailing, resulting in a disappointing performance of the separation system. The use of an end-capped packing material will improve the performance, but this study was not focused on the optimum separation of this type of compound. By applying a voltage over the separation column an electrophoretic component will be superimposed on the chromatographic migration. Fig. 4b shows the chromatogram of the same test mixture, but under pEC conditions. It is clear that the application of a voltage over the capillary influences the separation characteristics considerably.

An even stronger example is given by the separation of a test mixture of some nucleotides. Nucleotides are charged polar compounds possessing different numbers of phosphate moieties, which make them very well suited for separation techniques in which the electrophoretic mobility is involved.

Although much effort has been put into analyses based on MS using flow injection as an introduction technique applying different types of interface [11–16], to our knowledge no systems for nucleotide analysis by LC–MS have been reported. For UV detection-based analysis, Willis *et al.* [17] studied the use of triethylamine as an "ion-pairing" agent for the separation of a large number of nucleotides and related compounds. With respect to volatility, triethylamine looks very promising, but in practice it turned out that the concentration must be above 10 mmol/l in order to achieve sufficient retention of nucleotides. The use of such high TEA concentrations causes excessive ion-source contamination while at same time various chromatographic parameters such as selectivity and resolution are substantially affected. Haastert [18] described the use of various alkylamines for the separation of cyclic nucleotide derivatives, and reported the influence of the alkyl chain length, the number of alkyl chains, the pH of the mobile phase and the concentration of the alkylamine in

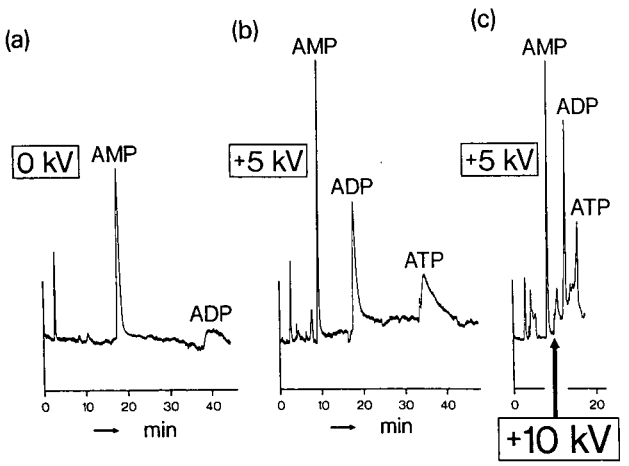

Fig. 5. Separation of 17 ng of AMP, ADP and ATP. Column, 200 mm × 220 μm I.D. packed with 5-μm Nucleosil $100C_{18}$; mobile phase, 10% methanol in 2 mmol/l dibutylamine at pH 5.0; UV detection at 260 nm, 0.0025 a.u.f.s. (a) Isocratic conditions; (b) applied voltage +5 kV; (c) starting voltage +5 kV, increased to +10 kV at $t = 9$ min.

question. The longer alkyl chains of dibutylamine (DBA) gave indeed sufficient retention of nucleotides even when used at concentrations as a low as 1–2 mmol/l.

Fig. 5a shows the chromatogram of three adenosine phosphates, separated under isocratic conditions. Retention was obtained, but ADP and ATP are eluted with a poor performance. In Fig. 5b the chromatogram of the same mixture is given, but in this case a voltage of +5 kV was applied to the downstream electrode, implying that the anionic compounds are accelerated. Although the symmetry of the later eluting compounds is far from ideal, it can be seen that a real peak compression takes place. Nevertheless, it must be realized that the same effect should be obtained by applying solvent-generated gradient elution by increasing the content of modifier in the mobile phase. In that event, however, the compatibility with the CF-FAB ionization may be diminished as the FAB conditions are affected by the change in the mobile phase composition.

The influence of the application of a voltage over the capillary is even clearer in Fig. 5c, in which after the elution of AMP the applied voltage of +5 kV was increased to +10 kV. It can easily be predicted that by using voltage-programmed elution, further optimization of the performance can be obtained. This aspect is currently under investigation.

Fig. 6 represents the mass chromatograms of inosine-5k'-triphosphate (ITP), (a) under isocratic conditions and (b) under pEC conditions. These data were obtained by applying MS in the negative-ion CF-FAB (NI-CF-FAB) mode. The signal-to-noise ratio is improved by a factor of about 10. In both instances the amount injected was about 50 ng, implying that 10–50 pmol amounts are needed for the full-scan detection of this nucleotide.

Fig. 7 gives another example of the potential of pEC, showing the mass chromatograms of suramin. Suramin is an antiviral drug with six sulphonate groups, which means that the compound will be in the form of a 6− anion that will be strongly influenced by an electric field. Fig. 7a shows the result obtained with a modifier gradient and Fig. 7b was obtained using pEC. The theoretical plate numbers of 5000 and 34 000, respectively, demonstrate an improvement that cannot be due only to an on-column concentration caused by isotachophoresis effect. With injection of an analyte dissolved in a buffer with an ionic strength below that of the running buffer, a discontinuous buffer system is used, which leads to peak sharpening during

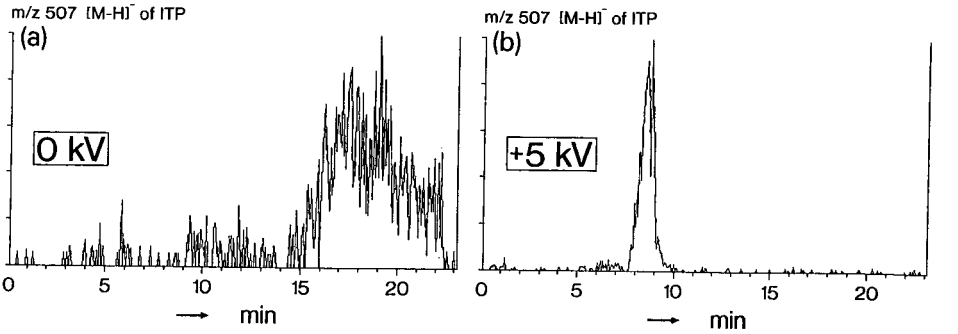

Fig. 6. Mass chromatograms of the $[M-H]^+$ ion of 50 ng of ITP obtained by (a) isocratic chromatography and (b) pEC. Conditions as in Fig. 5.

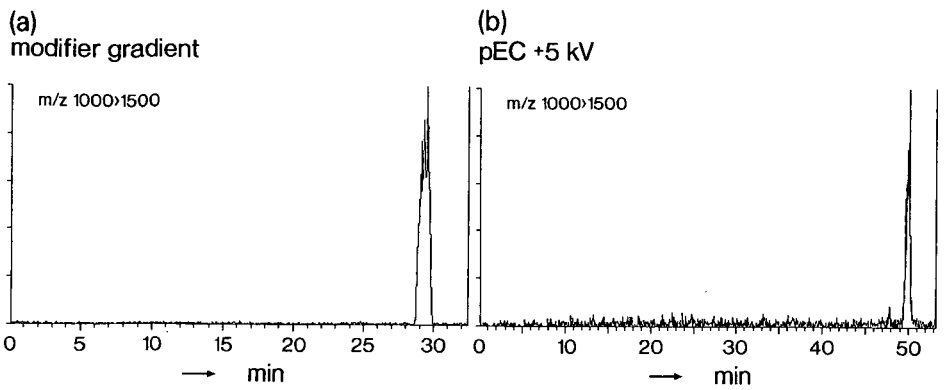

Fig. 7. Summed mass chromatograms (m/z ranging from 1000 to 1500) of 250 ng of suramin (MW 1296). Conditions as in Fig. 5. (a) Modifier gradient (5–60% methanol in 30 min); (b) pEC, modifier content 30%, applied voltage 5 kV.

the injection [19,20]. Such a compression results in a negligible injection volume, meaning that the peak broadening should only be caused by the separation processes and the detection. Taking these aspects in consideration, the obtained plate number of 34 000 is still better than expected and cannot be fully explained. A more systematic study to the peak broadening is in progress.

Fig. 8a shows the pEC–CF-FAB-MS results obtained by adding the $[M-H]^-$ ion of uridine disposphate (UDP, m/z 403) and uridine triphosphate (UTP), m/z 483). The negative-ion FAB mass spectra were obtained after injection of 10 ng of both compounds into the pEC system.

In the negative-ion mode no nucleotide ions were observed when the matrix contained TFA. However, when DBA was used instead of TFA, intense $[M-H]^-$ ions were observed. Fig. 8b and c show the negative-ion mass spectra of UDP and UTP. Ions at m/z 159 ($[P_2O_6H]^-$), 177 ($[P_2O_7H_3]^-$), 239 ($[P_3O_9H_2]^-$) and 257 ($[P_3O_{10}H_4]^-$) give information about the number of phosphate groups. Similar ions at m/z 97 ($[PO_4H_2]^-$) and 79 ($PO_3]^-$) are expected for the monophosphate nucleosides [21], but were not observed because scans were made starting at m/z 100.

Interface performance

Postcolumn addition allows any FAB matrix to be used without impairing the chromatographic separation process. The only requirement is that this should be done without (significant) decreases in chromatographic resolution. Both the coaxial and the liquid junction type of interface meet this requirement. Nevertheless, the liquid junction was chosen because the coaxial interface had some practical disadvantages, the first being the difficulty of inserting a 200 μm O.D. capillary in a 220 μm I.D. capillary over a length of 75 cm. Owing to small irregularities in the capillaries used this is sometimes impossible, or the sheath capillary is damaged. The second is that the success of this procedure depends heavily on only small between-batch differences in the fused-silica capillaries used.

This postcapillary addition results in dilution of the analytes, but with a mass flow-sensitive detector this will not affect the detection limits.

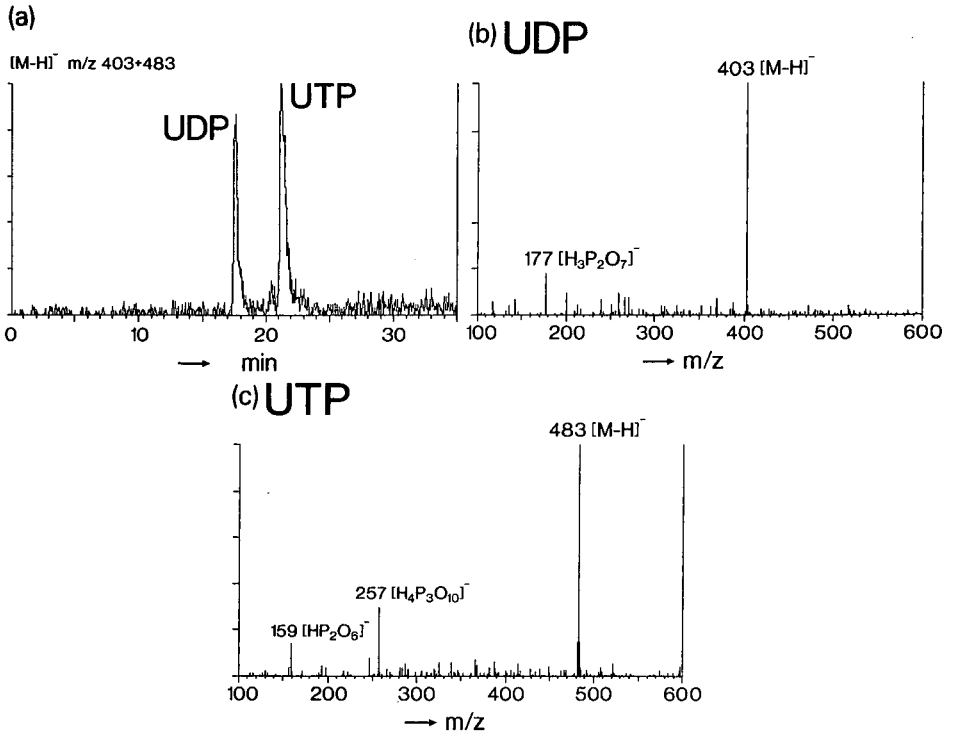

Fig. 8. (a) Mass chromatograms of the $[M-H]^+$ ions of 10 ng of UDP and UTP and (b) and (c) the corresponding negative-ion FAB mass spectra as obtained with pEC. Conditions as in Fig. 5c; applied voltage, starting voltage 5 kV, increased to 10 kV at $t=8$ min.

Limitations

The use of a hydrodynamic flow of several microlitres per minute makes the electroosmotic flow negligible. This means that for neutral compounds pEC cannot be distinguished from capillary chromatograhpy. Further, dilute buffers are required in pEC using 220 μm I.D. columns in order to avoid excessive heat generation within the capillary and simultaneously a greater risk of air bubble formation. Buffer concentrations exceeding 5 mmol/l result in unacceptably high electric currents and lower the performance of the system considerably.

CONCLUSIONS

pEC appeared to be a good supplementary technique for capillary LC. The method is useful for obtaining improved chromatographic performance for ionic compounds. The selectivity in pEC can be tuned easily by voltage programming. pEC appears to be readily compatible with CF-FAB-MS. In the analysis of charged compounds the use of an expensive gradient system can be avoided by the application of pEC. The described system allows the full-scan detection of nucleotides in 10–50 pmol amounts without the necessity for derivatization.

REFERENCES

1 Y. Ito, T. Takeuchi, D. Ishii and M. Goto, *J. Chromatogr.*, 346 (1985) 161.
2 R. M. Caprioli, T. Fan and J. S. Cottrell, *Anal. Chem.*, 58 (1986) 2949.
3 J. van der Greef, W. M. A. Niessen and U. R. Tjaden, *J. Pharm. Biomed. Anal.*, 6 (1988) 565.
4 P. S. Kokkonen, W. M. A. Niessen, U. R. Tjaden and and J. van der Greef, *Rapid Commun. Mass Spectrom.*, 5 (1991) 19.
5 J. H. Knox and I. H. Grant, *Chromatographia*, 24 (1987) 135.
6 T. Tsuda, *Anal. Chem.*, 59 (1987) 521.
7 L. J. Deterding, M. A. Moseley, K. B. Tomer and J. W. Jorgenson, *Anal. Chem.*, 61 (1989) 2504.
8 R. D. Minard, D. Chin-Fatt, P. Curry, Jr., and A. G. Ewing, presented at the *36th Annual Conference on Mass Spectrometry and Allied Topics, ASMS, San Francisco, CA, 1988*, p. 950.
9 N. J. Reinhoud, E. R. Verheij, L. G. Gramberg, W. M. A. Niessen, U. R. Tjaden and J. van der Greef, *Rapid Commun. Mass Spectrom.*, 3 (1989) 348.
10 S. Hoffmann and L. Blomberg, *Chromatographia*, 24 (1987) 416.
11 C. G. Edmonds, F. F. Hsu and J. A. McCloskey, presented at the *33rd Annual Conference on Mass Spectrometry and Allied Topics, ASMS, San Diego, CA, 1985*, p. 516.
12 C. R. Blakley, J. J. Carmody and M. L. Vestal, *J. Am. Chem. Soc.*, 102 (1980) 5931.
13 C. M. Whitehouse, R. N. Dreyer, M. Yamashita and J. B. Fenn, *Anal. Chem.*, 57 (1985) 675.
14 M. Sakairi and H. Kambara, *Anal. Chem.*, 60 (1988) 774.
15 C. G. Edmonds, J. A. Loo, C. J. Barinaga, H. R. Udseth and R. D. Smith, *J. Chromatogr.*, 474 (1989) 21.
16 K. W. M. Siu, G. J. Gardner and S. S. Berman, *Org. Mass. Spectrom.*, 24 (1989) 931.
17 C. L. Willis, C. K. Lim and T. J. Peters, *J. Pharm. Biomed. Anal.*, 4 (1986) 247.
18 P. J. M. Haastert, *J. Chromatogr.*, 210 (1981) 229.
19 J. L. Beckers and F. M. Everaerts, *J. Chromatogr.*, 508 (1990) 3.
20 D. S. Stegehuis, H. Irth, U. R. Tjaden and J. van der Greef, *J. Chromatogr.*, 538 (1991) 393.
21 J. Eagles, C. Javanaud and R. Self, *Biomed. Environ. Mass. Spectrom.*, 11 (1984) 41.

Journal of Chromatography, 554 (1991) 351–358
Elsevier Science Publishers B.V., Amsterdam

CHROMSYMP. 2252

Ionization mechanisms in capillary supercritical fluid chromatography–chemical ionization mass spectrometry

ROBERT J. HOUBEN, PIET A. LECLERCQ* and CAREL A. CRAMERS
Laboratory of Instrumental Analysis, Eindhoven University of Technology, P.O. Box 513, 5600 MB Eindhoven (Netherlands)

ABSTRACT

Ionization mechanisms have been studied for supercritical fluid chromatography (SFC) with mass spectrometric (MS) detection. One of the problems associated with SFC–MS is the interference of mobile phase constituents in the ionization process, which complicates the interpretation of the resulting mass spectra. This interference can be reduced by adding a reagent gas to the ion source. It was found that the properties and the pressure of this reagent gas control the ionization process. In this study ammonia was used as a chemical ionization (CI) reagent gas. An increase in the reagent gas pressure generally resulted in higher abundances of the protonated molecular ion. The presence of an excess of reagent gas suppresses charge exchange processes between the mobile phase constituents and the solutes. Charge exchange causes a more pronounced fragmentation than proton transfer in CI processes. The spectra obtained by charge exchange ionization, with helium as the reagent gas at moderately high pressures, are comparable to electron ionization spectra from standard MS libraries.

INTRODUCTION

The combination of capillary supercritical fluid chromatography (SFC) and mass spectrometry (MS) offers a powerful analytical technique. With SFC it is possible to analyse thermally labile and high-molecular-weight components which cannot be analysed directly by gas chromatography (GC) [1]. The properties and the low flow-rate of the SFC mobile phase (*e.g.*, carbon dioxide) allows direct interfacing with MS; liquid chromatography (LC) is more difficult to couple with MS. The application of MS provides a sensitive and general detection technique which gives structural information for unknown components. Organic mobile phase modifiers (*e.g.*, alcohols) preclude the use of flame ionization detection (FID), but are compatible with MS [2].

Prerequisites for the analysis of unknown samples are a good chromatographic separation efficiency and mass spectral integrity, yielding interpretable mass spectra. Obtaining a good separation efficiency can be a problem whenever the sample components interact with the column wall. In addition, the properties of the mobile phase are sometimes not favourable for dissolving the solutes. In both instances this may lead to deformed peaks and thus to a decreased separation efficiency. Adding polar

0021-9673/91/$03.50

mobile phase modifiers can have a positive effect on the separation. The modifier molecules can give rise to a deactivation of the active sites on the column wall and to an increase of the mobile phase polarity and density [3].

For the identification of the separated solutes, information about the molecular weight can be obtained from the mass spectrum produced whenever the molecular ion is stable enough. The spectrum can be compared with electron ionization (EI) mass spectra in computer databases or can be interpreted by the fragmentation pattern. In this way, unknown substances can be identified.

The identification process for SFC–MS can be complicated. The mobile phase constituents are ionized and collide with the sample molecules. Charge exchange ionization can occur between the ionized mobile phase constituents and the solutes [4,5] and, in addition, protic mobile phase modifiers can give rise to chemical ionization (CI) of the solutes [6]. The mass spectrum obtained thus depends on the composition and the pressure of the mobile phase in the ion source, both of which can change during the analysis.

To reduce the interference of the mobile phase in the ionization process two different approaches can be followed. One is to open the ionizer to improve pumping in this section and to effectively remove the mobile phase constituents. This approach leads to a reduced sensitivity; the reason for the reduction is not yet well known [6,7]. The improved pumping probably also causes the removal of sample constituents.

The other approach is to use a reagent gas to achieve relatively high-pressure conditions in the ionizer. The excess of reagent gas in the ionizer suppresses charge exchange and CI reactions between the solutes and the mobile phase constituents. In this way the solutes are primarily ionized by collisions with the reagent gas ions. The high-pressure conditions in the ionizer also break up clusters of solutes, which would otherwise lead to a decrease in sensitivity [8]. This cluster formation is caused by the rapid expansion of the supercritical fluid to low-pressure conditions. The expansion causes adiabatic cooling of the flow restrictor (Joule–Thompson cooling), necessitating heating of the restrictor [8]. Under high-pressure conditions the clusters formed will be broken up because an average molecule undergoes about 10^5 collisions before ionization [8]. Under low-pressure conditions the solutes may not have enough time to volatilize prior to ionization [8].

There are several reports of SFC–MS in the CI and charge exchange mode of operation. However, systematic studies on the influence of the ion source pressure on the ionization processes have not yet been published. This paper reports experiments which were carried out to acquire a better insight into the ionization processes occurring in SFC–MS. Methods to reduce the influence of the mobile phase constituents on the ionization process are described. It is shown that these methods are useful in obtaining mass spectra which are less dependent on the composition and the pressure of the mobile phase during SFC analysis.

EXPERIMENTAL

Supercritical fluid chromatography

All experiments were conducted on a Carlo Erba SFC 3000 instrument (Milan, Italy) equipped with a dual-syringe pump system. This system allows the pressure, temperature, density and composition of the mobile phase to be programmed. In the

pump system one of the two syringe heads was cooled to 5°C to facilitate filling with carbon dioxide. Carbon dioxide of 99.996% grade purity (Intermar, Breda, Netherlands) was used. An activated carbon filter was installed between the carbon dioxide bottle and the pump to further purify the mobile phase [9]. In the case of a modified mobile phase, carbon dioxide of 99.5% grade purity (Hoekloos, Schiedam, Netherlands) was used with ethanol (p.a. grade, Merck, Darmstadt, Germany) as the modifier.

The samples were dissolved in dichloromethane at concentrations of about 1 g/l. These samples were introduced onto the column by a switching valve (NI4W, Valco, Schenkon, Switzerland) actuated by helium. This valve was operated at 30°C with an injection time of 200 ms. The internal loop of the valve had a volume of 100 nl. In this way about 10 ng of the solute were introduced onto the column. No extra flow splitting was applied to reduce the amount of sample.

For small percentages of modifier, the volumetric flow-rate of the mobile phase modifier was too low to operate the pump under stable conditions. Therefore, the total flow was increased by incorporating a flow splitter before the injection valve.

The separation column was an 8 m × 50 μm I.D. fused-silica capillary, coated with a 0.25-μm film of SB-Methyl 100 stationary phase (Lee Scientific, Salt Lake City, UT, USA). The separations were performed at 100°C, except where indicated otherwise. A polished integral restrictor [10] was fabricated at the end of the column to depressurize the SFC mobile phase.

Interface design

Fig. 1 shows the laboratory-made SFC–MS interface for Finnigan MAT 4000/4500/4600 instruments (Sunnyvale, CA, USA) which required only minor modifications of the mass spectrometer inlet system.

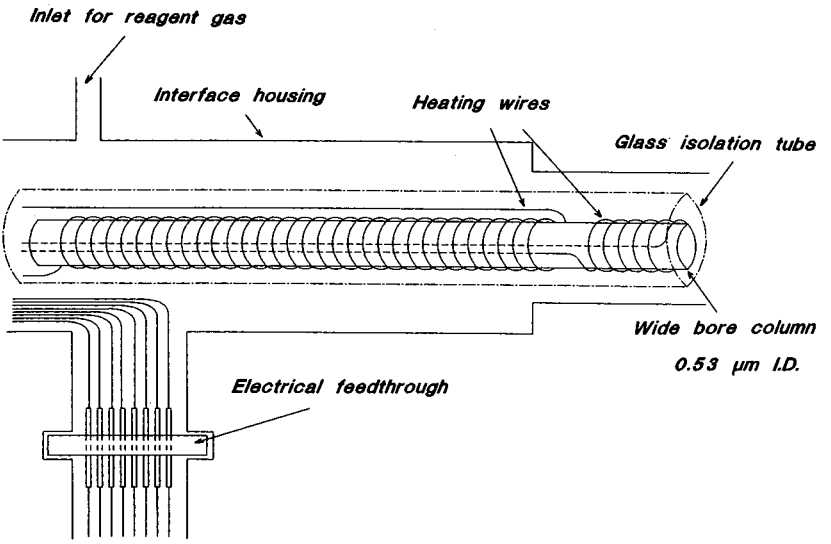

Fig. 1. Schematic diagram of the laboratory-made SFC–MS interface.

The heart of this interface is a 0.53 μm I.D. uncoated fused-silica column, wrapped with 0.2 mm O.D. Kanthal heating wire. The heating wires are electrically isolated by glass tubes (0.1 mm wall thickness) which are placed around the coil. The standard GC–MS inlet system incorporates a 5 cm × 2 mm I.D. tube, which can be switched to close the ion source (CI mode). The dimensions of this tube restrict a part of the SFC–MS interface to < 2 mm O.D.

The interface consists of two separately heated sections. A section of 55 cm maintains the SFC oven temperature up to the ion source housing, and is heated by a 50-V power supply (Delta Electronics TPS 050-5, Zierikzee, Netherlands). A 2-cm-long section controls the temperature of the restrictor and compensates for the Joule–Thompson cooling effect [8]. This section is heated by a 30-V power supply (Delta Electronics E 030-1) and is kept at a temperature of 350°C.

A glass plate in which molybdenum pins are embedded forms a vacuum feed-through for the electrical connections. To obtain a vacuum seal between this plate and the metal housing of the interface, two Kalrez rings (DuPont, Wilmington, DE, USA) were used on both sides of the plate.

Mass spectrometry

Mass specta were acquired on a Finnigan 4000 instrument with a dual electron ionization (EI)–CI source. The ion source can be switched between the EI and the CI mode by automatic mechanical and electrical readjustment. The quadrupole mass filter has a mass range of 4–1000 dalton. The vacuum system consists of two diffusion pumps, backed up by a 300 l/s mechanical forepump. The ion source and the quadrupole analyser are differentially pumped to ensure high vacuum conditions in the analyser section.

The mass spectrometer was operated in the positive-ion chemical ionization mode with a gastight ion source. The electron energy and emission current were held at 75 eV and 0.3 mA, respectively. The electron multiplier was operated at −1900 V. Under CI conditions ammonia (10% in methane) was used as the reagent gas. Under charge exchange conditions helium was used as the reagent gas. Both reagent gases were fed coaxially to the SFC effluent. In this way better results were obtained compared with feeding the gases perpendicularly to the SFC effluent.

The MS data were acquired and processed using a Data General NOVA 4/S system (Southboro, MA, USA) with custom-written software.

RESULTS AND DISCUSSION

Fig. 2 shows the influence of the CI reagent gas pressure on the ionization process. Partial mass spectra of the polymer additive Irgafos 168 [tris(2,4-di-*tert.*-butylphenyl) phosphite] are plotted as a function of the pressure in the mass analyser. This pressure was applied by adding ammonia to the ion source. The pressure in the mass analyser was used as an indication of the pressure in the ion source. From Fig. 2 it can be seen that the abundance of the protonated molecular ion, at m/z 647, increases with increasing reagent gas pressure. At low pressure the solutes are partly ionized by charge exchange, with carbon dioxide. The relative contribution of charge exchange ionization with carbon dioxide decreases when more reagent gas is introduced into the ion source. A maximum in the abundance of the protonated molec-

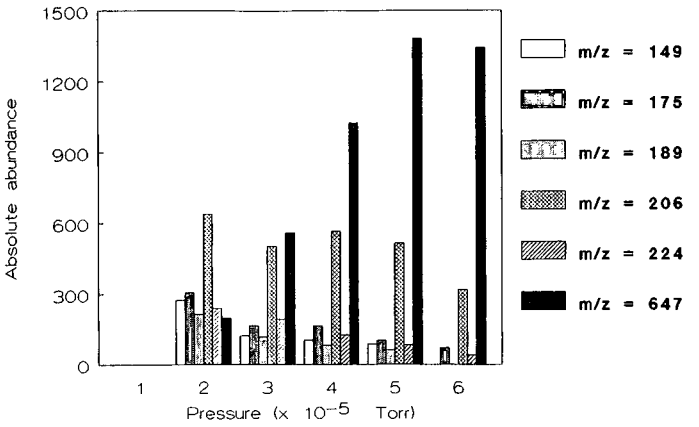

Fig. 2. Partial mass spectra of Irgafos 168 as a function of the reagent gas pressure in the mass analyser. SFC pressure programme, 150 bar (5 min), ramp of 10 bar/min to 320 bar, isobaric for 5 min. The MS was scanned at a rate of 2 s per scan with a mass range of 100–1000. The ion source temperature was 200°C.

ular ion was found at a pressure of $5 \cdot 10^{-5}$ Torr in the mass analyser. This pressure corresponded with a pressure of 0.3 Torr in the ion source (as measured with a Pirani gauge). These results show that the pressure of the reagent gas in the ion source controls the ionization and fragmentation process. During the course of an SFC pressure programme, increasing the mobile phase pressure will change the conditions in the ion source continuously. This indicates that at lower mobile phase pressures, CI spectra are obtained, but that higher mobile phase pressures result in mixed charge exchange–CI spectra. However, Fig. 2 indicates that CI conditions can be obtained for the component Irgafos 168, which eluted at a SFC mobile phase pressure of about 310 bar.

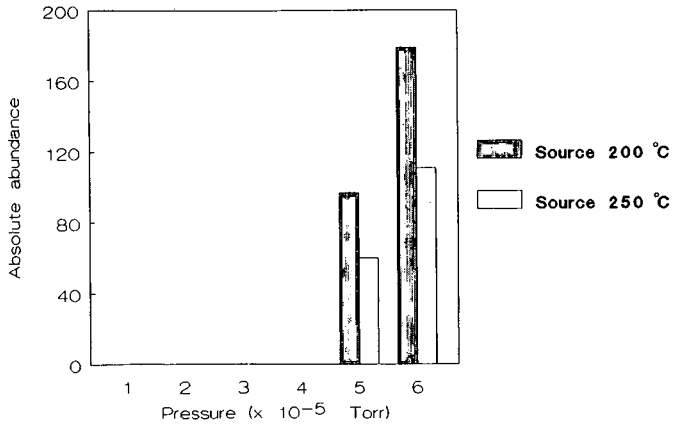

Fig. 3. Abundance of the protonated molecular ion of Tinuvin 770 as a function of the reagent gas pressure in the mass analyser. The ion source was held at 200 and 250°C, respectively. Other experimental conditions as in Fig. 2.

For some types of samples, relatively high-pressure conditions are necessary to detect the protonated molecular ion. The energy transferred at the ionization of the sample molecules should be low enough to prevent extensive fragmentation. For the polymer additive Tinuvin 770 [bis(2,2,6,6-tetramethyl-4-piperidinyl) sebacate], no protonated molecular ions, at m/z 481, were found at pressures lower than $5 \cdot 10^{-5}$ Torr in the mass analyser (see Fig. 3). Lowering the source temperature also resulted in more abundant molecular ions and less fragmentation as is also shown in Fig. 3.

One way to obtain mass spectra similar to EI spectra, which can be found in libraries, is to use charge exchange [11]. In the charge exchange process the sample constituents are ionized by collisions with a reagent gas that does not contain protons. Carbon dioxide [4,5], helium [6], nitrogen [11] and air [12] have been used as reagent gases. During the ionization process a relatively high amount of energy is transferred to the solutes [13]. This means that charge exchange ionization causes a high degree of fragmentation, comparable to the fragmentation process in EI. For SFC–MS this implies that spectra similar to those seen with EI can be produced while relatively high-pressure conditions are maintained in the ion source [6]. A comparison between the spectra obtained with SFC–MS with helium as the reagent gas and GC–EI-MS is given in Figs. 4–6. This comparison was made by transferring the SFC–charge exchange MS data from the NOVA 4/S computer to a VAX 8530 computer. Using MASS-LIB (Max-Planck-Institut für Kohlenforschung, Mülheim/Ruhr, Germany), a software package for library searching of mass spectra, the SFC–charge exchange MS spectrum was matched with the EI spectra available in the

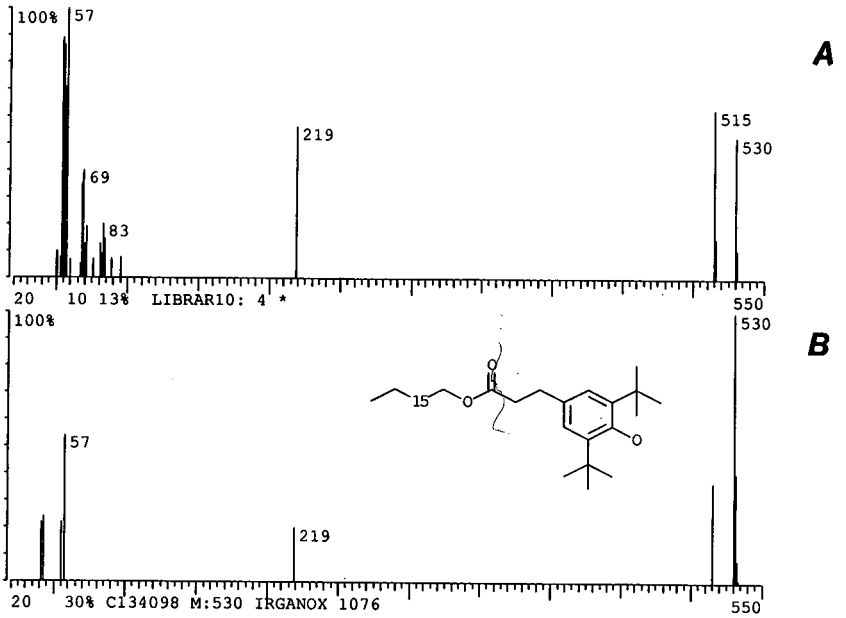

Fig. 4. Mass spectra of Irganox 1076 (A) under SFC–charge exchange MS conditions and (B) from the MASS-LIB library (best hit). The pressure in the analyser under SFC–charge exchange MS conditions was $2.5 \cdot 10^{-5}$ Torr. Other experimental conditions as in Fig. 2.

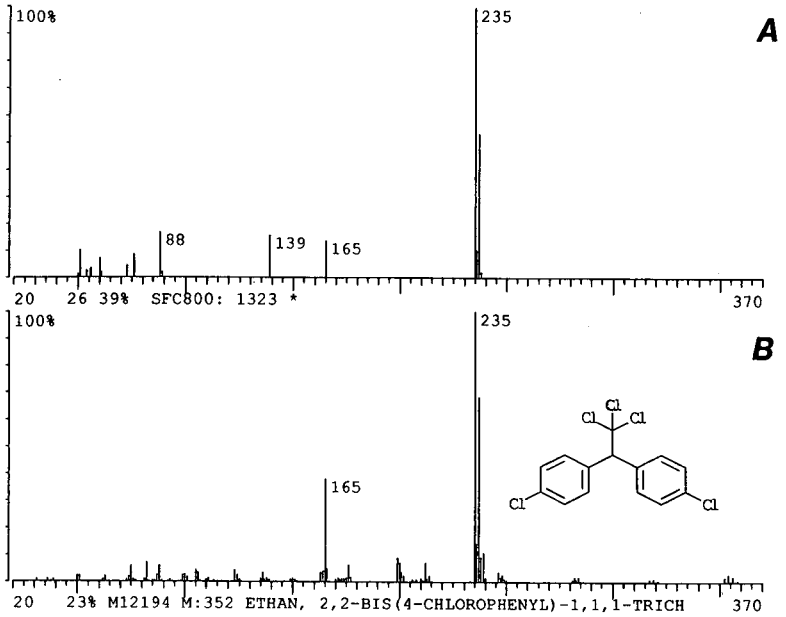

Fig. 5. Mass spectra of *p,p'*-DDT (A) under SFC–charge exchange MS conditions and (B) from the MASS-LIB library (best hit). SFC pressure programme, 100 bar (5 min), ramp of 10 bar/min to 320 bar. The MS was scanned at a rate of 1 s per scan with a mass range 50–500. The pressure in the analyser was $2.5 \cdot 10^{-5}$ Torr.

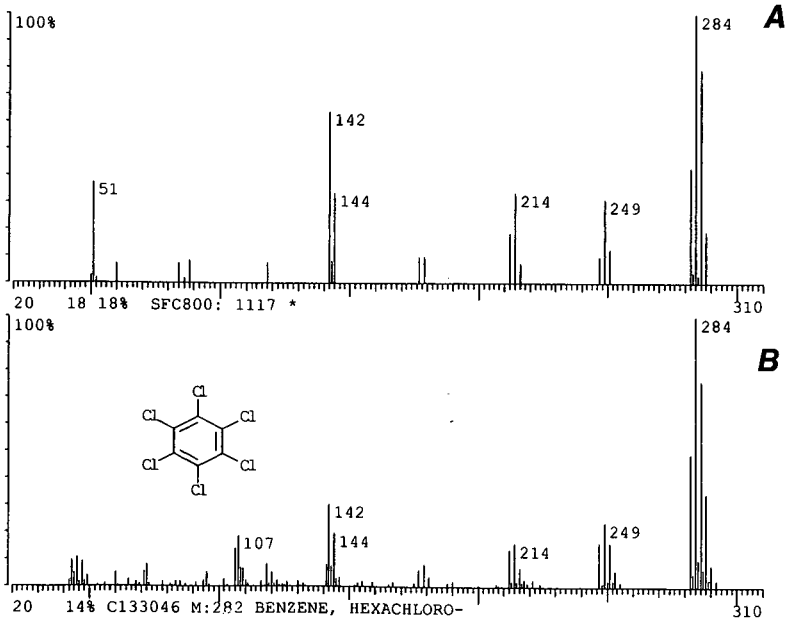

Fig. 6. Mass spectra of hexachlorobenzene (A) under SFC–charge exchange MS conditions and (B) from the MASS-LIB library (best hit). Experimental conditions as in Fig. 5.

libraries. The unknown compound can be identified by finding the spectrum with the highest similarity index ("best hit"). In Fig. 4 the spectra of the polymer additive Irganox 1076 [octadecyl-3-(3,5-di-*tert.*-butyl-4-hydroxyphenyl) propionate] are shown. Figs. 5 and 6 give the results for *p,p'*-DDT and hexachlorobenzene, compounds of environmental interest. The SFC–charge exchange MS spectra differ from the GC–EI-MS spectra in two ways, namely in the relative intensity of the different ions and in the presence of ions produced from mobile phase constituents. The relative intensity of the different ions can be tuned by selecting the pressure and the properties of the charge exchange reagent gas. It was found that SFC–charge exchange MS with helium as the reagent gas resulted in a higher degree of fragmentation than that found with GC–EI-MS. The degree of fragmentation decreased when more helium was introduced into the ion source. At the same time, a decrease in sensitivity was found. Good results were obtained at a moderately high pressure of $2.5 \cdot 10^{-5}$ Torr in the mass analyser (ion source pressure 0.2 Torr). In contrast, contributions found from mobile phase impurities (such as hydrocarbons) can only be reduced by the use of more highly purified carbon dioxide [9].

CONCLUSIONS

In coupled SFC–MS, the ionization process can be controlled by applying a relatively high reagent gas pressure to the ion source. In this way ionization primarily occurs by collisions between the reagent gas ions and the solute molecules. The influence of the composition and the pressure of the SFC mobile phase on the ionization process is thus reduced. The properties and the pressure of the reagent gas control the ionization process resulting in charge exchange spectra similar to EI, or in CI spectra.

REFERENCES

1 C. M. White and R. K. Houck, *J. High Resolut. Chromatogr. Chromatogr. Commun.*, 9 (1986) 4.
2 B. W. Wright, H. T. Kalinoski, H. R. Udseth and R. D. Smith, *J. High Resolut. Chromatogr. Chromatogr. Commun.*, 9 (1986) 145.
3 J. G. M. Janssen and C. A. Cramers, *J. Chromatogr.*, 505 (1990) 19.
4 J. D. Pinkston, D. J. Bowling and T. E. Delaney, *J. Chromatogr.*, 474 (1989) 97.
5 J. Cousin and P. J. Arpino, *J. Chromatogr.*, 398 (1987) 125.
6 E. D. Lee, S.-H. Hsu and J. D. Henion, *Anal. Chem.*, 60 (1988) 1990.
7 R. D. Smith, H. R. Udseth and H. T. Kalinoski, *Anal. Chem.*, 56 (1984) 2971.
8 R. D. Smith, H. T. Kalinoski and H. R. Udseth, *Mass Spectrom. Rev.*, 6 (1987) 445.
9 H. J. Houben, J. G. M. Janssen, P. A. Leclercq, J. A. Rijks and C. A. Cramers, *J. High Resolut. Chromatogr.*, 13 (1990) 669.
10 E. J. Guthrie and H. E. Schwartz, *J. Chromatogr. Sci.*, 24 (1986) 236.
11 D. F. Hunt and P. J. Gale, *Anal. Chem.*, 56 (1984) 1111.
12 S. Huang, *Org. Mass Spectrom.*, 24 (1989) 1065.
13 A. G. Harrison, *Chemical Ionization Mass Spectrometry*, CRC Press, Boca Rotan, FL, 1983, p. 14.

Author Index

PUBLICATION SCHEDULE FOR 1991

Journal of Chromatography and Journal of Chromatography, Biomedical Applications

MONTH	D 1990–M 1991	J	J	A	S	O	N	D
Journal of Chromatography	Vols. 535–545/1	545/2 546/1 + 2 547/1 + 2	548/1 + 2 549/1 + 2 550/1 + 2	552/1 + 2 553/1 + 2 554/1 + 2 555/1 + 2	556/1 + 2 557/1 + 2 558/1	558/2 559/1 + 2		
Cumulative Indexes, Vols. 501–550				551/1 + 2				
Bibliography Section	560/1	560/2			561/1			561/2
Biomedical Applications	Vols. 562–566	567/1	567/2 568/1	568/2	569/1 + 2 570/1	570/2	571/1 + 2	572/1 + 2

INFORMATION FOR AUTHORS

(Detailed *Instructions to Authors* were published in Vol. 522, pp. 351–354. A free reprint can be obtained by application to the publisher, Elsevier Science Publishers B.V., P.O. Box 330, 1000 AH Amsterdam, The Netherlands.)

Types of Contributions. The following types of papers are published in the *Journal of Chromatography* and the section on *Biomedical Applications:* Regular research papers (Full-length papers), Review articles and Short Communications. Short Communmications are usually descriptions of short investigations, or they can report minor technical improvements of previously published procedures; they reflect the same quality of research as Full-length papers, but should preferably not exceed six printed pages. For Review articles, see inside front cover under Submission of Papers.

Submission. Every paper must be accompanied by a letter from the senior author, stating that he/she is submitting the paper for publication in the *Journal of Chromatography*.

Manuscripts. Manuscripts should be typed in double spacing on consecutively numbered pages of uniform size. The manuscript should be preceded by a sheet of manuscript paper carrying the title of the paper and the name and full postal address of the person to whom the proofs are to be sent. As a rule, papers should be divided into sections, headed by a caption (*e.g.*, Abstract, Introduction, Experimental, Results, Discussion, etc.). All illustrations, photographs, tables, etc., should be on separate sheets.

Introduction. Every paper must have a concise introduction mentioning what has been done before on the topic described, and stating clearly what is new in the paper now submitted.

Abstract. All articles should have an abstract of 50–100 words which clearly and briefly indicates what is new, different and significant.

Illustrations. The figures should be submitted in a form suitable for reproduction, drawn in Indian ink on drawing or tracing paper. Each illustration should have a legend, all the *legends* being typed (with double spacing) together on a *separate sheet.* If structures are given in the text, the original drawings should be supplied. Coloured illustrations are reproduced at the author's expense, the cost being determined by the number of pages and by the number of colours needed. The written permission of the author and publisher must be obtained for the use of any figure already published. Its source must be indicated in the legend.

References. References should be numbered in the order in which they are cited in the text, and listed in numerical sequence on a separate sheet at the end of the article. Please check a recent issue for the layout of the reference list. Abbreviations for the titles of journals should follow the system used by *Chemical Abstracts.* Articles not yet published should be given as "in press" (journal should be specified), "submitted for publication" (journal should be specified), "in preparation" or "personal communication".

Dispatch. Before sending the manuscript to the Editor please check that the envelope contains four copies of the paper complete with references, legends and figures. One of the sets of figures must be the originals suitable for direct reproduction. Please also ensure that permission to publish has been obtained from your institute.

Proofs. One set of proofs will be sent to the author to be carefully checked for printer's errors. Corrections must be restricted to instances in which the proof is at variance with the manuscript. "Extra corrections" will be inserted at the author's expense.

Reprints. Fifty reprints of Full-length papers and Short Communications will be supplied free of charge. Additional reprints can be ordered by the authors. An order form containing price quotations will be sent to the authors together with the proofs of their article.

Advertisements. Advertisement rates are available from the publisher on request. The Editors of the journal accept no responsibility for the contents of the advertisements.

This comprehensive book covers all important separation methods

Chromatography Today

by **C.F. Poole** and **S.K. Poole**, Wayne State University, Detroit, MI, USA

Chromatography Today provides an extensive coverage of all important chromatographic methods in a single text. Gas, liquid, thin layer and supercritical fluid chromatographic and capillary electrophoretic methods are handled with an emphasis on the contemporary practice.
Particular attention is given to the optimization of these techniques. Method selection then becomes a more logical process.
As an integral part of the total analytical technique, sample preparation methods as well as preparative scale separations are treated fully. The most common hyphenated techniques used for sample identification are also discussed.

Scope and level of **Chromatography Today** make the book suitable for:
- graduate level students as a textbook in separation science;
- professional institutes offering short courses in chromatography;
- chromatographers who may use the book to refresh their knowledge in the field.

Chromatography Today offers:
- a comprehensive collation of all relevant equations, physical constants and general information used by chromatographers;
- extensive bibliography of recent literature to facilitate the location of specific items or areas of interest.

Chromatography Today is illustrated with over 200 figures, 110 tables and contains more than 3,330 references to contemporary literature.

Contents:

1991 x + 1026 pages
Price: US $ 147.50 / Dfl. 295.00
ISBN 0-444-88492-0

Paperback:
Price: US $ 75.00 / Dfl. 150.00
ISBN 0-444-89161-7

Elsevier Science Publishers

P.O. Box 211, 1000 AE Amsterdam, The Netherlands
P.O. Box 882, Madison Square Station, New York, NY 10159, USA